Physics Division
Physics Division
Physics Division
Physics Division
Physics Division
Physics Division
Physics Division
Physics Division

Physics Division Annual Report 1999

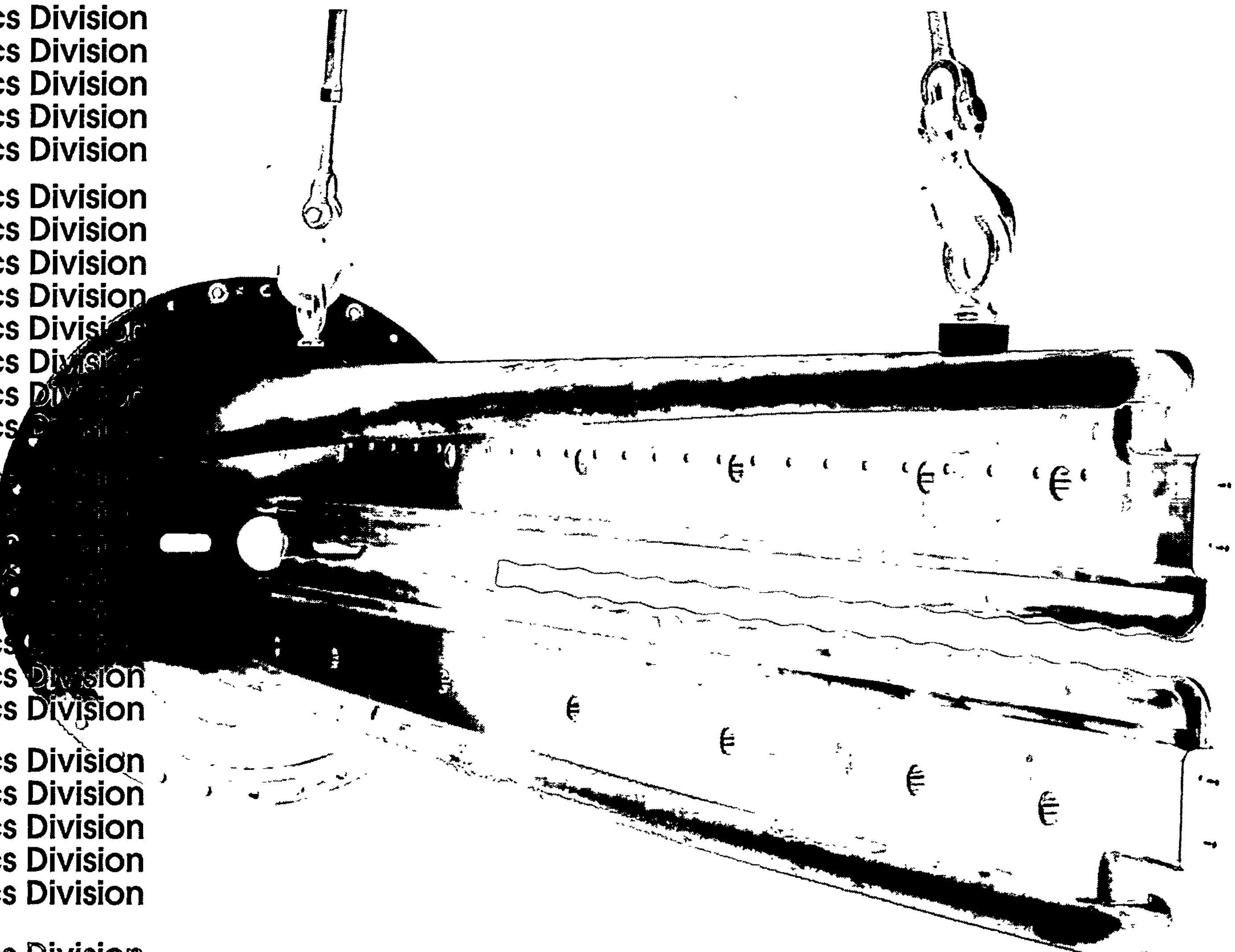

Argonne National Laboratory

operated by The University of Chicago

for the United States Department of Energy under Contract W-31-109-Eng-38

ARGONNE NATIONAL LABORATORY UNIVERSITY OF CHICAGO

Physics Division
Physics Division

Available electronically at http://www.doe.gov/bridge

Available for a processing fee to U.S. Department of Energy and its contractors, in paper, from:

U.S. Department of Energy
Office of Scientific and Technical Information
P.O. Box 62
Oak Ridge, TN 37831-0062
phone: (865) 576-8401
fax: (865) 576-5728
email: reports@adonis.osti.gov

ANL-00/20

ARGONNE NATIONAL LABORATORY
9700 S. Cass Avenue
Argonne, Illinois 60439-4801

PHYSICS DIVISION ANNUAL REPORT

1999

Donald F. Geesaman
Director

October 2000

Preceding Annual Reports
ANL-97/14 1996
ANL-98/24 1997
ANL-99/12 1998

Edited by Karen J. Thayer

FOREWORD

This report summarizes the research performed in the past year in the Argonne Physics Division. The Division's programs include operation of ATLAS as a national heavy-ion user facility, nuclear structure and reaction research with beams of heavy ions, accelerator research and development especially in superconducting radio frequency technology, nuclear theory and medium energy nuclear physics. The Division took significant strides forward in its science and its initiatives for the future in the past year. Major progress was made in developing the concept and the technology for the future advanced facility of beams of short-lived nuclei, the Rare Isotope Accelerator. The scientific program capitalized on important instrumentation initiatives with key advances in nuclear science.

In 1999, the nuclear science community adopted the Argonne concept for a multi-beam superconducting linear accelerator driver as the design of choice for the next major facility in the field, a Rare Isotope Accelerator (RIA) as recommended by the Nuclear Science Advisory Committee's 1996 Long Range Plan. Argonne has made significant R&D progress on almost all aspects of the design concept including the fast gas catcher (to allow fast fragmentation beams to be stopped and reaccelerated) that, in large part, defined the RIA concept, the superconducting rf technology for the driver accelerator, the multiple-charge-state concept (to permit the facility to meet the design intensity goals with existing ion-source technology), and designs and tests of high-power target concepts to effectively deal with the full beam power of the driver linac. An NSAC subcommittee recommended the Argonne concept, and set as the design goal Uranium beams of 100-kwatt power at 400 MeV/u. Argonne demonstrated that this goal can be met with an innovative, but technically in-hand, design.

The heavy-ion research program focused on Gammasphere, the premier facility for nuclear structure gamma-ray studies. One example of the ground-breaking research with Gammasphere was the first study of the limits of stability with angular momentum in the shell stabilized nobelium isotopes. It was found that these heaviest nuclei could be formed at surprisingly high angular momentum, providing important new insight into the production mechanisms for super-heavy elements. Another focus continues to be experiments with short-lived beams for critical nuclear astrophysics applications. Measurements revealed that ^{44}Ti is more readily destroyed in supernovae than was expected. Major progress was made in collecting and storing unstable ions in the Canadian Penning Trap. The technique of stopping and rapidly extracting ions from a helium gas cell led directly to the new paradigm in the production of rare isotope beams that became RIA.

ATLAS provided a record 6046 hours of beam use for experiments in FY99. The facility pressed hard to support the heavy demands of the Gammasphere research program but maintained an operational reliability of 93%. Of the 29 different isotopes provided as beams in FY99, radioactive beams of ^{44}Ti and ^{17}F comprised 6% of the beam time.

The theoretical efforts in the Division made dramatic new strides in such topics as quantum Monte Carlo calculations of light nuclei to understand microscopic many-body forces in nuclei; QCD calculations based on the Dyson-Schwinger approach which were extended to baryon systems and finite temperatures and densities; the structure of heavy nuclei; and proton decay modes of nuclei far from stability.

The medium-energy program continues to focus on new techniques to understand how the quark-gluon structure of matter impacts the structure of nuclei. The HERMES experiment began making measurements of the fraction of the spin of the nucleon carried by the glue. Drell-Yan experiments study the flavor composition of the sea of the proton. Experiments at Jefferson lab search for clues of QCD dynamics at the hadronic level. A major advance in trace isotope analysis was realized with pioneering work on Atom Trap Trace Analysis, exploiting the exquisitely sensitive nature of laser-

atom traps to detect, background free, ^{81}Kr at the 10^{-13} level. This technique provides a valuable new approach to such diverse problems as dating old ground water, the solar neutrino problem, measuring charge radii of exotic nuclei and medical applications.

The performance of the Division in 1999 is, in large part, a result of the seven years of leadership of Walter Henning. Walter left the Division in the fall of 1999 to become the Director of GSI. His mark on the Division was unmistakable. I will endeavor to ensure that Walter's spirit of creative, world-class research and gracious behavior remains the hallmark of the Division in the next millennium.

Donald Geesaman, Director, Physics Division

TABLE OF CONTENTS

I. HEAVY-ION NUCLEAR PHYSICS RESEARCH

OVERVIEW

The Heavy-Ion program in the Argonne Physics Division addresses key questions about the structure and dynamics of the nuclear many-body system. Nuclear structure and reactions are studied in collisions between complex nuclei with heavy-ion beams mostly from the Argonne Tandem-Linac Accelerator (ATLAS), a national heavy-ion users facility. Some important studies are performed at forefront facilities elsewhere. The major thrusts of this program are three-fold: a) the understanding of the nucleus as a many-body system built of protons and neutrons and governed by the strong force, b) the exploration of the origin of the chemical elements and their role in shaping the reactions that occur in the cataclysmic events of the cosmos and c) tests of the limits of validity of the Standard Model, the fundamental theory that currently best represents our understanding of the laws and fundamental symmetries of Nature. The specific current research topics include the development and acceleration of short-lived nuclei and their use in measurements of cross-sections of astrophysics interests as well as in nuclear structure and reaction dynamics studies; the production and study of nuclei at the very limits of stability, in particular the discovery of new proton emitters near the drip line and the study of the level structure of very heavy elements ($Z > 100$); the study of exotic nuclear shapes, including superdeformation; the delineation of the essential parameters governing dynamics of reactions between heavy nuclei such as fusion, fission, transfer and deep inelastic reactions; tests of current descriptions of the weak force. Smaller scale efforts complementary to the main research program focus on the behavior of cooled ions confined in storage rings and ions traps, and on the study of collisions between heavy ions at relativistic energies. These efforts are based on forefront instrumentation available at ATLAS which includes Gammasphere, the Fragment Mass Analyzer (both systems are also used in combination), the Canadian Penning Trap, and exploit the unique capabilities of the accelerator to produce radioactive beams either through reactions in a production target or directly from the ion source. Participation to the PHOBOS detector construction is at the core of the research with relativistic heavy ions.

Some of the main goals of the program can be summarized as follows:

- Develop and utilize short-lived nuclear beams (1) to measure reactions of astrophysics interest (^{17,18}F, ^{21}Na and the break-out of the hot CNO cycle, ^{25}Al, ^{44}Ti and ^{56}Ni and the rp process), (2) to study the properties of proton-rich nuclei (single-particle states near the unstable doubly-magic nucleus ^{56}Ni), and (3) to investigate aspects of reaction dynamics (the impact of weakly bound states on fusion).

- Discover new isotopes and determine the properties of these nuclei at the limits of proton-stability by measuring (1) groundstate quantum numbers, (2) particle decay modes (proton, alpha and beta decay) and (3) gamma decay of excited states taking advantage of the resolving power of Gammasphere and the selectivity offered by the Fragment Mass Analyzer (FMA).

- Study the importance of shell effects on nuclear structure as a function of mass, excitation energy and spin. In particular, understand the properties of heavy nuclei ($Z > 82$), of superdeformed nuclei, and of light ($A < 30$) nuclei (in the regime where particle and gamma decay compete) by comprehensive measurements with the highest detection sensitivity (Gammasphere).

- Determine time scales of dissipation processes in nuclei through the characterization of the gamma decay of giant dipole resonances (utilizing the LEPPEX array of BaF_2 detectors) with mass or angular momentum selection.

- Measure with high precision nuclear masses with the CPT, in particular the mass of super-allowed 0^+ to 0^+ beta emitters ($50 < A < 100$). These mass determinations have a direct impact on the determination of the fundamental weak vector coupling constant and the unitarity test of the top row of the Cabbibo-Kobayashi-Maskawa matrix.

- Use the high quality beams of ATLAS to pursue unique applications with energetic heavy-ion beams such as defects in high Tc superconductors, and accelerator mass spectrometry of heavy (transactinide) radioisotopes.

- Understand the behavior of nuclear matter at high density by exploring collisions between relativistic heavy ions. Studies focus on particle production, phenomena associated with collective flow and in-medium modification of meson masses.

A. EXPERIMENTS WITH SECONDARY BEAMS

Over the last few years, a number of secondary (e.g. radioactive) beams of short-lived nuclei have been produced and accelerated at ATLAS. So far, beams of ^{18}F ($t_{1/2}$ = 110 m), ^{56}Ni ($t_{1/2}$= 61 d), ^{56}Co ($t_{1/2}$ = 77d), ^{44}Ti ($t_{1/2}$ = 60 y) have been produced and accelerated via the so-called two-accelerators method where beam material is being produced at another accelerator, and subsequently transformed into a cone for the SNICS source of the tandem. Beams of shorter lived isotopes have been produced directly at ATLAS with the in-flight technique where a primary beam undergoes a reaction in a gas cell. These beams are: ^{17}F ($t_{1/2}$ =65 s), ^{21}Na ($t_{1/2}$ = 22.5 s), ^{25}Al ($t_{1/2}$ = 7.2 s) and ^{8}B ($t_{1/2}$ = 770 ms). The experiments being performed cover issues of interest in nuclear astrophysics and in nuclear structure. This section also contains a description of efforts by members of the Heavy-Ion group towards the Rare Isotope Accelerator (RIA) described in detail elsewhere in this report.

a.1. Spin Determination of States in ^{18}Ne via the ^{17}F(p,p)^{17}F Reaction

(B. Harss, J. Caggiano, P. Collon, J. P. Greene, D. Henderson, A. Heinz, R. V. F. Janssens, C. L. Jiang, J. Nolen, R. C. Pardo, T. Pennington, K. E. Rehm, J. P. Schiffer, R. H. Siemssen, I. Wiedenhoever, M. Paul,* R. E. Segel,† and P. Parker‡)

Our measurements of the ^{17}F(p,α)^{14}O reaction (see annual report 1998) identified several new levels in ^{18}Ne which contribute to the breakout from the hot CNO cycle via the ^{14}O(α,p)^{17}F reaction. The angular distributions of the (p,α) reactions, however, are not very sensitive to the angular momentum transfer and therefore for some of the states no definite spin assignment could be made. Elastic proton scattering on ^{17}F, on the other hand, is expected to provide a better signature between positive and negative parity states. We have therefore measured elastic and inelastic scattering of ^{17}F on a hydrogen target.

The ^{17}F beam was produced by the in-flight technique via the d(^{16}O,^{17}F)n reaction with a ^{16}O beam from ATLAS incident on a gas cell filled with deuterium. Details of the production technique can be found in the 1998 annual report.

Elastic scattering of ^{17}F on hydrogen was separated from scattering of the beam contaminant ^{16}O by detecting the scattered protons in kinematic coincidence with the heavy beam particle (^{17}F or ^{16}O) which was identified with respect to mass and Z by an annular parallel plate avalanche counter/Bragg Curve ionization chamber combination. The protons were detected by two annular Si detectors surrounded by six 5 × 5 cm^2 Si strip detectors. The detection efficiency of the whole array was typically 60%.

Excitation functions for two states in ^{18}Ne at E_x = 7.16 and 7.60 MeV were measured with this setup. The data are presently being analyzed.

*Hebrew University, Jerusalem, Israel, †Northwestern University, ‡Yale University

a.2. Production of a ^{44}Ti Beam at ATLAS

(K. E. Rehm, I. Ahmad, J. P. Greene, J. Nolen, R. C. Pardo, A. A. Sonzogni, B. Zabransky, D. L. Bowers, F. Brumwell,* G. McMichael,* and M. Paul†)

Satellite-based gamma detector arrays have recently been used to identify remnants of supernovae through the detection of the ^{44}Ti afterglow. Nuclei of ^{44}Ti($T_{1/2}$ = 60 y) are produced in supernovae in the so-called alpha-rich freeze-out. The amount produced in the explosion is governed by a subtle interplay between nuclear reactions that produce it and those that destroy it. Network calculations have shown that the number of ^{44}Ti nuclei produced in a supernova depends strongly on the cross section of the ^{44}Ti(α,p)^{47}V reaction. For a first measurement of this reaction in the laboratory we have developed a ^{44}Ti beam at ATLAS. The ^{44}Ti material was produced via the ^{45}Sc(p,2n) reaction, using a 50-MeV, 20-μA proton beam from the linac injector of Argonne's Intense Pulsed Neutron Source (IPNS) facility. The target, a 25 mm diameter, 5 mm-thick disk of Sc, was mounted inside a water-cooled Cu holder, whose front face was made of graphite, acting both as a collimator and an energy degrader. The irradiation lasted ~70 hours. Two weeks later, the Sc disk was removed from the holder and placed in front of a Ge detector. The dominant source of gamma radiation originated from the decay of ^{44}Sc. Nuclei of ^{46}Sc ($T_{1/2}$ = 83.8 d) were also produced by neutron capture. A ^{44}Ti activity of ~180 μCi was obtained from the γ spectrum, which represents ~ 1.8×10^{16} atoms or ~ 1.3 μg of ^{44}Ti.

About four weeks later, the ^{44}Ti activity was chemically separated from the Sc material. The Sc disk was dissolved in a HNO_3/HCl solution and the Sc then precipitated by the addition of HF. The solution containing the Ti activity was then dried and heated. A part of the resulting material, left as a $^{44}TiO_2$ compound, was mixed with 50 mg of $^{nat}TiO_2$ and placed inside a copper insert for a negative-ion Cs-sputter source. The ^{44}Ti activity from the pellet was measured to be ~38 μCi. From the ion source a beam of $^{44}TiO^-$ was extracted and injected into the tandem accelerator at ATLAS. After stripping in the terminal of the tandem, a $^{44}Ti^{8+}$ beam was accelerated in the linac part of ATLAS to an energy of 133.5 MeV. Two guide beams were used to optimize the beam tuning of the ATLAS accelerator for the weak $^{44}Ti^{8+}$ beam: the optics of the ion source and the tandem injector were tuned with $^{48}TiO^-$, while the superconducting linac was tuned with $^{66}Zn^{12+}$.

In order to measure the composition of the accelerated mass 44 beam, a 2 mg/cm^2 Ti foil was used to degrade its energy and the Fragment Mass Analyzer (FMA) was set to separate the beam particles in m/q. Ions with the same m/q value but different nuclear charge experience a different energy loss in this foil and can thus be easily identified in the focal plane of the FMA. Figure I-1 shows a ΔE--E plot measured in an ionization chamber in the focal plane of the FMA. The different components of the beam are indicated. From these measurements it was concluded that 38% of the beam consisted of ^{44}Ti, 54% of ^{44}Ca while ^{33}S and ^{11}B accounted for the remaining 8%. The ^{33}S and ^{11}B ions are injected as mass 60 molecules from the ion source and ions with the same charge-to-mass ratio are accelerated to the same velocity in the linear accelerator. Intensities of ~ 5×10^5 ^{44}Ti/s on target were observed. This allowed a first measurement of the ^{44}Ti(α,p)^{47}V reaction (see Sec. a.3).

*Intense Pulsed Neutron Source, ANL, †Hebrew University, Jerusalem, Israel

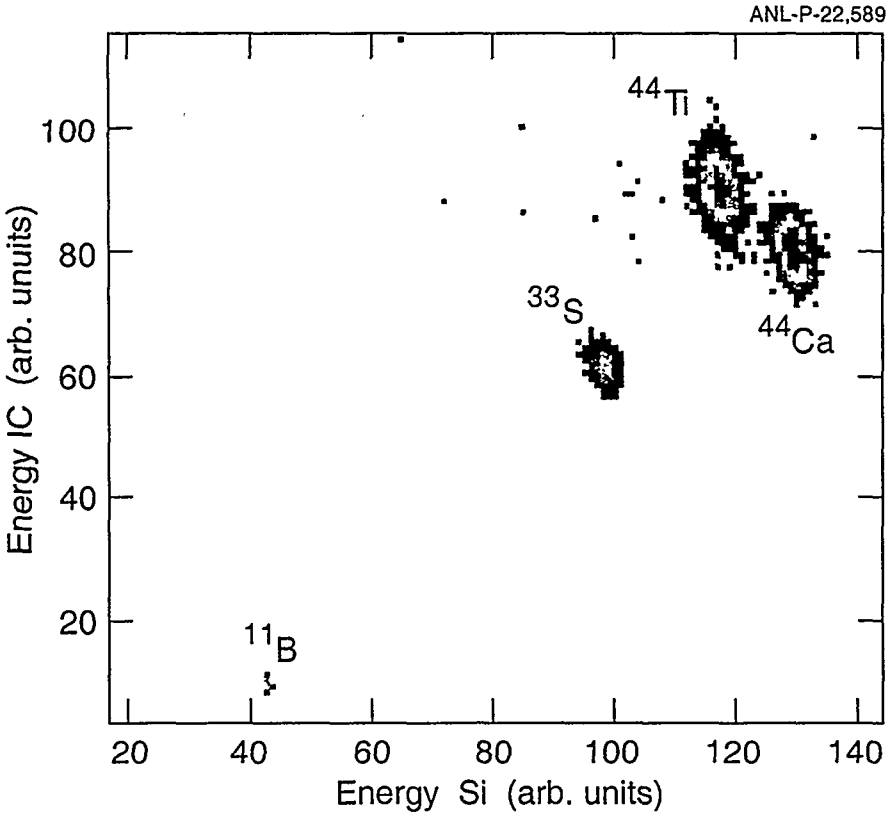

Fig. I-1. Energy loss (measured in the ionization chamber) vs. residual energy (measured in a Si detector) for particles detected in the focal plane of the Fragment Mass Analyzer. The different components of the beam are indicated.

a.3. The ^{44}Ti(α,p) Reaction and Its Implication on the ^{44}Ti Yield in Supernovae

A. Sonzogni, K. E. Rehm, I. Ahmad, J. Caggiano, C. N. Davids, J. P. Greene, B. Harss, A. Heinz, D. Henderson, R. V. F. Janssens, C. L. Jiang, J. Nolen, R. C. Pardo, J. P. Schiffer, D. Seweryniak, R. H. Siemssen, J. Uusitalo, I. Wiedenhöver, B. Zabransky, F. Borasi,† D. L. Bowers,¶ F. Brumwell,* G. McMichael,* M. Paul,‡ R. E. Segel,† and J. W. Truran§)

The recent observation of γ rays associated with the decay of ^{44}Ti by the COMPTEL space telescope from the Cassiopeia A and from the Vela supernova remnants have demonstrated that the ^{44}Ti gamma afterglow can be used to locate individual supernova remnants. It is expected that with the next-generation of space-based gamma-ray observatory INTEGRAL (scheduled for launch in 2001), new supernova remnants will be discovered and the total mass of ^{44}Ti ejected in the supernova events will be determined. The use of the ^{44}Ti afterglow of supernovae for distance or age determination depends critically on the amount of ^{44}Ti produced in the explosion which is governed by a subtle interplay between the nuclear reactions that produce it and those that destroy it. This subject was studied in detail for type II supernovae by The et al.[1] From these calculations, it was concluded that the amount of ^{44}Ti produced in a supernova depends strongly on the cross section of the ^{44}Ti(α,p)^{47}V reaction. Since ^{44}Ti(α,p)^{47}V reaction destroys ^{44}Ti, an increase in its rate will decrease the final amount of ^{44}Ti and vice-versa. Due to the relatively high value of the Coulomb barrier for the ^{4}He + ^{44}Ti system, the influence of this reaction is felt at temperatures of 2.2-4.2 × 10^9 K. This temperature range corresponds to center-of-mass energies (Gamow peak values) of 4-6.1 MeV. In order to put the nuclear astrophysics part of ^{44}Ti production in supernovae on a more solid ground we have performed the first measurement of the ^{44}Ti(α,p)^{47}V reaction.

The production of the ^{44}Ti sample and details of the beam production are described in a separate contribution (see Sec. a.2). The ^{44}Ti beam bombarded a ^{4}He gas target consisting of a 2.2-mm-long cell with two 1.3 mg/cm^2 titanium metal windows, filled with 600 mbar of ^{4}He and cooled to LN_2 temperature. The areal density was 80 μg/cm^2. For the separation of the ^{47}V reaction products emitted at small scattering angles (typically 2°) from the primary mass 44 beam particles the Fragment Mass Analyzer (FMA) was used. To further identify the ^{47}V particles an Ionization Chamber (IC) and a Si detector were placed behind the Parallel Grid Avalanche Counter (PGAC) at the focal plane of the FMA. The PGAC provided position and timing signals, while the IC-Si detectors gave energy and Z information.

To avoid a re-tuning of the linac at each energy change, which, for low intensity beams, can be quite time-consuming, Ti degrader foils ranging in thickness from 0.6 to 2 mg/cm^2 were used. The energy measurements of the beam were done by time-of-flight using the isochronous property of the FMA. Before the ^{44}Ti experiment the experimental arrangement was tested with stable ^{40}Ca and ^{46}Ti beams. For ^{40}Ca as well as for ^{44}Ti, the (α,p) reaction dominates in the energy range of interest. With a transport efficiency through the FMA which was calculated taking the charge-state distributions, the kinematics and small angle scattering into account, the measured excitation function for the ^{40}Ca(α,p)^{43}Sc reaction was found to be in very good agreement with the results from the literature.

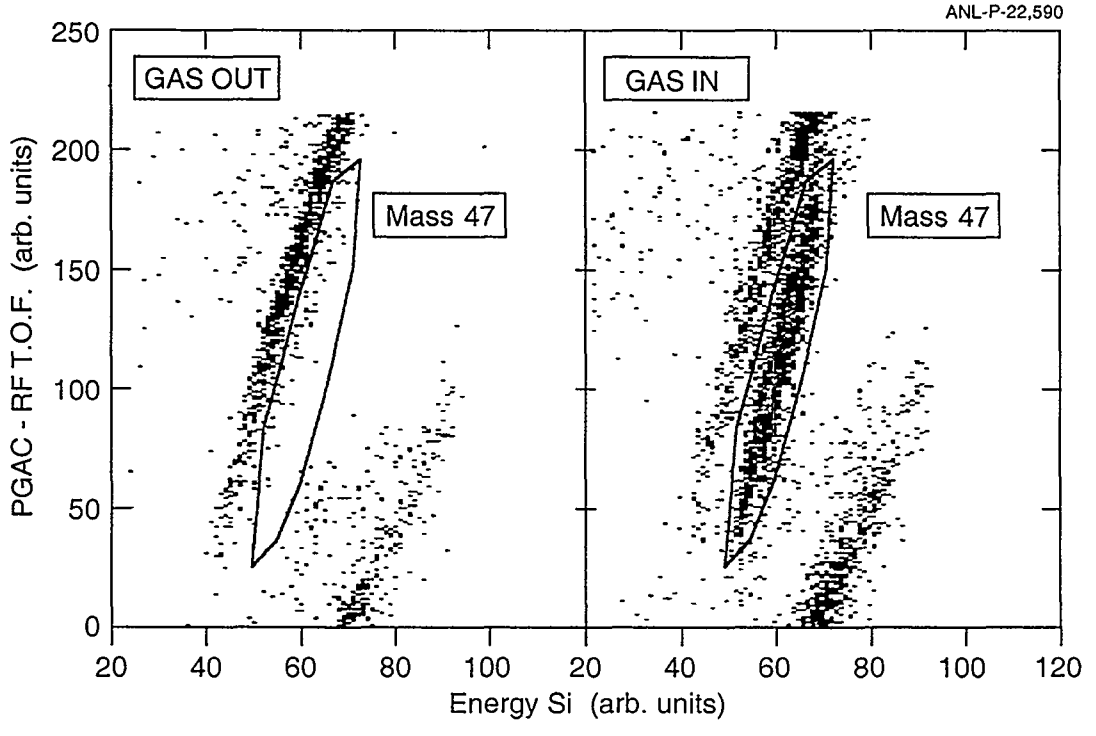

Fig. I-2. Time of flight (measured with the parallel-grid-avalanche-counter relative to the rf timing from the accelerator) vs. energy (measured in the Si detector). The left panel corresponds to an empty gas cell, the one at the right to a full gas cell. The reaction products with mass 47 are indicated by the solid contour line.

Plots of the time-of-flight through the FMA versus the energy measured in the Si detector behind the focal plane are shown in Fig. I-2 for an incident ^{44}Ti energy of 122.1 MeV. The left panel corresponds to an empty gas cell, the right one to a gas cell filled with 600 mbar of He. With the empty cell only mass 44 particles are observed, produced by beam particles scattered in the gas cell windows or on various components in the FMA. The plot for the full gas cell shows the mass 47 reaction products, well separated from the scattered mass 44 particles. To measure the contributions from the reactions products from the ^{44}Ca component of the beam (mainly ^{47}Ti and ^{47}Sc produced via the ^{4}He(^{44}Ca,n) and ^{4}He(^{44}Ca,p) reactions) a pure beam of ^{44}Ca was used. To correct for the charge-state distribution of ^{47}V detected in the focal plane, the

distributions were measured in a separate experiment (see Sec. a.4) using stable ^{51}V beams in the energy range E_{lab} = 25-110 MeV and adjusted to the same velocities.

The resulting cross sections for the $^{44}Ti(\alpha,p)^{47}V$ reaction can be seen in Fig. I-3. The solid line is the result from the statistical model code SMOKER[2] which is used in many astrophysical network calculations to estimate astrophysical reaction rates that cannot be studied in the laboratory. At the two higher energies the agreement between our experiment and the theoretical prediction is excellent. However, the falloff in the cross section due to the penetration of the Coulomb barrier appears to be shifted towards lower energies resulting in cross sections that are larger by about a factor of two compared to the SMOKER predictions. The astrophysical reaction rate for the $^{44}Ti(\alpha,p)$ reaction is shown by the solid line in Fig. I-4. The reaction rates from the SMOKER calculations as well as those by Woosley et al.[3] are given by the dashed and dot-dashed curves, respectively. These two sets of theoretical calculations give basically the same result for the $^{44}Ti(\alpha,p)^{47}V$ reaction rates, which is lower than the experimentally determined rate by about a factor of two.

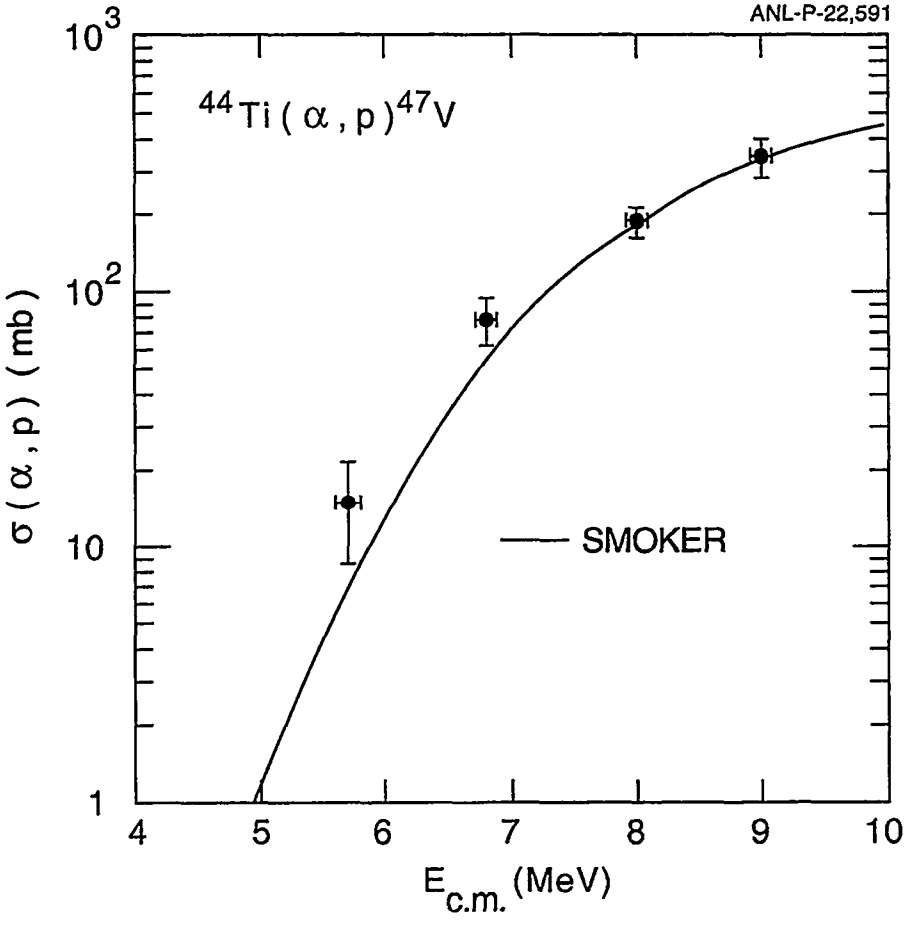

Fig. I-3 Measured excitation function for the $^{44}Ti(\alpha,p)^{47}V$ reaction. The solid line corresponds to a calculation done with the code SMOKER.

The higher astrophysical reaction rate results in a reduction of the amount of ^{44}Ti produced in supernovae explosions. With the increased reaction rate shown in Fig. I-4 one expects a 25% decrease in the ^{44}Ti yield of a type II supernova. For a measurement of the ^{44}Ti gamma-ray flux from a supernova, this decrease in yield translates into a 12% larger distance or a 20 y earlier occurrence. It should be noted that changes in other reaction rates which have not been measured so far (e.g. the $^{45}V(p,\gamma)$ reaction) could effect the ^{44}Ti yield as well.

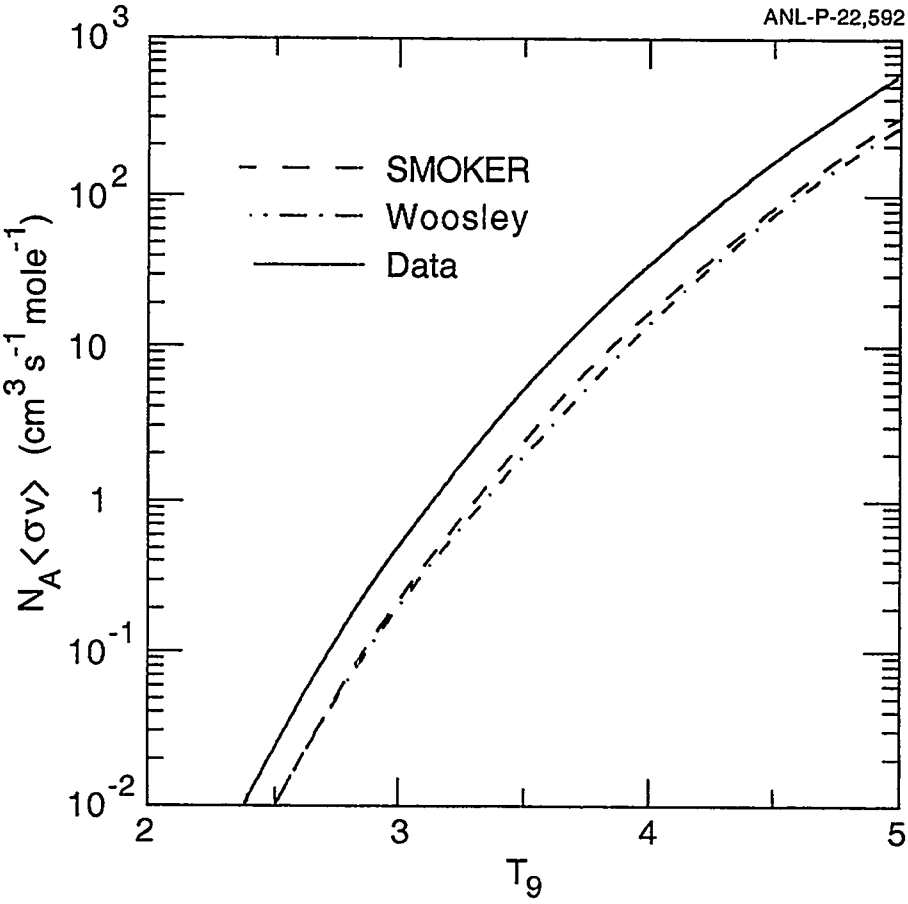

Fig. I-4. Astrophysical reaction rates for the $^{44}Ti(\alpha,p)^{47}V$ reaction. The solid line was obtained from the experimental information as described in the text. The dashed line corresponds to a SMOKER calculation and the dot-dashed line to a calculation by Woosley et al. [Ref. 3].

In addition to its effects on the energetics of the light curve of supernova 1987A, and for searches for ^{44}Ti decay γ rays from galactic supernova remnants, these new experimental results also hold important implications for galactic nucleosynthesis. Observational determinations of the abundances of (elemental) titanium in the oldest (most metal deficient) stars in our galaxy reveal that titanium is over-abundant relative to iron by a factor of ~ 2-3. Preliminary calculations of supernova nucleosynthesis indicate that the higher rate for $^{44}Ti(\alpha,p)^{47}V$ might result in an increased production of ^{48}Cr which decays into the most abundant Ti isotope ^{48}Ti.

*Intense Pulsed Neutron Source, ANL, †Northwestern University, ‡Hebrew University, Jerusalem, Israel, §University of Chicago, ¶Chemical Technology, ANL

[1]L.-S. The *et al.*, Astrophys. Jrnl. **504**, 500 (1998).
[2]F-K. Thielemann *et al.*, Advances in Nucl. Astrophys., Editions Frontiere, **525** (1987).
[3]S. E. Woosley and T. A. Weaver, Astrophys. Journ. Suppl. **101**, 181 (1995).

a.4. Measurement of ^{51}V Charge State Distributions

(A. Sonzogni, K. E. Rehm, I. Ahmad, C. N. Davids, J. P. Greene, B. Harss, D. Henderson, R. V. F. Janssens, C. L. Jiang, J. Nolen, R. C. Pardo, J. P. Schiffer, D. Seweryniak, J. Uusitalo, I. Wiedenhöver, F. Borasi,* M. Paul,† and R. E. Segel*)

As mentioned in Sec. a.3, cross sections for the $^{44}Ti(\alpha,p)^{47}V$ reaction which are of interest in nuclear astrophysics were measured using the Fragment Mass Analyzer (FMA). An important part of this project was a knowledge of the transmission efficiency of the FMA, i.e. the probability that ^{47}V nuclei produced by the reaction will reach the detector at the focal plane of the FMA. This efficiency is given by the product of two terms: the geometric transport efficiency determined by the acceptance of the FMA and the charge state distribution of the particles of interest.

In order to improve the accuracy on the measured cross sections, the charge state distributions for ^{51}V were measured at energies of 25-120 MeV using the Enge split pole magnetic spectrograph. A Ti target, whose thickness was chosen to simulate the energy loss in the ^{4}He gas cell windows, was used to scatter ^{51}V beam particles, which were detected at the focal plane of the Enge split-pole spectrograph, using the standard focal plane detector.

Since the FMA separates ions in M/Q, its capabilities to distinguish ^{47}V from beam-like particles ^{44}Ti particles can be improved by choosing an appropriate foil after the Ti windows, which will maximize the charge state distribution in a region of charge state where it is unlikely to find beam particles with the same M/Q. Several exit foil options (Be,C..) were explored and it was concluded that a thin Au foil was the most suitable one for our project.

As an example, a charge state distributions for ^{51}V ions measured at 0.5 MeV/u with a Carbon exit foil can be seen in Fig. I-5, together with calculations from Ref. 1 (full line) and Ref. 2 (dashed line).

This extensive body of data, corrected for the mass difference and interpolated to the energies of interest, was used to obtain the charge state distributions for ^{47}V.

*Northwestern University, †Hebrew University, Jerusalem, Israel

[1]K. Shima *et al.*, At. Data and Nucl. Data Tables **51**, 173 (1992).
[2]Y. Baudinet-Robinet, Nucl. Instrum. Methods **190**, 197 (1981).

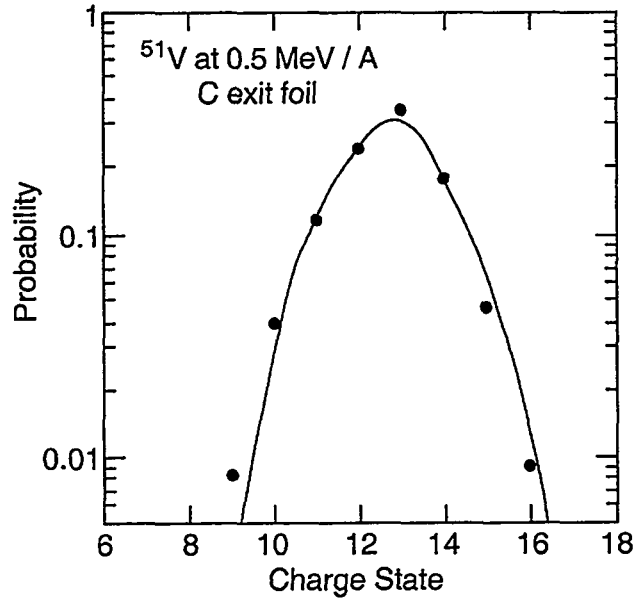

Fig. I-5. Charge-state distribution measured with a 0.5-Mev/u ^{51}V beam and a C foil.

a.5. Study of Proton-Unbound States in Astrophysically-Interesting Nuclei

(J. A. Caggiano and K. E. Rehm)

An important task in nuclear astrophysics is linking observational gamma ray astronomy to laboratory studies of nuclei. The availability of data from COMPTEL/CGRO has provided measurements to constrain for models used to understand explosive events such as nova and supernova in the heavens. For example, the ability to detect gamma rays from ^{26}Al and ^{44}Ti, and the absence of gamma rays from ^{22}Na have provided such constraints.

^{26}Al and ^{22}Na are predominantly made as unstable proton rich nuclei in the rp process and then decay to these nuclei as daughters. Thus, in order to understand how much of these isotopes was made in the event, an understanding of the production rates of their parents is important.

Many of the proton rich nuclei have been studied with the (p,t) or (^{3}He,n) reactions which very preferentially populate natural parity states. As a consequence, many of the unnatural parity states in these nuclei remain missing (based on mirror nucleus considerations). Furthermore, investigation of the production of certain isotopes (^{26}Al for example) show that unnatural parity states can dominate proton capture rates. In these cases, where the data is missing, the models rely on reaction rates that are based solely on theoretical predictions of where the levels are, which have uncertainties of ~100 keV or so. Because the rate depends exponentially on the resonance energy (level energy less the Q-value), a 100 keV uncertainty can mean orders of magnitude uncertainty in the rates, which renders the calculation essentially useless.

The (^{3}He,^{6}He) reaction will be used to populate important states in proton rich nuclei, such as ^{26}Si (ATLAS proposal #835) and ^{22}Mg (experiment at Yale University to be done in February 2000). The Enge split-pole spectrograph will be used to identify and measure the energy of the ^{6}He. This method has many advantages:

- Cross sections are of the order of 1 μb/sr, making the measurement possible.
- Resolution of 40 keV or better is possible.
- The reaction can populate unnatural parity states.
- When studying even-even nuclei, because the starting nucleus usually has an extra neutron, the Q-value gets much less negative (~ -15 to -20 MeV). This makes the cross sections larger and enables easy separation from the reactions on the inevitable target contaminants carbon and oxygen (Q-values of ~ -30 MeV), leaving no question as to the origin of the states.
- Because of this fact, carbon in the target backing provides no interference, and hence targets don't have to be self-supporting.

Many proton-rich nuclei will be studied in this manner during the course of next year (2000).

a.6. Yield Calculations for an Advanced Rare Isotope Accelerator Facility

(C. L. Jiang, B. B. Back, I. Gomes, A. M. Heinz, J. A. Nolen, K. E. Rehm, G. Savard, and J. P. Schiffer)

Over the last ten years, intense worldwide effort has been devoted to the design of facilities which can produce a broad range of radioactive nuclei at high intensities[1]. The scientific opportunities offered by these facilities have been discussed extensively at many recent national and international conferences[2].

In the course of the development of these concepts and designs, the calculation of production yields using different kinds of reaction mechanisms at different energies and different beam-target combinations plays a fundamental role.

An exciting new concept for an advanced facility of the ISOL type (Isotope Separation On Line) for beams of exotic short-lived nuclei has been developed at Argonne National Laboratory[3,4]. Such a facility is based on a high intensity driver beam that produces short-lived nuclear species which are stopped in a suitable medium. The desired isotopes are then selected, and accelerated to the appropriate energy in a second accelerator. Most importantly, it includes a novel approach that avoids the most serious drawbacks of an ISOL facility for a broad range of beams: delay between the production of the short-lived isotopes and their acceleration and the underlying sensitivity to the chemistry of the extracted species. Many reaction mechanisms (related with a special beam-target assemblies) can be used. The most important are the following four: spallation reactions, two-step fast neutron fission, projectile fragmentation and in-flight fission.

The ANL concept is based on a high-power superconducting linac providing a broad range of beams. With the intense beams and high target power densities expected from the driver linac, target cooling becomes a central issue. The four reaction mechanisms are all associated with different beam-target assemblies, optimized for the cooling problems and the extraction of the reaction products. These beam-target assemblies have been described in Ref. 4.

Predictions of production yields of secondary beam should be based on experimental data as much as possible. However, in many cases experimental cross sections are not available, and therefore yields need to be estimated using theoretical calculations. In this contribution the aim is not to calculate precise yields for some special nuclide, but to create a general idea of what yields a next generation ISOL facility can provide over the whole region of a Z-N map. Even with an uncertainty of a factor of ten, the relative trends and ratios still supply important information.

Data bases for either reaction cross sections or yields have been generated for all reaction mechanisms discussed above.

For spallation reactions (Standard ISOL method) many data have been published in the literature[5]. From the tables obtained at E_{proton} = 600 or 1000 MeV, a yield data base was created. Since in many cases the experimental data do not cover a wide enough mass region, extrapolations have been performed to obtain the yields for some isotopic chains.

For the two-step fission reaction mechanism, data bases for yields at $E_{deuteron}$ = 200, 400, 800 and 1200 MeV (at constant power 100 kW) have been generated using Lahet[6] calculations. The actual target geometry (a cooled tungsten neutron production target and a uranium carbide fission target) has been used in the calculations and contributions from fast and from slow neutrons were included. Yields for nuclides at the neutron-rich region with very small cross sections were obtained by extrapolations.

For fragmentation reactions, most of the data were obtained from calculations. For each desired product, several beams can be used for the production, and an optimum beam has to be selected. ISAPACE[7], a computer program based on the internuclear cascade program incorporated with the evaporation code PACE, requires considerable computing time. EPAX, a parametrization of the fragmentation process[8], on the other hand, provides also good estimates within very short computing time.

A program was developed to produce a data base for fragmentation reactions for all nuclides in the Z-N plane at 100 MeV/u and 100 kW with yields higher than 10^{-6}/sec. An automatic searching was done using EPAX for each desired product, by comparing the yields from all possible beams. The target thickness in the calculations was determined by the requirement that the energy of the beam after the target was 50 MeV/u, since for energies < 50 MeV/u the production yields

were found to decrease rapidly. To produce different isotopes for a given element, several beams have to be used. For example, for the Sn isotopes of A = 125-128, 129-132, 133-139 and 140-145, the optimum beams are ^{130}Te, ^{136}Xe, ^{150}Nd and ^{160}Gd respectively. The target used in the calculations was ^{7}Li, since with liquid lithium the cooling problem can be solved using existing technologies as mentioned in Ref. 4.

For in-flight fission reactions, experiments with ^{238}U beams (750 MeV/u) at GSI supply a good base of reaction cross sections for the production of neutron-rich nuclide[9]. From these data we have generated a data base for in-flight fission reaction method using also calculations with the Abrasion-Ablation Model[10]. For some isotopes in the neutron-rich region extrapolations have been performed.
From these data bases predicted yields at different energies (MeV/u) and different beam power can be calculated, and various yields for nuclides in the Z-N plane can be displayed.

In the following we compare the yields from the four production methods to find out which method can provide the most intense beam for each nuclide. The resulting two-dimensional Z-N map is shown in Fig I-6. For simplification, the ISOL mechanism and two-step mechanism are combined and shown in green,

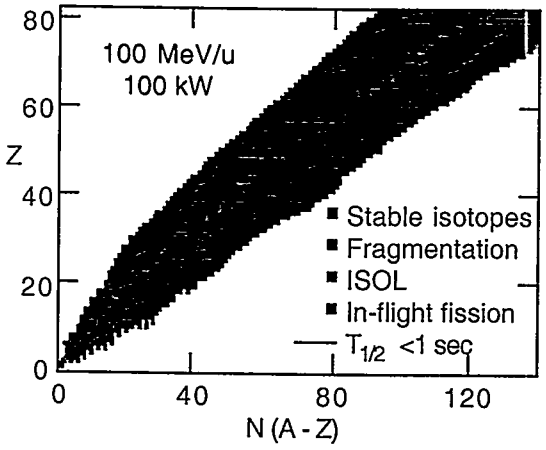

Fig. 1-6. Reaction mechanisms which give the highest yields of each separated isotope assuming 100 kW of beam power and 100 MeV/u.

the fragmentation mechanism in red, and the in-flight fission method in blue. It should be noted that this plot extends to isotopes for which the yield with a next generation ISOL facility would be on the order of a few per day (10^{-4}), and which are, for the most part, totally unknown. The assumptions in Fig. I-6 are for a facility with 100 kW of beam power at 100 MeV/u. Different assumptions (e.g. 400 MeV/u) will not change the results appreciably.

Contour plots of the production yields are shown in Fig. I-7, which gives the intensities for a next generation RIA facility, using for any nuclide the highest yield from any of the four production methods.

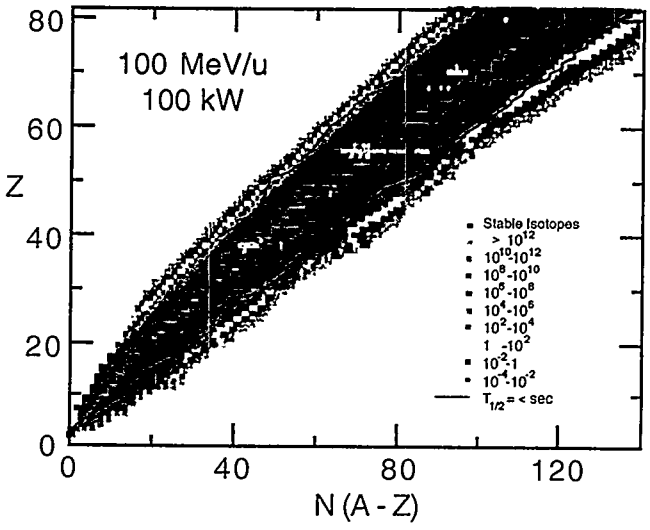

Fig. I-7. Mass-separated yields (ions/sec) for an advanced ISOL facility, assuming 100 kW of beam power and primary beams of 100 MeV/u.

The absolute production yields depend very much on the bombarding energy. At higher beam energies, thicker targets can be used. However, there are additional effects which influence the yields and have to be included in the calculations (attenuation effects of the beam and of the reaction products, production through the secondary reactions, and multiple scattering which influences the transmission efficiency of the mass separator). These effects are usually small at E_{beam} = 100 MeV/u but become more significant at higher beam energies (higher target thicknesses) especially for the fragmentation and in-flight fission production methods.

The calculations indicate that there is an optimum target thickness at each higher incident energy, which gives the maximum yields. Absolute yields for some nuclei are shown in Fig. I-8 as a function of the bombarding energy assuming a constant primary beam current (100 kW at 400 MeV/u). From Fig. I-8 we observe the wide range of intensities that can be produced by the different reaction mechanisms. Yields from the fragmentation method are shown in red, for in-flight fission method in blue, and from the standard ISOL and

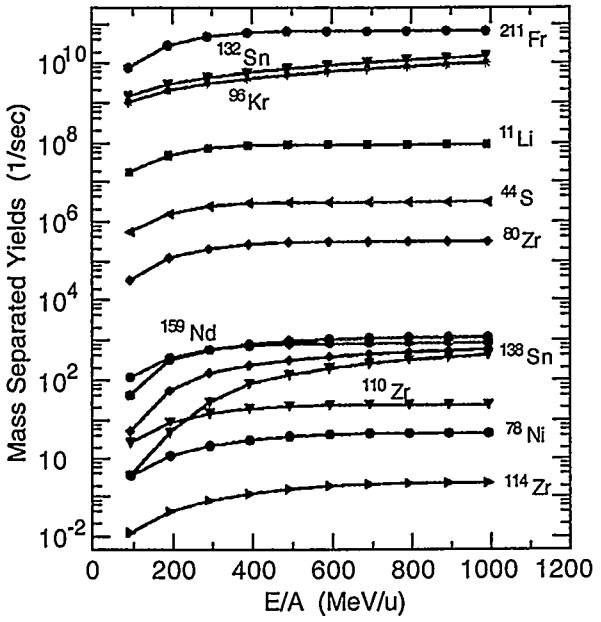

Fig. I-8 Absolute yields versus Energy (in MeV/u) for some nuclei assuming constant current (100 kW at 400 MeV/u). The green curves are for either standard ISOL or two-step fission, the red curves are for fragmentation reactions and the blue curves are for in-flight fission reactions.

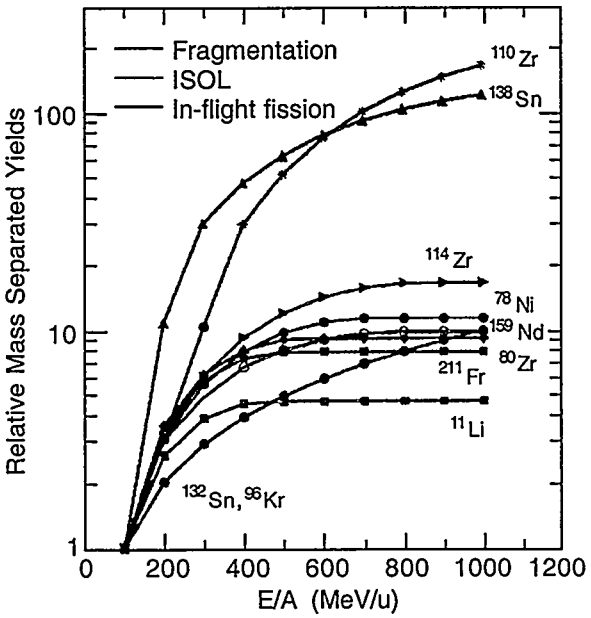

Fig. I-9. Relative yields (normalized to the values at 100 MeV/u) versus bombarding energy for some nuclei for constant current (100 kW at 400 MeV/u). The color code is the same as in Fig. I-8.

two-step fission into green. The highest intensities are observed by using the ISOL and two-step fission methods.

To emphasize the energy dependence, the same data are shown normalized to the yields at 100 MeV/u in Fig. I-9. It is clear that the production yields from the ISOL and the two-step fission methods, as well as from the fragmentation method, give a factor of 5-10 increase in yields between 100 MeV/u and 400 MeV/u. For the in-flight fission case, however, the increase is nearly two orders of magnitude. The reason for this is the relatively large momentum and angular spread that is introduced between the fragments in the fission process at low energies. Furthermore, attenuation losses of the beam and of the fragments in the target for the fission method are less pronounced, because the range of ^{238}U is short and thus the targets are thinner. It should be noted that Figs. I-8 and I-9 are calculated for constant current. For constant power, a factor of 1/10 has to be multiplied to the points at 1000 MeV/u as shown in Fig. I-10.

[1]Proceedings of the Fourth International Conference on Radioactive Beam, Omiya, Japan, 3-7 June, 1996, Nucl. Phys. **A616**, (1997).

[2]Scientific Opportunities with an Advanced ISOL Facility, Workshop at Columbus, OH, July 30-August 1, 1997.

[3]Concept for an Advanced Exotic Beam Facility Based on ATLAS (1995).

[4]Report to Users, ATLAS Facilities, March, 1999, ANL-ATLAS-99-1.

[5]ISOL Task Force Information, CERN-ISOLDE part; J. Lettry *et al.*, Nucl. Instr. Meth. **B126**, 138 (1997).

[6]R. G. Alsmiller *et al.*, Nucl. Instrum. Methods **A278**, 713 (1989); R. E. Price and H. Lichtenstein, Los Alamos National Laboratory Report, LA-UR-89-3104 (1989).

[7]Y. Yariv and Fraenkel, Phys. Rev. C **20**, 2227 (1979); M. Fauerbach (private communication).

[8]K. Sümmerer, W. Brüchle, D. J. Morrissey, M. Schädel, B. Szweryn, and Y. Weifan, Phys. Rev. C **42**, 2546 (1990).

[9]C. O. Engelmann, Dissertation, Kernspaltung relativistischer Uranprojectile und Erzeugung Extrem Neutronenreicher Isotope, 1998, GSI.

[10]J. J. Gaimard, K. H. Schmidt, Nucl. Phys. **A531**, 709 (1991); J. Benlliure *et al.*, Nucl. Phys. **A660**, 87 (1999); T. Enqvist *et al.*, Nucl. Phys. **A658**, 47 (1999).

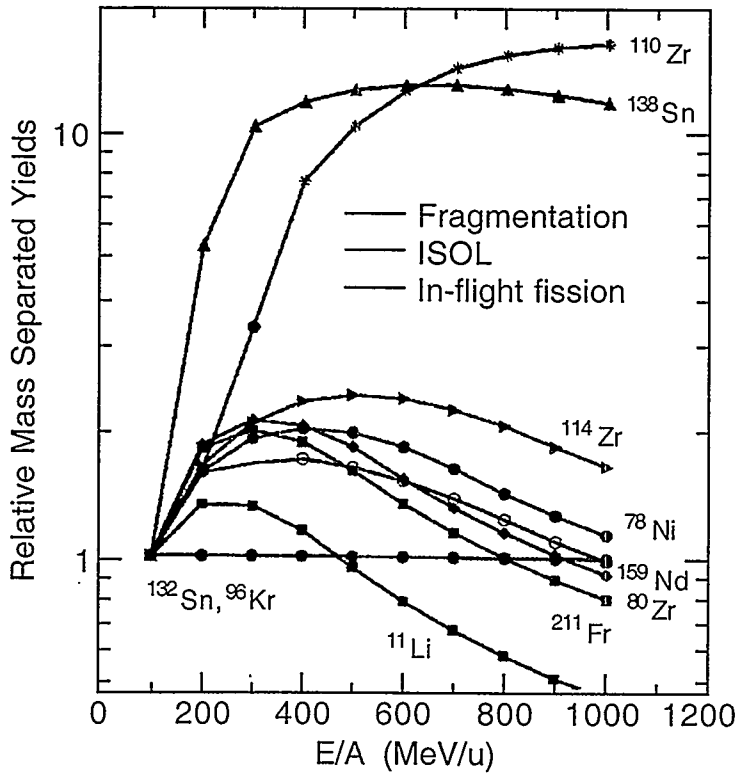

Fig. I-10. Relative yields (normalized to the values at 100 MeV/u) versus bombarding energy for some nuclei for constant power (100 kW). The color code is the same as in Fig. I-8.

a.7. The Rare Isotope Accelerator Web Page (J. A. Caggiano and R. V. F. Janssens)

The planning for the Rare Isotope Accelerator (RIA) facility has created the desire for a visible presence on the World Wide Web. A white paper was published stating the case for the construction of the facility, and a link to the file exists on the first page. The goal of the web page was to incorporate all the information in a user-friendly, navigable fashion.

Such a web page now exists and, while still in the development, provides a resource on the WWW to learn about the RIA project. There are three main categories: (1) the science case, (2) the technical aspects and (3) a short history. Figure I-11 shows the home page. To view the page and its links, go to http://www.phy.anl.gov/ria.

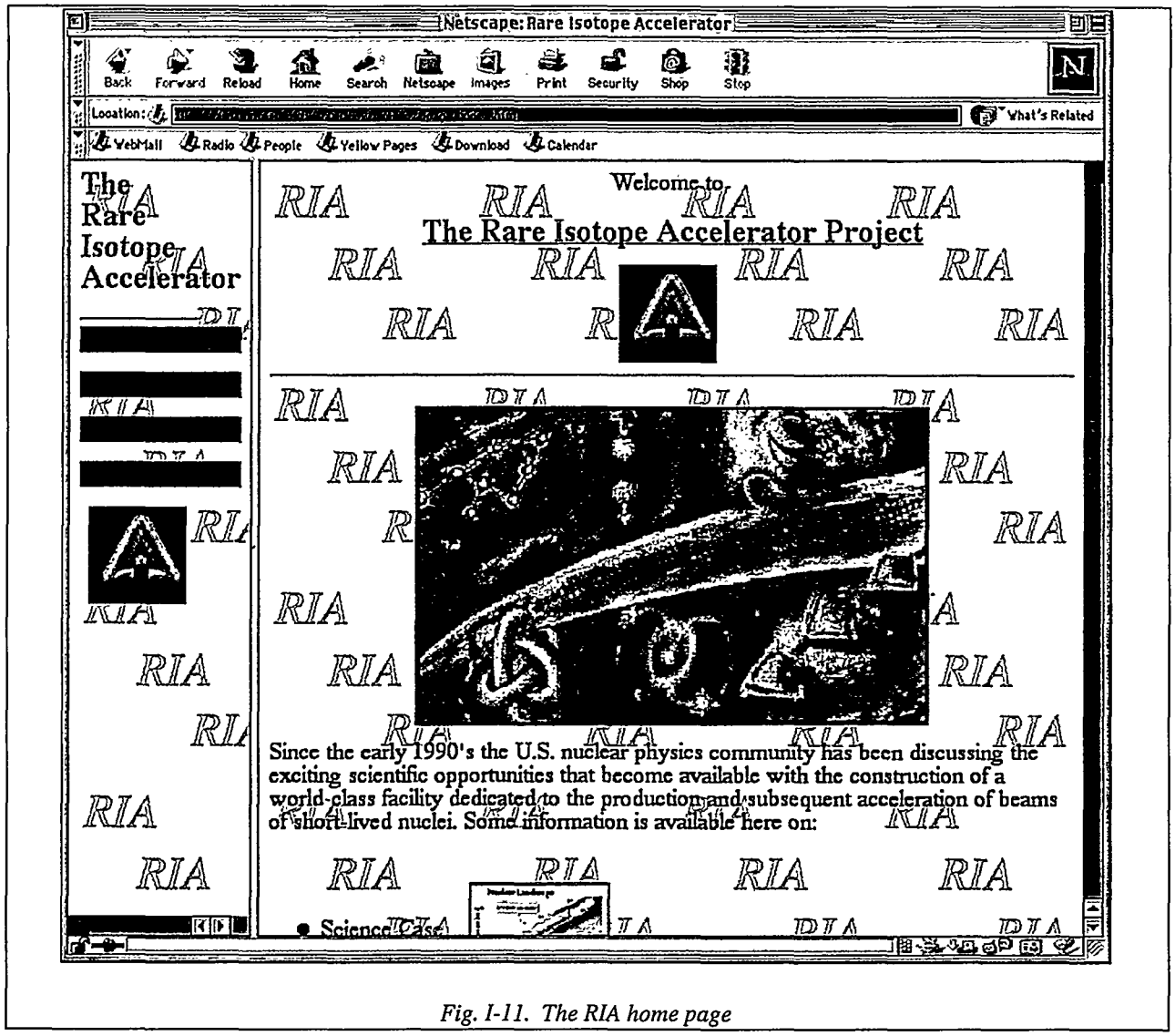

Fig. I-11. The RIA home page

B. STRUCTURE OF NUCLEI AT THE LIMITS OF STABILITY

The study of the properties of nuclei at the very limits of stability is currently a subject of great interest. Gammasphere was installed at the target position of the FMA late in 1997. A vigorous research program taking advantage of the unique capabilities brought about by the coupling of the two devices has developed since, accounting for a large fraction of the available beam time. In particular, the technique of recoil decay tagging has been used with success to investigate nuclei near or at the proton drip line. Spectroscopy information is now available on states produced at the sub-microbarn level. Other experiments have taken advantage of other auxiliary detectors such as microball and/or the neutron array. This section also presents results of studies where Gammasphere was used to explore nuclei located either along the valley of stability or on the neutron-rich side. Most of these studies used either Coulomb excitation of radioactive, actinide targets or spectroscopy following fission.

b.1. Spectroscopy of ^{24}Mg Using Gammasphere

(C. J. Lister, M. P. Carpenter, D. J. Henderson, A. M. Heinz, R. V. F. Janssens, I. Wiedenhöver, and A. H. Wuosmaa)

In the first year of operation of Gammasphere at ANL, a promising experiment was performed using the Fragment Mass Analyzer as a zero-degree time-of-flight reaction spectrometer. Using two-body reactions the time-of-flight method allowed the selection of individual states which were directly populated from the reaction. The ^{12}C(^{16}O,α)^{24}Mg reaction was ideal for this purpose. The technique was found to be particularly sensitive for states which are particle-unbound, but have small radiative branches, perhaps 10^{-4} of their total width. The sensitivity arises as a surviving ^{24}Mg ion is detected in the final channel. A follow-up experiment was performed in which Gammasphere was used as a full calorimeter, with the data from the 700 BGO elements retained on tape for analysis. This increases the experimental sensitivity by a factor five. The increase should especially enhance the ability to reconstruct high energy gamma-ray information. These data have still to be evaluated.

b.2. First Identification of a 10$^+$ State in ^{24}Mg

(I. Wiedenhöver, A. H. Wuosmaa, H. Amro, J. Caggiano, M. P. Carpenter, A. Heinz, R. V. F. Janssens, F. G. Kondev, T. Lauritsen, C. J. Lister, S. Siem, A. Sonzogni, P. Bhattacharyya,* M. Devlin,† D. G. Sarantites,† and L. G. Sobotka†)

The level structure of ^{24}Mg provides a crucial testing ground for theoretical approaches as different as the spherical shell model or α-cluster descriptions. High-spin states with $I \geq 8$ are especially sensitive to the assumptions underlying the different models. To identify candidate states with $I \geq 8$ we performed an experiment at ATLAS using a high granularity Si strip array with 160 channels inside the target chamber of Gammasphere. The states of interest in ^{24}Mg were populated in the ^{12}C (^{16}O, α) ^{24}Mg reaction. The α-particles emitted from the compound nucleus, the subsequent α-decay to states of ^{20}Ne and the characteristic γ-rays emitted from the ^{20}Ne nucleus were observed in coincidence.

The technique for spin determination is based on the observation of the fivefold directional correlations between the beam axis, the two α particles and two photons, which are emitted in the decay path leading from the compound state in ^{28}Si (m = 0) to the ground state of ^{20}Ne (see Fig. I-12). The main concept of the method is illustrated by Fig. I-12. All steps of one individual decay path, i.e. two α and two γ rays must be observed in the event in order to produce a characteristic angular correlation, which permits a spin determination. If one gamma ray of the decay path remains unobserved, the α particles lose their characteristic correlations and spin determination becomes impossible. The necessity of detecting $\alpha\alpha\gamma\gamma$ events with high efficiency lead to the design of a compact experimental setup of 5 DSSD detectors in the target chamber of Gammasphere.

The other difficulty in this project lay in the data analysis: In order to determine the correlation patterns of this five dimensional problem, a new technique was developed that relies on the expansion into coefficients of an orthogonal basis and allows the concentration of the relevant information into only few spectra. Employing this technique, we were able to assign spins to nine levels and confirm previous assignments unambiguously. The most notable result is the identification of a 10^+ state at 19.1 MeV (see Fig. I-14). The first unambiguous identification of this level in ^{24}Mg resolves a long-standing problem of nuclear physics. The energy of the 10^+ state lies on the continuation of the ground state rotational band, indicating that the rotational sequence continues far beyond the α-binding threshold. This 10^+ state is with $\hbar\omega \approx 2.9$ MeV one of the fastest rotating nuclear systems ever observed.

*Purdue University, †Washington University

[1]R. K Sheline, I. Ragnarsson, S. Aberg, and A. Watt, Jrnl. Phys. G **16**, 1201 (1988).
[2]S. Marsh and W. D. M. Rae, Phys.Lett. **B180**, 185 (1986).

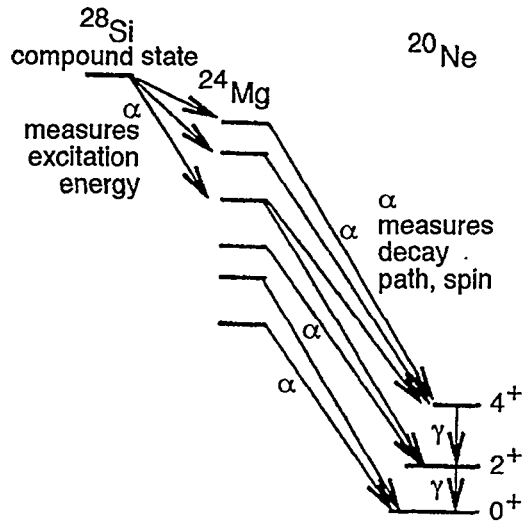

Fig. I-12 Schematic decay path from the ^{28}Si (m = 0) state to the ground state of ^{20}Ne.

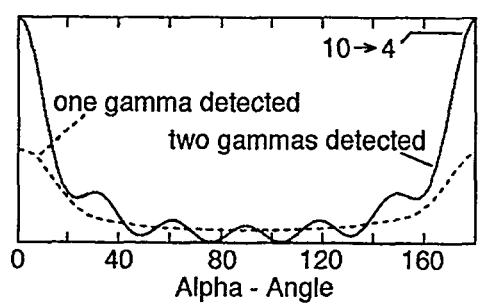

Fig. I-13 Angular distributions calculated for the emission of an α-particle from a 10^+ state of ^{24}Mg populating the 4^+ state of ^{20}Ne. Solid line: in coincidence with two γ-rays, detected at (θ,φ)=(45°,0) and (45°,180°). Dashed line: in coincidence with only one γ-ray at (θ,φ)=(45°,0) (dashed line), not observing the $4^+ \rightarrow 2^+$ transition.

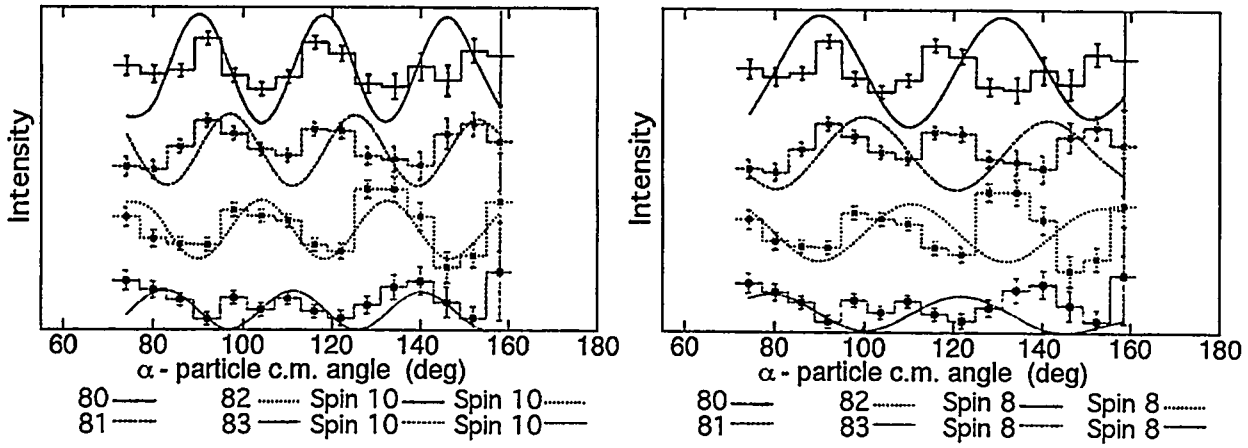

Fig. I-14 Experimental γγ correlated angular distributions of α-particles ^{24}Mg, 19.1 MeV → ^{20}Ne (4^+), compared to the theoretical curves for spin 10^+ (left) and 8^+ (right). Plotted are the correlations with the (k,q) =(8,0),(8,1),(8,2),(8,3) components of the γγ patterns detected with Gammasphere.

b.3. Deformed Excitations in ^{71}As and ^{72}Br

(M. P. Carpenter, C. J. Lister, C. N. Davids, R. V. F. Janssens, D. Seweryniak, T. L. Khoo, T. Lauritsen, D. Nisius, P. Reiter, J. Uusitalo, I. Wiedenhoever, N. Fotiades,* J. A. Cizewski,* A. O. Macchiavelli,† and R. W. MacLeod‡)

The nuclei in the A = 70 mass region exhibit a complicated interplay between single-particle and collective degrees of freedom, reflecting the influence of competing shell gaps in the single-particle levels. As a result, gamma sequences built on configurations corresponding to different shapes are observed in the same nucleus, e.g. ^{72}Se[1]. In order to understand better the single-particle excitations responsible for the deformed structures, we have recently studied with Gammasphere the level structure of ^{71}As and ^{72}Br.

High-spin states in both ^{71}As and ^{72}Br were investigated using the ^{16}O + ^{58}Ni reaction at a beam energy of 59.5 MeV. The ^{16}O beam was supplied by the ATLAS accelerator at Argonne National Laboratory. Gamma rays at the target position were detected by the Gammasphere array which was coupled to the Fragment Mass Analyzer (FMA) in order to separate evaporation residues from other reaction products. Mass 71 and 72 were the strongest evaporation residue channels observed in this reaction. In addition to ^{71}As (*3p*) and ^{72}Br (*pn*), ^{68}Ge (*2pα*), ^{71}Se (*2pn*), ^{72}Se (*2p*) have also been identified in this data set.

The previous reported level structure[2] for ^{71}As has been confirmed and extended in this experiment. In addition, a new sequence of negative-parity levels have been observed at moderate excitation. This sequence consists of two rotational bands connected to each other by dipole transitions which compete favorably with the quadrupole cross-over transitions. Based on the extracted B(*M*1)/B(*E*2), the band has been given a 7/2$^-$[303] ($f_{7/2}$) assignment with $\varepsilon_2 \sim 0.37$. This is the first observation of a deformed proton $f_{7/2}$ configuration in the A = 70 mass region.

*Rutgers University, †Lawrence Berkeley National Laboratory, ‡Thomas Jefferson National Accelerator Facility

[1] J. H. Hamilton *et al.*, Phys. Rev. Lett. **32**, 239 (1974).
[2] R. S. Zighelboim *et al.*, Phys. Rev. C **50**, 716 (1994).
[3] S. Ulbig *et al.*, Z. Phys. **A329**, 51 (1988).
[4] R. Bengtsson *et al.*, Nucl. Phys. **A415**, 189 (1984).
[5] N. Fotiades *et al.*, Phys. Rev. C **59**, 2919 (1999).
[6] N. Fotiades *et al.*, Phys. Rev. C **60**, 057302 (1999).

For ^{72}Br, the level scheme deduced in the present study has been extended with respect to previous work[3]. Two of the gamma-sequences observed have been associated with the $\pi g_{9/2} \otimes \nu g_{9/2}$ deformed configuration. The observed signature splitting between the two bands is larger than that observed for similar decoupled bands in the heavier odd-odd Br isotopes due to the lower-Ω = 3/2, $g_{9/2}$ orbitals involved. In addition, the low-frequency signature inversion observed in the heavier Br isotopes is absent in ^{72}Br in accordance with theoretical predictions[4].

Two papers reporting the results from this experiment have been published this past year in Phys. Rev. C[5,6].

b.4. Spectroscopy of N = Z ^{68}Se, ^{72}Kr, ^{76}Sr, ^{80}Zr, ^{84}Mo and ^{88}Ru

(C. J. Lister, M. P. Carpenter, A. M. Heinz, D. J. Henderson, R. V. F. Janssens, J. Schwartz, D. Seweryniak, I. L. Wiedenhöver, J. Cizewski,* N. Fotiades,* A. Bernstein,† Becker,† Bauer,† S. Vincent,‡ A. Aprahamian,‡ P. Hausladen,§ D. Balamuth,§ and S. M. Fischer¶)

The nuclei with N = Z above ^{56}Ni continue to attract attention, because of their importance in understanding explosive nucleosynthesis, and as they are fertile testing ground for nuclear models and for testing fundamental symmetries of nuclear forces. However, the nuclides of greatest interest lie far from stability, sometimes only one nucleon from the proton dripline. The systems are weakly bound and difficult to produce. Only recently has experimental technique advanced sufficiently to allow detailed spectroscopy in the nuclei of greatest interest. A series of experiments have been conducted using Gammasphere to study properties of these nuclei.

A) ^{68}Se This nucleus was predicted to provide an interesting example of shape coexistence. For many years it has been expected to be one of the few nuclei in nature with substantial ($\beta \sim -0.3$) oblate deformation in its groundstate. An FMA-Gammasphere experiment aimed at low-spin shape coexistence was performed, using the "Daresbury" method of tagging recoils by their stopping properties in an ion chamber. The reaction used, ^{12}C(^{58}Ni,2n)^{68}Se at the Coulomb barrier is ideal for populating low-spin non-yrast states. Despite the low production cross section of about 200 μb, two bands were found as is shown in Fig. I-15. The bands appear to both be collective, but have very different characteristics, the ground state band appearing to be characteristic of an oblate band while the excited band behaves similarly to the many prolate bands known in the region. The oblate groundstate appears about 600 keV more bound than the prolate shape. However, the prolate configuration has larger moments of inertia, so becomes yrast at spin J = 8. The oblate-prolate barrier is lowest in the triaxial plane at β = 0.3, and is predicted to be a few hundred keV high. The rather weak oblate-prolate mixing found in experiment indicates the barrier is higher than anticipated. These results have been published as a Physical Review Letter. A follow-up experiment by the Berkeley group using the microball has extended the yrast sequence to higher spin, through a two-alpha evaporation channel. It is clear the FMA gated, 2n evaporation studies and the microball-gated 2α measurements are very complimentary, the former favoring low-cross section, low-multiplicity, low-spin non-yrast structure and the latter high-spin phenomena.

B) ^{72}Kr At low spin, ^{72}Kr exhibits signs of coexistence similar to ^{68}Se, although the prolate shape dominates the yrast landscape and the oblate band could not be identified as it has become non-yrast even by spin J = 2. However, at high spin in the prolate sequence, a new challenge has been pursued. It has been suggested that new neutron-proton collective pairing modes, characteristic only of N = Z nuclei would require greater rotational Coriolis force to destroy, so alignments would be delayed to higher frequency. Two issues arise: what would one expect the "normal" frequency to be, and experimentally how large is the delay? We have performed a microball-Gammasphere experiment and through the ^{40}Ca(^{40}Ca,2α)^{72}Kr reaction have developed the decay scheme well past the backbending region, to spin J = 28 or higher. We have found the alignment is indeed delayed relative to other krypton isotopes and have identified several new bands. These data are in the final stages of analysis.

C) ^{76}Sr By N = Z = 38 the oblate shapes are gone and prolate shapes dominate. This should be an ideal place to find further evidence of "delayed alignment" and also quantify the stiffness of this nucleus which is the most deformed in the region with β_2 = 0.4. An experiment has just been completed. Using a new triggering mode, Gammasphere was operated in free-running "singles" mode, interrupted only when a recoil-gamma coincidence was detected in "external" electronic logic. This arrangement substantially

reduced dead time and thus enhanced the size of the data set. On-line sorting indicated it should be possible to extend the yrast line from spin J = 4 to above J = 16, well past the expected alignment frequency.

D) ^{80}Zr Another good rotor studied for "delayed alignment". This was the test experiment for the novel triggering described above. Despite some technical hitches, an excellent data set was collected and the yrast sequence advanced from J = 4 to J = 12. Clear evidence for delayed alignment was found, as the moment of inertia rises smoothly to the highest identified state, well above the frequency at which alignment is found in the other deformed zirconium nuclei.

E) ^{84}Mo Formed as a by-product in the ^{88}Ru study described below, evidence for this nucleus was found at an intensity level sufficient to suggest the structure may be investigated to higher spin than the J = 4 which is presently known. Analysis is in progress.

F) ^{88}Ru This nucleus has been sought in many structure studies. To date, no excited states are known. Using the ^{32}S(^{58}Ni,2n)^{88}Ru reaction and the "Daresbury" method, an attempt was made to elucidate its structure. One challenge was to produce a sulfide target of sufficient robustness to withstand bombardment with about 10 pnA of 200 MeV ^{58}Ni. This has been a stumbling block in previous studies. In this experiment a MoS_2 target was prepared and mounted on a rotating target wheel. This arrangement was very satisfactory, and after some initial "conditioning" with a small loss of sulfur, the target stabilized for extended running. A substantial data set was collected and data are being analyzed, though ion-chamber gain drifts and dead time issues compromised this data set, which was one of the first in this series of studies.

*Rutgers University, †Lawrence Livermore National Laboratory, ‡University of Notre Dame, §Pennsylvania University, ¶DePaul University

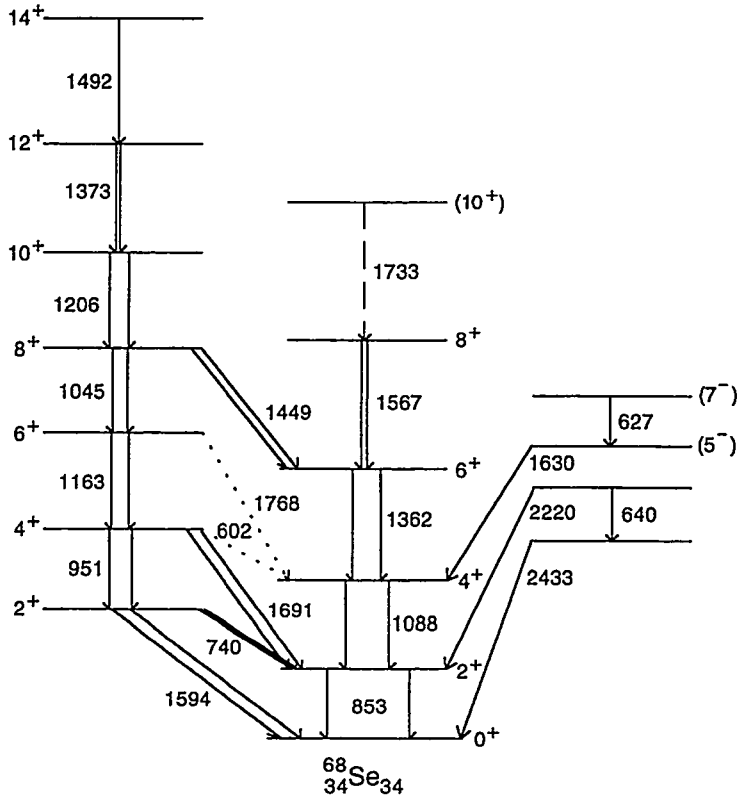

Fig. I-15. The two bands observed in ^{68}Se. The groundstate band has all the characteristics of an oblate shape, while the excited band is consistent with prolate deformation.

b.5. Yrast and Near-Yrast Excitations up to High Spin in ^{100}Cd

(M. P. Carpenter, R. V. F. Janssens, D. Seweryniak, I. Wiedenhöver, R. M. Clark,* J. N. Wilson,† D. Appelbe,‡ C. J. Chiara,§ M. Cromaz,* M. A. Deleplanque,* M. Devlin,† R. M. Diamond,* P. Fallon,* D. B. Fossan,§ D. J. Jenkins,¶ N. Kesall,¶ T. Koike,§ D. R. LaFosse,§ G. L. Lane,* I. Y. Lee,* A. O. Macchiavelli,* K. Starosta,§ F. S. Stephens,* C. E. Svensson,* K. Vetter,* R. Wadsworth,¶ J. C. Waddington,‡ D. Ward,* and B. Alex Brown‖)

In recent years, there has been an increasing experimental effort devoted to the study of nuclei near the doubly-magic, N = Z nucleus, ^{100}Sn. Gamma-ray spectroscopic studies are edging ever closer to this goal, but the very low (microbarn) cross sections and high backgrounds from other reaction products make it difficult to identify gamma transitions with nuclides produced with these low cross sections.

Recently, we have studied high-spin states in ^{100}Cd (Z = 48,N = 52) a close lying isobar to ^{100}Sn in order to learn more about the location of single-particle states near N = Z = 50. In this study, states in ^{100}Cd were populated in the ^{46}Ti(^{58}Ni,2p2n) reaction with a beam of energy of 215 MeV. Gamma rays emitted at the target were measured with Gammasphere. In order to identify gamma transitions in ^{100}Cd, the evaporated particles from this reaction were measured using Microball and a 20 element array of NE213 liquid scintillator detectors. The former was used to detect light charged particles while the later was used to detect neutrons. In addition, an Au catcher foil was placed immediately behind the target with the aim of stopping all recoils in order to allow for a tag on delayed γ transitions coming from isomeric states.

Before this study, excited states in ^{100}Cd were known up to the 60 ns 8^+ isomer[1]. In this study, a prompt γ-ray spectrum consisting of transitions lying above the 8^+ isomer was produced by gating on delayed transitions lying below the isomer in coincidence with the detection of two protons and at least one neutron. To build the level scheme, a $E_\gamma - E_\gamma$ matrix was formed by incrementing events which were in coincidence with any of the four prompt delayed transitions lying below the 8^+ isomer. No other gates on evaporated particles were required.

From the analysis of the data, the level scheme of ^{100}Cd has been extended up to 20 $\hbar$ in angular momentum and 10 MeV in excitation energy. Spin and multipolarity assignments were made based on angular correlation ratios. In an attempt to understand the single-particle nature of the states, shell model calculations were performed and compared with the data. The spectrum of the yrast states up to I = 14 $\hbar$ is generally well reproduced by the shell-model calculations. Above this spin and excitation energy, high-energy γ-ray transitions are observed. These transitions can be viewed as a ``fingerprint" of either core excitations or excitations involving $h_{11/2}$ neutrons. It is clear that a full quantitative description of the decay scheme requires extended shell-model calculations. Indeed, the recent advances in γ-ray spectroscopy of nuclei near ^{100}Sn are clearly outstripping the theoretical descriptions and it is our hope that experimental efforts such as presented here will encourage renewed theoretical effort.

A paper reporting the results of this work was published recently in Physical Review C[2].

*Lawrence Berkeley National Laboratory, †Washington University, ‡McMaster University, Hamilton, Ontario, §SUNY at Stonybrook, ¶University of York, United Kingdom, ‖Michigan State University

[1]Gorska *et al.*, Z. Phys. **A350**, 181 (1994).
[2]R. M. Clark *et al.*, Phys. Rev. C **61**, 044311 (2000).

b.6. Spectroscopy of ^{103}Sn and the Development of a Technique to Observe ^{101}Sn

(C. J. Lister, M. P. Carpenter, D. Seweryniak, C. Baskill,* S. Freeman,* J. Durell,* B. J. Varley,* M. Leddy,* D. Balamuth,† P. Hausladen,† S. Fischer,§ and D. Sarantites‡)

The approach to the doubly-magic nucleus ^{100}Sn has proven very difficult using fusion evaporation reactions. In "inbeam" spectroscopy ^{104}Sn is the closest isotope studied, although a high-spin isomer has been found and studied in ^{102}Sn, yielding the effective charge for neutrons beyond the doubly magic shell closure.

An attempt was made to populate ^{103}Sn using the ^{50}Cr(^{60}Ni,α3n) reaction and using microball, neutron detectors, the FMA and an ion-chamber to over define the reaction products, while gamma rays were detected in Gammasphere. The aim of the experiment was two-fold: evaluation of channel selection techniques in order to plan a future study of ^{101}Sn using the same reaction but with a ^{58}Ni beam, and secondly to identify states in ^{103}Sn, particularly the 3-neutron multiplets to evaluate residual interactions and state mixing.

The data are still undergoing evaluation. The 16-detector Penn-Manchester array of scintillators had an efficiency of about 14% for one neutron, about that achieved using the more recently commissioned UW-LBNL-Penn 30 detector arrangement. However, the neutron-gamma separation was very good. The microball was very clean in identifying alpha particles downstream, but upstream alphas in this inverse reaction were very difficult to identify efficiently, so the overall detection efficiency was lower than estimated. Buildup of light contaminants on the target was also an impediment to clean channel selection. The efficiency of the FMA was also less than originally estimated, due to its operation at 90 cm, forced by the size of Gammasphere. Very few events had correlated mass A = 103 ions detected at the FMA focal plane and identified alphas in microball due to the alpha-residue angular correlation. Finally, after target and window losses, the ion-chamber resolution was less clean that expected and electronic gain drifts were found which needed correction. Thus, in almost all respects the channel selection techniques were poorer than originally expected. However, many aspects can be worked on and technically improved for the future.

Despite these shortcomings, a very large data set was collected, and a spectrum for ^{103}Sn may emerge. However, at present the information from this experiment seems most valuable for designing an optimum experiment for the future. Many aspects of the project can be improved and tested without Gammasphere. A Manchester student is pursuing this project for his Ph.D. thesis project.

*University of Manchester, United Kingdom, †University of Pennsylvania, ‡Washington University, §DePaul University

b.7. In-Beam γ-Ray Spectroscopy of the Proton Emitter ^{109}I

(M. P. Carpenter, C. N. Davids, R. V. F. Janssens, C. J. Lister, D. Seweryniak, J. Uusitalo, C. H.-Yu,* A. Galindo-Uribarri,* S. D. Paul,*† and B. D. McDonald‡)

The recoil decay tagging (RDT) technique has proven to be a powerful tool in the study of proton-rich nuclei. With the placement of Gammasphere in front of the FMA, this technique has been successfully used to probe excited states in nuclei which lie at the edges of stability. In the past two years a number of RDT measurements have been performed with the Gammasphere + FMA setup. These studies have attempted to characterize the nuclear structure built on top of the proton emitting states. One such experiment was performed on ^{109}I, a nuclide which had been studied previously at the Daresbury tandem accelerator using the EUROGAM I array and the Daresbury Recoil Mass Spectrometer[1].

In the experiment at Gammasphere, excited states in ^{109}I were populated using the ^{54}Fe(^{58}Ni,$p2n$) reaction at a beam energy of 220 MeV. Gamma rays in ^{109}I were identified using the RDT technique. The analysis of the γ-γ data yielded the yrast sequence in ^{109}I which has been interpreted as an excitation built on the $h_{11/2}$ proton orbital. Interestingly, the sequence of gamma-rays assigned to this band in ^{109}I is different than that reported in Ref. 1. Since the Gammasphere assignments are based on a significantly larger number

of gamma-proton correlated events, we believe that the sequence reported in Ref. 1 is incorrect.

Previous systematic analyses of proton emitters have shown that most known proton emitters have spectroscopic factors close to unity. ^{109}I stands out as one of the few which have very small spectroscopic factors. The proton emitting ground state of ^{109}I has been assigned to the $d_{5/2}$ configuration, however, its spectroscopic factor is very small (S = 0.055), and this fact has been sited as evidence that the ground state has substantial prolate deformation. Unfortunately, the current experiment was unable to identify states associated with the ground state configuration, and thus, no information on the deformation of the ground-state could be extracted. The trend of the $h_{11/2}$ sequence indicates a decrease in deformation with decreasing N which is supported by theoretical predictions.

A paper reporting the results of this work was published this past year in Physical Review C.[2]

*Oak Ridge National Laboratory, †Oak Ridge Institute for Science and Education, ‡Georgia Institute of Technology
[1]E. S. Paul, P. J. Woods, *et al.*, Phys. Rev. C **51**, 78 (1995).
[2]C. H.-Yu *et al.*, Phys. Rev. C **59**, R1834 (1999).

b.8. Lifetimes of High-Spin States in Proton Rich A ≈ 130 Nuclei

(F. G. Kondev, M. P. Carpenter, A. Heinz, R. V. F. Janssens, D. J. Hartley,* L. L. Riedinger,* A. Galindo-Uribarri,† R. W. Laird,‡ W. Reviol,§ M. A. Riley,‡ and O. Zeidan*)

The mass 130 region is a rich field for shape coexistence phenomena where bands with axial, triaxial, and oblate deformations are present in the vicinity of the yrast line. In addition, highly deformed bands (with β_2 = 0.3-0.4) are observed in these nuclei which result from the occupation of shape-driving $\nu i13/2$ and/or $\pi g9/2$ orbitals as well as from the proximity of neutron shell gaps at higher deformations at N = 72,74. A previous experiment was performed with the Gammasphere spectrometer in conjunction with the Washington University Microball charged-particle detection array using the ^{40}Ca + ^{94}Mo reaction. Several possible highly deformed structures were identified in $^{130,131}_{60}$Nd, $^{127-131}_{59}$Pr, and $^{128,130}_{58}$Ce from this experiment.

In order to confirm that the new structures have large deformation, a lifetime measurement was recently performed at the ATLAS facility where once again the power of Gammasphere was combined with the selectivity of the Microball. The same reaction was performed, but a target consisting of ~ 1 mg/cm^2 of ^{94}Mo on ~ 14 mg/cm^2 of Au was used instead of a self-supporting ^{94}Mo foil as in the previous experiment. Lifetimes of the states will be extracted by applying a lineshape analysis (Doppler shift attenuation method (DSAM), which will allow us to determine the quadrupole moments (and thus the deformations) of some of these bands. By populating so many highly deformed bands under the same experimental conditions, we are able to compare the deformations of the bands without concern for systematic differences that occur when comparing quadrupole moments deduced in different measurements. The analysis is in progress.

*University of Tennessee, †Oak Ridge National Laboratory, ‡Florida State University, §University of Tennessee and Washington University

b.9. Gamma-Ray Studies of Few-Valence-Particle Nuclei Around Doubly Magic ^{132}Sn

(I. Ahmad, M. P. Carpenter, R. V. F. Janssens, T. L. Khoo, T. Lauritsen, C. J. Lister, P. Reiter, D. Seweryniak, I. Wiedenhöver, C. Constantinescu,* P. Bhattacharyya,* C. T. Zhang,* P. J. Daly,* Z. W. Grabowski,* B. Fornal,† R. Broda,† and J. Blomqvist‡)

We have been investigating the yrast excitations in the Z = 50-54, N = 80-84 range of nuclei, which are important to obtain information on nucleon-nucleon interactions and effective charges in the poorly studied ^{132}Sn region. Our ongoing analysis of the extensive high-quality γ-ray data recorded in 10 days of Gammasphere measurements using a sealed ^{248}Cm source delivering ~ 6 × 10^4 fissions/sec has led to substantial advances in the spectroscopy of N = 81, 82 and 83 isotones of ^{132}Sn. For example, we have made considerable improvement in the ^{134}Sb and ^{135}Te level schemes (0.5 μs isomer occurs along the yrast line in ^{135}Te) over our earlier scheme deduced from the EUROGAM2 run[1]. The level scheme of ^{135}Te from the new analysis is shown in Fig. I-16. We have tentatively assigned spin-parity of the levels and assigned them probable three-particle assignment. The results on ^{134}Sb and ^{135}Te will be published in Phys. Rev. C.

*Purdue University, †IFJ, Cracow, Poland, ‡Royal Institute of Technology, Stockholm, Sweden

[1]P. Bhattacharyya *et al.*, Phys. Rev. C **56**, R2363 (1997).

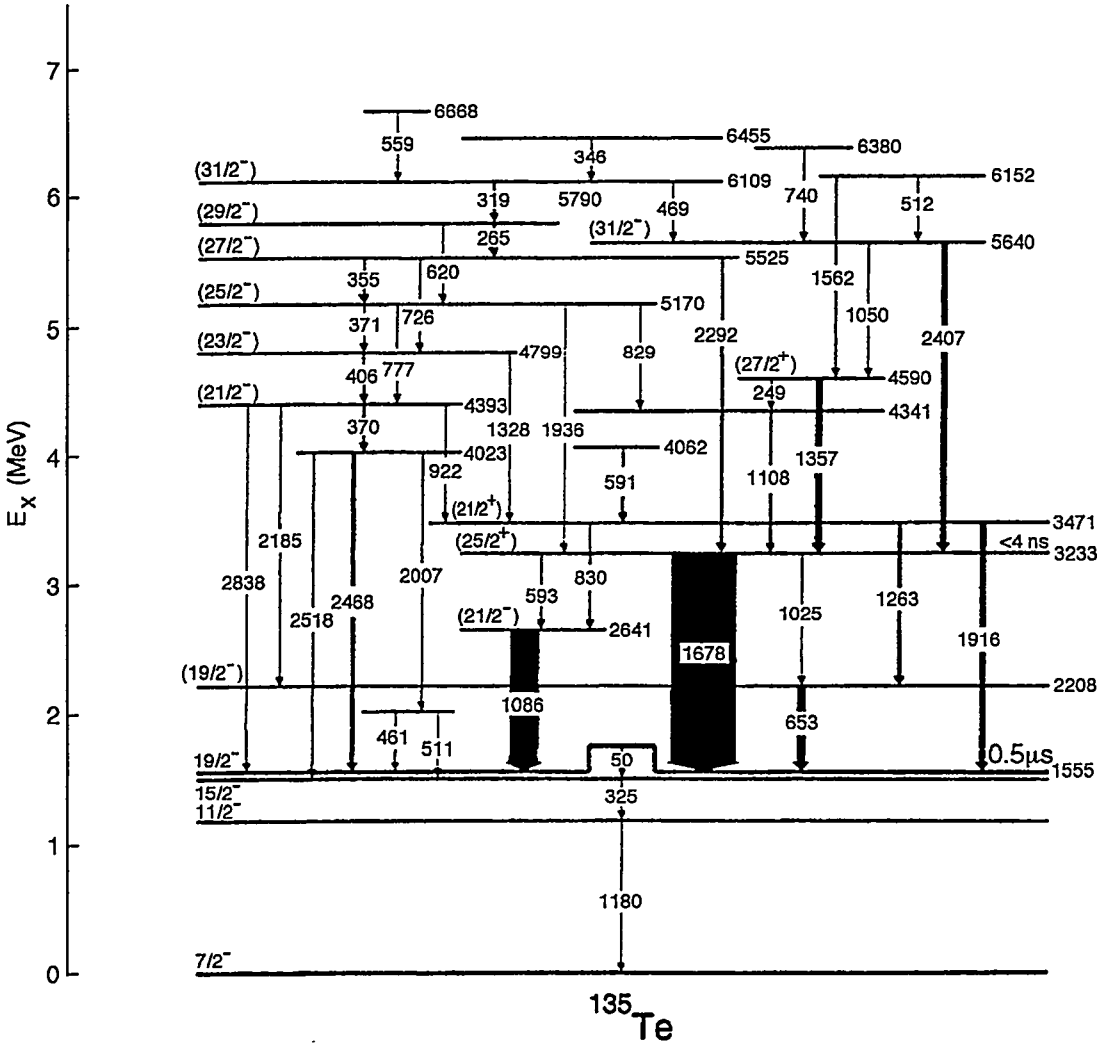

Fig. I-16. Level scheme of three-particle nucleus ^{135}Te deduced from the 1998 Gammasphere run.

b.10. Properties of N = 84 Even-Even Nuclei Populated in the Spontaneous Fission of ^{248}Cm

(I. Ahmad, A. Korgul,* W. Urban,* T. Rzaca-Urban,* M. Rejmund,* J. L. Durell,† M. J. Leddy,† M. A. Jones,† W. R. Phillips,† A. G. Smith,† B. J. Varley,† N. Schulz,‡ M. Bentaleb,‡ E. Lubkiewicz,‡ and L. R. Morss§)

Systematic studies of the N = 84 isotones were made in order to test the limits of the region around ^{132}Sn where the shell-model description still applies. The ^{134}Sn nucleus, identified in our earlier study, was reinvestigated. The 2509 keV level in ^{134}Sn obtained in the present work was interpreted as the $\nu(f_{7/2}\, h_{9/2})$ configuration. Its excitation energy fits very well the shell-model description, providing further confirmation of the $\nu h_{9/2}$ single-particle assignment of the 1561-keV level in ^{133}Sn. On the other hand, ^{138}Xe, which also has two valence neutrons, displays an excitation pattern characteristic of vibrational, collective motion. This nucleus cannot be described by the shell model. Between these two limits is ^{136}Te, having two valence protons and two valence neutrons. The maximum aligned configurations $[\pi(g_{7/2})^2\ 0^+\ \nu(f_{7/2})^2\ 6^+]$, $[\pi\,(g_{7/2})^2\ 0^+\ \nu(f_{7/2}h_{9/2})8^+]$ and $[\pi(g_{7/2})^2\ 6^+\ \nu(f_{7/2}h_{9/2})8^+]$ which in ^{136}Te correspond to the 6^+, 8^+ and 14^+ levels are well described by the shell-model code OXBASH. On the other hand the $[\pi(g_{9/2})^2\ 6^+\ \nu(f_{7/2})^2\ 6^+]$ configuration is observed at an excitation energy higher than predicted and does not produce the expected isomerism in ^{136}Te. We explained this difference as the result of collective motion admixtures in ^{136}Te, only four valence nucleons away from the ^{132}Sn core. The results of this study were published.[1]

*University of Warsaw, Poland, †University of Manchester, United Kingdom, ‡IReS, Strasbourg, France, §Chemistry Division, ANL

[1]A. Korgul *et al.*, Euro. Phys. J. **A7**, 167 (2000).

b.11. Medium Spin Structure of Single Valence-Proton Nucleus ^{133}Sb

(I. Ahmad, W. Urban,* W. Kurcewicz,* A. Korgul,* P. J. Daly,† P. Bhattacharyya,† C. T. Zhang,† J. L. Durell,‡ M. J. Leddy,‡ M. A. Jones,‡ W. R. Phillips,‡ A. G. Smith,‡ B. J. Varley,‡ M. Bentaleb,§ E. Lubkiewicz,§ N. Schulz,§ L. R. Morss,¶ and J. Blomqvist||)

Excited states in ^{133}Sb populated in the spontaneous fission of ^{248}Cm were studied with the EUROGAM2 array. The ^{133}Sb nucleus, having one valence proton, provides direct information on the single-particle excitations. Its structure can be described as the excitations of the single valence proton coupled to the ^{132}Sn core. We have identified excited levels in ^{133}Sb corresponding to the $\nu(h_{11/2}^{-1}f_{7/2})$ core excitations coupled to the $\pi g_{7/2}$ proton level. The $13/2^+$, $15/2^+$ and $17/2^+$ yrast members of the $[\pi g_{7/2}\nu(h_{11/2}^{-1}f_{7/2})]$ configurations were observed. Our calculations give the energy of the $19/2^+$ member higher than that of the $21/2^+$ level, which in turn is predicted to lie only ~ 30 keV above the $17/2^+$ level. This is the cause for the 16 μs isomerism, reported previously. Another important finding in ^{133}Sb was the identification of the 4297 keV level, corresponding to the 3^-, octupole vibration of the core. Work is in progress to determine the rate of the E3 transition associated with this excitation. The results of this investigation have been submitted to Phys. Rev. C.

*Warsaw University, Poland, †Purdue University, ‡University of Manchester, United Kingdom, §IReS, Strasbourg, France, ¶Chemistry Division, ANL, ||Royal Institute of Technology, Stockholm, Sweden

b.12. First Observation of Excited States in ^{137}Te and the Extent of Octupole Instability in the Lanthanides

(I. Ahmad, W. Urban,* A. Korgul,* T. Rzaca-Urban,* N. Schulz,† M. Bentaleb,† E. Lubkiewicz,† J. L. Durell,‡ M. J. Leddy,‡ M. A. Jones,‡ W. R. Phillips,‡ A. G. Smith,‡ B. J. Varley,‡ and L. R. Morss§)

Studies of neutron-rich lanthanides have revealed a region of octupole instability around N = 88. To understand the dependence of octupole correlations on neutron numbers we have studied the structures of heavy Te isotopes. Excited states in ^{137}Te were investigated in the spontaneous fission of ^{248}Cm by measuring coincidence spectra with the gamma ray array EUROGAM2. To find transitions in ^{137}Te, spectra were obtained by placing gates on γ rays in the complementary Ru fragments. Several new γ rays were observed. To assign the new transitions to ^{137}Te, mass correlation technique was used. By gating on transitions in a given Te isotope, the γ ray intensities of the Ru isotopes were obtained. The weighted mass of the Ru isotopes was plotted against the mass of each Te isotope. The excellent correlation confirms the assignment of transitions to ^{137}Te.

The level scheme of ^{137}Te as deduced from the present work is displayed in Fig. I-17. The structure of ^{137}Te is similar to those of heavier N = 85 isotones and can be interpreted as due to three valence nucleons in the $\nu(f_{7/2}^3)j$ or $\nu[h_{9/2}(f_{7/2}^2)]j$ configurations. The data indicate a decrease in octupole correlations as one is approaching Z = 50 shell. The results of this study were published.[1]

*Warsaw University, Poland, †IReS, Strasbourg, France, ‡University of Manchester, United Kingdom, §Chemistry Division, ANL

[1] W. Urban *et al.*, Phys. Rev. C **61**, 041301(R) (2000).

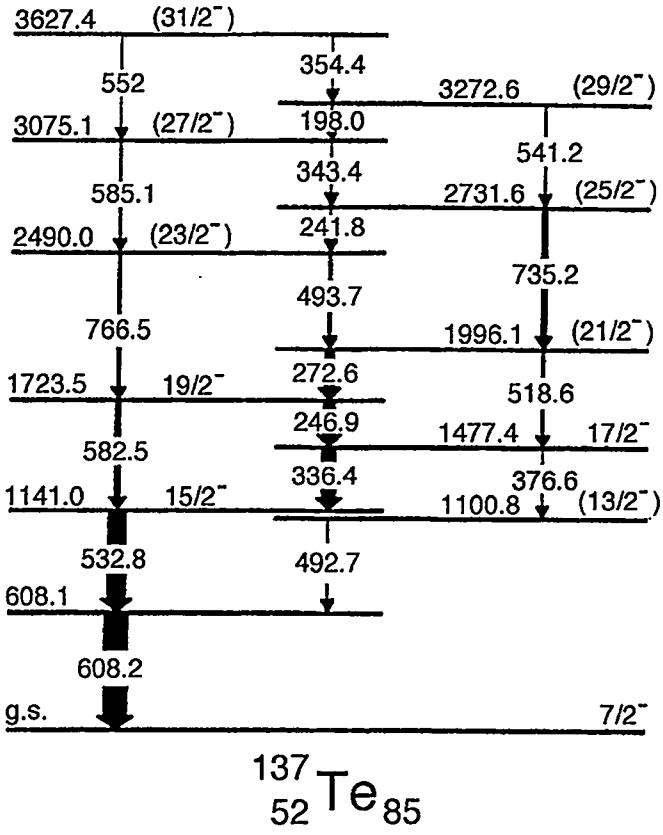

Fig. I-17. The level scheme of ^{137}Te deduced from the results of the present study.

b.13. First Observation of Excited States in the Neutron-Rich Nucleus ^{138}Te

(I. Ahmad, F. Hoellinger,* B. P. J. Gall,* N. Schulz,* W. Urban,† M. Bentaleb,* J. L. Durell,‡ M. A. Jones,‡ M. Leddy,‡ E. Lubkiewicz,§ L. R. Morss,¶ W. R. Phillips,‡ A. G. Smith,‡ and B. J. Varley‡)

Levels in ^{138}Te have been observed for the first time. Gamma rays produced in the spontaneous fission of ^{248}Cm were measured with the EUROGAM2 array of Ge detectors. Several new γ rays were observed in coincidence with the γ rays of complementary light Ru isotopes. The mass assignment of the new γ rays was made on the basis of the mass correlation technique. By gating on the transitions in Te isotopes, intensities of γrays in the Ru isotopes were measured. The weighted mass of the Ru isotopes was plotted against the mass of each Te isotope. The excellent correlation, shown in Fig. I-18, confirms the assignment of transitions to ^{138}Te. The level scheme obtained from the present work is displayed in Fig. I-19 The level scheme indicates a β soft prolate minimum consistent with theoretical predictions. The results were published[1].

*IReS and Universite Louis Pasteur, Strasbourg, France, †Warsaw University, Poland, ‡University of Manchester, United Kingdom, ¶Chemistry Division, ANL, §Jagiellonian University, Cracow, Poland

[1]F. Hoellinger *et al.*, Eur. Phys. J. A **6**, 365 (1999).

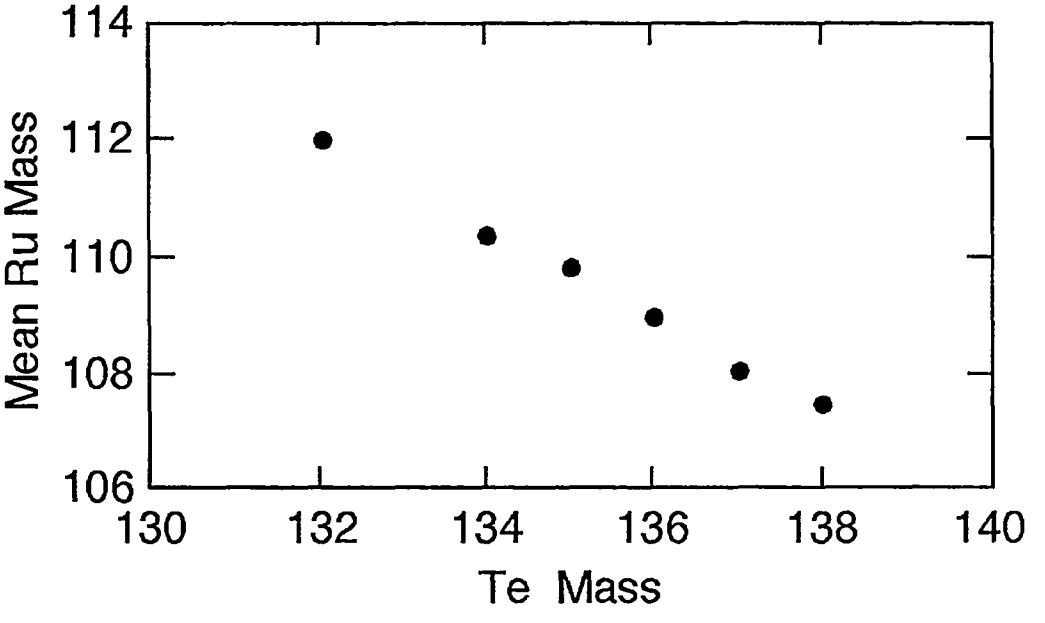

Fig. I-18. Plot of mean mass of Ru isotopes against the mass of the Te isotope. The smooth trend in the data points is the basis for the assignment of new gamma lines to ^{138}Te.

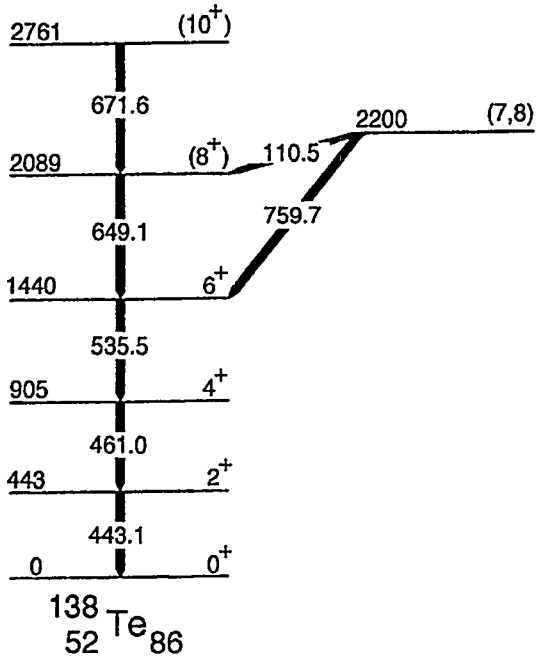

Fig. I-19. Level scheme of ^{138}Te obtained in the present work.

b.14. Measurements of g-Factors of Excited States of Fission Fragments Implanted into Fe

I. Ahmad, M. P. Carpenter, J. P. Greene, R. V. F. Janssens, F. Kondev, D. Seweryniak, A. G. Smith,* O. J. Onakanmi,* D. Patel,* G. S. Simpson,* J. F. Smith,* R. M. Wall,* J. P. Gall,† B. Roux,† and O. Dorveaux†)

An experiment was performed with Gammasphere to measure g-factors of excited states in neutron-rich fission fragments using the time-integral perturbed angular correlation functions between pairs of secondary-fragment γ rays. The experiment involved the use of a ^{252}Cf source of total activity 100 μCi sandwiched between two layers of Fe metal. Prior to the deposition of the californium, the Fe metal foils (each 10 mg cm^{-2} thick) were annealed in an oven at 650°C for ten minutes. The magnetization of these foils as a function of temperature and applied field was measured using a magnetometer. The results of this measurement showed that the magnetic moment of the iron reached saturation at room temperature in an applied field of 0.1 T. The Cf was then electroplated onto the surface of one of the iron foils and a layer of indium metal (200 μg cm^{-2} thick) was evaporated over the second iron foil. A pair of small permanent magnets applying a field of around 0.2 T were placed either side of the source in the direction normally reserved for the beam to Gammasphere. The direction of the applied field could be reversed by rotating the magnet assembly through an angle of 180°. The experiment ran for two weeks during which time 9×10^9 events of fold three (or greater) were collected. A preliminary check on the precessions of angular correlations in the fragments ^{100}Zr, ^{104}Mo and ^{144}Ba has revealed impurity hyperfine fields of -26(5), -24(3) and -4.5(7) T, respectively. These fields are largely in line with tabulated values and represent a huge improvement relative to a previous attempt to measure g-factors in fission fragments using a cooled Gd/Cf/Gd sandwich in conjunction with the Euroball array[1]. In the previous experiment, no precessions could be measured in either Zr or Mo fragments, which indicated impurity hyperfine fields of less than 1 Tesla for these species. Since there is no reason to expect that the impurity hyperfine fields in other species should not follow tabulated values for implantation into saturated Fe foil, the current data set is likely to provide a large number of new g-factor measurements for low-lying excited states in very neutron-rich nuclei.

*University of Manchester, United Kingdom, †IReS and Universite Louis Pasteur, Strasbourg, France

[1]A. G. Smith *et al.*, Phys. Lett. **B453**, 206 (1999).

b.15. Measurements of g-Factors of Excited States in Ba and Ce Nuclei Using γ Rays from Secondary Fission Fragments

(I. Ahmad, J. P. Greene, A. G. Smith,* G. S. Simpson,* J. Billowes,* P. J. Dagnall,* J. L. Durell,* S. J. Freeman,* M. Leddy,* W. R. Phillips,* A. A. Roach,* J. F. Smith,* A. Jungclaus,† K. P. Lieb,† C. Teich,† B. J. P. Gall,‡ F. Hoellinger,‡ N. Schulz,‡ and A. Algora§)

An experiment was performed to measure the g-factors of excited states in neutron-rich fission fragments through the time-integral perturbed angular correlation functions between pairs of secondary-fragment γ rays. The experiment involved the use of a ^{252}Cf source of total activity 120 μCi sandwiched between two layers of gadolinium metal. Prior to the deposition of the californium, the gadolinium metal foils (each 20 mg cm^{-2} thick) were annealed in an oven at 650° for ten minutes. The magnetization of these foils as a function of temperature and applied field was measured using a magnetometer. The results of this measurement showed that the magnetic moment of the gadolinium reached 87% of its calculated maximum value with the temperature held at 80 K and an applied field of 0.2 T. The californium was then electroplated onto the surface of one of the gadolinium foils and a layer of indium metal (200 μg cm^{-2} thick) was evaporated over a second gadolinium foil. The layer of indium acted as an aid to adhesion between the active foil and the second foil, which was rolled on top to produce a closed source in which the fission fragments stop in gadolinium. The source was placed in a specially designed chamber at the center of the Euroball array. In this chamber the source was clamped between a copper strip and an aluminum plate, the copper strip being attached to a cold copper block that was maintained at 86 K by a constant flow of liquid-nitrogen. A pair of small permanent magnets applying a field of 0.2 T were placed either side of the source in the direction normally reserved for the beam to Euroball. The direction of the applied field could be reversed by rotating the magnet assembly through an angle of 180°. Even with the rather poor field strengths obtained here, it has proved possible to measure precessions for several states with nanosecond lifetimes. Measurements have been made for the first $I^{\pi} = 2^+$ states in ^{144,146}Ba and ^{146,148}Ce, as well as for the $9/2^-$ state at 117 keV in ^{143}Ba, the $7/2^-$ state at 114 keV in ^{145}Ba and the yrast 4^+ state in ^{150}Ce. The deduced g-factors are presented in Fig. I-20 and compared with those compiled in reference[1]. It can be seen from this comparison that in general the results obtained here are consistent with previously known g-factors, for those cases where measurements have been made. The measurement of the 2^+ state in ^{146}Ba is consistent with the previous result and provides supporting evidence for a downward trend in the g-factors of the 2^+ states of even-even barium isotopes. It has been suggested[2] that this decrease may be explained within the framework of the Interacting Boson Model (IBM2) as due to the increasing number of neutron valence bosons that occurs in the first half of a neutron shell, together with the quenching of the Z = 64 shell gap for N > 88. Within the IBM2, g-factors for even-even nuclei in this region can easily be calculated following reference[3], where the g-factors for neutron and proton bosons are taken as $g_\nu = 0.05$ and $g_\pi = 0.63$. The results of these calculations are shown in Fig. I-20 to give good agreement with the data. The ^{150}Ce result is the first g-factor measurement in this nucleus and is consistent with the IBM2 predictions. The results of this study were published[4].

*University of Manchester, United Kingdom, †University of Göttingen, Germany, ‡IReS and University of Louis Pasteur, Strasbourg, France, §Laboratori Nazionali Legnaro, Italy

[1] P. Raghavan, At. Data Nucl. Data Tables **42**, 189 (1989).
[2] A. Wolf *et al.*, Phys. Lett. **B123**, 165 (1983).
[3] R. L. Gill *et al.*, Phys. Rev. C **33**, 1030 (1986).
[4] A. G. Smith *et al.*, Phys. Lett. **B453**, 206 (1999).

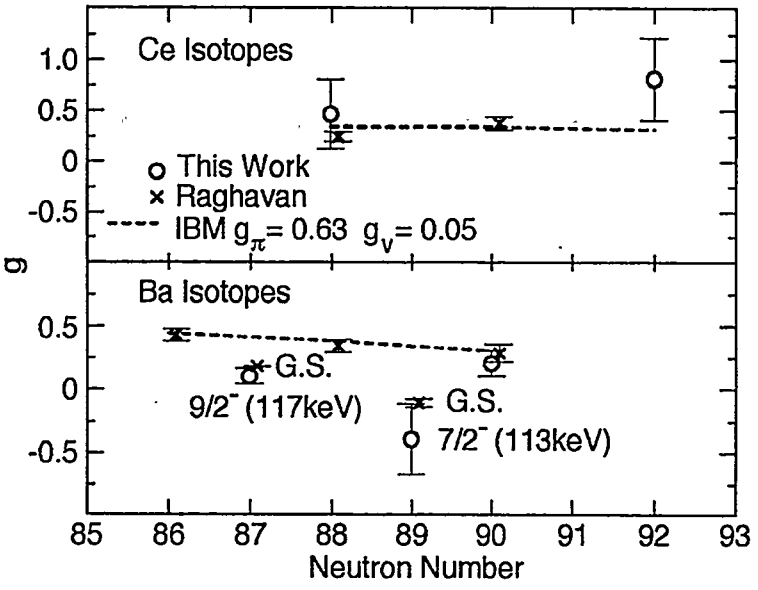

Fig. I-20. The g-factor results from this work are compared with those compiled in Ref. 1. The first 2^+ states in ^{144}Ba and ^{148}Ce are used to calibrate the field strengths.

b.16. In-Beam Gamma-Ray Spectroscopy of the Proton Emitter ^{131}Eu

(J. J. Ressler,† D. Seweryniak,* J. Caggiano, M. P. Carpenter, C. N. Davids, A. Heinz, R. V. F. Janssens, T. L. Khoo, F. G. Kondev, T. Lauritsen, C. J. Lister, P. Reiter, A. A.Sonzogni, J. Uusitalo, Wiedenhöver, P. J. Woods,‡ W. B. Walters,† J. A. Cizewski,§ B.T. Davinson,‡ and J. Shergur†)

A Recoil-Decay Tagging experiment was carried out to study excited states in the deformed proton emitter ^{131}Eu. Prompt γ rays were detected using Gammasphere and were tagged with decay protons observed in a Double-Sided Si Strip detector placed behind the focal plane of the Fragment Mass Analyzer. The ^{58}Ni(^{78}Kr,p4n)^{131}Eu reaction was used to produce ^{131}Eu nuclei. Fig. I-21 shows the spectrum of γ rays correlated with the ground-state proton decay in ^{131}Eu. The spectrum in Fig. I-21 is very complex. At least two rotational bands are present in the spectrum. However, statistics are too low to observe coincidences between observed γ-ray transitions, and no firm level scheme could be established so far. The data analysis is in progress.

It should be noted that the proton decay to the 2+ excited state in ^{130}Sm[1] was confirmed in the present experiment. In fact, the γ-ray spectrum tagged by the fine structure proton line resembles the spectrum corresponding to the ground-state proton line. This proves that both lines originate from the same state.

*Argonne National Laboratory and University of Maryland, †University of Maryland, ‡University of Edinburgh, United Kingdom, §Rutgers University

[1]A. A. Sonzogni *et al.*, Phys. Rev. Lett. **83**, 1116 (1999).

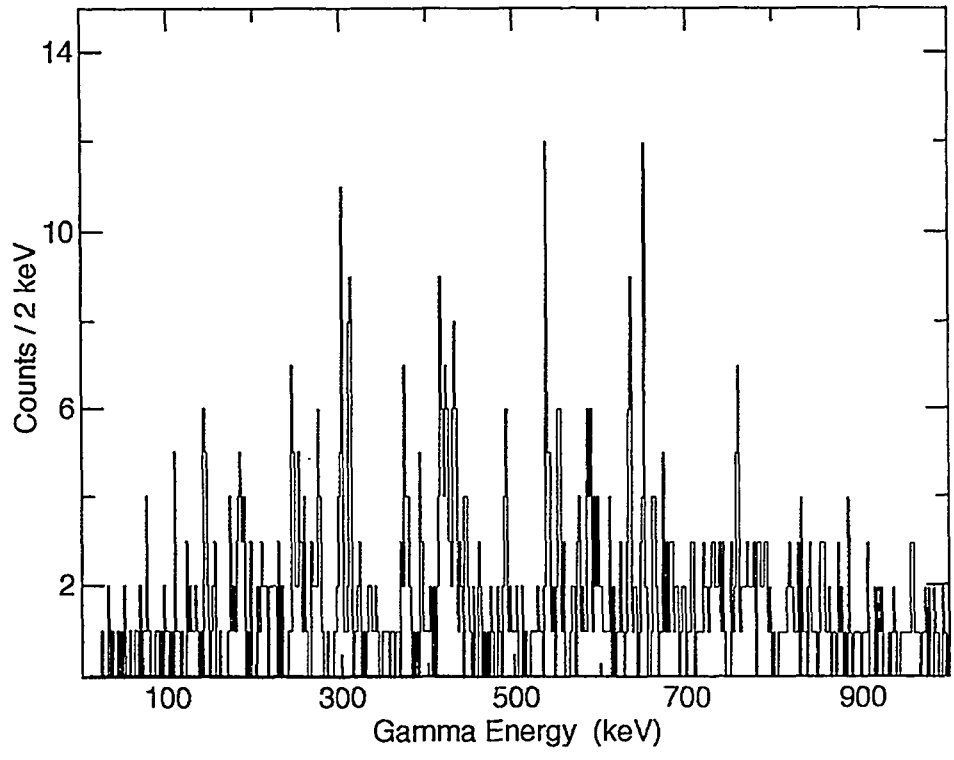

Fig. I-21. The spectrum of γ rays correlated with the ground-state proton decay of ^{131}Eu.

b.17. Rotational Bands in the Proton Emitter ^{141}Ho

(D. Seweryniak,* J. A. Caggiano, M. P. Carpenter, C. N. Davids, A. Heinz, R. V. F. Janssens, T. L. Khoo, F. G. Kondev, T. Lauritsen, C. J. Lister, P. Reiter, A. A. Sonzogni, J. Uusitalo, I. Wiedenhöver, W. B. Walters,† J. A. Cizewski,§ T. Davinson,‡ K. Y. Ding,§ N. Fotiades,§ U. Garg,¶ J. Shergur,† P. J. Woods,‡ and J. J. Ressler†)

The results of the first in-beam studies of the deformed proton emitter ^{141}Ho were presented in the previous annual report. A second Recoil-Decay Tagging experiment was carried out to obtain data on excited states in ^{141}Ho with better statistics. Prompt γ rays were detected using Gammasphere and were tagged with decay protons observed in a Double-Sided Si Strip detector placed behind the focal plane of the Fragment Mass Analyzer. The ^{54}Fe(^{92}Mo,p4n)^{141}Ho reaction was used to produce ^{141}Ho nuclei. Compared to the first experiment inverse kinematics was used this time to narrow the recoil emission cone. As a result about a factor of about 4 more protons were collected and coincidence relationships were established between γ rays observed in the first experiment. Figure I-22 shows the sum of selected γ-ray gates from the ground-state band. As can be seen from Fig. I-22, the ground-state band was extended to spin 35/2 ħ. In addition, evidence was found for the unfavored signature partner of the ground-state band.

The dynamic moment of inertia deduced for the ground-state band increases gradually up to the rotational frequency of ω ~ 0.45 MeV indicating that the alignment of the $h_{11/2}$ proton pair at ω ~ 0.25 MeV is blocked. It confirms the $\pi h_{11/2}$ origin of the ground-state band. Particle-rotor calculations show that the large signature splitting of the ground-state band can be explained only if a significant hexadecapole deformation (β_4 = -0.06 was calculated by Möller and Nix[1]) and triaxiality is assumed. The B(M1)/B(E2) ratios deduced for the lower states are also consistent with the $\pi h_{11/2}$ assignment. The dynamic moment of inertia deduced for the band feeding the isomeric state indicates a band crossing at low rotational frequencies. Since only one signature partner was observed the band has to have a large signature splitting. Among non-

$h_{11/2}$ orbitals near the Fermi surface only the band based on the $1/2^+[411]$ configuration is expected to have a large signature splitting. The above single-particle assignments are in agreement with the ones proposed based on the proton-decay rates[2].

In addition to new information on excited states, more precise energy, 1235(9) keV, and half-life, 6.5(-0.7+0.9) μs, was measured for the proton decay from the isomeric state. Despite better statistics, the decay from the ground state and the isomeric state to the 2^+ state in ^{140}Dy was not observed and only an upper limit of 1 % was established for this decay branch.

*Argonne National Laboratory and University of Maryland, †University of Maryland, ‡University of Edinburgh, United Kingdom, §Rutgers University, ¶University of Notre Dame

[1]P. Möller *et al.*, At. Nucl. Data Tables **59**, 185 (1995).
[2]C. N. Davids *et al.*, Phys. Rev. Lett. **80**, 1849 (1998).

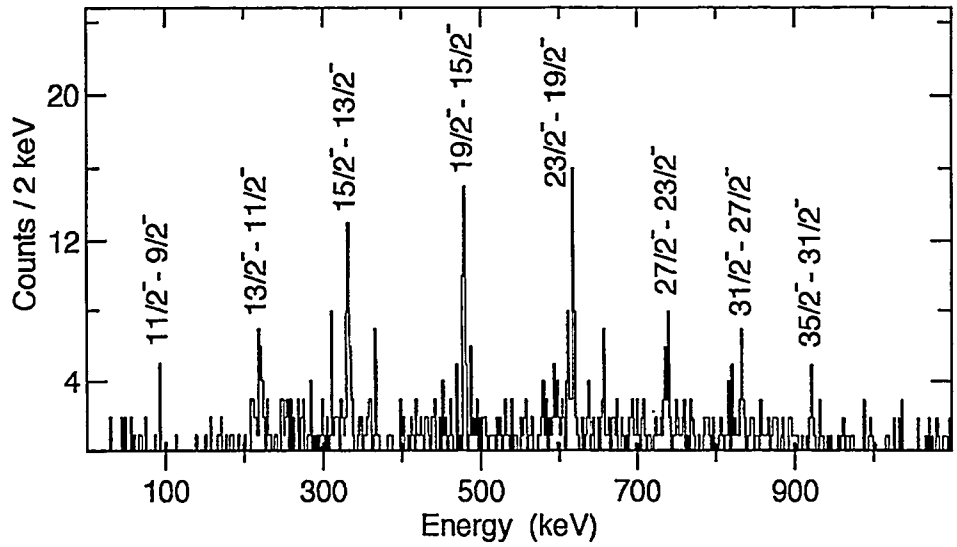

Fig. I-22. The sum of selected γ-ray gates correlated with the ground-state proton decay of ^{141}Ho.

b.18. Complex Band Interactions in ^{170}Er

(M. P. Carpenter, R. V. F. Janssens, I. Wiedenhöver, C. Y. Wu,* D. Cline,* M. W. Simon,* R. Teng,* and K. Vetter†)

Two low-lying quadrupole vibrational modes of motion are ascribed to β and γ vibrations. While there is considerable and compelling evidence for the presence of low-lying γ-vibrational collective excitations, experimental evidence for low-lying β-vibrational modes is sparse and often ambiguous. In ^{170}Er both the β and γ vibrations are located at nearly the same excitation energy, making this nucleus an ideal case to study the β-vibrational mode of motion. In addition, low-lying octupole and hexadecapole vibrational bands also have been identified in ^{170}Er[1]. The closeness in the phonon excitation energies associated with all of these collective modes provides an opportunity to study second-order interactions among them which in turn can help elucidate the validity of collective model descriptions and the microscopic structure underlying these low-lying excitations.

We have recently completed a study of the inelastic excitation of ^{170}Er targets using a ^{238}U beam provided by ATLAS. This experiment exploited the combination of the 4π heavy-ion detector array, CHICO[2], for the kinematics measurement, and Gammasphere for γ-ray detection. In this work, the ground state band was extended to 26^+ and the γ-vibrational band to 19^+ ($K\pi = 2^+$). The presumed β-vibrational band ($K\pi = 2^+$) and the $K\pi = 3^+$ were observed up to spin 22^+. Figure I-23 shows the partial level scheme for these four bands deduced from this work. The following observations and conclusions were drawn from the data.

- Strong population of the $K\pi = 0^+$, β-vibrational band, brought about by strong mixing with the γ-vibrational band.
- The $K\pi = 0^+$ band gains spin alignment faster than the ground band and becomes yrast at

spin 22^+ due to strong mixing with the rotationally aligned two-quasiparticle band.

- Appreciable population of the low-lying $K^\pi = 3^+$ hexadecapole vibrational band due to its mixing with the quadrupole γ-vibrational band.

While mixing between the different phonon's does take place, the weakness of the interaction strength between the β- and γ-vibrational motions and between the quadrupole and hexadecapole vibrational motions ensures that their interactions are of second order in nature and that their collective classification remains justified.

The results of this study have been recently published in Phys Rev C[3].

*University of Rochester, †Lawrence Berkeley National Laboratory

[1]C. M. Baglin, Nucl. Data Sheets **77**, 125 (1996) and references therein.
[2]M. W. Simon *et al.*, Nucl. Instrum. Methods Phys. Res. A (to be published).
[3]C. Y. Wu *et al.*, Phys Rev C **61**, 021305(R) (2000).

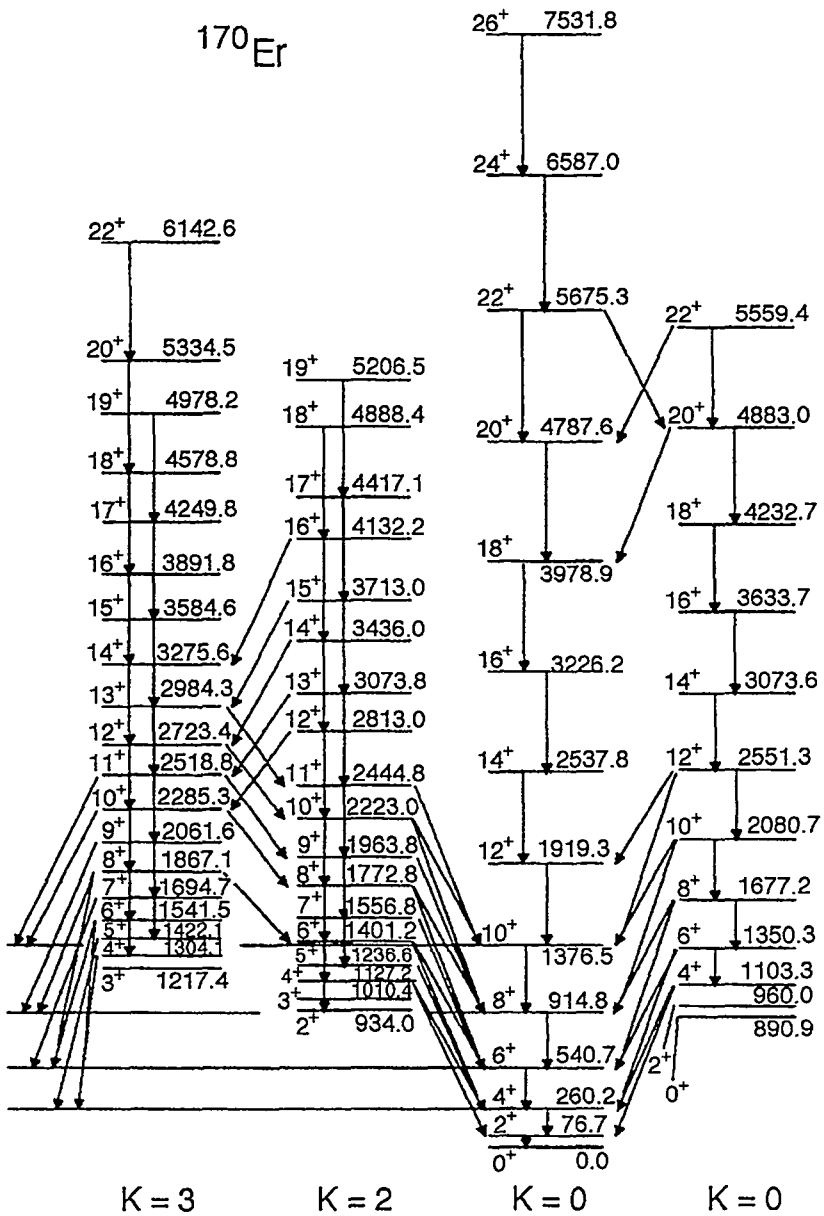

Fig. I-23. Partial level scheme of the $K^\pi = 3$, γ-vibrational, ground-state, and β-vibrational bands for ^{170}Er.

b.19. Entry Distributions and Fusion Dynamics in the Radiative Capture Reaction of $^{90}Zr + ^{90}Zr$

(M. P. Carpenter, K. Abu Saleem, I. Ahmad, J. Caggiano, C. N. Davids, A. Heinz, R. V. F. Janssens, R. A. Kaye, T. L. Khoo, F. G. Kondev, T. Lauritsen, C. J. Lister, J. Ressler, D. Seweryniak, A. A. Sonzogni, I. Wiedenhöver, S. Siem,* B. Heskind,‡ H. Amro,† W. C. Ma,‡ W. Reviol,§ L. L. Riedinger,¶ D. G. Sarantites,§ and P. G. Varmette†)

Some years ago, the surprising observation of fusion without subsequent particle evaporation was reported for the $^{90}Zr + ^{90}Zr$ system at the Coulomb barrier[1,2]. The process was found to have cross sections as high as ~ 40 μb.

An experiment dedicated to a further study of radiative capture in the $^{90}Zr + ^{90}Zr$ system was recently performed at the ATLAS facility with Gammasphere and the Fragment Mass Analyzer (FMA). With the calorimetric capabilities of the spectrometer and the selectivity of the FMA, it was possible to investigate in detail the gamma decay of ^{180}Hg using the recoil decay tagging (RDT) technique for channel selection.

In such measurements, the isotopic purity of the target is an important consideration given the much stronger cross sections for evaporation channels. For this reason, measurements were performed not only with a ^{90}Zr target, but also with ^{91}Zr and ^{92}Zr targets. For all projectile-target combinations, the properties of the various reaction channels were investigated at beam energies ranging from 369 up to 410 MeV.

By utilizing the RDT technique, spectra for the γ-ray total energy and multiplicity were produced for the capture channel, ^{180}Hg. In both cases, the distributions were wider than the corresponding spectra for the evaporation channels. This is due to the fact that our ^{90}Zr target is not isotopically pure, allowing ^{180}Hg to be produced in reactions involving the impurities ^{91}Zr and ^{92}Zr. However, when the contribution of these impurities are subtracted from each spectrum, the resulting distributions in total energy and multiplicity lie at higher excitation energy and multiplicity than those distributions associated with evaporation channels. This clearly shows that the capture channel is produced at the highest excitation energies and angular momentum produced by the reaction.

*Argonne National Laboratory and University of Oslo, Norway, †Mississippi State University, ‡Niels Bohr Institute, Roskilde, Denmark, §Washington University, ¶University of Tennessee

[1] J. G. Keller *et al.*, Nucl. Phys. **A452**, 173 (1986).
[2] K.-H. Schmidt *et al.*, Phys. Lett. **B168**, 39 (1986).

b.20. First Observation of Excited Structures in Neutron Deficient, Odd-Mass Pt, Au and Hg Nuclei

(F. G. Kondev, K. Abu Saleem, I. Ahmad, M. Alcorta, P. Bhattacharyya, L. T. Brown, J. Caggiano, M. P. Carpenter, C. N. Davids, S. M. Fischer, A. Heinz, R. V. F. Janssens, R. A. Kaye, T. L. Khoo, T. Lauritsen, C. J. Lister, G. L. Poli, J. Ressler, D. Seweryniak, A. A. Sonzogni, I. Wiedenhöver, H. Amro,* S. Siem,† J. Uusitalo,‡ J. A. Cizewski,§ M. Danchev,¶ D. J. Hartley,¶ B. Heskind,‖ W. C. Ma,** R. Nouicer,†† W. Reviol,‡‡ L. L. Riedinger,¶ M. B. Smith,§ and P. G. Varmette**)

The neutron deficient nuclei near $Z = 82$ play a seminal role in elucidating the contributions of various orbitals to the many different nuclear shapes seen in this mass region. The microscopic understanding of the excited prolate structures discovered recently in the near drip line isotopes ^{176}Hg and ^{178}Hg[1,2,3] requires spectroscopic knowledge of the level structures in neighboring odd-mass Hg and Au nuclei as the latter provide the possibility to isolate the shape driving effects of individual orbitals.

A number of dedicated experiments have been performed at ATLAS using Gammasphere in conjunction with the recoil-decay tagging technique. By combining the simplicity of α- decay spectroscopy following mass selection with the complexity of in-beam γ-ray coincidence techniques, comprehensive level schemes of many neutron deficient isotopes were established for the first time. Among these are: ^{173}Pt, $^{173\text{-}177}$Au and $^{175\text{-}179}$Hg. In addition, we have significantly extended the previously known level schemes of $^{174\text{-}176}$Pt. Special attention was devoted to level structures built upon the intruder $\pi h_{9/2}$ and $i_{13/2}$ proton orbitals, as well as to those associated with the $p_{3/2}$ and $\nu i_{13/2}$ neutron configurations. A sample γ-ray spectrum showing γ rays associated with the $1/2^-[521]$ ($p_{3/2}$) band in ^{179}Hg is presented in Fig. I-24. Surprisingly, the odd-mass, neutron-deficient Au and Hg isotopes exhibit persistent collectivity at relatively low excitation energy. This should be contrasted with the rapid rise of the excitation energy of the prolate band for the $N < 100$ even-even Hg neighbors. In addition to the in-beam spectroscopy studies, we have also performed a detailed investigation of the α-decay properties of these isotopes. We have revised many of the decay schemes and this provides for a better understanding of the structure of these nuclei. Alpha energy spectra showing the main decays of ^{177}Au and its daughter isotope ^{173}Ir are presented in Fig. I-25. Sample spectra of γ rays in coincidence with selected ^{174}Au α lines are shown in Fig. I-26.

The analysis of the data is still in progress.

*Argonne National Laboratory and Mississippi State University, †Argonne National Laboratory and University of Oslo, Norway, ‡Argonne National Laboratory and University of Jyväskylä, Finland, §Rutgers University, ¶University of Tennessee, ‖The Niels Bohr Institute, Roskilde, Denmark, **Mississippi State University, ††University of Illinois at Chicago, ‡‡Washington University

[1] M. P. Carpenter *et al.*, Phys. Rev. Lett. **78**, 3650 (1997).
[2] M. Muikku *et al.*, Phys. Rev. C **58**, R3033 (1998).
[3] F. G. Kondev *et al*, Phys. Rev. C **61**, 011303(R) (2000).

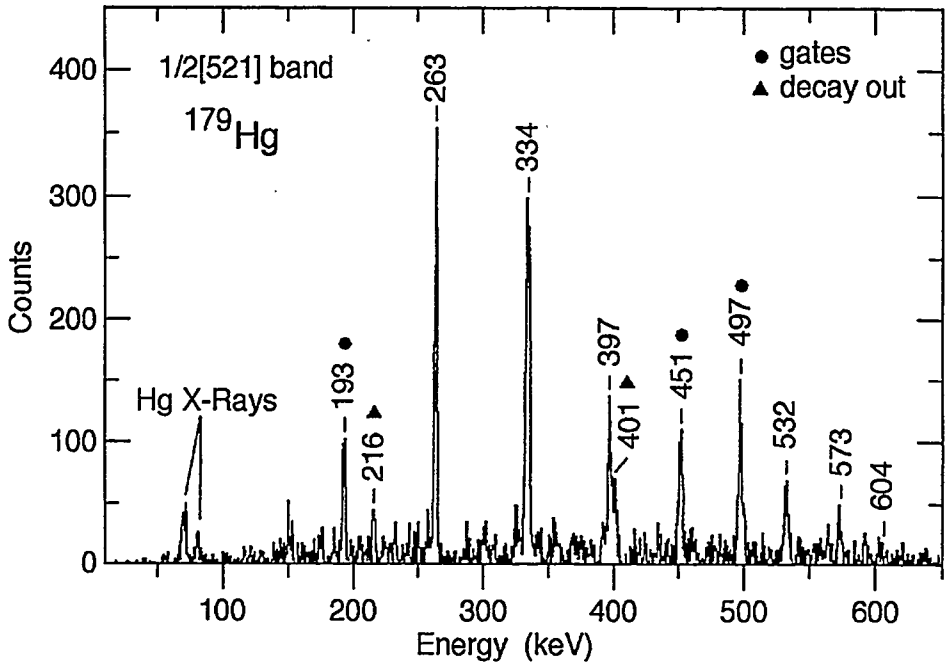

Fig. I-24. Sample spectrum obtained from the mass-gated coincidence data for the 1/2⁻[521] ($p_{3/2}$) band observed in ^{179}Hg. The spectrum is the result of sums of coincidence gates placed on the transitions marked with the black dots.

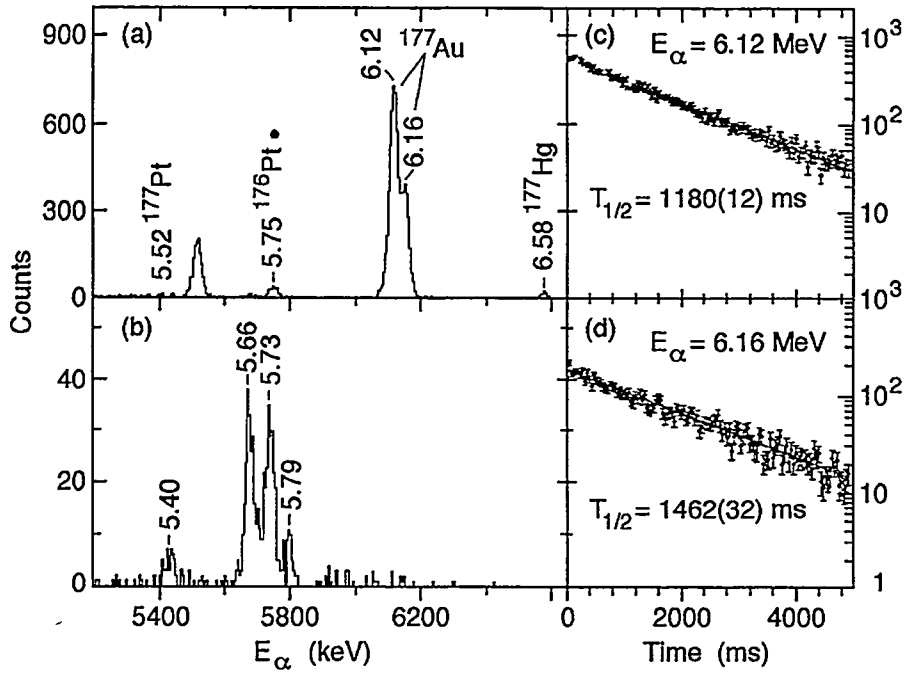

Fig. I-25(a). First generation α-energy spectrum for A = 177 selected recoils. (Note, that the presence of the 5.75 MeV line of ^{176}Pt is due to the subsequent β^+ decay of ^{177}Au.) (b) Second generation α-energy spectrum correlated with the E_α = 6.12 MeV line. Time decay spectra for the E_α =6.12 MeV (c) and 6.16 MeV (d) lines. The fitted curves are shown with solid lines.

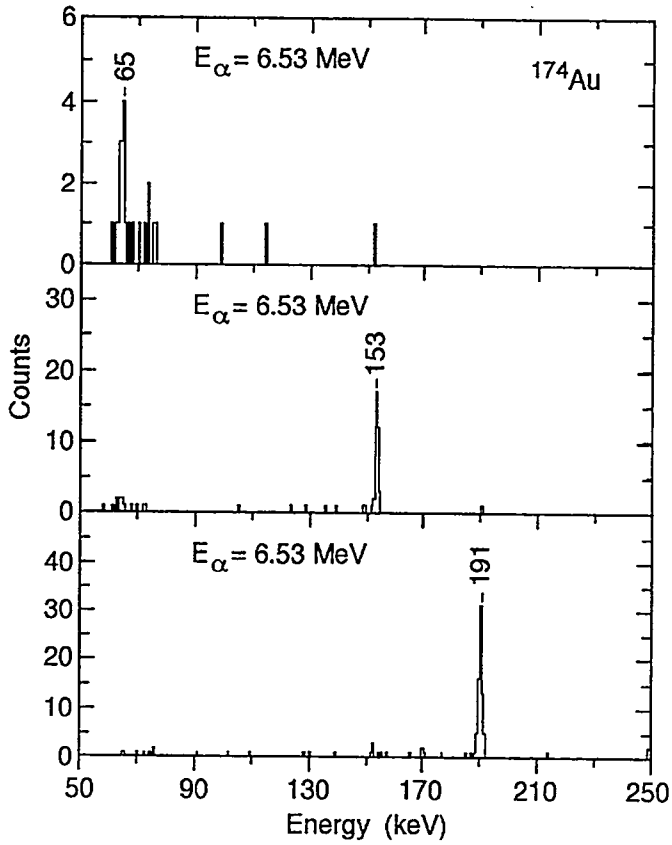

Fig. I-26. Spectra of γ-rays in coincidence with the ^{174}Au characteristics α-lines.

b.21. Spectroscopy of Neutron Deficient Even-Even Hg Nuclei

(F. G. Kondev, K. Abu Saleem, I. Ahmad, M. Alcorta, P. Bhattacharyya, L. T. Brown, J. Caggiano, M. P. Carpenter, C. N. Davids, S. M. Fischer, A. Heinz, R. V. F. Janssens, R. A. Kaye, T. L. Khoo, T. Lauritsen, C. J. Lister, J. Ressler, D. Seweryniak, A. A. Sonzogni, I. Wiedenhöver, H. Amro,* S. Siem,† J. Uusitalo,‡ B. Heskind,§ W. C. Ma,¶ R. Nouicer,‖ W. Reviol,** L. L. Riedinger,†† and P. G. Varmette¶)

Neutron deficient Hg nuclei are characterized by level structures associated with prolate and oblate deformations. The prolate bands find their origin in multi-particle-hole excitations across the $Z = 82$ shell gap involving several proton intruder orbitals[1,2]. Mean field calculations by Nazarewicz[3] predict that the prolate minimum for Hg and Pb isotopes with $N < 98$ evolves towards much larger deformations ($\beta^2 \sim 0.50$-0.56), but its excitation energy rises up to ~ 3.5 MeV. Nuclei in this region also exhibit a variety of collective excitations. For example, due to the presence of pairs of orbitals with $\Delta j = \Delta l = 3\ \hbar$ near both the proton and neutron Fermi surfaces, octupole vibrations should be enhanced at low spin. Such structures will compete along the yrast line with collective excitations built on specific quasiparticle configurations. This situation provides an opportunity to study the interplay between these collective modes.

In last year's Annual Report a study was reported of yrast structures in ^{178}Hg, as a part of our program to investigate properties of very neutron deficient Hg nuclei in this region. The level scheme for this nucleus, deduced from this work, is presented in Fig. I-27 and its investigation has now been completed[4]. At the ATLAS facility, we have investigated this year the ^{180}Hg isotope, which was produced as a by-product of an experiment dedicated to the study of fusion dynamics in the vicinity of the Coulomb barrier. A sample γ-ray spectrum showing the main transitions in ^{180}Hg is presented in Fig. I-28. Particular attention was paid to the low-lying negative parity excitations which have been observed for the first time in ^{178}Hg and ^{180}Hg. They exhibit a complex decay towards the low spin states arising from both the prolate-deformed and the nearly spherical coexisting minima. These structures are associated at low spin with an octupole vibration and are crossed at moderate frequency by shape driving, two-quasiproton excitations. Striking similarities are noted and a consistent interpretation appears to emerge based on detailed comparisons with various model calculations.

A brief account of the data on the ^{178}Hg nucleus has been published[4] and a full report on ^{180}Hg has been submitted for publication.

*Argonne National Laboratory and Mississippi State University, †Argonne National Laboratory and University of Oslo, Norway, ‡Argonne National Laboratory and University of Jyväskylä, Finland, §The Niels Bohr Institute, Roskilde, Denmark, ¶Mississippi State University, ‖University of Illinois at Chicago, **Washington University, ††University of Tennessee

[1] J. L. Wood, K. Heyde, W. Nazarewicz, M. Huyse, and P. Van Duppen, Phys. Rep. **215**, 103 (1992).
[2] K. Heyde, P. Van Isacker, M. Waroquier, J. L. Wood, and R. A. Meyer, Phys. Rep. **102**, 293 (1983).
[3] W. Nazarewicz, Phys. Lett. **B305**, 195 (1993).
[4] F. G. Kondev *et al.*, Phys. Rev. C **61**, 011303(R) (2000).

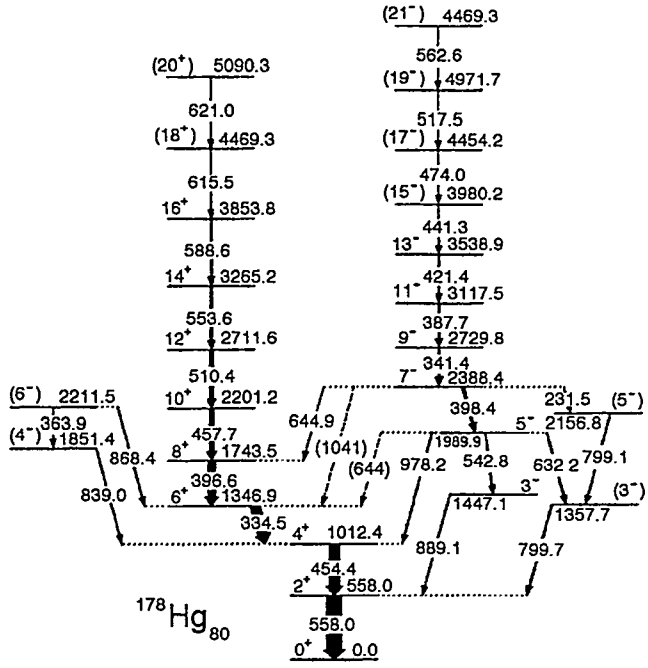

Fig. I-27. Proposed ^{178}Hg level scheme. Quantum numbers are given in parenthesis when reliable multipolarity information was not obtained. For each transition, the width of the arrow is proportional to the measured intensity.

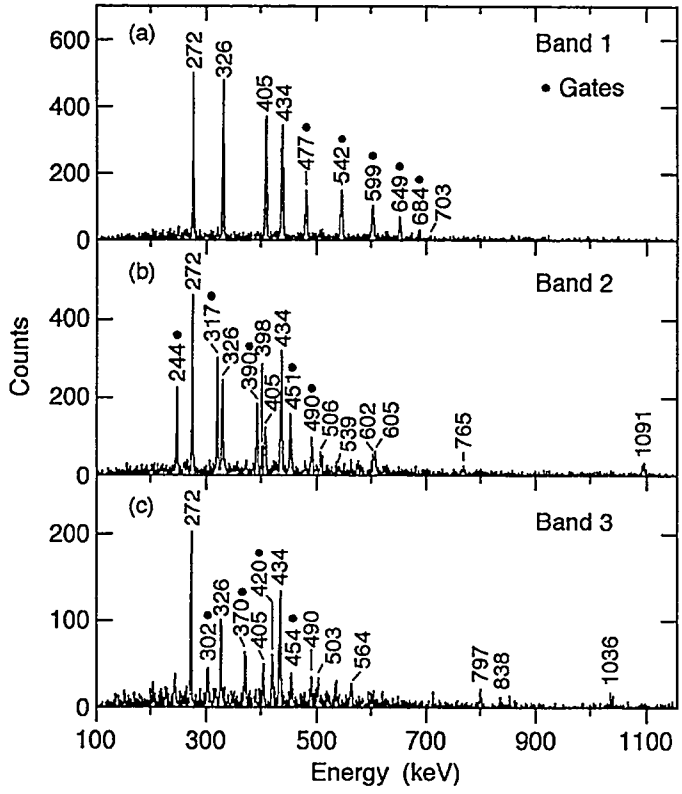

Fig. I-28. Sample spectra obtained from the mass-gated coincidence data for bands observed In ^{180}Hg. The spectraare sums of coincidence gates placed on the transitions marked with the black dots.

b.22. High-Spin Collective Structures in ^{178}Pt

(F. G. Kondev, M. Alcorta, P. Bhattacharyya, L. T. Brown, M. P. Carpenter, C. N. Davids, S. M. Fischer, R. V. F. Janssens, T. L. Khoo, T. Lauritsen, C. J. Lister, D. Seweryniak, A. A. Sonzogni, I. Wiedenhöver, S. Siem,* J. Uusitalo,† R. Nouicer,‡ W. Reviol,§ and L. L. Riedinger¶)

Despite their close proximity to the Z = 82 shell closure, the Pt (Z = 78) nuclei of the A ~ 180 region are characterized by level structures associated with prolate, oblate and triaxial deformations. In these nuclei, excitations based on the intruder orbitals have received considerable attention because of their ability to affect the nuclear shape. While in the Os (Z = 76) nuclei the quadrupole deformation is approximately constant over a wide range of isotopes, there is evidence in the Hg (Z = 80) isotopes that structures built upon specific intruder orbitals impact the nuclear shape significantly. Specifically, Ma *et al.*[1] have shown in ^{186}Hg that the occupation of the 1/2$^+$[651] ($g_{9/2}$) and 1/2$^-$[770] ($j_{15/2}$) neutron orbitals drives the nucleus towards a prolate deformation value of β_2 ~ 0.35 which is intermediate between those associated with the normally deformed (β_2 ~ 0.25) and the superdeformed (β_2 ~ 0.50) minima. In this general context the study of Pt nuclei is worthwhile as it is likely to add information on the relative importance of various orbitals for the collective excitations in this mass region.

Excited states in ^{178}Pt were populated with the ^{103}Rh(^{78}Kr,3p) reaction using 350-MeV beams provided by the ATLAS superconducting linear accelerator at the Argonne National Laboratory. An extended level scheme for ^{178}Pt, shown in Fig. I-29, was obtained by combining the selectivity of the FMA with the high detection efficiency and resolving power of the Gammasphere spectrometer. Specifically, the ground state band was observed beyond the first crossing which is attributed to the alignment of a pair of $i_{13/2}$ neutrons. The previously known excited band was firmly assigned odd-spin and negative parity, and was considerably extended in spin. A new negative parity band was observed for the first time. The configurations of these structures were interpreted as octupole vibrations at low spin which are crossed at higher frequency by two-quasiparticle excitations. The latter are most likely neutron excitations. Such assignments were aided by examining a range of properties including (a) the excitation energy of the bands, (b) the E1 transition probabilities and (c) alignments (see Fig. I-30). In addition, the α-decay reduced widths for the Pt isotopes were also investigated. The large reduction of the width for the odd-mass Pt isotopes is explained through the weakening of neutron pairing due to the blocking effect. As illustrated in Fig. I-31, such a behavior is reproduced by blocked Nilsson-Lipkin-Nogami calculations.

A full report of this work has been accepted for publication.

*Argonne National Laboratory and University of Oslo, Norway, †Argonne National Laboratory and University of Jyväskylä, Finland, ‡University of Illinois at Chicago, §Washington University, ¶University of Tennessee

[1] W. C. Ma *et al.*, Phys. Rev. C 47, R5 (1993).

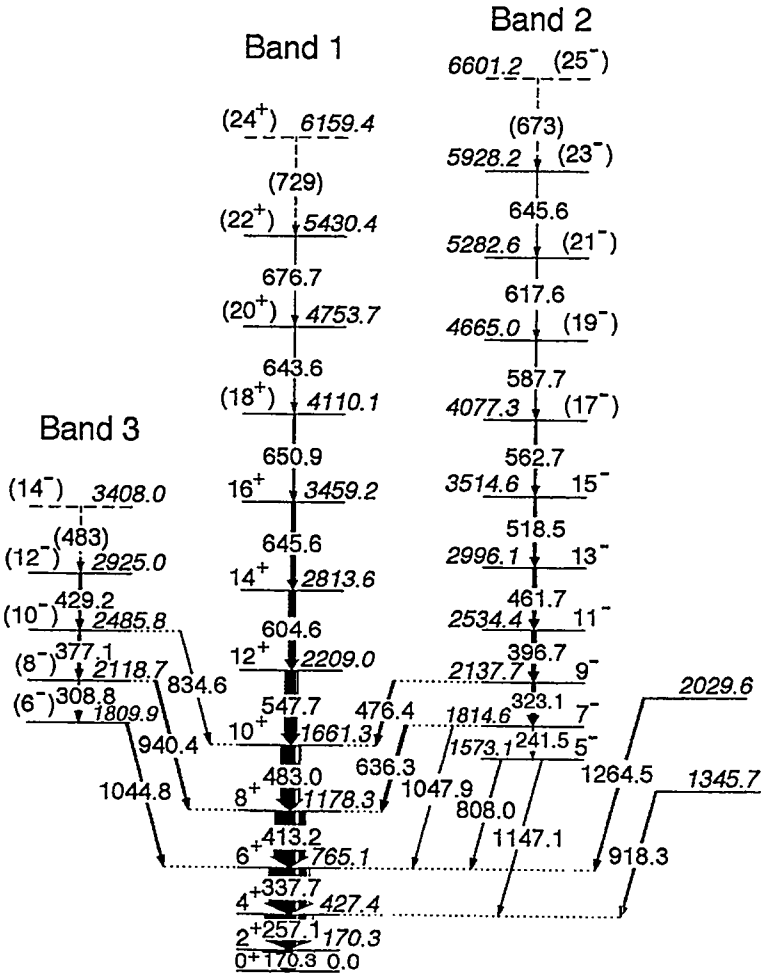

Fig. I-29. Level scheme of ^{178}Pt deduced from this work. Tentative placements are indicated by dashed lines. Tentative spin-parity assignments are given in brackets.

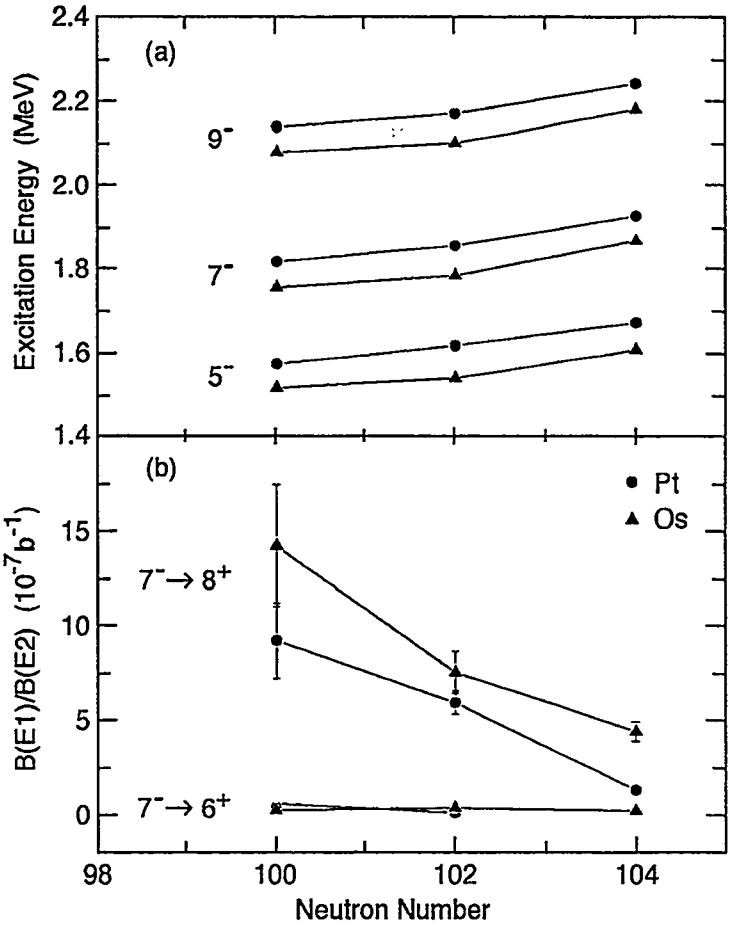

Fig. I-30. Excitation energies for the 5⁻, 7⁻ and 9⁻ levels (a) and B(E1)/B(E2) ratios for selected transitions (b) in ^{178}Pt and neighboring even-even Os and Pt isotopes.

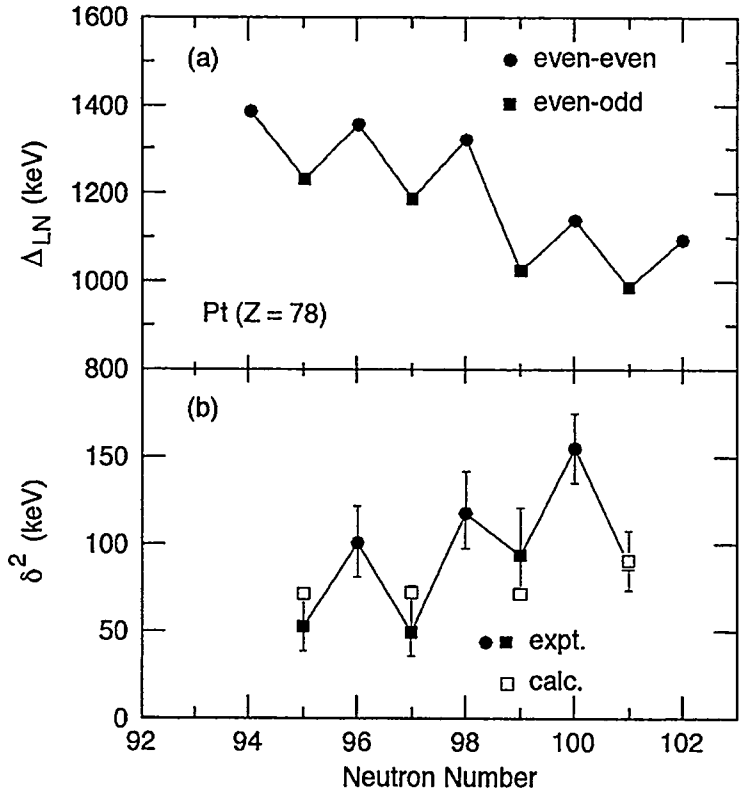

Fig. I-31. (a) Calculated Lipkin-Nogami pairing gap parameter Δ_{LN} for selected even-even and odd-A Pt isotopes. (b) Experimental (filled symbols) and calculated (open symbols) α-decay reduced widths for several Pt isotopes. The calculated δ^2 values were deduced from the predicted F_α values and the experimental data for the reduced widths of the even-even neighboring nuclei (see the text for details).

b.23. Spectroscopy of ^{183}Tl with Recoil-Mass and Z Identification

(M. P. Carpenter, R. V. F. Janssens, T. Lauritsen, D. Seweryniak, J. Uusitalo, I. Wiedenhöver, W. Reviol,* D. Jenkins,† K. S. Toth,‡ C. R. Bingham,* L. L. Riedinger,* W. Weintraub,* J. Cizewski,§ R. Wadsworth,† A. N. Wilson,† C. J. Gross,‡¶ J. C. Batchelder,¶ S. Juutinen,‖ and K. Helariutta‖)

The spectroscopy of ^{183}Tl has been the focus of an experiment with Gammasphere coupled to the FMA. The ^{182,183}Tl nuclei have also been studied as byproducts of a search for ^{182}Pb at RITU in Jyväskylä[1]. In these two experiments, the yrast sequence in ^{183}Tl has been observed for the first time (see Fig. I-32). The results reported here and in Ref. 2 are mainly based on the spectroscopy of ^{183}Tl with mass identification. The identified yrast sequence in ^{183}Tl resembles the well-deformed (prolate) excited bands in adjacent nuclei of Hg, Tl, and Pb, but its decay-out properties are different from those cases in two respects. (*i*) The rotational-like sequence is observed from medium spin to the 13/2$^+$ state, *i.e.* the population intensity stays within the band down to the bandhead. (*ii*) A strong γ-decay branch from the prolate band to a slightly-oblate structure, like in heavier Tl nuclei, is not observed. These features suggest that the prolate energy minimum in ^{183}Tl has dropped significantly compared to ^{185}Tl[3]. In the present level scheme it is not clear how the ^{183}Tl band decays and, therefore, upper and lower-limit estimates for the energy of the 13/2$^+$ bandhead relative to the 9/2$^-$ isomeric state (oblate) have been made (95 keV ≤ E_{rel} ≤ 424 keV[2]). However, with the estimated upper limit, the basic conclusions for the $i_{13/2}$ band in ^{183}Tl are not affected by the uncertainty for the decay out of the band.

*University of Tennessee, †University of York, United Kingdom, ‡Oak Ridge National Laboratory, §Rutgers University, ¶Oak Ridge Associated Universities, ‖University of Jyväskylä, Finland

[1]D. Jenkins, *et al.*, to be published.

[2]W. Reviol *et al.*, Proceedings of the Conference "Nuclear Structure '98", Gatlinburg, TN, AIP-Conference Proceedings, in print.

[3]G. Lane *et al.*, Nucl. Phys. **A586**, 316 (1995).

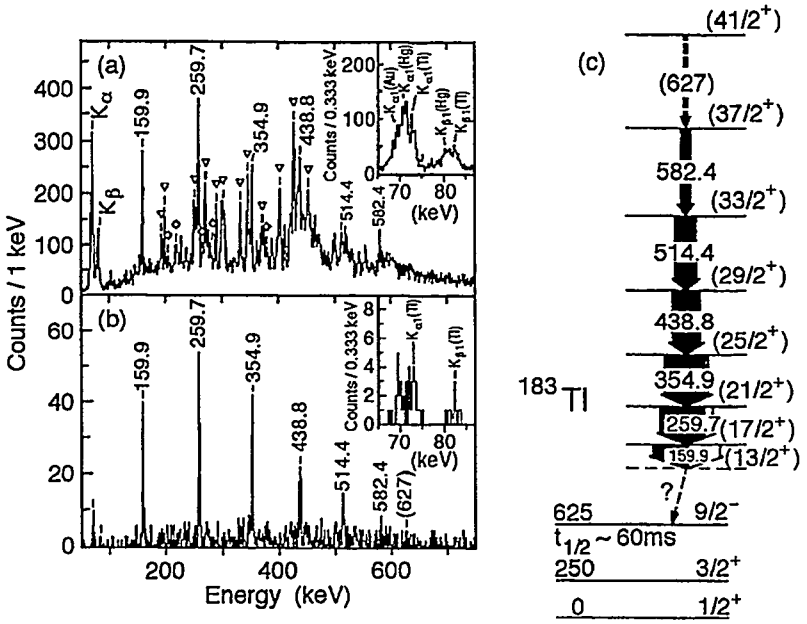

Fig. I-32. (a) Gamma rays in coincidence with A = 183 residues. Known transitions in ^{183}Hg and ^{183}Au are labeled by triangles and diamonds. Newly observed transitions are labeled by their energies in keV. (b) Summed spectrum of gates on the 159.9-, 259.7-, 354.9-, 438.8-, and 514.4-keV lines from the A = 183 Eγ-Eγ coincidence data. (c) Deduced level structure for ^{183}Tl.

b.24. Identification of a $t_{1/2} > 1$ ms K-Isomer in Neutron-Rich ^{185}Ta

(I. Ahmad, M. P. Carpenter, G. Hackman, R. V. F. Janssens, T. L. Khoo, D. Nisius, P. Reiter, C. Wheldon,* P. M. Walker,* R. D'Alarcao,† P. Chowdhury,† C. J. Pearson,* E. H. Seabury,† and D. M. Cullen‡)

Our program of using pulsed heavy beams to populate long-lived high-K isomers in neutron-rich nuclei in the $A \approx 180$ region has proven to be extremely successful. Experiments with U beams on Lu, Hf, Ta and W isotopes have yielded many new multi-quasiparticle isomers, overcoming the limitations of fusion-evaporation reactions in reaching the neutron-rich nuclei in this region. The results of the strongest reaction channels have been published[1,2], and we are now making progress on the weaker channels involving nucleon transfer. Here we report on a new long-lived isomer in neutron-rich ^{185}Ta, populated via 1-proton transfer with a 1600 MeV pulsed ^{238}U beam incident on a thick target of ^{186}W. The γ rays were measured by the ANL/Notre-Dame BGO array.

The out-of-beam spectra are dominated by the strong inelastic excitation of K isomers in the target nucleus[1]. However, a new band has been observed from the particle transfer channels, (see Fig. I-33) fed by a $t_{1/2} >$ 1 ms isomer. The population intensity and careful analysis of the weak x-ray coincidences suggest that the new band is in the isotope ^{185}Ta (1-proton from the target). An earlier (t,α) experiment[3] identified 3 low-lying states in the $K\pi = 9/2$ band in ^{185}Ta, the energies of which are in excellent agreement with the corresponding levels in the new band. In addition, intensity balancing arguments have been used to extract an electron conversion coefficient for the 175 keV transition, leading to an E1 assignment. This is consistent with a K-allowed decay from the $K\pi = 9/2^-$ bandhead to the $K\pi = 7/2^-$ ground state, and is also of approximately the right energy to continue the systematics observed in the lighter isotopes. Examination of the in-band γ-ray branching ratios supports the $9/2^-[514]$ Nilsson configuration assignment.

Adding one unit of spin for each level above an $I\pi = 9/2^-$ bandhead would mean that the transition directly de-populating the isomer feeds the $19/2^-$ member of the band (see Fig. I-33 inset for proposed level scheme). This transition has not been observed but can be given upper energy limits of 100 keV (M1) and 80 keV (E1) on the basis of detection-efficiency and conversion-coefficient considerations. Comparison with Nilsson model calculations favors a $K^\pi = 21/2^-\{5/2^-[402], 7/2^+[404], 9/2^-[514]\}$ 3-quasiproton configuration for the isomer, consistent with an isomeric M1 transition. This is the most neutron-rich seniority > 2 K-isomer identified and the results have been published[4].

*University of Surrey, United Kingdom, †University of Massachusetts, ‡University of Liverpool, United Kingdom

[1]C. Wheldon *et al.*, Phys. Lett. **B425**, 239 (1998).
[2]R. D'Alarcao *et al.*, Phys. Rev. C **59**, R1227 (1999).
[3]G. Lovhoiden, D. G. Burke, E. R. Flynn, and J. W. Sunier, Phys. Scr. **22**, 203 (1980).
[4]C. Wheldon *et al.*, Eur. Phys. J. **A5**, 353 (1999).

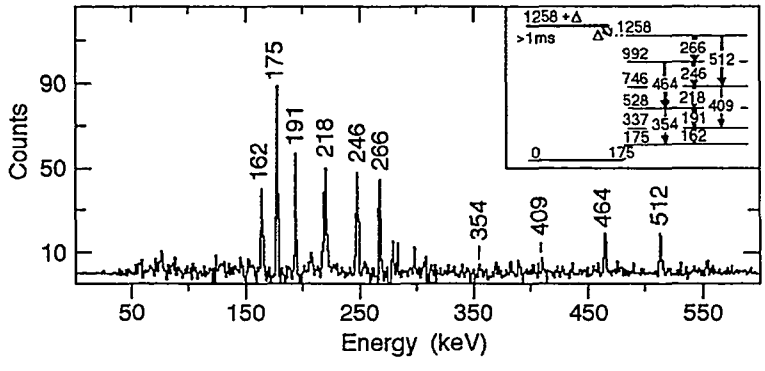

Fig. I-33. The gamma-ray spectrum gated on transitions in the new band. A level scheme is proposed (see inset panel), with a well formed rotational structure being fed by an isomeric state. The low energy isomeric transition has not been observed leading to an offset of triangle for the isomeric level.

b.25. Studies of the Excited States and the Decay of ^{185}Bi

(G. L. Poli, D. Seweryniak,* M. P. Carpenter, C. N. Davids, A. Heinz, R. V. F. Janssens, T. L. Khoo, F. G. Kondev, A. A. Sonzogni, I. Wiedenhöver, P. J. Woods,† T. Davinson,† J. A. Cizewski,§ J. J. Ressler,‡ J. Shergur,‡ and W. B. Walters‡)

A Recoil-Decay Tagging experiment was carried out to study the proton decay and excited states of ^{185}Bi. Prompt γ rays were detected using Gammasphere and were tagged with decay protons observed in a Double-Sided Si Strip detector placed behind the focal plane of the Fragment Mass Analyzer. The ^{96}Mo(^{92}Mo,p2n)^{185}Bi reaction was used to produce ^{185}Bi nuclei. The decay spectrum is shown in Fig. I-34. Compared to the first discovery experiment[1] a factor of about 4 more protons and α particles associated with ^{185}Bi were detected. An energy of 1618(11) keV and a half-life of $50(^{7}_{9})$ μs was obtained for the decay of ^{185}Bi. An energy of 1618(11) keV was measured for the protons and 8080(30) keV for the α particles. The proton-decay branching ratio was deduced to be 85%. The analysis of γ-ray data is in progress.

*Argonne National Laboratory and University of Maryland, †University of Edinburgh, United Kingdom, ‡University of Maryland, §Rutgers University

[1] C. N. Davids *et al.*, Phys. Rev. Lett. **76**, 592 (1995).

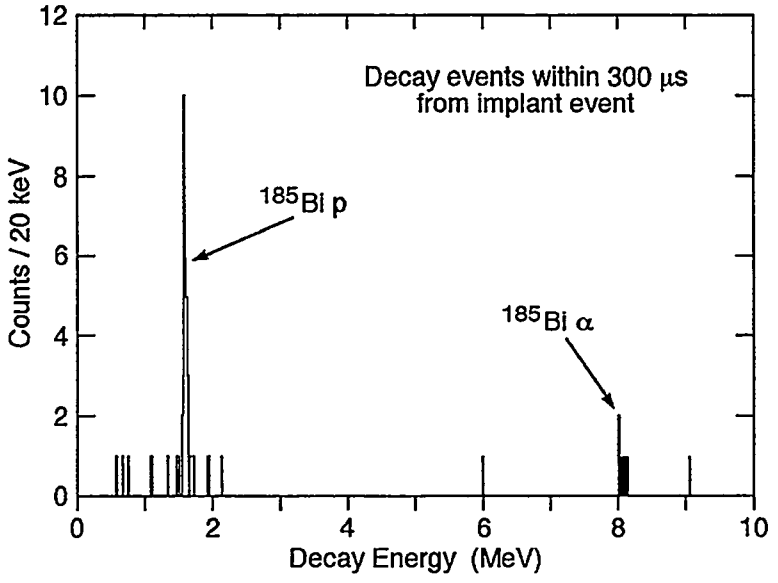

Fig. I-34. The decay spectrum associated with ^{185}Bi.

b.26. Coulomb Excitation and Few Nucleon Transfer Reactions for the ^{209}Bi + ^{232}Th System

(R. V. F. Janssens, I. Ahmad, J. Caggiano, M. P. Carpenter, J. P. Greene, A. Heinz, T. L. Khoo, F. G. Kondev, T. Lauritsen, C. J. Lister, D. Seweryniak, A. Sonzogni, I. Wiedenhoever, H. Amro,* K. Abu Saleem,† G. Hackman,‡ P. Chowdhury,§ D. Cline,¶ A. O. Machiavelli,‖ and C. Wu¶)

For the past two years, we have studied the high-spin collective behavior of long-lived actinide nuclei with the so-called "unsafe" Coulomb excitation technique with DC beams of very heavy ions at energies a few % above the Coulomb barrier and multi-detector arrays with a large number of Compton-suppressed Ge detectors. Some of this work has been published[1,2], while other parts are described elsewhere in this report. From the perspective of extending the "unsafe" Coulex technique, a tantalizing result was the observation and isotopic assignment of bands populated in transfer reactions. For example, in our study of the ^{208}Pb + ^{244}Pu reaction, two new rotational cascades were assigned to the yrast band of ^{243}Pu from cross-coincidence relationships with transitions in ^{209}Pb. Such a transfer reaction was subsequently used to gather data on ^{238}Pu with the ^{207}Pb + ^{239}Pu reaction at 1300 MeV. The choice of the odd-neutron ^{207}Pb projectile was determined by the desire to enhance neutron pick-up from the target.

The success encountered in these measurements led to the suggestion that exciting possibilities might exist to use proton transfer channels to study high-Z nuclei beyond Pu and Cm by using the appropriate projectile, e.g. ^{209}Bi. The ^{209}Bi + ^{232}Th reaction at 1400 MeV was studied at ATLAS with the Gammasphere spectrometer in order to answer the following questions: (1) how large are the cross sections for proton transfers, compared to Coulex? (2) how many reaction channels are actually open? (3) how large is the angular momentum transfer? (4) what types of excitations are observable? (5) are more complex reactions corresponding to the transfer of large number of nucleons observed?

While the data are still under analysis, the following general conclusions have already been reached: (i) One proton transfer and pick-up reactions to ^{233}Pa and ^{231}Ac have been observed with a yield of ~ 5% with respect to the intensity of ^{232}Th. This yield is comparable to that seen in the neutron transfer channels on the Pu targets. (ii) The yield for the two-proton transfer channel is lower by roughly one order of magnitude, again in line with expectations. (iii) States with spins as high as ~ 25 $\hbar$ have been observed. (iv) In addition to proton transfer, the neutron channels to ^{233,231,230}Th have also been observed. The intensities and spins reached are similar to those of the proton channels. Figure I-35 presents partial levels schemes obtained for ^{231}Ac and ^{233}Pa. The level scheme of ^{232}Th was considerably extended as well. The latter will be combined with results obtained in a similar experiment at the 8PI spectrometer[3].

*Argonne National Laboratory and North Carolina State University, †Argonne National Laboratory and Illinois Institute of Technology, ‡University of Kansas, §University of Massachusetts-Lowell, ¶University of Rochester, ‖Lawrence Berkeley National Laboratory

[1] G. Hackman *et al.*, Phys. Rev. C **57**, R1506 (1998).
[2] I. Wiedenhoever *et al.*, Phys. Rev. Lett. **83**, 2143 (1999).
[3] D. Ward *et al.*, private communication.

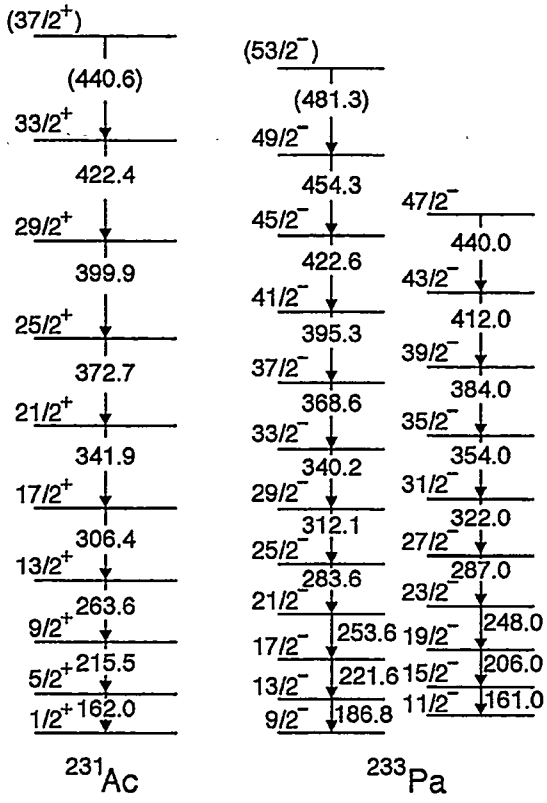

Fig. I-35. Preliminary level schemes for ^{233}Pa and ^{231}Ac obtained with the $^{209}Bi + ^{232}Th$ reaction.

b.27. Octupole Correlations in Pu Isotopes Studied by Coulomb Excitation

(I. Wiedenhöver, R. V. F. Janssens, K. Abu-Saleem, I. Ahmad, M. Alcorta, H. Amro, M. P. Carpenter, J. P. Greene, G. Hackman, T. L. Khoo, T. Lauritsen, C. J. Lister, D. T. Nisius, P. Reiter, D. Seweryniak, J. Uusitalo, S. Siem,* J. Cizewski,† A. O. Macchiavelli,‡ P. Chowdhury,§ E. H. Seabury,§ D. Cline,¶ and C. Y. Wu¶)

We performed a series of measurements with Gammasphere at ATLAS, using the technique of "Unsafe Coulomb Excitation" to investigate the nuclear structure of Actinide nuclei around Plutonium. These experiments rely on a combination of facilities, which at this moment is only available at Argonne: The access to radiochemical and target production facilities to handle targets of Actinide Isotopes, the ATLAS accelerator, which provides beams of the heaviest ions at the required energy and intensity and Gammasphere, the world's most powerful gamma detector array.

In our experiments, we bombarded targets of the isotopes ^{240}Pu and ^{244}Pu with a ^{208}Pb beam and ^{239}Pu, and ^{242}Pu targets with a ^{207}Pb beam at energies above the Coulomb barrier. The data includes Coulomb excitation of the target isotope as well as one- - and two neutron transfer channels, which were central to establish detailed spectroscopic data for nuclei which are too short-lived to be used as target material, like ^{238}Pu ($T_{1/2}$ = 8 y), ^{241}Pu($T_{1/2}$ = 14 y) and ^{243}Pu ($T_{1/2}$ = 5 *h*).

A common feature for the excited states known in many actinide nuclei is the presence of a positive parity rotational band and a negative parity excited band, which is interpreted to be based on an octupole surface vibration. The combined data of our experiments yielded a detailed picture of nuclear structure for the odd and even mass nuclei between ^{238}Pu and ^{244}Pu

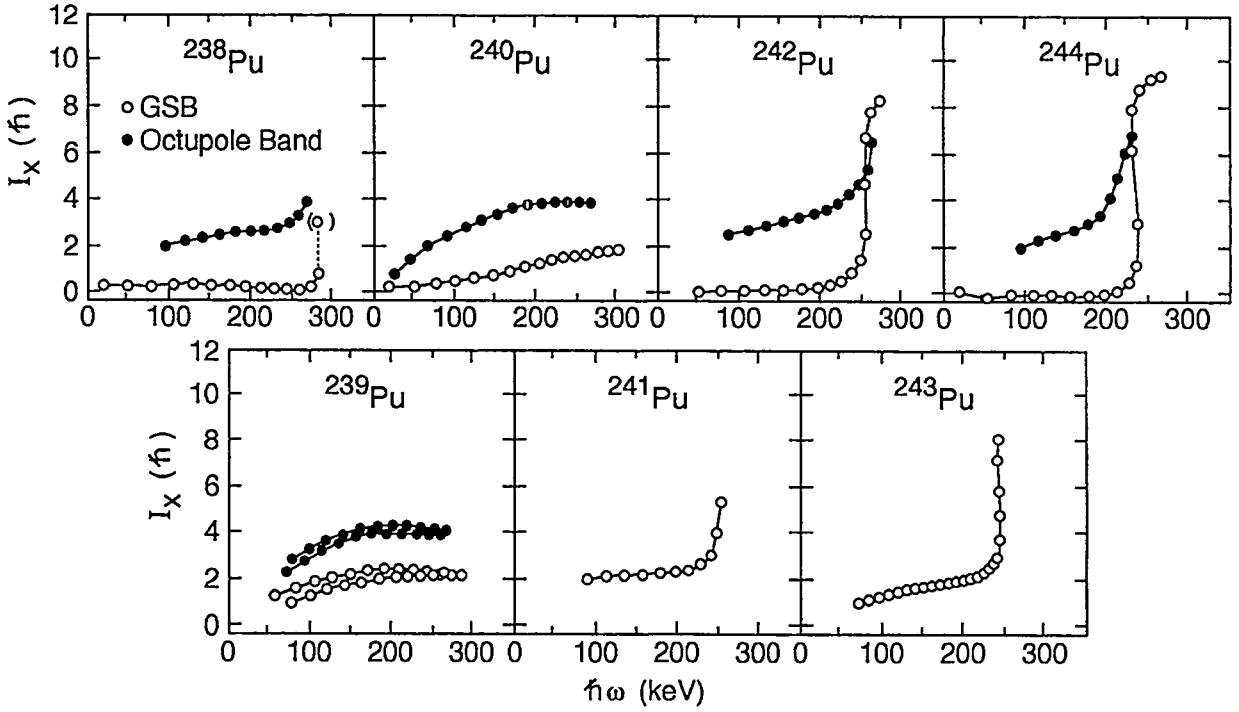

Fig. I-36. Aligned spins i_x of the yrast and octupole rotational bands in the Pu isotopes. In all cases the same reference is subtracted, with the Harris Parameters $J_0 = 65\ \hbar^2\ MeV^{-1}$ and $J_1 = 369\ \hbar^2\ MeV^{-3}$.

and allowed us to investigate the properties of these two bands systematically. The results discussed below show an unexpected contrasting behavior between ^{239}Pu and ^{240}Pu and the other isotopes[1]. Figure I-36 shows the aligned angular momentum as a function of rotational frequency. For ^{242}Pu and ^{244}Pu, the curves show a behavior typical for the alignment of a pair of $i_{13/2}$ protons due to the Coriolis force. The odd mass nuclei ^{243}Pu and ^{241}Pu show the same behavior. With the same certainty that this phenomenon was established in ^{242}Pu and ^{244}Pu, it was established to be missing in ^{240}Pu. The absence or delay of such quasiparticle alignment was theoretically predicted in the presence of octupole deformation[2].

Figure I-37 compares the relative energy position of the negative parity and positive parity bands for the even mass nuclei as a function of angular momentum. For high angular momenta, the negative parity band in ^{240}Pu comes down to the energy of the ground state band. At the same time we could observe the two negative parity bands of ^{239}Pu approach their respective positive parity partner, forming so-called ``parity-doublets" at high angular momenta, which again is an expected property of octupole-deformed nuclei.

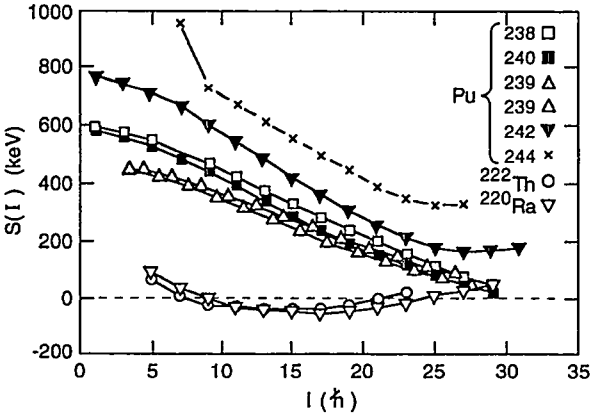

Fig. I-37 Comparison of the energy staggering S(I) as a function of spin I in the Pu isotopes and in ^{220}Ra and ^{222}Th, two of the best examples of octupole deformed nuclei.

Figure I-38 displays the electric dipole (E1)-transition matrix elements observed in the decay of the negative parity band to the positive parity partner. The decay of the ^{240}Pu negative-parity band exhibits the largest transition dipole moments among the isotopes under investigation. This fact also points to the presence of strong octupole correlations or octupole deformation, which are expected to enhance E1-decays.

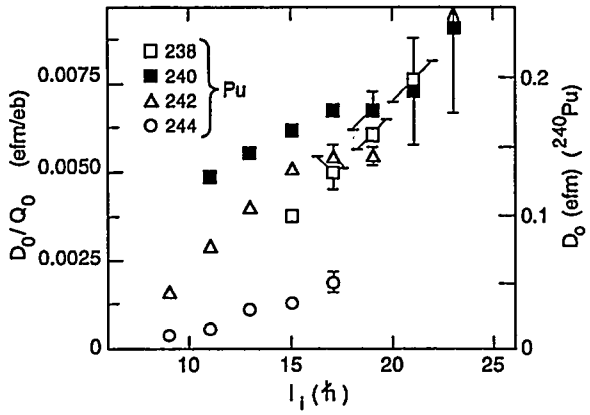

Fig. I-38. Ratio of transition dipole and quadrupole moments extracted from the E1 and E2 branchings E1: $I^-_i \rightarrow (I_i\text{-}1)^+$/E2: $I^-_i \rightarrow (I_i\text{-}2)^-$ as a function of the spin I_i. The values of the transition dipole moment D_0 given on the right hand side are for ^{240}Pu only, where they have been calculated assuming rotational E2-matrix elements with the Q_0 moment of the ground state band.

These three observables suggest that for the cases of ^{240}Pu and ^{239}Pu a transition has occurred from a situation, where octupole vibrations coexist with rotational behavior into a situation, where the ground state and octupole vibrational bands merge into one excitation associated with an octupole deformed shape. Although this transformation had been postulated for other nuclei, such as the neutron-deficient Th and Ra-isotopes, this is the first observed case in nuclei with a strong quadrupole deformation. Furthermore, the octupole collectivity develops in a sharp transition along the Pu-isotope chain, which is a strong indication for a microscopic origin of this phenomenon. This observation at the same time poses a challenge for detailed microscopic calculations.

*Argonne National Laboratory and University of Oslo, Norway, †Argonne National Laboratory and Rutgers University, ‡Lawrence Berkeley National Laboratory, §University of Massachusetts, ¶University of Rochester

[1]I. Wiedenhöver *et al.*. Phys. Rev. Lett. **83**, 2143 (1999).
[2]S. Frauendorf and V. Pashkevitch, Phys. Lett. **B141**, 23 (1984).

b.28. Proton Transfer Reactions on ^{237}Np, ^{241}Am and ^{248}Cm

(R. V. F. Janssens, Ahmad, D. L. Bowers, J. Caggiano, M. P. Carpenter, J. P. Greene, A. Heinz, T. L. Khoo, F. G. Kondev, T. Lauritsen, C. J. Lister, D. Seweryniak, I. Wiedenhoever, K. Abu Saleem,* G. Hackman,† P. Chowdhury,‡ D. Cline,§ M. Devlin,¶ N. Fotiades,¶ A. O. Macchiavelli,‖ E. H. Seabury,¶ and C. Wu§)

Following the successful study of proton transfer reactions with ^{209}Bi beams on ^{232}Th at energies ~ 20% above the Coulomb barrier, the resolving power of Gammasphere was used to study similar reactions on ^{237}Np, ^{241}Am and ^{248}Cm. The main goals of the measurements can be summarized as follows:

1. Study the behavior with spin and frequency of the proton excitations in ^{237}Np and ^{241}Am in relation to the alignment in the Pu and Cm even-even isotopes (possible blocking of proton alignment).

2. Study the octupole excitations in ^{237}Np and ^{241}Am and see whether they follow the pattern found for the same excitation in ^{239}Pu (i.e. a transition from octupole vibration to octupole rotation) or whether they exhibit a particle alignment instead (as in the heavier Pu isotopes).

3. Study the yrast and the lowest octupole band in ^{242}Cm and determine whether the band sequences mirror those of the isotone ^{240}Pu indicating similar octupole strength or whether they are similar to the patterns seen in the heavier Pu isotopes and in the isotone ^{238}U (upbending or backbending in both the yrast and octupole bands).

4. Delineate for the first time excitations to high spin in ^{249}Bk and ^{250}Cf as well as in all other transfer channels populated in the reaction.

The 6 days experiment was performed with a 1450 MeV ^{209}Bi beam. For each target a large statistical data set was collected. The data is under analysis.

*Argonne National Laboratory and Illinois Institute of Technology, †University of Kansas, ‡University of Massachusetts-Lowell, §University of Rochester, ¶Los Alamos National Laboratory, ‖Lawrence Berkeley National Laboratory

b.29. Spectroscopy of the Transfermium Nucleus ^{252}No

(T. L. Khoo, C. J. Lister, R.-D. Herzberg,* P. A. Butler,* N. Amzal,* A. J. C. Chewter,* N. Hammond,* G. D. Jones,* R. D. Page,* C. Scholey,* O. Stezowski,* M. Leino,† R. Julin,† J. F. C. Cocks,† O. Dorvaux,† P. T. Greenlees,† K. Helariutta,† P. M. Jones,† S. Juutinen,† H. Kankaanpaa,† H. Kettunen,† P. Kuusiniemi,† M. Muikku,† P. Nieminen,† P. Rahkila,† W. H. Trzaska,† F. Heβberger,‡ J. Gerl,‡ Ch. Schlegel,‡ H. J. Wollersheim,‡ W. Korten,§ F. Becker,§ Y. Le Coz,§ K. Hauschild,§ M. Houry,§ R. Lucas,§ Ch. Theisen,§ P. Reiter,¶ and K. Eskola‖)

The motivation for studying nobelium isotopes is given in Sec. b.34. This section reports on results from an experiment on ^{252}No, conducted with JUROSPHERE II and RITU at Jyväskylä, with R. Herzberg as spokesperson. The behavior at high-spin of the moment of inertia of the ground state band and the comparison with that of ^{252}No will reveal indirect information on the single-particle orbitals near the Fermi level, especially on the high-j ones, which align and increase the moment of inertia. In particular, the influence of the $j_{15/2}$ orbitals is expected to lead to a larger increase in the moment of inertia in ^{252}No than in ^{254}No.

From the experiment, the ground state band of ^{252}No has been tentatively identified up to spin 20. The moment of inertia of ^{252}No starts out lower than that of ^{254}No at low frequency, but becomes larger at $\hbar\omega \sim$ 0.14 MeV, as it increases more rapidly. These results support the expectations based on the cranked shell model, using single-particle levels given by a Wood-Saxon potential with the measured deformation[1].

*University of Liverpool, United Kingdom, †University of Jyväskylä, Finland, ‡GSI Darmstadt, Germany, §DAPNIA/SPhN CEA-Saclay, France, ¶Ludwig Maximilians Universität München, Germany, ‖University of Helsinki, Finland

[1]P. Reiter *et al*, Phys. Rev. Lett. **82**, 509 (1999).

b.30. Entry Distribution of ^{220}Th — The Measurement of Fission Barriers at High Angular Momentum

(T. L. Khoo, I. Ahmad, M. P. Carpenter, C. N. Davids, J. P. Greene, A. Heinz, W. F. Henning, R. V. F. Janssens, F. G. Kondev, T. Lauritsen, C. J. Lister, D. Seweryniak, A. A. Sonzogni, J. Uusitalo, I. Wiedenhöver, P. Reiter,* P. Bhattacharyya,† J. A. Cizewski,‡ G. D. Jones,§ R. Julin,¶ and S. Siem‖)

Today, more than 60 years after the discovery of nuclear fission, the number of nuclei, whose fission barriers have been experimentally determined, is still very limited. In the past, fission induced by neutrons or charged particles allowed an accurate measurement of fission barriers of fissile nuclei in the vicinity of stable or long-lived targets. Fission induced by photons and electrons provided similar information.

Far off stability different methods have been applied. Pioneering work has been done using beta-delayed fission or electromagnetic interaction of relativistic secondary beams with Pb targets. These methods are limited as well: in the former case only nuclei which show beta-delayed fission are accessible. In the latter case, an intense primary beam is needed, which excludes elements heavier than Pu. The fission barriers of the heaviest elements are particularly interesting, as they are essential for understanding the production mechanisms of superheavy elements.

We have introduced a new method, which uses the entry distribution for an evaporation residue, to set constraints on the fission barrier of the shell stabilized nucleus ^{254}No - see Ref. 1.

Here, we report on the measurement of the entry distribution of ^{220}Th. A ^{48}Ca beam at 206 MeV was used to produce ^{220}Th in a fusion reaction with a 810 μg/cm^2 target of ^{176}Yb. The energy was chosen in order to maximize the production cross section, which is expected to be about 1 mb (Ref. 2). As the fission barrier of ^{220}Th has been determined before using electromagnetic interaction of relativistic secondary beams[3], it provides a calibration of the entry distribution method. In addition, the method provides the first direct measurement of the spin dependence of

the fission barrier. The fission barrier of ^{220}Th should be dominated by its liquid drop term; therefore a strong spin dependence is expected. This is in contrast to ^{254}No, where the fission barrier arises predominantly from the shell energy. Our entry distributions[1] in ^{254}No suggest that the shell-correction energy and, hence, the fission barrier is robust against rotation.

The preliminary entry distribution of ^{220}Th is shown in Fig. I-39. The distribution does not extend beyond the neutron separation energy S_n - as expected - and is mainly confined within the locus of the saddle-point energy E_{saddle}. The data suggest that the fission barrier, at e.g. spin 20, is larger than 6.5 MeV, which is somewhat higher than the predicted value of 5.7 MeV. This compares to the value $B_f = 6.8$ obtained by Grewe *et al.*[3] at spin 0.

Further analysis, especially of a data set at higher excitation energies, is in progress.

*LMU University of Münich, Germany, †Purdue University, ‡Argonne National Laboratory and Rutgers University, §University of Liverpool, United Kingdom, ¶University of Jyväskylä, Finland, ||Argonne National Laboratory and University of Oslo, Norway

[1]P. Reiter *et al.*, see Sec. b.34; Phys. Rev. Lett., in press; Phys. Rev. Lett. **82**, 509 (1999).
[2]C. C. Sahm *et al.*, Nucl. Phys. **A441**, 316 (1985).
[3]A. Grewe *et al.*, Nucl. Phys. **A614**, 400 (1997).

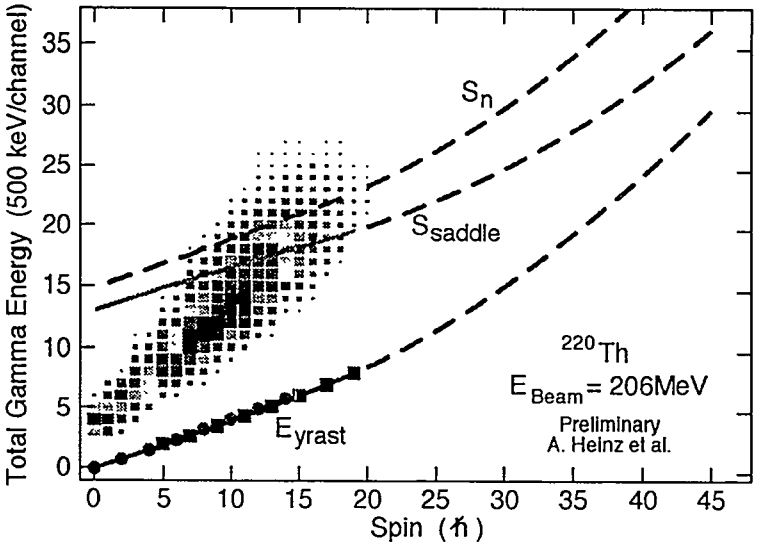

Fig. I-39. Preliminary entry distribution of ^{220}Th. The yrast line, the neutron-separation energy S_n and the saddle-point energy E_{saddle} are shown. The saddle-point energy is defined as $E_{saddle}(I) = E_{yrast}(I) + B_f(I)$, with $B_f(I)$ being the fission barrier at a given angular momentum I. $B_f(I)$ is calculated as the sum of a liquid drop and ground-state shell correction terms. The dashed lines are extrapolations. The neutron separation energy is calculated according to $S_n(I) = S_n(I = 0) + E_{yrast}(I)$.

b.31. Correlated Spins of Complementary Fragment Pairs in the Spontaneous Fission of ^{252}Cf

(I. Ahmad, J. P. Greene, A. G. Smith,* G. S. Simpson,* J. Billowes,* P. J. Dagnall,* J. L. Durell,* S. J. Freeman,* M. Leddy,* W. R. Phillips,* A. A. Roach,* J. F. Smith,* A. Jungclaus,† K. P. Lieb,† C. Teich,† B. J. P. Gall,‡ F. Hoellinger,‡ N. Schulz,‡ and A. Algora§)

Investigations of the properties of fission-fragment angular momentum provide one of the few means open to the experimentalist to explore the behavior of the fissioning system near the point of scission, providing a particularly crucial test in the case of spontaneous fission where the initial angular momentum of the system is well defined.

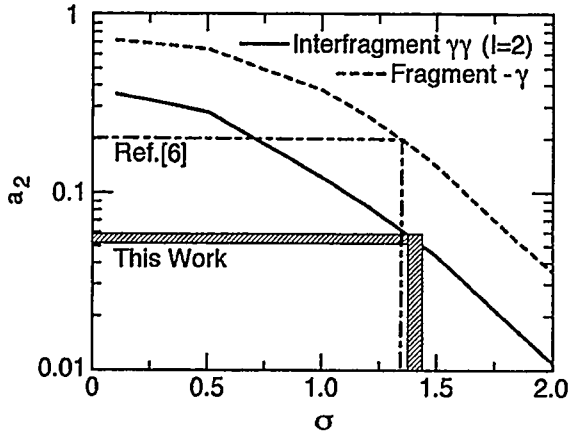

Fig. I-40. Results of calculations of m-substate smearing and its effect on the a_2 coefficient for fragment-γ angular distributions, as well as γγ correlations between the 2 → 0 decays of complementary fragment pairs.

A 120 μ Ci ^{252}Cf source, sandwiched between two 20 mg cm^{-2} Gd foils, was used as a source of neutron-rich fission fragments, whose γ-ray decays were detected in the Euroball array of germanium detectors. In this experiment measurements were made of angular correlations between γ rays emitted from one fragment with γ rays from the complementary fragment, for decays from low-lying excited states. For a range of complementary fragment pairs, the inter-fragment correlation was measured between the $2_1 \rightarrow 0_1$ γ-ray in the heavy fragment and the $2_1 \rightarrow 0_1$ γ-ray in the light fragment. Measurements were also made of the inter-fragment angular correlations between $4_1 \rightarrow 2_1$ γ rays. For complementary even-even fragments the weighted mean inter-fragment anisotropy, for $2 \rightarrow 0, 2 \rightarrow 0$ coincidences was found to be A = 0.101(7) with weighted mean values $a_2 = 0.057(4)$ and $a_4 = 0.021(5)$. The corresponding result for $4 \rightarrow 2, 4 \rightarrow 2$ inter-fragment coincidences was $A = 0.05(1)$ with weighted mean values of $a_2 = 0.035(5)$ and $a_4 = -0.003(8)$. Data from a previous experiment using a ^{248}Cm fission source[1] was re-analyzed with a method analogous to that used for ^{252}Cf. The weighted mean inter-fragment γ-ray anisotropy for $2 \rightarrow 0, 2 \rightarrow 0$ coincidences was found to be $A = 0.016(4)$ with weighted mean coefficients $a_2 = 0.014(2)$ and $a_4 = -0.009(3)$. We adopt a similar Gaussian smearing technique to that used by Yamazaki[2] for parameterizing the degree of alignment in heavy-ion fusion-evaporation reactions. The z-direction is defined by the γ ray from one fragment and full alignment corresponds to the m-substate populations in the two fragments being equal. Figure I-40 shows the effect of varying σ on the a_2 coefficient for inter-fragment γγ correlations, assuming two quadrupole $2 \rightarrow 0$ transitions, as well as for fragment-γ distributions with a quadrupole $2 \rightarrow 0$ γ decay. The measured value of $a_2 = 0.057(5)$ for the inter-fragment γγ correlations in ^{252}Cf indicates a statistical width $\sigma_{\gamma\gamma} = 1.40(5)$. The magnitude of the corresponding theoretical $a_4(= -0.01)$ is very much attenuated at this value of sigma. The fragment-γ distributions of Wilhelmy et al.[3] for $2 \xrightarrow{E2} 0$ decays in ^{100,102}Zr, ^{104,106}Mo, ^{110}Ru, ^{144}Ba and ^{148}Ce, produced in the spontaneous fission of ^{252}Cf, have a mean value of $a_2 = 0.20(4)$. As seen in Fig. I-40, this translates into a statistical substate smearing with $\sigma_{f\gamma} = 1.35(5)$. The similarity in the smearing widths for inter-fragment γγ

*University of Manchester, United Kingdom, †University of Göttingen, Germany, ‡IReS and University of Louis Pasteur, Strasbourg, France, §Laboratori Nazionali Legnaro, Italy

[1]M. A. Jones *et al.*, Nucl. Phys. **A605**, 133 (1996).
[2]T. Yamazaki, Nucl. Data. **3**, 1 (1967).
[3]J. B. Wilhelmy *et al.*, Phys. Rev. C **5**, 2041 (1972).
[4]A. G. Smith *et al.*, Phys. Rev. C **60**, 064611 (1999).

correlations and fragment-γ distributions in ^{252}Cf fission is somewhat surprising given that the γγ correlations suffer from substate smearing from two independent statistical processes, the deexcitation to the 2^+ states in two fragments, whereas the fragment-γ distributions suffer attenuation due to the statistical decay in one fragment only. This suggests that there is an additional statistical process which contributes to the substate smearing in fragment-γ distributions, but does not affect the inter-fragment γγ correlations. One possible explanation is that the fragment spins are not mutually parallel, but are tilted out of the plane perpendicular to the fission axis. The results of this investigation were published[4].

b. 32. Relative Cross Sections for Production of ^{253,254}No and Their Detection Efficiencies

(T. L. Khoo, I. Ahmad, M. P. Carpenter, C. N. Davids, A. Heinz, W. F. Henning, R. V. F. Janssens, F. Kondev, T. Lauritsen, C. J. Lister, D. Seweryniak, S. Siem, A. A. Sonzogni, I. Wiedenhöver, P. Reiter,* N. Amzal,† P. A. Butler,† J. Chewter,† J. A. Cizewski,‡ P. T. Greenlees,† K. Helariuta,§ R. D. Herzberg,† G. Jones,† R. Julin,§ H. Kankaanpää,§ W. Korten,¶ M. Leino,§ J. Uusitalo,§ K. Vetter,|| H. Kettunen,§ P. Kuusiniemi,§ and M. Muikku§)

In order to study the nuclear structure of the shell-stabilized nuclei, it is necessary to first know the production cross sections. The relative cross sections for the ^{207,208}Pb(^{48}Ca,2n) ^{253,254}No reactions have been measured with the gas-filled separator RITU at Jyväskylä. By taking a cross section[1] of 2 μb for ^{254}No, the cross section of ^{253}No was determined to be 0.46 μb, with an uncertainty of ~30%. During a subsequent experiment to investigate the structure of ^{253}No with Gammasphere and the Fragment Mass Analyzer (FMA), it was unexpectedly found that the focal-plane detection rates of the two nobelium isotopes was about the same (within 30%). This implies that the FMA detection efficiency of the mass 254 isotope is about a quarter that of the mass 253 isotope. The probable explanation is that there is an isomer, with half life 0.1-3 μs, in ^{254}No. The decays within the FMA, with a flight time of 1.5 μs, would change the charge state, resulting in trajectories that do not land on the focal-plane detectors. On the other hand, rapid re-equilibration of the charge state in the gas of RITU would keep the trajectories of the evaporation residues close to normal, so that there is no loss of detection efficiency. Confirmation of this hypothesis would come from detection of an isomer in ^{254}No, with a lifetime in the μs range, in a future experiment.

These results have implications in the search for superheavy elements, which are likely to have isomers, especially in spherical nuclei with doubly-closed shells. (There are many known isomers near ^{208}Pb.) If the lifetimes are similar to the flight times through vacuum-based separators, such as the FMA and SHIP (at GSI), then the detection efficiencies of superheavy elements would be reduced. This may be a possible explanation for the different results on element 118: three events were detected in the gas-filled BGS separator at LBNL, whereas none were detected at SHIP with comparable integrated beam. Although this is only a speculation at this time, nevertheless one has to seriously take into account the role of isomers in the search for superheavy elements. Our investigations on the nobelium isotopes have emphasized that, to reach the ground state, an evaporation residue has to decay by gamma cascades from excited entry states of moderate spin. Isomers along the cascade have more deleterious consequences if the decay occurs within vacuum separators than in gas-filled separators.

*Ludwig-Maximilians-Universität, Garching, Germany, †University of Liverpool, United Kingdom, ‡Rutgers University, §University of Jyväskylä, Finland, ¶DAPNIA/SPhN, CEA Saclay, France, ||Lawrence Berkeley National Laboratory

[1]M. Leino *et al.*, Eur. Phys. J **A6**, 63 (1999).

b.33. Structure, Fission Barrier and Limits of Stability of ^{253}No

(T. L. Khoo, I. Ahmad, M. P. Carpenter, C. N. Davids, A. Heinz, W. F. Henning, R. V. F. Janssens, F. Kondev, T. Lauritsen, C. J. Lister, D. Seweryniak, S. Siem, A. A. Sonzogni, I. Wiedenhöver, P. Reiter,* N. Amzal,† P. A. Butler,† A. J. Chewter,† J. A. Cizewski,‡ P. T. Greenlees,† K. Helariuta,§ R. D. Herzberg,† G. Jones,† R. Julin,§ H. Kankaanpää,§ W. Korten,¶ M. Leino,§ J. Uusitalo,§ K. Vetter,|| H. Kettunen,§ P. Kuusiniemi,§ and M. Muikku§)

For the heaviest nuclei, including the superheavy nuclei, a large shell-correction energy provides additional binding, thereby creating a fission barrier where none (or a small one) would have existed. Knowledge of the single-particle energies of the heaviest nuclei is important for calculating the shell-correction energy. The most direct information on the single-particle energies comes from an odd nucleus, ^{253}No in this case. The entry distribution gives information on the fission barrier – see Secs. b.30 and b.34. It is interesting to determine the mass dependence of the fission barrier around N = 152 for two reasons. First, the barrier has been found to vary rapidly near N = 152 for lighter nuclei. Second, barriers of a sequence of isotopes provide a good test of theory.

For these reasons, we have performed an experiment to study the levels of ^{253}No, with the use of the ^{207}Pb(^{48}Ca,2n) reaction. In a first experiment with the gas-filled separator RITU at Jyväskylä, the production cross section of ^{253}No was measured as ~ 0.5 μb (by comparing with the known cross section for the ^{208}Pb(^{48}Ca,2n) ^{254}No reaction). This showed that a γ-ray experiment was feasible.

In a subsequent experiment at Argonne, the γ rays were detected with Gammasphere, in coincidence with the FMA, as described in Sec. b.34. It is clear that in ^{253}No the spectrum is dominated by the K X-rays and that the transitions connecting excited states are much weaker relative to the x-rays. (The integrated beam for the odd-nucleus experiment was about three times larger.) The explanation for the difference lies in a huge conversion electron branch for ΔI = 1 intraband transitions in the odd nucleus. Even with a small M1 branching ratio, there is an overwhelmingly large conversion electron yield. Analysis is in progress in an attempt to assign the observed transitions within rotational bands. However, it is likely that many of the observed gamma rays probably represent interband transitions (probably of E1 character, which have smaller conversion coefficients.

We have also measured the two-dimension distribution in detector multiplicity vs. the sum energy. A tail of high fold, with low sum energy, is observed, in ^{253}No, which is absent in ^{254}No. This tail is most likely from dipole transitions. There is nonetheless a significant contribution from stretched E2 transitions in both nuclei. This component suggests smaller sum energy, but a higher fold, in the odd nucleus. Although the analysis is preliminary at this stage, the lower sum energy already points towards a lower fission barrier in ^{253}No than in ^{254}No.

*Ludwig-Maximilians-Universität, Garching, Germany, †University of Liverpool, United Kingdom, ‡Rutgers University, §University of Jyväskylä, Finland, ¶DAPNIA/SPhN, CEA Saclay, France, ||Lawrence Berkeley National Laboratory

b.34. Entry Distribution, Fission Barrier, Formation Mechanism and Structure of $^{254}_{102}$No

(P. Reiter, T. L. Khoo, I. Ahmad, M. P. Carpenter, C. N. Davids, J. P. Greene, A. Heinz, W. F. Henning, R. V. F. Janssens, F. G. Kondev, T. Lauritsen, C. J. Lister, D. Seweryniak, A. Sonzogni, J. Uusitalo, I. Wiedenhöver, N. Amzal,* P. Bhattacharyya,† P. A. Butler,* J. Chewter,* J. A. Cizewski,‡ K. Y. Ding,§ N. Fotiades,§ P. T. Greenlees,* R.- D. Herzberg,* G. D. Jones,* W. Korten,¶ M. Leino,‖ S. Siem,** and K. A. Vetter††)

The heaviest nuclei, with Z > 100, are at the limit of Coulomb instability. They would be unstable against spontaneous fission but for a large shell-correction energy, which leads to additional binding and creates a sizeable fission barrier of up to 8 MeV. The existence of these very heavy elements is a striking manifestation of shell structure in nuclei, and arises from the identical mechanism responsible for the proposed stability of an "island" of superheavy elements around Z = 114, N = 184. Recent reports[1,2] of the detection of elements 114 and 116, 118 provide support for the stability of superheavy elements. Shell-stabilized nuclei could be different from ordinary nuclei, where the binding is largely derived from the liquid-drop energy. However, there is little experimental information on the properties of shell-stabilized nuclei. Their high-spin behavior, e.g. the variation with spin of the moment of inertia and of the fission barrier, would provide information about the angular momentum dependence of the shell energy, which is not only interesting in its own right, but also provides a new test of theories that calculate the properties of superheavy elements. Since the heaviest nuclei are only weakly bound in the ground state, it is interesting to determine the limiting spin and excitation energy that they can sustain. The limits of stability in spin and excitation energy are governed by the fission barrier. Knowledge of the barrier is also essential for understanding the production mechanism of superheavy nuclei.

In lighter actinide nuclei the fission barrier parameters are most directly obtained in nucleon-transfer or neutron-capture reactions from the variation of the fission probability as a function of excitation energy E*. Since no suitable target exists, this method is not applicable to the heaviest elements. We propose a new method that may be used to deduce the fission barrier Bf(I) and also its variation with spin I. The method is based on a measurement of the entry distribution, which represent the distribution of initial states from which gamma decay to the ground state start. Hence, the entry distribution reflect states where gamma emission successfully compete with fission and the distribution is generally located below the fission barrier.

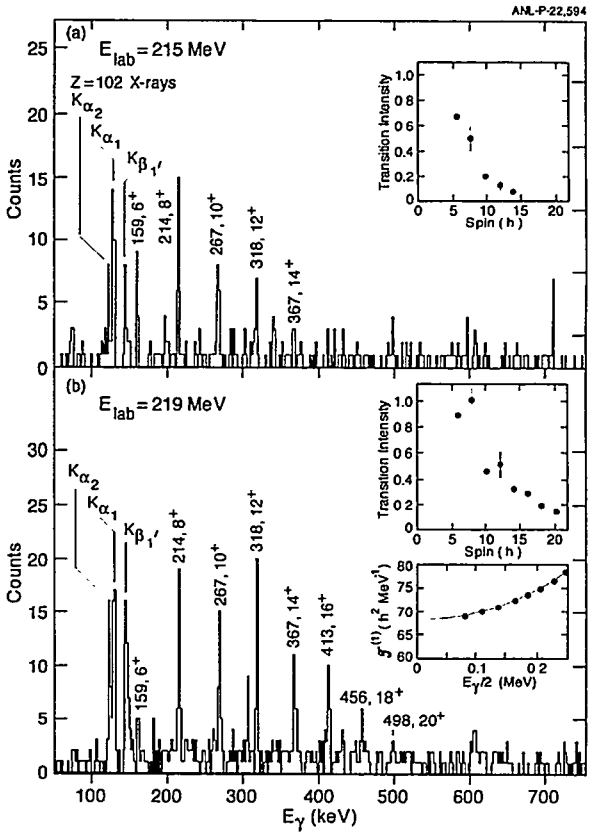

Fig. I-42. ^{254}No γ spectra at beam energies of (a) 215 MeV and (b) 219 MeV. The gsb transitions are labeled by their energies (in keV) and initial spins. Note the large increase in high-spin population at the higher beam energy, which is also seen in the insets that show relative intensities (with some typical statistical errors). A second inset in Fig. I-42(b) shows the moment of inertia $\mathfrak{I}$ (I) vs. $E_{\gamma/2}$.

We have measured the entry distributions of ^{254}No, which is an example of a shell-stabilized nucleus. The reaction ^{208}Pb(^{48}Ca,2n)^{254}No was used to populate states in ^{254}No. Gammasphere was used to measure not only the γ rays with high resolution, but also the γ-ray multiplicity and sum energy. The γ rays from ^{254}No nuclei were extracted from a background due to fission, which was > 10^4 times more intense, by requiring coincidences with evaporation residues. The latter were unambiguously identified with the Argonne

Fragment Mass Analyzer (FMA). To minimize deterioration of the ^{208}Pb targets (~ 0.5 mg/cm^2), they were mounted on a rotating wheel and the beam was wobbled vertically ±2.5 mm across the target with a magnetic steerer. Beams with energies of 215 MeV and 219 MeV and intensities of 9 pnA to 12 pnA were provided by ATLAS. The compound nucleus (CN) excitation energies (at mid target) were 19.3 MeV and 22.7 MeV, respectively. The γ spectra obtained at 215 MeV, which we have previously published[3], and at 219 MeV are compared in Fig. I-42. Transitions from higher-spin members of the ground state band (gsb) are clearly enhanced at the higher bombarding energy and the gsb could be extended up to spin 20$^+$ [Fig. I-42(b)]. The relative transition intensities, given in the insets, show that the population has saturated by spin 8 at the higher beam energy.

In order to determine the initial angular momentum and excitation energy of the ^{254}No residues, we measured the number of detector modules that fired and the total energy emitted by γ radiation. Based on measured response functions, a two-dimensional Monte Carlo unfolding procedure transformed the two-dimensional distribution of detector multiplicity vs. γ sum energy into a distribution of γ multiplicity vs. excitation energy. (To correct for the effect of the trigger requirement of two Compton suppressed Ge events, the efficiency dependence on multiplicity was taken into account.) The initial spin of the evaporation residue is deduced from the γ multiplicity. For high-Z nuclei, the internal conversion coefficients can be very large for low-energy transitions and estimates for electron multiplicities are made from the measured properties of the gsb.

The entry distributions, which represent the starting point for γ decay and formation of ^{254}No, are shown in Fig. I-43 for the two beam energies. The one-dimensional spin and excitation energy distributions are also given. It is evident that a small increase in beam energy leads to noticeably higher initial spins and excitation energies. The entry distribution at the lower beam energy reveals that it is the maximum allowable energy E^*_{max} after neutron emission that imposes a 16 $\hbar$ limit on the angular momentum and not the fission barrier. At the higher beam energy, states up to spin 22 $\hbar$ and E* = 8.5 MeV (up to 6 MeV above the yrast line) are populated in the entry distribution, showing that the nucleus clearly can survive against fission up to these limits. At the higher beam energy, the entry distribution no longer extends to E^*_{max}, perhaps an indication of fission competition.

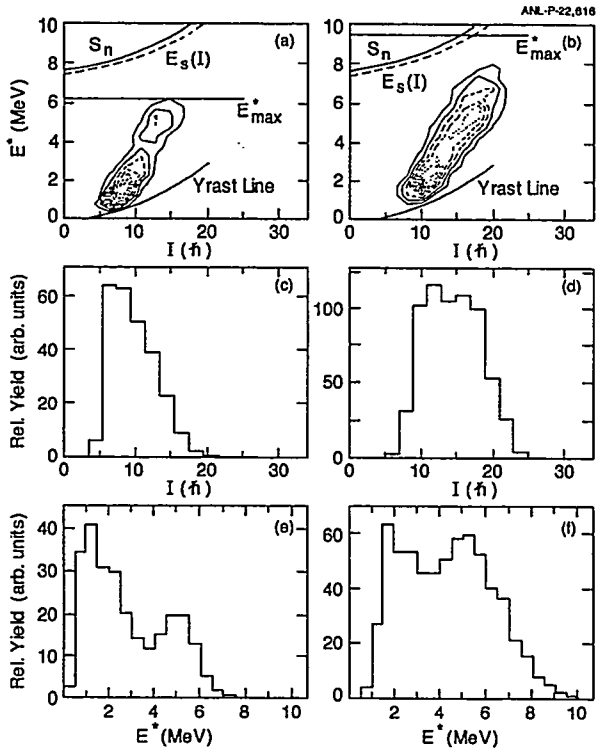

Fig. I-43. Contour plots (a,b) of the entry distributions in spin and excitation energy and their projections at E_{Lab} = 215 (left panels) and 219 (right panels) MeV. The measured yrast line, the neutron-separation energy S_n, a theoretical saddle-point energy $E_s(I)$ and the maximum allowable energy, $E^*_{max} = E_{CN} - S_{n1} - S_{n2}$, in ^{254}No are indicated. The distributions in spin (c,d) and excitation energy (e,f) are also shown.

Gamma decay to the ground state originates from the entry distribution, implying successful γ competition over fission. The highest-energy point of the entry distribution for each spin lies below the saddle energy, $E_s(I) = E_{yrast}(I) + Bf(I)$, (or within 0.5 MeV), so that a lower bound on Bf(I) can be obtained. Only a lower bound on Bf can be deduced since the decreasing population with increasing excitation energy could, in principle, also be due to a reduced cross section after neutron emission. Energy distributions for individual spin bins, projected from the entry distributions in Fig. I-43(a,b), show that the half-maximum points correspond to 5 MeV above the yrast line for I ≥ 12. This suggests that, even at high spin, Bf > 5 MeV, a surprisingly large value for a nucleus as fissile as ^{254}No.

There are no calculations of the shell-correction energy at higher spin, but if it were to remain constant with spin, the saddle-point energy, Es(I), would lie along the dashed line in Fig. I-43. The slight decrease from the

solid line denoting the neutron separation energy is due to the diminution of the liquid-drop term.

Our data provide new information important for understanding the synthesis of superheavy nuclei. Previously, the only constraints on theory have come from excitation function measurements of ground-state cross sections. The present results reveal that high partial waves contribute to the formation of evaporation residues, as predicted by Smolanczuk[4]. The fission barrier governs the survival of the compound nucleus, as it evaporates neutrons and γ rays in competition with fission decay. Fusion-evaporation calculations suggest that a barrier of 5 MeV would lead to a much larger cross section for production of ^{254}No than is observed[5]. This suggests either that there is a hindrance in the formation of the compound nucleus or that the fission barrier damps rapidly with excitation energy.

An unexpected feature of our entry distribution is the sharp tilt angle with respect to the yrast line. This is due, at least in part, to the small excitation energy of the low-spin entry states, which appears to be a distinct component [see Fig. I-43 (a,b,e,f)]. This feature cannot be easily explained by a simple statistical model. At low excitation energy, the level density is small, so that states near the yrast line should have only small population. The deviation of the entry distribution from the line representing E^*_{max} gives the energy removed by the 2 neutrons. Hence, evaporation residues with low partial waves appear to be associated with unusually energetic neutrons. On the other hand, at higher spin ($I \geq 14$) the high excitation energy above the yrast line is more normal. Hence, there is a hint of at least two mechanisms in the formation of superheavy nuclei: a normal statistical one responsible for high-spin formation and another one with emission of higher energy (perhaps pre-equilibrium) neutrons, which is important at lower spins.

In summary, we have measured the entry distribution for a shell-stabilized nucleus. The limiting angular momentum and excitation energy are deduced for excited states in ^{254}No after the ^{208}Pb(^{48}Ca,2n) reaction. The data provide direct information on the fission barrier and on the shell-correction energy, based on a novel experimental technique to determine a lower bound of the barrier height. In the synthesis of very heavy nuclei, the entry distributions suggest that high partial waves contribute and that there may be more than one reaction mechanism. A paper on this work has been submitted to Physical Review Letters.

---

*University of Liverpool, United Kingdom, †Purdue University, ‡Argonne National Laboratory and Rutgers University, §Rutgers University, ¶DAPNIA/SPhN, CEA Saclay, France, || Ludwig-Maximilians-Universität, Garching, Germany, **Argonne National Laboratory and University of Oslo, Norway, ††Lawrence Berkeley National Laboratory

[1]Yu. Ts. Oganessian *et al.*, Nature **400**, 242 (1999); Phys. Rev. Lett. **83**, 3154 (1999).
[2]V. Ninov *et al.*, Phys. Rev. Lett. **83**, 1104 (1999).
[3]P. Reiter *et al.*, Phys. Rev. Lett. **82**, 509 (1999).
[4]R. Smolanczuk, Phys. Rev. C **59**, 2634 (1999).
[5]H. W. Gäggeler *et al.*, Nucl. Phys. **A502**, 561c (1989).

b.35. Jyväskylä Experiment on Excited States in ^{254}No

(T. L. Khoo, M. Leino,* F. P. Hessberger,† R.-D. Herzberg,‡ Y. Le Coz,§ F. Becker,§ P.A. Butler,‡ J. Chewter,‡ J. F. C. Cocks,* O. Dorvaux,* K. Eskola,¶ J. Gerl,† P. T. Greenlees,‡ K. Helariutta,* M. Houry,§ G. D. Jones,‡ P. M. Jones,* R. Julin,* S. Juutinen,* H. Kankaanpää,* H. Kettunen,* W. Korten,§ P. Kuusiniemi,* R. Lucas,§ M. Muikku,* P. Nieminen,* R. D. Page,‡ P. Rahkila,* P. Reiter,‖ A. Savelius,* Ch. Schlegel,† Ch. Theisen,§ W. H. Trzaska,* and H.-J. Wollersheim†)

The nucleus ^{254}No is one of the heaviest for which there is a possibility of investigating the excited states. The motivation for studying it has already been discussed above (see Sec. b.34). An experiment was conducted at Jyväskylä, which employed the SARI detector array together with the gas-filled recoil separator RITU to study the structure of ^{254}No. The production reaction was ^{48}Ca + ^{208}Pb. SARI consisted of four unshielded, segmented clover detectors placed at 50 degrees relative to the beam direction. Stationary ^{208}Pb targets of 250-700 μg/cm^2 thickness were used. The beam current was 10 pnA. An excitation function measurement found the maximum cross section of ~2 μb at a beam energy of 216 MeV (two-thirds into the target), corresponding to 21 MeV excitation in the compound system. The method of recoil decay tagging (RDT) was used to identify in-beam gamma rays observed in the SARI detectors, on the basis of the 8.09 MeV alpha particles emitted by ^{254}No.

The same transitions are observed in the RDT spectrum but with lower intensity due to the loss of escaping alpha particles. Ground state band transitions are observed up to 414 keV. The results confirm the transitions observed in the Argonne experiment and extend the ground band by one transition ($16^+ - 14^+$).

This work has been published in Euro. Phys. J.

*University of Jyväskylä, Finland, †GSI, Darmstadt, Germany, ‡University Liverpool, United Kingdom, §DAPNIA/SPhN CEA-Saclay, France, ¶University of Helsinki, Finland, ‖Ludwig-Maximilians University, Munich, Germany

b.36. Spectroscopic Studies Beyond N = 152 Neutron Gap: Decay of ^{255}Md and ^{256}Md

(I. Ahmad, R. R. Chasman, and P. R. Fields*)

Energies of single-particle states in the heaviest nuclei accessible are needed to understand the structure of superheavy elements. In the early seventies we produced Md isotopes by the irradiation of ^{253}Es with 35-45 MeV alpha particles from the Argonne 152 cm cyclotron. The recoiling Md atoms were stopped in He gas and were removed by a gas jet system. Alpha, gamma and alpha-gamma coincidence spectra of purified Md isotopes were measured by Si and Ge detectors. Gamma rays were assigned to ^{255}Md and ^{256}Md isotopes on the basis of their measured half-lives. The ^{256}Md gamma rays could not be placed in a level scheme because the $2^+ \rightarrow 0^+$ transition energy in ^{256}Fm ground state band was not known. The publication of the levels in ^{256}Fm by Hall et al.[1] provided us the necessary information to interpret our data. In the case of ^{255}Md, two gamma rays of energy453.1 and 405.5 keV were observed in coincidence with ^{255}Md alpha particles.

[1]H. L. Hall *et al.*, Phys. Rev. C **39**, 1866 (1989).
[2]I. Ahmad *et al.*, Phys. Rev. C **17**, 2163 (1978).
[3]I. Ahmad *et al.*, Phys. Rev. C **61**, 044301 (2000).
*deceased

The same transitions were also seen in the electron capture decay of ^{251}Fm and were interpreted as transitions deexciting the 7/2-[514] single particle state at 460.4 keV. Since the 460.4 keV level in ^{251}Es is populated by the favored alpha decay, the ground state of 255Md is established as the 7/2-[514]. This is the only nucleus in which a definite identification of the 7/2-[514] orbital has been made.

The ^{256}Md nucleus is found to populate low spin states in ^{256}Fm. The 2+ vibrational band previously observed by Hall et al.[1] has been identified in the ^{256}Md decay. In addition, four other levels have been identified which are given spin-parity assignments of 1+, 2+, 1-, 2-. The level scheme of ^{256}Fm is shown in Fig. I-45. These levels are interpreted as the nn{7/2+[613;9/2+[615]}1+ and pp{7/2+{633];7/2-[514]}0- bands. The results of this investigation were published.[3]

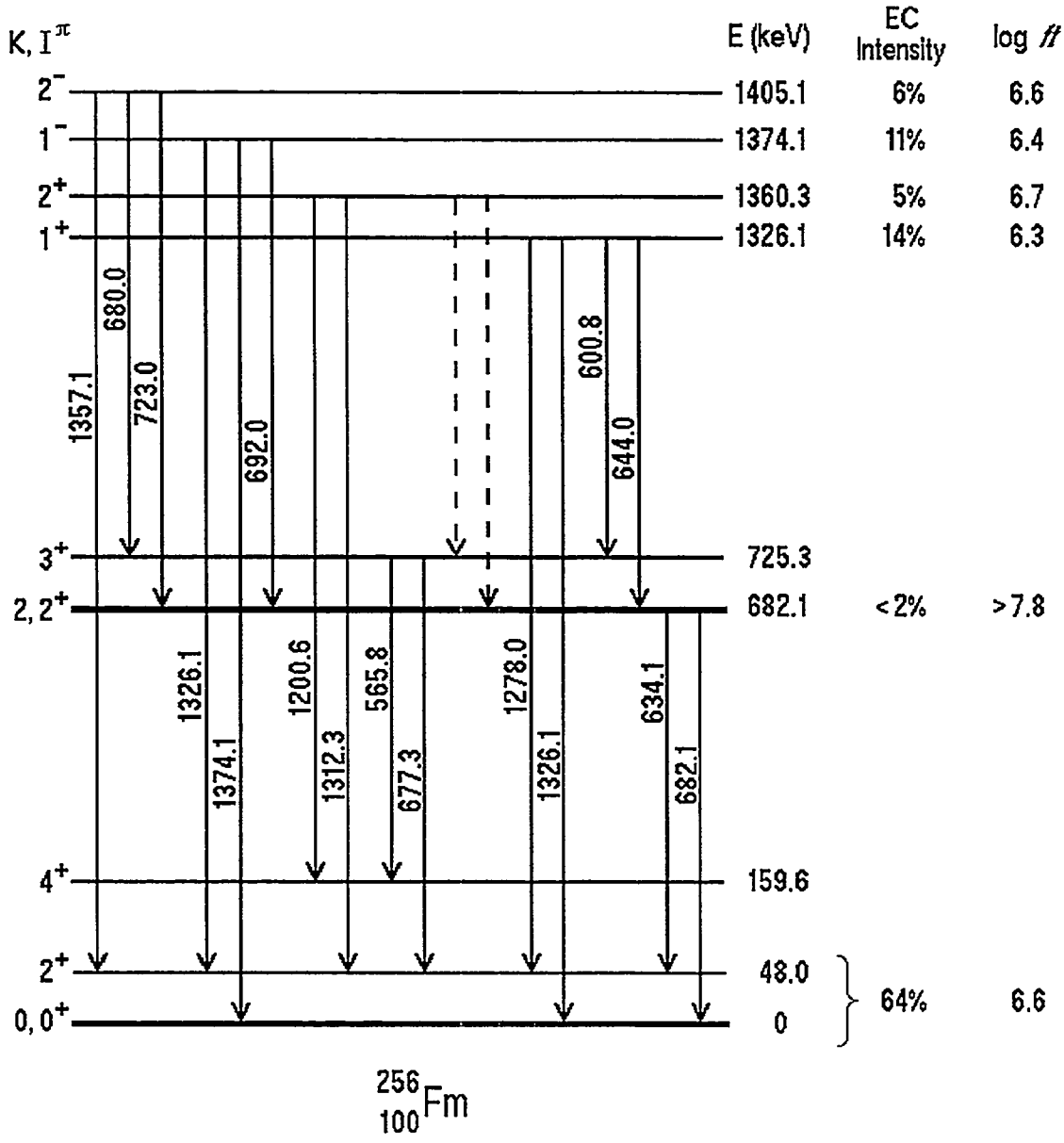

Fig. I-45. Electron capture decay scheme of ^{256}Md deduced from the results of the present investigation. Dashed lines represent transitions expected but whose energies overlap with the stronger transitions.

C. SUPERDEFORMATION AND OTHER SPECTROSCOPY TOPICS

Studies of the properties of nuclei under extreme conditions, and in particular, of superdeformed nuclei remain a topic of intense investigation within the Division. Over the last few years, research has emphasized the properties associated with the decay out of superdeformed bands, and searches for hyperdeformation. Other efforts utilizing gamma-ray spectroscopy techniques are also summarized here.

c.1. A Superdeformed Band in the N = Z Nucleus ^{36}Ar

(R. V. F. Janssens, M. P. Carpenter, D. Seweryniak, C. E. Svensson,* A. O. Macchiavelli,* A. Juodagalvis,† C. Baktash,‡ R. M. Clark,* M. Cromaz,* M. A. Deleplanque,* R. M. Diamond,* P. Fallon,* M. Furlotti,§ A. Galindo-Uribarri,‡ G. J. Lane,* I. Y. Lee,* M. Lipoglavsek,‡ S. D. Paul,‡ D. C. Radford,‡ D. G. Sarantites,§ F. S. Stephens,* V. Tomov,§ K. Vetter,* D. Ward,* C. H. Yu,‡ I. Ragnarsson,† and S. Aberg†)

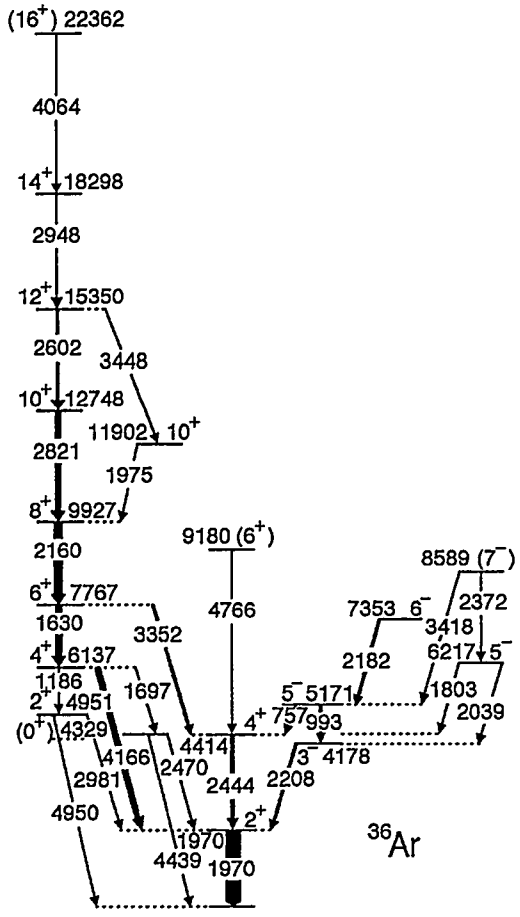

Fig. I-46. Partial decay scheme for ^{36}Ar showing the superdeformed band (left). Transition and level energies are given to the nearest keV.

With the Gammasphere spectrometer and the microball array, a superdeformed band has been identified in the N = Z nucleus ^{36}Ar following the ^{28}Si(^{16}O, 2α) reaction at 75 MeV. The band is firmly linked to known low-spin states in this nucleus: the relevant level scheme is shown in Fig. I-46. The band is observed to its presumed termination (spin 16). Deformed mean field and spherical shell model calculations lead to a configuration assignment in which four fp-shell orbitals are occupied. This band involves the cross-shell correlations typical of rotational motion in heavier nuclei, while the number of active particles remains sufficiently small to be confronted with the spherical shell model. The latter calculations support the $(fp)^4$ assignment, but suggest that the entire sd-shell is also essential for the full description of this band. Hence, ^{36}Ar provides an ideal case to investigate the microscopic origin of collective rotation in nuclei. A paper reporting these results has recently been submitted for publication[1]. In addition, an experiment to determine the lifetimes of the superdeformed states, to deduce the associated deformation (predicted to be $\varepsilon_2 \sim 0.4$) and to characterize the transitions linking the new cascade to the low-lying level structure has also been performed recently. The analysis of the latter experiment is underway.

*Lawrence Berkeley National Laboratory, †Lund Institute of Technology, Sweden, ‡Oak Ridge National Laboratory, §Washington University

[1] C. E. Svensson *et al.*, submitted to Phys. Rev. Lett.

c.2. Decay Out of the Doubly Magic Superdeformed Band in the N = Z Nucleus ^{60}Zn

(M. P. Carpenter, G. Hackman, R. V. F. Janssens, P. Reiter, D. Seweryniak, C. E. Svensson,* D. Rudolph,† C. Baktash,‡ M. A. Bentley,§ J. A. Cameron,* M. Devlin,¶ J. Eberth,|| S. Flibotte,* A. Galindo-Uribarri,‡ D. S. Haslip,* D. R. LaFosse,¶ T. J. Lampman,* I. Y. Lee,** F. Lerma,¶ A. O. Macchiavelli,** J. M. Nieminen,* S. D. Paul,‡ D. C. Radford,‡ L. L. Riedinger,†† D. G. Sarantites,¶ B. Schaly,* O. Thelen,|| H. G. Thomas,|| J. C. Waddington,* D. Ward,** W. Weintraub,†† J. N. Wilson,¶ C. H. Yu,‡ A. V. Afanasjev,†‡‡ and I. Ragnarsson†)

Investigations throughout the chart of the nuclides have led to the observation of many superdeformed (SD) rotational bands in the A ~ 190, 150, 80 and 60 nuclei. Although it has been relatively straightforward to observe the long cascades of rotational transitions in these bands with modern γ-ray arrays, discrete transitions connecting SD bands to states in the first well have been more difficult to identify. As a result, the excitation energy, spin, and parity of levels in these superdeformed bands are unknown. Recently, significant progress has been made in studying the decay out of SD bands in the A ~ 190 region where the observation of linking transitions in ^{194}Hg[1] and ^{194}Pb[2] has led to definite quantum number assignments for SD states in these nuclei. In addition, a consistent description of the decay out process in A ~ 190 SD bands in terms of a statistical process governed by the weak mixing of SD states with a ``sea" of hot ND states has been developed[3]. The nature of the decay out process for SD bands in other mass regions remains an open question.

Recently, an SD band in ^{60}Zn built on the SD shell gaps at N,Z = 30 has been identified for the first time from data taken with the Gammasphere array. Two different experiments were conducted. In the first experiment, a 125-MeV ^{28}Si beam from the 88-Inch Cyclotron at Lawrence Berkeley National Laboratory accelerated onto a ^{40}Ca produced ^{60}Zn via the 2α channel. In the second experiment, a 134-MeV ^{32}S beam provided by the ATLAS facility at Argonne impinging onto a ^{40}Ca target produced ^{60}Zn via the 3α channel. In both experiments, evaporated charged particles were detected with the Microball, a 4π array of CsI scintillators, in order to isolate weak reaction channels.

From the analysis of these data, a previously unknown rotational band was found consisting of 11 transitions. The quadrupole moment, Q_t of the band was measured to be 2.75 ± 0.45 *e*b. The corresponding quadrupole deformation of 0.47 ± 0.07 confirms the SD character of the band. Of equal interest is the observation of linking transitions connecting the SD band to the yrast line, thus establishing the spins, parities and excitation energies of the SD states. Unlike the A = 190 region where linking transitions are found to have dipole character, these transitions in ^{60}Zn are dominated by ΔI = 2 E2 transitions, indicating that the decay-out process in ^{60}Zn differs substantially from that observed in the A ~ 190 region.

A paper reporting the results from these two experiments was published this past year in Physical Review Letters[4].

*McMaster University, Hamilton, Ontario, †Lund University, Sweden, ‡Oak Ridge National Laboratory, §Staffordshire University, United Kingdom, ¶Washington University, ||University of Cologne, Germany, **Lawrence Berkeley National Laboratory, ††University of Tennessee, ‡‡Technical University of Münich, Germany

[1] T. L. Khoo *et al.*, Phys. Rev. Lett. **79**, 1233 (1996); G. Hackman *et al.*, Phys. Rev. Lett. **79**, 4100 (1997).
[2] A. Lopez-Martens *et al.*, Phys. Lett. **B380**, 18 (1996).
[3] R. G. Henry *et al.*, Phys. Rev. Lett. **73**, 777 (1994).
[4] C. E. Svensson *et al.*, Phys. Lett. **82**, 3400 (1999).

c.3. Level Structure of ^{94,95,96}Tc at High Spins and Shell-Model Calculations

(R. V. F. Janssens, M. P. Carpenter, T. L. Khoo, T. Lauritsen, S. S. Ghugre,* B. Kharraja,* U. Garg,* W. F. Mueller,† W. Reviol,† L. L. Riedinger,† and R. Kaczarowski‡)

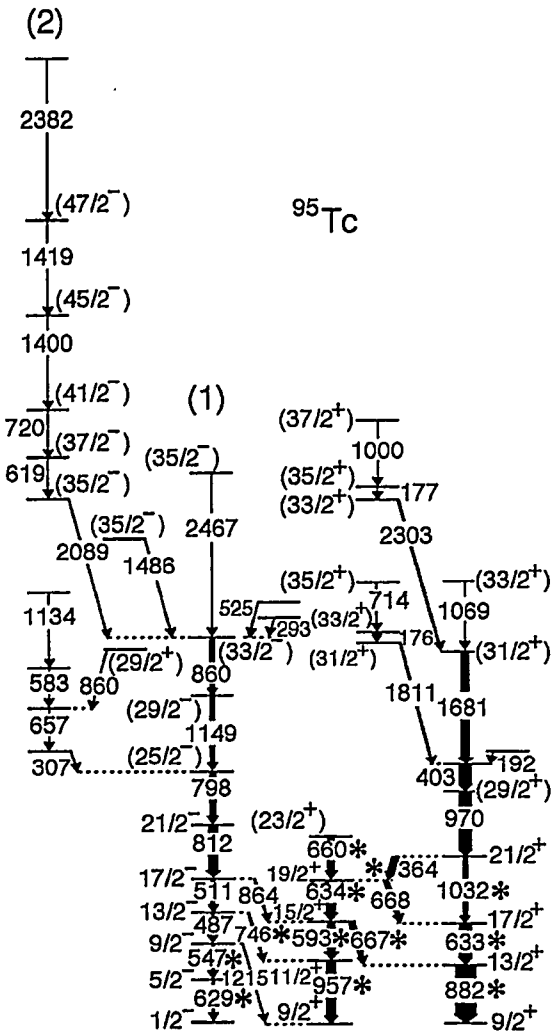

*Fig. I-47. Level scheme for ^{95}Tc as established from the present study. The previously-known transitions are indicated by a * sign.*

High spin states in the ^{94,95,96}Tc (N = 51, 52 and 53) nuclei have been investigated using the ^{65}Cu + ^{36}S reaction at a beam energy of 142 MeV with the Gammasphere spectrometer. More than 60 new transitions have been identified and placed in their respective level schemes, which now extend up to spin ~ 22 $\hbar$ and excitation energies Ex ~ 12 MeV. The ^{95}Tc scheme is given as an example in Fig. I-47. Spherical shell-model calculations have been performed using different model spaces. A restricted model space, using ^{88}Sr as the core and the proton (p1/2, g9/2) and neutron (d5/2, s1/2) valence orbitals, reproduces the experimental excitation energies up to spin 14 $\hbar$. The higher-angular-momentum states are dominated by the excitation of a g9/2 neutron across the N = 50 magic core, as indicated by large-basis shell model calculations. A paper summarizing these results has recently been published[1].

*University of Notre Dame, †University of Tennessee, ‡Soltan Institute for Nuclear Studies, Swierk, Poland

[1] S. S. Ghugre *et al.*, Phys. Rev. C **61**, 024302 (2000).

c.4. Recoil-Distance Lifetime Measurements in ^{96,97,98}Ru: Search for Onset of Collectivity Above the N = 50 Shell Closure

(R. V. F. Janssens, I. Ahmad, M. P. Carpenter, T. L. Khoo, T. Lauritsen, B. Kharraja,* S. S. Ghugre,* U. Garg,* H. Jin,* W. F. Mueller,† W. Reviol,† L. L. Riedinger,† R. Kaczarowski,‡ E. Ruchowska,‡ S. Fischer,§ W. C. Ma,¶ and I. M. Govil‖)

Lifetimes of high-spin states in the N = 52-54 Ru nuclei have been investigated using the recoil-distance Doppler-shift technique for low- and moderate-spin transitions. The data were collected in coincidence mode at the Argonne-Notre Dame BGO gamma-ray facility using ^{65}Cu(^{36}S,p2-4n) reactions with 142 MeV beams from ATLAS. Lifetimes were obtained for both the positive and negative parity states in the even Ru isotopes. In the odd isotope, lifetimes could only be measured along the yrast line. The main purpose of the experiment was to investigate whether the observed E2 "band-like" cascades seen in these nuclei[1] are of collective nature. The deduced transition probabilities B(E2) and B(M1) do not exhibit the enhancement that would be expected for collective behavior. Rather, good agreement with shell model calculations was found. The data have recently been published[2].

*University of Notre Dame, †University of Tennessee, ‡Soltan Institute for Nuclear Studies, Swierk, Poland, §DePaul University, ¶Mississippi State University, ‖Panjab University, Chandigarh, India

[1]B. Kharraja *et al.*, Phys. Rev. C **57**, 83 (1998).
[2]B. Kharraja *et al.*, Phys. Rev. C **61**, 024301 (2000).

c.5. Search for Hyper-Deformation in the A = 150 Region

(T. Lauritsen, I. Ahmad, M. P. Carpenter, C. Davids, R. V. F. Janssens, T. L. Khoo, C. J. Lister, P. Reiter, A. A. Sonzogni, S. Siem, J. Uusitalo, I. L. Wiedenhöver, A. Korichi,* H. Amro,† S. M. Fischer,§ F. Hannachi,* and A. Lopez-Martens‡)

Several attempts have been made to experimentally verify the existence of a hyper-deformed (HD) minimum in the nuclear potential energy surface. Such a minimum, created by shell effects and stabilized by rapid rotation, has been predicted by a number of theorists[1,2], and is calculated to become yrast at very high spins (> 70 $\hbar$).

Searches for the discrete band transitions emitted while the nucleus is trapped and cold in this minimum have been unsuccessful[3-5]. It is likely that the nucleus never gets cold enough over a sufficiently long time period for a cascade of closely spaced discrete gamma rays to be emitted. The only evidence that we therefore may get for the existence of the HD minimum is from the gamma rays emitted while the nucleus is relatively hot in this minimum. In that case, because the level density is high and there are many bands, a quasicontinuum (QC) of gamma rays are emitted which will exhibit characteristic ridges in a gamma-gamma matrix or planes in a gamma-gamma-gamma cube. The first hints of evidence for HD were indeed found in QC spectra (of ^{153}Dy[6-7]).

*CSNSM, Orsay, France, †North Carolina State University, ‡IReS, Strasbourg, France, §University of Pennsylvania

[1]Dudeck *et al.*, Phys. Rev. B **211**, 252 (1988).
[2]Chasman, Phys. Lett. **B302**, 134 (1993).
[3]LaFosse *et al.*, Phys. Rev. C **54**, 1585 (1996).
[4]LaFosse *et al.*, Phys. Rev. Lett. **74**, 5186 (1996).
[5]J. N. Wilson *et al.*, Phys. Rev. C **56**, 2502 (1997).
[6]Galindo-Uribarri *et al.*, Phys. Rev. Lett. **71**, 231 (1993).
[7]Lunardi *et al.*, Proceedings from the Conference on Nuclear Structure at the Limits, ANL, July 22-26, 1996, p. 29 and Lunardi *et al.*, Heavy Ion Physics **6**, 241 (1997).

A new search for hyper-deformation was performed with Gammasphere (GS) coupled to the Fragment Mass Analyzer (FMA). ^{80}Se at 340 MeV impinged on two stacked ^{76}Ge targets. The 4n reaction channels populated ^{152}Dy at very high spins (~70-80 $\hbar$). The FMA coupled to Gammasphere (GS) provides a unique opportunity to optimize the experimental conditions at which the weak HD signal in a strong channel can be extracted. With the FMA it is possible to study reaction channels at much higher spins than usual -- and still get clean spectra -- by populating the channels at much higher bombarding energies than their optimum. The strong competition from fission and other reaction channels at these extreme spins can be overcome by the mass gating of the FMA!

The number of gamma cascades that pass through the HD minimum is probably very small. Thus, one must think of ways to extract the very weak signal from these cascades from the overwhelming number of gamma cascades that do not pass through the HD minimum. One way is to selectively gate on very high spin and relatively low energy entry points (H,K) of a reaction channel. The HD minimum will only be low in energy at very high spins, thus, such a gating should further enhance the HD signal. GS without the heavy-mets mounted in front of the BGO Compton shields is a ≈72% efficient calorimeter. This allows us to efficiently place gates on the sum-energy and multiplicity (~spin) at which the residues are created.

In essence, the performed experiment was tailored to use the Fragment Mass Analyzer (FMA) to cleanly tag on the residues that are populated at high spins; but against all odds survived fission!

The data from this experiment has now been partially analyzed. Figures I-48 and I-49 show diagonal cuts of mass gated (A = 152) gamma-gamma matrices -- with cut parameters identical to those used in Ref. 6. As can be seen, no HD signal is observed. Furthermore, the SD ridges are clearly seen in Fig. I-49 - whereas that is not the case in Ref. 6. This data analysis is still ongoing and the data in Figs. I-48 and I-49 were not HK gated. Preliminary analysis where this energy and spin (HK) gating is used has so far not produced hints of the reported[6] 30 keV HD ridges.

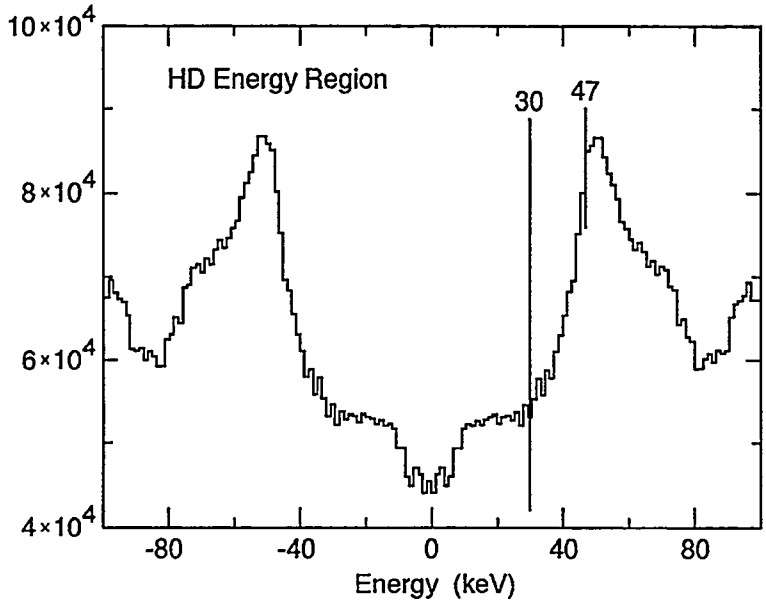

Fig. I-48. Diagonal projection of a gamma-gamma matrix with mass gated (A = 152) data from this experiment. The projection parameters are the same as in Ref. 6 panel a (i.e., the HD region of [6]).

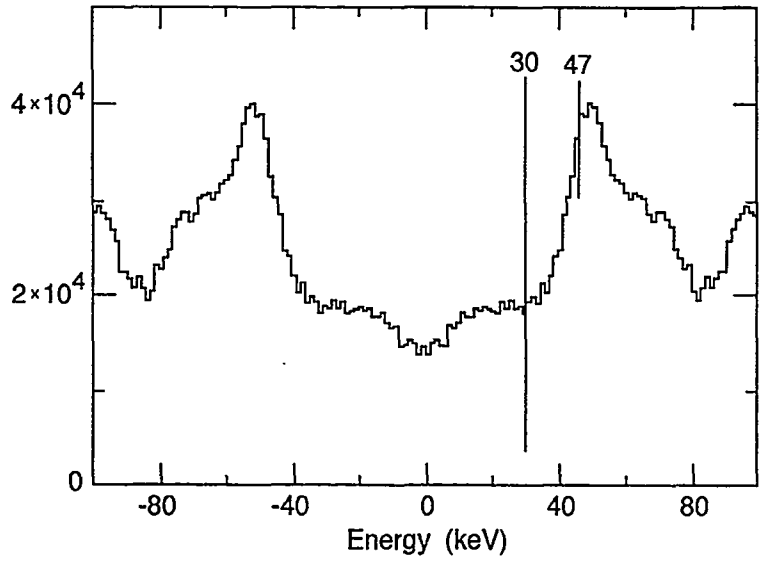

Fig. I-49. Diagonal projection of a gamma-gamma matrix with mass gated (A = 152) data from this experiment. The projection parameters are the same as in Ref. 6 panel b (i.e., the SD region of [6]).

c.6. Quasicontinuum and Discrete Gamma Rays Linking Superdeformed Bands in ^{151,152}Dy

(T. Lauritsen, I. Ahmad, M. P. Carpenter, C. Davids, J. P. Greene, R. V. F. Janssens, T. L. Khoo, F. G. Kondev, C. J. Lister, S. Siem, A. Sonzogni, R. C. Vondrasek, I. L. Wiedenhöver, A. Korichi,* H. Amro,† T. Døssing,§ F. Hannachi,* B. Herskind,§ and A. Lopez-Martens‡)

With the possible exception of ^{149}Gd[1], no firm transitions have been found which link the decaying superdeformed (SD) states to the normal (ND) states in the A = 150 mass region. Thus, the spins and excitation energies of the many SD bands in this mass region have not been experimentally determined. A preliminary analysis, based on data from a Gammasphere (GS) experiment in 1998, of (QC) gamma rays in coincidence with the yrast SD bands in ^{151,152}Dy has been performed. The analysis reveals that the spectra of decay QC gamma rays are very different from what is seen in the A = 190 region! No high energy statistical component is seen; rather an excess strength at low energy is observed, see Fig. I-50. This could indicate that the decay of SD bands in the A = 150 region is different from the decay of SD bands the A = 190 region.

Due to the scope and goals of the experiment in 1998, the data set was marginal for the extraction of the QC in coincidence with the SD bands. Thus, a new long run, optimized for the QC analysis, was proposed and accepted by the ATLAS PAC. ^{80}Se at 320 MeV impinged on two stacked ^{76}Ge targets mounted on the Gammasphere target wheel. The 5n,4n reaction channels populated ^{151,152}Dy at optimum energies to populate the SD bands in these residues. The large area fragile stacked germanium targets for the target wheel required significant target developments. Due to the almost symmetric reaction, the transmission of the ^{151,152}Dy were detected in the FMA with as high efficiency as possible. The new analysis of the QC from this dedicated experiment is still ongoing.

*CSNSM, Orsay, France, †North Carolina State University, ‡IReS, Strasbourg, France, §The Niels Bohr Institute, Copenhagen, Denmark

[1]Ch. Finck, Phys. Lett. **B467**, 15 (1999).

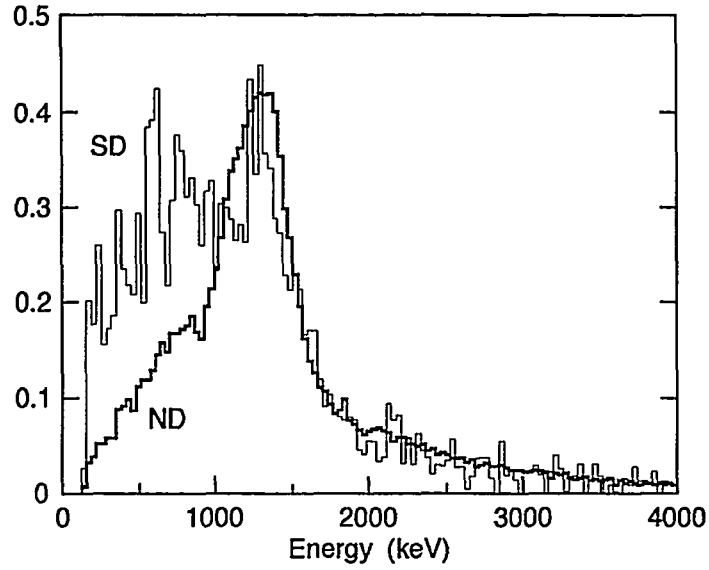

Fig. I-50. Quasicontinuum when double gates are place on ND gamma rays (thick line) and when triple gates are place on SD gamma rays (thin line). Both spectra have been corrected for detector efficiency, corrected for summing effects, unfolded and normalized to the same number of gamma cascades.

However, the new dataset has already revealed a number of high energy one-step primary transitions linking the yrast SD band in ^{152}Dy to the ND states the band decays into! Figure I-51 shows some of these lines. In particular, the 4014 keV line is promising. Figure I-52 show spectra where gates have been placed on the two strongest one-step primary transitions, 4014 and 2895, and any combination of two SD lines. It is clearly seen that the spectrum gated on the 4014 one-step primary transitions does not include the 647 keV line, establishing that the decay of the SD band via this line is from the level feed by the SD 693 line and it feeds into the level feed by the 221 ND transition. However, from this dataset it probably cannot be determined if the decay proceeds via any intermediate states. The 2895 keV transition most likely comes from the SD level feed by the 647 keV line and eventually feeds into the ND level feed by the 541 keV line. The 2895 keV transition is not as clean as the 4014 keV line since it has a larger background. The intensities of the 4014 keV and 2895 keV one-step primary transitions are only 0.4% and 0.3%, respectively, of the intensity of the SD band.

The analysis of the one-step primary is still ongoing; but it is clear that it will be necessary to gather more statistics to finally be able to link the yrast SD band in ^{152}Dy. A new, much longer run will be proposed to the LBNL PAC when Gammasphere is moved back to Berkeley in the spring of year 2000.

The 4014 keV line allow us to determine that the SD level feed by the 693 keV SD line has an energy of at least 11,675 keV and probably a spin around 26 $\hbar$.

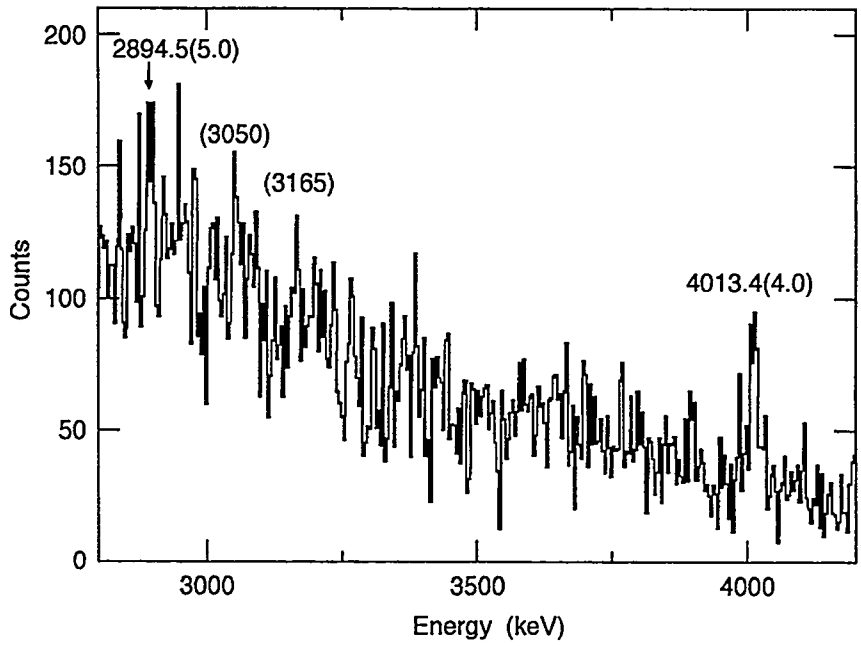

Fig. I-51. The high energy end of a spectrum where gates have been placed on three clean SD lines from the yrast SD band in ^{152}Dy. Further analysis indicates that the 4014 keV line is from the level fed by the SD 693 line and it feeds into the level fed by the 221 ND transition. It is, however, not clear from this dataset if the decay proceeds via any intermediate states. The data analysis is still ongoing.

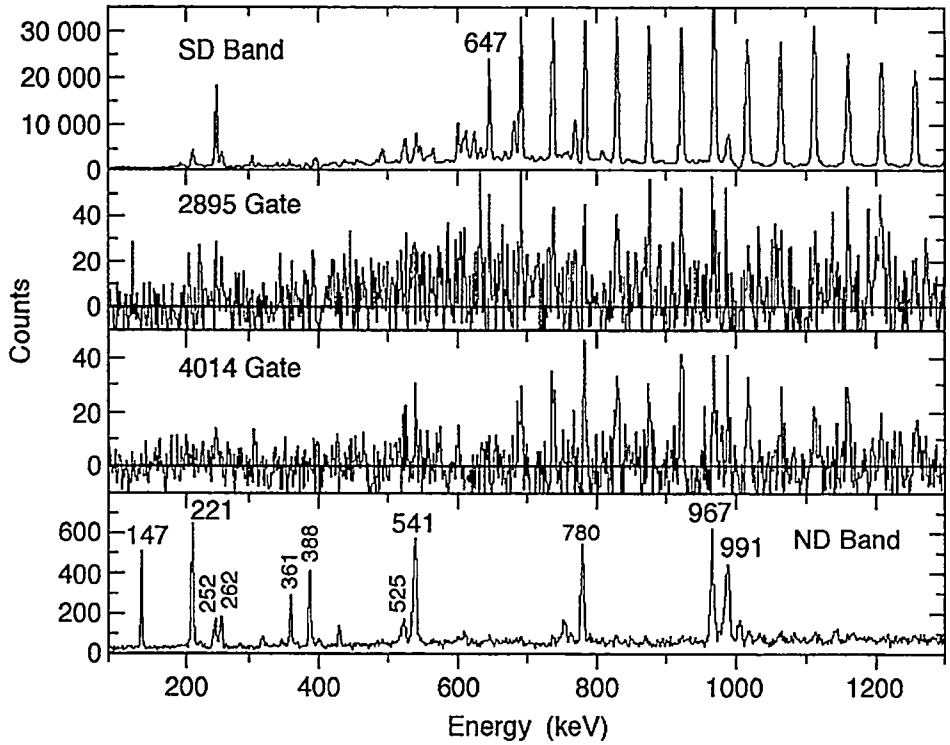

Fig. I-52. Spectra where gates have been placed on the two strongest one-step primary transitions, 4014 and 2895, and any combination of two SD lines. Also shown on top is a spectrum after gates have been placed on three SD lines and, on the bottom, the sum of spectra when gates are placed on ND lines above the 147 keV line in the normal level scheme of ^{152}Dy (i.e., selecting gamma cascades fed at high spins).

c.7. Phase Transitions Above the Yrast Line in ^{154}Dy

(T. L. Khoo, I. Ahmad, M. P. Carpenter, R. V. F. Janssens, T. Lauritsen, D. Nisius, P. G. Varmette, W. C. Ma,* V. Martin,† J. L. Egido,‡ P. Bhattacharyya,§ P. J. Daly,§ Z. W. Grabowski,§ J. H. Hamilton,¶ A. V. Ramayya,¶ and C. T. Zhang§)

Mean-field theory suggests that nuclei can undergo phase transitions. An especially interesting example is the transitional nucleus ^{154}Dy, which is predicted[1] to change from a collective to an oblate aligned-particle structure with increasing spin and temperature. In a mesoscopic system, such as a nucleus, thermal shape fluctuations are expected to smear the phase transition and a question is whether remnant signatures of the phase transition persist at high excitation energies. A sudden change from collective to aligned-particle configurations at spin 34 $\hbar$ has indeed been confirmed along the zero-temperature yrast line in ^{154}Dy[2]. However, in excited states, where thermal fluctuations are dominant even at moderate temperature, it remains a challenge to obtain unambiguous signatures for a phase transition.

Calculations[3] based on results of mean-field theory and incorporating fluctuations have suggested that the quasicontinuum (QC) collective E2 spectrum can provide such a signature. Specifically, an E2 spectrum consisting of a unique two-peak feature was predicted[3] for ^{154}Dy, when the gamma cascade straddles the two regions on either side of the phase-transition boundary. In contrast, only one broad QC peak is detected in the vast majority of nuclei. This two-peak feature in the QC E2 spectrum has been, in fact, previously observed[4]. The calculations of Ref. 3 suggest that, while fluctuations indeed smear out the phase transition, they also play a critical role in providing an observable signature via the E2 spectrum. That is because no collective E2 spectrum would normally be expected in the oblate phase; it arises only because thermal fluctuations cause admixtures of collective (prolate and triaxial) shapes. This has been amply demonstrated in Ref. 3, where the calculated E2 spectra reproduce the different features observed[4,5] in ^{152,154,156}Dy. A stringent test of the calculations consists of proving that the different E2 peaks indeed arise from the two phase regions, as will be done in this work.

The hot excited states in nuclei remain a little explored frontier since there are only few experimental investigations of excited nuclear states above the yrast line, compared to studies of cold yrast states. This is partly because there has been no clear-cut way to specify the spin-excitation energy being studied. We propose a new, but simple, way to provide this specification. By demanding that cascades feed the yrast line at a particular spin, the precursor QC spectrum then arises from states of higher spins. This can be simply accomplished by setting coincidence gates on specific yrast transitions. For example, cascades which feed into a low-spin region of the yrast line can be selected; in this case we predict two E2 peaks, one from each phase region. On the other hand, cascades selected by demanding entry into the yrast line at high spin traverse only the nominally oblate region; only the upper E2 peak is then expected. Furthermore, the average initial point of the cascade is also deduced from the resulting QC spectrum. It is this knowledge of *both the initial and final points* that allows the decay pathways to be constrained.

The experiment was performed at the Lawrence Berkeley 88" Cyclotron. Excited states in ^{154}Dy were populated via the ^{36}S(^{122}Sn,4n) reaction with a 165-MeV beam. The γ rays were detected with the early-implementation phase of the Gammasphere spectrometer, which consisted of 36 Compton-suppressed Ge detectors at that time.

*Mississippi State University, †Universidad Politécnica de Madrid, Spain, ‡Universidad Autónoma de Madrid, Spain, §Purdue University, ¶Vanderbilt University

[1] V. Martin and J. L. Egido, Phys. Rev. C **51**, 3084 (1995).
[2] W. C. Ma *et al.*, Phys. Rev. Lett. **61**, 46 (1988).
[3] V. Martin *et al.*, Phys. Rev. C **51**, 3096 (1995).
[4] R. Holzmann *et al.*, Phys. Rev. Lett. **62**, 520 (1989).
[5] R. Holzmann *et al.*, Phys. Lett. **B195**, 321 (1987).
[6] K. Kumar and M. Baranger, Nucl. Phys. **A110**, 529 (1968).

Spectra were obtained for ^{154}Dy at three detector angles (forward, 90°, backward), coincident with selected pairs of yrast transitions. Each spectrum was analyzed with corrections for neutron interaction, coincidence summing, detector response (unfolding) and photopeak efficiency. Discrete peaks (originating from the yrast region) were removed to obtain the QC portion of the γ-ray spectra (from excited states above the yrast region). The E2, dipole and statistical components of the spectra were extracted. From the multiplicity and average energy of each component, the total spins and energies removed by all γ rays entering each selected spin region could be deduced. The average entry point for the total ^{154}Dy channel was thus found to be 56.1 and 31 MeV.

The spectra feeding the different regions of the yrast line are given in Fig. I-53, where they are compared to equivalent theoretical spectra. A distinct and unusual feature is the occurrence of two broad peaks. The spectrum of E2 transitions from excited states of a nucleus of approximately fixed deformation normally consists of a single broad peak since the transition energy, $E_\gamma = (2I-1)\,\hbar^2/\Im$, grows monotonically with spin I. ($\Im$ is the moment of inertia.) Hence, the two-peak spectra provide a clear signal of a deviation from constant deformation

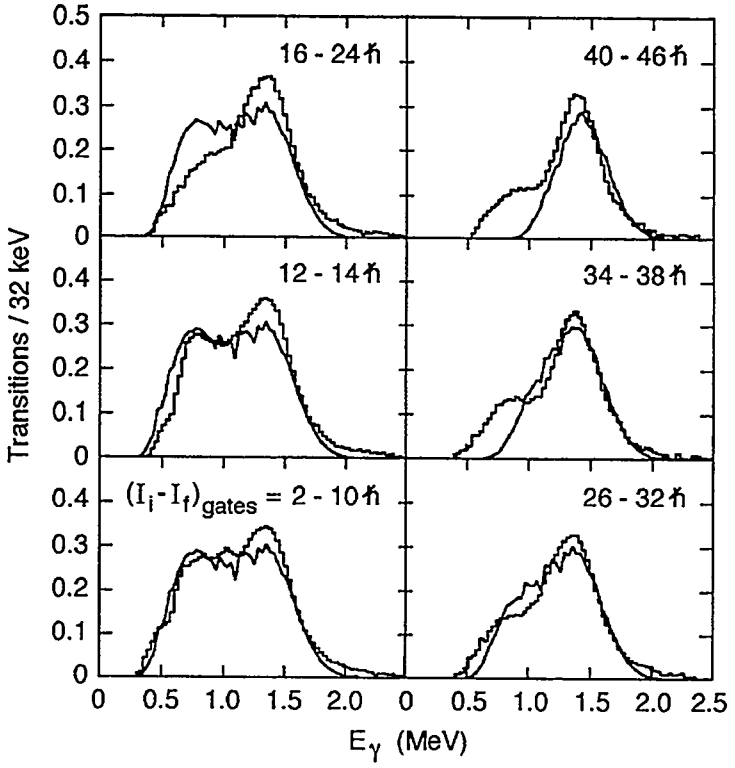

Fig. I-53. Integral spectra of the quasicontinuum E2 transitions feeding into and above the indicated spin intervals. Histograms represent experimental results, solid lines the theoretical calculations. The labels I_i-I_f gates denote the spin interval of the transitions used for coincidence gates.

To quantitatively understand the origin of the two peaks, we have performed theoretical calculations to simulate the QC decay of this nucleus by using a Monte Carlo method[3]. The collective E2 strengths, which carry information about the structure and phase transition, are microscopically calculated as a function of spin I and excitation energy E from finite-temperature Hartree-Fock (FTHF) theory, with the standard set of Pairing-Plus-Quadrupole force parameters and configuration space[6]. In order to reproduce the features of a finite system, we have to go beyond mean field theory by including fluctuations in the shape degrees of freedom[1]. The average entry spin and energy for the reaction are obtained directly from the experiment. The procedure produces spectra that are equivalent to the experimental ones, where the discrete lines are removed.

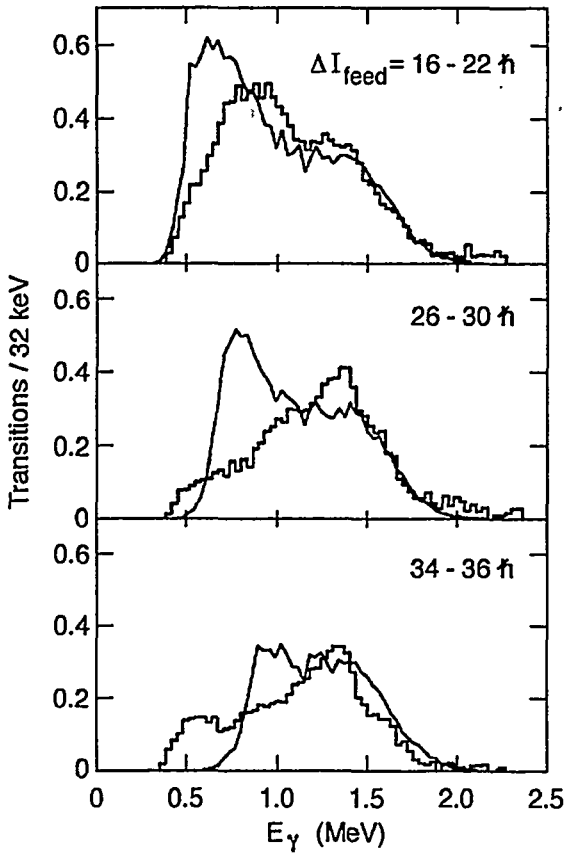

Fig. I-54. Differential E2 spectra feeding into the yrast line only in the indicated spin region ΔI_{feed}. Histograms and solid lines correspond to experiment and theory.

Figure I-53 shows the experimental and theoretical QC E2 spectra from coincidence gates from different spin regions. The spectra are normalized such that the area under each spectrum gives the total multiplicity of the associated γ rays. Two peaks, centered around 0.8 and 1.4 MeV, are prominent in the spectra from low-spin gates — as found in a previous study[4] at Argonne.

The two-peak feature indicates a redistribution of γ-ray energies along the deexcitation pathways. In the later decay stages, when the cascades approach the yrast line at medium and low spins, the moment of inertia increases and transition energies shift downwards, causing the clustering around 800 keV and the dip around 1.1 MeV. In the spectra gated at higher spins, contributions of cascades traversing the low-spin prolate region of the I-E plane are eliminated, thus reducing the strength of the low-energy component. This demonstrates that the low-energy component originates mainly from regions of lower spins. The high-energy peak begins to dominate over the low-energy one for cascades feeding regions as low as 16-24 ħ and, in the theoretical spectra, becomes almost the only component for feeding above 32 ħ. This clearly identifies the region I > 32 ħ as the one with the smaller average moment of inertia.

The spectra in Fig. I-53 might be termed integral spectra. Each spectrum, which is obtained from coincidence gates on yrast transitions of specific spin, selects all QC cascades that feed into the yrast line above that spin. As the spin threshold increases, the QC pathways become more narrowly defined in spin, thus better specifying the I-E region being studied. However, as the threshold spin is lowered, the selectivity of such integral spectra decreases since all contributions from higher spins persist. It is possible to emphasize the particular QC cascades from a lower-spin region, by using differential spectra that feed *only* a narrow spin interval. For example, the QC spectrum feeding into the yrast states with only I = 16-22 ħ can be extracted by subtracting the spectra gated on the transitions depopulating the 16^+ and 24^+ levels (after correct normalization) — see Fig. I-54. The low-energy E2 component is now significantly stronger than in the integral I = 16-24 ħ spectrum (Fig. I-53). Again this emphasizes that this component must arise from the low-spin region. In contrast, in the differential spectrum feeding the spin interval 26-30 ħ, this low-energy component is markedly smaller, indicating that the γ cascade crosses the phase-transition boundary around spin 32 ħ. Although the trend of a low-energy component that diminishes with yrast entry spin is reproduced by theory, discrepancies in details indicate that, in the calculation, the γ cascade crosses the phase boundary at higher spin, I > 36 ħ.

In conclusion, two broad peaks are observed in both experimental and theoretical quasicontinuum spectra. The pronounced change in relative strengths of the two peaks, when going from low-spin gates to high-spin gates, provides an incisive probe of the change in nuclear structure in the two zones of the I-E plane. The low-energy E2 component originates from the lower spin region, with prolate deformation. The high-energy component is largely from the nominally oblate region of the phase diagram, where strong fluctuations give rise to E2 transitions. Despite the fluctuations present in a finite system, signatures of a phase transition are seen to clearly persist in both the experimental and theoretical spectra. A paper has been submitted to Physical Review Letters.

c.8. Lifetimes of Triaxial Superdeformed Bands in ^{168,169}Hf

(T. Lauritsen, M. P. Carpenter, T. L. Khoo, C. J. Lister, R. V. F. Janssens, S. Siem, P. G. Varmette,* H. Amro,* M. Bergstrom,* A. Bracco,** J. Domsheit,‡ G. B. Hagemann,* B. Herskind,* G. Sletten,* K. A. Smith,* S. Odegaard,* W. C. Ma,§ D. Hartley,† L. L. Riedinger,† H. Hubel,‡ S. Frattini,** and B. Million**)

Superdeformed (SD) shapes, coexisting with normal prolate shapes, have been predicted in N ~ 94 and Z ~ 71 nuclei[1,2]. These shapes are unusual and interesting in that they are predicted to be triaxial -- as opposed to all other SD bands which have identical minor axes. Such triaxial bands were first observed in the odd proton Lu isotopes[3]. Last year, in a Gammasphere experiment at ANL, two triaxial superdeformed band candidates were found in the even proton ^{168,169}Hf isotopes. The spectrum from ^{168}Hf is shown in Fig. I-55. The ultra cold semi-symmetric reaction, ^{76}Ge + ^{96}Zr at 310 MeV from the ATLAS accelerator, was used to populate these bands at very high spins.

In order to verify that these bands indeed are i) superdeformed and ii) triaxial a new experiment was performed - this time with a thick target - in order to measure the lifetime of the states using the DSAM technique. The same reaction as mentioned above with a beam intensity of 5 pnA over 6 days was used. For the fragile target to sustain this intense beam, the beams from ATLAS were wobbled in both the x and y direction. Thus the beam was distributed over a 5 × 5 mm area. The data analysis is in progress.

*Niels Bohr Institute, Copenhagen, Denmark, †University of Tennessee, ‡University of Bonn, Germany
§Mississippi State University, **University of Milan, Italy

[1]I. Ragnarsson, Phys. Rev. Lett. **62**, 2084 (1989).
[2]S. Aaberg, Nucl. Phys. **A520**, 35c (1990).
[3]W. Schmitz, Phys. Lett. **B303**, 230 (1993).

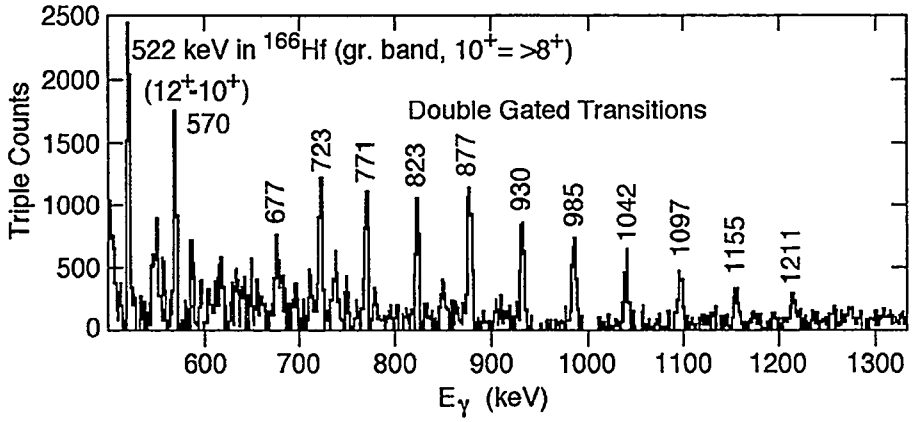

Fig. I-55. Spectrum where double gates have been placed on the transitions in the triaxial SD band in ^{168}Hf.

c.9. Spins and Excitation Energy of the Yrast Superdeformed Band in ^{191}Hg

(S. Siem,* P. Reiter, T. L. Khoo, M. P. Carpenter, T. Lauritsen, D. Gassmann, I. Ahmad, I. Calderin, S. M. Fischer, G. Hackman, R. V. F. Janssens, D. Nisius, H. Amro,‡ T. Døssing,† U. Garg,§ F. Hannachi,¶ B. Kharraja,§ A. Korichi,¶ A. Lopez-Martens,¶ E. F. Moore,‡ and C. Schuck¶)

The total gamma-spectrum following the decay out of the yrast SD band in ^{191}Hg has been extracted using the methods described in[1]. The gamma-rays following the ^{174}Yb(^{22}Ne,5n)^{191}Hg reaction were collected with Gammasphere and the beam was provided by the 88" Cyclotron at LBNL. From the total gamma-spectrum the excitation energies and spins of the yrast SD band members have been determined. The level fed by the 351 keV transition (the decay-out level) has an excitation energy of 5.73 ± 1.0 MeV and spin 17.0 ± 0.7 $\hbar$, leading to two possible spins: 33/2 $\hbar$ or 35/2 $\hbar$.

The result from the quasicontinuum analysis is in good agreement with the previous result from a one-step linking transition[2]. A second one-step transition of 3310 keV, with 3 σ statistical significance, has been tentatively assigned to feed a 33/2$^-$ known normal-deformed level. There are now two one-step transitions; both place the decay-out level at 6000 keV. The angular distribution of the stronger one-step line (2778 keV) shows a big positive value for the A2 coefficient (0.57 ± 0.48), which is consistent with ΔI = 0, suggesting a 35/2 $\hbar$ spin assignment for the decay-out level. We rule out the possibility of it being an E2 transition, because that would make the other one-step transition a M3 transition competing with a M1 transition that is not observed. The spin is consistent with a $j_{15/2}$ particle configuration assignment[3]. However, the experimental data do not allow for a parity assignment. For the parity of the SD band to be consistent with a $j_{15/2}$ particle configuration assignment, the one-step lines must be M1 transitions. From neutron capture experiments it is known that the ~8 MeV E1 transitions are about 5 times more likely than M1 transitions. However, in ^{191}Hg the 1-step lines have significantly lower energy (~ 3 MeV). In fact, M1 transitions around this energy are observed both in neutron capture and also from the decay of the SD band in ^{194}Pb.

In conclusion, the excitation energy and spin of the yrast SD band in ^{191}Hg has been determined to be 6000 keV and 35/2 $\hbar$ for the decay-out level. The energy above yrast of the SD band at the point of decay out is 2.778 MeV. The excitation energy of the yrast SD band extrapolated to 13/2 $\hbar$, the spin of the ground state, is 4.74 MeV. It is important to obtain these quantities in an odd-even nucleus since that gives information on the relative pair correlation energies in ND and SD states, thereby providing a stringent test for theory. Information on pair quenching in excited states will be obtained by comparing the quasicontinuum spectra following the decay of the SD bands in ^{191,192,194}Hg. In addition, these spectra will be compared with theoretical statistical decay spectra[4] from excited states in even-even and odd-even nuclei.

A paper on this work is being written.

---

*ANL and University of Oslo, Norway, †The Niels Bohr Institute, Copenhagen, Denmark, ‡North Carolina State University, §University of Notre Dame, ¶CSNSM, Orsay, France

[1] R. G. Henry *et al.*, Phys. Rev. Lett. **73**, 777 (1994); T. Lauritsen et al., Heavy Ion Physics **6**, 229 (1997), Proc. Symp. on Nucl. Structure at the Limits, ANL (1996).

[2] P. Reiter *et al.*, Physics Division Annual Report for 1997, ANL-98/24, p. 38.

[3] M. P. Carpenter *et al.*, Phys. Rev. C (1995).

[4] T. Døssing *et al.*, Phys. Rev. Lett. 75 (1995) 1276.

c.10. Determination of Spin and Excitation Energy of Superdeformed Bands in ^{192,194}Hg from the Quasicontinuum Gamma Rays

(T. Lauritsen, T. L. Khoo, I. Ahmad, M. P. Carpenter, R. V. F. Janssens, A. Lopez-Martens,* H. Amro,† S. Berger, L. Calderin, T. Døssing,¶ S. M. Fischer,§ G. Hackman, D. T. Nisius, F. Hannachi,* A. Korichi,* and E. F. Moore†)

Superdeformed (SD) bands in the mass 190 region decay suddenly, over a few states, at relatively low spin and high excitation energy. The decay path is very fragmented and only in a few cases have one-step or two-step decays been seen. Presently, in this mass region, only three superdeformed bands have been linked to the normal states they decay to via discrete one step links[1,2,3]. Most of the gamma rays from the decay of the SD bands form a quasicontinuum. Thus, for most SD bands in this mass region, the excitation energy and spins of the bands are not known experimentally.

However, by extracting and analyzing the decay quasicontinuum spectrum in coincidence with the SD bands it is also possible to determine the excitation energy and spin of the bands. This "quasicontinuum analysis method" (QC) was tested in ^{194}Hg, which is one of the few cases where the excitation energy and spin of the first superdeformed band is known, and was then applied to the first superdeformed band in ^{192}Hg, where no one-step decays been seen.

The derived excitation energy and spin in ^{194}Hg, using the quasicontinuum analysis method, were found to be in excellent agreement with the exact result determined from one-step and two-step decay lines in the nucleus. The extracted spin and energy of the 10^+ SD state in the yrast SD band was determined to be 10.8(1.0) $\hbar$ and 6.6(5) MeV, respectively, using the QC method. This should be compared to the exact result: 10 $\hbar$ and 6.6 MeV of reference[1,4]. For ^{192}Hg, extrapolated to zero angular momentum, the excitation energy of the SD band was found to be 5.3(5) MeV using the QC method. Figure I-56 shows a composite plot of the continuum spectra in coincidence with the SD band in ^{192}Hg. The statisticals, quadrupole and M1/E2 dipoles are from the feeding of the SD band. The remainder, after the latter quasicontinuum components have been subtracted from the total continuum, are the quasicontinuum gamma rays from the decay of the SD band.

A paper with these results has been submitted to Phys. Rev. C.

---

*CSNSM, Orsay, France, †North Carolina State University, ‡IReS, Strasbourg, France, §University of Pennsylvania, ¶Niels Bohr Institute, Copenhagen, Denmark

[1]T. L. Khoo, Phys. Rev. Lett. **76**, 1583 (1996).
[2]A. Lopez-Martens, Phys. Lett. **B380**, 18 (1996).
[3]D. P. McNabb, Phys. Rev. C **56**, 2474 (1997).
[4]G. Hackman, Phys. Rev. Lett. **79**, 4100 (1997).

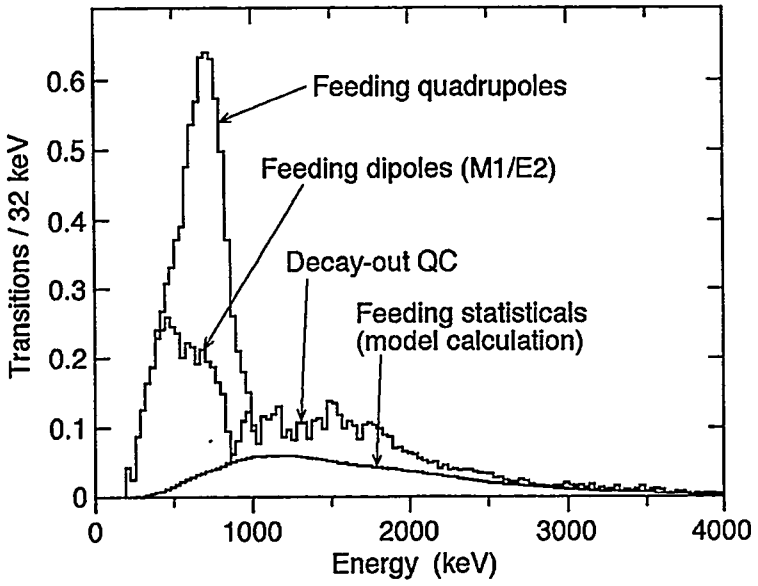

Fig. I-56. Composite plot of the continuum spectra in coincidence with the SD band in ^{192}Hg. The feeding components are: the statisticals, quadrupole and M1/E2 dipoles. The decay-out QC are the quasicontinuum gamma rays from the decay of the SD band.

c.11. Fluctuations in the Strengths of Primary Transitions from Decay Out of a Superdeformed Band

(T. L. Khoo, T. Lauritsen, I. Calderin, M. P. Carpenter, G. Hackman, I. Ahmad, S. Fischer, R. V. F. Janssens, D. Nisius, A. Lopez-Martens,† T. Døssing,* A. Korichi,† F. Hannachi,† and E. F. Moore§)

The decay from SD states is precipitated by sufficient mixing with one or two of the nearest normal-deformed (ND) states among which they are embedded. The decay spectrum is then governed by the admixed highly-excited ND state. In analogy with neutron-capture gamma rays, we call the transitions that directly deexcite the state primary gamma rays. In the decay spectrum of ^{194}Hg (band 1), 34 primary transitions above 2.6 MeV have been detected above a 3σ level. These transitions have a distribution in strength.

The fluctuations in the strength distribution can provide an indicator of the chaoticity of excited ND states around 4.3 MeV. In the fully chaotic limit, where the wavefunction is complex, the distribution is expected to be a χ^2 distribution, with the number of degrees of freedom ν equal to 1, giving the so-called Porter-Thomas distribution.

A technique based on the maximum likelihood method has been developed for analyzing the distribution of the transition strengths. The analysis shows that the observed distribution is consistent with a χ^2 distribution with $\nu = 1$ (Porter–Thomas distribution). However, the uncertainties in ν and in the average strength θ are very large because the observed primary transitions represent the high-intensity tail of the maximum-likelihood distribution. In fact, some of the 1-step lines exhibit strengths up to 9 times the average strength, raising the possibility that there may be some perseverance of selection rules for decay from states at ~ 4.3 MeV. Since it is difficult to explain why this happens in only ^{194}Hg, a more likely explanation is that chance (and fortune) is responsible for the large 1-step strengths. (In ^{194}Pb, where the excitation energy of the SD band is significantly lower, the primary transitions are expected to be stronger.) In summary, the distribution of the strength of primary decay lines in ^{194}Hg is consistent with decay from a chaotic state.

This work has been published in Nuclear Physics A.

*Niels Bohr Institute, Copenhagen, Denmark, †CSNSM, Orsay, France, ‡IN2P3-CNRS, Orsay, France, §North Carolina State University

c.12. Superdeformation in ^{193}Pb: Observation of Three Additional Excited Bands

(M. P. Carpenter, R. V. F. Janssens, D. Roβbach,* A. N. Wilson,† C. Barton,† D. M. Cullen,‡ H. Hubel,* S. L. King,‡ A. Korichi,§ and A. T. Reed‡)

The occurrence of superdeformation in nuclei with mass numbers around A ~ 190 results from large gaps in the single-particle spectra (N = 112 and Z = 80) at large deformation (β_2 ~ 0.5). The nucleus ^{193}Pb, with 82 protons and 111 neutrons, lies just below the neutron shell closure, and thus, provides an ideal system for studying neutron excitations around the N = 112 shell gap. The properties of excited superdeformed (SD) bands allow the identification and characterization of orbitals lying close to the neutron Fermi surface and provides information on the excitations across the shell gap.

Previous work[1,2] identified six SD bands in ^{193}Pb. Bands 1 and 2 are assigned to $j_{15/2}$ intruder orbital. Bands 3 and 4 show a small signature splitting at high rotational frequency and have been assigned to the [642]3/2 quasineutron configuration. Cross-talk was observed between the weakest pair of bands (bands 5 and 6), allowing an estimate of the g-factor to be made. The result suggests that the [624]9/2 was the favorable assignment.

We have recently performed a new measurement on ^{193}Pb using the Gammasphere spectrometer array at Lawrence Berkeley National Laboratory. In addition to the previously known six SD bands, three new bands have been observed. Two of them are a pair of signature partner bands which show similar transition energies to bands 5 and 6. These two new bands have been assigned the [512]5/2 quasineutron configuration. The third new band has been assigned to the favored signature of the [752]5/2 Nilsson orbital. In addition, a more reliable gyromagnetic factor, g_K has been obtained for bands 5 and 6 which is in good agreement with calculations for the [624]9/2 state.

A paper reporting results from this study has recently been published in Nuclear Physics A[3].

*University of Bonn, Germany, †Yale University, ‡University of Liverpool, United Kingdom, §CSNSM Orsay, France

[1] J. R. Hughes *et al.*, Phys. Rev. C **51**, R447 (1995).
[2] L. Ducroux *et al.*, Phys. Rev. C **53**, 2701 (1996).
[3] D. Roβbach *et al.*, Nucl. Phys. **A660**, 393 (1999).

c.13. Quasicontinuum Spectrum of Gamma Rays Which Depopulate SD States in ^{194}Pb

(T. L. Khoo, T. Lauritsen, D. P. McNabb,* J. A. Cizewski,* K.-Y. Ding,* W. Younes,* D. Archer,† R. W. Bauer,† J. A. Becker,† L. A. Bernstein,† K. Hauschild,† R. M. Clark,‡ M. A. Deleplanque,‡ R. M. Diamond,‡ P. Fallon,‡ I. Y. Lee,‡ A. O. Macchiavelli,‡ F. S. Stephens,‡ and W. H. Kelley§)

Primary gamma rays from the decay out of the SD band in ^{194}Pb have been identified and the spins, likely parity and excitation energies of the band have been determined[1] from experiments performed with both Eurogam and Gammasphere. The focus of this work is the analysis of Gammasphere data for the total decay spectrum. As for ^{192,194}Hg, this spectrum consists of both sharp primary transitions and an unresolved quasicontinuum component. In ^{194}Pb, however, the primary lines have a significantly larger fraction of the total decay yield, due largely to the smaller excitation energy of the SD band, which reduces the phase space for the unresolved component. The total decay spectrum out of SD states has been extracted. The energy of the decaying SD states that is derived from

*Rutgers University, †Lawrence Livermore National Laboratory, ‡Lawrence Berkeley National Laboratory, §Iowa State University

[1] A. Lopez-Martens *et al.*, Phys. Lett. **B380**, 18 (1996); K. Hauschild *et al.*, Phys. Rev. C **55**, 2819 (1997).
[2] T. Døssing *et al.*, Phys. Rev. Lett. **75**, 1276 (1995).

the total decay spectrum agrees with that determined from the discrete lines. About 0.9 MeV below the end point, the spectrum rises rapidly. This feature, which has been predicted by Døssing et al.,[2] reflects a region of low level density located immediately above the normal-deformed yrast line, to which decay is naturally reduced. This work, which constituted part of the Ph. D. thesis of D. McNabb from Rutgers, has been accepted as a Rapid Communication in Physical Review C.

c.14. Actinide Signature Measurements for Spent-Fuel Characterization

(R. V. F. Janssens, I. Wiedenhöver, J. D. Cole,* M. W. Drigert,* R. Aryeinejad,* E. L. Reber,*and J. K. Jewell*)

Experiments to study the radiation emitted from neutron-induced fission on selected actinide targets have continued at the ANL Intense Pulsed Neutron Source. Following the irradiation of ^{235}U samples performed in 1998, a new set of data with a 5 gram ^{239}Pu target was collected in 1999. The measurements are performed with 8 Compton-suppressed spectrometers of the Argonne-Notre Dame BGO gamma-ray facility. The results will be applied to the problem of determining fissile isotopic ratios for arms control issues and are also forming the basis for techniques addressing concerns about the disposal and storage of spent nuclear fuel. Of particular importance is the study of gamma rays above 1 MeV in prompt fission fragments as it offers the possibility of relatively straightforward isotopic assignments. A preliminary report of this work has been published[1]. Another campaign of measurements is scheduled for 2000.

*Idaho National Engineering Laboratory

[1]J. D. Cole *et al.*, Proceedings of International Conference on Perspectives in Nuclear Physics, J. H. Hamilton, H. K. Carter and R. B. Piercey editors, World Scientific, p. 35 (1999).

D. REACTION DYNAMICS

Over the last few years studies of various aspects of reaction dynamics using heavy-ion beams within the Division have steadily moved from measurements performed with ATLAS beams in the vicinity of the Coulomb Barrier towards higher beam energies. At present, the measurements at ATLAS focus mainly on reactions with exotic beams and on studies involving gamma-ray detection with Gammasphere: these are discussed elsewhere in this report. In addition to one contribution on inelastic scattering studies performed at ATLAS, this section presents work being performed at relativistic energies; i.e. the analysis of the AGS E917 experiment and the preparations for the PHOBOS experiment at RHIC.

d.1. Angular Correlation, Spin Alignment, and Resonance Behavior in $^{12}C(^{12}C, ^{12}C)\,^{12}C(3^-)$ Inelastic Scattering

(A. H. Wuosmaa, B. B. Back, R. R. Betts, D. J. Blumenthal, S. Fischer, B. G. Glagola, D. J. Henderson, D. Hofman, R. V. F. Janssens, C. J. Lister, V. Nanal, D. Nisius, M. D. Rhein, P. R. Wilt, and M. Freer*)

Many previous studies of inelastic scattering in the $^{12}C + ^{12}C$ system have revealed strong resonance-like behavior. Several theoretical pictures have emerged which attempt to describe this behavior, either as super-deformed cluster states in the compound system ^{24}Mg, or as potential scattering resonances whose strength is enhanced due to favorable angular momentum coupling conditions at particular energies. These models make predictions about the angular momenta expected to dominate the scattering process at resonance energies. Many of the reaction channels in which the strongest resonances are observed have non-zero channel spin, making the extraction of a resonance angular momentum difficult, if not impossible, using the traditional technique of angular distribution measurements. If, however, the radiation from the decay of the level in the inelastically excited nucleus can be detected, the angular correlations between that radiation, and the scattered nucleus, becomes sensitive to the total angular momentum of the system and, hence, the resonance spin. Furthermore, such angular correlations may be used to study the alignment of the spin of the excited, scattered partner. Such data can provide information about the inelastic scattering process.

We have used these techniques to study features in the excitation functions of inelastic scattering in the $^{12}C + ^{12}C$ system to the 3^- state at 9.64 MeV in ^{12}C, which decays to the alpha-particle unbound ground state of ^{8}Be. Reilly *et al.*[1] and Fulton *et al.*[2] have reported the excitation function for this channel.[1] The three alpha particles from the decay of this level in ^{12}C were detected in an array of double-sided silicon strip detectors (DSSDs). The data were sorted in order to extract the scattering yield as a function of the $^{12}C + ^{12}C$ scattering angle, as well as the angle between the direction of the α-^{8}Be relative velocity and the beam direction. These correlated angular distributions, or angular correlations, were studied in order to learn about the reaction mechanism and to attempt to extract the spins of resonances in this channel. Some of the results of this work have appeared elsewhere.[3]

*University of Birmingham, United Kingdom

[1] W. Reilly *et al.*, Nuovo Cimento **13A**, 913 (1973).
[2] B. R. Fulton *et al.*, Phys. Rev. C **21**, 198 (1980).
[3] A. H. Wuosmaa *et al.*, Phys. Rev. C **54**, 2463 (1996).
[4] Y. Kondo, Y. Abe, and T. Matsuse, Phys. Rev. C **19**, 1356 (1980).
[5] S. Marsh and W. D. M. Rae, Phys. Lett. **B153**, 21 (1985).

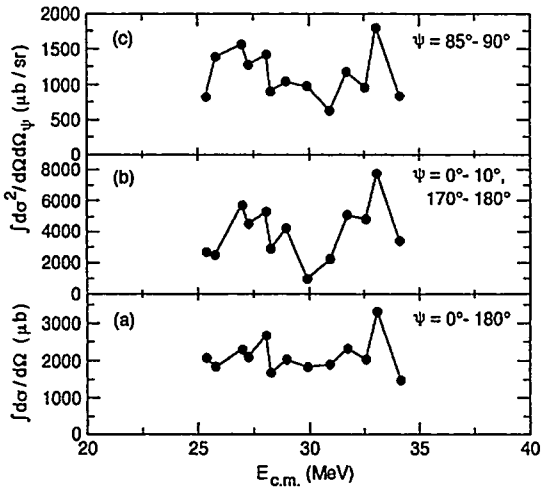

Fig. I-57. Excitation function for $^{12}C + {}^{12}C(3^-)$ inelastic scattering, for events with the angle between the α-^{8}Be relative velocity and the beam direction of (a) all values between 0^o and 180^o (b) 0^o-10^o and 170^o-180^o, and (c) 85^o-95^o.

A model-independent analysis of the angular correlation data may be obtained for events in which the alpha particle from the $^{12}C(3^-)$ decay is detected at 0^o with respect to a particular quantization axis, here chosen to lie along the beam direction. In this case, as there is no projection of the total angular momentum along the beam direction, the only magnetic substate which can contribute to the scattering is that with $m = 0$. Figure I-57 shows excitation function data for the 3^- inelastic channel for the total cross section integrated from $\theta_{C.M.} = 40^o$-105^o degrees in the lab and for the primary alpha particle detected at (a) all angles between 0^o and 180^o, (b) 0^o -10^o and 170^o-180^o, and (c) 85^o-95^o. The data in (b) and (c) correspond to scattering to the $m = 0$, and predominantly $m = 1$ substates, respectively. The $m = 0$ cross section shows the most significant variation in the cross section, with a peak-to-background ratio nearly a factor of two larger than that seen in (c). Such behavior is an indication that at the resonance energies, the spin of the 3^- state aligns predominantly perpendicular to the quantization axis, i.e. the assumption of a fully aligned system with the total angular momentum J = L + S, where L is the orbital angular momentum and S is the spin of the excited ^{12}C state, the magnetic sub-state populations are expected to be approximately proportional to the Clebsch-Gordan coefficients $|\langle L3\text{-}mm|J0\rangle|^2$. Taking into account the solid angle $\Delta\Omega_{\psi\_}$ for each bite in the alpha-particle correlation angle ψ, one expects the ratio of $\sigma(\psi = 0^o + 180^o)/\sigma(\psi = 90^o)$ to be approximately 2, close to that which is observed in Fig. I-57.

Figure I-58 shows inelastic scattering angular distribution data for the $m = 0$ substate obtained at several energies between 25 and 34 MeV. The solid curves represent Legendre polynomial partial-wave fits with three partial waves, L = 11, 13, and 15. The dashed curves correspond to pure squared Legendre polynomials of order 13, at $E_{C.M.} = 27.0$ MeV, and 15, at $E_{C.M.} = 33.1$ MeV. These energies correspond to resonances reported by Fulton *et al.* Figure I-59 shows the energy dependence of the extracted partial cross sections σ_L. The enhancements in σ_{13} at 27 MeV, and σ_{15} at 33 MeV are clear, and consistent with the expectations from visual inspection of the $m = 0$ angular distributions and comparison to the Legendre polynomial curves in Fig. I-59. These results confirm that the dominant orbital angular momenta are 13, and 15, for $E_{C.M.} = 27$ and 33 MeV, respectively, and this information, combined with the observed alignment of the spin are consistent with spin assignments of $J^\pi = 16^+$ and 18^+ for the two resonances, respectively, two units of angular momentum higher than those predicted by the band crossing model.[4] Finally, the spacing between the resonances is consistent with that expected for that between two rotational states with moments of inertia similar to that of two touching spheres, or of an extended deformed configuration resembling two orbiting ^{12}C nuclei.[5]

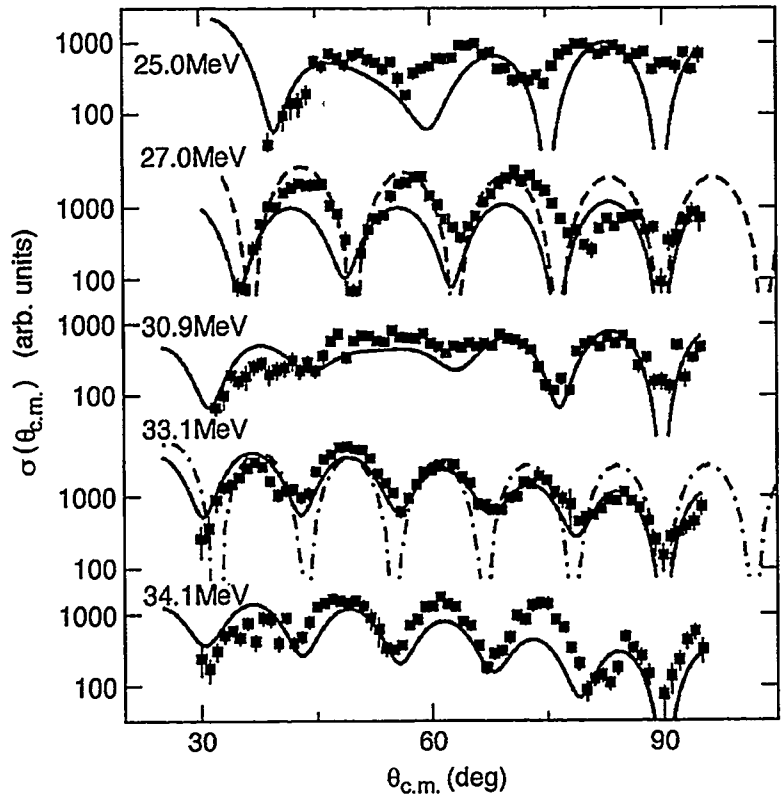

Fig. I-58. $^{12}C + ^{12}C(3^-)$ *m = 0 angular distribution data for several bombarding energies. The solid curves represent the Legendre-polynomial fits described in the text. The dashed, and dashed dotted curves represent pure squared Legendre polynomials of order 13, and 15 respectively.*

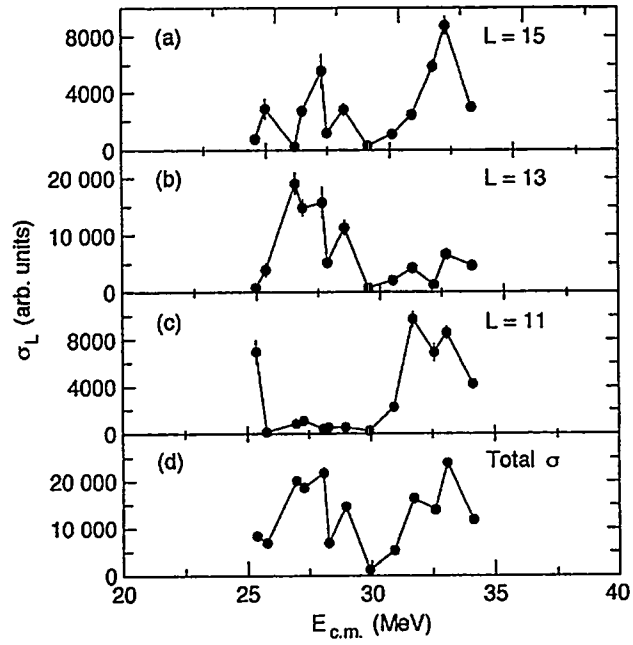

Fig. I-59. Energy dependence for partial wave cross sections σ_L, *where L = 11 (a), 13 (b) and 15 (c), and* $\Sigma_L(\sigma_L)$ *(d), from Legendre-polynomial fits to the m = 0 angular distributions.*

d.2. Studies of Au + Au Collisions at 6, 8, 10.8 GeV/Nucleon at the AGS

(E917 collaboration: B. B. Back, R. R. Betts,§ D. J. Hofman, V. Nanal, A. Wuosmaa, W. C. Chang,‡ C. Y. Chi,§§ Y. Y. Chu,† J. B. Cumming,† J. C. Dunlop,*** W. Eldredge,‡ S. Y. Fung,‡ R. Ganz,‡‡‡ E. J. Garcia-Solis,†† A. Gillitzer,¶¶ G. Heintzelman,† W. F. Henning,††† B. Holzman,§ J. H. Kang,†† E. J. Kim,** S. Y. Kim,** Y. Kwon,** D. McLeod,§ A. C. Mignerey,†† M. Moulson,§§ C. A. Ogilvie,¶ R. Pak,‡‡ A. Ruangma,†† D. E. Russ,†† R. Seto,‡ P. J. Stankas,†† G. S. F. Stephans,¶ H. Q. Wang,‡ F. Wolfs,‡‡ H. Xiang,‡ G. Xu,‡ H. B. Yao,¶ and C. Zou‡)

Introduction

Nuclear matter is compressed to high baryonic density in central collisions of heavy nuclei at relativistic energies. This opens the possibility of generating a new state of matter, the Quark-Gluon Plasma (QGP), in which quarks are not confined to baryons and mesons as is the case for normal matter. The question of whether sufficient densities can be achieved to generate the QGP at the beam energies available at the AGS accelerator at Brookhaven National Laboratory hinges critically on the degree of "stopping" that can be achieved, i.e. the pile-up of a large number of nucleons within a small interaction volume. Although it may be virtually impossible to study the instantaneous state of the interaction region, since the particles that are finally observed in the detectors may have undergone severe rescattering and/or coalescence processes during the later stages of the reaction, such information may still be embedded in the final distribution of particles.

In the E917 experiment at the AGS we have measured the spectra of protons, deuterons, pions, kaons, Λ's, and Φ-mesons as well as some of their anti-particles emitted from the interaction volume and analyzed both their transverse and longitudinal components.

The collision dynamics was studied further by the way of the emission pattern relative to the reaction plane and by means of Hanbury-Brown Twiss analysis of two-particle correlations.

The E917 collaboration is now in its final phase of data analysis and the main results are presently being prepared for publications. Many preliminary results have been presented at various conferences, and included in conference proceedings.

Experiment

The experimental arrangement is shown in Fig. I-60. It consists of a magnetic spectrometer which allows for momentum analysis of particles emerging from the target. Particle trajectories are tracked by several multiwire ionization chambers located both in front and behind the magnet. The time-of-flight wall provides particle identification when combined with the measured particle momentum.

Several beam counters located upstream of the target provide timing and trajectory information on each beam particle. When combined with the spatial location of the projectile remnant at the Hodoscope it is possible to determine the orientation of the reaction plane, with reasonable accuracy. The centrality of the collision (impact parameter) is obtained either by observing the multiplicity of particles (mostly pions) in the New Multiplicity Array (NMA) or the total energy of the projectile remnant in the Zero Degree Calorimeter (Z_{cal}).

Proton Spectra - Stopping

Proton spectra vs. transverse mass, m_t, have been measured over a wide range of rapidity and centrality. Each m_t-spectrum has been fit by a Boltzmann distribution in order to extrapolate into large m_t regions. The resulting integrated yields dN/dy for 5% most central collisions are shown as solid points in Fig. I-61(a-c); open points represent measured points reflected about mid-rapidity. Panels 4d-f shows the corresponding inverse slopes of the m_t spectra, T(y). All data points are shown as a function of rapidity, y-y_{cm}, relative to the center-of-mass system. The dN/dy and inverse

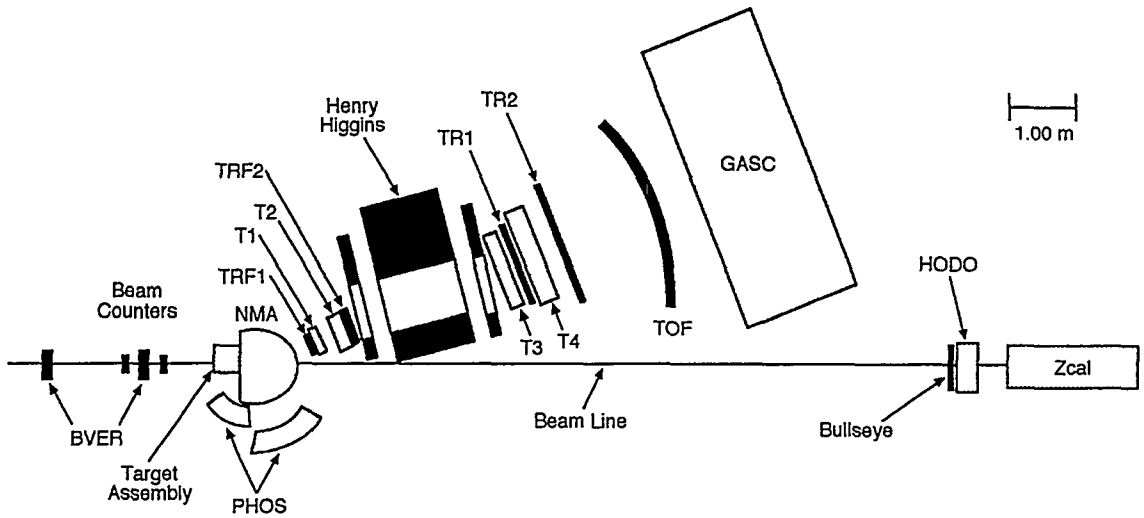

Fig. I-60. Experimental setup. See text for details.

slope data have been fit with a simple model, resulting in the solid curves. In this model the measured protons are assumed to be emitted isotropically from a continuous distribution of sources, which are uniformly distributed over a rapidity range from $-y_b-y_{cm}$ to y_b-y_{cm}. However, in order to simultaneously reproduce the data for the effective temperature, Fig. I-61(d-f), it was necessary to assume that the source temperature decreases with rapidity away from y_{cm} following

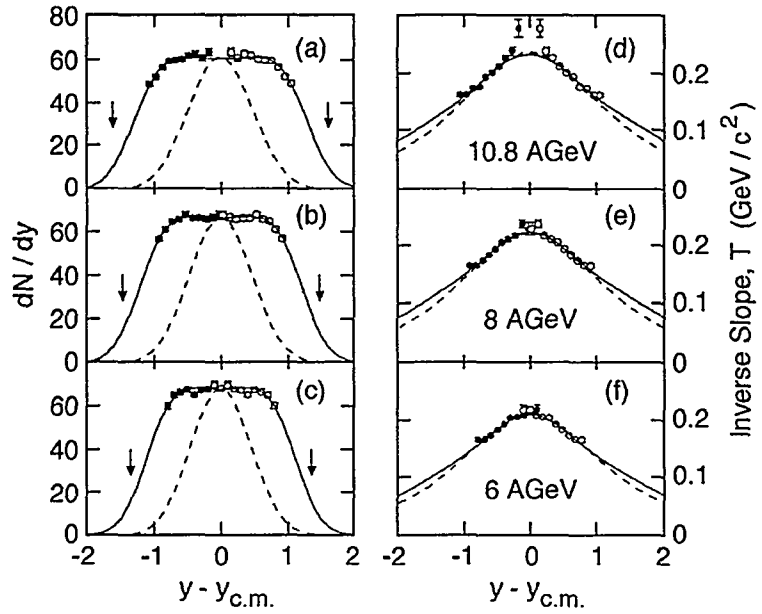

Fig. I-61. Measured (solid points) reflected (open circles) proton radidity distributions and inverse slopes are shown as a function of rapidity $y-y_{cm}$ for beam energies of 6,8, and 10.8 GeV nucleon. The arrows indicate the target and beam rapidities. The dashed curves represent the expected distribution for isotropic emission from a thermal source at rest in the center-of-mass system ($y=y_{cm}$), whereas the solid curves correspond to an optimum fit to the data for a uniform distribution of sources within a range of rapidities $(y_{cm}-y_b) < (y_{xm}+y_b)$ with a Gaussian profile of $T_{eff}(y)$ centered at y_{cm} (see text). The parameters obtained from a least squares fit to the data are y_b=0.990, 1.086, 1.166, T^{o}_{eff}=0.253, 0.267, 0.279 GeV/c² and σ_T=0.697, 0.762, 0.809 for E_{beam}=6,8,10.8 GeV/nucleon, respectively.

a Gaussian profile. We observe that this crude model is capable of reproducing the data very well, despite the fact that its basic assumptions are probably flawed. Thus it is generally accepted that the transverse m_t spectra is a result of both thermal and radial collective motion. However, in this analysis the fitted curves serve only to provide a reasonable extrapolation into the unmeasured region, which is required in order to obtain a standard measure of the degree of "stopping" in the process, namely the mean rapidity loss, $\langle\delta_y\rangle$ of the projectile/target protons. The results are listed in Table 1 for the present data as well as Pb + Pb collisions at 158 GeV/nucl from the CERN SPS program (NA49 collaboration). We observe that the absolute mean rapidity loss $\langle\delta_y\rangle$ increases with beam energy (projectile rapidity). However, it is interesting to note that when the mean rapidity loss is normalized to the maximum possible rapidity loss, $\delta_y^{max} = y_{beam}/2$, there is only a slight increase with beam energy.

To further evaluate the degree of "stopping" we have estimated the maximum fraction of the observed protons which can originate from an isotropically emitting source at rest in the c.m. system. The emission pattern from such a source is represented by the dashed curves in Fig. I-61. We first observe that the measured longitudinal distributions [Fig. I-61(a-c)] are significantly wider than expected for a thermal source in the c.m. system indicating a substantial degree of "transparency" in the collision. In one interpretation, this observation indicates that the only a relatively small fraction, f_{iso}, Table 1, of the incoming beam energy is converted to heat and particle production in the interaction region. Exactly how this translates to estimates of the maximum baryon density achieved in the collision does not follow directly and must be determined on the basis more realistic model calculations. This topic is discussed in further detail in Refs. 1-2.

Table 1. Measures of stopping in central heavy-ion collisions

E_{beam} (A*GeV)	$\langle\delta_y\rangle$	$\langle\delta_y\rangle/\delta_y^{max}$	f_{iso}
6.0	0.74 ± 0.01	0.55 ± 0.01	0.49 ± 0.01
8.0	0.82 ± 0.01	0.56 ± 0.01	0.46 ± 0.01
10.8	0.93 ± 0.01	0.57 ± 0.01	0.45 ± 0.01
158	1.68 ± 0.01	0.58 ± 0.01	0.23 ± 0.02

Pion and Kaon Spectra

The pion and kaon production measured at 6 and 8 GeV/nucleon in the E917 experiment have been augmented with measurements at 2, 4, and 10.7 GeV/nucleon obtained in the predecessor experiment E866 to obtain a rather complete excitation function.

As expected, we find that both K^+ and π^+ production, i.e. the rapidity density dN/dy at mid-

†Brookhaven National Laboratory, ‡University of California at Riverside, §University of Illinois at Chicago, ¶Massachusetts Institute of Technology, **Yonsei University, Seoul, Korea, ††University of Maryland, ‡‡University of Rochester, §§Columbia University, ¶¶Forschungzentrum Julich, Germany, ***Yale University, †††GSI, Germany, ‡‡‡MPI, Germany

[1] Advances in Nuclear Dynamics 5, Plenum Publishers, New York 1999, Eds. Bauer and Westfall, p. 131.

[2] B. B. Back *et al.*, submitted to Phys. Rev. Lett. (Feb. 2000).

rapidity y = y_{cm} increases drastically with beam energy as illustrated Fig. I-62. On the other hand, the mean transverse mass of the K^+ and π^+ spectra increase by less than 75% over the same beam energy range indicating that most of the increase in beam energy is converted to particle production.

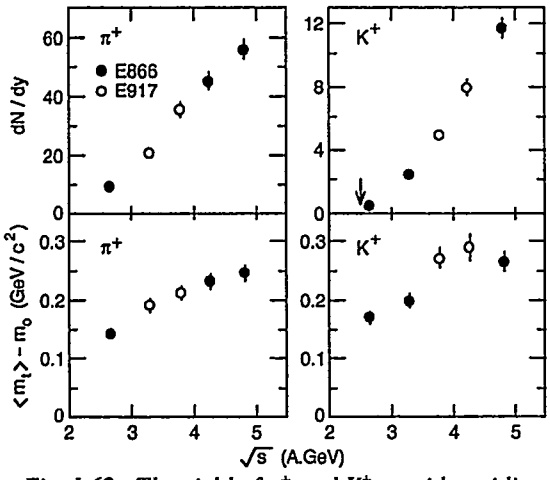

Fig. I-62. The yield of π^+ and K^+ at mid-rapidity (top panels) for central Au + Au reactions as a function of the initial available beam energy. The data from E866 are shown in filled circles and the data from E917 are shown as open circles. The lower panels show the mean m_t minus the rest mass for π^+ and K^+ at the same rapidity. The errors include both statistical and a 5% (dN/dy), 5% (mean m_t) point-to-point systematic uncertainty. The arrow indicates the threshold energy for producing K^+ in a p + p reaction.

By comparing the ratio of K^+ to π^+ at mid rapidity we find, however, a substantially stronger, but smooth increase in strangeness production (K^+) than expected from pure p + p collisions shown as circular points and the hatched area in Fig. I-63, respectively. This enhancement of strangeness production in nucleus-nucleus collisions is thought to arise from hadronic re-scattering processes within the hot interaction volume. There is, however, no experimental evidence for a sudden increase in strangeness production with beam energy, which has been suggested as a possible signal for the phase transition from hadronic matter to the quark-gluon plasma. A manuscript presenting this analysis has been accepted for publication in Physics Lett. B.[3]

It has been predicted that mass of K^+ and K^- may be modified in a dense medium, such as the one encountered in relativistic nucleus-nucleus collisions. This effect arises from the difference in the interaction between the two kaon species and the hadronic medium. Thus it is known that the mean-field interaction of K^- with baryons is attractive, whereas K^+ interaction is repulsive. We have therefore studied the differences in K^+ and K^- production with beam energy, which is expected to increase the density of the medium. In Fig. I-64 we show the ratio of rapidity density at mid-rapidity for K^- and K^+ production as a function of c.m. energy $\sqrt{s}$. The kaon production thresholds in p + p collisions at $s^{1/2}$ = 2.548 GeV for K^+ and $s^{1/2}$ = 2.864 GeV for K^- are indicated by the arrows. It is clear that the difference in phase space for the two production mechanisms has a strong effect also in heavy-ion collisions, although the production of both K^- and K^+ extend well into the sub-threshold region. However, when the data are plotted as a function of energy relative to the production threshold $s^{1/2} - s_{th}^{1/2}$ we find a distinctly different behavior above and below the threshold as shown in Fig. I-65. The earlier K^-/K^+ ratios measured for Ni + Ni (triangles) and C + C (open squares) by the KaoS collaboration at GSI cluster near unity whereas the data from the E866 and E917 experiments at the AGS result in K^-/K^+ ratios near 0.2.

The reason for this apparent discrepancy between the two data sets is not yet understood. However, a manuscript demonstrating these findings has been submitted to Phys. Rev. Lett.[4] A preliminary report on the pion and kaon data has been published,[5] and these data are the basis for the Ph.D. thesis of J. C. Dunlop, MIT.[6]

[3] L. Ahle *et al.*, Phys. Lett. **B476**, 1 (2000).
[4] L. Ahle *et al.*, submitted to Phys. Rev. Lett.
[5] W.-C. Chang *et al.*, "Advances in Nuclear Dynamics 5", Plenum Press, New York 1999, Eds. Bauer & Westfall, p. 215.
[6] J. C. Dunlop, Ph.D. Thesis, MIT 1999.

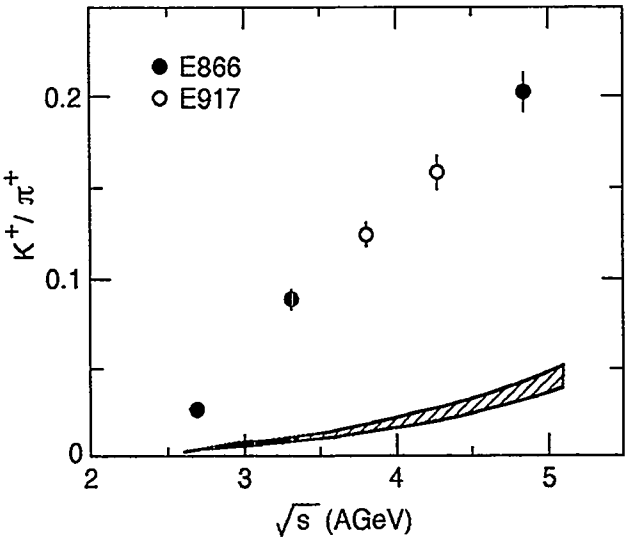

Fig. I-63. The radio of dN/dy for K^+/π^+ at mid-rapidity ion central Au+Au reactions as a function of the initial available energy. The data from E866 are shown as filled circles and the data from E917 are shown as open circles. The errors include a 5% systematic uncertainty. The hashed region is the K^{π}/π^+ ratio from the parameterized K and π yields from p+p reactions (see text for details). The hashed regon covers $\pm 1\sigma$ around the p+p K^+/π^+ ratio.

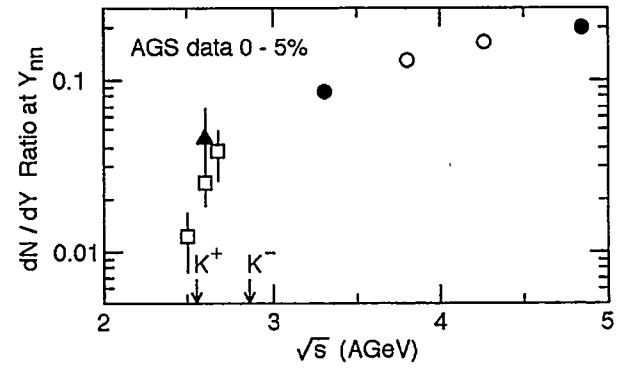

Fig. I-64. The K^-/K^+ ratio as a function of $s^{1/2}$ for central 0-5% Au+Au reactions. The data from E866 are shown as filled circles and the data from E917 are shown as open circles. Also shown are the K^-/K^+ ratios measured by KaoS in Ni+Ni (trangles) and C+C (open squares)

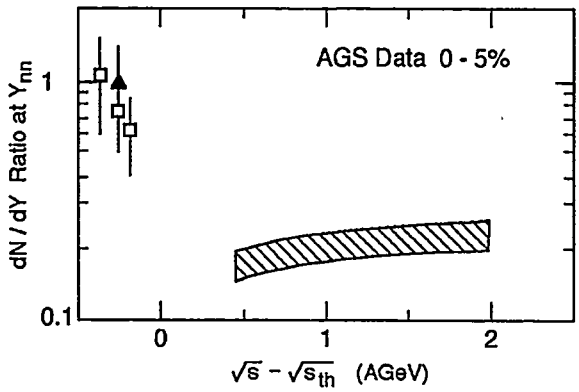

Fig. I-65. The K^-/K^+ ratio as a function of $s^{1/2} - s_{th}^{1/2}$. The hashed bands represent the data as $\pm 1\sigma$ bands calculated from the fitted K^+ and K^- yields for central 0-5% Au+Au reactions. Also shown in both panels are the K^-/K^+ ratios measured by KaoS in Ni+Ni (triangle) and C+C (open squares).

$\bar{\Lambda}$ and $\bar{p}$ Production

Recently, there has been particular interest in the strange anti-baryon channel in relativistic heavy-ion collisions because it combines the QGP signatures of antimatter and strangeness. Recent results from silicon beams at the AGS and from attempts to resolve a discrepancy between AGS experiments both suggest that the $\bar{\Lambda}$ to $\bar{p}$ ratio may be anonymously large. In this context it is of interest that E917 can provide direct information on both the $\bar{p}$ and $\bar{\Lambda}$ production, the latter being obtained directly from the $\bar{p}\pi^+$ decay channel.

The anti-proton production was measured at a beam energy of 10.8 GeV/nucleon over four rapidity bins of y = 1.0-1.1, 1.1-1.2, 1.2-1.3 and 1.3-1.4 and four centrality bins, namely 0%-5%, 5%-12%, 12%-23%, 23%-39%, and 39% - 77% of the total interaction cross section.

The $\bar{\Lambda}$ production was obtained from analysis of the invariant mass spectrum of $\bar{p}\pi^+$ pairs. Because of lack of statistics, only two bins in centrality namely 0%-23% and 23%-77% over the rapidity region y = 1.0-1.4, were obtained. Assuming that the $\bar{\Lambda}$ decay into $\bar{p}\pi^+$ is the only source of hyperon feed-down into the $\bar{p}$ channel, we calculate the direct $\bar{p}$ yield as $dN(\bar{p}_{direct})/dy = dN(\bar{p}_{measured})/dy - 0.64\ dN(\bar{\Lambda})/dy$, by correcting for the 64% branching ratio of $\bar{\Lambda}$ decays into the $\bar{p}\pi^+$ channel. The results of this analysis are listed in Table 2.

Table 2: This results in a $\bar{\Lambda}$ yields and inverse slope T of m_t spectra for 0%-23% centrality over the rapidity range y = 1.0-1.4 for 10.8 GeV/nucleon Au-Au collisions.

Particle	dN/dy	T (MeV)
$\bar{\Lambda}$	$1.56 \pm 0.64\text{-}0.45 \times 10^{-2}$	232^{+92}_{-51}
$\bar{p}$	$1.50 \pm 0.06 \times 10^{-2}$	196 ± 11

This results in a $\bar{\Lambda}$ to $\bar{p}$ production ratio of $N(\bar{\Lambda})/N(\bar{p}_{direct}) = 3.3^{+2.0}_{-1.7}$ which is consistent with the lower limit of 2.3 reported by the E864 collaboration.[7] A preliminary analysis of these data has been published,[8] and they were the basis for the Ph.D. thesis of George Heintzelman, MIT.[9]

[7] T. A. Armstrong *et al.*, Phys. Rev. C **59**, 2699 (1993).
[8] G. Heintzelman *et al.*, "Heavy Ion Physics from Bevalac to RHIC", Ed. Richard Seto, World Scientific, Singapore, 1999, pp. 205-209.
[9] G. Heintzelman, Ph.D. Thesis, MIT (1999).

Phi-mesons

The possibility of in-medium modifications of the width and/or centroid of the Φ-meson in Au - Au collisions at AGS energies was one of the original motivations for the E917 experiment. In this experiment the Φ-meson is measured via its decay in to the K^+K^- channel by construction of an invariant mass spectrum. The yields of Φ's were measured over the rapidity interval y = 0.9-1.4 and the data were divided into two independent centrality bins, namely 0-23% and 23-77% of the total interaction cross section. An intermediate, but overlapping, centrality bin of 12-39% was also studied. The yields, dN/dy and inverse slopes, T, of the m_t spectra are listed in Table 3.

Table 3: Inverse slopes, T, and yields, dN/dy of the Φ-meson as a function of the number of participants <NP>. (Preliminary results).

Centrality	$\langle N_p \rangle$	T (MeV)	dN/dy
0-23%	301	174 ± 56	0.252 ± 0.107
12-39%	200	229 ± 55	0.129 ± 0.027
23-77%	104	199 ± 44	0.058 ± 0.015

The Φ-yields and the ratio of Φ-meson to K^- production at mid-rapidity is also shown in Fig. I-66(a). We note that the Φ yield is proportional to the number of participants in the collisions, $\langle N_p \rangle$, although a larger than linear dependence cannot be ruled out on the basis of the data. In addition, we observe that the Φ/K^- ratio is essentially constant with $\langle N_p \rangle$. Concerning the centroid and width of the Φ mass peak in the invariant mass spectrum, we observe good agreement with the adopted values of m_Φ = 1019.4 MeV/c^2 and Γ = 4.4 MeV/c^2 in p-p scattering as listed in the Particle Data Book. The analysis of the Φ data is still in progress and additional statistical accuracy will be obtained. Preliminary results have been reported in conference proceedings,[10-12] and they are the basis for the Ph.D. Thesis of Hong Xiang, UC Riverside.[13]

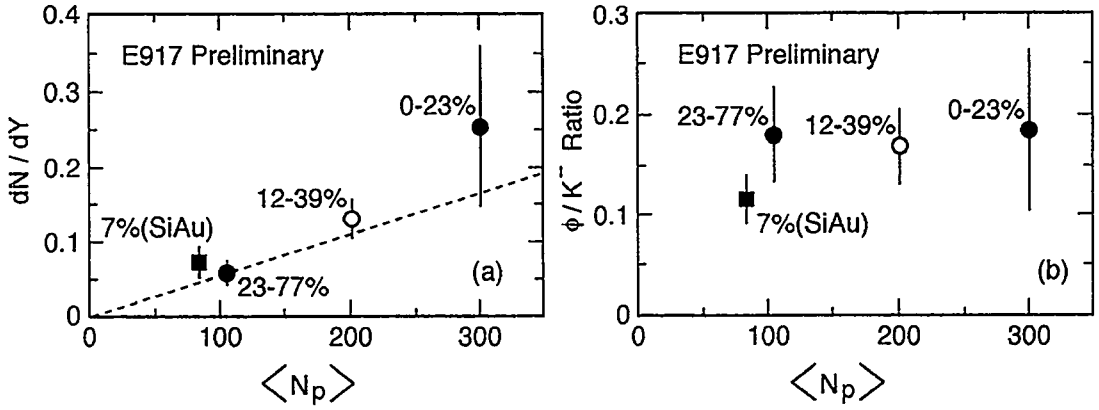

Fig. I-66. (a) Φ yield as a function of $\langle N_p \rangle$ and 0.9<y<1.4 from Table 3. (b) Φ/K^- ratio as a function of $\langle N_p \rangle$. The ratio for Si + Au is taken from ref. 5 and is for total yields.

[10] W.-C. Chang *et al*, Advances in Nuclear Dynamics 5, Plenum Press, New York 1999, Eds. Bauer and Westfall, p. 215.

[11] H. Xiang *et al.*, "Heavy Ion Physics from Bevelac to RHIC", Ed. Richard Seto, World Scientific, Singapore, 1999, p. 291.

[12] R. K. Seto *et al.*, Nucl. Phys. **A661**, 506c (1999).

[13] H. Xiang, Ph.D. Thesis, UC Riverside, 1999.

Reaction Plane and Collective Flow Studies

The study of flow phenomena in relativistic heavy ion collisions provides a method for obtaining information on the collective properties of the hot and dense system produced in such reactions. These studies require accurate information on the initial trajectory of the beam particle, which was obtained from the two upstream beam vertex detectors, built at Argonne. Each detector consists of two perpendicular planes of scintillating fibers, which are read out with position sensitive photomultiplier tubes. A detailed description of this detector system and its performance in the E917 experiment has been published.[14] An estimate of the orientation of the reaction plane is obtained by locating the azimuthal angle of the projectile remnant after the collision using the zero degree hodoscope. We have demonstrated that the accuracy of obtaining the reaction plane in this manner is approximately $\sigma_\phi = 50$ degrees.

The directed flow signal for protons and pions has been obtained using the Fourier analysis of the azimuthal distribution of particles. i.e.

$$dN/d\phi|_y = A(1 + 2\, v_1 \cos\phi)$$

where v_1 corresponds to the first Fourier moment of the ϕ-distribution.

As an example, we show in Fig. I-67(a-e) the ϕ distribution of protons for 10.8 GeV/nucleon beam energy and the 12-17% centrality bin. The rapidity bins are indicated in Fig. I-67. The solid curves represent the best fits to the data using the above expression. The resulting first Fourier moments, v_1 are shown as a function of rapidity bin in panel f; the open points are reflected around mid-rapidity. We observe a clear positive flow signal for protons in this centrality bin. Preliminary analysis of the flow signals from π^+, and π^- both show somewhat weaker flow signals, but in the opposite direction, i.e. anti-flow.

The data analysis of the collective flow characteristics obtained in E917 is continuing and is presently being extended to the 8 GeV/nucleon beam energy.[15] This work will constitute the Ph.D. thesis of John-Peter Stanskas, University of Maryland.[16]

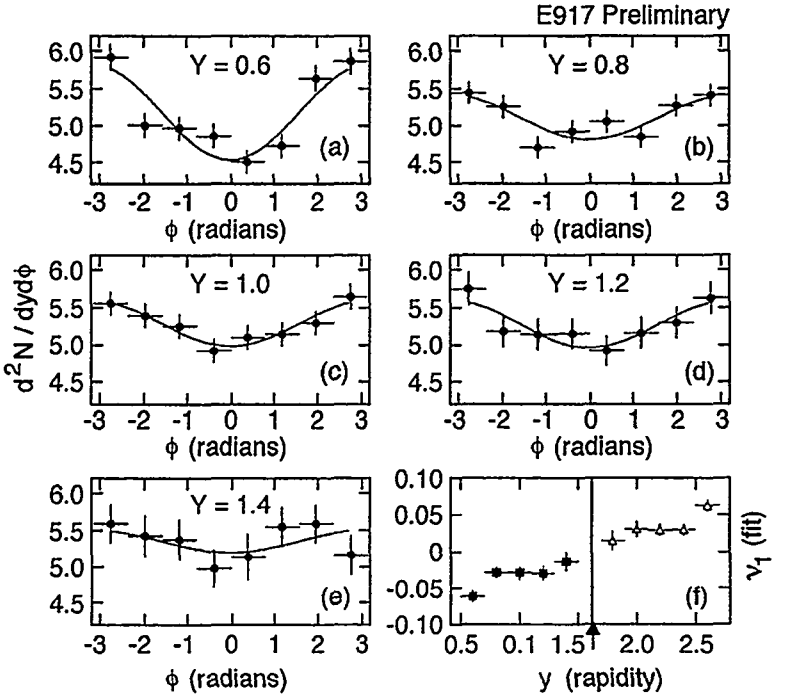

Fig. I-67. Proton directed flow signal. See text for details.

[14] Y. Akiiba *et al*, Phys. Rev. Lett. **76**, 2021 (1996)

[15] B. B. Back, R. R. Betts, A. Gillitzer, W. F. Henning, D. J. Hofman, V. Nanal, A. H. Wuosmaa, R. Ganz, B. Holzman, D. McLeod, W. R. Winns, and J. W. Epstein, Nucl. Instrum. Methods **A412**, 191 (1998)

[16] D. J. Hofman *et al.* "Heavy Ion Physics from Bevalac to RHIC", Ed. Richard Seto, World Scientific, Singapore, 1999, p. 98.

Two Particle Correlations

Applying the Hanbury-Brown Twiss analysis to correlations between identical particles is an important tool for studying the size and possibly the shape of the hot fireball, from which these particles are emitted, provided certain conditions are fulfilled. We are applying this type of analysis to pairs of π^+ π^+ and π^- π^- pairs from Au - Au collisions at 6, 8, and 10.8 GeV/nucleon. If sufficient data are available this analysis will also be applied to pion-pairs emitted at specific azimuthal angular bins relative to the reaction plane in order to attempt to determine possible non-spherical momenta of the fireball and/or shadowing effects of the spectators. Preliminary results from this analysis have been published in conference proceedings.[17-18] This work will also constitute the Ph.D. thesis for Burt Holzman, University of Illinois at Chicago.

[17]B. Holzman *et al.* "Advances in Nuclear Dynamics 5", Plenum Press, New York, 1999, Eds. Bauer and Westfall, p. 189.

[18]B. Holzman *et al.*, "Heavy Ion Physics from Bevalac to RHIC", Ed. Richard Seto, World Scientific, Singapore, 1999, p. 59.

d.3. Heating of Nuclei with Pions and Anti-Protons

(B. Back, T. Lefort,* K. Kwiatkowski,* W.-C. Hsi,* L. Pienkowski,† L. Beaulieu,* H. Breuer,‡ S. Gushue, ¶ G. Korteling, ¶ R. Laforest,** E. Martin,** E. Ramakrishnan,** L. Remsberg,§ D. Rowland,** A. Ruangma,**V. E. Viola,* E. Winchester,** and S. J. Yennello**)

Studies of the heating of heavy nuclei (Au) using antiprotons and π^- projectiles of momentum 8 GeV/c have been carried out at the Brookhaven AGS accelerator using the Indiana Silicon Sphere 4π detector array. It is found that enhanced energy deposition is achieved with anti-protons as compared to negative pions at this energy as illustrated in Fig. I-68. The results indicate the formation of thermal-like heavy residues with excitation energies of up to 1.5 GeV. The results are compared with the intra nuclear cascade model. Some of the results are published in Refs. 1-2.

[1]Lefort *et al.*, Phys. Rev. Lett. **83**, 4033 (1999).

[2]L. Beaulieu *et al.*, Advances in Nuclear Dynamics, 5, Eds. Bauer & Westfall, Plenum Publishers, New York, 1999, p. 1.

*Indiana University, †Warsaw University, Poland, ‡University of Maryland, §Brookhaven National Laboratory, ¶Simon Fraser University, Canada, **Texas A&M University

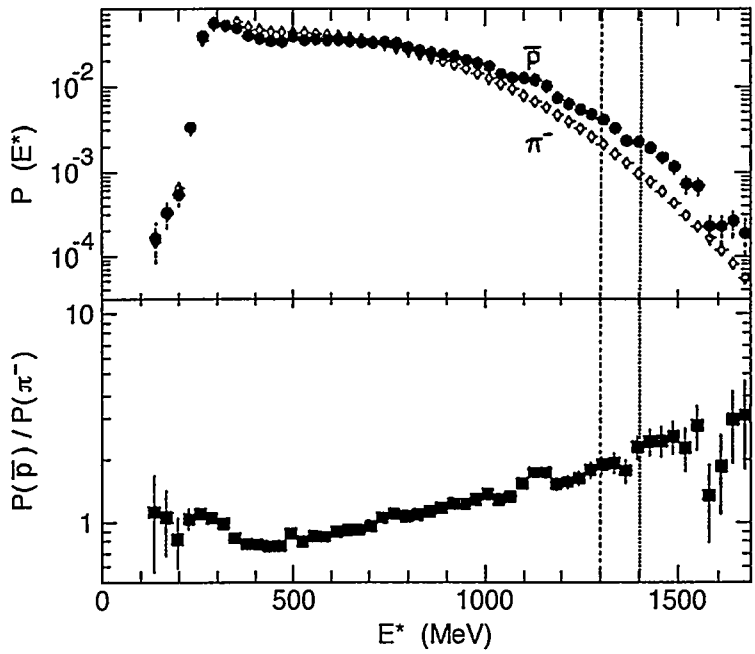

Fig. I-68. Upper panel: Excitation-energy probability distributions for reactions of 8 GeV/c π^- (diamonds) and $\bar{p}$ (circles) with ^{197}Au. Lower panel: Ratio of excitation-energy probability for $\bar{p}$ relative to that for π^-. E^* values beyond the vertical lines (dashed: π^-; solid: $\bar{p}$) account for 1% of events.

d.4. The PHOBOS Experiment at RHIC (B. B. Back, N. George, A. H. Wuosmaa and the PHOBOS Collaboration - ANL, BNL, Krakow, MIT, NCU Taiwan, ORNL, U. of Rochester, UIC, and U. of Maryland)

Overview

At RHIC, heavy ions will collide at center of mass energies an order of magnitude higher than have previously been available anywhere. There, it is expected that a baryon-free region of extremely high energy density will remain after the two colliding nuclei have passed through each other. It is believed that this situation will be more than sufficient to create a system of deconfined quarks and gluons - the "Quark Gluon Plasma". After formation, the plasma should expand and cool before passing into the normal hadronic phase which in turn further expands until the hadrons cease to interact with each other ("freezeout"). The questions are then what are the direct probes and signatures of the plasma phase, and what identifiable traces of the quark-gluon phase remain in the observed hadronic final state? The PHOBOS experiment seeks to address these questions.

The PHOBOS experiment focuses on measurements of hadronic observables for a very large sample of events. The PHOBOS apparatus consists of a 4π multiplicity detector and two multi-particle spectrometers capable of measuring and identifying particles with very low transverse momenta. The multiplicity detector will provide event-by-event charged-particle multiplicity distributions, which can be used to find interesting events for study in more detail using the spectrometers. The multiplicity distributions are interesting on their own, and contain information on fluctuations and correlations, which relate to some of the proposed signatures of the plasma.

An overall view of the PHOBOS apparatus is shown in Fig. I-69; several different components are identified. The fabrication of the multiplicity and Vertex detectors is the responsibility of the groups at Argonne and UIC. Together, these systems contain over 22000 channels of silicon pad detector.

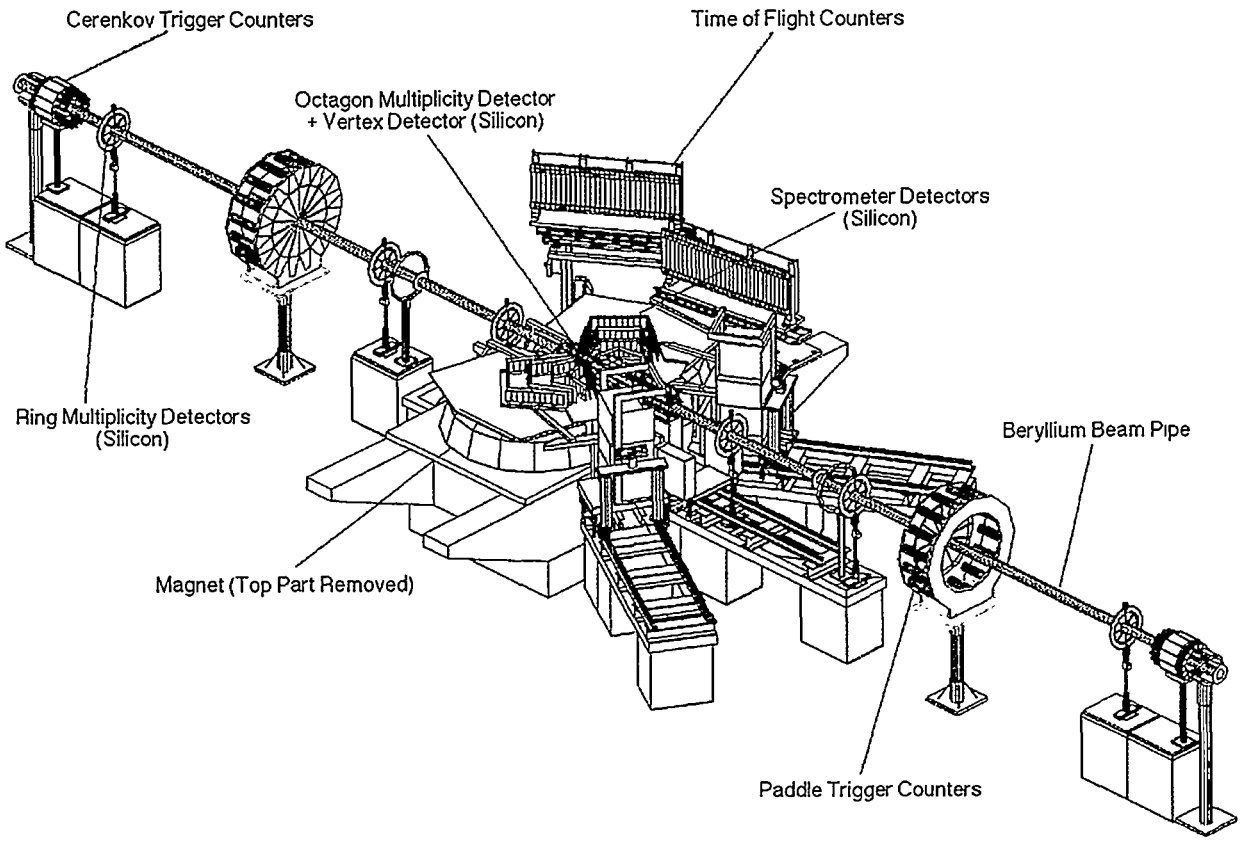

Fig. I-69. Overview of the PHOBOS experimental setup. The top half of the spectrometer magnet has been removed for clarity.

The Multiplicity detector will provide event-by-event information on the charged particle multiplicity distributions over ±5 units of pseudo-rapidity, with complete azimuthal coverage. For central Au + Au collisions at RHIC, the total charged particle multiplicity in this pseudo-rapidity range is expected to be of order 6000 or greater. The multiplicity measurement is made using a centrally located, 11000 channel "Octagon" array of silicon pads supplemented with six 512 channel "Ring" counters placed up and down the beam pipe. These detectors will measure the energy deposited as a function of angle with respect to the collision vertex. Multiple hits can be handled in an average way by dividing the measured energy by the average expectation for a single charged particle at that point in the detector. Monte Carlo studies have shown that the charged particle multiplicity distributions for central Au + Au collisions can be reconstructed with systematic errors small compared to normal Poisson fluctuations.

The Vertex detector is designed to locate the position of the interaction vertex on an event by event basis. It is composed of two pairs of planes of silicon pad detectors, each plane segmented into 2048 channels so that the occupancy is low. Particles emitted from the collision vertex can be tracked by combining pairs of hits on the inner and outer Vertex planes such that the position of the reconstructed interaction point can be determined to a precision of better than 300 μm. Vertices may be reconstructed over the entire range of the RHIC collision diamond, corresponding to ±20 cm about the center of the intersection region.

In the past 12 months, the PHOBOS experiment has undergone a tremendous amount of progress, and at this writing, all of the detector components required for the experiment for the first years running are complete. The following sections describe the status of elements which are the primary responsibility of the ANL/UIC collaboration, i.e. the multiplicity and vertex detectors.

Assembly and Testing Status

The assembly and quality control testing procedures of the detector modules that make up the Multiplicity and Vertex detectors in PHOBOS are carried out at the University of Illinois at Chicago, ANL, and the Silicon Detector Facility at Fermi National Accelerator Laboratory. The hybrids that carry the front-end electronics chips for each detector module are initially fabricated under the supervision of the MIT electronics laboratory. These circuits, which consist of either 128, or 64, channels of charge-sensitive preamplifier and shaping elements, are mounted on the hybrids. Micro-wire bonding of electronics connections between the preamplifier chip and the hybrid was carried out at FNAL, and the units are subsequently electronically tested at ANL. Those that pass the initial quality control evaluation are returned to UIC, where the silicon sensors are affixed to them. The now fully-fledged detector modules are returned to FNAL, where the individual channel connections are made by additional wire bonding. The resulting detector modules return to ANL where they are further evaluated, both with electronic testing, as well as with radioactive sources. Those modules that pass all quality control evaluations are then used for installation in the experiment.

At present, all silicon modules needed for the multiplicity and vertex detector arrays are complete. This complement includes 128 Multiplicity Octagon and 50 Multiplicity Ring modules, and 21 Vertex detector modules, containing over 33000 channels, all of which have been subjected to the various acceptance tests. These have been delivered to BNL.

Installation and Testing of the Complete PHOBOS Detector

At the end of 1999, the modules that make up the Year 1 physics detector for PHOBOS were mounted on their respective frames. The assembled mid-rapidity frame carrying 94 Octagon, and 12 Vertex detectors, and the six high-η ring multiplicity arrays each carrying 8 ring detector modules, were assembled at BNL. Figure I-70 shows the assembled octagon, and two ring detectors, in the assembly laboratory at BNL.

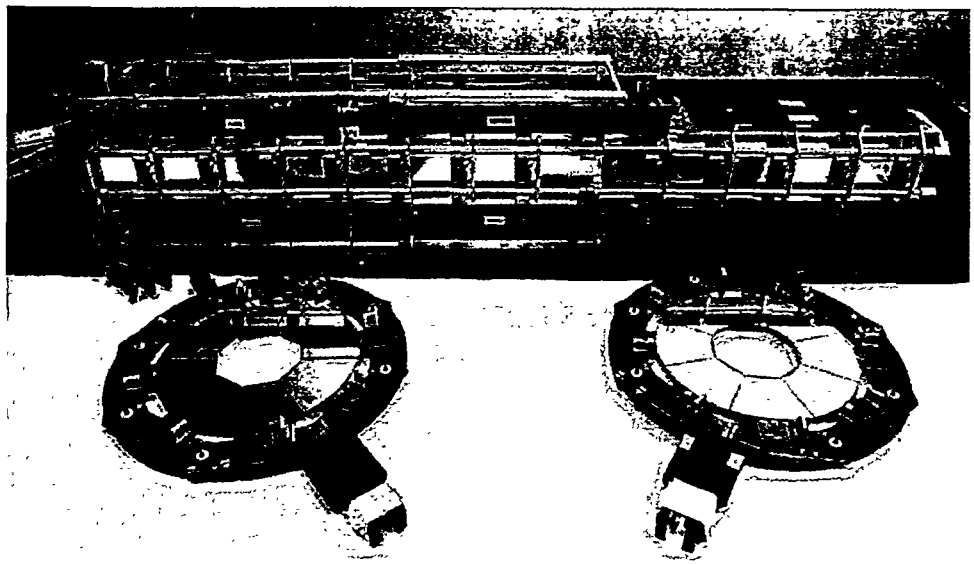

Fig. I-70. Assembled Octagon and Ring detectors for PHOBOS in the assembly laboratory at Brookhaven National Laboratory.

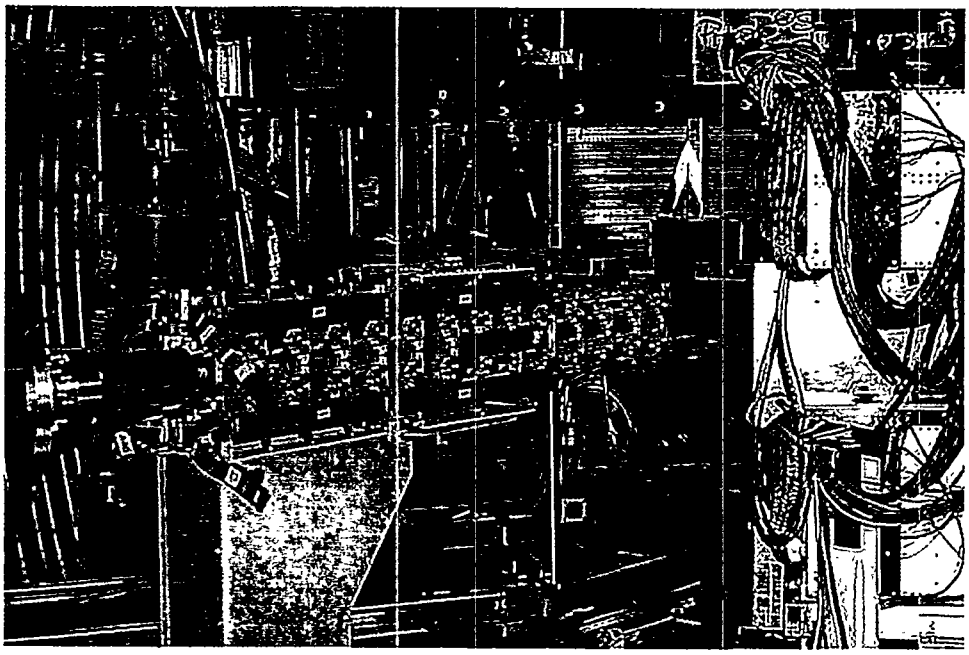

Fig. I-71. Central multiplicity and vertex detector assembly installed in the RHIC tunnel around the beam pipe, prior to insertion into the central magnet gap.

After the detector modules were mounted on their respective frames, these frames were installed in the experimental hall in the RHIC tunnel. Figure I-72 shows the loaded octagon frame in position around the beam pipe, prior to insertion into the central magnet gap. Figure I-72 shows one of the six ring arrays, as well as one of the two high-η Cerenkov trigger detector arrays, also in position around the beam pipe. With this installation, the construction of PHOBOS is essentially complete, signifying a major milestone for the PHOBOS experiment.

The stability and performance of the system was evaluated over a 4-day period in early 2000. Detector leakage currents, pedestals, noise and gain for each of the approximately 70000 channels in the full experiment were monitored for stability, and also as a test of the full data acquisition system. The stability of the full system was excellent, with gain and pedestal variations of order 1% or less. The temperature and leakage current stability was also excellent, owing to the performance of the chilled water cooling system that keeps all silicon detector elements of the experiment at a constant temperature. Subsequent to this test, the full complement of the detectors to be used in the Year-1 physics run was removed, and replaced with a limited subset of silicon modules. This was done in order to protect the silicon and front-end electronics chips from the harsh radiation conditions expected during the tuning and commissioning stages of beam development for Year-1 physics running (see below).

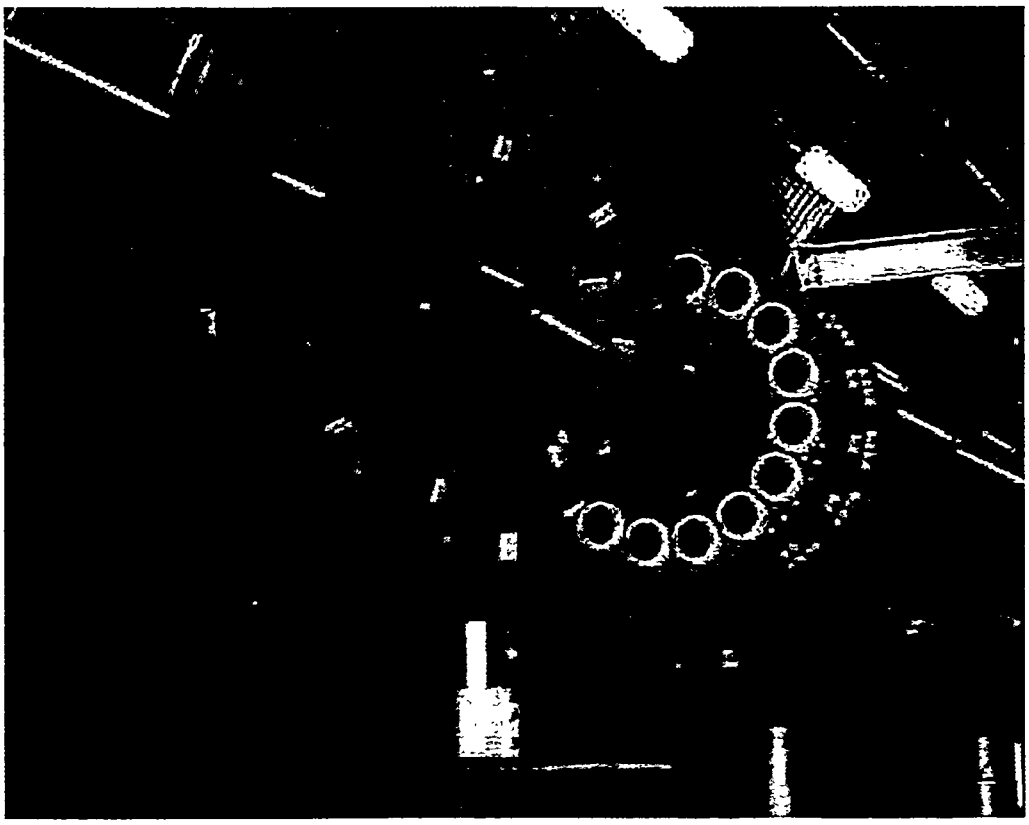

Fig. I-72. One of six multiplicity ring detectors, and one of two high-η trigger detectors installed around the RHIC beam pipe.

The Summer Engineering Run and First Beam in RHIC

During the summer of 1999, the first Au beams were injected and circulated in the RHIC rings. The purpose of this running period was to commission the accelerator, to understand the collider optics, and to provide the experiments with the first possibility to obtain data with injected beams. During this period Au beams from the BNL AGS were injected with an energy of 10.8 GeV/nucleon, and were circulated in the two RHIC rings individually. In one of the two rings (the "Blue" ring), reasonable tuning conditions were achieved and stable orbits with lifetimes of the order of 1000s of turns were obtained. For the second ("Yellow") ring, somewhat poorer results, with beam lifetimes of order only 100s of turns, were obtained before termination of the Engineering Run. In addition to evaluation of the collider optics, the RF system was exercised and capture was achieved (a necessity for long beam lifetimes), and some acceleration was performed for beams in the Blue ring. At no time were beams present simultaneously in the two rings, and consequently no collisions were produced. Despite this, there were events from the scattering of the Au ions from residual gas, as well as from beamline components that produced particles that could be detected in the experiments.

PHOBOS employed a subset of its full physics detectors for data taking during the engineering run. A single "ladder" of octagon multiplicity modules, two vertex detectors, and a component of trigger and plastic-scintillator detectors, were installed in the RHIC tunnel. These were read out with at prototype version of the PHOBOS data acquisition system. The trigger detectors were capable of firing either on beam-induced, or Cosmic-ray particles. Figure I-73 shows a histogram of the energy deposited by cosmic-ray particles passing through the octagon detectors. A clear minimum-ionizing peak is observed at an energy of approximately 100 keV deposited in the detector.

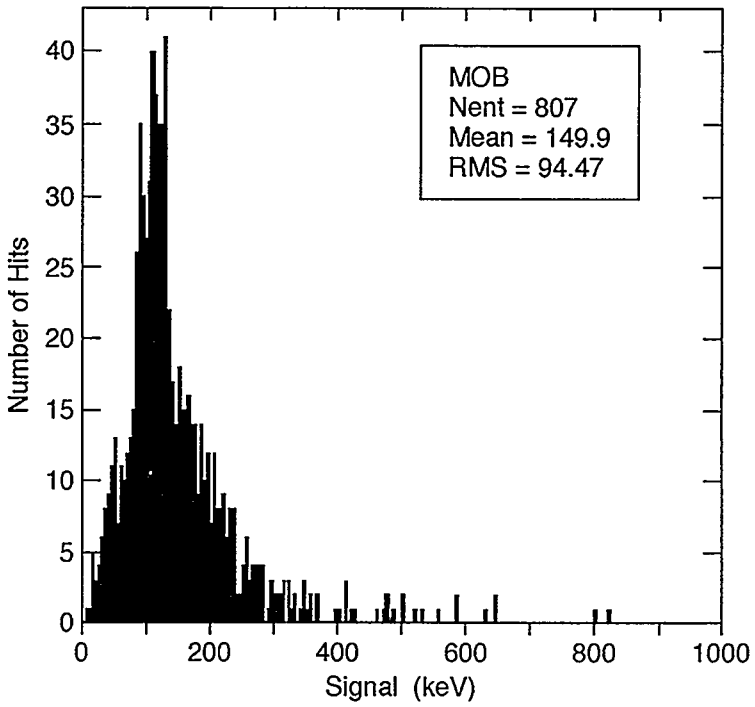

Fig. I-73. Histogram of energy loss in the Engineering run octagon detector. The peak corresponding to minimum ionizing particles is at an energy of 100 keV.

Figures I-74 and I-75 show spectra of energy deposited in the octagon and vertex detectors from particles produced by interactions of the Au beam with either residual gas or components of the RHIC beamline. The differences in the widths of the two minimum-ionizing peaks arises from the fact that most of the beam induced particles are produced moving nearly parallel to the beam, and intersect the silicon detectors at very small angles. The vertex detectors possess much

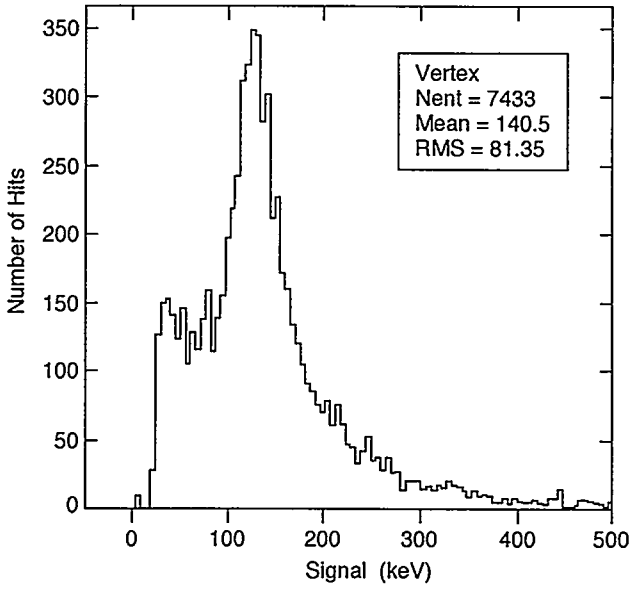

Fig. I-74. Energy-loss spectrum for beam induced particles detected in a Vertex sensor.

smaller pads than those in the octagon sensors, and therefore the particles traverse a smaller volume of silicon, and deposit a correspondingly smaller amount of energy in the vertex pads, as compared to the octagon.

On occasion, there would be events that produced very large numbers of particles resulting in large observed energy deposition signals in all channels of the silicon detectors. These so-called "blast" events, presumably arising from an entire bunch of Au ions impacting a beamline magnet or other component, had a detrimental effect on the silicon performance, and often resulted in a phenomenon known as "CMOS latchup". Under this condition, the front-end electronics chips fail to work properly, although generally this failure condition was recoverable. A consequence of this observation was that the front-end control electronics was modified to identify this condition and to protect the front-end electronics chips from it. In addition, the decision was made to postpone installation of the full detector system for the initial physics run until stable beam conditions were achieved in the RHIC rings.

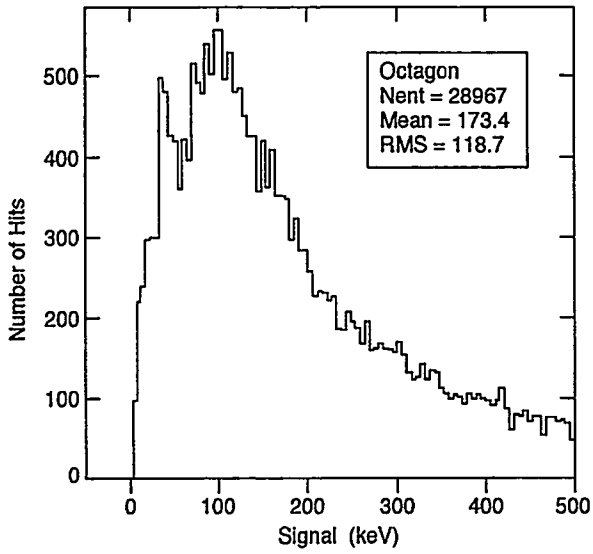

Fig. I-75. Energy-loss spectrum for beam induced particles detected in an Octagon sensor.

Multiplicity Reconstruction and Early Physics Analyses

In preparation for the first data from PHOBOS, much consideration is being given to the first data analyses, and to the extraction of physics results. Chief among these are the values of the rapidity density $dN/d\eta$ at mid-rapidity, and the multiplicity distribution for charged particles as a whole. For the important quantity $dN/d\eta|_{\eta=0}$, data from the central region of the octagon, as well as from the vertex detectors and the forward spectrometer planes, are all important. The chief uncertainties in any analysis of charged-particle multiplicity in PHOBOS arise from both the contributions of secondary particles, and from the transformation of measured energy-deposition signals to the number of particle tracks within a given pad in the silicon detectors. Near mid-rapidity, the vertex detectors and most highly segmented spectrometer planes are able to resolve individual particle tracks. A comparison of these measurements to the multiplicity determined from the energy deposited in the larger octagon detector pads constitutes a valuable crosscheck for the multiplicity determination. Analyses of Monte-Carlo data designed to study this problem are currently underway.

Beyond mid-rapidity, the octagon is the primary tool for measuring charged-particle multiplicity, although these determinations will be compared with, and augmented by, other measurements from the trigger counters and zero-degree calorimeters in order to correlate the multiplicity data with other experimental parameters, such as impact parameter. Away from mid-rapidity, it is expected that the backgrounds from secondary particle production will be considerable. One task of the early data analysis will be to understand these backgrounds and to determine how they affect the reconstructed multiplicity distributions. Once these issues are resolved, the multiplicity data will be used to confront the predictions of the various event generators, to identify possibly interesting events with large multiplicities, and to search for unusual fluctuations in

dN/dη as possible evidence of new physics. An example of the kind of data that may be obtained with the multiplicity detector array appears in Fig. I-76, which shows typical multiplicity distributions for central events obtained from the event generator HIJING. Shown in Fig. I-76 are the distribution from a single event as predicted by HIJING, that same distribution as reconstructed by PHOBOS, and the average multiplicity distribution from 200 such events. Current indications are that the systematic uncertainties introduced by the multiplicity reconstruction procedure will be comparable to, or smaller than, the statistical uncertainties inherent in the data.

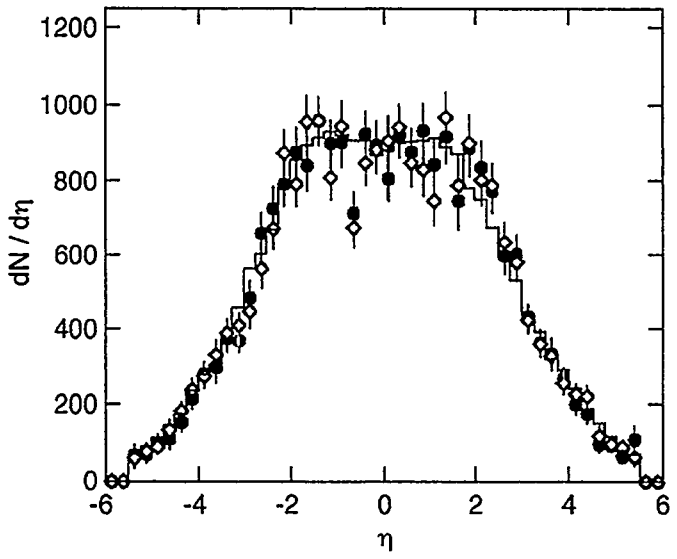

Fig. I-76. Multiplicity distribution from one HIJING event (solid symbols), the same event reconstructed (open symbols) and the average of 200 HIJING events (histogram).

Status and Schedule

RHIC is presently scheduled to begin injection and tuning of Au beams for the Year-1 physics run in April-May 2000. As discussed above, while the PHOBOS hardware is complete, for the initial beam tune of RHIC, the full PHOBOS apparatus will not be present in the tunnel. Instead, a subset of detectors including one ladder of octagon sensors, 1/4 of the Vertex detector, 4 planes of tracking spectrometer, and trigger detectors will be installed. The initial beam tune is expected to take of order 1 month, from injection to tuning for collisions. Following this tuning period, the commissioning setup will be removed from the tunnel, and replaced with the full apparatus. As previously noted, this installation is projected to require no more than approximately two weeks. Data taking with the full physics setup will continue until the conclusion of the Year-1 run, at the end of August 2000.

E. FUNDAMENTAL INTERACTIONS AND OTHER TOPICS

This section covers research activities with the Canadian Penning Trap (CPT), an instrument operated by a large collaboration of Canadian and American scientists. The device aims at high-precision determination of atomic masses of short-lived isotopes. One of the main directions of research is high-precision measurements of the mass of super-allowed 0^+ to 0^+ beta emitters ($50<A<100$). These mass determinations have a direct impact on the determination of the fundamental weak vector coupling constant and the unitarity test of the top row of the Cabbibo-Kobayashi-Maskawa matrix. This year the trap was brought into full operation.

This section also describes efforts devoted to a number of other topics such as: (1) the physics of cooled, confined beams; (2) the search for the first excited state in ^{229}Th; (3) the development of a new method to measure the electric dipole moment of the neutron; (4) recent efforts in accelerator mass spectrometry; (5) the study of nuclear excitation by electronic transitions; and (6) the determination of the half-life of ^{44}Ti.

e.1. Progress at the Canadian Penning Trap Mass Spectrometer

(G. Savard, R.C. Barber,* F. Buchinger,† J. Caggiano, J. Clark,* J.E. Crawford,† H. Fukutani,* S. Gulick,† J.C. Hardy, ‡ J.K.P. Lee,† R.B. Moore,† J. Schwartz, D. Seweryniak, K.S. Sharma,* J. Vaz*

The Canadian Penning Trap (CPT) Mass Spectrometer installed at ATLAS is a device aiming at the precise determination of the atomic masses of short-lived isotopes. It uses a combination of two ion traps, a radio-frequency quadrupole (RFQ) trap and a precision Penning trap, to capture and accumulate short-lived isotopes and confine them at rest in vacuum. This then enables properties of these isotopes to be precisely determined using a sample size as small as a few ions injected in the measurement trap. The radioactive ions to be injected in the CPT are produced at the target location of the area II gas-filled Enge spectrograph, separated and collected at the focal plane in a RF gas cooler designed to stop, cool and accumulate these unstable isotopes and transfer them as a pulsed low-energy beam to the CPT. The main components of the system are shown below in Fig. I-77.

*University of Manitoba
†McGill University
‡Texas A&M

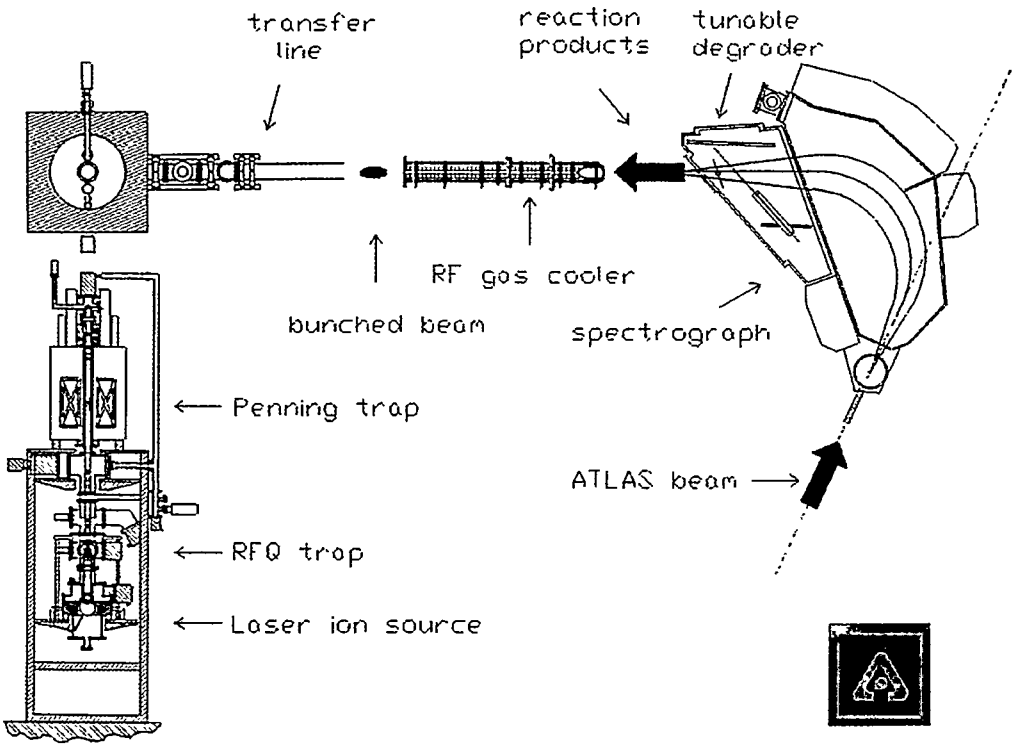

Fig I-77. Main components of the CPT spectrometer and its injection system at ATLAS.

The work performed this year at the CPT mass spectrometer centered around the completion of the injection system and transfer line, together with various improvements in the operation of the CPT itself. Progress on the various subsystems will be described below in the order in which the beam sees them.

The production of the radioactive isotopes takes place in the target chamber of the area II split pole spectrograph. The spectrograph is used in the gas-filled mode with a rotating window located at the entrance of the chamber and the production target sitting in the gas. Various window materials have been tested and we have now settled on 200 $\mu g/cm^2$ Carbon and 250 $\mu g/cm^2$ Aluminum for applications where low gas pressures (below 5 Torr) are required in the magnet. The light materials minimize scattering in the window which created significant background in the diagnostics tools in the spectrograph. These windows, together with most targets, can tolerate high currents since they are cooled by the gas in the chamber and we now routinely operate with beam currents of 0.5 μA or higher. A small tantalum beam stop has also been added at 0 degrees at the entrance of the spectrograph to minimize the amount of direct beam entering it.

The gas-filled magnet itself has seen a number of changes. The main magnet power supply was not aging well and overheated above 13 kGauss. It has been replaced by a more modern supply which was available and as a result it can now run at the full magnet specification which is 17 kGauss. The gas-filled magnet is now also operated with helium gas instead of nitrogen gas for medium mass nuclei. This significantly improved the separation between the reaction products and the beam tails at the focal plane. The RAYTRACE program used to simulate operation of the Enge spectrograph in the gas-filled mode has also been upgraded to better reproduce the target and zero degree cup geometry and modified acceptance. In the same vein, a large area PPAC was modified to run in transmission mode and is now used for diagnostics in the spectrograph. The PPAC provides clean identification of the reaction products via position and timing against the accelerator RF structure (see Fig. I-78). Since the PPAC is now a transmission device it can be left in location when we stop the recoils in the gas cell system; the unbiased PPAC then becomes an energy degrader. Finally, a tunable degrader was installed at the entrance of the gas cell and is used to center the range of the recoils into the gas cell.

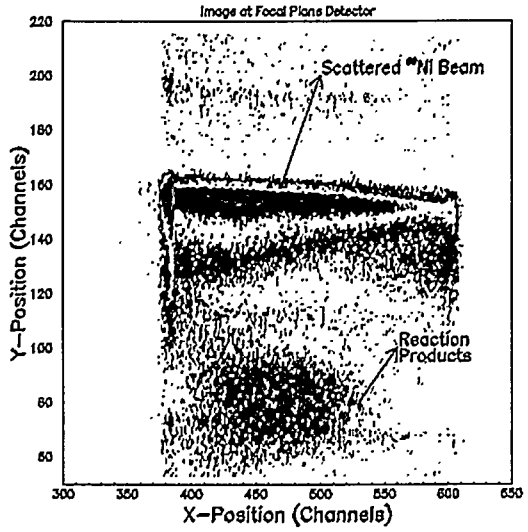

Fig. I-78. Timing vs position signal obtained with the PPAC. During tuning of the Enge, the accelerator is run with one RF bucket out of every four filled giving a 340 ns time window between beam pulses. The reaction products for this particular reaction arrive at the detector about 150 ns after the tail of the beam (time runs down on the ordinate of the graph at a rate of about 2 ns per channel).

The gas cell and RF cooler system have also been significantly improved over the course of the year. As reported in section f.6, the gas cell extraction plate has been modified to obtain higher focusing fields inside the cell which resulted in a significant increase in efficiency. The segmented rod structures in the RF cooler have also been modified to eliminate shorting problems observed across previously used thin mica insulators and improve mechanical alignment. The RF power distribution to the different sections has also been modified with the first section now operating as a tuned circuit at high frequency to obtain maximum transmission while sections 2 and 3 have their RF coupled through broadband systems providing more flexibility when operating in different mass ranges. Sections 2 and 3 are used in a mass selective mode which allows distant contaminants to be removed early on in the process of injection into the CPT minimizing space-charge related problems.

The transfer line connecting the RF gas cooler and the CPT was completed this year. The transport of the bunched ions is done at low potential (about 1500 eVs) by a purely electrostatic system. The transport line is shielded from the stray field of the CPT superconducting magnet by μ-metal and diagnostics is provided by sets of micro-channel plate and Si detectors which can be moved in and out of the ions path. They provide both ion signals and radioactivity signals depending on the species being transported. The transport line was commissioned with stable ions and activity produced on-line by fusion-evaporation reactions.

The ions transported by the transfer line are captured first in the RFQ trap of the CPT. The control system was modified to synchronize the ejection out of the RF gas cooler to bring the ions at a well-defined injection phase into the RFQ trap. To handle the wide range of masses that the system must cover we have also modified the RFQ trap which now operates with the RF provided by a high-power switching system delivering high-voltage square waves to the ring instead of the usual sinusoidal waveform. This greatly simplifies the computer control and phasing of the different systems since no tuned circuits are necessary to feed in the RF power. This eliminates the phase shifts in the feeding circuits which made the synchronization of the different components difficult to achieve over a wide mass range. The ejection from the RFQ trap and transfer to the precision Penning trap has also been significantly improved with a more sturdy high-voltage linear amplifier for the ramp cavity used to match the phase-space of the ions ejected from the RFQ trap to the acceptance of the Penning trap.

The Penning trap itself has seen few modifications except for a more flexible ensemble of pulse generators to improve the electrostatic potential during the ion capture phase and operation of the trap with a 10 volts potential depth which increases the capture efficiency. Modifications of the control system also allow for more versatile cleaning of the ions inside the Penning trap so that contaminants can be removed more effectively before the actual mass measurement is performed.

The completion of the system and the numerous improvements and fine tuning steps have led to the

successful stopping and cooling of radioactive ions in the gas cell, bunching in the RF cooler, transfer to the RFQ trap and finally to the high-precision Penning trap where they have been identified and their mass measured. In this process, the effectiveness of the various cleaning processes used in the system has been demonstrated, as was the ability to separate isobars (see Fig. I-79).

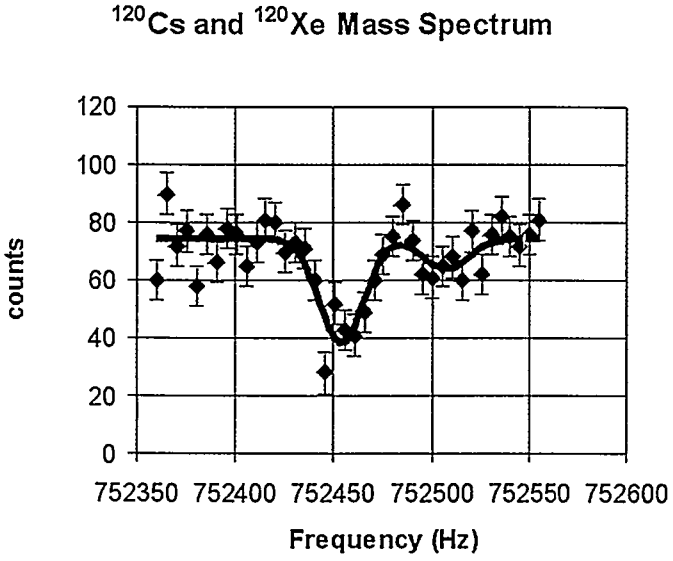

Fig. I-79. Mass spectra showing the separation between ^{120}Cs and ^{120}Xe with both species loaded simultaneously in the Penning trap. The ordinate is the number of ions left in the trap after the excitation, demonstrating that two close isobars can be independently manipulated in the trap.

e.2. Development of a Large Accelerated Gas Cell System for the Collection of Fast Recoiling Radioactive Ions

(G. Savard,* J. Schwartz,* J. Caggiano,* J. Clark,† H. Fukutani,† J. Greene,* M. Maier,*,† D. Seweryniak,* K.S. Sharma,† B. Zabransky*)

A large gas cell system was developed last year for the injection of radioactive ions into the CPT mass spectrometer system at ATLAS. It uses a large high-purity helium gas volume where fast reaction products separated by the area II gas filled spectrometer are stopped and thermalized as 1+ ions before being extracted by a combination of gas flow and DC and RF electric fields. The efficiency with this seminal system was of the order of 20% which demonstrated both i) the fast extraction possible with large gas cells when electric fields are used to assist the extraction process and ii) the large efficiencies that can be achieved with large gas cells when the ionizing primary beam does not enter the stopping gas volume.

While the stopping volume used is much larger than in standard IGISOL type system, other possible applications require rapid thermalization of fast ions covering even larger effective stopping ranges. In particular, as part of an application initially proposed at Argonne and which has now become an integral part of the RIA concept, it is proposed to use intense energetic heavy-ion beams to produce short-lived nuclei by projectile fragmentation, perform in-flight fragment analysis and separation on the fast moving recoils and stop the fragments in a large helium gas cell from which they would be quickly extracted as singly-charged ions and reaccelerated. This scheme combines the intrinsic advantages of in-flight fragmentation – short delay times – with those of the ISOL concept – high-quality beams of precise energy as required by experiments. It does, however, require much larger stopping volumes than even what was achieved with the original cell at the CPT. For this reason, development of a gas cell which would provide a larger stopping range while maintaining the fast extraction time was initiated.

*University of Manitoba
†GSI

The delay time studies performed last year on the initial gas cell with Argon as a stopping gas were first extended to helium gas. Calculations performed with the complex simulation package we have developed to model the gas cell behaviour predicted very fast extraction times even at modest DC gradients inside the cell with helium as a stopping gas. These studies, performed by pulsing the ATLAS beam on a slow time cycle and observing the delay between the ions extracted from the cell and the primary beam, confirmed these predictions. As shown in Fig. I-80, we observed mean extraction delay times as long as 200 ms without fields which decreased to as low as 7 ms for the highest extraction field that could be applied at that time. It was also noted that at even higher extraction fields the extraction efficiency was starting to decrease from which we concluded that higher focusing forces were needed at the extraction region to further decrease the delay times.

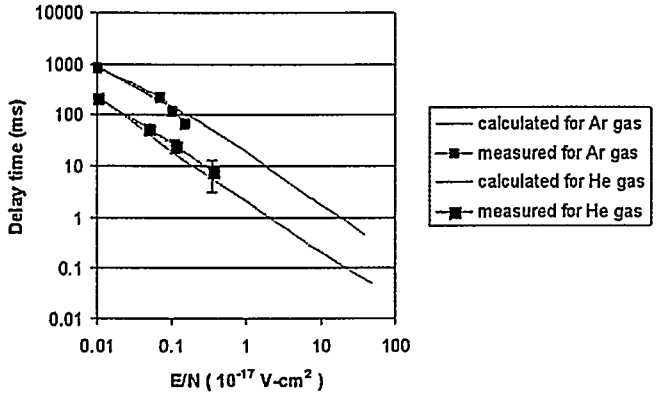

Fig. I-80. Mean delay time between injection of a pulsed beam in the gas cell and extraction of the ions out of the cell as a function of the electric field gradient applied inside the cell.

Major efforts during the year were therefore put at increasing the focusing strength at the extraction end of the cell and at the same time increasing the purity of the stopping gas. The gas delivery system was modified to purify the gases by the addition of a Monotorr (SAES getter inc.) getter system, a totally stainless steel delivery system with high-purity valves, pressure regulators and fittings, and a UHV quality construction for the components of the cell. The focusing at the extraction of the cell was improved with an improved geometry for the extraction system which allowed for the RF focusing used along the body of the gas cell to be more effective close to the extraction aperture. The effective RF-focusing force exerted on the ions inside the gas scales as where $\partial E/\partial r$ is the

$$F_{RF} = -\frac{eA}{2}\frac{\partial E}{\partial r}\cos\theta$$

RF-field gradient, A the amplitude of the RF motion and θ the phase of the motion in the RF field. The modified geometry allows us to increase the RF-field gradient and hence the effective focusing force. The new gas cell is shown in Fig. I-81.

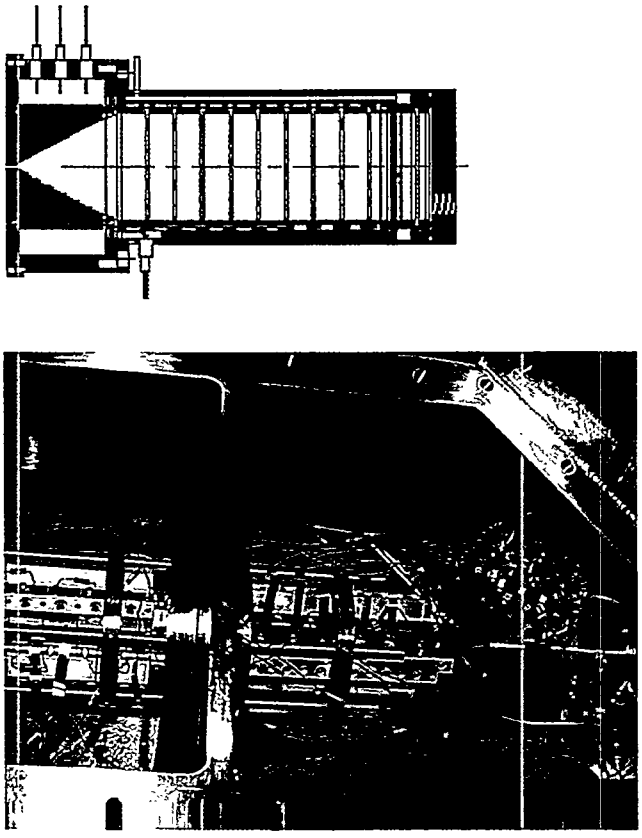

Fig. I-81. A schematic drawing of the gas cell with the modified extraction cone is shown on the top figure. On the bottom figure is shown the extraction end of the gas cell and the first section of the RF cooler in location at the focal plane of the gas-filled Enge split pole spectrograph in area II.

These modifications have been tested both off-line and on-line and have allowed us to increase the total efficiency of the gas cell to close to 50% (see Fig. I-82). The behaviour of the focusing forces again follows closely what is expected from our detailed simulations. Studies of the focusing forces as a function of the pressure of the gas inside the cell are now ongoing.

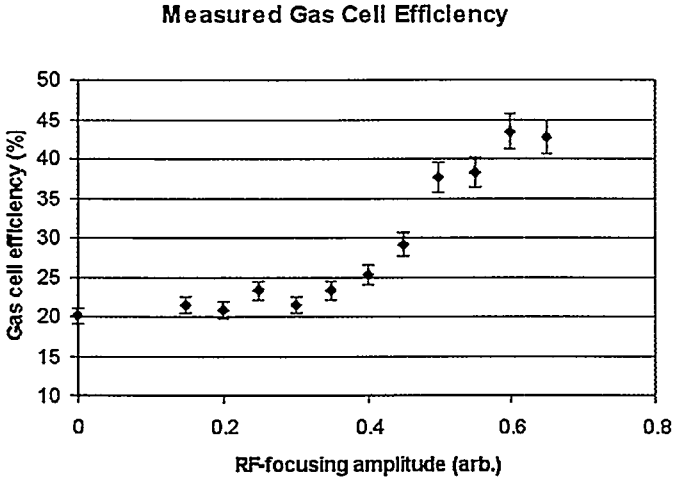

Fig. I-82. Measured efficiency for the gas cell system as a function of the RF focusing amplitude applied to the cell.

The results obtained with this system, together with the success in on-line operation with the CPT spectrometer, have clearly demonstrated that the gas cell can fulfill the requirements of the RIA concept. The main task remaining is to scale the working prototype to the 0.5 to 5 helium atmosphere-meter of stopping length required for RIA operation. This requires both a larger cell and higher helium density. This development is being performed in two steps. First a new cell is being developed that will operate at higher gas density. The RF cooler chamber where the present gas cell was tested was modified to accept this new cell for testing and characterization. From these tests a second cell at the full RIA scale will be constructed and first tested at ATLAS where it will be fully characterized before being moved to GSI to be tested at the full RIA energy behind the FRS fragment separator.

e.3. Temperature, Ordering, and Equilibrium in Radiofrequency Confinement

(J. P. Schiffer, M. Drewsen,* J. S. Hangst,* and L. Hornekaer*)

The meaning of temperature and equilibrium and how these relate to ordering are apparently not well studied in classical systems with rapid time-varying fields, with the rate of variation in the Hamiltonian faster than the natural periods for the characteristic motion of the system. This is the case for charged particles in radio-frequency traps. Cold crystalline ordering characteristic of mK temperatures had been observed in such traps with laser cooling, where the kinetic energy associated with motion in the rf field is on the order of several hundred degrees K.

Simulations using the technique of molecular dynamics were carried out with a Silicon Graphics Origin 200 4-processor parallel computer. The effective time-averaged confining force in the quadrupole (x,y) directions was taken as equal to the confining force in the non-rf (z) direction to produce a cloud whose time-averaged shape was spherical.

A 1000 particle system subjected to the sinusoidally varying field was followed in the simulations as the cooling proceeded. The average kinetic energies in the axial z-direction gradually approached the targeted value in about 25000 rf periods. The kinetic energies associated with the x and y directions are huge in comparison, because of the time-variation of the confining field: some seven orders of magnitude greater than the target temperature. Because of the time-varying confining force, the x and y components of energy are not going to be reduced. Instead, we use an effective temperature that uses velocities computed from displacements in complete rf periods, in other words motion that is not periodic with the rf voltage. The components of this 'effective temperature' reduce more slowly in these dimensions and require about 50000 rf periods (roughly 50 ms) to reach the target value.

The temperature reached is sufficient for crystallization. Indeed, as is shown in Figs. I-83 and I-84, an ordered system was obtained. As in statically confined systems, the density in the interior shows a series of spherical shells.

Systems cooled to various temperatures were allowed to propagate in the simulation with no temperature control applied, and the effective temperature was monitored. The rate at which the applied rf motion heats the system, introducing increasing random motion, is shown in Fig. I-85. For the coolest systems the coupling was too small to be observed in the simulations, corresponding to lifetimes for order of this type in a real trap of hours -- though other sources are likely to be more limiting. For increasing temperatures the dependence of this coupling between the periodic motion and the "temperature" seems to increase quadratically.

Our results show that the definition of an effective temperature in terms of the non-periodic motion is valid in a system where the distances between particles are continually changing due to external forces. How to justify the thermodynamic description of such a system is not clear. The very small coupling, corresponding to very low viscosity, between the driven motion and the random thermal excitations is surprising and qualitatively consistent with the successes in getting crystallization for large clouds in such ion traps. The quadratic dependence of this coupling on temperature is evident, but not understood at present.

*University of Århus, Denmark

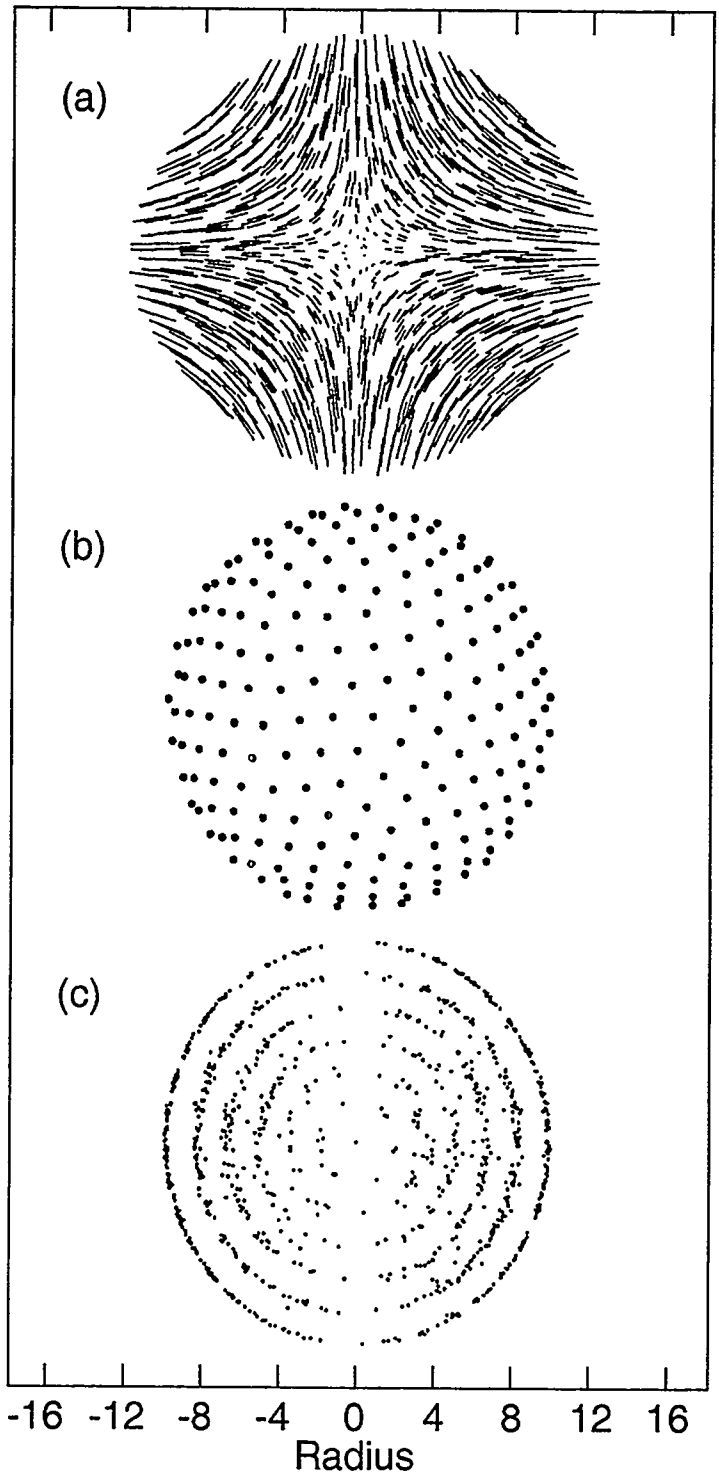

Fig. I-83. The order and motion of particles in rf confinement is shown. The trajectory followed by all of the 1000 particles is shown as lines in (a). The shape of the cloud oscillates in the x-y plane. The time-average positions of ions in the outer shell is shown in (b), while the radial positions of the ions are shown in the r-z plane with r the cylindrical radius $r = \sqrt{y^2 + z^2}$.

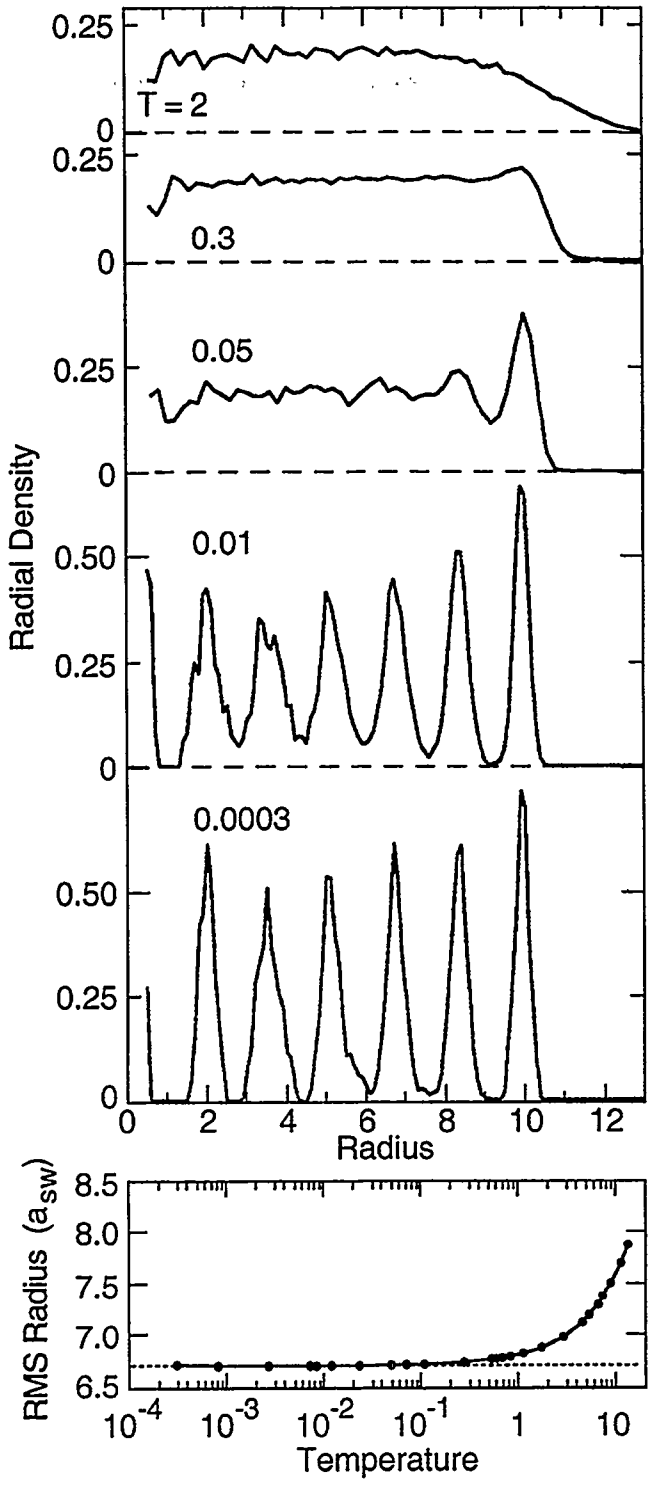

Fig. I-84. The top part of the figure shows the time-averaged (spherical) radial density profile of the cold cloud at different temperatures illustrating the onset of ordering as the system gets colder. The temperature is in dimensionless units where ordering comes about around T = .01, though there is no sharp phase transition with temperature for these finite systems. The bottom plot shows related information: the increase in the rms radius of the cloud as a function of temperature.

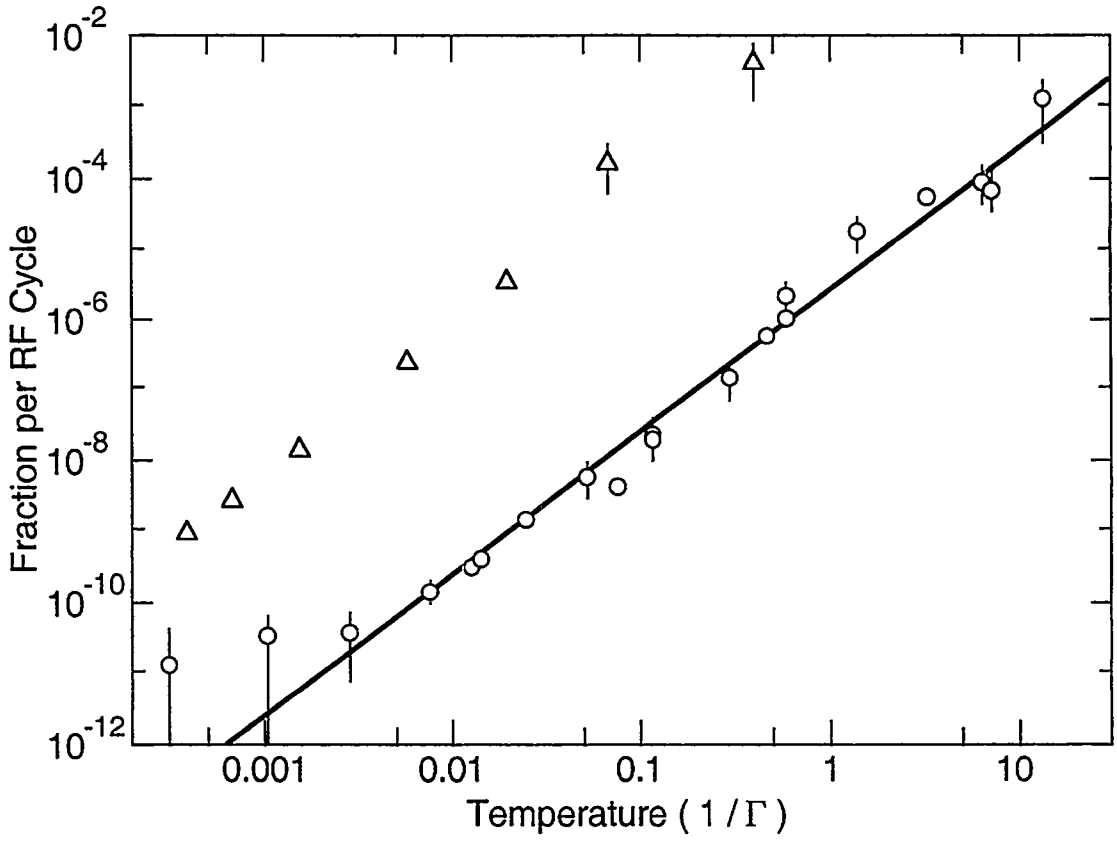

Fig. I-85. The coupling between the kinetic energy in the periodic motion of trapped ions into aperiodic, thermal motion is shown: the fraction of the kinetic energy in the periodic motion that is mixed into heat per rf period is plotted as a function of effective temperature. The line represents a quadratic temperature dependence of this coupling. The error bars represent an estimate due to the fluctuations in a finite system. For the lowest points, the bars show the limits that can be set for this coupling. The open circles represent simulations with the ratio of rf frequency to the characteristic frequency of one particle in the average confining field (the secular motion frequency) of 15.5. The triangles represent simulations with this ratio reduced to 4.7.

e.4. Search for the First Excited Level in the ^{229}Th Nucleus (I. Ahmad, J. A. Dunmore, K. Bailey, Z.-T. Lu, D. L. Bowers,* and D. G. Graczyk*)

The first excited level of the ^{229}Th nucleus was deduced to be 3.5 ± 1.0 eV above the ground-level[1]. As nuclear transitions are normally found on the order of keV to MeV, this would be the lowest known nuclear excited level and a unique case in which nuclear excitation energy is below the atomic ionization energy. A nuclear level this low provides an opportunity to study the interaction of the nucleus with its atomic surroundings and alternative ways to excite nuclei, such as with lasers.

*Chemical Technology Division, ANL

[1]R. G Helmer and C. W. Reich, Phys. Rev. C **49**, 1845 (1994).

[2]G. M. Irwin and K. H. Kim, Phys. Rev. Lett. **79**, 990 (1997). D. S. Richardson *et al.*, *ibid.* **80**, 3206 (1998). R. W. Shaw *et al.*, *ibid.* **82**, 1109 (1999). S. B. Utter *et al.*, *ibid.* **82**, 505 (1999).

The present experiment was formed in order to clarify discrepancies between results of earlier experiments[1,2]. Rather than using a ^{233}U source, fresh samples of ^{229}Th extracted from ^{233}U were used. Theoretically, this extraction would have left a large number of excited thorium nuclei, which could be observed by detecting ultraviolet photons with a sensitive photomultiplier tube.

We extracted ^{229}Th from a 100 mg isotopically pure ^{233}U sample ($^{232}U/^{233}U < 10^{-9}$). We obtained three samples with different growth time in order to check a range of possible half-lives for the isomer. The first source used in the experiment was a 200 Bq sample of fresh ^{229}Th deposited on a surface of quartz disk. Assuming that the isomer has a half-life of two days[1], this source should have produced an initial photon count rate of 106 cpm (counts per minute). This source displayed a consistent count rate at $(9 \pm 3) \times 10^2$ cpm over the PMT background (3×10^4 cpm) for three days. Because this rate did not decrease over the period, we believe that the detected photons were due to alpha emission only and not the isomer. The rate that was observed was approximately what was expected from the alpha-induced background. A second and a third source of fresh ^{229}Th electroplated to a thin steel disk had activities of 7 Bq and 50 Bq, respectively. No photon counts above the background were seen with these two sources.

The goal of this experiment was to verify the unique energy level in ^{229}Th, to get a more accurate measurement of its energy, and to measure the lifetime of this level. We were unable to make these measurements because the photon signal was not observed. Possible explanations are that we did not have a source thin enough for the optical photons to escape, the half-life of the isomer could be much more or less than expected, or the photons may be emitted at a wavelength beyond the spectral response range of our PMT (1.5-6 eV). Transitions from this particular isomer in the ^{229}Th nucleus have yet to be observed directly and the question of whether this nucleus would be suitable for studying nuclear-atomic interaction remains.

e.5. A Proposed Method for Measuring the Electric Dipole Moment of the Neutron by a Large Improvement of the Shull Method (T. W. Dombeck,* M. Peshkin, and G. R. Ringo)

Experiments to measure the electric dipole moment (EDM) of the neutron by subjecting neutrons to an external magnetic field and observing their spin precession currently find that the EDM vanishes with an uncertainty of 1×10^{-25} e-cm, that sensitivity being limited by systematic errors. We have been doing feasibility studies for a different kind of experiment which will have completely different, and possibly smaller, systematic errors. In this new experiment, polarized neutrons will undergo several thousand Bragg reflections in a slot cut in a perfect silicon crystal. At each reflection, their polarization will be rotated by the action of the crystalline electric field on the neutron's EDM, and the accumulated rotation will be measured. The hoped-for improvement in sensitivity relies upon the great magnitude of the crystalline electric field, which is four orders of magnitude stronger than external electric fields that can be achieved practically in the Ramsey experiments. This method should be simpler and less expensive than the interferometeric measurement that we proposed in 1997,[1] but possibly somewhat less sensitive.

An experiment by Shull and Nathans in which neutrons were transmitted through a crystal has confirmed the effective crystalline field by observing the stronger interaction with the neutron's magnetic dipole moment (MDM). The moving MDM interacts with the electric field as an effective EDM equal to (v/c) times the MDM. Our experiment will amplify the effect of the EDM interaction by having thousands of bounces from the crystal while the moving MDM effect will be suppressed by suitable arrangement in magnetic guide fields.

Preliminary experiments at the Missouri reactor have encouraged us to try an experiment with greater sensitivity to the Bragg-angle reflectivity of the perfect silicon crystal, which is required to allow several thousand Bragg reflections without significant loss of neutrons. Such an experiment is planned at the Missouri reactor in the year 2000. That should lead to a full-scale design that we hope to try on a higher flux source, possible HIFR at Oak Ridge National Laboratory.

*Fermi National Accelerator Laboratory

[1]M. S. Freedman, G. R. Ringo and T. W. Dombeck, Nucl. Instrum. Methods **A396**, 181 (1997).

e.6. Accelerator Mass Spectrometry of Heavy Elements with an ECR Positive Ion Source and the ATLAS Linear Accelerator

(I. Ahmad, F. Borasi, J. Caggiano, C. Davids, J. P. Greene, B. Harss, A. Heinz, D. J. Henderson, W. Henning, C. L. Jiang, R. Pardo, K. E. Rehm, R. Rejoub, D. Seweryniak, A. Sonzogni, J. Uusitalo, R. Vondrasek, M. Paul,* and D. Berkovits†)

Detection of naturally-occurring and artificial isotopes in the heavy element region has a wide-ranging interest in geophysical and environmental sciences. The elements in the actinide region have traditionally been detected by alpha spectrometry and mass spectrometry but both methods have limited sensitivity for low isotopic abundance nuclides. Accelerator Mass Spectrometry (AMS) has been recently expanded towards the detection of actinide elements using tandem accelerators. In this work we use accelerator mass spectrometry with the ECRIS-ATLAS-FMA (Electron Cyclotron Resonance Ion Source-Argonne Linear Accelerator-Fragment Mass Analyzer) system. The use of the ECR-ATLAS system for AMS of heavy elements has two advantages: (i) the efficient production of high-charge state ions in the ECR source ensures the elimination of molecular ions at the source stage, a highly attractive feature for any mass-spectrometric use which has not been exploited so far, (ii) the linear acceleration based on velocity matching acts as a powerful mass and background filter. We have shown that our system reaches an abundance sensitivity of 1×10^{-14} for Pb isotopes. The use of the system for rare isotopes e.g. ^{236}U ($T_{1/2}$ = 23.4 My), requires the determination of the transmission efficiency with a pilot beam of nearly equal charge to mass (q/m) ratio. The large number of stable xenon isotopes with suitable charge states available in the ECR source allow to match various heavy nuclides and offer the advantage of short memory effects in the ion source. The sensitivity for ^{236}U detection (q = 21) is $^{236}U/U \gtrsim 1 \times 10^{-12}$, limited mainly by the ion source output. A large number of background ion groups (Fig. I-86) (q/m degeneracies) are observed but they are well resolved using the high separation power of the FMA and a measurement of the residual energy. Figure I-87 shows the identification of ^{236}U in a natural pitchblende mineral from Joachimsthal (Bohemia). Previous use of the ECR with present-day commercial U material ($^{236}U/U \sim 1 \times 10^{-5}$) however impeded the quantitative measurement of ^{236}U in the natural samples due to source contamination.

*Hebrew University, Jerusalem, Israel, †Soreq Nuclear Research Center, Yavne, Israel

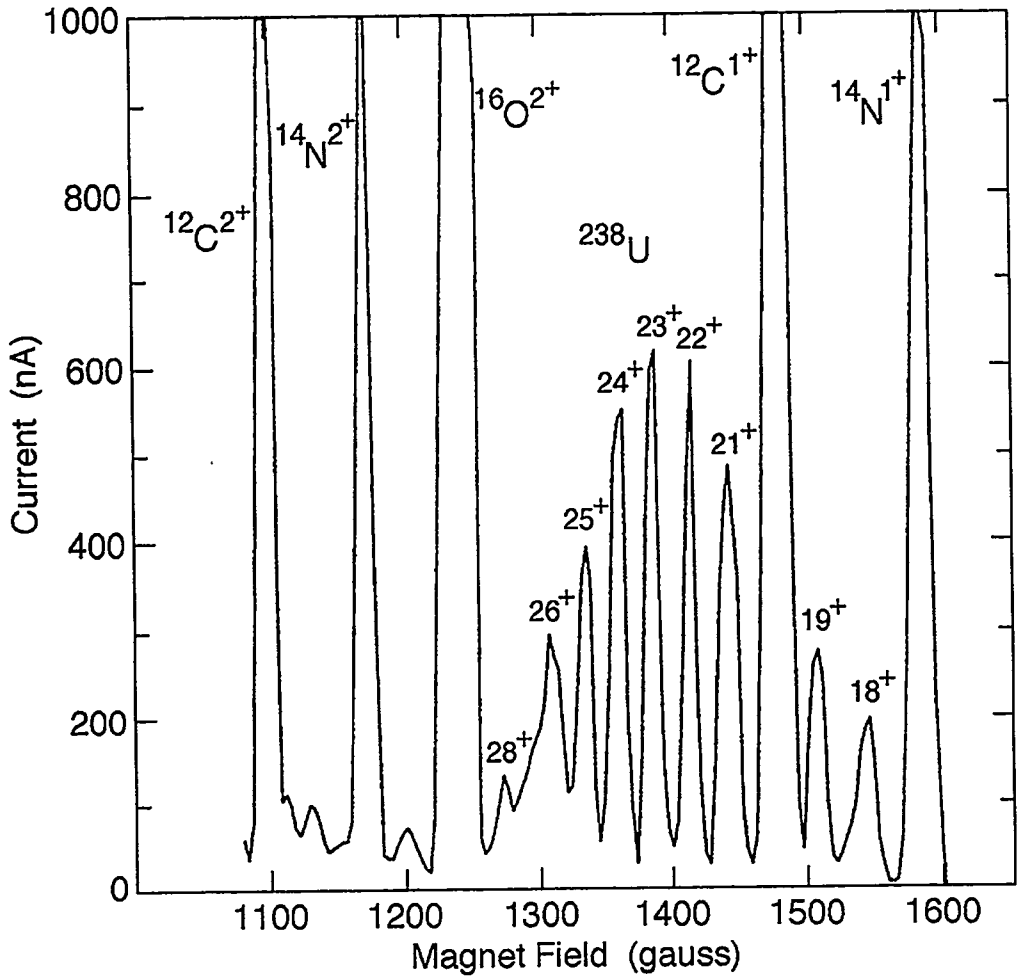

Fig. I-86. ECRIS mass over charge (m/q) spectrum. The beam was analyzed by a 90° low-resolution magnet and measured in the ECR HV platform Faraday cup. A natural pitchblende (U_3O_8) sample mixed with graphite was used in the sputtering positon and biased with 2.3 kV. Oxygen was used as a support gas for the ECR plasma. The electrons in the plasma were driven by a 630-Watt microwave power source. The ions were extracted from the source with a potental of 14.0 kV.

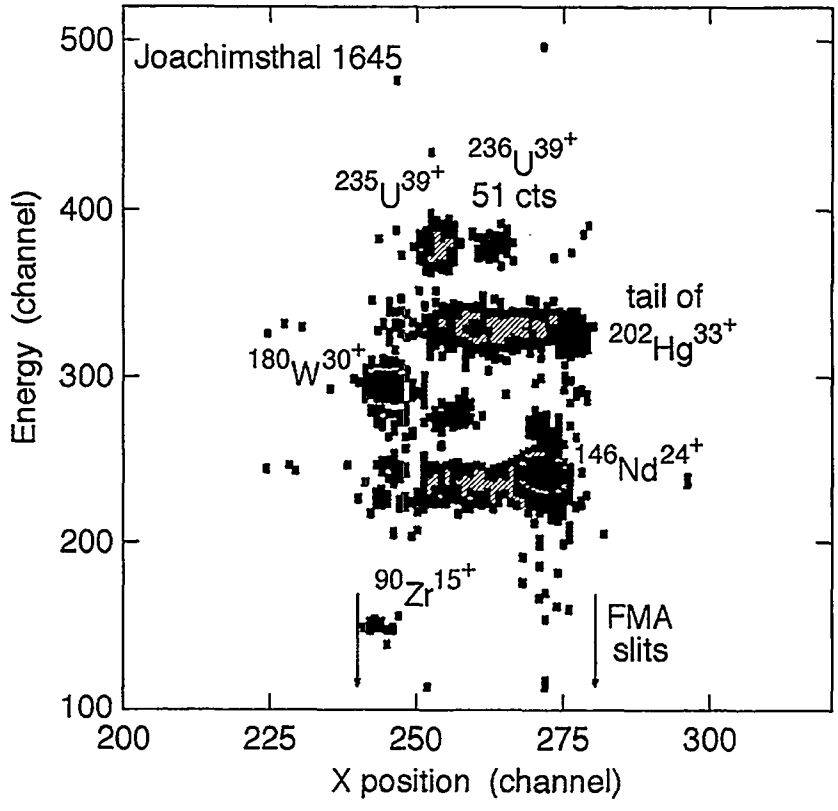

Fig. I-87. Energy versus FMA position for a natural ore from Joachimsthal (see text). FMA slits were closed around $^{236}U^{39+}$. Measurement time was 643 sec.

e.7. Nuclear Excitation by Electronic Transition (NEET) in ^{189}Os

(I. Ahmad, R. W. Dunford,* H. Esbensen, D. S. Gemmell, E. P. Kanter,* C. J. Lister, U. Rütt,† R. H. Siemssen, and S. H. Southworth*)

Tunable monochromatic 100-keV x-rays from the Advanced Photon Source have been used to explore the phenomenon of Nuclear Excitation by Electronic Transition (NEET) in the ^{189}Os atomic/nuclear system. NEET is a rare but fundamental mode of decay of an excited atomic state. It is a process by which the energy of the atomic state is transferred via the exchange of a virtual photon into excitation of the atom's nucleus. It can only occur when the atomic and nuclear states have closely matching transition energies and also involve the same changes in spin and parity. The NEET process, which competes with the "normal" decay modes involving x-ray and/or Auger-electron emission, was first postulated in 1973 by Morita[1] and is similar to related processes seen in the decay of muonic atoms. We have developed a new theoretical approach to calculating this process and predict a value for the "NEET probability", P_{NEET}, of 1.310^{-10}. P_{NEET} is the probability that a given atomic excitation, (in this case a K-vacancy) will result in the excitation of a specific nuclear state (in this case the 69.5-keV level in ^{189}Os). This value is much lower than most of the calculated values given in the literature for this system. Our measurement used an intense (5101^{1} photons/s) beam of monoenergetic 98.7-keV x-rays to make large numbers of K-vacancies in the atoms of an enriched metallic ^{189}Os target. Some small fraction of these vacancies are expected to result in excitation of the 69.5-keV nuclear level via NEET. This level has a branch to a 6-hr half-life metastable state at 31-keV. We followed 20-hour x-ray irradiations with sensitive detection measurements, also for about 20 hours, of the decay of the metastable state. This gave the result $P_{NEET} < 9 \times 10^{-10}$, an upper limit which is several

orders of magnitude lower than the values found in previous measurements, but which is consistent with our new calculation. We established the half-life of the metastable state to be 5.65 ± 0.15 h. In FY2000 we plan further measurements whose increased sensitivity (approx. a factor of 100) should permit us to quantify the NEET probability more precisely.

*Chemistry Division, ANL, †Materials Science Division, ANL
[1]M. Morita, Prog. Theor. Phys. **49**, 1574 (1973).

e.8. Half-Life of ^{44}Ti (I. Ahmad, J. P. Greene, W. Kutschera,* and M. Paul†)

The half-life of ^{44}Ti is needed for the determination of the ^{44}Ti mass produced in a supernova. For this reason, we started a measurement of ^{44}Ti half-life in 1992. The result obtained following 5 years of decay was published in 1998[1]. We have continued the measurement at Argonne and Jerusalem because a longer measurement provides a more precise value for the half-life. The same set up used for the 1998 paper has been used and data have been obtained for additional three years. Additional measurements do not change the published half-life of 59.0 ± 0.6 yr. A decay curve with the additional data points obtained at Jerusalem is displayed in Fig. I-88.

*University of Vienna, Austria, †Hebrew University, Jerusalem, Israel
[1]Ahmad *et al.*, Phys. Rev. Lett. **80**, 2550 (1998).

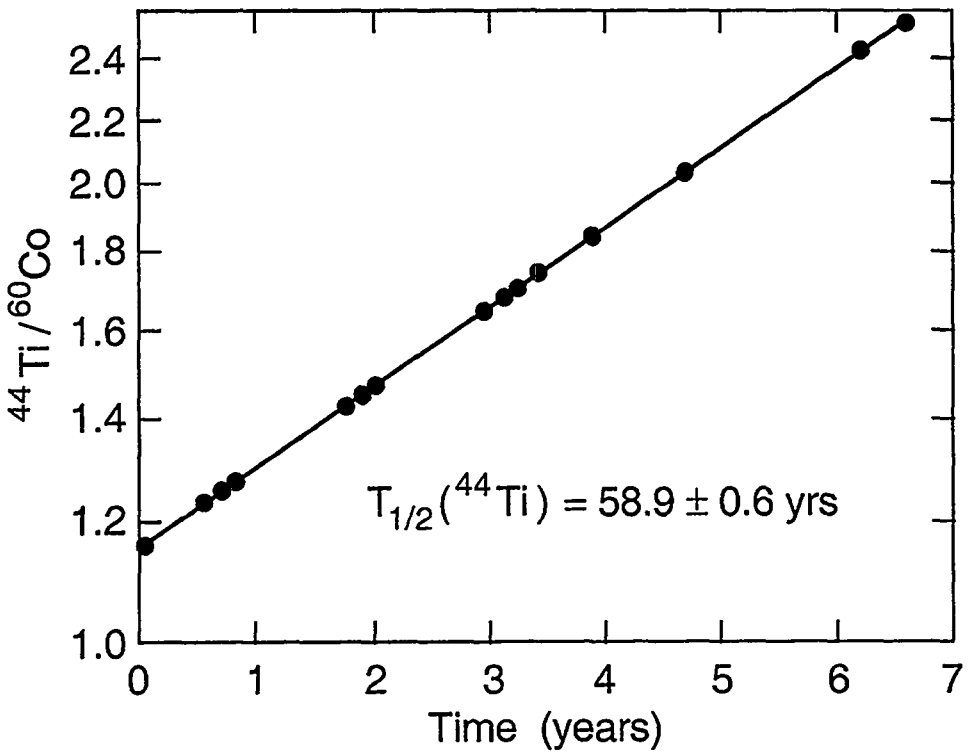

Fig. I-88. Semilogarithmic plot of the ratios of counts in the 1157-keV peak of ^{44}Ti to the counts in the 1173 keV peak of ^{60}Co measured at Jerusalem. The last two points were obtained after the publication of our paper.

F. EQUIPMENT DEVELOPMENT AT THE ATLAS FACILITY

This section describes the various technical developments linked with the experimental program associated with Heavy-Ion research within the Division.

During 1999 Gammasphere completed its second full year of operation at ATLAS, and much effort was devoted to the effective operation of the device. Nevertheless, a large number of other developments have taken place and these are described hereafter.

This section also contains a description of new developments associated with target making and computing.

f.1. Gammasphere Operations (M. P. Carpenter, C. J. Lister, R. V. F. Janssens, F. Kondev, T. Lauritsen, D. Seweryniak, and I. Wiedenhöver)

On March 15, 2000, Gammasphere will have completed its cycle at ATLAS marking two years and two months of experimental activity. In that time, 100 experiments were performed. Many of the nuclei studied in these investigations lie at or near the proton drip line as Fig. I-89 clearly illustrates. Approximately 60% of the Gammasphere experiments used the Argonne Fragment Mass Analyzer to provide mass identification of residues. Nearly all of the experiments performed utilized one or more of the 19 auxiliary detectors available for use in tandem with Gammasphere.

The operation of Gammasphere has proceeded smoothly while the device has been at ATLAS. For nearly all experiments, Gammasphere has run with its full compliments of Ge detectors (101 maximum). Table 1 summarizes the beam on target hours for Gammasphere while operating at Argonne. A total of 9864 hours of beam time was available for experimental research. This represents 72% of the total ATLAS beam time delivered to the experimental areas for the period January 15, 1998 to March 15, 2000. In addition, 1224 experimental hours were utilized for Gammasphere experiments with radioactive sources bringing the total time of Gammasphere operations at ATLAS to 11088 hours.

Table 1: Beam on target hours for ATLAS and Gammasphere for the period of Jan. 15, 1998 to March 15, 2000.

Year	ATLAS Hours	GS Hours	% of Beam time
FY1998[1]	4597	3011	65%
FY1999	6046	4719	78%
FY2000[2]	3096	2134	69%
Total	13739	9864	72%

[1]ATLAS ran a total of 5749 hours in FY98, including the period GS was not available for experiments.
[2]For the period Oct. 1, 1999 to March 15, 2000.

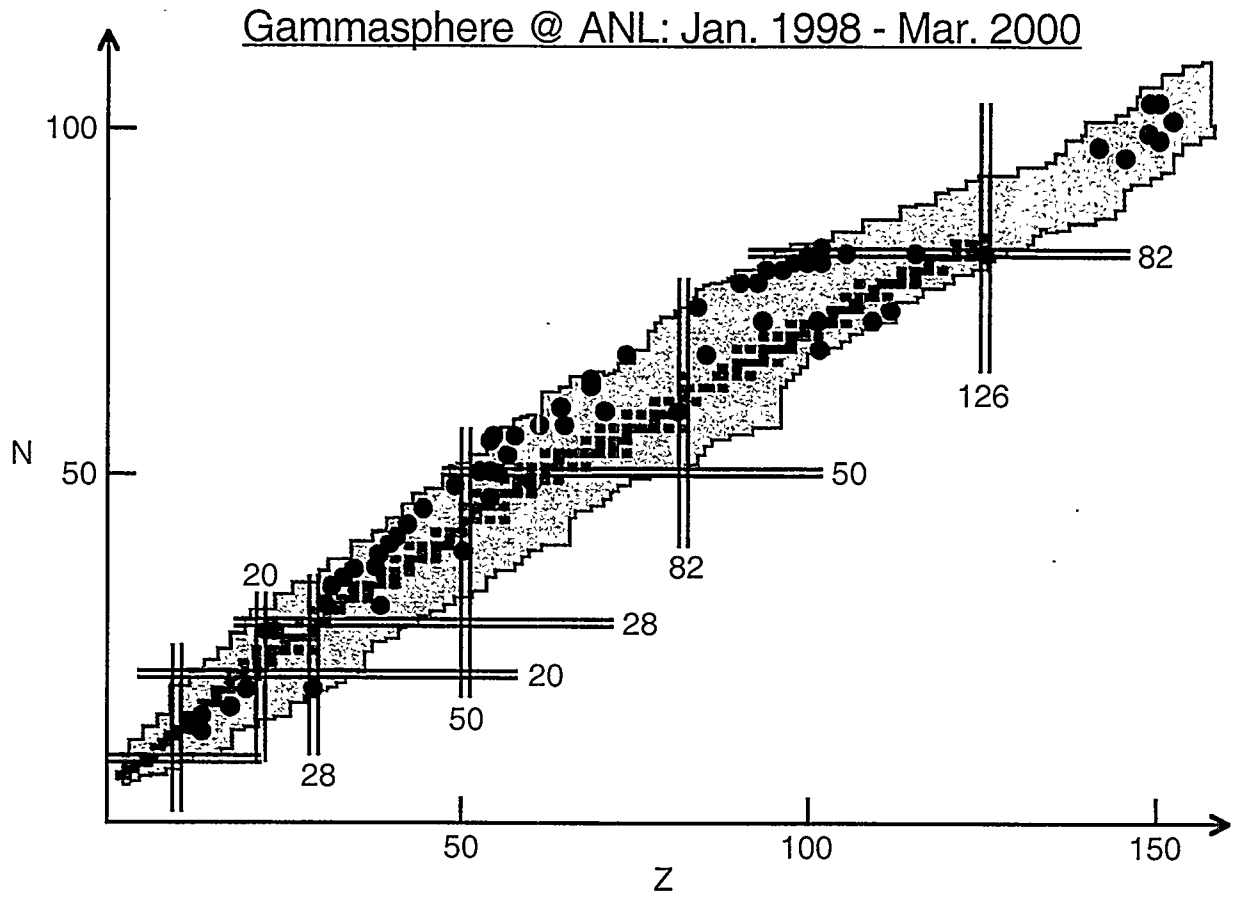

Fig. I-89. Known chart of the nuclides. Black squares represent stable nuclei. Black circles represent nuclei which have been measured with Gammasphere at ATLAS between January 1998 and March 2000.

f.2. Maintenance of Gammasphere's Germanium Detectors (I. Wiedenhöver, K. Abu-Saleem, R. V. F. Janssens, F. Kondev, C. J. Lister, and P. Wilt)

The Germanium detectors of Gammasphere continued to perform outstandingly in their second year of operation at ATLAS. In the standard configuration at the FMA, Gammasphere can hold 101 γ detectors with their respective escape-suppression systems. Most of the Gammasphere experiments ran with the maximal number of detectors possible.

One major reconfiguration of Gammasphere was undertaken for a series of experiments in the period of September-November 1999, when the newly built Neutron wall from Washington University was installed. For these experiments, 22 Germanium detectors had to be removed in order to make room for neutron-detectors. The Ge detectors in these most forward positions are usually exposed to an increased flux of high-energy neutrons, which slowly deteriorates the detector's performance during normal in-beam operation. Thus, the opportunity to repair the effects of neutron radiation on these 22 detectors was used. Most of the defects induced into the Germanium crystals by neutrons can be repaired by heating the crystal to temperatures around 105 C for 3-5 days. During this process, the vacuum around the crystal is maintained by a turbo-pump to avoid contamination of the crystal surfaces. After the annealing, 20 of the Germanium detectors could be restored to their original performance, while two detectors developed a more serious problem and had to be returned to the manufacturer. Twenty-two detectors were returned to the array, incorporating two spare systems.

Apart from this planned operation, six other detector systems developed problems during this year of

intensive use and had to be taken out of the setup for repair. Also in these cases the detectors were replaced by spare systems so that the normal configuration could be restored after a short time, while the repair took place. Two of these detectors had developed vacuum leaks, which were repaired by welding in house. In another case, a leak proved to be mechanically unaccessible and the cryostat-vacuum housing of the detector had to be replaced by the manufacturer. The other problems were due to failing electronic components, which usually could be repaired in-house.

The overall performance of Gammasphere's Germanium detector systems remains excellent.

f.3. The Gamma-Ray Box Project (GARBO) (C. J. Lister, M. P. Carpenter, R. V. F. Janssens, D. G. Jenkins, F. G. Kondev, T. L. Khoo, T. Lauritsen, B. Phlips,* and R. Kroeger*)

The next generation of gamma-ray detectors, beyond Gammasphere and Euroball, will be designed to meet the needs of RIA-based physics projects. These include: high efficiency (both in discrete transitions and for calorimetry), excellent Doppler correction capability for swiftly-moving sources (up to 7% c for accelerated ISOL beams, or 50% for fragmentation beams), polarization sensitivity for all events, excellent timing characteristics (for "chance" coincidence suppression, and for electronically measuring the lifetime of states in the nano-second regime), and finally high countrate capability to allow operation in an environment where radiation from beam-decay is an issue. To achieve these goals the detectors will have to be more highly pixelated, have higher data collection capability, and be more hermetic for high-resolution calorimetry, ideally consisting of a pure germanium shell. Around the world, many groups are investigating technologies which may satisfy the needs of these arrays. The implications of these investigations go far beyond nuclear structure studies. New detector systems could have profound impact on medical imaging, space science and on environmental monitoring.

One promising technology involves the development of large-area planar germanium detectors. These counters can be made position sensitive through using orthogonal "strip" electrodes on their front and back faces. Depth information can be gained from the risetimes of pulses, thus allowing a full x,y,z location of the electromagnetic interaction, and tracking of photons in material. The parallel-plate electric field should make "tracking" of multiple interactions between a photon and the germanium, through Compton, pair, and photoelectric interactions, more straightforward than for more complicated geometries.

At present, many technical challenges have been surmounted, but many remain. The basic physics of tracking the interaction in a uniform, parallel-plate field seems to be on a sound footing. We have continued to work on this technology to see how far it can be developed. We have procured the worlds largest planar detector, from EG&G Ortec. It is a 90 mm × 90 mm × 20 mm crystal, with 16 × 5mm strips on each side. The prototype is mounted in a large cryostat to avoid thermal problems, and had 32 individually mounted preamplifiers to allow easier individual adjustments. The detector was delivered in March 2000 and is undergoing preliminary testing. The Li-implanted side with room temperature electronics meets specifications, with a resolution of 1.8 keV at 122 keV, but the B-implanted strips, with cold FET's still experience noise problems and have resolutions between 3.0 and 4.0 keV.

We are also working on GEANT simulations of an array of such detectors. Using 24 streamlined modules, arranged in stacks of 3 in a single cryostat, we have been evaluating the performance of an array which we call the GAmma-Ray BOx, GARBO. The simulations are interesting and educational. However, until a true detector "module" has been built and evaluated it is difficult to develop a clear picture of what the working array would look like or how well it might perform. It would appear that a full 4-π coverage detector is very difficult, but a very powerful device could be built which covers 3-π with germanium and which would be ideal for radioactive beam physics.

*Naval Research Laboratory

f.4. Refinement of Channel Plate Detectors: Second Generation Design (C. J. Lister, D. J. Henderson, and T. O. Pennington)

The use of Channel-Plate detectors at the FMA has continued. Considerable operational experience has been gained for a wide variety of ions, count rates and energies. Continuous small modifications of the design continues to make the system more reliable, and the detectors operational characteristics more clear-cut. New interlocked power supplies built by the Physics Division Electronics group have proved extremely useful and reliable. The detectors are very sensitive to the state of the FMA electric fields and to the vacuum in the beam line. More careful shielding of the detectors has reduced the noise level from these background sources, so "false" firing has been eliminated. A new vacuum system using cold-cathode gauges allows continuous pressure monitoring, and automatic shut-down of the channel-plate system is vacuum irregularities occur. Normal operation now has a two-foil arrangement, one in the focal plane for generating mass spectra and one about 25 cm behind the focal plane for generating a clean, efficient identification trigger.

It is clear that the experience gained from the current detectors has been very useful, but an entirely new detector is needed to remedy the remaining problems which are three-fold: insufficiently good mass resolution, modest time-resolution, and in-efficient "fringe" regions at the counter periphery. Indeed, our most recent measurements indicate the response is only highly efficient for the central 2-3 cms of the counter. We believe that most of the problems can be solved with a new foil-and-mirror system, which will shorten the electron trajectories and have larger mirror surfaces which extend well beyond the active area. A new design is in progress, and a new prototype should be ready for testing by summer 2000.

f.5. Current Modifications of the Focal Plane Ion Chamber Detector (T. Pennington, D. Henderson, and C. J. Lister)

The Focal Plane Ion Chamber Detector Window has been redesigned. It is now much easier to change the window because of breakage, leakage, or if a different window thickness is needed. There are three different sized windows: 5 cm × 5 cm, 5 cm × 10 cm (there are three window frames for each size), and 5 cm × 15 cm (this window frame and wire support frame has currently not been constructed). The wire support system has also been redesigned for a 0.9 μm thick Mylar window (125 $\mu g/cm^2$) and 33 Torr of pressure. Plans are being made to construct and to conduct tests to see if 0.5 μm thick Mylar window (70 $\mu g/cm^2$) is workable. Another modification to the ion chamber is the front electric field gradient wires have been removed from the window frame and have been permanently mounted inside the ion chamber. The final modification to the ion chamber that has been implemented is the ability to install a 5 cm × 5 cm silicon detector. This detector will allow the measurement of the total energy of the particles that have not completely lost their energy in the ion chamber. This preserves Z resolution capability of the ion chamber while allowing for thinner windows, which reduces energy straggling and allows for lower operating pressures.

f.6. Degrader Foils for Gas Catcher Cell (J. A. Caggiano, J. P. Greene, G. Savard, and B. J. Zabransky)

The gas catcher cell after the Area II spectrograph is designed to stop reaction products and then reaccelerate them through a small potential for transport to an ion trapping system, i.e. the Canadian Penning Trap. Since the cell is only 18 cm long and runs at a maximum of 180 Torr, the stopping power of the gas is limited. Furthermore, the combined system is required to stop even the most energetic light ions, such as ^{6}He. Thus, it is required to slow down the ions to an energy of 0.3-0.5 MeV/u. Decelerating the ions was attempted by increasing the pressure in the spectrograph (in gas filled mode) to slow the ions, but this method was unsuccessful.

A method was developed and implemented to degrade the ions prior to entering the gas cell but without increasing the pressure in the magnet. The method is based on a ladder of degrader foils that can be fine-tuned to stop almost any ion in the gas cell. The degrader foils had to be large enough to accommodate the ~ 4 cm diameter beam spot, and span a range of thicknesses from 0 to 100 mg/cm^2 continuously. A ladder of 5 foils that could rotate up to 60° was chosen to be the most flexible and easiest to implement.

The degrader ladder was designed to be rotated up to 60° and still allow a window (bigger than the beam spot) of 5 × 5 cm^2 for the reaction products to pass through. Thus, the foils had to be 5 cm by 10 cm to accommodate a ~ 4 cm diameter beam spot when rotated to 60°. Three sets of five aluminum foils were made to allow thicknesses of 0.1-100 mg/cm^2. Each set of 5 foils are designed to span one decade of thickness using the 60 degree rotation, i.e. 0.1-1 mg/cm^2, 1-10 mg/cm^2, and 10-100 mg/cm^2.

The degrader ladder is mounted on a small turntable. The small turntable is mounted on an arm attached to a linear drive mechanism. One motor is used to control the height of the ladder by moving the arm up and down, while the other is used to rotate the ladder. Speedometer cables transfer the power from the motors, mounted outside the focal plane detector housing, to the drives. The cable is coupled to the linear drive through a 90°, 3:1 reducing gear box. The threaded rod in the linear drive has a pitch of 10 threads/inch, and vertical motion is readout at the motor, with a pitch of 10 numbers/revolution. Thus the vertical motion is controlled and accurate to 0.003", adequate for our purposes.

The ladder is rotated by rotating the turntable that is mounted on a 3:1 reducing gear box. The turntable is a timing-belt sprocket, and a timing belt is run to another sprocket mounted on a rotation encoder for reading the angle. The rotation encoder is 12-bit for one revolution, for a reading accurate to 0.09°. To control the motor at this level, the motor was coupled to the gear box through a 360:1 speed reducer, which gives control at the 0.03° level, well matched with the rotation encoder readout. Figure I-90 shows photographs of the ladder as installed in the spectrograph.

The ladder has been tested during experimental runs and works well.

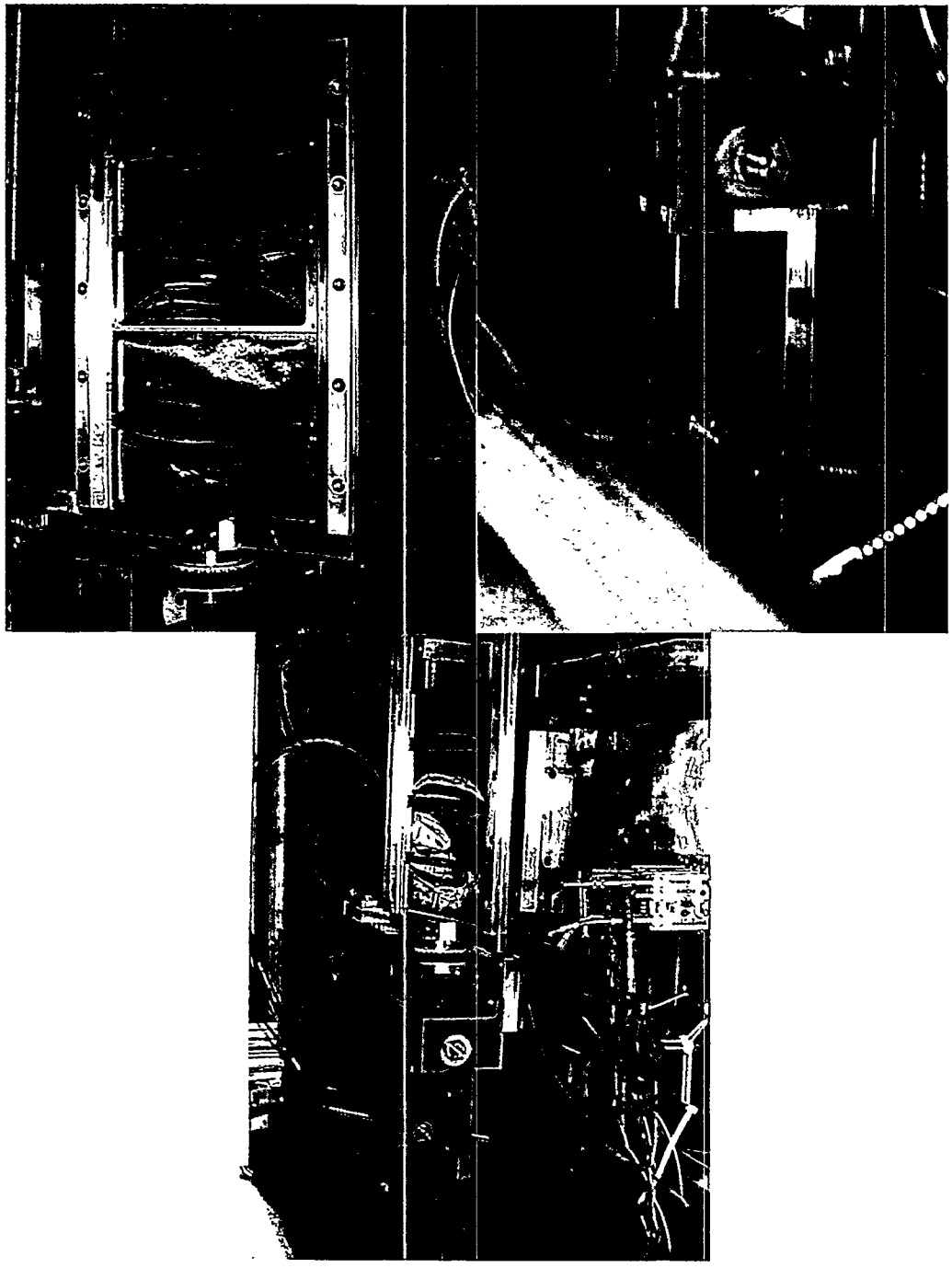

Fig. I-90. Pictures of the degrader ladder. Top left: Just the ladder itself with 4 of the 5 foil positions filled. Top right: The two gear boxes that control the height and rotation of the ladder. Bottom: The whole ladder, as it is installed in the spectrograph.

f.7. Status of the Beam Monitoring Circuit (P. Wilt, B. Harss, R. Pardo, and P. Ostroumov)

The Beam Monitoring project is being developed to allow operators and experimenters to determine the position of weak beams as they are accelerated through ATLAS. This is accomplished by placing a set of 64 scintillation fibers in the path of the beam; thirty-two of which are horizontal and the thirty-two others are vertical. As the beam passes through the fibers, they scintillate, producing a light that follows the fiber to an X-Y grid photomultiplier tube. With the information produced from the photomultiplier tube and some post acquisition calculations the intensity, location and size of the beam in the X and Y directions can be determined.

An additional requirement is to place the entire system into a CAMAC module. This includes amplification, trigger logic, acquisition (ADC′ s), post acquisition calculations, a multichannel analyzer and oscilloscope display driver circuit.

A number of design criteria needed addressed. They were:

1. Design a Track and Hold circuit that could track 5 ns pulses to 2.5V.
2. Design an acquisition system that could convert >1M events per second.
3. Design a Ratio Conversion circuit that operates at the desired event rate.
4. Design the complete circuit into a one or two slot wide CAMAC module.
5. Construct the complete system at a reasonable cost.

Because of the design criteria and the speed at which this system would have to operate to accommodate all the acquisition, conversion and display functions, it was decided that prototypes of the individual circuits would be built and tested to determine the feasibility of this project. This approach would then also provide guidance for the final lay-out.

At present, the basic logic design has been completed. It is based on a fast microprocessor which uses a fast SRAM memory for the display, and EPRoM for the data transfer and various operations. The analog circuit has been designed and built as well. Considerable attention has been devoted to the design and signal compatibility of the PMT base.

The various sub-systems have undergone an extensive number of tests, some of which were performed with beam. A number of design changes are currently being implemented as a result of these tests.

f.8. LEPPEX Development (D. Hofman, B. B. Back, D. Henderson, and I. Dioszegi*)

The machining and assembly of the LEPPEX scattering chamber has been completed. The fabrication of the eight PPAC chambers has been completed at Stony Brook. The printed circuit boards for the wire planes have been fabricated. Vacuum tests of the scattering chamber have been completed successfully. Remaining items are: design, fabrication and installation of the target wheel mechanism, procurement of vacuum system, installation of old Apex gas handling system, assembly and testing of PPAC's.

*University of Milan, Italy

f.9. BaF_2 GDR Measurement Collaboration

(D. Hofman, B. B. Back, M. Carpenter, P. Collon, A. Heinz, D. Henderson, M. Kelly, T. L. Khoo, F. Kondev, C. Lister, T. Pennington, R. Siemssen, V. Nanal,* I. Dioszegi,† A. Bracco, † F. Camera, † R. Varner, ‡ M. Thoennessen,§ and U. Garg¶)

A collaboration with participation from Argonne, Oak Ridge, Michigan State University, Texas A&M University, Stony Brook, Notre Dame University, and INFN Milano has been formed with the goal of studying Giant Dipole Resonance γ emission from well identified hot nuclei formed in heavy-ion fusion reactions. The experiments will be carried out at Argonne using the FMA augmented with the BGO Spin spectrometer to identify the spin range and the mass (M/q) of the nuclei under study. The high energy (GDR) gamma rays will be measured in a high efficiency array of BaF_2 detectors arranged on four packs of 30-37 BaF_2 crystals centered at ±90 and ±135 degrees w.r.t. the beam axis. The BaF_2 detectors will be provided by ANL, ORNL, MSU and TAMU.

An organizing workshop was held at ANL on January 22-23, 2000 in order to discuss the scientific opportunities and technical details of this program.

Proposals for a comprehensive study of hot GDR emission and other topics using this setup has been submitted to the ATLAS Program Advisory Committee for the Spring-summer 2000 period.

*Tata Institute of Fundamental Research, India, †University of Milan, Italy, ‡Oak Ridge National Laboratory, §Michigan State University, ¶University of Notre Dame

f.10. Nuclear Target Development

(J. P. Greene and G. E. Thomas)

The Physics Division operates a target development laboratory that produces targets and foils of various thicknesses and substrates, depending on the requirements, for experiments performed at the ATLAS and Dynamitron accelerators. The targets are prepared from both naturally occurring materials and stable isotopes that are supplied either in pure, elemental form or as stable compounds. Targets are made not only for the Physics Division but also for other divisions at the Laboratory and occasionally for other laboratories and universities.

In the past year, numerous targets were fabricated either as self-supporting foils, on various substrates or as "sandwich" targets. Targets produced included AgS, Al, Au, Be, Bi, $^{12,13}C$, $^{40,48}Ca$, Co, ^{52}Cr, Cu, CD_2, Fe, formvar, $^{72,76}Ge$, Havar, ^{180}Hf, kapton, $^{24,26}Mg$, $^{94,95}Mo$, MoS_2, mylar, ^{58}Ni, $^{206,207,208}Pb$, ^{208}PbO, PbS, ^{106}Pd, polyethylene, polypropylene, Pt, $^{102,104}Ru$, Se, $^{30}SiO_2$, Ta, ^{130}Te, Th, $^{46,50}Ti$, Ti/V/Al, U, UC_2, ^{176}Yb and $^{90,91,92,96}Zr$. Many of these target foils have been fabricated via mechanical rolling using our small rolling mill. Approximately 400 targets have been prepared for various experiments during this calendar year. With second full year of Gammasphere operation at ATLAS, support continues for both researchers in-house, as well as others outside the Division. Preparation of targets absorbers, reset foils, etc. has progressed steadily. A new rotating target wheel was developed based on designs previously employed at APEX so as to increase lifetimes and allow for higher beam currents on target. This Gammasphere target wheel is now in routine use for many experiments where high beam currents are necessary. Successful runs employing auxiliary detector systems other than the FMA have included μBall, CHICO and fission source studies, each employing specialized target holders. The Physics Division Target Laboratory fabricated approximately 260 targets for the research effort at Gammasphere this year.

As part of ATLAS support, the target lab routinely produces carbon stripper foils of 2 $\mu g/cm^2$ for use in the Tandem as well as other thickness for additional stripping throughout the accelerator. A total of 304 carbon stripper and gold foils of various types were prepared for ATLAS in 1999. In addition, there continues to be an increase in the preparation of various dilutions of isotopic source material into a form and shape suitable for introduction into PIIECR and SNICS sources to produce enriched beams at ATLAS. This includes reducing separated isotopes. Some examples include ^{40}Ca, ^{76}Ge, ^{54}Fe, FeS, ^{26}Mg, ^{58}Ni, ^{6}LiH and

$^{44}TiO_2$ which was the first accelerated beam of ^{44}Ti produced by ATLAS and delivered to the FMA for experiments of astrophysical significance. This material, used in the SNICS source at the Tandem, was obtained by bombarding a scandium disk target with protons at IPNS, producing a small quantity of ^{44}Ti, which was then chemically separated by CMT Division. The resulting oxide precipitate was mixed with natural TiO_2 and packed in a source cone for use in the Tandem. Future experiments are planned. The continuing procurement of stable and enriched material for ATLAS consumption and maintenance of isotope inventories for enriched beam production is being provided by the target laboratory staff.

The target development laboratory includes state-of-the-art equipment used for thin-film fabrication. The available techniques consist of multiple resistive heating, focused ion beam sputtering, glow-discharge plasma deposition, electron beam and electron bombardment evaporation, electrodeposition and mechanical rolling. The evaporators are maintained under high vacuum and each vessel contains a quartz-crystal film-thickness monitor with deposition rate indicators. Also included are movable shutters, quartz-lamp substrate heaters and thermocouple temperature sensors, allowing for complete process monitoring during target deposition.

Other auxiliary equipment used for target development includes electrodeposition equipment, a small rolling mill, an alpha particle counting chamber, inert atmosphere glove box, laminar flow clean bench, pellet press, a reduction furnace, and a variety of precision balances. A turbo-pumped target storage facility is in operation for maintaining, under high vacuum, those targets that readily oxidize in air. This system utilizes computer-controlled circuitry to prevent targets from exposure to atmosphere during power interruptions. A second storage system employing a bank of vacuum desiccators and connected to a mechanically pumped manifold is available for use by individual experimenters. Similar systems are in operation at ATLAS just inside the entrance to Target Area II. A new additional set-up, consisting of two large glass desiccators evacuated using a small turbo-pump system, is in operation for long-term material storage. This allows a separation of material storage from target storage, hence eliminating repeated exposure when transferring and retrieving targets.

A low-level radioactive source and target preparation laboratory exists at a separate location within the Division that is dedicated to the production of these sources and targets. Available preparation techniques include multiple resistive heating, employing a diffusion-pumped vacuum evaporator. A second, smaller evaporator system was constructed for close proximity evaporations of higher activity materials, to be used as targets as well as radioactive sources. The small size of this system allows for installation within a hood. Preparation of actinide targets by electrodeposition is continuing, most notably Cm and Pu for Coulomb excitation studies using Gammasphere at ATLAS. The Physics Division finds itself in the unique position of having the ability to obtain, process and handle actinide elements and, therefore, prepare the thin deposits used as targets for these experiments while Gammasphere presents the necessary experimental opportunity to accomplish this effort. Production also continues for natural and depleted uranium and natural thorium foils by mechanical rolling. A large effort went into the preparation of several geologic samples for an AMS run involving ^{236}U. Ore and mineral samples were received from many locations and needed processing into forms acceptable for the ECR source. A clean hood, work area and special tools were procured so as to avoid contamination of the samples. This work is still in progress.

Outside of target development, support is being provided for the production of thin films and foils for use in various new detector systems developed for experiments at ATLAS. Several variations of metallized plastic foils were prepared for use in the channel plate detector at the FMA. A variety of windows employed in CPT experiments at the SPS in Area II were produced. These included windows of Ti, Ni, Kapton and Havar. Also developed for the SPS II focal plane was an energy degrader system consisting of a ladder of various thickness, large area, aluminum foils, which were prepared by mechanical rolling. Support of the efforts involving fragmentation/high-pressure He gas stopper cell as a means to produce secondary exotic beams also being pursued at the SPS in Area II has required foils and gas cell window technologies previously developed for the production targets used in the ^{17}F experiments at ATLAS. This support is continuing. One area of considerable importance is the ability to manufacture and measure the thickness of large area foils of various kinds. In particular, for the preparation of formvar films for the channel plate detectors at the FMA. To accomplish this, we have constructed a new alpha particle counting system with a chamber large enough to accommodate these mounted foils.

Another area of increased research effort has been toward development of radioactive beams employing the ISOL technique involving neutron producing targets which induce fission in uranium or a uranium compound production target. One aspect of this development has been the design of a liquid uranium target for testing at the Dynamitron accelerator. Melts of uranium samples attempted via resistive heating using the Cooke evaporation in the Radioactive Target Laboratory have met with only little success. A higher temperature source is needed and will require the installation of the electron beam evaporator system obtained by ANL from Florida State University. In addition, the first direct measurements of the thermal conductivity of uranium carbide samples have been made using the method of heating by electron bombardment and measuring the surface temperature of thin UC_2 disks with an optical pyrometer. The uranium carbide sample disks are first prepared by the reduction of uranium oxide using carbon in a resistively heated source in the Radioactive Target Laboratory. Next, the samples are heated by a 10 kV electron beam provided by a mortar source in a vacuum evaporator in the target lab (R-154) and the temperature measured as a function of beam current using a two-color pyrometer. This work is still in progress.

f.11. Portable Data-Acquisition System (T. Pennington, D. Henderson, and P. Wilt)

A portable data-acquisition system for detector testing has been constructed. The system is composed of a 100 MHz Pentium PC (A 600 MHz Pentium III PC was purchased), a NIM bin, and a CAMAC crate with a GPIB Interface. The software that is being used is Labview 5.0. Currently, an EG&G ORTEC AD811 ADC is being used, but the system can be adapted for any CAMAC configuration (i.e. ADC, TDC, QDC, etc.).

A MCA program with real-time analysis was written, but this program is extremely slow. The count rate is approximately 6 Hz and the average dead time is approximately 100–120 microseconds. The lack of speed is mainly due to the large amount of overhead from the real time analysis and the speed of the PC being used.

Two low overhead programs were written that basically writes the ADC output to disk to increase speed of the data acquisition (which can be read by a spreadsheet program for data analysis and plotting). There is no real time analysis or real time spectra for these programs. The first program reads a single channel from the ADC. The count rate of the program is approximately 19 Hz. The second program reads two channels from the ADC. The count rate of this program is approximately 14.5 Hz. Both programs were tested on a 333-MHz Pentium II PC and the count rates of the programs increased by approximately 3 times.

The data-acquisition system is expandable to as many ADCs and ADC channels that can fit into the CAMAC Crate. All the low overhead programs are easily altered for the addition of more ADCs and ADC channels. Each ADC and ADC channel that is added will decrease the overall count rate of the system due to more program overhead and CAMAC read and writes. Also, any online analysis can be included in the system but at the cost of speed, i.e. average dead time, centroid, etc.

f.12. Physics Computing Facilities (K. Teh, D. R. Cyborski, and T. Lauritsen)

The Physics Division maintains several computer systems for data analysis, computation, and general computing. These systems are conveniently grouped into various clusters and are described briefly below.

The Division's Unix cluster consists of Suns Sparcstations and Linux PC workstations. Its primary function is data analysis and general computing. The VMS Analysis cluster consists of three Alphastations hosted by an Alphaserver. It is used primarily for sorting data obtained from ATLAS based experiments. In addition, the Division maintains a 4-processor SGI Origin 200 for numerically intensive computations.

The Vax cluster continues to provide general computing services, primarily mail, and serves as a disk storage to Windows PCs and Macintoshes. Last year, a dual processor Linux PC was installed as a possible replacement for the Vax cluster. It is now online and available.

The Division also operates four additional clusters. The Theory Group maintains a pair of IBM RS/6000 workstations that serve several X-window terminals. They also make use of the ANL IBM SP2 and the SGI Origin 2000, both massively parallel machines, for large numerical computations. The Medium Energy Group has two clusters: a Compaq Unix cluster and a VMS cluster which is used for data analysis and general computing. Finally, the ATLAS accelerator group maintains its own cluster of controlling the ATLAS accelerator.

f. 13. Data-Acquisition Systems (K. Teh, D. R. Cyborski, and T. Lauritsen)

The Division operates three MSU/Daphne data-acquisition systems. Each consists of an MSU VME front-end and a VMS Alphastation back-end running Daphne for online data monitoring.

Work continues on the SCARLET acquisition system which is intended to replace the MSU/Daphne system. This system is based on a custom CAMAC controller that is being built in-house. It is expected that it will be ready for use by the end of summer.

G. ASSISTANCE TO OUTSIDE USERS OF ATLAS

D. J. Hofman

This year has seen a continuation of a large number of outside Users of ATLAS due to the very active, successful program utilizing Gammasphere. Outside Users were involved in about 95% of all experiments performed in fiscal year 1999. David J. Hofman has been available in a user liaison capacity to handle the scheduling of ATLAS experiments, provide assistance in experiment proposal submission matters, and help facilitate the effective performance of research at ATLAS by outside scientists. In addition, a large portion of the Heavy-Ion in-house scientific staff has spent time in experiment setup, preparation and assistance for the many different Gammasphere experiments.

The program advisory committee met twice during the 1999 fiscal year. Program advisory committee meetings were held on November 9-10, 1998 and May 21-22, 1999 to recommend experiments for running time at ATLAS. In FY 1999 the Program Advisory Committee members were:

David Balamuth	University of Pennsylvania
Russell Betts	Argonne National Laboratory
Bernard Haas	Institut de Recherches Subatomiques (Strasbourg)
I-Y. Lee (chair)	Lawrence Berkley Laboratory
Witek Nazarewicz	University of Tennessee
Lee Riedinger	University of Tennessee
Bradley Sherrill	Michigan State University
Robert Tribble	Texas A&M University

The PAC reviewed 40 proposals for 198 days of requested running time and 45 proposals for 225 days of running time at the two meetings, respectively. Of the submitted proposals for both meetings, the program advisory committee recommended acceptance of 33 proposals for a total of 159 days of running time.

The ATLAS User Executive Committee organized a joint User Group meeting chaired by David Fossan in conjunction with the Gammasphere and Berkley 88" Cyclotron User Groups during the October 1999 Division of Nuclear Physics APS meeting held at Pacific Grove, CA. Approximately 100 scientists attended the meeting. The main topics of discussion concerning Argonne were the status of ATLAS, updates on various experimental programs and issues surrounding Gammasphere. In FY 1999 the ATLAS Executive Committee consisted of David Fossan (SUNY Stony Brook) as Chairperson, Michael Wiescher (University of Notre Dame), and Frank Wolfs (University of Rochester).

A wide variety of experiments were carried out at ATLAS during the last year, with emphasis placed on utilization of Gammasphere during its tenure at ATLAS. The strength and diversity of the research program at ATLAS continues to rely heavily on active involvement by universities and other institutions.

a. Experiments Involving Outside Users

All experiments in which outside users directly participated during FY 1999 are listed below. The spokesperson for each experiment is given in square brackets after the title, and the collaborators who were present for the experiment are given with their home institution below each entry.

(1) Heavy-Ion Lithography on High Temperature Superconductors [Kwok]
L. Paulius, Western Michigan University; W. Kwok, R. Olsson, Material Science Division, Argonne National Lab; D. Hofman, Argonne National Lab.

(2) Ion Irradiations of Anisotropic High-Tc Superconductors: Probing Dynamics of Magnetic Vortices [Miller]
P. Berghuis, D. Kim, D. Miller, Material Science Division, Argonne National Lab; D. Hofman, Argonne National Lab.

(3) Preparation of the FMA and Auxiliary Detectors for Operation with Gammasphere [Lister]
J. Schwartz, Yale University; P. Hausladen, University of Pennsylvania; P. Chowdhury, E. Seabury, University of Massachusetts, Lowell; W. Walters, University of Maryland; R. Macleod, Thomas Jefferson Nat'l. Accelerator Facility; J. Cizewski, K. Ding, N. Fotiadis, Rutgers University; P. Reiter, Ludwig Maximilians-Universität München; P. Fallon, A. Macchiavelli, M. Maier, Lawrence Berkeley National Lab.; M. Carpenter, C. Davids, D. Henderson, R. Janssens, T. Khoo, T. Lauritsen, C. Lister, D. Nisius, D. Seweryniak, J. Uusitalo, Argonne National Lab.

(4) Accelerator-Mass-Spectrometry Measurements of Natural ^{236}U Concentrations with the ECR-ATLAS System [Paul]
B. Harss, Tu Munich; D. Berkovits, Soreq Nuclear Research Center; F. Borasi, Ludwig Maximilians-Universität München; M. Paul, Hebrew University of Jerusalem; I. Ahmad, J. Caggiano, J. Greene, A. Heinz, C. Jiang, R. Pardo, K. Rehm, R. Rejoub, D. Seweryniak, A. Sonzogni, R. Vondrasek, Argonne National Lab.

(5) Study of $^{44}Ti(\alpha,p)^{47}V$ at Energies of Astrophysical Interest [Sonzogni]
B. Harss, Tu Munich; F. Borasi, R. Segel, Northwestern University; M. Paul, Hebrew University of Jerusalem; I. Ahmad, C. Davids, J. Greene, D. Henderson, W. Henning, R. Janssens, C. Jiang, J. Nolen, R. Pardo, K. Rehm, J. Schiffer, D. Seweryniak, R. Siemssen, A. Sonzogni, J. Uusitalo, I. Wiedenhoever, Argonne National Lab.

(6) Test of ^{86}Kr Beam Production and Heavy Element Synthesis [Janssens]
P. Reiter, Ludwig Maximilians-Universität München; J. Caggiano, J. Greene, A. Heinz, W. Henning, R. Janssens, C. Jiang, T. Khoo, F. Kondev, T. Lauritsen, R. Pardo, J. Schiffer, D. Seweryniak, I. Wiedenhoever, Argonne National Lab.

(7) Measurement of the $^{3}He(^{25}Al,d)^{26}Si$ Reaction: Production of an ^{25}Al Beam [Champagne]
D. Bardayan, P. Parker, Yale University; A. Champagne, University of North Carolina-Chapel Hill; B. Harss, Tu Munich; J. Blackmon, Oak Ridge National Laboratory; R. Janssens, C. Jiang, R. Pardo, K. Rehm, A. Sonzogni, J. Uusitalo, Argonne National Lab.

(8) A Study of Radiative Decay from High Lying States in ^{24}Mg [Lister]
J. Schwartz, Yale University; W. Catford, University of Surrey; J. Cizewski, Rutgers University; M. Carpenter, R. Janssens, T. Lauritsen, K. Lister, I. Wiedenhoever, A. Wuosmaa, Argonne National Lab.

(9) A Measurement of the Radiative Decay from High Lying States in ^{24}Mg [Lister]
M. Carpenter, A. Heinz, R. Janssens, F. Kondev, C. Lister, I. Wiedenhoever, Argonne National Lab.

(10) Determination of the Nuclear Diffuseness Parameter from Deep Sub-Barrier Fusion [Dasgupta]
G. Lane, Lawrence Berkeley National Lab.; A. Byrne, M. Dasgupta, D. Hinde, C. Morton, Australian National University; B. Back, C. Lister, Argonne National Lab.

(11) Spectroscopy of Odd Tin Isotopes Approaching ^{100}Sn [Freeman]
J. Schwartz, Yale University; M. Devlin, D. Sarantites, Washington University; D. Balamuth, University of Pennsylvania; C. Baskill, S. Freeman, M. Leddy, A. Qadir, S. Robinson, J. Smith, B. Varley, University of Manchester; J. Wilson, University of Copenhagen; M. Carpenter, C. Lister, D. Seweryniak, Argonne National Lab.

(12) Alpha and Proton Calibration of Microball [Sarantites]
M. Devlin, F. Lerma, D. Sarantites, Washington University; A. Axelsson, M. Weiszflog, Uppsala University; H. Eberth, T. Steinhardt, Universität zu Köln; W. Reviol, University of Tennessee; J. Wilson, University of Copenhagen; C. Andreoiu, C. Fahlander, D. Rudolph, Lund University; R. Clark, Lawrence Berkeley National Lab.; S. Fischer, De Paul University; M. Carpenter, Argonne National Lab.

(13) Deformation and Proton Decay in ^{185}Bi [Davids]
J. Ressler, University of Maryland; T. Davinson, P. Woods, University of Edinburgh; J. Cizewski, Rutgers University; J. Caggiano, M. Carpenter, C. Davids, A. Heinz, F. Kondev, T. Lauritsen, D. Seweryniak, I. Wiedenhoever, Argonne National Lab.

(14) Exploring Methods to Measure the Missing 3^+-State in ^{26}Si [Lister]
J. Schwartz, Yale University; B. Harss, Tu Munich; R. Janssens, C. Lister, K. Rehm, Argonne National Lab.

(15) Isospin Symmetry and Identical Bands in the A ~ 80 Region – Mirror Nuclei Across the N = Z Line [Leddy]
J. Schwartz, Yale University; C. Baskill, S. Freeman, M. Leddy, A. Qadir, S. Robinson, B. Varley, University of Manchester; L. Bernstein, P. Garrett, Lawrence Livermore National Lab.; L. McLean, Duke University; C. Lister, R. Janssens, Argonne National Lab.

(16) Spectroscopy of Nuclei Near N = Z = 40 Using Gammasphere and the FMA [Bernstein]
N. Fotiadis, Rutgers University; E. Tavukcu, North Carolina State Univ.; R. Bauer, J. Becker, L. Bernstein, K. Hauschild, Lawrence Livermore National Lab.; C. Lister, I. Wiedenhoever, Argonne National Lab.

(17) Superdeformation, Shell Structure and Neutron-Proton Correlations at A ~ 90, N ~ Z [Cederwall]
M. Devlin, D. Sarantites, Washington University; M. Hausmann, A. Jungclaus, Universität Göttingen; J. Wilson, University of Copenhagen; T. Bäck, B. Cederwall, E. Ideguchi, K. Jonsson, W. Klamra, Royal Institute of Technology; D. Napoli, Lab. Nazionali di Legnaro; Ö. Skeppstedt, Chalmers University of Technology; M. Carpenter, R. Janssens, D. Seweryniak, Argonne National Lab.

(18) Study of Excited States in ^{181}Tl and ^{179}Au - Spectroscopy Beyond the Neutron Midshell [Reviol]
D. Jenkins, R. Wadsworth, University of York; D. Balabanski, C. Bingham, D. Hartley, W. Reviol, L. Riedinger, O. Zeidan, University of Tennessee; W. Mueller, University of Leuven; M. Carpenter, R. Janssens, T. Khoo, F. Kondev, T. Lauritsen, C. Lister, D. Seweryniak, I. Wiedenhoever, Argonne National Lab.

(19) Proton Decay Fine Structure and γ-Decays of ^{141}Ho [Woods]
U. Garg, S. Zhu, University of Notre Dame; S. Tumey, W. Walters, University of Maryland; T. Davinson, P. Woods, University of Edinburgh; J. Cizewski, Rutgers University; M. Carpenter, C. Davids, R. Janssens, T. Khoo, D. Seweryniak, A. Sonzogni, J. Uusitalo, Argonne National Lab.

(20) Deformation and Superdeformation in N = Z = 44 Nuclide ^{88}Ru [Lister]
J. Schwartz, Yale University; M. Quinn, A. Teymurazyan, S. Vincent, University of Notre Dame; J. Durell, S. Freeman, B. Varley, University of Manchester; T. Bäck, K. Jonsson, Royal Institute of Technology; C. Lister, I. Wiedenhoever, Argonne National Lab.

(21) Study of the Symmetric Reaction ^{90}Zr + ^{90}Zr using Gammasphere and the Fragment Mass Analyzer [Carpenter]
J. Schwartz, Yale University; M. Furlotti, D. Sarantites, Washington University; W. Reviol, University of Tennessee; B. Herskind, University of Copenhagen; W. Ma, P. Varmette, Mississippi State University; I. Ahmad, J. Caggiano, M. Carpenter, C. Davids, A. Heinz, R. Janssens, R. Kaye, Jr., T. Khoo, F. Kondev, T. Lauritsen, C. Lister, D. Seweryniak, I. Wiedenhoever, Argonne National Lab.

(22) Formation Mechanism, Fission Barrier and Structure of ^{254,255}No at High Angular Momentum [Reiter]
S. Siem, University of Oslo; A. Chewter, R. Herzberg, University of Liverpool; H. Kankaanpää, University of Jyväskylä; J. Cizewski, N. Fotiadis, Rutgers University; P. Reiter, Ludwig Maximilians-Universität München; K. Vetter, Lawrence Berkeley National Lab.; M. Carpenter, A. Heinz, R. Janssens, T. Khoo, F. Kondev, T. Lauritsen, C. Lister, D. Seweryniak, A. Sonzogni, J. Uusitalo, I. Wiedenhoever, Argonne National Lab.

(23) Study of the Odd-Odd N = Z Nucleus ^{70}Br [Fallon]
R. Charity, M. Furlotti, D. Sarantites, V. Tomov, Washington University; N. Kelsall, R. Wadsworth, University of York; W. Reviol, University of Tennessee; S. Vincent, University of Notre Dame; G. Ball, TRIUMF; D. Rudolph, Lund University; R. Clark, M. Cromaz, P. Fallon, A. Macchiavelli, C. Svensson, Lawrence Berkeley National Lab.; S. Fischer, De Paul University; M. Carpenter, C. Lister, D. Seweryniak, Argonne National Lab.

(24) Recoil Decay Tagging Study of the Highly Deformed Proton Emitter ^{131}Eu [Woods]
J. Ressler, J. Shergur, W. Walters, University of Maryland; J. Uusitalo, University of Jyväskylä; P. Woods, University of Edinburgh; J. Cizewski, Rutgers University; M. Carpenter, C. Davids, R. Janssens, D. Seweryniak, Argonne National Lab.

(25) Is the Superdeformed Decay-Out Mechanism in the Mass 150 Region Different than in the 190 Region? [Lauritsen]
I. Ahmad, M. Carpenter, R. Janssens, T. Khoo, F. Kondev, T. Lauritsen, C. Lister, I. Wiedenhoever, Argonne National Lab.

(26) Fission Barrier, Limits of Stability, Formation Mechanism and Structure of ^{252}No [Reiter]
G. Jones, University of Liverpool; R. Julin, University of Jyväskylä; J. Cizewski, Rutgers University; P. Bhattacharyya, Purdue University; P. Reiter, Ludwig Maximilians-Universität München; I. Ahmad, J. Caggiano, M. Carpenter, R. Janssens, T. Khoo, F. Kondev, T. Lauritsen, C. Lister, D. Seweryniak, I. Wiedenhoever, Argonne National Lab.

(27) Unsafe Coulex of the ^{238,239}Pu Nuclei [Janssens]
S. Siem, University of Oslo; G. Hackman, University of Kansas; H. Amro, North Carolina State Univ.; P. Reiter, Ludwig Maximilians-Universität München; A. Macchiavelli, Lawrence Berkeley National Lab.; I. Ahmad, M. Carpenter, R. Janssens, T. Khoo, T. Lauritsen, C. Lister, A. Sonzogni, J. Uusitalo, I. Wiedenhoever, Argonne National Lab.

(28) Coupling Between Single-Particle and Collective Modes in ^{235}U [Cline]
M. Devlin, Washington University; P. Napiorkowski, Warsaw University; D. Cline, M. Simon, R. Teng, C. Wu, University of Rochester; A. Macchiavelli, K. Vetter, Lawrence Berkeley National Lab.; J. Gerl, H. Wollersheim, GSI, Darmstadt; M. Carpenter, R. Janssens, I. Wiedenhoever, Argonne National Lab.

(29) The Fragmentation of the Two-Phonon Octupole Strength in ^{208}Pb [Vetter]
D. Cline, C. Wu, University of Rochester; M. Cromaz, A. Macchiavelli, M. Stephens, K. Vetter, Lawrence Berkeley National Lab.; R. Janssens, Argonne National Lab.

(30) Study of the $J^{\pi} = 38^{+}\,\hbar$ Heavy-Ion Resonance in ^{48}Cr [Sanders]
V. Rauch, M. Rousseau, Université Louis Pasteur; P. Delurgio, A. Dummer, K. Farrar, G. Hackman, F. Prosser, S. Sanders, University of Kansas; R. Nouicer, University of Illinois-Chicago; A. Szanto de Toledo, Universidade de São Paulo; M. Carpenter, R. Janssens, F. Kondev, I. Wiedenhoever, A. Wuosmaa, Argonne National Lab.

(31) Spectroscopy of $^{98}_{48}Cd^{50}$ [Clark]
M. Devlin, D. Sarantites, Washington University; D. Jenkins, N. Kelsall, R. Wadsworth, University of York; J. Wilson, University of Copenhagen; C. Chiara, D. Fossan, T. Koike, D. LaFosse, K. Starosta, S.U.N.Y. at Stony Brook; D. Appelbe, J. Waddington, McMaster University; R. Clark, M. Cromaz, P. Fallon, G. Lane, C. Svensson, Lawrence Berkeley National Lab.; R. Janssens, D. Seweryniak, Argonne National Lab.

(32) B(M1)-Values in the Band Crossing Region of the Strongest Shears Band in ^{197}Pb [Krücken]
C. Beausang, J. Cooper, R. Krücken, J. Novak, Yale University ; A. Dewald, G. Kemper, T. Klug, Universität zu Köln; R. Clark, Lawrence Berkeley National Lab.; I. Wiedenhoever, R. Janssens, Argonne National Lab.

(33) Spectroscopy of Proton-Decay Links from Superdeformed Minima in Mass 60 Nuclei [Rudolph]
R. Charity, M. Devlin, F. Lerma, D. Sarantites, L. Sobotka, Washington University; H. Eberth, T. Steinhardt, Universität zu Köln; D. Balamuth, P. Hausladen, University of Pennsylvania; J. Wilson, University of Copenhagen; C. Baktash, A. Galindo-Uribarri, Oak Ridge National Lab.; C. Andreoiu, C. Fahlander, D. Rudolph, Lund University

(34) Study of K-Forbidden Transitions in ^{178}Hf by Coulomb Excitation [Gerl]
M. Devlin, Washington University; P. Napiorkowski, J. Srebrny, Warsaw University; D. Cline, C. Wu, University of Rochester; K. Vetter, Lawrence Berkeley National Lab.; J. Gerl, C. Schlegel, H. Wollersheim, GSI, Darmstadt; R. Janssens, I. Wiedenhoever, Argonne National Lab.

(35) Spectroscopy of Exotic, Neutron-Rich Nuclei at and above the Doubly-Closed Shell at $^{208}_{82}Pb_{126}$ [Lane]
R. Clark, G. Lane, A. Macchiavelli, K. Vetter, Lawrence Berkeley National Lab.; R. Broda, B. Fornal, Institute of Nuclear Physics; A. Byrne, G. Dracoulis, Australian National University; M. Carpenter, R. Janssens, K. Lister, I. Wiedenhoever, Argonne National Lab.

(36) Off-Line Studies in Very Heavy Nuclei with Gammasphere [Ahmad]
J. Uusitalo, University of Jyväskylä; P. Bhattacharyya, Purdue University; P. Reiter, Ludwig Maximilians-Universität München; I. Ahmad, M. Carpenter, R. Chasman, J. Greene, R. Janssens, T. Khoo, F. Kondev, T. Lauritsen, C. Lister, D. Seweryniak, A. Sonzogni, I. Wiedenhoever, Argonne National Lab.

(37) Dynamics of the Ternary Fission of ^{252}Cf with Gammasphere [Ramayya]
C. Beyer, J. Hwang, J. Kormicki, A. Ramayya, X. Zhang, Vanderbilt University; G. Chubaryan, Texas A & M University; W. Ma, Mississippi State University; A. Fomichev, J. Kliman, L. Krupa, A. Rodin, Joint Institute for Nuclear Research; I. Ahmad, J. Greene, R. Janssens, K. Lister, D. Seweryniak, I. Wiedenhoever, Argonne National Lab.

(38) Superdeformation in Neutron-Rich A ~ 70 Nuclei [Devlin]
M. Devlin, M. Furlotti, D. Sarantites, V. Tomov, Washington University; T. Steinhardt, O. Thelen, Universität zu Köln; M. Carpenter, R. Janssens, K. Lister, D. Seweryniak, Argonne National Lab.

(39) Spectroscopy of Neutron-Rich $50 < A < 90$ Nuclei via Fusion-Fission Reactions [Devlin]
M. Devlin, F. Lerma, D. Sarantites, Washington University; D. Cline, C. Wu, University of Rochester; S. Vincent, R. de Haan, University of Notre Dame; J. Wilson, University of Copenhagen; N. Fotiadis, Rutgers University; M. Carpenter, R. Janssens, I. Wiedenhoever, Argonne National Lab.

(40) Proton Transfer Reactions in Actinide Nuclei: Spectroscopy Beyond Pu and Cm? [Janssens]
D. Cline, University of Rochester; S. Siem, University of Oslo; G. Hackman, University of Kansas; J. Caggiano, M. Carpenter, A. Heinz, R. Janssens, F. Kondev, T. Lauritsen, A. Sonzogni, J. Uusitalo, I. Wiedenhoever, Argonne National Lab.

(41) High-K Isomers in Neutron-Rich ^{182,184}Hf Nuclei via Transfer Reactions [Chowdhury]
C. Pearson, Z. Podolya'k, P. Walker, C. Wheldon, University of Surrey; P. Chowdhury, R. D'Alarcao, I. Shestakova, University of Massachusetts, Lowell; D. Cullen, University of Liverpool

(42) A Search for Chiral Doubling in Nuclei [Clark]
R. Clark, P. Fallon, M. Stephens, C. Svensson, Lawrence Berkeley National Lab.

(43) Lifetimes of Exotic Bands in ^{168,169}Hf [Varmette]
C. Beyer, Vanderbilt University; D. Hartley, University of Tennessee; S. Siem, University of Oslo; A. Bracco, B. Million, University of Milano; G. Hagemann, B. Herskind, T. Saitoh, G. Sletten, J. Wilson, University of Copenhagen; W. Liu, W. Ma, S. Phillips, R. Piercey, J. Terry, P. Varmette, J. Winger, Mississippi State University; M. Carpenter, R. Janssens, T. Khoo, C. Lister, Argonne National Lab.

(44) Feeding and Decay of the Doubly-Magic SDB in ^{60}Zn [Svensson]
M. Furlotti, D. Sarantites, Washington University; T. Steinhardt, O. Thelen, Universität zu Köln; W. Reviol, University of Tennessee; R. Austin, T. Rodinger, J. Waddington, McMaster University; C. Andreoiu, D. Rudolph, Lund University; R. Clark, C. Svensson, Lawrence Berkeley National Lab.; M. Carpenter, R. Janssens, T. Khoo, T. Lauritsen, Argonne National Lab.

(45) High Spin States in ^{100}Pd: Search for 'Anti-Magnetic Rotation' [Garg]
P. Boutachkov, E. Kharraja, S. Zhu, University of Notre Dame; S. Chintalapudi, S. Ghugre, IUCDAEF-Calcutta Center; R. Janssens, Argonne National Lab.

(46) Study of High-Spin α-Decaying States in 24Mg by α–α–γ–γ Angular Correlations at Gammasphere [Wiedenhoever]
M. Devlin, D. Sarantites, L. Sobotka, Washington University; S. Siem, University of Oslo; P. Bhattacharyya, Purdue University; H. Amro, North Carolina State University; J. Caggiano, M. Carpenter, A. Heinz, R. Janssens, F. Kondev, T. Lauritsen, K. Lister, D. Seweryniak, A. Sonzogni, I. Wiedenhoever, A. Wuosmaa, Argonne National Lab.

(47) Band Termination, Superdeformation and Complex Clusters in ^{32}S [Baktash]
M. Furlotti, D. Sarantites, V. Tomov, Washington University; C. Baktash, A. Galindo-Uribarri, A. Huerta-Hernardcz, E. Padilla-Rodal, S. Pascual-Vazquez, S. Paul, D. Radford, C. Yu, Oak Ridge National Laboratory; M. Cromaz, A. Macchiavelli, Lawrence Berkeley National Lab.; M. Lipoglavsek, Jozef Stefan Institute; M. Carpenter, D. Seweryniak, Argonne National Lab.

(48) Landau-Zener Crossing Between the First and Second Minima in ^{131}Nd [Hartley]
D. Sarantites, Washington University; D. Balabanski, D. Hartley, W. Reviol, L. Riedinger, O. Zeidan, University of Tennessee; A. Galindo-Uribarri, Oak Ridge National Laboratory; R. Laird, M. Riley, Florida State University; F. Kondev, Argonne National Lab.

(49) Studies of the Continuum Gamma-Ray Spectrum [Lee]
G. Lane, I. Lee, F. Stephens, M. Stephens, D. Ward, Lawrence Berkeley National Lab.; R. Janssens, M. Carpenter, Argonne National Lab.

(50) Search for Discrete Energy Proton and Alpha-Particle Decay of Nanosecond Isomers in the ^{100}Sn Region: Spectroscopy of $^{105\text{-}107}$Sb, $^{106\text{-}107}$Te, and $^{102\text{-}104}$Sn [Sarantites]
R. Charity, M. Furlotti, D. Sarantites, V. Tomov, Washington University; W. Reviol, University of Tennessee; D. Rudolph, Lund University; R. Clark, M. Cromaz, P. Fallon, A. Macchiavelli, Lawrence Berkeley National Lab.; M. Carpenter, D. Seweryniak, Argonne National Lab.

(51) High-Accuracy Mass Determination of Neutron-Deficient Hg Isotopes: On-Line Commissioning of the CPT Spectrometer [Savard]
J. Schwartz, Yale University; J. Clark, J. Fingler, H. Fukutani, K. Sharma, University of Manitoba; J. Hardy, Texas A & M University; C. Boudreau, F. Buchinger, A. Cassidy, J. Crawford, S. Gulick, J. Lee, McGill University; M. Maier, Lawrence Berkeley National Lab.; D. Hofman, G. Savard, D. Seweryniak, J. Uusitalo, Argonne National Lab.

(52) High-Accuracy Determination of the Q-Value of Superallowed 0^+ to 0^+ Beta-Emitters with the CPT Mass Spectrometer [Savard]
J. Schwartz, Yale University; J. Clark, J. Fingler, University of Manitoba; C. Boudreau, F. Buchinger, A. Cassidy, S. Gulick, McGill University; M. Maier, Lawrence Berkeley National Lab.; J. Caggiano, H. Fukutani, A. Heinz, G. Savard, D. Seweryniak, Argonne National Lab.

(53) Study of the Breakout from the Hot CNO Cycle to the (rp) Process via the $^{18}Ne(\alpha,p)^{21}Na$ Reaction [Rehm]
P. Crotty, University of Chicago; B. Harss, Tu Munich; F. Borasi, R. Segel, Northwestern University; R. Janssens, C. Jiang, J. Nolen, R. Pardo, K. Rehm, J. Schiffer, A. Sonzogni, J. Uusitalo, I. Wiedenhoever, Argonne National Lab.

(54) Measurement of the $^{17}F(p,\alpha)^{14}O$ Reaction [Harss]
A. Chen, P. Parker, Yale University; P. Crotty, University of Chicago; B. Harss, Tu Munich; J. Blackmon, M. Smith, Oak Ridge National Laboratory; F. Borasi, Northwestern University; R. Janssens, C. Jiang, R. Pardo, K. Rehm, J. Schiffer, A. Sonzogni, J. Uusitalo, I. Wiedenhoever, Argonne National Lab.

(55) Measurement of the $^{17}F(p,\alpha)^{14}O$ and $^{17}F(p,p)^{17}F$ Reactions [Harss]
P. Parker, Yale University; B. Harss, Tu Munich; R. Segel, Northwestern University; D. Rudolph, Lund University; J. Caggiano, A. Heinz, R. Janssens, C. Jiang, R. Pardo, K. Rehm, J. Schiffer, R. Siemssen, I. Wiedenhoever, Argonne National Lab.

(56) Decay Properties of Particle-Unbound States in ^{19}Ne [Borasi]
R. Teng, University of Rochester; B. Harss, Tu Munich; F. Borasi, R. Segel, Northwestern University; M. Paul, Hebrew University of Jerusalem; J. Caggiano, A. Heinz, R. Janssens, C. Jiang, R. Pardo, K. Rehm, J. Schiffer, R. Siemssen, A. Sonzogni, J. Uusitalo, I. Wiedenhoever, A. Wuosmaa, Argonne National Lab.

b. Outside Users of ATLAS During the Period October 1, 1998 - September 30, 1999

This list includes all outside Users who were an experiment spokesperson (a), alternate spokesperson (b), student (*) or collaborator actually present at ATLAS for an experiment. An additional 110 Users listed as collaborators on the various experiment proposals were not at ATLAS in person, and thus are not represented in the list below.

(1) Australian National University
A. Byrne
M. Dasgupta
G. Dracoulis
D. Hinde
C. Morton

(2) Chalmers University of Technology
b Ö. Skeppstedt

(3) De Paul University
S. Fischer

(4) Duke University
* L. McLean

(5) Florida State University
* R. Laird
M. Riley

(6) GSI, Darmstadt
J. Gerl
C. Schlegel
H. Wollersheim

(7) Hebrew University of Jerusalem
M. Paul

(8) IUCDAEF-Calcutta Center
S. Chintalapudi
S. Ghugre

(9) Institute of Nuclear Physics
b R. Broda
B. Fornal

(10) Joint Institute for Nuclear Research
A. Fomichev
J. Kliman
L. Krupa
A. Rodin

(11) Jozef Stefan Institute
* M. Lipoglavsek

(12) Lab. Nazionali di Legnaro
D. Napoli

(13) Lawrence Berkeley National Lab.
- b R. Clark
- M. Cromaz
- b P. Fallon
- G. Lane
- I. Lee
- b A. Macchiavelli
- M. Maier
- b F. Stephens
- M. Stephens
- C. Svensson
- K. Vetter
- D. Ward

(14) Lawrence Livermore National Lab.
- R. Bauer
- J. Becker
- L. Bernstein
- P. Garrett
- b K. Hauschild

(15) Ludwig Maximilians-Universität München
- F. Borasi
- P. Reiter

(16) Lund University
- * C. Andreoiu
- C. Fahlander
- D. Rudolph

(17) Material Science Division, ANL
- P. Berghuis
- b G. Crabtree
- b K. Gray
- D. Kim
- a W. Kwok
- D. Miller
- * R. Olsson

(18) McGill University
- * C. Boudreau
- F. Buchinger
- * A. Cassidy
- J. Crawford
- S. Gulick
- J. Lee

(19) McMaster University
- D. Appelbe
- * R. Austin
- * T. Rodinger
- b J. Waddington

(20) Mississippi State University
- * W. Liu
- b W. Ma
- * S. Phillips
- R. Piercey
- * J. Terry
- P. Varmette
- J. Winger

(21) North Carolina State University
- * H. Amro
- E. Tavukcu

(22) Northwestern University
- * F. Borasi
- R. Segel

(23) Oak Ridge National Laboratory
- C. Baktash
- J. Blackmon
- A. Galindo-Uribarri
- * A. Huerta-Hernardcz
- * E. Padilla-Rodal
- * S. Pascual-Vazquez
- S. Paul
- D. Radford
- M. Smith
- C. Yu

(24) Purdue University
- P. Bhattacharyya

(25) Royal Institute of Technology
- * T. Bäck
- B. Cederwall
- E. Ideguchi
- * K. Jonsson
- W. Klamra

(26) Rutgers University
- J. Cizewski
- * K. Ding
- N. Fotiadis

(27) S.U.N.Y. at Stony Brook
- * C. Chiara
- D. Fossan
- * T. Koike
- D. La Fosse
- K. Starosta

(28) Soreq Nuclear Research Center
- D. Berkovits

(29) TRIUMF
- G. Ball

(30) Texas A & M University
G. Chubaryan
J. Hardy

(31) Thomas Jefferson Nat'l. Accelerator Facility
R. Macleod

(32) Tu Munich
b* B. Harss

(33) Universidade de São Paulo
A. Szanto de Toledo

(34) Universität Göttingen
* M. Hausmann
A. Jungclaus

(35) Universität zu Köln
A. Dewald
H. Eberth
* G. Kemper
* T. Klug
* T. Steinhardt
* O. Thelen

(36) Université Louis Pasteur
V. Rauch
M. Rousseau

(37) University of Chicago
* P. Crotty

(38) University of Copenhagen
G. Hagemann
B. Herskind
* T. Saitoh
G. Sletten
b J. Wilson

(39) University of Edinburgh
T. Davinson
b P. Woods

(40) University of Illinois-Chicago
R. Nouicer

(41) University of Jyväskylä
R. Julin
* H. Kankaanpää
J. Uusitalo

(42) University of Kansas
P. Delurgio
* A. Dummer
K. Farrar
b G. Hackman
F. Prosser
S. Sanders

(43) University of Leuven
W. Mueller

(44) University of Liverpool
* A. Chewter
D. Cullen
R. Herzberg
G. Jones

(45) University of Manchester
* C. Baskill
J. Durell
S. Freeman
M. Leddy
* A. Qadir
* S. Robinson
J. Smith
B. Varley

(46) University of Manitoba
* J. Clark
* J. Fingler
* H. Fukutani
b K. Sharma

(47) University of Maryland
* J. Ressler
* J. Shergur
* S. Tumey
W. Walters

(48) University of Massachusetts, Lowell
P. Chowdhury
* R. D'Alarcao
E. Seabury
* I. Shestakova

(49) University of Milano
A. Bracco
B. Million

(50) University of North Carolina-Chapel Hill
A. Champagne

(51) University of Notre Dame
* P. Boutachkov
* R. de Haan
U. Garg
b E. Kharraja
* M. Quinn
* A. Teymurazyan
b S. Vincent
* S. Zhu

(52) University of Oslo
* S. Siem

(53) University of Pennsylvania
D. Balamuth
* P. Hausladen

(54) University of Rochester
b D. Cline
M. Simon
R. Teng
b C. Wu

(55) University of Surrey
W. Catford
C. Pearson
Z. Podolya'k
b P. Walker
* C. Wheldon

(56) University of Tennessee
D. Balabanski
C. Bingham
D. Hartley
W. Reviol
b L. Riedinger
* O. Zeidan

(57) University of York
* D. Jenkins
* N. Kelsall
R. Wadsworth

(58) Uppsala University
* A. Axelsson
M. Weiszflog

(59) Vanderbilt University
* C. Beyer
J. Hwang
b J. Kormicki
A. Ramayya
* X. Zhang

(60) Warsaw University
* P. Napiorkowski
J. Srebrny

(61) Washington University
R. Charity
b M. Devlin
* M. Furlotti
* F. Lerma
b D. Sarantites
L. Sobotka
V. Tomov

(62) Western Michigan University
L. Paulius

(63) Yale University
* D. Bardayan
C. Beausang
* A. Chen
J. Cooper
R. Krücken
* J. Novak
P. Parker
* J. Schwartz

II. OPERATION AND DEVELOPMENT OF ATLAS

OVERVIEW

This and the following section report on the operation of the Argonne Tandem Linear Accelerator System (ATLAS) as a national user facility and related accelerator physics R&D projects. ATLAS is used for basic research in nuclear and atomic physics, and occasionally for other areas of research and development, such as material science. Over half of the beam time is allocated to experiments for which the spokesperson is an outside user. Recent ATLAS operating performance and related development projects are described. ATLAS personnel are also involved in developing technology in support of a future advanced facility for beams of short-lived nuclei based on ATLAS. Projects related to the exotic beam facility are also described.

ATLAS operates on a seven-day-per-week schedule. The installation of GAMMASPHERE was completed in December 1997 and the experimental program with GAMMASPHERE began in January 1998. For the 1999 fiscal year, ATLAS provided 6054 hours of beam time for research, surpassing the 6000-hour goal. Beams were provided from twenty-nine different isotopes at intensities up to 250 pnA. Statistics about beam hours and users are given in Table II-1. 74% of all beam time was used by GAMMASPHERE in FY1999. The GAMMASPHERE research program will end in mid-March, 2000 after which ATLAS plans to enter a maintenance period for approximately six weeks.

ATLAS continued to provide a range of radioactive species with intensities generally in the range of 10^5 to 10^6 particles per second. This year 6.4% of all beam-time went to radioactive beams. The fraction of beam time devoted to these low-intensity rare beams decreased this year due to the demands of the GAMMASPHERE research program. Beams of long-lived ($T_{1/2}$ > 2 hours) species produced at other facilities and placed in the ATLAS tandem ion source and beams of short-lived species produced in-flight by inverse-kinematics reactions have been developed at ATLAS. See the Heavy-Ion Research section for a summary of recent physics results from experiments using radioactive beams.

Table II-1. SUMMARY of ATLAS EXPERIMENTS and USER STATISTICS

	FY 1999 (actual)	FY 2000 (extrap.)	FY 2001 (pred.)
Beam Use for Research (hr)			
Nuclear Physics	5586	5000	4600
Atomic Physics	292	250	150
Accelerator R & D	48	100	150
Other	120	110	100
Total	6046	5460	5000
Number of Experiments Receiving Beam	56	50	45
Number of Scientists Participating in Research	251	150	130
Institutions Represented			
Universities (U.S.A.)	23	14	14
DOE National Laboratories	5	5	5
Other	33	20	20
Usage of Beam Time (%)			
In-House Staff	38	35	35
Universities (U.S.A.)	35	38	40
Other DOE National Laboratories	12	12	10
Other Institutions	15	15	15
Total	100%	100%	100%

A. OPERATION OF THE ACCELERATOR

(R.C. Pardo, D. Barnett, B. Batzka, J. Bogaty, B. E. Clifft, S. Daley, A. Deriy, R. Jenkins, A. Krupa, S. McDonald, B. Millar, F. H. Munson, Jr., A. Peevy, D. R. Phillips, D. Quock, A. Ruthenberg, R.H. Scott, J. R. Specht, P. Strickhorn, R. C. Vondrasek, G. P. Zinkann)

a.1. Operations Summary

The operation of ATLAS during FY1999 was dominated by the presence of GAMMASPHERE and the associated fragment mass analyzer (FMA). For FY1999, approximately 74% of all beam time provided by ATLAS went to experiments using GAMMASPHERE. The primary goal of operation was to provide the requested beams with as little unscheduled downtime and as high a reliability as possible. The results for FY1999 are tabulated in Table II-2 and show that ATLAS provided 6046 research hours with beam-on-target or available. This performance was achieved with an operational reliability of 93.2%.

The excellent facility performance was achieved during a period of high personnel turnover. During a significant portion of FY1999, ATLAS operated with only three fully qualified operators and one operations supervisor. Even so, not one shift was left uncovered during that period. The dedication of the operator group to providing coverage for ATLAS deserves our sincere thanks and appreciation.

ATLAS provided a total of 29 different isotopes for research in FY1999. The distribution of species is shown in Figure II-1. The demand for these isotopes was amazingly uniform, with no single species accounting for more than 10.7% of all beam time during the year. Over 37% of all beam time was for isotopes heavier than ^{58}Ni, a return to a more typical distribution for ATLAS from last year's rather light-weight distribution when only 20% of all beam time went to beams heavier than nickel.

The new ion source, ECR-II, is now fully operational and provided approximately 13% of all beam time during the 1999 calendar year. The associated new bunching system is still undergoing development, especially the traveling-wave chopper. That system is now nearly fully operational and with the ECR-I upgrade project nearing the construction phase, ECR-II will provide a significantly increased portion of all beam time during FY2000.

With two ECR sources in operation it had become imperative that additional effort be directed to the operation of these sources. A second ECR source operator/engineer position has been created and staffed with a person from the operator pool (R. H. Scott). This enhancement to the staffing addresses a crisis situation in which the facility was effectively dependent on a single person for 7-day 24-hour coverage.

The tandem injector continues to be a useful component of the ATLAS facility. The tandem was used for beam delivery 35% of the scheduled time. The tandem has assumed an important role in the ongoing radioactive beam program at ATLAS today. It is used for the acceleration of long-lived isotopes made at other facilities such as ^{18}F, ^{56}Ni, and ^{44}Ti. The development of these beams was described in past annual reports.

A new SNICS negative ion source was purchased in FY1999 so that one source may be dedicated to radioactive beam production. As the ongoing RIB activity has progressed, longer-lived species have become the focus. The problem of maintenance of these, now radioactive, source bodies has become more difficult. Dedicating one source to stable beams will improve the situation. In additional, a new hot lab facility will be constructed in FY2000 for servicing these ion sources. This facility will be constructed in a room adjacent to the tandem vault which previously was used for negative ion source development activities.

The use of the original linac target area, Area II, has increased significantly during the past year as the Canadian Penning Trap Facility gears up for operation. This area had fallen into almost total disuse over the past few years and was bypassed in the various improvements implemented at ATLAS over the past 15 years. This year we started the process of bringing that area up to the standards of the rest of ATLAS including a fully functioning ARIS implementation and computer control of all beamline components. These upgrade activities will be completed in FY2000.

Table II-2. ATLAS Reliability and Hours of Operation

Time Period	Research Beam Hours	Reliability*
FY1999	6046	93.2%
Calendar 1998	6176	92.7

Reliability = 100(Total Research Hours)/(Total Research Hours+Unscheduled Maintenance)

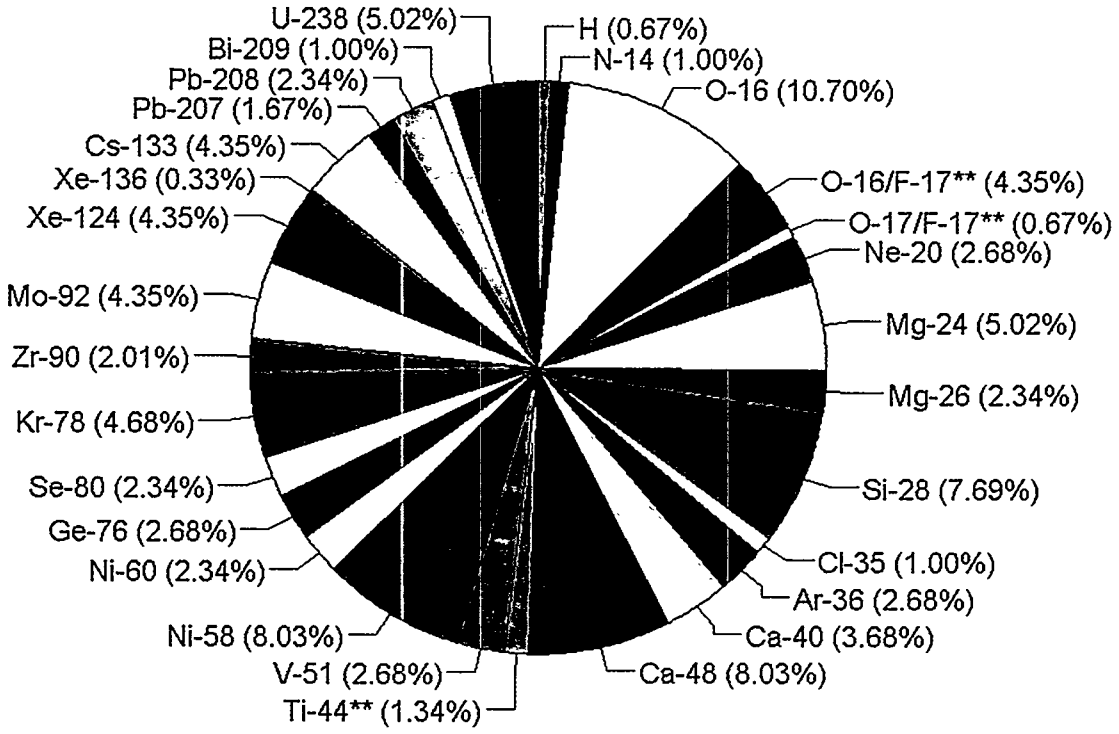

Figure II-1. Distribution of beam time, by isotope, provided by ATLAS in FY1999. A total of 29 different isotopes were provided to the research program. Radioactive beams of ^{17}F and ^{44}Ti comprised 6.4% of all beam time in FY1999.

B. DEVELOPMENTS RELATED TO ATLAS

b.1. Status of the 14-GHz ECR Ion Source (ECR-2) (R. Vondrasek and R. H. Scott)

ECR-2 has continued to be used for the injection of beams into the PII linac. Due to its higher beam output it has been used for most of the runs using gas as a feed material. Solid material development has continued with an emphasis on the sputtering technique (employed at ECR-1) as well as the introduction of magnetic materials (Fe, Ni, Co). The high temperature oven has been used to produce beams of ^{76}Ge, ^{84}Sr, ^{152}Sm, and ^{208}Pb.

The sputtering technique has been used at ECR-1 very successfully for the past several years. A solid piece of sample material is introduced into the plasma chamber and a negative voltage is applied to it. The plasma ions accelerate towards the sample and sputter material from its surface. This technique was utilized with many materials (iron, nickel, molybdenum, lead, and uranium) with great success. We are developing this technique at ECR-2 as well. We have made good progress except with magnetic materials. Due to the

close proximity of the sample to the edge of the plasma chamber slot, as well as the presence of the high magnetic field from the hexapole, material sputtered from the sample creates a short between the sample and the chamber. Further work in this area is required. In the interim we are delivering these beams (iron and nickel) out of the high temperature oven.

We used the sputtering technique at ECR-2 to produce stable beams of ^{208}Pb and ^{238}U. The uranium was produced using a sample of depleted uranium metal, which was biased to 3.0 kV. The lead was produced using a natural metal sample with a bias voltage of 1.1 kV. A lead beam was produced using the oven under the same source conditions and the results confirm that the oven technique produces a higher peak charge state than the sputtering technique. However, both techniques are capable of producing >1 puA of lead. Results are summarized in Table II-3.

Table II-3. Performance of ECR-2 for Heavy Metal Beams

Q	^{238}U Sputtering	^{208}Pb Sputtering	^{208}Pb Oven
23		27.5	14.5
25	11.8	31.0	21.5
27	8.2		
28	6.5	12.5	24.0
32			8.8

All intensities are in euA as measured on the source platform.

An issue reported in the 1998 status report was the electrical noise generated by the ALPHA power supplies used to power the source solenoid coils. An interim fix was implemented using spare power supplies as well as heavy filtering of the power line on the deck. We replaced the power supplies with Lambda EMI high frequency switching power supplies. These power supplies do not produce the line noise present from the SCR-based supplies and all systems on the deck are now fully functional.

b.2. Upgrade of ATLAS ECR-1 Ion Source (D. P. Moehs, R. H. Scott, R. Vondrasek, and R. C. Pardo)

Renovation of the ATLAS 10 GHz ECR-1 ion source, which began operation in 1987, is in the construction and testing phase. The original ion source has served ATLAS well, but a major redesign of the magnetic confinement fields and plasma chamber should significantly improve performance. The primary goal for the upgrade is to improve the average charge state distribution produced by the source, shifting the average charge state up by approximately 10%. A secondary goal is to increase the total useful extracted beam current by up to a factor of two.

To accomplish these goals, while maintaining a source design that continues to emphasize the importance of solid feed materials, the old two-stage source is being converted to a single-stage design similar to ECR-2. The new source will utilize an electron donor disk and high gradient magnetic field design that preserves radial access for solid material feeds and pumping of the plasma chamber. A rail-mounting system for the injection coil provides flexibility and easy access to the plasma chamber. The overall magnetic field profile should allow for the possibility of a second ECR zone at a frequency of 14 GHz (see Fig. II-2).

An open hexapole configuration with radial ports 2.8-cm long and 1.7-cm wide through the plasma chamber allows access to the plasma chamber for solid feed materials. Pumping of the chamber will be provided through all six of the radial ports as well as through the extraction tank. Measurements of the magnetic field strength near the surface of the plasma chamber are in good agreement with computer calculations. At the chamber wall, 4 cm in radius, the field strength is nearly 9.3 kG along the magnet poles and 5.7 kG along the pole gaps. Eight solenoid coil pancakes from the existing ECR are being reused to produce the axial mirror in conjunction with a 2-inch-thick iron yoke. These coils can carry a current of up to 500 A and computer models predict a minimum B field of 3 kG with injection and extraction mirror ratios of 4.4 and 2.9, respectively. The parameters are summarized in Table II-4. The rebuilt source is expected to begin operation in the summer of 2000.

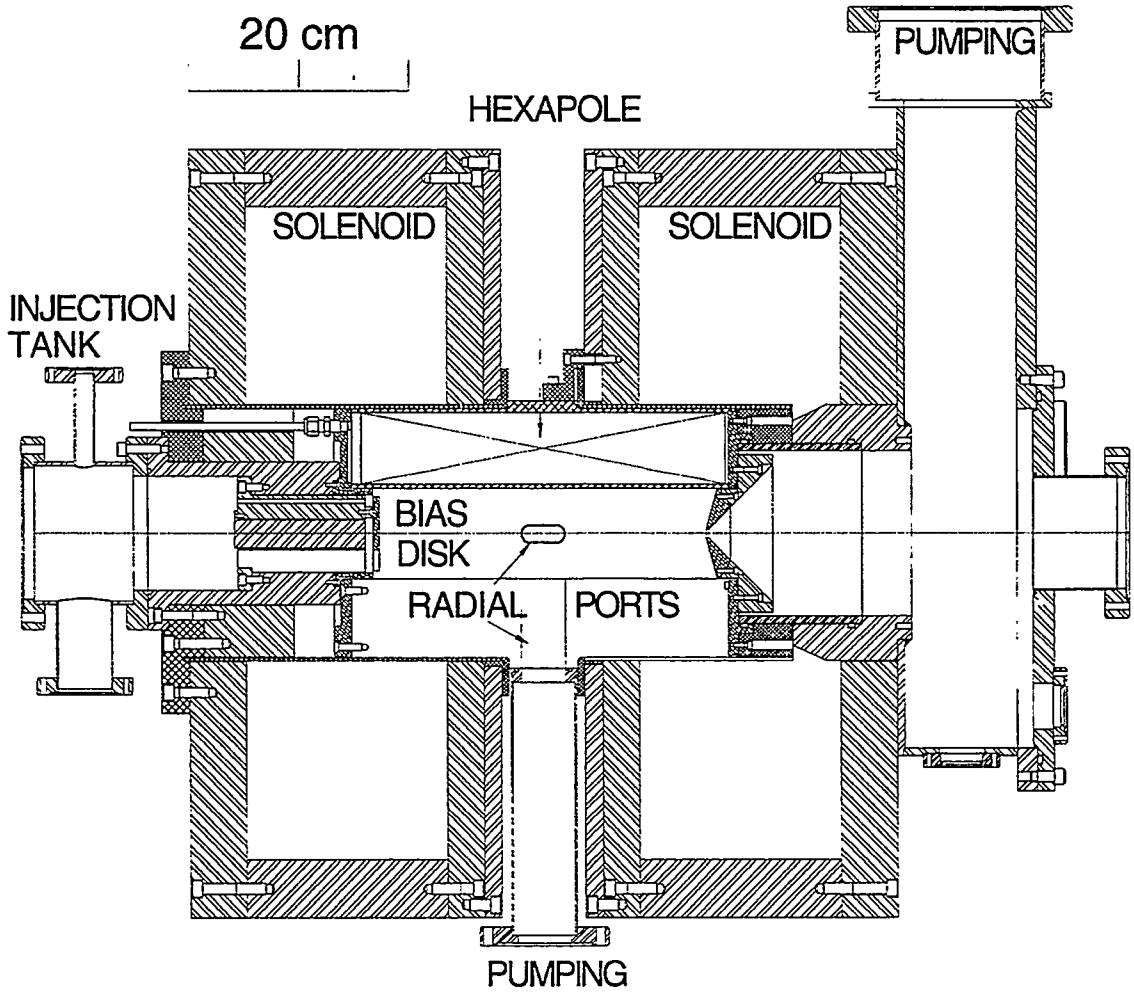

Figure II-2. Schematic of the upgraded ECR-1 10-GHz ECRIS with the injection tank on the left. Pumping of the plasma chamber will be provided through two of the radial ports and through the extraction region.

Table II-4. Summary of the upgraded ECR-1 parameters.

Microwave Frequency	10 GHz 14 GHz possible		
Aluminum plasma chamber		Hexapole	
Inner Diameter	8.0 cm	Length	33.0 cm
Radial ports	2.8 cm by 1.7 cm	Easy axis angle (radial ref.)	38.0°
Water channel cross section	0.38 cm^2	B_r Pole tip field, r = 4 cm	≈ 9.3 kG
		B_Φ Gap field, r = 4 cm	≈ 5.6 kG
Solenoid coils		Cooling water	
Current range for 10 GHz	350 – 500 A	Input temperature	≈ 11° C
Minimum Field (500 A)	3.0 kG	Head pressure	80 psi
Injection side MR	4.4 kG	Max. expected $\Delta T_{hexapole}$	< 10° C at 1.0
Extraction side MR	2.9 kG	For a 2 kW input	gpm per channel
		Max. expected ΔT_{coils}	< 30° C at 4.0
		For a current of 500 A	gpm per coil

b.3. Vibration Damper (A. Facco*, G. P. Zinkann, and K. W. Shepard)

Phase stability of low-velocity superconducting accelerating structures is limited by ambient acoustic noise that excites mechanical vibrations in the cavities. In the PII section of the accelerator, these effects are most troublesome in the heavily loaded very low beta (.008 and .016) four-gap quarter wave resonators. A vibration damper has been designed and installed in a $\beta = 0.016$ (I2) resonator to reduce such phase noise. Figure II-3 illustrates the components of the Vibration Damper. The mechanical damper consists of a stainless steel holding tube and a sliding load. The load sits on the holding tube terminating disk and it is free to slide over it while being maintained in a coaxial position with the inner conductor by three centering rods. Every vibration of the inner conductor makes the load slide, producing mechanical power dissipation and reducing the mechanical Q.

*INFN- Laboratori Nazionali di Legnaro,via Romea 4, I-35020 Legnaro (Padova) Italy

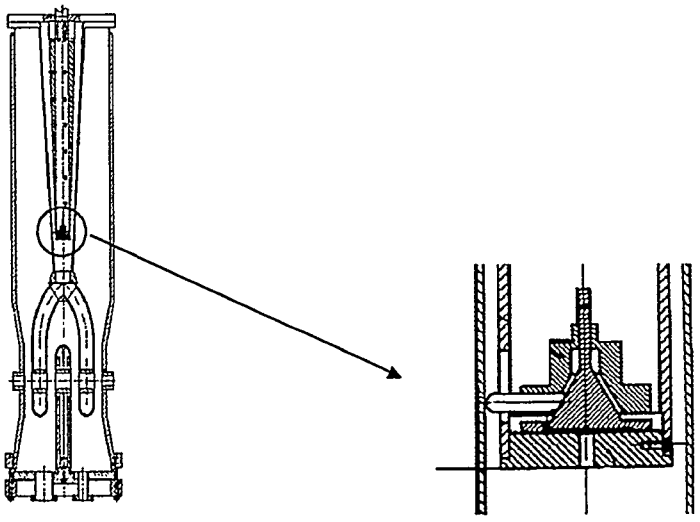

Figure II-3. Components of the Vibration Damper

An I2 class resonator with the largest amount of mechanical vibration was chosen to test the damper design. Calculations were done to compute the mass needed to dampen the I2-type resonator. The damper was constructed in November 1998 and installed in December during a scheduled maintenance period. Room temperature testing and optimization could not be done given the short duration of the downtime available. The results of the damper are given in Table II-5

Table II-5. Table of Vibration Damper Results

	R112		R113 (control cavity)
	Noise Frequency (Hz)	Vibration Decay Time (s)	Noise Frequency (Hz)
Without damper	~375	28	~125
With damper in R112	~40– 80	0.5	

The success of the Vibration Damper enables the reduction of the tuning window on the fast tuner. This has several benefits.

1. The reactive power that the PIN diodes are required to switch is lower.
2. The output power required of the drive amplifier is lower.
3. The energy spread of the beam is smaller due to less phase wobble from the fast tuner.

Plans to install another Vibration Damper in the other $\beta = 0.008$ resonator are underway.

b.4. Status of the Transmission-Line Chopper for ATLAS (R.C. Pardo, J.M. Bogaty, B.E. Clifft)

A ten-segment transmission-line chopper (Fig. II-4) whose job is to remove unbunched tails from a partially bunched heavy-ion beam in order to avoid undue emittance growth in the linac and eliminate undesirable satellite beam bunches has been installed on the PII low-energy beamline. This chopper is designed to work with a new PII bunching system geometry that requires a bunch width of approximately 16-17 ns at the chopper location.

When poorly bunched beams traverse the traditional sine-wave chopper, unacceptable transverse emittance growth and unnecessary beam loss result. Significant reduction in the emittance growth and beam losses compared to a sine-wave chopper was reported last year. The chopper was rebuilt with a new water-cooled semi-rigid delay line to allow CW operation at 12 MHz. A new driver and power supply was constructed and operated off-line at 6 MHz, but 12 MHz operation has continued to elude us. New driver circuitry is being designed and initial testing is planned for the spring of 2000.

b.5. ATLAS Control System (F. H. Munson, D. Quock, J. Figueroa, B. Chapin)

A number of new features and improvements were made during this reporting period. The more significant changes involved ion source control and monitoring, data acquisition, and record keeping.

The original ECR ion source was incorporated into the main control system. Ion sources at ATLAS make use of two levels of high voltage. In the past, insulated rods were required to control devices at one of these levels on the ECR sources. Hardware and appropriate software have been added to allow the use of fiber optic cable to control and monitor the entire ion source from any one of the control consoles. Faraday cup currents originating on the high-voltage platform can now be read using a new process that makes use of a graphical analog meter.

The control system's data-acquisition software comprises in-house written processes, and Vista Inc.'s Vsystem graphical interface. Therefore, it is integrated seamlessly into the overall system. Improvements were made to the method of setting cursors about peaks in graphical energy and timing plots. In addition, a new data-acquisition diagnostic region was added providing a more flexible user interface for modifying constants.

Record keeping is an important function of the control system. One feature of this effort is the ability to store and retrieve complete accelerator tune configurations. Previously only three possible charge-state stripping - foil configurations were allowed. Recently a fourth was added at the exit of ATLAS.

b.6. ATLAS Cryogenic System (J. R. Specht, B. Millar, and S. W. MacDonald)

Improving operational reliability and safety has been the goal for cryogenic enhancements this year. Condensation and ice were a problem with the lines and heaters venting cold nitrogen from the various cryostat shields etc. We rebuilt all the cold gas heaters to move the ac power leads to the warm end of the heater. In addition the on-off type temperature controllers were replaced with proportional ones with SCR outputs. This should eliminate controller failures due to output relay problems.

Vacuum insulated hoses were installed on one cryostat to eliminate the condensation problem with the interconnecting hose. This test went very well and as a result during the next few years all the lines will be replaced on the remaining six cryostats.

We designed, built, and operated an automatic LHe fill system for a superconducting magnet used in radioactive beam experiments. This system increased beam time while eliminating worker exposure to radiation.

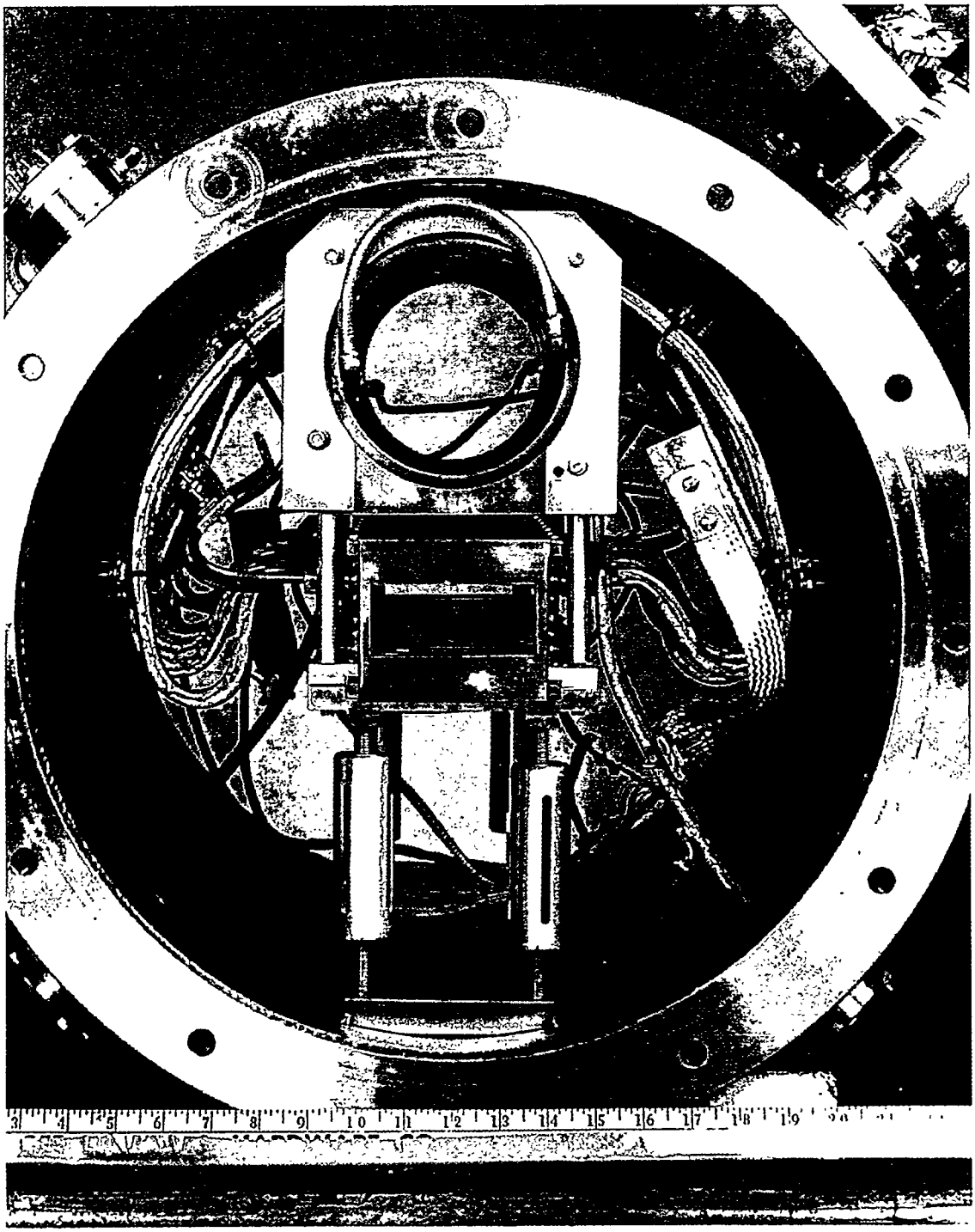

Figure II- 4. Photograph of the assembled transmission-line chopper in its vacuum housing. Shown is a portion of the semi-rigid delay-lines connecting the sequential electrodes visible in the rectangular beam aperture.

C. RESONATOR DEVELOPMENT AND CONSTRUCTION FOR THE NEW DELHI LINAC

c.1. Resonator Construction Project (K. W. Shepard, P. Potukuchi*, S. Ghosh*, and M. Kedzie)

Construction of the first twelve niobium quarter-wave cavities has been completed. Shipment of the cavities to New Delhi awaits removal of the Nuclear Science Centre from the proscribed entity list by the U. S. DOE Office of Non-Proliferation. The completion of twelve cavities within the budget and schedule allotted for ten cavities was made possible by the increase in productivity in the electron-beam welding process that was achieved during this project in collaboration with the e-beam welding vendor, Sciaky, Inc.

c.2. Slow-tuner Development (M. P. Kelly, P. Potukuchi*, S. Ghosh*, K. W. Shepard, M. Kedzie, and B. E. Clifft)

Tests of a niobium-bellows slow tuner fully assembled with a production version of the New Delhi 97-MHz quarter-wave cavity were completed. Accelerating gradients as high as 5 MV/m can be stably maintained with no measurable performance decrease due to rf-loss-induced heating of the bellows assembly as was observed in an earlier design. Figure II-5 shows the niobium-bellows tuner and the flange for attaching to the quarter-wave resonator. Internally, a newly re-designed Belleville washer assembly provides an additional restoring force which increases the range of motion to 2 millimeters for applied (He) gas pressures of 0 - 1 atmosphere. The corresponding tuning range was measured to be 45 kHz at 4.2 K.

* Nuclear Science Centre, New Delhi, India

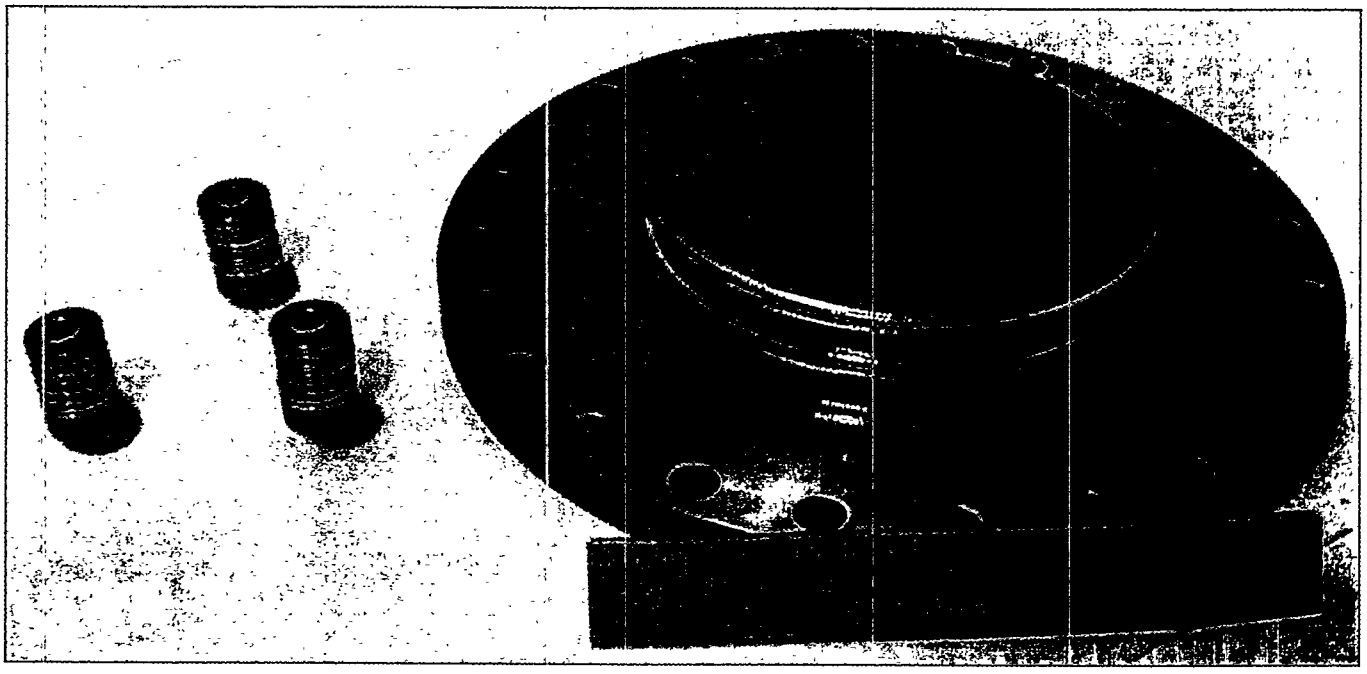

Figure II-5. The niobium-bellows tuner assembly together with three Belleville washer stacks used to provide an additional restoring force.

III. R & D RELATED TO A FUTURE RARE ISOTOPE ACCELERATOR FACILITY

A. INTRODUCTION

Intense efforts over the past few years, supported in part by Argonne Laboratory Directed Research and Development (LDRD) funds, have led to an exciting concept for an advanced facility for beams of exotic short-lived nuclei of the ISOL (Isotope Separation On Line) type. Such a facility is based on an intense driver beam that produces short-lived nuclear species which are stopped, the desired isotope is selected, and accelerated to the appropriate energy in a second accelerator.

The recent Argonne work involves a number of technical innovations. Most importantly, it includes a novel approach that avoids the most serious drawbacks of an ISOL facility for a broad range of beams: delay between the production of the short-lived isotopes and their acceleration and the underlying sensitivity to the chemistry of extracted species. A scheme has been developed which provides for shorter delay times and insensitivity to the chemical properties. It is based on intense heavy-ion beams from the production linac, the use of the projectile fragmentation mechanism, and subsequent extraction of the desired fragment from a high-pressure helium-gas stopper cell.

The overall Argonne concept aims squarely at providing the intense beams of short-lived nuclei needed to carry out the research described in the community White Paper (1997) on the Science Opportunities with an ISOL Facility. Our initial plans, described in the 1995 Argonne Working Paper (*ANL Yellow Book*), have found widespread attention. The concept of using a high-power primary linac for light and heavy ions, including the generation of fast neutrons from a deuteron beam for a two-step production scheme, has triggered broad international interest.

The current concept builds and expands on these initial ideas, with several new developments: *i) a **superconducting cw production linac***, providing intense beams of light and light heavy-ions with beam power of up to 400 kW, and heavy ions up to uranium at 100 kW; *ii) **2- step targets*** to handle beam powers in excess of 100 kW; *iii)* utilization of a ***range of reaction mechanisms*** to optimize yields of radioactive ions

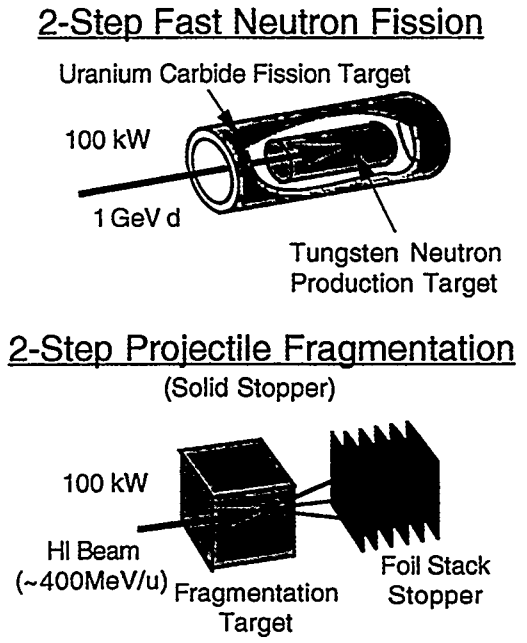

Fig. III-1 Production target concepts RIA.

and to match the high-power target concepts; *iv)* development of a cw injector into ATLAS, with a new ***RFQ accelerator for 1^+ ions*** and non-equilibrium low-velocity stripping; and *v)* ***superconducting acceleration and focusing structures*** for efficient injection into ATLAS.

The ISOL Task Force, which met throughout 1999, concluded that an advanced exotic beam facility, now called the Rare Isotope Accelerator (RIA), should utilize a powerful heavy ion driver. The present concept for a CW superconductivity driver is summarized below.

A variety of target concepts developed to handle 100 kW beam powers are illustrated schematically in Figure III-1

B. RADIOISOTOPE PRODUCTION AND HIGH-POWER TARGETRY

(J. Nolen, C. Reed,* I. Gomes,* and A. Hassanein†)

The most critical issues for an advanced ISOL facility concern the generation of radioisotopes in the ISOL production target, and their subsequent extraction as an ion beam. The key technical challenges (target power density, chemical aspects of diffusion, fast effusion geometries, high ionization yields, and ion-source beam emittances) tie into aspects of production mechanisms and target geometry.

The ANL concept for the advanced ISOL facility is based on a high-power superconducting linac providing a broad range of beams, up to uranium. Projected intensities range from close to 10^{16} protons/s to 10^{13} uranium ions/s.

With these intense beams and the high target power densities expected from the Argonne driver linac, target cooling becomes a central issue. In conventional ISOL production schemes the target and ion source are integrally coupled so that cooling the primary target may interfere with the extraction of the radioactive nuclides. With the two-step schemes these functions are physically separated. The ohmic heating by the beam is restricted to the primary target. Advantage is taken of recent developments in cooling with liquid lithium.

*Technology Development Division, ANL; †Energy Technology Division, ANL.

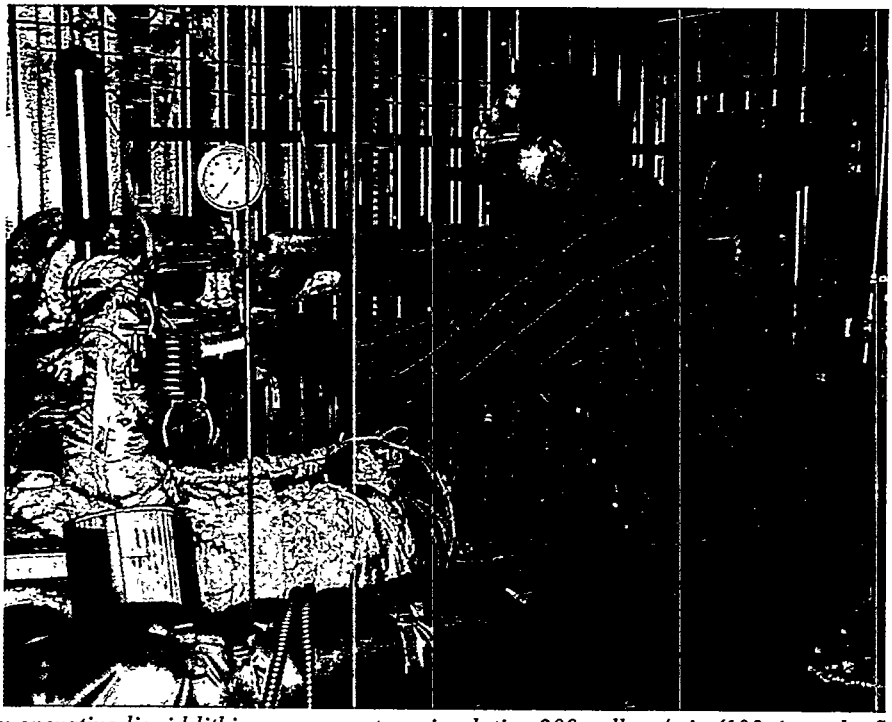

Figure III-2. An operating liquid-lithium pump system circulating 200 gallons/min (100 times the flow needed for the ISOL target) in the Argonne Technology Development Division.

Engineering designs of windowless flowing liquid lithium targets exist at Argonne in the Energy Technology Division and the Technology Development Division, which were developed for stopping 10-MW deuteron beams for the thermonuclear fusion program. Figure III-2 shows a photograph of an operating lithium pump system at Argonne National Laboratory.

C. DEVELOPMENT OF LINAC TECHNOLOGY FOR THE RIA PROJECT

(K. W. Shepard, P. N. Ostroumov, J. Nolen, A. Kolomiets*, M. Kedzie, M. Kelly, M. Portillo, S. Aseev,† and T. Tretyakova*)

The scope of the conceptual design for a driver linac for RIA has been expanded to encompass an unprecedented range of capabilities, including:

- CW beams of the full mass range of ions, from protons through uranium
- Continuously variable output energies up to 400 MeV/nucleon for uranium and higher energies, e.g. 900 MeV protons, for the lighter ions.
- Multiple charge state operation, so that several hundred kilowatts of beam power are available from existing ECR sources for most of the mass range.
- RF beam switching to provide simultaneous CW operation of several targets.

As presently conceived, the linac will provide more than 1.3 GV of accelerating potential, and will consist of an array of more than 400 independently-phased superconducting (SC) cavities of eight different types, ranging in frequency from 58 to 700 MHz. Development of elements of the driver linac is being carried forward at several national laboratories. The technical capabilities developed for the ATLAS SC linac are central in this regard, and are being further developed and extended in several distinct aspects.

Of the eight required cavity geometries, six are low-velocity, low-frequency types of the sort pioneered at ATLAS, and detailed designs for these classes of cavity are being developed with the goal of testing prototypes as soon as feasible. Detailed designs for cryostats, including RF couplers, are also being developed.

The large transverse and longitudinal acceptance available in a SC ion linac opens the possibility of accelerating multiple charge state beams. Such operation can greatly extend the limits of present-day ECR ion source performance, which for the heaviest ions restricts the available beam power in a single-charge-state beam to less than the initial goal of 100 kW, let alone the ultimate goal of 400-kW beams. By operating in a multiple charge state mode, the efficiency of the stripping process is effectively increased by a factor of 3 – 4. This innovation provides directly an increase in the effective beam current and also makes possible the use of multiple strippers, reducing the size of the linac. A further benefit of accelerating multiple charge states is the great reduction in the amount of beam dumped at the stripping points, reducing shielding requirements.

Using numerical simulation techniques, the dynamics of multiple charge state beams are being studied extensively and details of the driver linac lattice, diagnostics, and tuning techniques are being developed. Additionally, experiments are being planned to study several aspects of multiple charge beams that can be tested using the existing ATLAS SC ion linac.

*Institute for Theoretical and Experimental Physics, Moscow, Russia.
†Institute for Nuclear Research, Troitek, Russia.

D. MULTIPLE-CHARGE BEAM DYNAMICS IN AN ION LINAC

(P. N. Ostroumov and K. W. Shepard)

An advanced facility for the production of nuclei far from stability could be based on a high-power driver accelerator providing ion beams over the full mass range from protons to uranium. A beam power of several hundred kilowatts is highly desirable for this application. At present, however, the beam power available for the heavier ions would be limited by ion source capabilities. A simple and cost-effective method to enhance the available beam current would be to accelerate multiple charge states through a superconducting ion linac. The driver linac will consist of two strippers, at ~12 MeV/u and ~85 MeV/u. After the first, the charge state distribution is centered at the charge state q_0=75 for uranium beam. The beam fraction for charge state 75 is 20%; five charges encompass 80% of the incident beam. After the second stripper, 98% of the beam is in four charge states neighboring q_0 = 89, all of which can be accelerated to the end of the linac. The simultaneous acceleration of neighboring charge states becomes possible because the high charge-to-mass ratio makes the required phase offsets small. Figure III-3 shows synchronous phase as a function of charge state calculated for uranium ions at $\varphi_{s,q_0} = -30°$. This particular example shows that if the linac phase is set for charge state q_0=75, it can accelerate a wide range of charge states. If all charge state are injected at the same time then the bunches of different charge state will oscillate. Therefore one can expect effective emittance growth for multiple charge state beams. The results of numerical simulation of all 5 charge state bunches at the linac portion up to 85.5 MeV/u, just before the second stripper, is shown in Fig. III-4. After the second stripper, the effective longitudinal emittance of the multiple charge state beam is increased by a factor of ~6. We note, however, that this longitudinal emittance is still substantially less than the acceptance of the remaining portion of the SC linac which has been calculated by particle ray tracing and also shown in Fig. III-4.

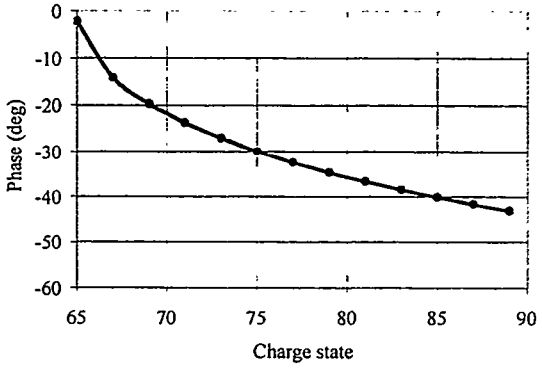

Figure III-3. Synchronous phase as a function of uranium ion charge state. The designed synchronous phase is -30° for q_0 = 75.

Numerical simulations were performed to estimate the effects of various types of errors in accelerator, for both single-charge-state and also for multiple-charge-state beams. In existing SC linacs, phase noise in SRF cavities is generally of the order or less than ±0.3°, and amplitude fluctuations are typically less than ±0.3%. For such systems the effective emittance growth due to multiplicity of charge states in the beam is smaller than the growth due to rf noise. Note that even including both these effects, the total increase in longitudinal emittance is still well below the acceptance of the high energy part of the driver linac.

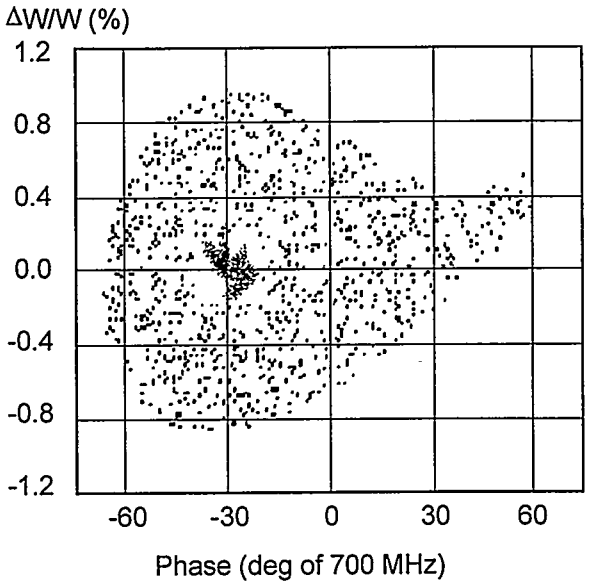

Fig. III-4. Phase space plots of 5 charge state uranium beam at the location of second stripper (85 MeV/u). The large dotted area represents the longitudinal acceptance of the following high-beta linac.

In the ideally tuned linac without any alignment errors the multiplicity of charge states does not produce any emittance growth in transverse phase space. However, in the presence of transverse errors the emittance growth is more severe and less correctable for multiple charge state beams than for single charge state beams. The transverse emittance of multiple charge state beams can grow mostly due to two error effects. The first type of error, mismatch, is caused by errors in tuning or matching the beam into the linac and arises because of errors in measurement of the input beam parameters. The second type of error, a misalignment of the focusing elements, can generally be corrected by using steering magnets to offset any measured deviation of the beam centroid. For a single charge state beam, coherent transverse oscillations and rotation in phase space will not increase effective transverse emittance. In the case of a multiple charge state beam, however, the different charge states have different betatron periods. As the beam proceeds along the linac, the transverse oscillations of the various charge states eventually become uncorrelated and the effective total emittance, summed over all charge states, increases. As we show, the usual corrective steering, can partially correct this situation. Monte Carlo simulations of the dynamics of multiple charge state beams in the presence of alignment errors were performed. A five charge state uranium beam in that portion of the linac between the first and second strippers. Then we tracked the multiple charge state beam through this portion of the linac and noted the increase in transverse emittance resulting from the positioning errors. This entire simulation was then repeated two hundred times, each time with a different, random set of alignment errors. Even for multiple charge state beams, however, emittance growth can be substantially reduced by simple corrective steering procedures. We modeled this by assuming a measurement of beam centroid position and corrective steering to be performed once every four focussing periods. This interval would correspond to the space between cryomodules in the benchmark linac design. The results of our studies show that the transverse emittance growth will not exceed a factor of three for multiple charge state beams in the linac with all types of errors.

In summary, these simulations indicate that it is quite feasible to accelerate 5 charge states of uranium after the first stripper and 4 charge states after the second stripper in this linac.

E. SUPERCONDUCTING CAVITY DEVELOPMENT

e.1. Cavity Production and Testing

(K. W. Shepard, M. P. Kelly, P. Potukuchi,** M. Kedzie, S. Ghosh,** and B. E. Clifft)

Shielding of the test cryostats for ambient magnetic fields has been improved, enabling Q's greater than 10^9 to be observed in, for example, the New Delhi quarter-wave cavities.

RF power available at 350 MHz was upgraded to 400 watts, enabling fields greater than 5 MV/m, as shown in Figure III-5, to be reached in the 350 MHz spoke cavity prototypes for the RIA project. Completion of the testing of these cavities requires high-power pulse conditioning, which awaits the delivery of a 5-kW, 350-MHz amplifier, expected shortly.

Two 97-MHz split-ring cavities were re-built, using off-site vendors for both forming and electron-beam welding procedures. The successful test of these re-built cavities indicate that we established the capability to manufacture these structures through commercial vendors.

*Nuclear Science Centre, New Delhi, India

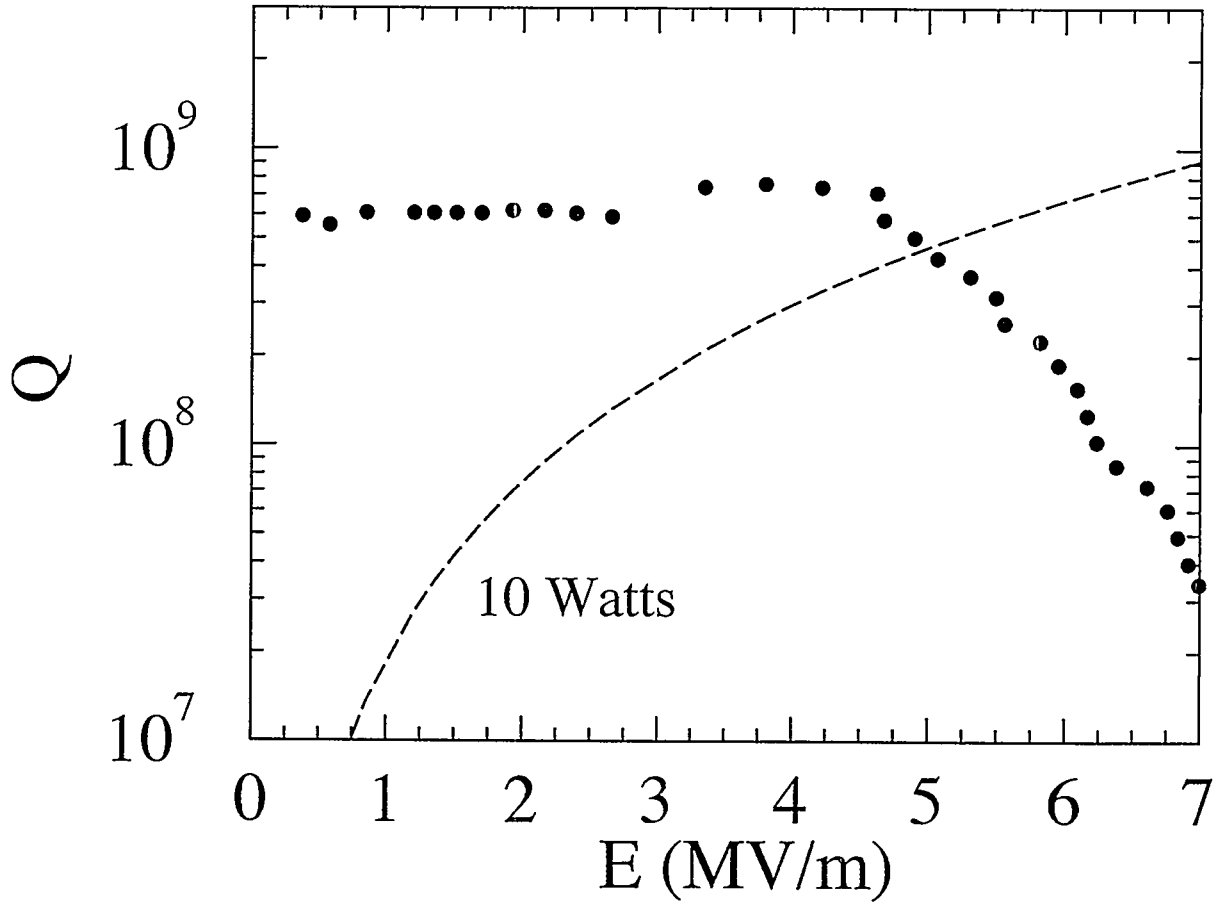

Figure III-5. Measured Q-curve data (filled circles) for 350 MHz spoke cavity. Dashed curve - constant input RF power of 10 W.

e.2. Surface Preparation Laboratory Upgrade (K. W. Shepard, M. Kedzie)

The cavity surface preparation laboratory in Building 203, G150, is being upgraded to, firstly, use vendor-prepared acid mixtures in 55-gallon drum quantities. This upgrade will eliminate most of the hands-on handling of acid required for cavity processing. Secondly, we are adding a capability to perform buffered chemical polishing (BCP) of cavities in addition to the electropolishing procedures that we have used exclusively up to the present. Safety reviews of the additional hardware and procedures are completed, and hardware upgrades are in progress. A high-pressure water-rinser system will also be installed in the near future.

e.3. Superconducting Cavity Design for RIA (K. W. Shepard, T. Tretyakova*)

Six different superconducting drift-tube cavity geometries will be required for the RIA driver, and several more for the secondary accelerator. Initial MAFIA modeling is complete for all six driver cavities, spanning a frequency range from 57 MHz to 350 MHz, and a velocity range from 0.02c to 0.5c. Designs for all six cavities were developed which have satisfactory electromagnetic properties. Mechanical modeling remains to be done before the designs can be finalized.

*Institute for Theoretical and Experimental Physics, Moscow

F. ION SOURCE DEVELOPMENT AT DYNAMITRON

(M. Portillo, J. Nolen, C. Batson, P. Billquist)

A surface ionization source was constructed and tested for use in release studies. The target cup is capable of holding about 15 cm^3 of refractory materials and its centroid lies 3 cm from a primary target which can produce neutrons from $^{9}Be(d,n)$ or $^{11}B(d,n)$ reactions. New refractory materials, such as yttria, were tested as electrical insulators at high temperatures to allow direct contact between the heating filament and the target cup. Also, porous forms of zirconia were used to provide heat shielding for making the target oven as efficient as possible. Target temperatures as high as 1600° were achieved with this scheme at a filament power as low as 200 W. Thus, the power requirements were reduced to almost a factor of 2.5 compared to other heat shielding methods used in the past.

An emittance measurement system was built and used to characterize the ion source. The device is made up of two linear feedthroughs driven by step motors to scan a wire and slit that are 30 cm apart. The slit was 0.5 mm wide and the wire is 0.25 mm in diameter. Figure III-6 shows a plot of the transverse emittance phase space is the x-plane. Simulations using a Monte Carlo model for thermal velocity distributions from a hot surface along with trajectory reconstruction using the code Simion 6.0 agree with the results obtained by measurement.

Figure III-7 shows the resulting analysis applied in order to characterize the phase space area. Integrating the area from the most intense regions to the weakest, the area occupied by the specified current is plotted.

The Dynamitron's performance was tested under high deuteron current conditions. Currents as high as 4.5 μA of the d+ ion were delivered to a ^{9}Be target at the 8°E+25°W beam line at an energy as high as 3.5 MeV. Beam currents of d+ as high as 35 uA have been delivered at 1 MeV, and tests are on-going to deliver such currents at higher energies. Such beams could be used to generate sufficient production rates for measuring time release curves of various refractory materials to survey possible refractory materials for isotope production.

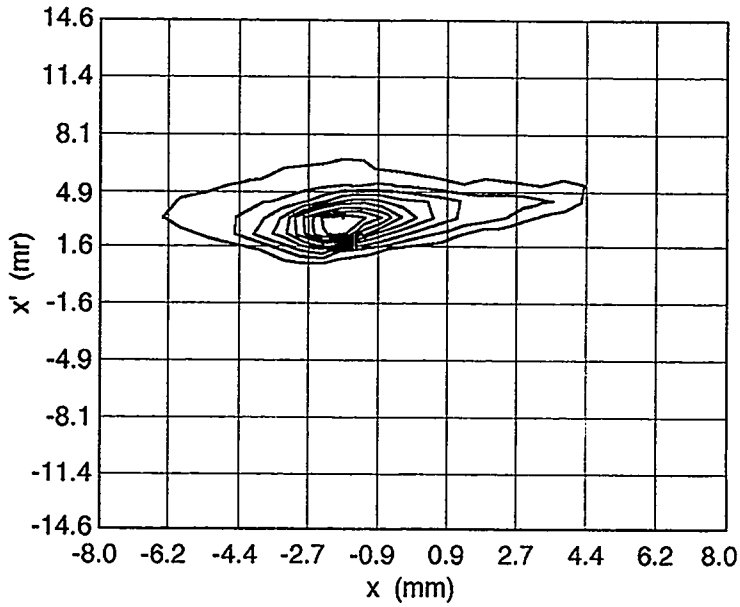

Figure III-6. Transverse phase space emittance plot in the x-plane. The lens after extraction was left off to allow parallel beam to enter the scanning slit.

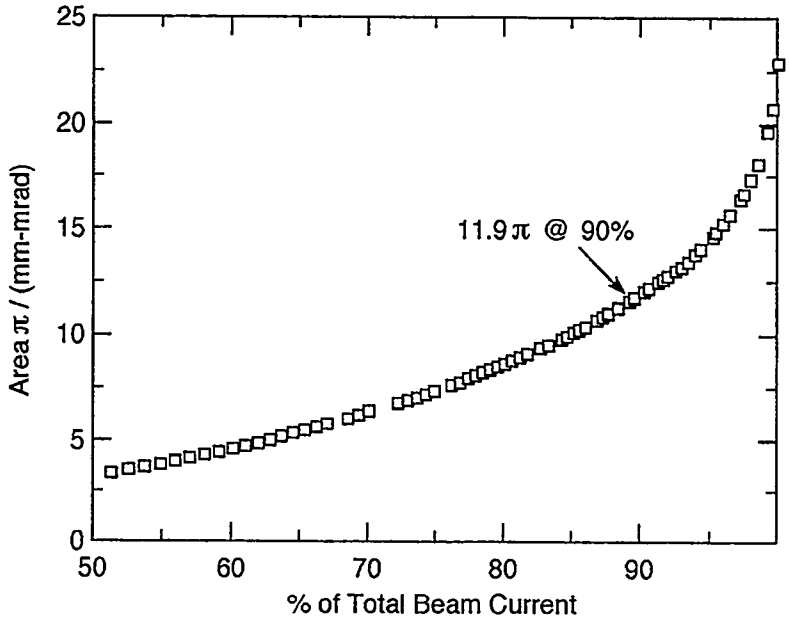

Figure III-7. Phase space area calculated from measurements of the x-plane emittance from a surface ionization source. The area is integrated starting from contour regions of the highest beam intensity. The extraction voltage was 10 kV.

G. THERMAL CONDUCTIVITY MEASUREMENTS OF POROUS MATERIALS AT HIGH TEMPERATURES

(J. A. Nolen, M. Petra and J. Green)

The target materials which are used for ISOL-type radioactive beam facilities are often porous forms of refractory compounds, such as calcium oxide and uranium carbide. At high primary beam power the temperature distribution within such targets depends on the thermal conductivity of these forms of the materials. Very little data exist on the thermal conductivity of such materials at the temperatures of interest, typically 1500 – 2000 °C, or even higher.

In the present research a simple method based on steady-state electron beam heating was developed to measure the thermal conductivity of porous materials. The emissivity and subsequently the thermal conductivity are evaluated by measuring the temperatures of the hot and cold faces of the specimen (that is T_{hot} and T_{cold} respectively). Three UC_x powder specimens of approximately 1/4 the theoretical density of UC_2 were examined. The total hemispherical emissivity and thermal conductivity were evaluated over a broad temperature range (approximately 850-1750 °C). The method can be extended to other porous materials that are of interest to ISOL-type facilities.

T_{hot} and T_{cold} were recorded as a function of electron-beam current at an applied voltage equal to 8.7 kV. Calculation of the unknown emissivity of the sample was done by performing an energy balance in the system. The power supplied to the specimen is equal to the power radiated by the cold and hot faces of the sample and the power irradiated by the periphery (Fig. III-8).

The thermal conductivity and emissivity derived from the energy balance in the system were then used as initial input in TAS-TRASYS, a general-purpose thermal modeling code that incorporates a precompiled version of TRASYS. Then, successive iterations in order to match the experimental and computational results yield the final values for the emissivity and thermal conductivity of the specimens (Fig. III-9a-b). An average thermal conductivity (k_{avg}) of those calculated for each specimen was inferred and is plotted as a function of temperature in Fig. III-9a. In Fig. III-9 is also shown the thermal conductivity of theoretical density UC_2 as well as the emissivity of UC for comparison. The simulations assumed that the heating of the lower face of the specimen is uniform and that the specimen is radiating to the environment from the two faces as well as the periphery with a view factor equal to 1. The simulated temperature contour in the specimen calculated with TAS-TRASYS is shown in Fig. III-10a-b for specimen #1. The temperature contour internal to the specimen can be seen in the simulation of one radial brick of the UC_x specimen.

The results for porous UC_x specimens prepared by the ISOLDE prescription is k_{avg} ranging between approximately 0.04 W/cm K and 0.01 W/cm K in the temperature range of approximately 850 °C and 1750 °C.

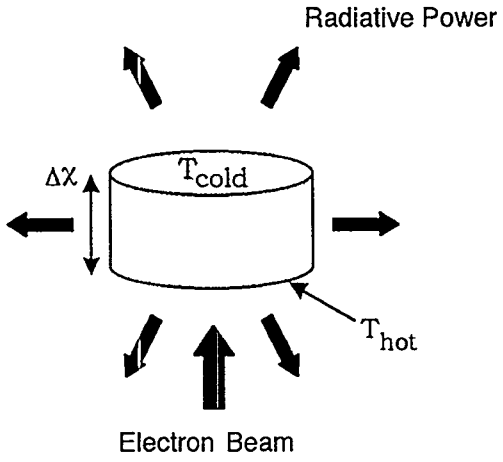

Figure III-8. Enlarged view of the specimen (not to scale). The electron beam heats the lower side of the specimen (of thickness Δx) raising the temperature at T_{hot}. Heat is radiated from the lower and upper sides as well as the periphery of the specimen.

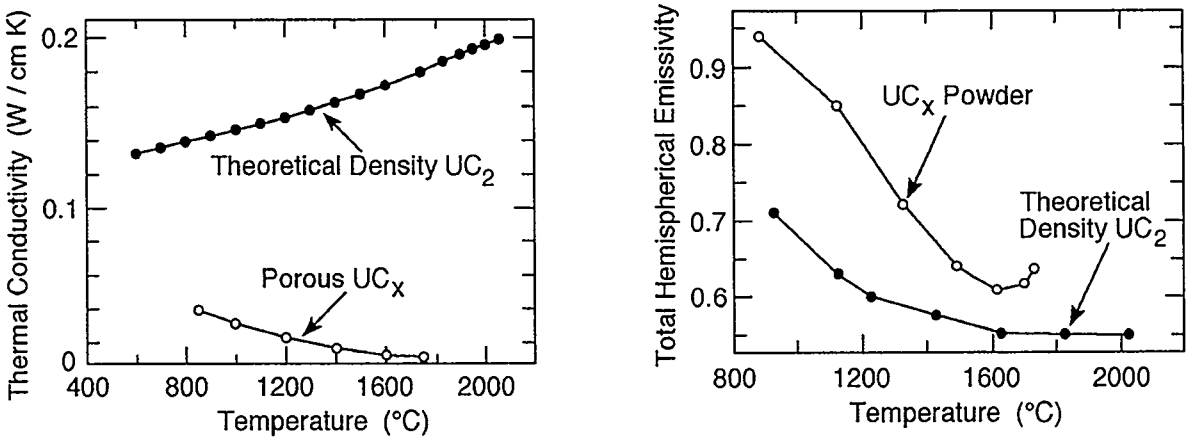

(a) (b)

Figure III-9. a) Variation of the thermal conductivity of theoretical density UC_2 and porous UC_x as a function of temperature. The values shown for the porous UC_x represent average values (that is k_{avg} as a function of T_{avg}). b) Total hemispherical emissivity of theoretical density UC as a function of temperature and UC_x (specimen #1) as a function of T_{avg}.

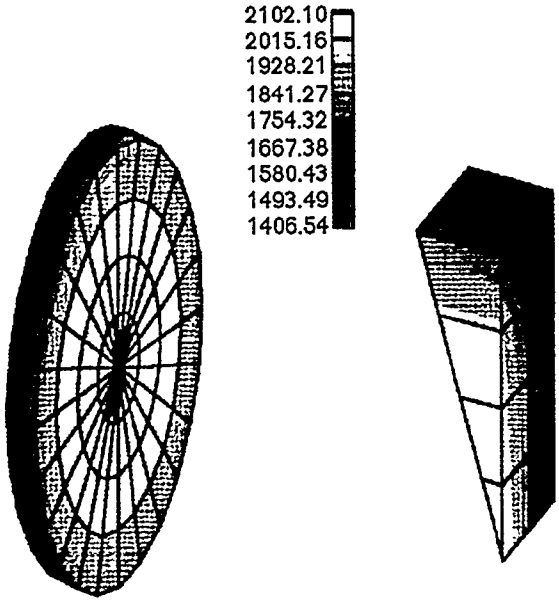

Figure III-10. a) Simulation of the temperature contour in UC_x (specimen #1) performed with TAS-TRASYS. The thermal conductivity and total hemispherical emissivity were assumed equal to 0.0134 W/cm K and 0.634 respectively (Temperatures shown are in °C). b) Temperature contour in one 15° radial brick of the 24 used to simulate the UC_x specimen.

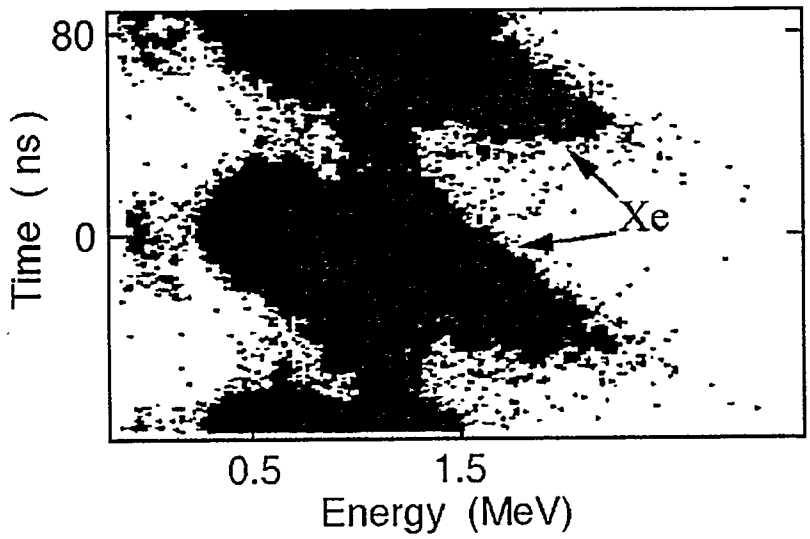

Figure III-11. Measured energy versus time-of-flight spectrum for beam at the RFQ exit for an initially DC beam. Arrows indicate events due to accelerated Xe beam centered at an energy of 1.5 MeV

H. RIB LINAC RFQ BEAM TESTS USING SINGLY-CHARGED A=132 IONS

(P. N. Ostroumov, M. P. Kelly, K. W. Shepard, R. A. Kaye, M. Kedzie, B. E. Clifft)

We performed detailed experimental measurements of singly charged ^{132}Xe beams accelerated through the ANL 12 MHz RFQ for inter-vane voltages up to the design value of 100 keV[1]. As part of an injector to a RIB linac for RIA (Rare Isotope Accelerator) the RFQ would accelerate low energy, low charge-to-mass ratio ion beams with high efficiency (*ie.* CW operation) while simultaneously introducing minimal transverse or longitudinal emittance growth.

We show here some results of a series of measurements using ^{132}Xe beams ranging in energy from 360 to 450 keV injected into the RFQ using the ANL 4 MV Dynamitron. Measured energy versus time-of-flight spectra clearly show events due to accelerated ^{132}Xe ions at the exit of the RFQ. These events are contained in well resolved bunches (~10 ns wide) as measured in a recently constructed silicon detector apparatus placed 30 cm beyond the RFQ exit.

Figure III-11 shows a typical energy versus time-of-flight spectrum for a beam injection energy of 400 keV and an inter-vane voltage of 92 kV. Calibration of the horizontal (energy) axis was performed by direct implantation of 1.3 to 1.7 MeV ^{132}Xe ions into the detector with the RFQ off. The vertical (time) axis contains two complete RF (~80 ns) periods and was measured using standard TOF (time-of-flight) techniques. The two intense regions centered near 1.5 MeV are due to accelerated ^{132}Xe while the events at lower energies are due primarily to detector noise (DC component) and RF pickup. These tests clearly demonstrated the feasibility of CW operation of a room temperature RFQ for low energy, low Z/A ions.

Detailed measurements of emittance and beam transport efficiency using pre-bunched beams, as well as, studies of the long term thermal stability of the RFQ at the highest inter-vane voltages (~100 kV) are underway.

[1]Beam Tests of the 12 MHz RFQ RIB Injector for ATLAS, R. A. Kaye, K. W. Shepard, B. E. Clift, M. Kedzie, PAC99 Meeting, March 29-April 2, (1999)

IV. MEDIUM-ENERGY NUCLEAR PHYSICS RESEARCH

OVERVIEW

In order to understand how to incorporate the quark-gluon structure of the nucleon into a fundamental description of nuclear forces, the medium-energy research program in the Argonne Physics Division emphasizes the study of processes in nuclei in which interactions with the constituents of the nucleon describe the basic physics. Examining related physics topics at both the quark and hadronic levels in complementary experiments is most revealing of the low-energy structure of the strong interactions. Because energetic leptons provide an accurate, well-understood probe of these phenomena, primary emphasis is placed on the experiments involving electron and muon scattering.

The electron beams of the Thomas Jefferson National Accelerator Facility (TJNAF) are ideally suited for studies of nuclei at hadronic scales and represent one center of the experimental program. Staff members led in the construction of experimental facilities, serve as spokesmen for three experiments and are actively involved in several others. The group completed construction of the broad-purpose Short Orbit Spectrometer which forms half of the coincidence spectrometer pair that is the base experimental equipment in Hall C. We continue to upgrade the SOS detector package and improve the understanding of the spectrometer optics and acceptance. Argonne led the first experiment to be carried out at TJNAF in FY1996 and has completed six other experiments. In FY1999 measurements were made with a 5.5 GeV electron beam to extend our results on the d(γ,p)n and (e,e'p) reactions to higher scales. An experiment was also completed to measure the ratio of the longitudinal to transverse inelastic electron scattering response in the resonance region. We also measured kaon electroproduction on targets of ^{3}He and ^{4}He to study the reaction mechanism of electroproduction of hypernuclei and to search for bound Σ-hypernuclear states.

The first results from TJNAF build upon previous ANL experiments at Stanford Linear Accelerator Center (SLAC), MIT-Bates and Saclay (ALS). For the first time, forward-backward angle measurements of the (e,e'p) reaction have been used to perform longitudinal-transverse separations of the proton spectral function at high momentum transfers. Exclusive deuteron photo-disintegration experiments have established that this reaction obeys quark-counting-rule scaling arguments at large transverse momenta. The simplest extension of this work, to coherent pion photo-production on the deuteron, did not see evidence of the quark counting rule behavior. Measurements of kaon production on hydrogen, deuterium, ^{3}He and ^{4}He provide important information on the basic strangeness production mechanisms, the poorly known low energy hyperon-nucleon interaction and the electromagnetic form factor of the K^+. Pion production measurements on hydrogen, deuterium, ^{3}He and ^{4}He will

determine the charge form factor of the pion and measure the change in the pion field in the nuclear medium. Since the pion contains valence antiquarks, these measurements complement our high energy Drell-Yan measurements of the antiquark distributions in nucleons and nuclei. Results of new measurements of inclusive electron scattering in the resonance region provide evidence for the concept of semi-local duality in relating averaged resonance and deep inelastic scattering yields.

HERMES, a broadly based North American-European collaboration is studying the spin structure of the nucleon using internal polarized targets in the HERA storage ring at DESY. Deep inelastic scattering has been measured with polarized electrons on polarized hydrogen and ^{3}He. Argonne has concentrated on the hadron particle identification of HERMES, a unique capability compared to other spin structure experiments. In 1999, the Argonne-led dual-radiator ring imaging Cerenkov counter (RICH) was brought into operation at the design specifications to provide complete hadron identification in the experiment. This will allow HERMES to make decisive measurements of the flavor dependence of the spin distributions. HERMES is beginning to make measurements of the spin dependence of the glue in the photoproduction of pairs of high transverse momenta pions. The HERMES experiment is also making significant advances in unpolarized deep-inelastic scattering physics with its coincident hadron detection. Argonne scientists have extended the physics program in studies of exclusive vector meson production in polarized-beam-polarized-target measurements and also measurements on nuclear targets. Clear evidence is seen on the nuclear targets for the effect of coherence in the production mechanism. An unexpected strong nuclear dependence of the ratio of longitudinal to transverse deep inelastic scattering cross sections has been observed at low x and Q^2. This will be explored further in a TJNAF experiment in 2000.

Measurements of high mass virtual photon production in high energy proton-induced reactions have determined the flavor dependence of the sea of antiquarks in the nucleon. These measurements give insight into the origin of the nucleon sea. In the same experiment, the nuclear dependence of the Drell-Yan process and the nuclear dependence of the production of heavy quark resonances such as the J/ψ and Υ have been determined. The Drell-Yan results demonstrate that the energy loss of quarks in the nuclear medium is significantly less than theoretical expectations. The heavy vector meson results provide constraints on the gluon distributions of nucleons and nuclei and a significant baseline for attempts to use heavy vector meson production as a signal of the formation of the quark-gluon plasma in relativistic heavy-ion experiments. A new initiative is underway to continue these measurements with much higher luminosity at the FNAL Main Injector.

The technology of laser atom traps provides a unique environment for the study of nuclear and atomic systems and represents a new thrust for the group. Initially the efforts focus on developing high efficiency and high sensitivity trapping techniques for the isotope analysis of noble gases. The isotope Krypton-81 was detected at natural (10^{-13}) abundance and the technique was demonstrated to be free of contamination from other isotopes and elements. This atom trace analysis (ATTA) technique provides a new approach to such diverse problems as dating old ground water or mapping out the atmospheric concentration of fission products. Work has begun on applying ATTA to the detection of ^{41}Ca. A longer term goal is to make nuclear moment measurements of trapped short-lived atoms and to apply these techniques to a variety of weak interaction problems.

A. SUBNUCLEONIC EFFECTS IN NUCLEI

a.1. The Energy Dependence of Nucleon Propagation in Nuclei as Measured in the (e,e'p) Reaction

(D. F. Geesaman, J. Arrington, K. Bailey, W. J. Cummings, D. DeSchepper, H. E. Jackson, C. Jones, S. Kaufman, T. O'Neill, D. Potterveld, J. Reinhold, J. P. Schiffer, B. Zeidman, P. Bosted,* A. Lung,† D. Abbott,‡ R. Carlini,‡ J. Dunne,‡ R. Ent,‡ J.-O. Hansen,‡ D. Mack,‡ D. Meekins,‡ J. Mitchell,‡ S. Wood,‡ C. Yan,‡ Jae-Choon Yang,§ E. Belz,¶ E. Kinney,¶ D. van Westrum,¶ P. Markowitz,‖ K. A. Assamagan,** O. K. Baker,**| K. Beard,** J. Cha,** T. Eden,** P. Gueye,** W. Hinton,** C. Keppel,** R. Madey,** G. Niculescu,** I. Niculescu,** L. Tang,** Wooyong Kim,†† C. Bochna,‡‡ H. Gao,‡‡ R. Holt,‡‡ M. Miller,‡‡ A. Nathan,‡‡ B. Terburg,‡‡ A. Ahmidouch,§§ R. Suleiman,§§ E. Bruins,¶¶ L. Kramer,¶¶ J. Martin,¶¶ A. Mateos,¶¶ R. Milner,¶¶ W. Kurchinetz,¶¶ C. Williamson,¶¶ W. Zhao,¶¶ E. Beise,‖ ‖ H. Breuer,‖ ‖ N. Chant,‖ ‖ F. Duncan,‖ ‖ J. J. Kelly, ‖ ‖ R. Mohring,‖ ‖ M. Khandaker,*** K. McFarlane,*** C. Salgado,*** S. Beedoe,†††S. Dangoulian,††† C. Jackson,††† D. Dutta,‡‡‡@ R. E. Segel,‡‡‡ Pat Welch,§§§ A. Klein,¶¶¶ S. Barrow,‖ ‖ ‖ D. Beatty,‖ ‖ ‖ H. T. Fortune,‖ ‖ ‖ D. Koltenuk,‖ ‖ ‖ W. Lorenzon,‖ ‖ ‖ J. Yu,‖ ‖ ‖ V. Frolov,**** J. Pricel**** P. Stoler,**** R. Gilman,†††† J.-E.Ducret,‡‡‡‡ C. Cothran,§§§§ D. Day,§§§§ B. Zihlmann,§§§§ C. Armstrong, ¶¶¶¶ T. Amtuoni,‖ ‖ ‖ ‖ H. Mkrtchyan,‖ ‖ ‖ ‖ and V. Tadevosyan‖ ‖ ‖ ‖)

ANL led the first experiment to be carried out at TJNAF in 1995-1996. This experiment built upon earlier ANL work at MIT and SLAC using the (e,e'p) reaction to study the propagation of 0.35-3.3 GeV protons through nuclear material and the reaction mechanism in the quasifree region. The Hall C collaboration selected this experiment as one of the two commissioning experiments. Electrons were detected in the High Momentum Spectrometer and protons were detected in the Short Orbit Spectrometer except at the highest Q^2 setting where the roles of the spectrometers were reversed. The experiment utilized TJNAF beams of 0.845, 1.645, 2.445, and 3.245 GeV with up to 50 μA intensity on targets of C, Fe and Au. Hydrogen targets were used to check the normalization at each kinematic setting. Full commissioning studies of each spectrometer were performed to calibrate this experiment and to serve as a baseline for future experiments.

Measurements were made at Q^2 values of 0.64, 1.3, 1.8 and 3.3 $(GeV/c)^2$ corresponding to average proton kinetic energies of 0.35, 0.70,0.97 and 1.8 GeV to span the threshold for pion production in p-p collisions where the nature of the p-p cross section changes from dominantly elastic to dominantly inelastic. At Q^2 of 0.64 and 1.8 $(GeV/c)^2$ data were taken at two values of the virtual photon polarization to examine the separate contributions of longitudinal and transverse photon exchange. In all aspects the experimental performed as expected. The statistics, kinematic coverage and experimental precision significantly exceed those of previous measurements. This data set provides precise measurements of nuclear transparency as well as a broad survey of nuclear spectral functions from recoil momentum of 0 to 300 MeV and missing energy of 0 to 150 MeV.

The measurements of the average nuclear transparency were published in 1998. Radiatively corrected spectral functions have been extracted for each target and momentum transfer. These spectral functions suggest that the widths of deeply bound hole states in Fe and Au may be somewhat larger than had been expected. Figure IV-1 shows the results of the separation of the longitudinal and transverse spectral functions on carbon for missing momenta from 0 to 80 MeV at the two momentum transfers and the difference between the transverse and longitudinal strength at Q^2 of 0.6 and the difference in the transverse strength at the two Q^2. The longitudinal and transverse spectral functions of the p-shell knockout strength are consistent with each other. There is a substantial excess of transverse strength compared to the longitudinal strength in the missing energy region from 30-50 MeV at Q^2 of 0.6 $(GeV/c)^2$ (bottom panel of Fig. IV-1). At 1.8 $(GeV/c)^2$, the transverse strength is reduced (middle panel). Similar results are observed for iron and gold. The missing energy and nucleus dependence suggest that meson exchange mechanisms are important for the transverse strength, especially at the lower Q^2. The longitudinal strength is observed to extend to the highest missing energies measured signaling the effects of short range correlations.

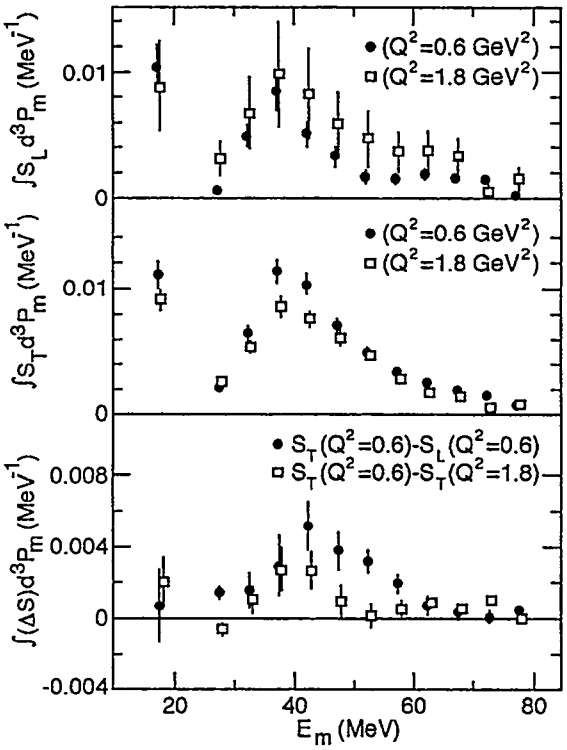

Fig. IV-1. The integrals of S_L (top panel) and S_T (middle panel) from $0<p_m<80$ MeV are shown at Q^2 of 0.64 (circles) and 1.8 $(GeV/c)^2$ (squares). In the bottom panel the differences: S_T - S_L at 0.64 $(GeV/c)^2$ (circles) and $S_T(Q^2=0.6)$ - $S_T(Q^2=1.8)$ (open squares) are shown. The errors are the sum in quadrature of the statistical and systematic uncertainties. The lowest E_m point is an average over $10 < E_m < 25$ MeV. The response functions at 1.8 $(GeV/c)^2$ are corrected for differences in proton attenuation by factors of 1.075 for $E_m < 25$ MeV and 1.18 for $E_m > 25$ MeV.

*American University; †Caltech; ‡TJNAF; §Chungnam National University, Taejon, Korea; ¶University of Colorado; ||Florida International University; **Hampton University; ††Kyungpook National University, Taegu, S. Korea; ‡‡University of Illinois, Urbana; §§Kent State University; ¶¶MIT; || ||University of Maryland; ***Norfolk State University; †††North Carolina A&T University; ‡‡‡Northwestern University; §§§Oregon State University; ¶¶¶Old Dominion University; || || ||University of Pennsylvania; ****Rensselaer Polytechnic Institute; ††††Rutgers University; ‡‡‡‡CE Saclay, France; §§§§University of Virginia; ¶¶¶¶William and Mary; || || || ||Yerevan Physics Institute, Armenia; @This experiment formed the basis for the Ph.D. theses of these students.

a.2. Electroproduction of Kaons and Light Hypernuclei

(J. Arrington, K. Bailey, F. Dohrmann, D. F. Geesaman, K. Hafidi, H. E. Jackson, B. Mueller, T. G. O'Neill, D. Potterveld, P. Reimer, J. P. Schiffer, B. Zeidman, and E91-016 Collaboration

Jefferson Lab experiment E91-016, "Electroproduction of Kaons and Light Hypernuclei" is a study of quasifree production of Kaons on targets of H, D, ^{3}He, and ^{4}He at an incident electron energy of 3.245 GeV. For H and D targets, data were also obtained at E_e =2.445 GeV. The scattered electron and emergent K^+ were detected in coincidence with the use of the HMS and SOS spectrometers, respectively, in Hall C. Angular distributions for the (e,e'K^+)Y reactions were measured at forward angles with respect to the virtual photon for Q^2 = 0.34, 0.37, and 0.5(GeV)^2. Particle identification utilizing time-of-flight detectors together with Aerogel Cerenkov detectors yields clean missing mass spectra, e.g. Report ANL/99-12, Fig III-6, and allows subtraction of random backgrounds.. The experiment was run in two time periods. The H and D targets were studied over a period of months near the end of CY 1996 while the balance of the experiment, namely the ^{3,4}He targets were investigated during the last few months of CY 1999.

The fundamental interaction being studied is N(e,e'K^+)Y where Y is either a Λ or Σ and N represents a nucleon. For the H target, the final state can only be a Λ or Σ, but for heavier targets, there is relative motion between the nucleons in the target that results in broadening of the peaks. For the D target, it is possible to separate the two peaks inasmuch as the Fermi broadening is not large compared to the mass difference between Λ and Σ. For ^{3}He and ^{4}He, very preliminary missing mass spectra being shown in Fig. IV-2, it will be much more difficult to separate the yields for the various final states. Even in this very early stage of analysis, it is quite clear that the widths of the quasifree peaks are greater in ^{4}He than in ^{3}He (more binding and larger Fermi momenta).

For D, it is known that there is no bound Lambda-nucleon state, but for both ^{3}He and ^{4}He targets we anticipate bound hypernuclear states. Although the data shown in the figure are quite preliminary, it appears that bound Λ hypernuclear states are indeed seen. The possibility of bound Sigma hyper-nuclei also exists, but it is conjectural at this time. Construction of an optimal Monte Carlo simulation will require considerably more effort before any conclusions can be drawn. The large number of final state configurations results in complications that must be analyzed prior to extracting final cross sections. The present data set provides a high-statistics study of the mass dependence of Kaon electroproduction on light nuclei. There are a number of issues that must be investigated in the near future. Students from Hampton University and the University of Pennsylvania utilize data from E91-016 for their Ph.D. Theses.

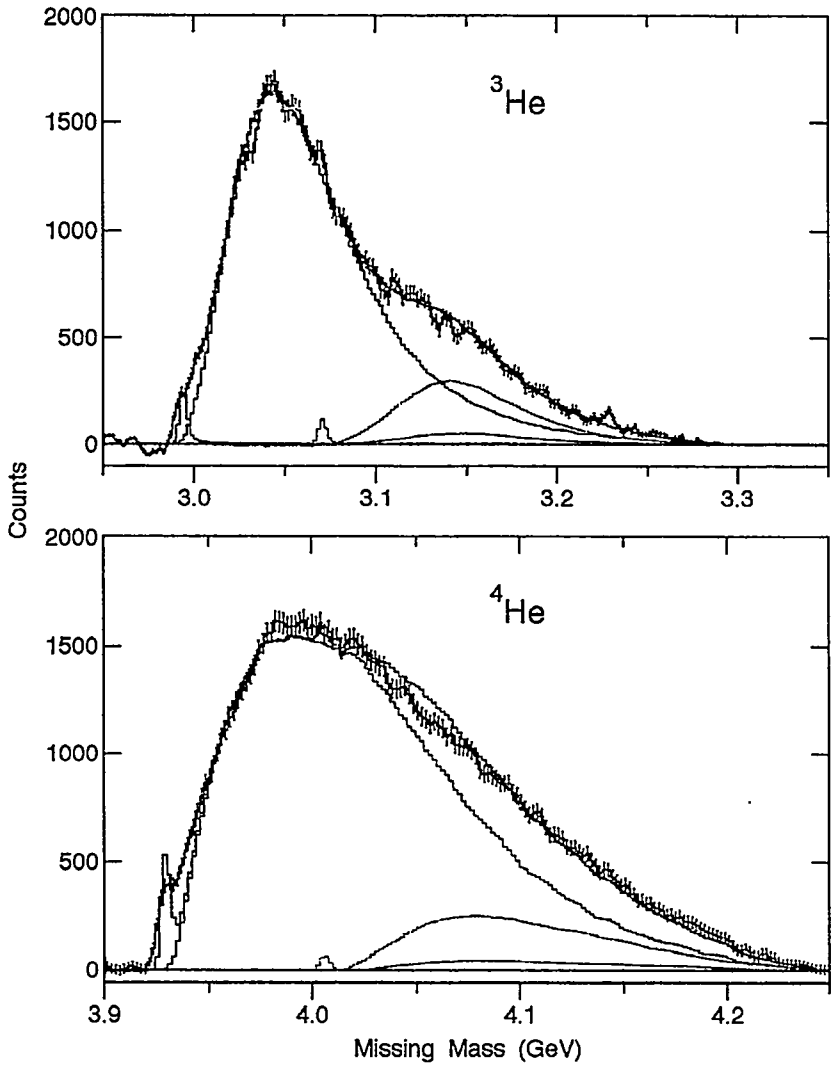

Fig. IV-2. Preliminary missing mass spectra for ^{3}He and ^{4}He(e,e'K$^+$) reactions. The broad curves that represent Monte-Carlo simulations for quasi-free production of Λ, Σ^0, Σ in decreasing magnitude respectively, are preliminary and relatively crude. The locations of possible "bound Λ and Σ states" are indicated by the narrow peaks (~ 5 MeV width and arbitrary magnitudes). The sums of the various contributions are also shown. It should be emphasized that it is very early and much analysis is required.

a.3. A Study of Longitudinal Charged-Pion Electroproduction in D, ^{3}He, and ^{4}He

(H. E. Jackson, J. Arrington, K. Bailey, D. De Schepper, D. Gaskell, D. F. Geesaman, B. Mueller, T. G. O'Neill, D. H. Potterveld, J. Reinhold, B. Zeidman, and the E91-003 Collaboration)

According to the simplest models of the nucleon-nucleon force, pion-exchange currents in nuclei should give rise to mass-dependent enhancement of the nuclear pion charge distribution. Longitudinal pion electroproduction should be a clean direct probe of the nuclear pion currents because of the dominance of the pion-pole process for charged-pion emission in the direction of the virtual photon. If current conceptions of pion-exchange currents in nuclei are correct, longitudinal electroproduction will be suppressed at lower momentum transfers and enhanced at higher momentum transfers. These currents should also manifest themselves in the quark-antiquark distribution functions as observed in deep-inelastic scattering on nuclei. However, analysis of parton distribution functions show no evidence for any mass enhancements of the sea quarks. Recent data from Drell-Yan studies which probe directly the quark-antiquark sea, show no mass dependence. These results, suggest that a reformulation of pion-exchange models of the medium- and short-range properties of nuclear forces may be required. In an attempt to probe exchange currents directly, we carried out a series of measurements of single-charged-pion electroproduction on the proton, deuteron, and ^{3}He at the TJNAF. The goal is to measure the longitudinal cross section in parallel kinematics by means of a Rosenbluth separation, and to search for target-mass dependent effects. The results from these measurements should provide insight into the absence of any enhancement of sea quark distributions in nuclei as measured in deep-inelastic scattering.

The measurements were carried out at Jefferson Lab in February-April 1998 using the Hall C facility. 0.845 to 3.245 GeV electrons were scattered from high-density cryo-targets. The scattered electrons were observed in the High Momentum Spectrometer in coincidence with pions observed in a short orbit spectrometer. The kinematic conditions corresponded to momentum transfers for which, in one case, the electroproduction is expected to be quenched, and a second, in which according to the standard pion-exchange model of nuclear forces, one expects a substantial enhancement. Measurements were made at kinematics corresponding to two virtual photon polarizations for each momentum transfer in order to use the data to carry out a Rosenbluth separation of the transverse and longitudinal cross sections. To date, measurements have been made for the proton, deuterium, and ^{3}He. A direct comparison of the cross sections for each target measured in the identical geometry will allow the determination of mass dependencies without measurements of absolute cross sections. The data analysis has been focused on careful simulations of the spectrometer acceptances, as well as other relevant instrumental effects. Monte Carlo distributions have been generated using the Hall C simulation, SIMC, which includes spectrometer acceptance, radiative processes, energy loss, and particle decay. The measured cross sections are established by comparing the results of the SIMC simulations to data with a hypothesied input cross section and then iterating until agreement with the data is achieved. The general features of the deuterium and ^{3}He pion spectra in missing mass, are typical of quasifree scattering. For the π^+ production on ^{3}He, in addition to the quasifree component which appears to be the same as for π^-, there is a sharp peak corresponding to coherent production leading to a triton in the final state, and a second component corresponding to a deuteron and neutron in the final state. Preliminary longitudinal-transverse separations have been reported and the analysis is being refined in order to obtain the maximum achievable accuracy for the longitudinal and transverse cross sections and their mass dependencies. To date, there is no evidence for any enhancement of the longitudinal cross sections above the quasifree values expected in a simple impulse approximation. Rather there appears to be substantial quenching, particularly in ^{3}He. Preliminary results, for the ratio of the observed cross sections to those expected from simple quasifree scattering are presented in Fig. IV-3. If an enhancement due to pion exchange currents were to occur, the effect would be expected to manifest itself in the region of virtual pion momenta near 400-500 MeV where we have an experimental point.

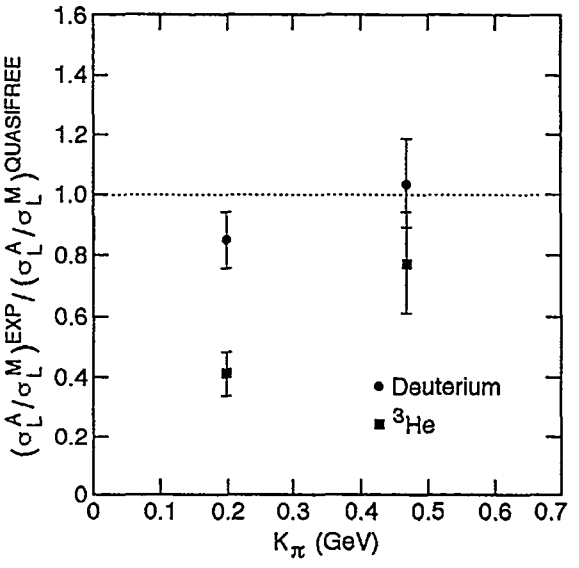

Fig. IV-3. Measured longitudinal cross section ratios for forward angle pion electroproduction on deuterium and ^{3}He corrected for kinematic effects induced by the quasifree scattering mechanism.

a.4. Pion Electroproduction from H_2 and D_2 at W=1.95 GeV (H. E. Jackson, J. Arrington, D. Gaskell, B. Mueller, and the E93-021 Collaboration)

The pion, as the lightest meson, is an ideal laboratory for studying the transition between the non-perturbative and perturbative regions of QCD. Experimental results for the value of the pion form factor, (F_π), at moderate and high Q^2 have large experimental uncertainties. Experiment E93-021 measured the H(e,e'π^+)n reaction at TJNAF for Q^2 values from 0.6-1.6 $(GeV/c)^2$. The forward longitudinal response in this process is dominated by the knockout of virtual pions, and is therefore sensitive to the pion form factor. Data analysis is in progress and is focused on obtaining longitudinal and transverse separated cross sections. The value of F_π at Q^2 of 0.6, 0.75, 1.0, and 1.6 $(GeV/c)^2$ will be obtained from this data. E93-021 has also measured the D(e,e'π^+)nn and D(e,e'π^-)pp reactions. The π^-/π^+ ratio is sensitive to contributions to the cross section which are unrelated to F_π. The hydrogen and deuterium data samples from E93-021 is also being analyzed to determine the ratio of the longitudinal part of the π^+ electroproduction cross section from deuterium to that from hydrogen. This analysis is performed as part of the E91-003 experiment, and will provide complimentary information about the enhancement of the nucleon pion field at W=1.95 GeV and Q^2 from 0.6-1.6 $(GeV/c)^2$.

a.5. Measurements of Deuteron Photo-disintegration up to 5.5 GeV (D. F. Geesaman, H. E. Jackson, T. G. O'Neill, D. H. Potterveld, B. Zeidman, J. Arrington, B. Mueller, and the E89-012 and E96-003 collaborations)

Constituent-counting-rule behavior was observed previously in high energy proton-proton scattering and photo-meson productions from the proton. Only one nuclear reaction thus far has exhibited this behavior. Argonne experiments NE8 and NE17 at SLAC showed that the deuteron photodisintegration d(γ,p)n reaction at a proton center-of-mass angle of 90° starts to show the scaling behavior at the unexpectedly low photon energy of around 1.0 GeV. Extending the SLAC measurements to higher photon energies and performing a detailed angular distribution study is essential to identify the limits of the kinematic regime of this behavior and to investigate the underlying mechanisms.

TJNAF experiment E89-012, one of the two hall-C commissioning experiments performed in 1996,

measured for the first time the differential cross section for d(γ,p)n up to 4.0 GeV at center-of-mass angles 36°, 52°, 69°, and 89°. The d(γ,d) π° reaction was also studied at E_γ = 0.8-3.2 GeV. The d(γ,p)n results[1], shown in Fig. IV-4, are in good agreement with the previous measurements and the data near 90° continue to show the scaling behavior up to 4 GeV and are also in fair agreement with an asymptotic meson-exchange model calculation[2]. The data at 36° and 52° do not exhibit the counting-rule behavior, but also do not extend to as high a region of transverse momenta as the 90° data. The d(γ,d) π^0 results are consistent with previous measurements at low photon energy, but do not show any signs of scaling at a center-of-mass angle of 90°. In contrast, the results at 136° are in good agreement with the constituent-counting-rule behavior.

This work was continued in TJNAF experiment E96-003, which ran in the spring of 1999. The d(γ,p)n cross sections were measured for beam energies of 5.0 and 5.5 GeV, at center-of-mass angles of 37° (5 GeV only), 53°, and 70°. The higher energy of these measurements should provide a more stringent test of the theoretical models for this reaction. The analysis of these data is currently in progress.

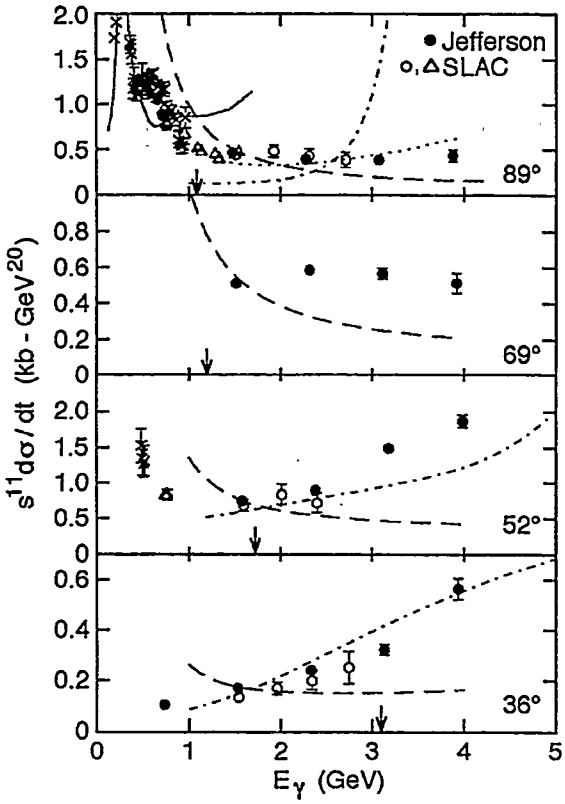

Figure IV-4. $s^{11}d\sigma/dt$ vs. E_γ for the d(γ,p)n reaction. The present work is shown as solid circles with statistical uncertainties only, the SLAC NE17 data are shown as open circles, the SLAC NE8 data are shown as open triangles, and other existing data are shown as crosses. The solid line is the meson-exchange model calculation of Lee[3]. The long-dashed line is the RNA analysis[4], and the dotted line is Nagornyi's[2] asymptotic meson-exchange calculation. The dash-dotted line is the QGS calculation[5]. The arrows indicate the photon energies where p_T^2 = 1.0 (GeV/c)^2. The previous data are shown above at nominal center of mass angles of 37°, 53°, and 90°.

[1] C.~Bochna *et al.*, Phys. Rev. Lett. **81**, 4576 (1998).

[2] S. I.~Nagornyi, Yu. A. Kasatikin, and I. K. Kirchenko, Sov. J. Nucl. Phys. **55** 189 (1992).

[3] T.-S. H. Lee, Argonne National Laboratory Report No. PHY-5253-TH-88; T.-S. H. Lee, in *Proceedings of the International Conference on Medium and High Energy Nuclear Physics, Taipei, Taiwan, 1988* (World Scientific, Singapore, 1988), p.563.

[4] S. J. Brodsky and J. R. Hiller, Phys. Rev. C **28**, 475 (1983).

[5] L. A. Kondratyuk *et al.*, Phys. Rev. C **48**, 2491 (1993).

a.6. HERMES, Measurements of Spin-Structure Functions and Semi-Inclusive Asymmetries for the Proton and Neutron at HERA

(J. Arrington, H. E. Jackson, T. G. O'Neill, D. H. Potterveld, D. De Schepper, and collaborators at 33 other institutions)

Since 1995, the HERMES experiment has provided fundamental new insights into the structure of the nucleon, especially on the composition of its spin. The unique capabilities of the experiment have produced data that were not possible with previous measurements at SLAC, CERN, and Fermilab. The collaboration has collected and analyzed millions of deep-inelastic scattering (DIS) events using longitudinally polarized electrons and positrons incident on longitudinally polarized internal gas targets of ^{1}H, ^{2}H, and ^{3}He, as well as thicker unpolarized gas targets. These data together with large sets of photo-production events have yielded several results that were unexpected and are provoking new work, both theoretical and experimental. Thanks to the large momentum and solid angle acceptance of the HERMES spectrometer, these results extend well beyond the principal HERMES role of studying nucleon spin structure.

The HERMES collaboration consists of approximately 30 institutions from North America and both western and eastern Europe. The HERMES experiment is located in the East straight section of the HERA storage ring at the DESY laboratory in Hamburg. Positron (or electron) beam polarizations are stable and reproducible at about 50%, and are monitored with systematic uncertainties of better than ±5% by two independent Compton backscattering polarimeters. The 27.5 GeV longitudinally polarized lepton beam interacts with polarized internal gas targets stored in an open-ended thin-walled storage cell. Data were taken on a polarized ^{3}He target in 1995, on a polarized ^{1}H target in 1996 and 1997, and on a polarized ^{2}H target in 1998 and 1999. The target densities are about 7.5 (5) x 10^{13} atoms/cm^2 for hydrogen (deuterium) and 3.5 x 10^{14} atoms/cm^2 for ^{3}He. Typical polarizations of the target are 90% (50%) for the hydrogen/deuterium (^{3}He) sources, and are measured to better than ±5% with polarimeters. Luminosities are in the range of 4-30 x 10^{31} nucleons cm^{-2} sec^{-1}. Unpolarized gases of hydrogen, deuterium, nitrogen, and krypton, with thicknesses of around 10^{15} atoms/cm^2, are also used for data taking.

The experimental apparatus is an open-geometry forward spectrometer with momentum analysis and background rejection provided by a 1.3 T-m dipole magnet. The spectrometer is constructed in two symmetric halves above and below the positron ring plane. Forty-two drift chamber planes and 6 micro-strip gas chamber planes provide tracking in each spectrometer half. Particle identification is provided by the combination of a lead-glass calorimeter, a pre-shower detector consisting of a scintillator hodoscope preceded by 2 radiation lengths of lead, a transition radiation detector, and a threshold Cerenkov detector. The Cerenkov counter was upgraded to a ring imaging configuration in 1998 (see section a.11). A detailed description of the spectrometer is found in Ref. 1. The angular acceptance of the experiment is $40 < \Theta < 220$ mrad. The kinematic range accessible is $0.02 < x < 0.8$ and $0.2 < Q^2 < 20$ (GeV/c)^2. Argonne provided the Cerenkov counter used for particle identification, led the RICH upgrade effort, and developed the drifilm coating technique for the ultrathin target cell required for this experiment.

HERMES has performed a measurement of the flavor asymmetry between up and down quarks in the nucleon sea[2], several studies of fragmentation of up and down quarks to pions, measurement of the DIS contributions to the generalized Gerasimov-Drell-Hearn integral for both the proton and neutron[3], a measurement of the spin transfer from virtual photons to Λ^0 hyperons, measurements of the effect of the nuclear environment on the hadronization process to study its time development, and most recently the observation at small Q^2 of a surprisingly large difference in the effects of the nuclear medium on the transverse and longitudinal DIS cross sections[4]. (Here $-Q^2 = q^2$ is the square of the invariant mass of the exchanged virtual photon, a measure of the resolution of the probe.) A broad program of measurements involving diffractive vector meson production is also underway with basic studies in ρ^0, ϕ^0, ω^0, and J/Ψ production, as well as the determination of photon $\rightarrow$ vector-meson spin density matrix elements through the analysis of the angular distribution of the decay products[5]. The ρ^0 semi-exclusive cross section has been found to have a large and unexpected spin dependence[6]. The study of diffractive ρ^0 production in nuclei has led to the observation of a lifetime (coherence length) effect on the initial-state nuclear interactions of the virtual quark pair that represent the hadronic structure of the photon[7].

The spin-dependence of inclusive DIS lepton scattering has been used by HERMES and other experiments to

provide information about the total contribution of all quark species to the nucleon spin. Much more detailed information about the spin content of the nucleon can be obtained from the spin-dependence of the semi-inclusive deep inelastic scattering (SIDIS) reaction, eN $\rightarrow$ eh$^{\pm}$X. (Here h$^{\pm}$ refers to a positive or negative hadron detected in coincidence with the scattered positron.) In the quark parton model, the factorization approximation relates the detected hadron to the struck quark. In this approximation, the asymmetries measured in inclusive and semi-inclusive DIS can be combined to extract the contribution of each quark flavor q (=up, down, or strange) to the nucleon spin, and to distinguish between the contributions of valence and sea quarks. Figure IV-5 exhibits the polarized distribution functions of valence and sea quarks measured at

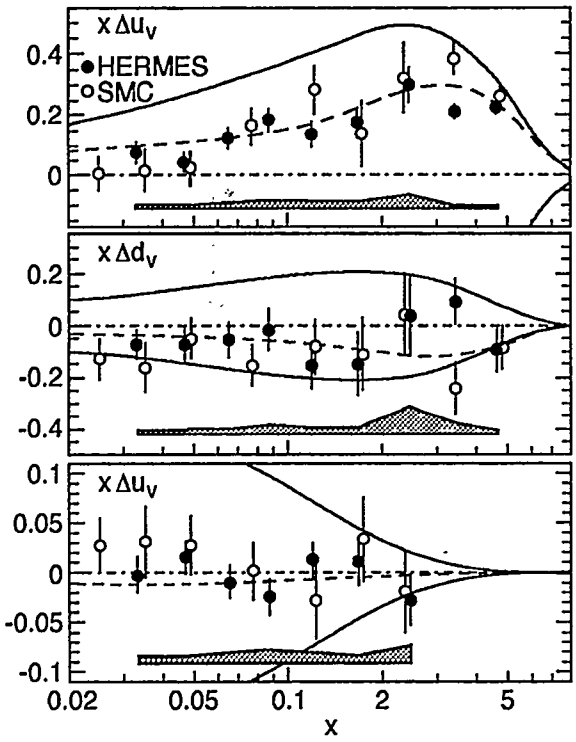

Fig. IV-5. The polarized valence and sea quark distributions measured at HERMES (1995-1997) and SMC (all data).

HERMES and SMC. In the figure, $\Delta q(x) = q^{+}(x) - q^{-}(x)$ where $q^{+}(x)$ [$q^{-}(x)$] is the probability of finding a quark of flavor q in a proton with spin oriented parallel (antiparallel) to the proton and carrying a fraction x of the proton's momentum in the infinite momentum frame. The valence contribution $\Delta q_v(x) = \Delta q(x) - \Delta \bar{q}(x)$ is found by subtracting the sea contribution $\Delta \bar{q}(x)$ from the distribution function for each flavor. (Here $\bar{q}$ refers to the antiquark of flavor q.) The HERMES results substantially improve the knowledge of the polarized parton distributions, especially on $\Delta u_v(x)$ and on the polarization of the sea quarks. The deuterium data being acquired in 1999/2000 will allow nearly as precise a determination of Δd_v. In addition the addition of the RICH detector in 1998 will allow the first measurement of the separate SIDIS asymmetries for the different hadron species (pions, kaons, and protons)--see section a.11. This will greatly improve the determination of the polarization of the different quark flavors, especially of the strange quark, whose polarization is presently weakly constrained.

The precise inclusive and semi-inclusive polarized deep-inelastic scattering data from SLAC, CERN and HERMES clearly show that the quark spins account for only about 20% of the nucleon's spin. Much of the remainder could be provided by a possible large positive polarization of the gluon field in the proton. It is important to test this hypothesis by measuring the gluon helicity distribution, $\Delta G(x)$. Phenomenogical LO QCD fits to the scaling violations observed in the polarized structure function $g_1(x,Q^2)$ suggest that the integral of $\Delta G(x)$ is positive, but some theoretical models predict a negative contribution to the nucleon spin[8]. Lepto-production reactions dominated by the direct coupling of the exchanged virtual photon to one of the gluons in the nucleon, a process known as photon-gluon fusion (PGF), allow more direct measurement of $\Delta G(x)$ because the gluon distribution enters in leading order. Monte Carlo studies indicate that in the HERMES experiment, PGF dominates the photo-production of pairs of hadrons with opposite charge and high transverse momentum. If so, the beam-target spin asymmetry can be used to determine the polarization of the glue because the PGF process has a strong negative polarization analyzing power.

For h^{+} h^{-} pairs where one hadron has a transverse momentum of at least 1.5 GeV/c and the other of at least 1.0 GeV/c, the asymmetry is found to be $A_{\parallel}$ = -0.28 $\pm$0.12 (stat) $\pm$0.02 (syst). Given the Monte Carlo prediction of PGF dominance, this indicates a significant *positive* polarization of the gluons. The negative value supports the Monte Carlo prediction, since none of the known background processes exhibit negative asymmetries (deep-inelastic scattering from protons is characterized by positive asymmetries). A leading order QCD model was implemented in the PYTHIA Monte Carlo generator to determine the effect on the asymmetry of the background processes, such as

the QCD Compton effect. Within the context of this model, the measured asymmetry implies a value $\Delta G(x)/G(x)$ of 0.41 ±0.18 ±0.03 for the fractional polarization of gluons with momentum fraction $\langle x_G \rangle$ = 0.17. The value is consistent with the phenomenological fits to the $g_1(x,Q^2)$ scaling violations. The contribution to the HERMES measurement from model uncertainty is unknown, and the Monte Carlo underpredicts by a factor of two the yield of hadron pairs with high transverse momentum. Nevertheless, in the absence of other sources of negative asymmetry, the data indicate that the glue is positively polarized.

HERMES has just begun to demonstrate the quality and variety of the results it can obtain. Results are being developed and finalized on many additional topics, and present and future running will greatly improve the statistical precision of the results already shown. Moreover, the HERMES apparatus has recently been upgraded and improved: a reduction in the diameter of the target storage tube has led to a 50% increase in the luminosity; a dual-radiator RICH has replaced the threshold Cerenkov counter, allowing identification of pions, kaons and protons over nearly the entire momentum acceptance of the detector (see section a.11); an instrumented iron wall was built, which enables the identification of muons; a wheel-shaped array of silicon counters is being installed just downstream of the target such that the acceptance for Λ^0 hyperons and J/Ψ mesons (in conjunction with new wide-angle scintillators behind the magnet) is increased by a factor of 4; a new set of quadrupoles behind the experiment is being equipped with tracking chambers between their pole faces that make it possible to reconstruct the virtual-photon energy ν for some of the photo-produced J/Ψ mesons. Furthermore, preparations are being made for the installation (in the first months of 2001) of a new silicon recoil detector below the target. Coupled with recent improvements in the HERA electron (or positron) beam current, these improvements will help lead to a rich future of HERMES physics results.

[1]HERMES, K. Ackerstaff *et al.*. "The HERMES Spectrometer", Nucl. Instr. & Meth. A **417**, 230 (1998).
[2]HERMES, K. Ackerstaff *et al.*. "The Flavor Asymmetry of the Light Quark Sea from Semi-inclusive Deep Inelastic Scattering", Phys. Rev. Lett. **81**, 5519 (1998).
[3]HERMES, K. Ackerstaff *et al.* "Determination of the Deep-Inelastic Contribution to the Generalized Gerasimov-Drell-Hearn Integral for the Proton and Neutron", Phys. Lett. B **444**, 531 (1998).
[4]HERMES, K. Ackerstaff *et al.* "Nuclear Effects on $R\sigma_L/\sigma_T$ in Deep-Inelastic Scattering", DESY 99-150, hep-ex/9910071, Phys. Lett. (in press).
[5]HERMES, K. Ackerstaff *et al.* "Measurement of Angular Distributions and $R= \sigma_L/\sigma_T$ in Diffractive Electroproduction of ρ^0 Mesons",
DESY 99-199.
[6]F. Meissner, "Double-Spin Asymmetry in Exclusive Vector Meson Production at HERMES", Proceedings of the 7th Int. Workshop on Deep Inelastic Scattering and QCD, DIS99, Zeuthen, Germany, April 1999, DESY HERMES 99-028.
[7]HERMES, K. Ackerstaff *et al.* "Observation of a Coherence Length Effect in Exclusive ρ^0 Electroproduction", Phys. Rev. Lett. **82**, 3025 (1999).
[8]R. L. Jaffe, Phys. Lett. B **365**, 359 (1996).

a.7. Results from Exclusive, Diffractive ρ^0 Electroproduction (T. G. O'Neill, J. Arrington, D. De Schepper, H. E. Jackson, D. H. Potterveld, and collaborators at 33 other institutions)

A signal for the exclusive electroproduction of the neutral ρ(770) meson was isolated as a subset of the standard HERMES deep inelastic scattering data. In this reaction, the electron or positron emits a virtual photon which then fluctuates into a quark-antiquark pair of lifetime l_c. A diffractive interaction with the target converts the quark-antiquark pair into the detected ρ^0. The ρ^0 meson, which decays into 2 pions, manifests itself in a peak at $M_\rho = 0.77$ GeV in the invariant mass of the 2-pion system. Energy and momentum conservation can be used to ensure that there are no additional particles in the final state, resulting in a clean signal for the exclusive $eN \rightarrow e\ \rho^0\ N$ reaction. Measurements of the reaction inside nuclei have confirmed that the lifetime of the quark-antiquark fluctuation is correctly given by l_c, and that it interacts with the nucleus like a physical ρ^0 meson[1]. Publications are being finalized on the unpolarized ρ^0 production cross section and on the $\rho^0 \rightarrow \pi^+ \pi^-$ decay angular distributions[2]. The cross section results will help illuminate the transition in the ρ production reaction mechanism from the low- to high-energy regimes, and constrain novel theories of the reaction in terms of off-forward parton distributions. The decay results provide unprecedented detail about the helicity structure of the reaction at HERMES energies. This information is complemented by the first observation of a non-trivial dependence of a vector meson production reaction on the relative orientation of beam and target spins[3], see Fig. IV-6. The discovery is especially interesting in the context of a preliminary SMC result showing no such dependence in ρ production at higher energy, where the reaction is dominated by exchange of the (presumably) spinless pomeron. The HERMES result suggests a violation of s-channel helicity conservation, which is approximately observed in diffractive reactions. It also casts new light onto the production of the ρ^0 by transverse photons which, unlike production by longitudinal photons, cannot presently be calculated in the context of perturbative QCD.

[1]HERMES, K. Ackerstaff *et al.* "Observation of a Coherence Length Effect in Exclusive ρ^0 Electroproduction", Phys. Rev. Lett. **82**, 3025 (1999).

[2]HERMES, K. Ackerstaff *et al.* "Measurement of Angular Distributions and $R = \sigma_L/\sigma_T$ in Diffractive Electroproduction of ρ^0 Mesons", DESY 99-199.

[3]F. Meissner, "Double-Spin Asymmetry in Exclusive Vector Meson Production at HERMES", Proceedings of the 7th Int. Workshop on Deep Inelastic Scattering and QCD, DIS99, Zeuthen, Germany, April 1999, DESY HERMES 99-028.

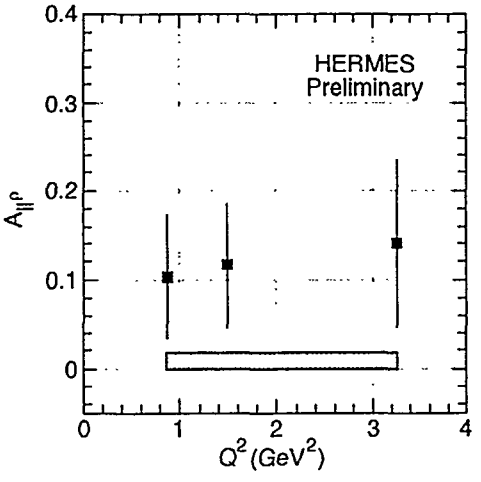

Fig. IV-6. Longitudinal beam-target asymmetry A_{11}^{ρ} (fractional dependence of the cross section on relative beam-target spin orientation) for exclusive ρ^0 production as a function of Q^2, with a systematic uncertainty band.

a.8. Measurements of Inclusive Cross Section and R = σ_L/σ_T in The Nucleon Resonance Region

(J. Arrington, D. F. Geesaman, H. Gao, T. G. O'Neill, D. Potterveld, J. Reinhold, C. Keppel,* K. Assamagan,* O. K. Baker,* W. W. Buck,* A. Cochran,* L. Gan,* A. Gasparian,* R. Green,* P. Gueye,* I. Niculescu,* E. Segbefia,* L. Tang,* C. Williams,* L. Yuan,* P. Bosted,† S. Rock,† B.D. Anderson,‡ G. Petratos,‡ J.W. Watson,‡ W. M. Zhang,‡ W. Lorenzon,§ J. Dunne,¶ S. Beedoe,‖ S. Danagoulian,‖ C. Jackson,‖ R. Sawafta,‖ V. V. Frolov,** J. Napolitano,** J. Price,** P. Stoler,** C. Armstrong,†† R. Carlini,†† R. Ent,†† K. Garrow,†† J. Gomez,†† A. Lung,†† D. Mack,†† J. H. Mitchell,†† A. Saha,†† W. Vulcan,†† S. Wood,†† C. Yan,†† C. Cothran,‡‡ D. Day,‡‡ M. Zeier,‡‡ B. Zihlmann,‡‡ H. P. Blok,§§ H. Mkrtchyan,¶¶ Ts. Amatuni,¶¶ V. Tadevosian,¶¶ D. Beck,‖‖ C. W. Bochna,‖‖ R. J. Holt,‖‖ M. A. Miller,‖‖ B. P. Terburg,‖‖ D. Dutta,*** R. E. Segal,*** B. W. Filippone,††† E. Kinney,‡‡‡ D. van Westrum,‡‡‡ D. M. Koltenuk,§§§ and R. M. Mohring¶¶¶)

Reliable global descriptions of inclusive electroproduction data are necessary for electron-nucleon scattering model development, accurate radiative correction calculations, and the extraction of form factors, structure functions, and parton distribution functions from inclusive electron scattering experiments.

A great deal of our understanding of the quark structure of the nucleon comes from inclusive electron scattering. However, most of the measurements focus on the deep inelastic region. High precision cross section measurements in the resonance region, combined with a separation of the longitudinal (σ_L) and transverse (σ_T) components, will substantially improve the global description of electroproduction at moderate to high Q^2 and large Bjorken-x. Measurements have been made to extract the ratio $R= \sigma_L/\sigma_T$ from deep inelastic cross sections at momentum transfers as high as $Q^2 = 50$ $(GeV/c)^2$, and from elastic electron-proton scattering up to $Q^2 = 8.83$ $(GeV/c)^2$. In contrast to both the elastic and the deep inelastic, there exist few separation measurements of the ratio R in the resonance region at moderate or high momentum transfers.

A series of measurements of inclusive electron scattering in the resonance region was taken during in Hall C at Jefferson Lab during 1995 and 1996 running. Data were obtained from both hydrogen and deuterium allowing extraction of the resonance production cross section from both the proton and the neutron. The cross sections were measured for momentum transfers between 0.5 and 5.0 $(GeV/c)^2$. Generating interest recently is an observed scaling relationship between resonance electroproduction and deep inelastic scattering, termed local duality. First observed by Bloom and Gilman, this duality suggests a common origin for both kinematic regimes. Local duality was observed both for the entire region and locally in the vicinity of each prominent resonance. In addition, the structure functions measured appear to be insensitive to sea quarks, giving a scaling curve that represents the valence quark distribution of the nucleon. Theoretical models indicate that both the longitudinal and the transverse structure functions should manifest Bloom-Gilman duality, but previous experiments that separated the longitudinal and transverse components did not have the precision necessary to study duality. A fundamental quark description of nucleons may be expanded to include information in the resonance region by studying duality with new resonance electroproduction data and better measurements of $R = \sigma_L/\sigma_T$. In 1999, experiment E94-110 was run in Hall C at Jefferson Lab. The experiment made a precision measurement of R in the resonance region, up to $Q^2= 7.5$ $(GeV/c)^2$. This new data should reduce the uncertainty in R from greater than 100% to approximately 10%. There is also an additional approved experiment to extend duality studies to higher Q^2, and a proposal has been submitted to the Jefferson Lab PAC to make additional measurements at low x and Q^2. The goal of this proposal is to more carefully examine the valence sensitivity of the data and to examine the low Q^2 evolution of the structure functions.

*Hampton University; †The American University; ‡Kent State University; §University of Michigan; ¶Mississippi State University; ‖ North Carolina A&T University; **Rensselaer Polytechnic Institute; ††Thomas Jefferson National Accelerator Facility; ‡‡University of Virginia; §§Vrije Universiteit; ¶¶Yerevan Physics Institute; ‖‖University of Illinois; ***Northwestern University; †††California Institute of Technology; ‡‡‡University of Colorado; §§§University of Pennsylvania; ¶¶¶University of Maryland

a.9. Measurements of the Nuclear Dependence of $R = \sigma_L/\sigma_T$ at Low Q^2

(J. Arrington, D. F. Geesaman, T. G. O'Neill, D. Potterveld, O. K. Baker,* A. Cochran,* L. Gan,* A. Gasparian,* T. Green,* P. Gueye,* B. Hu,* A. Johnson,* A. E. Keppel,* E. Segbefia,* L. Tang,* A. Bruell,† K. McIlhany,† R. G. Milner,† T. Shin,† J. Dunne,‡ R. B. Piercey,‡ C. S. Armstrong,§ R. Carlini,§ R. Ent,§ H. C. Fenker,§ K. Garrow,§ J. Gomez,§ A. Lung,§ D. Mack,§ J. H. Mitchell,§ W. F. Vulcan,§ S. A. Wood,§ E. Kinney,¶ B. van der Steenhoven,‖ B. Blok,** B. Zihlmann,** W. Lorenzon,†† B. Filippone,‡‡ and J. Martin‡‡)

Inclusive electron scattering is a well understood probe of the partonic structure of nucleons and nuclei. Deep inelastic scattering has been used to make precise measurements of nuclear structure functions over a wide range in x and Q^2. The ratio $R = \sigma_L/\sigma_T$ has been measured reasonably well in deep inelastic scattering at moderate and high Q^2 using hydrogen and deuterium targets. However, R is still one of the most poorly understood quantities measured in deep inelastic scattering and few measurements exist at low Q^2 or for nuclear targets. Existing data at moderate to large values of Q^2 rule out significant nuclear effects in R. However, evidence for substantial A-dependent effects has been recently reported by the HERMES collaboration at low x and Q^2. Figure IV-7 shows the ratio R_A/R_D for ^{3}He and Nitrogen, along with values extracted from NMC and SLAC data. While HERMES can not directly measure R (which requires data at multiple beam energies), they do measure the ratio of R_A to R_D. They see a significant deviation from unity in the ratio of $R_{^3He}/R_D$ and R_N/R_D for $x = 0.05$ and $Q^2 = 2.0$.

Jefferson Lab Experiment E99-119 is a direct measurement of R at low x (down to $x = 0.02$) and low Q^2 (down to 0.07 $(GeV/c)^2$). The measurement will be made on hydrogen, deuterium, and several nuclear targets (up to A=197). This will both significantly improve the measurement of R at low Q^2 for the proton, and examine the nuclear dependence of R in the region where the HERMES experiments has seen the A-dependence. Experiment E99-119 has been tentatively scheduled to run in Hall C in the summer of 2000.

*Hampton University; †Massachusettes Institute of Technology; ‡University of Colorado; §Thomas Jefferson National Accelerator Facility; ¶Mississippi State University; ‖ NIKHEV; ** Vrije Universiteit Amsterdam; ††University of Michigan; ‡‡California Institute of Technology

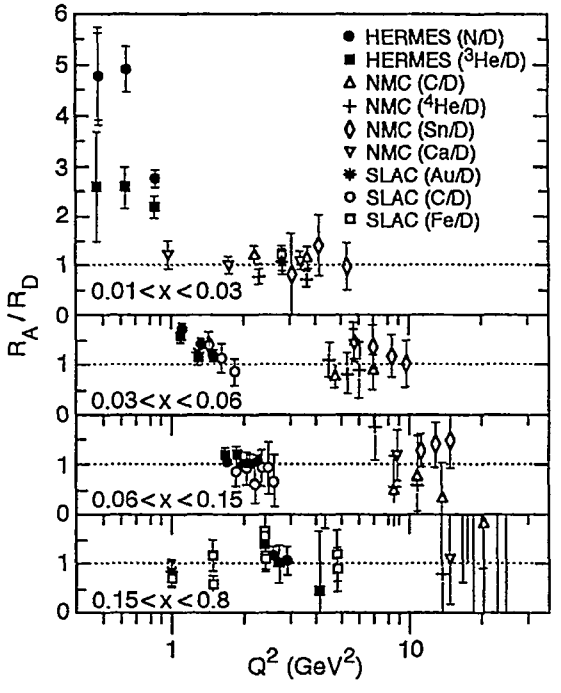

Fig. IV-7. The ratio of R_A to R_D as a function of Q^2 for four bins in x. Previous data from NMC and CLAC are consistent with one. The new HERMES data are consistent with the previous measurements, but show a significant deviation from unity for low values of x and Q^2.

a.10. Momentum Transfer Dependence of H(e,e'K$^+$)Y Reactions (J. Arrington, K. Bailey, D. F. Geesaman, H. E. Jackson, T. G. O'Neill, D. Potterveld, J. Reinhold, J. P. Schiffer, B. Zeidman, and E93-18 Collaboration)

In Jefferson Lab experiment E93-18, the momentum transfer dependence of the reaction H(e,e'K$^+$)Y, where Y is Λ or Σ^0, was studied at Q^2 = 0.5, 1.0, 1.5, and 2.0 (GeV/c)^2 at incident electron energies ranging from 2.445 to 4.045 GeV. The HMS and SOS spectrometers in Hall C were used for detection of the emergent electrons and K$^+$, respectively. For each Q^2, data were obtained at three different values of the polarization of the virtual photon in order to separate the longitudinal and transverse parts of the cross section. Together with data on the neutron (E91-16), this study is vital for understanding processes that lead to production of bound hypernuclei. Students from Hampton University[1] and the University of Maryland[2] utilized data from E93-18 for doctoral theses.

For Λ production, the ratio, $R = \sigma_L/\sigma_T$, was found to reach a maximum $\approx$1 at Q^2 = 0.75 (GeV/c)^2. The data were compared to calculations and provide significant constraints on theoretical models. These results were published.[3] The data for Σ^0 production agree with previous results for unpolarized cross actions as a function of Q^2 and with increasing Q^2, R decreases from a value $\approx$2 at $Q^2 \approx$ 0.5. Comparison with theoretical models is in progress.

[1] G. Niculescu, Ph.D. Thesis-Hampton University (1998)
[2] R. M. Mohring, Ph.D. Thesis-University of Maryland (1999)
[3] G. Niculescu *et al.*, Phys. Rev. Lett. **81**, 1805 (1998)

a.11. A Dual Radiator Ring Imaging Cerenkov Counter for HERMES

(H. E. Jackson, K. G. Bailey, D. M. De Schepper, T. P. O'Connor, T. G. O'Neill, D. H. Potterveld, J.-O. Hansen,* R. S. Kowalczyk,† and the HERMES Collaboration)

The HERMES experiment is unique among contemporary experimental studies of the spin structure of the nucleon in its emphasis on unambiguous measurement of pion, kaon, and nucleon semi-inclusive spin asymmetries in deep-inelastic scattering. These asymmetries provide information for the study of the flavor dependence of polarized structure functions and of the sea polarization. However, most of the hadrons produced in HERMES lie between 2 and 10 GeV, a region in which it has not been feasible to separate pions, kaons, and nucleons with standard PID techniques. RICH and threshold Cerenkov systems using heavy gases such as C_4F_{10}, at atmospheric pressure are useful only for energies above 10 GeV since the kaon threshold for Cerenkov radiation is typically higher than 9 GeV. Use of a high-pressure gas system is not technically feasible in HERMES. Clear liquid radiators are useful for hadron identification below roughly 2 GeV because of their correspondingly very low Cerenkov light thresholds.

To overcome these difficulties, the HERMES collaboration has replaced the existing threshold Cerenkov counters in the HERMES spectrometer with a dual-radiator RING Imaging Cerenkov Counter (RICH) which employs a new technology. The detector was designed and built by a collaboration of 8 institutions, led by Argonne (Argonne, Bari, CalTech, Frascati, Gent, Rome, Tokyo, and Zeuthen), in 12 months from concept to installation. The installation of the RICH was completed on 22 May, 1998 and has been commissioned during the past year. It is the first use of recently developed clear, hydrophobic aerogel as a Cerenkov radiator in a RICH system. In order to identify almost all of the pions, kaons and protons in the HERMES acceptance, the RICH is filled with a second radiator (C_4F_{10} gas) which in combination with the aerogel, provides complete hadron identification from 2 GeV/c to about 15 GeV/c. The basic geometry and radiator configuration are shown in Fig. IV-8. Rings from the aerogel (n = 1.03) provide identification up to about 9 GeV/c, while rings from the gas (n = 1.0015) are used for higher momenta. The RICH actually consists of a pair of identical counters, one in the upper half and second in the lower half of the HERMES spectrometer. Each photon detector is an array of 1934 3/4" photomultipliers arranged in a planar array of honeycomb packing. For a fully realistic particle, a typical ring pattern consists of a small inner ring generated by photons from the gas and a larger concentric ring of hits generated by photons from the aerogel. The ring pattern for a sample event is shown in Fig. IV-9.

The detector has operated routinely as part of the HERMES experiment since its installation in May 1998. After the mirror alignment, the single photon resolution of the detector is within 10% of the Monte Carlo predictions. The particle identification based on the inverse ray tracing technique has been implemented and its likelihood analysis is being optimized. More elaborate particle identification schemes, especially those that are based on event level algorithms, are currently under development. Hadron identification by the RICH detector will be a crucial feature of the analysis of the current (1998 and 1999) and future HERMES data.

*TJNAF; †Jet Propulsion Lab

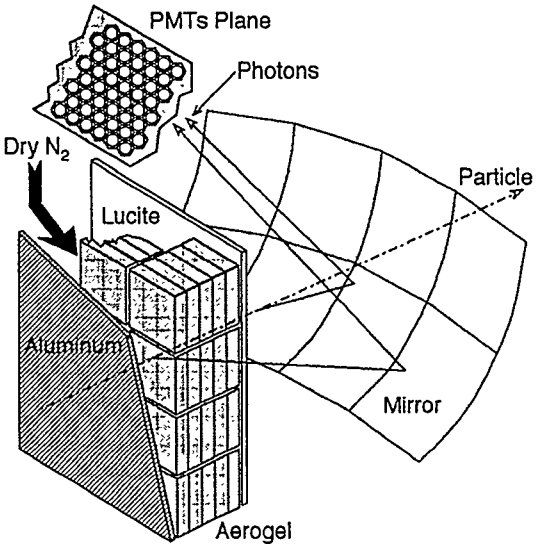

Fig. IV-8. Basic geometry and radiator configuration for the HERMES dual radiator RICH.

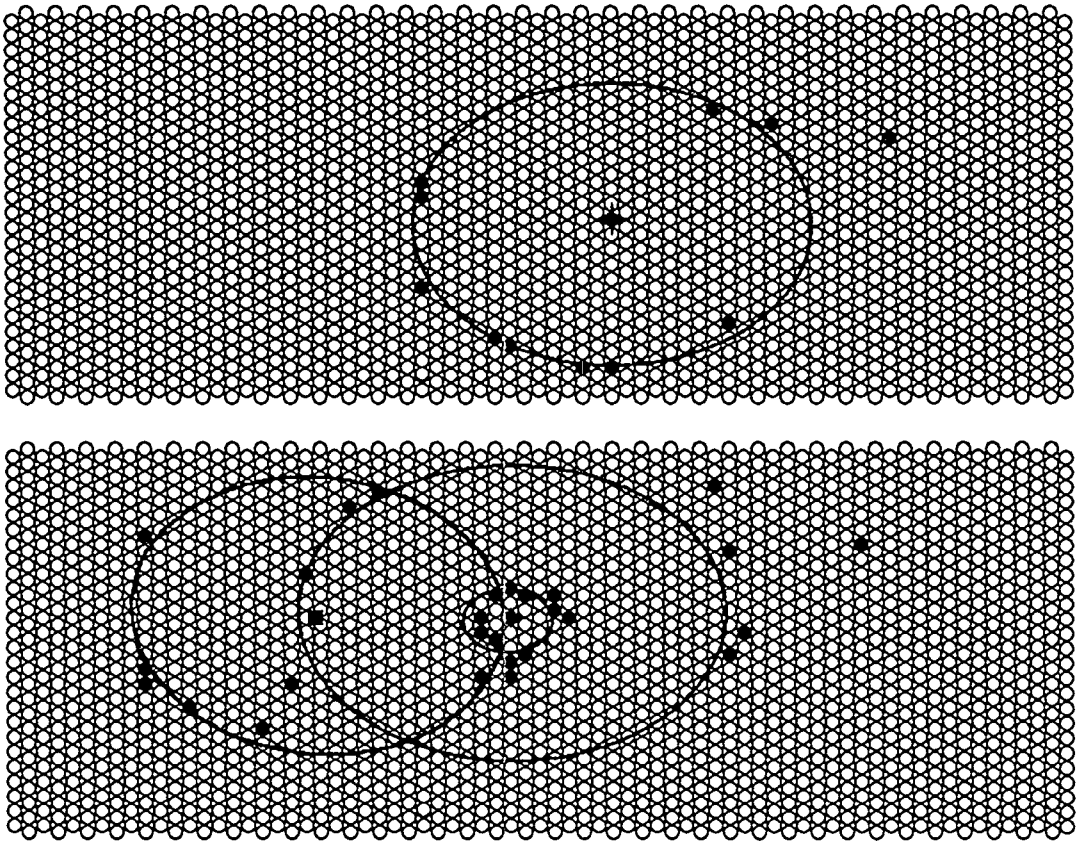

Fig. IV-9. HERMES RICH event display for an event with an electron and a pion in the lower half and a kaon in the upper half.

a.12. Lepton Pair Production with 800-Gev Protons to Explore the Antiquark Sea and ψ Production

(D. F. Geesaman, S. B. Kaufman, N. Makins, B. A. Mueller, P. E. Reimer, J. D. Bush,*L. D. Isenhower,* M. E. Sadler,* R. S. Towell,* J. L.Willis*, D. K.Wise*, C. N. Brown†, W. E. Cooper†, X. C. He‡,W. M. Lee‡, G. Peitt,‡ D. M. Kaplan,§ T. A. Cary;¶ G. T. Garvey,¶ D. M. Lee,¶ M. J. Leitch,¶ P. L. McGaughey,¶ T. N. Thompson,¶ P. N. Kirk,¶ Y. C. Wang,¶ Z. F. Wang,¶ M. E. Beddo,** T. H. Chang,** G. Kyle,** V. Papavassiliou,** J. Selden,** J. C. Webb,** T. C. Awes,†† P. W. Stankus,†† G. R. Young,†† E. A. Hawker,‡‡ G. A. Gagliardi,‡‡ R. E. Tribble,‡‡ M. A. Vasiliev,‡‡ D. D. Koetke,§§ and P. M. Nord§§)

While it is not required by any fundamental symmetry, it has—until recently—been widely assumed that distributions of anitdown ($\bar{d}$) and anti-up ($\bar{u}$) quarks in the proton sea were identical. After evidence from Deep Inelastic Scattering (DIS) of an integral difference between these distributions, the Fermilab 866/NuSea experiment measured the ratio of $\bar{d}/\bar{u}$ as a function of the momentum carried by the struck quark, x. Data were collected in 1996-1997 using the Meson East Spectrometer at Fermilab measuring Drell-Yan produced muon pairs from hydrogen and deuterium targets. Additional measurements of the nuclear dependence of J/ψ, ψ' and Drell-Yan production were made using Be, Fe and W targets.

The full analysis of the hydrogen and deuterium data is now complete. From the ratio of deuterium to hydrogen Drell-Yan cross sections, the ratio $\bar{d}/\bar{u}$ and the difference $\bar{d} - \bar{u}$ have been extracted. This revealed a striking, x -dependent asymmetry in the proton's antiquark sea. The flavor difference is a pure flavor non-singlet quantity: its integral is Q^2 independent and its Q^2 evolution, at leading order, does not depend on the gluon distributions in the proton. Therefore large differences seen in Fig. IV-10 must be nonperturbative in nature. Several approaches have been suggested to produce this difference[1], which include: (1) hadronic models of the meson cloud within the nucleon, (2) chiral quarks models which couple mesons directly to the constituent quarks, and (3) instanton models. These are illustrated by the curves in Fig. IV-10.

Although not well explained, the rate of production of the J/ψ and ψ' is diminished in nuclear targets relative to the same process with a proton target. Using nuclear targets, E866/NuSea is studying this suppression as a function of the kinematics variables Feynman- x (x_F) and transverse momentum. One significant observation, as shown in Fig. IV-11, is a difference between of the J/ψ and ψ' at low values of x_F, where the ψ' is suppressed more than the J/ψ. This affect might be attributable to the absorption of the $c\bar{c}$ pair in the nucleus before hadronization. Other effects, such as shadowing, also play important roles in the observed suppression.

Shadowing, which has been parameterized from DIS experiments, is also expected in Drell-Yan and J/ψ production data. By comparing the Drell-Yan yields from nuclear targets we were able to confirm that shadowing in Drell-Yan quantitatively matches predictions based on shadowing in DIS. In the Drell-Yan process, only initial state interactions are important since the final state muons do not interact with the nucleus. This, combined with the ability to correct for nuclear shadowing, makes Drell-Yan an ideal tool for the study of parton energy loss. Using the same data, corrected for shadowing, very tight limits were place on the energy loss of partons traveling through cold nuclear matter.

Analysis of the E866/NuSea Data continues, focusing on the following issues: (1) Extracting absolute Drell-Yan cross sections for hydrogen and deuterium. (2) Studying the angular distributions of ψ' production, which does not suffer from contamination by decays from higher $c\bar{c}$ states. (3) Extraction of Y angular distributions. The latter two compliment the already analyzed data on the polarization of J/ψ production which will be compared with models formulated to reproduce higher energy collider data.

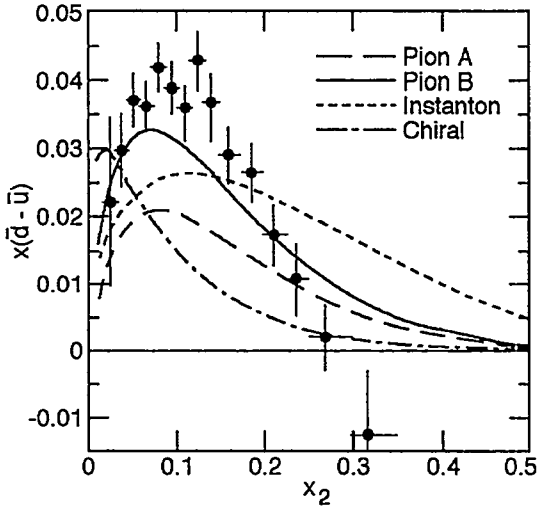

Fig. IV-10. The x dependence of the difference x ($\bar{d}$ − $\bar{u}$) of the proton at a mass scale of 7.353 GeV. The curves represent several model calculations[1]. The "pion cloud" curves show the effect of different vertex cutoffs.

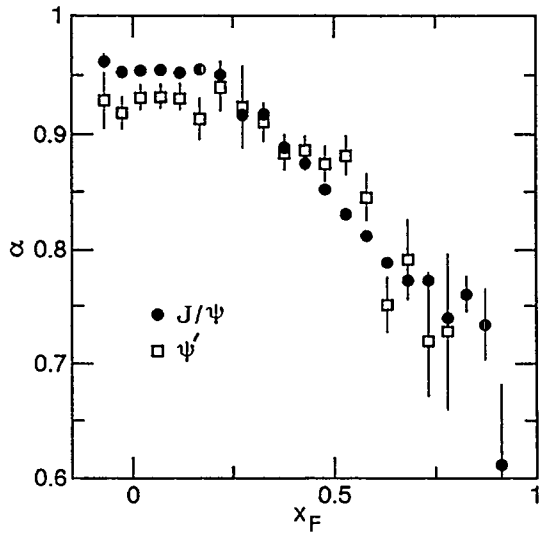

Fig. IV-11. Nuclear suppression of J/ψ and ψ' production parameterized in terms of a where $\sigma_A=\sigma_p A^{\alpha}$ and σ_A, σ_p represent the production cross section on a nuclear target and a free proton, respectively.

*Abilene Christian University; †Fermi National Accelerator Laboratory; ‡Georgia State University; §Illinois Institute of Technology; ¶Los Alamos National Laboratory; ||Louisiana State University; **New Mexico State University; ††Oak Ridge National Laboratory; ‡‡Texas A&M University; §§Valparaiso University

[1] J. C. Peng *et al.*, Phys. Rev. D **58** 092004 (1998).

a.13. Υ and J/ψ Production from 800-GeV Protons Incident on D_2 and H_2 Targets

(D. F. Geesaman, S. B. Kaufman, N. Makins, B. A. Mueller, J. D. Bush,* L. D. Isenhower,* M. E. Sadler,* R. S. Towell,* J. L. Willis,* D. K. Wise,* C. N. Brown,† W. E Cooper,† X. C. He,‡ W. M. Lee,‡ G. Petitt, ‡ D. M. Kaplan,§ T. A. Cary,¶ G. T. Garvey,¶ D. M. Lee,¶ M. J. Leitch,¶ P. L. McGaughey,¶ J. M. Moss,¶ B. K. Park,¶ J. C. Peng,¶ P. E. Reimer,¶ W. E. Sondheim,¶ T. N. Thompson,¶ P. N, Kirk,|| Y. C. Wang,|| Z. F. Wang,|| M. E. Beddo,** T. H. Chang,** G. Kyle,** V. Papavassiliou,** J. Selden,** J. C. Webb,** T. C. Awes,†† P. W. Stankus,†† G. R. Young,††, E. A. Hawker,‡‡ C. A. Gagliardi,‡‡ R. E. Tribble,‡‡ M. A. Vasiliev,‡‡ D. D. Koetke,§§ and P. M. Nord§§)

Fermilab experiment E866 is designed to detect pairs of oppositely charged muons produced in collisions between 800 GeV protons and variety of fixed targets. The primary motivation for E866 was to detect dimuon events generated in Drell-Yan reactions, but the detector is sensitive to any process which produces dimuon pairs. One such process is heavy quark vector meson production. Υ and J/ψ particles are produced when partons from the beam and target annihilate and form a virtual gluon which then hadronizes into a heavy resonance state. These states have several percent branching ratios into dimuon pairs and are detected during normal data acquisition. The virtual gluon which produce the resonance can be generated by the annihilation of either a quark/antiquark pair or a pair of gluons. Resonance production is therefore sensitive to both the quark and gluon distributions within the beam and target. J/ψ production is believed to occur dominantly via gluon-gluon fusion, while Υ production is thought to have contributions from both gluon-gluon fusion and quark-antiquark annihilation. Because the gluon distribution for the proton and neutron are thought be the same, the per nucleon J/ψ production cross section is expected to be the same for hydrogen

and deuterium. The Υ production ratio, on the other hand, is expected to be larger than unity since $\bar{u}_n(x) > \bar{u}_p(x)$ for the Bjorken-x values of Υ production accessed in E866.

The E866 hydrogen and deuterium data samples contain approximately 30000 Υ and 1 million J/ψ events. The production cross sections are determined by fitting the measured mass distribution to the simulated mass distributions of the relevant vector mesons and the underlying Drell-Yan continuum. This separation is performed for several bins in X-Feynman, to determine the kinematic dependence of the cross section. The absolute Υ and J/ψ production cross sections for hydrogen and deuterium are obtained from the extracted results by normalizing the yields to the integrated luminosity and correcting the results by the acceptance of the detector. The cross sections values can then be compared to predictions based various models using the various parton distributions available in the literature. Color evaporation model (CEM) calculations have been performed for both J/ψ and Υ production from H_2 and D_2. Although the CEM model is extremely simple and cannot predict the absolute value of the cross sections, the X-Feynman shape is reproduced by the CEM calculation. Further, the unknown scale factor in the CEM calculations cancels when the D_2/H_2 per-nucleon ratio is calculated. The extracted cross section ratio, D/2H , for J/ψ and Υ production are shown in Fig. IV-12. The J/ψ ratio is close to unity, which is consistent with expectations assuming gluon fusion production. The Υ ratio is also consistent with unity, which is in disagreement with the CEM calculation when either the MRST or CTEQ5M parton distribution functions (PDFs) are used. The deviation from the prediction may indicate that the PDFs underestimate the hard gluon ($x \approx 0.25$) distribution in the proton.

*Abilene Christian University; †Fermi Na;tional Accelrator Laboratory; ‡Georgia State University; §Illinois Institute of Technology; ¶Los Alamos National Laboratory; ‖ Louisiana State University; **New Mexico State University; ††Oak Ridge National Laboratory; ‡‡Texas A&M University; §§Valparaiso University

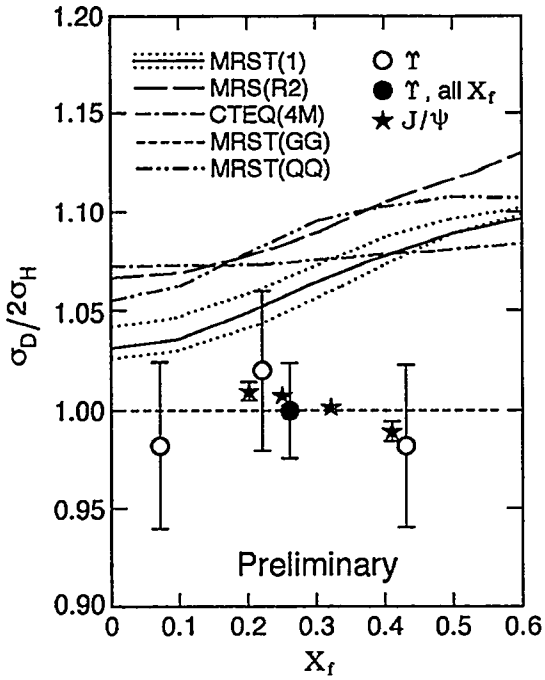

Fig. IV-12. The data points show the ratio of cross sections for υ and J/ψ production from deuterium and hydrogen. The curves correspond to color evaporation model calculations using several different parameterizations for the nucleon parton distributions.

a.14. Lepton Pair Production with 120-GeV Protons to Extend the Measurement of $\bar{d}/\bar{u}$ in the Nucleon

(D. DeSchepper, D. F. Geesaman, B. A. Mueller, T. G. O'Neill, D. H. Potterveld, P. E. Reimer, L. D. Isenhower*, M. E. Sadler*, C. N. Brown,† G. T. Garvey,‡ M. J. Leitch,‡ P. L. McGaughey,‡ J.-C. Peng,‡ R. Gilman,§ C. Glashausser,§ X. Jiang,§ R. Ransome,§ S. Strauch,§ C. A. Gagliardi,¶ R. E. Tribble,¶ M. A. Vasiliev,¶ and D. D. Koetkell)

The measurement by the Fermilab 866/NuSea Experiment revealed an unexpected dependence of the $\bar{d}$ / u ratio on the momentum fraction of the struck quark, x. For $x > 0.19$ the antiquark asymmetry began to decline, returning to a completely symmetric sea near the highest values of x accessible to the experiment. A significant extension of the x -range can be achieved with a higher-intensity, lower-energy beam, making this a study ideally suited for a "slow extraction" beam from the 120 GeV Fermilab main injector. The expected statistical errors which could be obtained from such a measurement are shown in Fig. IV-13.

After a favorably received letter of intent, a full proposal for this measurement was submitted to Fermilab in the spring of 1999. At that time, the Fermilab decided not to commit to a fixed target program based on a slow extraction because of its effect on the collider luminosity and the time scales of the other experiments which were proposed for this type of beam. The collaboration was encouraged to submit a proposal in the spring of 2001 when the impact of a fixed target program will be reconsidered. The collaboration intends to resubmit a new proposal at this time, and work is continuing toward this end.

*Abilene Christian University; †Fermi National Accelerator Laboratory; ‡Los Alamos National Laboratory; §Rutgers University; ¶Texas A&M University; ‖Valparaiso University

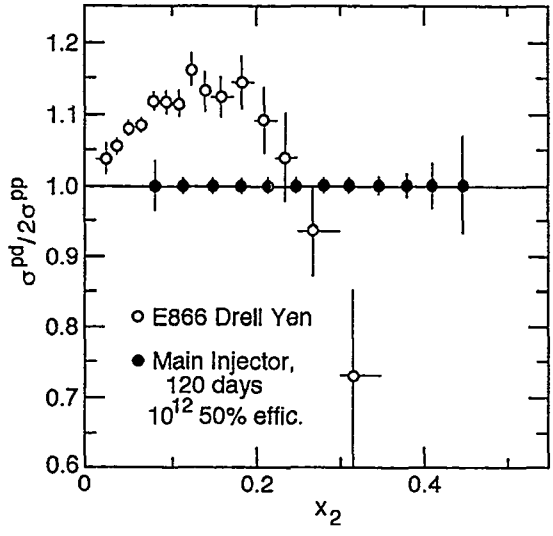

Fig. IV-13. Expected statistical precision for the proposed experiment (error bars with solid circles) arbitrarily plotted at a ratio of 1.0. Systematic errors are estimated to be less than 1%. Also shown are the Fermilab E866/NuSea results (open circles) for the x -dependence of the ratio of Drell-Yan cross sections from deuterium and hydrogen.

B. ATOM TRAP TRACE ANALYSIS

b.1. A New Method of Ultrasensitive Trace-Isotope Analysis

(K. Bailey, C. Y. Chen, X. Du, Y. M. Li, Z.-T. Lu, T. P. O'Connor, and L. Young*)

We have demonstrated a new method of ultrasensitive trace-isotope analysis[1]. Named Atom Trap Trace Analysis (ATTA), this method is based on the techniques of laser cooling and trapping of neutral atoms, and has been used to count individual $^{85}Kr(t_{1/2} = 10.8\,yr)$ and $^{81}Kr(t_{1/2} = 2 \times \supseteq 10^5\ yr)$ atoms present in a natural krypton gas sample with isotopic abundances in the range of 10^{-11} and 10^{-13}, respectively.

In 1999, we characterized and optimized the atomic beam machine that was built in 1998. With this machine, the abundant ^{83}Kr (11.5%) atoms could be loaded into the trap at $3 \times 10^8\ sec^{-1}$, or about 2×10^{-7} of the ^{83}Kr atoms injected into the vacuum system. The total efficiency resulted from a combination of the efficiency of metastable atom production ($\sim 10^{-4}$), losses due to atomic beam divergence ($\sim 10^{-3}$), and the fraction of atoms captured while passing through the trap ($\sim 10^{-1}$). In order to optimize both capture efficiency and the sensitivity of single atom detection, we implemented a procedure that alternated trap parameters between two sets that were optimized for capture and detection respectively. We could clearly detect a single trapped atom by observing its fluorescence, with a signal equal to 50 times the background noise (Fig. IV-14). We have detected and counted ^{81}Kr and ^{85}Kr atoms in an atmospheric krypton sample (Fig. IV-15), and measured the isotopic abundances to be $(1.5 \pm 0.4) \times 10^{-11}$ for ^{85}Kr and $(1.0 \pm 0.4) \times 10^{-12}$ for ^{81}Kr.

For real-world applications such as radio-krypton dating of ancient groundwater or polar ice, a much higher efficiency (10^{-4}-10^{-3}) is required. In order to improve the efficiency, we are currently investigating different methods of producing metastable krypton atoms. In addition, we plan to cool the atom source and recirculate the krypton atoms in the vacuum system.

In the future, ATTA can be used to analyze many other isotope tracers for a wide range of potential applications including measuring solar neutrino flux, searching for exotic particles, tracing atmospheric and oceanic currents, archeological and geological dating, medical diagnostics, and monitoring fission products in the environment for safe-guarding nuclear wastes.

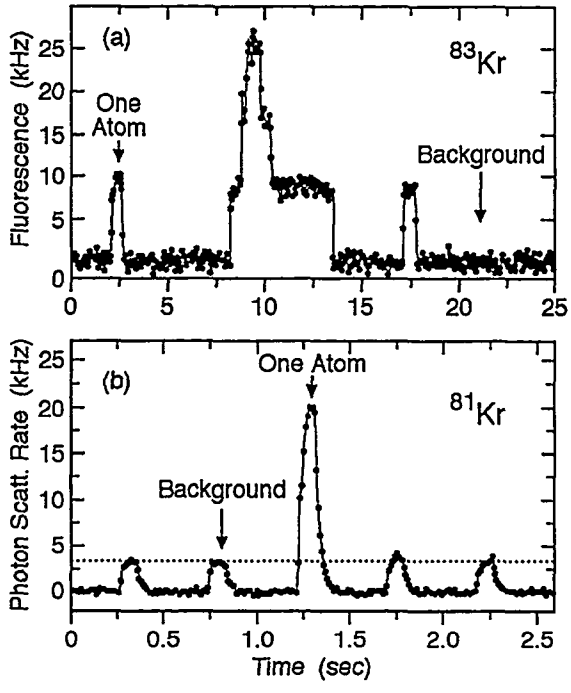

Fig. IV-14. Single atom counting. (a) Changes of the fluorescence signal of the abundant ^{83}Kr atoms mark the arrival and departure of individual atoms in the laser trap. (b) Signal of a single trapped ^{81}Kr atom. During loading time, the photon-count rate was low because the counter was blocked for protection from over-exposure.

*Chemistry Division, ANL

[1] C. Y. Chen et. al., Science **286**, 1139 (1999).

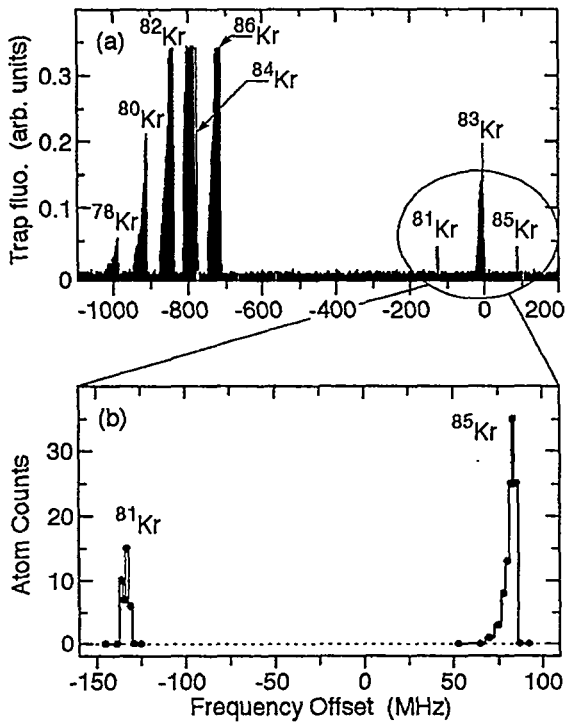

Fig. IV-15. The fluorescence signal from laser trapped metastable krypton atoms. Atoms of different isotopes are trapped at different laser frequencies due to isotope shifts. (a) The signal of abundant Kr isotopes; (b) Number of ^{81}Kr and ^{85}Kr atoms counted vs. laser frequency. Each data point represents the number of atoms counted in 3 hours for ^{81}Kr and 0.5 hours for ^{85}Kr.

b.2. Atom Trap Trace Analysis of ^{41}Ca (K. Bailey, X. Du, Y. M. Li, Z.-T. Lu, T. P. O'Connor, and L. Young*)

Calcium is an essential element in biological and geological objects. In particular, its abundance in human bones has motivated many works on the trace analysis of ^{41}Ca ($t_{1/2}$=103 kyr) for important applications in medicine and archaeology. In medicine, ^{41}Ca-tracer can be used to monitor bone-loss rates thereby providing an effective tool in the diagnosis of osteoporosis as well as in the evaluation of its treatment. In archaeology, ^{41}Ca is a potential tracer for dating bones in the age range of 10^5 years. This is an important era in human development, but is too old to be dated with ^{14}C ($t_{1/2}$=5.7 kyr)

So far, accelerator mass spectrometry (AMS) has been the only method available for these applications[1]. The natural isotopic abundance of ^{41}Ca(~10^{-15}) has been measured using AMS. A complete systematic study, however, has not been possible because the AMS detection limit is too close to the natural level. For medical applications, where the isotopic abundance of ^{41}Ca can be artificially raised to as high as 10^{-10}, AMS has proven to be an effective method in research works, however, its cost is likely to prevent it from being accessible to the general medical community.

We are developing a ^{41}Ca analyzer using the new Atom Trap Trace Analysis(ATTA) method[2], with the goal of advancing both of the aforementioned applications. ATTA is immune to contamination from other elements and isotopes, and has the potential to reach a detection limit far below the natural isotopic abundance of ^{41}Ca. Compared with a typical AMS facility, an ATTA apparatus is significantly cheaper and occupy a smaller area. Therefore, ATTA has a much better

chance of becoming a generally accessible medical instrument.

In 1999, we have installed a laser system that generates the 423nm laser light needed to trap calcium atoms. We have designed a calcium atomic beam machine and ordered various parts. Assembly and characterization of this system will be carried out in the following year.

*Chemistry Division, ANL

[1]W. Henning et. al., Science **236**, 725 (1987). D. Elmore et. al., Nucl. Instr. Meth. **B52**, 531 (1990).
[2]C. Y. Chen et. al., Science **286**, 1139 (1999).

b.3. Laser Spectroscopy of Rare Isotopes (K. Bailey, C. Y. Chen, X. Du, Y. M. Li, Z.-T. Lu, T. P. O'Connor, and L. Young*)

Laser spectroscopy on atoms has long been used to determine nuclear properties such as spins, magnetic dipole moments, electric quadrupole moments, and charge radii. In order to study unstable and rare isotopes, we have developed a sensitive atom trap trace analysis technique[1] to trap and conduct laser spectroscopy on individual atoms. When coupled with an ISOL source, this technique can be used to study, for example, short-lived cesium isotopes or neutron-rich ^{6}He and ^{8}He isotopes.

In 1999, we have conducted laser spectroscopy on individual ^{85}Kr atoms in the trap, and demonstrated the sensitivity of this technique. From a total of ~10^{9} ^{85}Kr atoms injected into the atom source, we trapped 145 atoms and obtained the spectrum shown in Fig. IV-16. The data points were on one side of the peak because trapping is only possible with the laser frequency tuned below the atomic resonance. A full and more precise spectrum can be obtained with improvements such as separating the processes of trapping and fluorescence collection.

*Chemistry Division, ANL

[1]K. Bailey et. al., A new method of ultrasensitive trace-isotope analysis, Physics Division Annual Report, ANL-99.
[2]B. D. Cannon, Phys. Rev. **A47**, 1148 (1993).

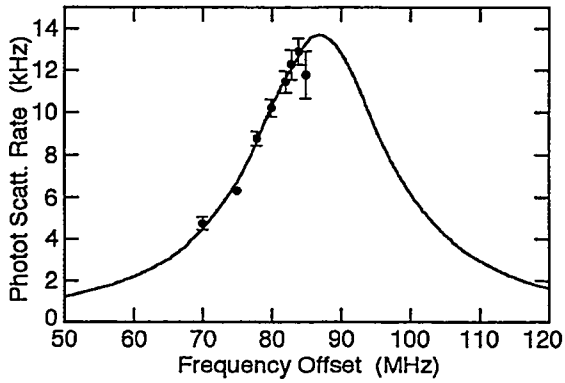

Fig. IV-16. Single atom fluorescence versus laser frequency offset. The measured photon-count rates are fitted to a Lorentzian function, rates $\propto [(f-f_r)^2 + (\gamma/2)^2]^{-1}$. Here, f_r is the resonant transition frequency of ^{85}Kr, f is the laser frequency, and $\gamma = \Gamma(1+s)^{1/2}$ is the power-broadened linewidth. We fixed f_r = 87 MHz and Γ = 5.3 MHz according to previous spectroscopy measurements[2]. The resulting saturation parameter $s = 19 \pm 1$. Error bars represent the change in fluorescence between different atoms. We attribute the cause of large fluctuations near resonance to the fact that the atom trajectory partially extends beyond the viewing region as the trap temperature increases near resonance.

V. THEORETICAL PHYSICS

OVERVIEW

Theoretical research in the Physics Division addresses a broad range of problems involving the structure and dynamics of hadrons and nuclei. There is a strong emphasis on comparison to data from Argonne's ATLAS facility, TJNAF, and other laboratories around the world. Our work includes the modeling and application of quantum chromodynamics to light- and heavy-hadron structure at zero temperature and density, and at the extremes of temperature and density appropriate to the early universe, neutron stars, and upcoming RHIC and LHC experiments. We develop reaction theories for meson and nucleon-resonance production experiments at JLab, and for medium effects on mesons and resonances in nuclei and dense matter also relevant to RHIC. We construct realistic two- and three-nucleon potentials that give accurate fits to NN elastic scattering data and trinucleon properties, and use them in detailed many-body calculations of light and closed-shell nuclei, nuclear matter and neutron stars, and in a variety of astrophysically important electroweak reactions. Our nuclear structure and reaction studies include coupled-channels calculations of heavy-ion reactions near the Coulomb barrier, and calculations of observables in breakup reactions of nuclei far from stability. We also study high-spin superdeformation, spectroscopy of the heaviest elements ($A \geq 250$), and nuclear structure near the proton-drip line. Additional research is made in atomic physics, neutron physics, quantum computing and fundamental quantum mechanics. Several of our projects involve major numerical simulations using the massively parallel computer systems at Argonne and NERSC.

A. NUCLEAR DYNAMICS WITH SUBNUCLEONIC DEGREES OF FREEDOM

The objective of this research program is to investigate the role of mesons, nucleon resonances, and quark-gluon degrees of freedom in nuclear dynamics.

The Dyson-Schwinger equations (DSEs) provide a nonperturbative approach to studying the continuum formulation of QCD, making accessible phenomena such as confinement, dynamical chiral symmetry breaking, and bound state structure and interactions. However, they also provide a generating tool for perturbation theory and hence their application is tightly constrained at high-energy. This is the particular feature of the phenomenological application of DSEs: their ability to furnish a unified description of high- and low-energy phenomena in QCD. This last year has seen many successful applications. For example, we developed a Fadde'ev amplitude model of the nucleon, and used it to calculate a wide range of leptonic and nonleptonic nucleon couplings and form factors, demonstrating that soft form factors are the natural outcome of quark substructure. We demonstrated that scalar and pseudoscalar bound states persist into the quark gluon plasma and that their widths remain large until very near the critical temperature for plasma formation. We also explored the consequences that non-Markovian effects in the quantum Vlasov equation's source term can have on the evolution to equilibrium of particles produced in an ultrarelativistic heavy ion collision.

At the level of meson and nucleon resonance degrees of freedom, we have developed a dynamical model for relating the structure of nucleon resonances (N*) as predicted by various QCD-based hadron models to the data on πN and γN reactions. The model has been used to test constituent quark models and to extract the Q^2-dependence of $\gamma \rightarrow \Delta$ transition factors from the recent data obtained at TJNAF, Mainz, and MIT-Bates. The amplitudes of vector meson photoproduction at a few GeV were analyzed based on the diffractive Pomeron-exchange and meson-exchange mechanisms to explain the latest data from TJNAF and DESY. Finally, models of hyperon-nucleon and hyperon-hyperon interactions constructed by using SU(3) symmetry were used to investigate the structure of hypernuclei.

"Relativistic effects" in nuclear dynamics depend strongly on definitions and assumptions. We have been concentrating on adjustments of standard Galilei covariant nuclear dynamics required for compliance with covariance under the inhomogeneous Lorentz group (Poincaré group). While covariants transform differently under the two groups, the invariants are effectively identical. We conclude that while it is essential to relate dynamically determined invariants to covariant observables by relativistic kinematics, Poincaré compliance at the 1% level does not require adjustments of standard nuclear Hamiltonians for two and three nucleons. We expect this result to hold for more nucleons as well.

a.1. A Dynamical, Confining Model and Hot Quark Stars (C. D. Roberts, S. Schmidt, D. Blaschke,* H. Grigorian,† and G. Poghosyan†)

We explored the consequences of an equation of state (EOS) obtained in a confining Dyson-Schwinger equation model of QCD for the structure and stability of non-strange quark stars at finite temperature, T, and compared the results with those obtained using a bag-model EOS. Both models support a temperature profile that varies over the star's volume and the consequences of this are model independent; *e.g.*, the maximum mass of a quark star is reduced as the central temperature is increased and the maximum attainable radius of a pure quark star is R ~ 8-10 km. However, in our model the analogue of the bag pressure is (T,μ)-dependent, which is not the case in the bag model. This is a significant qualitative difference and comparing the results effected a primary goal of elucidating the sensitivity of quark star properties to the form of the EOS. An article describing this work was published.[1]

*University of Rostock, Germany, †Yerevan State University, Armenia

[1]C. D. Roberts, D. Blaschke, S. Schmidt, H. Grigorian, and G. Poghosyan, Phys. Lett. **B450**, 207 (1999)

a.2. Mean Field Exponents and Small Quark Masses (C. D. Roberts, P. Maris, and A. Höll*)

We demonstrated that the restoration of chiral symmetry at finite-temperature in a class of confining Dyson-Schwinger equation (DSE) models of QCD is a mean field transition, and that an accurate determination of the critical exponents using the chiral and thermal susceptibilities requires very small values of the current-quark mass: $\log_{10}(m/m_u) \leq -5$, making their determination via lattice-QCD simulations very difficult. Other classes of DSE models characterized by qualitatively different interactions also exhibit a mean field transition. Incipient in this observation is the suggestion that mean field exponents are a result of the gap equation's fermion substructure and not of the interaction. This conclusion can likely only be false if $1/N_c$-corrections to the quark-gluon vertex are large in the vicinity of the transition. An article describing this work was published.[1]

*University of Rostock, Germany

[1]C. D. Roberts, P. Maris, and A. Höll, Phys. Rev. C **59**, 1751 (1999)

a.3. Survey of Heavy-meson Observables (C. D. Roberts, M. A. Ivanov,* and Yu. L. Kalinovsky†)

We employed a Dyson-Schwinger equation model to effect a unified and uniformly accurate description of light- and heavy-meson observables, which we characterized by heavy-meson leptonic decays, semileptonic heavy-to-heavy and heavy-to-light transitions: $B \to D^*, D, \rho, \pi$; $D \to K^*, K$; radiative and strong decays: $B^* \to B\gamma$; $D^* \to D\gamma$, $D\,\pi$; and the rare $B \to K^*\gamma$ flavor-changing neutral-current process. We elucidated the heavy-quark limit of these processes and, using a model-independent mass formula valid for all nonsinglet pseudoscalar mesons, demonstrated that their mass rises linearly with the mass of their heaviest constituent. In our numerical calculations we eschewed a heavy-quark expansion and relied instead on the observation that the dressed c,b-quark mass functions are well approximated by a constant, interpreted as their constituent-mass: we found $\hat{M}_c = 1.29$ GeV and $\hat{M}_b = 4.54$ GeV. The calculated heavy-meson leptonic decay constants and transition form factors are a necessary element in the experimental determination of CKM matrix elements. The results also show that this framework, as employed hitherto, is well able to describe vector meson polarization observables. An article describing this work was published.[1]

*BLTP, JINR, Dubna, †LCTA, JINR, Dubna,

[1]C. D. Roberts, M. A. Ivanov, and Yu. L. Kalinovsky, Phys. Rev. D **60**, 34018 (1999)

a.4. Electromagnetic Nucleon Form Factors (J. C. R. Bloch, C. D. Roberts, S. M. Schmidt, A. Bender,* and M. R. Frank†)

We calculated the nucleon's electromagnetic form factors on q^2 [0,3] GeV^2 using an *Ansatz* for the nucleon's Fadde'ev amplitude motivated by quark-diquark solutions of the relativistic Fadde'ev equation. In this first study only the scalar diquark is retained, and it and the quark are confined. A good description of the data requires a nonpointlike diquark correlation with an electromagnetic radius of 0.8 r_π. The composite, nonpointlike nature of the diquark is crucial. It provides for diquark-breakup terms that are of greater importance than the diquark photon absorption contribution. This is a first and important step in extending the successful, Dyson-Schwinger-equation-based meson phenomenology to the baryon sector, a long-held goal. An article describing this research was published.[1]

*University of Adelaide, Australia, †Institute for Nuclear Theory, Seattle

[1] J. C. R. Bloch, C. D. Roberts, S. M. Schmidt, A. Bender, M. R. Frank, Phys. Rev. C **60**, 062201 (Rapid Comm.) (1999)

a.5. Diquarks: Condensation without Bound States (J. C. R. Bloch, C. D. Roberts, and S. M. Schmidt)

We employed a bispinor gap equation to study superfluidity at nonzero chemical potential, $\mu < 0$, in two- and three-color QCD. The two-color theory, QC2D, is an excellent exemplar: the order of truncation of the quark-quark scattering kernel, K, has no qualitative impact, which allows a straightforward elucidation of the effects of μ when the coupling is strong. In rainbow-ladder truncation, diquark bound states appear in the spectrum of the three-color theory, a defect that is eliminated by an improvement of K. The corrected gap equation describes a superfluid (diquark condensed) phase that is semi-quantitatively similar to that obtained using the rainbow truncation. A model study suggests that the width of the superfluid gap and the transition point in QC2D provide reliable quantitative estimates of those quantities in QCD. The diquark superfluid may exist at the core of dense astrophysical objects. An article describing this research was published.[1]

[1] J. C. R. Bloch, C. D. Roberts, and S. M. Schmidt, Phys. Rev. C **60**, 065208 (1999)

a.6. Describing a_1 and b_1 Decays (J. C. R. Bloch, C. D. Roberts, S. M. Schmidt, and Yu. L. Kalinovsky*)

Two-body pion-radiating and weak decays of light axial-vector mesons and the ρ were studied as a phenomenological application of the QCD Dyson-Schwinger equations. We found that models based on the rainbow-ladder truncation are capable of providing a good description and, in particular, yield the correct sign and magnitude of the $a_1 \to \rho\pi$ and $b_1 \to \omega\pi$ D/S ratios, with no additional mechanism necessary. The study confirms that this ratio is sensitive to the long-range part of the quark-quark interaction and can be used to constrain model forms. An article describing this research was published.[1]

*LCTA, JINR, Dubna

[1] J. C. R. Bloch, Yu. L. Kalinovsky, C. D. Roberts, and S. M. Schmidt, Phys. Rev. D **60**, 111502 (Rapid Comm.) (1999)

a.7. Pair Creation: Back-Reactions and Damping (J. C. R. Bloch, C. D. Roberts, S. M. Schmidt, V. A. Mierny,* A. V. Prozorkevich,* S. A. Smolyansky,* and D. M. Vinnik*)

As a step toward understanding the kinetic evolution from a relativistic heavy-ion collision to a quark-gluon plasma we solved the quantum Vlasov equation for fermions and bosons, incorporating spontaneous pair creation in the presence of back-reactions and collisions. Pair creation is initiated by an external impulse field that models an energetic heavy-ion collision and the source term is non-Markovian; *i.e*, it is non-local in time. A simultaneous solution of Maxwell's equation in the presence of feedback yields an internal current and electric field that exhibit plasma oscillations with a period τ_{pl}, just as would a plasma in QED. Allowing for collisions, these oscillations are damped on a time-scale, τ_r determined by the collision frequency. We find that plasma oscillations cannot affect the early stages of the formation of a quark-gluon plasma unless $\tau_r \gg \tau_{pl}$ and $\tau_{pl} \approx 1/\Lambda_{QCD} \approx 1$ fm/c. That will make it difficult to observe this effect at RHIC. An article describing this research was published.[1]

*Saratov State University, Armenia

[1] J. C. R. Bloch, V. A. Mizerny, A. V. Prozorkevich, C. D. Roberts, S. M. Schmidt, S. A. Smolyansky and D. V. Vinnik, Phys. Rev. D **60**, 116011 (Rapid Comm.) (1999)

a.8. $K \to \pi\pi$ and a Light Scalar Meson (J. C. R. Bloch, C. D. Roberts, S. M. Schmidt, M. A. Ivanov,* and T. Mizutani†)

We explored the $\Delta I = 1/2$ rule and the fundamental CP violating gauge: ε'/ε in $K \to \pi\pi$ transitions using the Dyson-Schwinger equations. Exploiting the feature that QCD penguin operators direct K_S^0 transitions through 0^{++} intermediate states, we find an explanation of the enhancement of $I = 0$ $K \to \pi\pi$ transitions in the contribution of a light σ-meson, $m_\sigma \approx 0.5$ GeV. This mechanism also affects ε'/ε providing a significant enhancement. The study shows that the effect of this σ-meson should be understood before any conclusions can be drawn about non-Standard-Model effects in parity violating K-decays. An article describing this work was submitted for publication.

*BLTP, JINR, Dubna, †Virginia Polytechnic Institute and State University, Blacksburg, VA.

a.9. Memory Effects and Thermodynamics in Strong Field Plasmas (J. C. R. Bloch, C. D. Roberts, and S. M. Schmidt)

Continuing our exploration of nonequilibrium aspects of ultrarelativistic heavy-ion collisions, we studied the evolution of a strong-field plasma using a quantum Vlasov equation with a non-Markovian source term and a simple collision term. This provided calculated results for the time-dependence of the energy density and particle-number density. We found that the evolution of a plasma produced with RHIC-like initial conditions is well described by a low-density approximation to the source term, with non-Markovian effects and plasma oscillations unlikely to be observable. However, with the much larger initial energy density in an LHC-like collision, non-Markovian effects and plasma oscillations certainly influence the evolution of the plasma. These effects may even be observable in the spectrum of dileptons emitted before equilibration of the plasma. An article describing this work was published.[1]

[1] J. C. R. Bloch, C. D. Roberts, and S. M. Schmidt, Phys. Rev. D 61, 117502 (2000)

a.10. Selected Nucleon Form Factors and a Composite Scalar Diquark

(J. C. R. Bloch, C. D. Roberts, and S. M. Schmidt)

As an application and test of our quark-plus-scalar-diquark nucleon model, we calculated a wide range of leptonic and nonleptonic nucleon form factors: pseudoscalar, isoscalar- and isovector-vector, axial-vector and scalar. The last yields the nucleon σ-term and on-shell σ-nucleon coupling. The calculated form factors are soft and there is no sign that this is a model-dependent result, and the couplings are generally in good agreement with experiment and other determinations, as is evident in Table V-1. Elements in the dressed-quark-axial-vector vertex that are not constrained by the Ward-Takahashi identity contribute ~ 20% to the magnitude of g_A, as the comparison between the results labeled a) *etc.* in the table indicate. We anticipate a contribution of similar magnitude from the axial-vector diquark correlation, hitherto omitted. The calculation of the nucleon σ-term is particularly interesting because it illustrates the only method that allows an unambiguous off-shell extrapolation in the estimation of meson-nucleon form factors. The calculated form factor is depicted in Fig. IV-1. An article describing this work was submitted for publication.

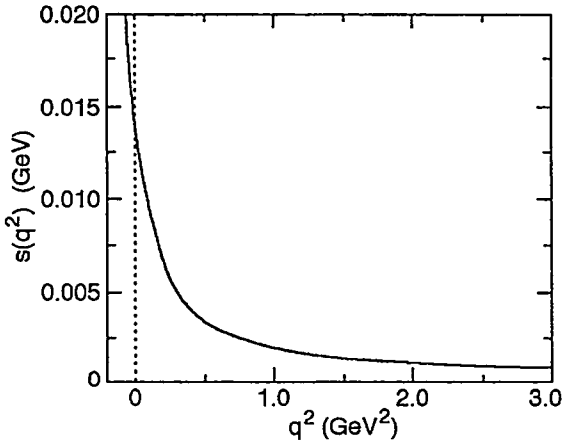

Fig. V-1. Calculated form of $\sigma(q^2)$. The rapid increase with decreasing q^2 is associated with the evolution to the σ-meson pole. A good fit to the result is: $\sigma(t) = g_\sigma(t), \frac{mn_\sigma}{1 - t/m_\sigma^2}$ with the renormalization group invariant product $mn_\sigma = 3.3$ MeV and $g_\sigma(t) = 1.61 + 2.61 \frac{1}{(1 - t/\Lambda_\sigma^2)^{10}}$ with $\Lambda_\sigma = 1.56$ GeV. The on-shell sigma-nucleon coupling is $g_\sigma NN = 27.7$.

Table V-1. Calculated nucleon couplings compared with: contemporary meson exchange model values, where available; experiment in the case of g_A, r_A; a lattice-QCD result for σ. For the VNN couplings the labels "a)" *etc.* identify the results obtained with different *Ansatze* for the vector meson Bethe-Salpeter amplitude; and for g_A and r_A the label b) indicates the inclusion of the a_1-meson's contribution to the dressed-quark-axial-vector vertex.

	Calc.	Estimates	Expt.
$g_{\pi NN}$	14.9	13.4	
$\langle r^2_{\pi NN}\rangle^{1/2}$	a) 0.71 b) 0.80	0.93 – 1.06 fm	
$g_{\rho NN}$	a) 5.92 b) 6.26 c) 4.82	6.4	
$f_{\rho NN}$	a) 15.4 b) 16.6 c) 12.6	13.0	
κ_ρ	a) 2.57 b) 2.64 c) 2.61	2.0	
$g_{\omega NN}$	a) 9.74 b) 10.2 c) 11.5	7 – 10.5	
$f_{\omega NN}$	a) 9.62 b) 10.7 c) 4.39		
κ_ω	a) 0.99 b) 1.04 c) 0.38		
g_A	a) 0.80 b) 0.99		1.259 ± 0.017
$\langle r^2_A\rangle^{1/2}$	a) 0.75 b) 0.75		0.68 ± 0.12 fm
σ/M_N	0.015	0.019 ± 0.05	
g_σ	9.3	10	
$\langle r^2_\sigma\rangle^{1/2}$	0.89	1.2 fm	

a.11. Temperature-Dependence of Pseudoscalar and Scalar Correlations

(C. D. Roberts, S. M. Schmidt, P. Maris,* and P. C. Tandy*)

In order to elucidate hadronic signals of quark-gluon plasma formation we solved the inhomogeneous pseudoscalar and scalar Bethe-Salpeter equations using a renormalization-group-improved rainbow-ladder truncation. The solutions exhibit bound state poles below and above T_c, the critical temperature for chiral symmetry restoration, *i.e.*, the bound states persist into the quark gluon plasma. Above T_c the bound state amplitudes are identical, as are the positions and residues of the pseudoscalar and scalar poles in the vertices, and so these composites are identical in the absence of dynamical chiral symmetry breaking. We found that in the chiral limit the $\pi^0 \to \gamma\gamma$ coupling vanishes at T_c, as do f_π, m_σ and $g_{\sigma\pi\pi}$. Furthermore, for light current-quark masses the 2π decay channel of the isoscalar-scalar meson remains open until very near T_c, and the widths of the dominant pion decay modes remain significant in the vicinity of the crossover. Therefore one cannot expect to identify the quark gluon plasma via a marked increase in the σ-meson lifetime. An article describing this research was submitted for publication.

*Kent State University

a.12. Axial-Vector Diquarks in the Baryon

(C. D. Roberts, S. M. Schmidt, and M. B. Hecht)

We have seen that a product *Ansatz* for the nucleon's Fadde'ev amplitude using only a scalar-diquark provides a very good description of leptonic and nonleptonic couplings and form factors, with some notable exceptions, *e.g.*, $\langle r_n^2 \rangle$ and g_A. We anticipate that the inclusion of axial-vector diquark correlations will significantly improve the description in these exceptional cases. Furthermore, without axial-vector diquark correlations we can't describe the Δ resonance, or the $N \to \Delta$ transition, which is an important probe of hadron structure and models. For example, resonant quadrupole strength in this transition can be interpreted as a signal of nucleon deformation. Hence we are currently working on improving the *Ansatz* by including these qualitatively important correlations.

a.13. J/Ψ Suppression as a Signal of Quark-Gluon Plasma Formation

(C. D. Roberts, S. M. Schmidt, M. B. Hecht, and D. B. Blaschke*)

We have developed a successful approach to describing heavy-meson observables at zero temperature. That makes possible a reliable extrapolation into the domain of nonzero temperature, which is relevant to the program at RHIC. The suppression of the J/Ψ production cross section has been touted as a unique signal for quark-gluon plasma formation, and such a suppression has been observed at CERN. We are studying J/Ψ production in the expectation that additional insight will follow from the Dyson-Schwinger equations' unique capacity to unify nonperturbative aspects of light- and heavy-meson observables via a microscopic description using QCD's elementary excitations. Our goal is to elucidate the mechanisms involved and the fidelity of J/Ψ suppression as a signal of quark gluon plasma formation.

*University of Rostock, Germany

a.14. Pre-equilibrium Signals of Plasma Formation (C. D. Roberts, S. M. Schmidt, and M. B. Hecht)

Nonequilibrium aspects of quark-gluon plasma formation remain an important focus and we aim to connect such pre-equilibrium effects as plasma oscillations and non-Markovian features of the source term with observable signals in the dilepton spectrum. A further improvement is to include a realistic description of quark propagation in the deconfined domain. Although chiral symmetry is restored, as evident in a marked suppression of the scalar piece of the dressed-quark's self energy, nonperturbative effects persist in the vector piece of the self energy. These have important, observable consequences in equilibrium, such as a softening of the equation of state, and may also quantitatively affect the pre-equilibrium phase.

a.15. Dynamical Test of Constituent Quark Models with πN Reactions (T.-S. H Lee, T. Yoshimoto,* T. Sato,* and M. Arima†)

A dynamical approach is developed to predict the πN scattering amplitudes starting with the constituent quark models. The first step is to apply a variational method to solve the three-quark bound state problem. The resulting wave functions are used to calculate the N* → πN, ηN, πΔ vertex functions by assuming that the π and η mesons couple directly to quarks. These vertex functions and the predicted baryon bare masses then define a Hamiltonian for πN reactions. We apply a unitary transformation method to derive from the constructed Hamiltonian a multi-channel and multi-resonance reaction model for predicting the πN scattering amplitudes up to W = 2 GeV. With the parameters constrained by the Δ(1232) excitation, we have shown that the πN scattering in S_{11} channel cannot be described by constituent quark models based on the one-gluon-exchange (OGE) or one-meson-exchange (OME) mechanisms. Our results are shown in Fig. V-2. It is found that the data seem to favor the spin-spin interaction due to one-meson-exchange and the tensor interaction due to one-gluon-exchange. A phenomenological quark-quark potential has been constructed to reproduce the S_{11} amplitude. A paper describing our results has been submitted to Physics Review C.

*Osaka University, Japan., †Osaka City University, Japan

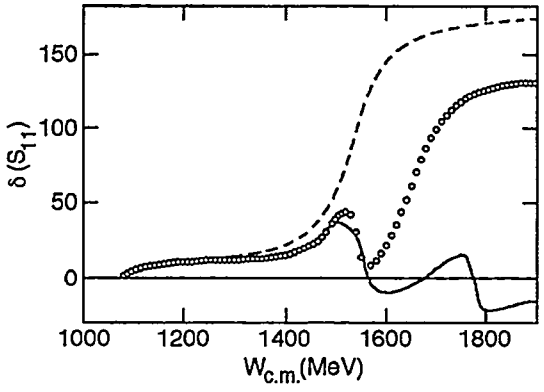

Fig. V-2. Phase shifts of πN scattering in the S_{11} channel. The solid and dashed curves are results from the OGE and OME models, respectively. Open circles are the data.

a.16. Determination of the N–Δ Form Factors with p(e, e′π^0) Reactions

(T.-S. H. Lee and T. Sato*)

The Hamiltonian model developed in Ref. 1 has been extended to investigate pion electroproduction on the nucleon. Guided by the results obtained from our previous study[1] of pion photoproduction, we assume that the strengths $G_M(0)$, $G_E(0)$, $G_C(0)$ of the bare $\gamma N \rightarrow \Delta$ vertex can be related to each other within the constituent quark model. For $G_M(0)$ = 1.85(1.95), $G_E(0)$ = 0.025(–0.025) determined in Ref. 1, we obtain $G_C(0)$ = -0.2241(0.2195). The only freedom in our calculations is the Q^2–dependence of the N–Δ form factors. In a first attempt, we have found that all of the available p(e, e′π^0) data can be described to a very large extent if we assume that the bare N–Δ form factor has the Q^2–dependence

$$F_{N\text{-}\Delta}(Q^2) = \left[1 + Q^2/4M_{ave}^2\right]^{1/2}\left[1 + Q^2/4\Lambda^2\right]^{-1} G_E^p(Q^2),$$

where $M_{ave} = (m_N + m_\Delta)/2$, $G_E^p(Q^2)$ is the usual proton electric form factor and Λ = 1.2 GeV. Some sample results are compared in Fig. V-3 with the recent data[2] at Q^2 = 2.7 $(GeV/c)^2$ from Jefferson Laboratory. More detailed results will be presented to give a more sophisticated quark model interpretation of the determined bare N–Δ form factors.

*Osaka University, Japan

[1]T. Sato and T.-S. H. Lee, Phys. Rev. C **54**, 2660 (1996)
[2]V. V. Frolov, *et. al.*, Phys. Rev. Lett. **82**, 45 (1998)

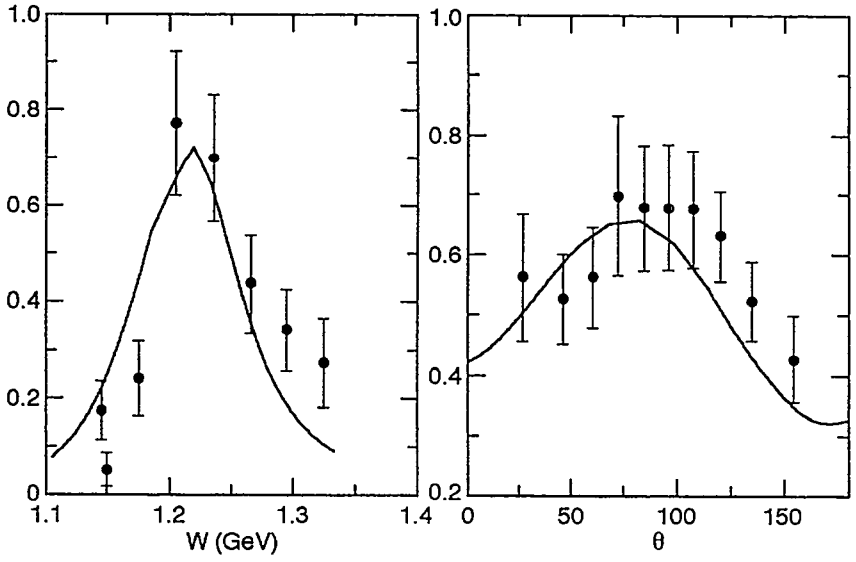

Fig. V-3. Differential cross section of p(e, e′π^0) at Q^2 =2.78 $(GeV/c)^2$.

a.17. Structure of the Vector Meson Photoproduction Amplitude at a Few GeV

(T.-S. H. Lee, A. I. Titov*, and H. Toki†)

The structure of the ϕ photoproduction amplitude in the $\sqrt{s}$~ 2-5 GeV region is analyzed based on Pomeron-exchange and meson-exchange mechanisms. The SU(3) symmetry and the ϕ decay widths are exploited to determine the parameters that are needed to predict the amplitudes due to pseudoscalar meson (π^0,η) exchange, scalar meson (σ, a_0, f_0) exchange, and the ϕ-radiation from the nucleon. In addition to the universally accepted Pomeron exchange with an intercept $\alpha(0)$ ~ 1.08, we investigate the role of a second Pomeron with $\alpha(0) < 0$, as inspired by the glueball ($J^{\pi} = 0^+$, M_b^2 ~ 3 GeV^2) predicted by Lattice QCD calculations and the Dual Landau-Ginsburg model. It is found that the existing limited data at low energies near threshold can accommodate either the second Pomeron or the scalar meson exchange. The differences between these two competing mechanisms are shown to have profound effects on various density matrices which can be used to calculate the cross sections as well as various single- and double-polarization observables. We predict a definite isotopic effect: polarization observables of ϕ photoproduction on the proton and neutron targets can have differences of a factor 2 and more. Two papers describing our results have been published[1,2].

*JINR, Dubna, Russia, †Osaka University, Japan

[1]A. I. Titov, T.-S. H. Lee, H. Toki, and O. Streltrslva, Phys. Rev. C **60**, 035205 (1999)
[2]A. I. Titov, T.-S. H. Lee, and H. Toki, Phys. Rev. C **59**, R2993 (1999)

a.18. Evidence for the Fourth P_{11} Resonance Predicted by the Constituent Quark Model

(T.-S. H. Lee, Simon Capstick,* W. Roberts,† A. Svarc‡)

It is pointed out that the third of five low-lying P_{11} states predicted by a constituent quark model can be identified with the third of four states in a solution from a three-channel analysis of πN scattering amplitudes. This is one of the so-called "missing" resonances, predicted at 1880 MeV. The fit to the $\pi N \rightarrow \eta N$ data is the crucial element in finding this fourth resonance in the P_{11} partial wave. A paper describing our results has been published[1].

*Florida State University, †National Science Foundation, ‡Rudjer Boskovic Institute, Croatia.

[1]T.-S. H. Lee, Simon Capstick, W. Roberts and A. Svarc, Phys. Rev. C **59**, R3002 (1999)

a.19. Strange Hadron Matter and SU(3) Symmetry

(T.-S. H. Lee and V. G. J. Stoks*)

We calculate saturation curves for strange hadron matter using the SU(3) baryon-baryon potentials of Ref. 1. All possible interaction channels within the baryon octet (consisting of N, Λ, Σ, and Ξ) are considered. It is found that a small Λ fraction in nuclear matter slightly increases binding, but that larger fractions (>10%) rapidly cause a decrease. Charge-neutral N, Λ, Ξ systems, with equal densities for nucleons and cascades, are only very weakly bound. The dependence of the binding energies on the strangeness per baryon, f_S, is predicted for various N, Λ, Ξ and N, Λ, Σ, Ξ systems. The implications of our results in relativistic heavy-ion collisions and the core of a dense star are discussed. We also discuss the differences between our results and previous hadron matter calculations. A paper describing our results has been published[2].

*University of Adelaide, Australia

[1]V. G. J. Stoks and Th. A. Rijken, Phys. Rev. C **59**, 21 (1999)
[2]V. G. J. Stoks and T.-S. H. Lee, Phys. Rev. C **60**, 024006 (1999)

a.20. Study of Hyperon-Nucleon Interactions with d(e,e'K) Reactions

(T.-S. H. Lee, P. Oswald,* and B. Saghai*)

The d(e,e' K^+) reaction has been investigated by using the kaon production amplitudes developed by the Saclay-Lyon collaboration. Our focus is on the dependence of the reaction cross sections on the final hyperon-nucleon interactions, aiming at testing the SU(3) models of baryon-baryon potentials. To fix the $\gamma N \rightarrow KY$ amplitude, we are refining the Saclay-Lyon amplitudes to fit the new data from TJNAF and extending the model to also account for kaon production on the neutron.

*CEA-Saclay, France

a.21. Particle-Hole Folded-Diagram Calculation of the Hypernucleus $^{16}_{\Lambda}O$ Using Meson-Exchange Interactions

(T.-S. H. Lee, Yiharn Tzeng,* S. Y. Tsay Tzeng,† and T. T. S. Kuo‡)

The $^{16}_{\Lambda}O$ hypernucleus is investigated by way of a folded-diagram method. The input G-matrix elements are calculated accurately from the Jülich-$\overline{B}$ and the Nijmegen realistic hyperon-nucleon potentials with the Pauli exclusion operator properly treated in the finite hypernuclear system. The effect of hyperon-nucleon-nucleon three-body forces is included through the consideration of core polarization diagrams. Although our predicted energy spectrum of the hypernucleus is in good agreement with experiments in general, there are significant differences between the positive parity energy levels obtained from these two realistic potentials. A folded-diagram calculation for the Λ single-particle energy has been performed. The spin-dependence parameters of Millener *et al.* calculated from the Jülich-$\overline{B}$ and Nijmegen potentials are significantly different from each other, and the contribution from the Λ–Σ three-body force to these parameters is important. A paper describing our results has been published[1].

*Academia Sinica, Taiwan, †National Taipei University of Technology, Taiwan, ‡SUNY, Stony Brook
[1]T.-S. H. Lee, Yiharn Tzeng, S. Y. Tsay Tzeng, and T. T. S. Kuo, Phys. Rev. C **60**, 044305 (1999)

a.22. Two-frequency Shell Model for Hypernuclei

(T.-S. H. Lee, T. T. S . Kuo,* and Y. Tzeng†)

A two-frequency shell model is proposed for investigating the structure of hypernuclei starting with a hyperon-nucleon potential in free space. In a calculation for $^{16}_{\Lambda}O$ using the folded-diagram method, the applicability of the model is demonstrated by showing that the predicted Λ single-particle energies have saturation minima at an oscillator frequency $\hbar\omega_\Lambda$ ~ 10 MeV, which is considerably smaller than $\hbar\omega_N$ =14 MeV for the nucleon orbits. A fairly strong dependence on $\hbar\omega_\Lambda$ has also been observed for the calculated Λ particle-nucleon hole interactions. The model has been applied to demonstrate that the ΛNN three-body force induced by the $\Lambda N \leftrightarrow \Sigma N$ transitions can significantly change the predicted spectrum. A paper describing our results has been published[1].

*SUNY at Stonybrook, †Academia Sinica, Taiwan
[1]T.-S. H. Lee, T. T. S. Kuo, and Y. Tzeng, Phys. Rev. C **61**, 031305 (2000)

a.23. Effect of Neutron Excess on Δ Excitations in Exotic Nuclei (T.-S. H. Lee, Mahmoud A. Hasan,* and James P. Vary†)

The effects of neutron excess on the formation of Δ(3,3) resonance states in exotic nuclei at equilibrium and under large amplitude compression have been investigated within the radial constraint spherical Hartree-Fock method. An effective Hamiltonian has been used which includes the Δ degree of freedom explicitly. Results are presented for ^{28}O, ^{60}Ca, and ^{70}Ca in a model space of seven major oscillator shells and eight Δ orbitals. The results show that the formation of the Δ's depends strongly on the amount of neutron excess in the nuclear system. In contrast to previous work where we found no Δ's in ^{16}O and ^{40}Ca at equilibrium, these results show that a significant amount of Δ's exists at equilibrium in exotic isotopes. In addition, as the nucleus is compressed to a density of 2.5 times the ordinary nuclear density, the percentage of the Δ's rises to 3%, 5%, and 7% of the total number of all baryons in ^{28}O, ^{60}Ca, and ^{70}Ca, respectively. This suggests a parameterization for the percentage of the Δ's created at 2.5 times the normal density of the form 0.25 (N–Z)%. The results are consistent with the theoretical prediction of the formation of Δ matter in neutron-rich matter at high compression. A paper describing our results has been published[1].

*Applied Science University, Jordan, †Iowa State University, Ames

[1]T.-S. H. Lee, Mahmoud A. Hasan, and James P. Vary, Phys. Rev. C **61**, 014301-1 (2000)

a.24. Quantum Monte Carlo Calculations of Pion Inelastic Scattering from Li (T.-S. H. Lee and R. B. Wiringa)

Quantum Monte Carlo methods have been successfully developed to predict the properties of low-lying states of light nuclei starting with realistic two- and three-nucleon potentials. The predicted proton transition densities were found to be in good agreement with the (e,e′) data both in shape and absolute magnitude. By carrying out the Distorted-Wave-Impulse-Approximation calculations of pion inelastic scattering from Li in the Δ region, we have found that the predicted neutron excitations are also in good agreement with the data. The large enhancement factors (about 2) for quadrupole excitations within the conventional shell-model are not needed in this calculation. This has resolved one of the long-standing structure problems encountered in the studies of pion-nucleus reactions. Our results are compared with the data in Fig. V-4 for ^{7}Li. Calculations for Be are now in progress.

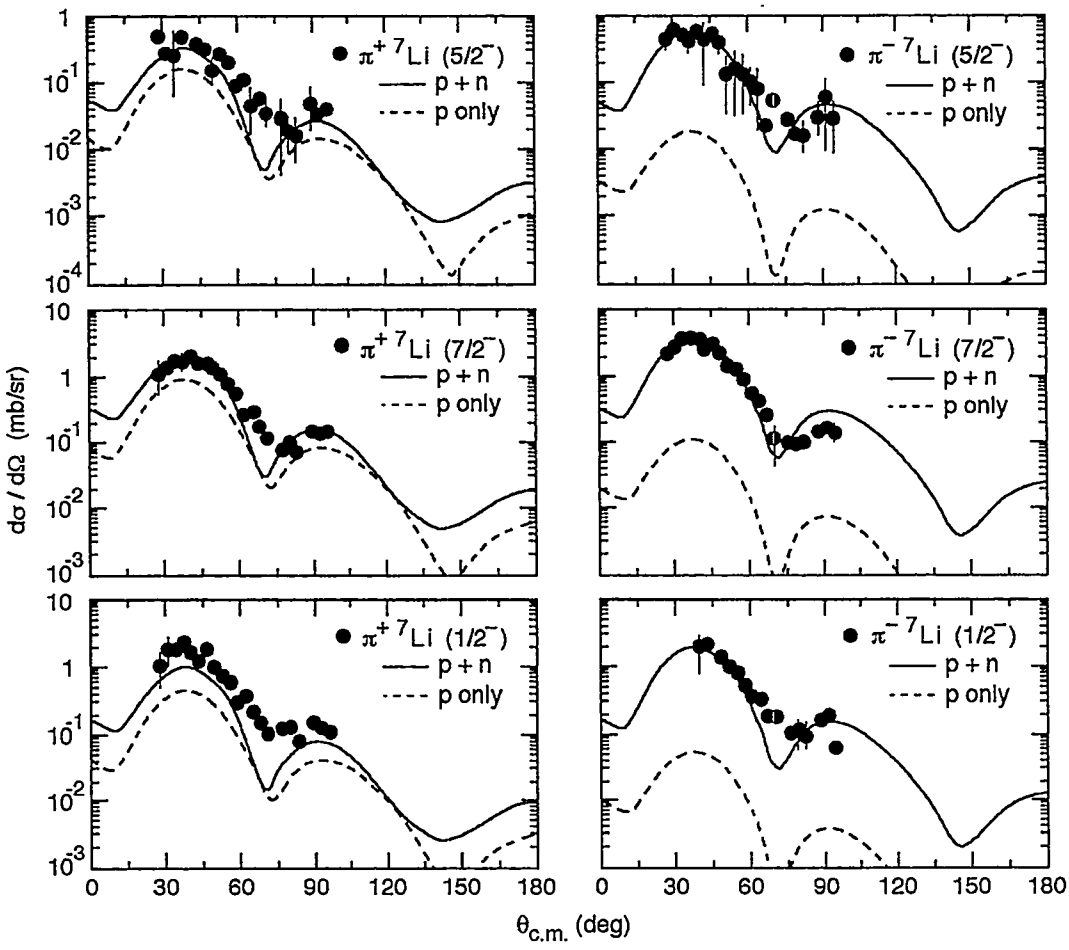

Fig. V-4. The differential cross section for ^{7}Li(π,π').

a.25. On "Ambiguities" of Spin-1 Form Factors in Null-Plane Dynamics
(F. Coester)

It is an inescapable feature of relativistic Hamiltonian dynamics that single-particle current density operators are covariant only under the kinematic subgroup. In practice the interaction dependence of fully covariant current matrices is obtained by transforming a subset of single-particle current matrix elements with the dynamic Poincaré representations. This process invariably involves physically motivated choices, specifically the choice of the kinematically-invariant hypersurface in relation to relevant four-vectors of the system. With null-plane dynamics the kinematic subgroup is determined by a null-vector, which for spin-1 systems can be related to three mutually orthogonal four-vectors: the four-momentum transfer Q, the projection $\tilde{P}$ of the four-momentum operator orthogonal to Q, and the transverse polarization four-vector $S_\perp$. In most applications the null-vector has been chosen orthogonal to Q. This choice has the virtue that $Q^2 = Q_\perp^2$ is a kinematic quantity independent of the masses. Subject to this constraint the null-vector can be any linear combination of $\tilde{P}$, $S_\perp$, and the unit vector perpendicular to both, as well as to Q. Different authors have used different prescriptions corresponding to different angles between the null-vector and $S_\perp$.[1] The matrix elements that determine the form factors also involve the longitudinal polarization vectors $S_{||}$ and $S'_{||}$ that are orthogonal to the initial and final four-momenta respectively. Only when the null-vector is perpendicular to the transverse polarization vector can the longitudinal polarization vectors be independent of the initial and final masses. This choice has the unique advantage that the current construction is equally applicable to inelastic transitions. The prescription resulting in this way is identical to that obtained by Karmanov treating the orientation of the null vector as an unphysical degree of freedom.[2,3]

[1] V.A. Karmanov, Nucl. Phys A **608**, 316 (1996)
[2] J. Carbonell *et al.*, Physics Reports **360**, 216 (1998)
[3] F. Coester, W. H. Klink, and W. N Polyzou Few Body Systems Supp. **10**, 115 (1999)

a.26. Poincaré Compliance of Standard Nuclear Dynamics[1] (F. Coester, W. H. Klink,* and W. N. Polyzou*)

Standard Hamiltonian nuclear dynamics[1] is a mathematically consistent framework for the quantitative description of nuclei. The form of the two-nucleon Hamiltonian is suggested by quantum field theory while the quantitative details are adjusted to fit a vast array of available two-nucleon data. Much smaller three-body forces are similarly determined. Assuming that higher-order multi-nucleon forces are negligible the Hamiltonian is then completely determined for any nucleon number. Conserved electromagnetic currents consistent with these nuclear forces are available.[2] Detailed numerical work has produced remarkable agreement with many data. Calculations of binding energies and energy levels of light nuclei are accurate to about 1% so that larger discrepancies with data can be attributed to an inadequacy of the Hamiltonian.

There is a possible objection of principle in that the standard nuclear dynamics does not respect the fundamental space time symmetry of the inhomogeneous Lorentz group (Poincaré group).[3] Crude estimates of "relativistic effects" suggest that they might be as large as 10%. In this context it is important to separate requirements suggested by features of relativistic quantum field theory from the space-time symmetry requirements. Standard nuclear dynamics is Galilei covariant. The question addressed here is what modification of the dynamics is required

*University of Iowa
[1] F. Coester, Symposium on Current Topics in the Field of Light Nuclei, Cracaow, (1999) p. 1000
[2] J. Carlson and R. Schiavilla, Rev. Mod. Phys. **70**, 743 (1009)
[3] S. Weinberg, Quantum Theory of Fields, Vol. **1**, Chapter 2
[4] F. Coester, Helv. Phys. Acta **38**, 7 (1965)
[5] B. D. Keister and W. N. Polyzou, Advances in Nuclear Physics, Vol. **20** p. 225 Sec. 3 (1991)

to achieve "Poincaré compliance", that is Poincaré covariance and cluster separability of the observables.[4] The answer depends on a comparison of the relevant irreducible unitary (projective) representations of the two groups.[3,5] For both groups the little group is SU(2). The Casimir operators of both groups are the square of the spin and the Casimir Hamiltonians related to the mass (rest energy) of the system. The Poincaré-Casimir Hamiltonian h of an A-nucleon system can be defined as a function of the mass operator M and the nucleon mass m by $h := (M^2 - A^2m^2)/2Am$. The operator h so defined has the same continuous spectrum including degeneracies as the Galilean Casimir Hamiltonian $h_{NR} := H - \vec{P}^2/2Am$. Thresholds and the point spectra (binding energies) differ by less than 1%. While covariants transform differently under the two groups the invariants are effectively identical. Dynamically-determined wave functions are not observable. Covariant observables, S-matrix elements and matrix elements of currents, are related to the invariants kinematically.

The realization of S-matrix cluster separability for more than 2 nucleons involve the Clebsch-Gordan and Racah coefficients, which differ for the two groups. For three nucleons it follows from properties of the Galilei and Poincaré Clebsch-Gordan coefficients that no adjustment of standard nuclear Hamiltonians is required to achieve Poincaré compliance. We expect that the required multi-nucleon forces for larger systems will be negligible.

We conclude that while it is essential to relate dynamically determined invariants to covariant observables by relativistic kinematics, Poincaré compliance at the 1% level does not require adjustments of standard nuclear Hamiltonians for two and three nucleons. We expect this result to hold for more nucleons as well.

B. NUCLEAR FORCES AND NUCLEAR SYSTEMS

The goal of this program is to achieve a description of nuclear systems ranging in size from the deuteron and triton to nuclear matter and neutron stars using a single parameterization of the nuclear forces. Aspects of our program include both the construction of two- and three-nucleon potentials and the development of many-body techniques for computing nuclear properties with these interactions. Detailed quantitative, computationally-intensive studies are essential parts of this program.

Quantum Monte Carlo (QMC) calculations of light ($A \leq 9$) nuclei with realistic interactions have been the main focus of our recent efforts. Our nonrelativistic Hamiltonian contains the accurate Argonne v_{18} two-nucleon (NN) potential, which includes charge-independence-breaking terms, and either the venerable Urbana IX three-nucleon (3N) potential, or one of several new Illinois 3N models. The QMC calculations include both variational (VMC) and Green's function (GFMC) methods. We begin with the construction of variational trial functions based on sums of single-particle determinants with the correct total $J^{\pi}T$ quantum numbers, and then act on them with products of two- and three-body correlation operators. Energy expectation values are evaluated with Metropolis Monte Carlo integration and parameters in the trial functions are varied to minimize the energy. These optimized variational wave functions then can be used to study other nuclear properties. They also serve as a starting point for the GFMC calculations, which systematically remove higher excited-state components from the trial wave functions by a propagation in imaginary time.

We are currently studying all $A \leq 9$ nuclei with experimentally known bound state or resonance energies, including some 50 (25) excited states in VMC (GFMC). These are the first and only calculations treating $A \geq 6$ nuclei directly with realistic NN and 3N interactions. In GFMC calculations, with the new Illinois 3N models, we can reproduce most of the experimental ground- and excited-state energies within 0.5 MeV. The VMC calculations, including two-body charge and current operators, are being used to study weak decays of A=6–8 nuclei and for various (e,e'p) and (e,e'n) reactions. They are also being used to obtain astrophysically

interesting cross sections, starting with the reaction ^{4}He(d,γ)^{6}Li. Finally, we are also studying the properties of neutron drops with the goal of providing additional constraints for the construction of Skyrme interactions that are used in the modeling of neutron-rich nuclei in neutron star crusts.

Studies of hypernuclei are also continuing. This year, we made major revisions to our calculations of Λ single-particle energies in matter, including density-dependent effective ΛN and ΛNN interactions. We also continue to examine the effect of Λ-induced distortion of nuclear cores in light hypernuclei.

b.1. Variational Monte Carlo Calculations of Light p-shell Nuclei

(R. B. Wiringa, S. C. Pieper, K. Varga, V. R. Pandharipande,* and J. Carlson†)

We have completed a major study of A = 8 nuclei, and initiated the first calculations for A = 9 nuclei. These calculations use the realistic Argonne v_{18} two-nucleon and Urbana IX three-nucleon potentials. The variational wave functions, $\Psi^V(\mathbf{R})$, obtained in these calculations are used as input to the more precise Green's function Monte Carlo (GFMC) calculations described below, and are also being used to study electron scattering and low-energy electroweak reactions of these nuclei. A major paper on the A = 8 calculations was recently accepted for publication.[1]

Construction of the variational trial function starts with a Jastrow core that includes single-particle orbitals LS-coupled to the desired JM values, as well as pair and triplet spatial correlations. This Jastrow core is then acted on by products of two-body spin, isospin, tensor, and spin-orbit correlation operators and three-body correlation operators for the 3N interaction. The wave functions are diagonalized in the small basis of different Jastrow spatial symmetry components to project out higher excited states with the same quantum numbers as the ground or first excited states.

To date we have made calculations for the ground states of all the A = 6–9 nuclei, and for 50 different excited states (not counting isobaric analogs); some recent results are shown in Table IV-2. The binding energies of the ground states are 3–10 MeV high compared to the final GFMC results. However, the excited state energies are in generally good agreement with those GFMC excitations (compared to their respective ground states) that have been calculated. Compared to experiment, these states generally occur in the correct order and with reasonable excitation energies. We have also computed all the isobaric analog multiplets to extract the isovector and isotensor energy differences, and we have calculated the isospin-mixing matrix elements in ^{8}Be excited states.

Current efforts focus on the search for low-lying even-parity intruder states in the A = 9 nuclei, and on the construction of improved variational wave functions that build in cluster substructure and have better asymptotic properties. For example, the present ^{8}B wave function treats all four p-shell nucleons equally, but there should be an asymptotic ^{7}Be + p behavior, with ^{7}Be itself having a significant α+τ cluster substructure. This behavior will be important in determining aspects of the proton halo, and in studying important reactions of astrophysical interest. Similar considerations will be even more important in the A = 9,10 nuclei.

*University of Illinois at Urbana-Champaign, †Los Alamos National Laboratory.

[1]R. B. Wiringa, S. C. Pieper, J. Carlson, and V. R. Pandharipande, Phys. Rev. C, to be published.

Table V-2. VMC and GFMC excitation energies (in MeV) computed with the Argonne v_{18} + Urbana IX interaction compared to the experimental spectrum for A = 8 nuclei.

$^{A}Z(J^{\pi};T)$	VMC	GFMC	Experiment
$^{8}He(2^{+};2)$	2.22(16)	3.01(23)	3.59
$^{8}He(1^{+};2)$	3.32(17)	4.42(25)	
$^{8}He(2^{+};2)$	4.72(18)		
$^{8}He(0^{+};2)$	5.01(17)		
$^{8}Li(1^{+};1)$	1.34(18)	1.03(27)	0.98
$^{8}Li(0^{+};1)$	2.83(19)	1.82(29)	
$^{8}Li(3^{+};1)$	3.35(18)	3.19(28)	2.26
$^{8}Li(2^{+};1)$	3.86(18)		
$^{8}Li(1^{+};1)$	4.22(19)		3.21
$^{8}Li(1^{+};1)$	5.32(19)		5.4
$^{8}Li(4^{+};1)$	6.08(18)	6.88(27)	6.53
$^{8}Li(2^{+};1)$	6.20(18)		
$^{8}Li(3^{+};1)$	7.31(18)		
$^{8}Li(0^{+};2)$	11.24(18)	12.10(25)	10.82
$^{8}Be(2^{+};0)$	2.39(25)	2.91(25)	3.04
$^{8}Be(4^{+};0)$	9.95(24)	9.58(27)	11.4
$^{8}Be(2^{+};1)$	18.60(23)	18.02(27)	16.63*
$^{8}Be(2^{+};0)$	20.29(24)		16.92*
$^{8}Be(1^{+};1)$	19.89(23)		17.64
$^{8}Be(1^{+};0)$	20.03(23)	18.09(33)	18.15
$^{8}Be(1^{+};0)$	21.73(24)		
$^{8}Be(3^{+};1)$	21.77(22)		19.07
$^{8}Be(3^{+};0)$	21.85(24)	19.53(33)	19.24
$^{8}Be(4^{+};0)$	25.85(22)		19.86
$^{8}Be(2^{+};0)$	23.61(23)		20.1
$^{8}Be(3^{+};0)$	25.53(23)		
$^{8}Be(0^{+};0)$	28.62(26)		20.2
$^{8}Be(0^{+};2)$	29.55(22)	29.93(25)	27.49

b.2. Green's Function Monte Carlo Calculations of Light p-shell Nuclei

(S. C. Pieper, R. Roncaglia, R. B. Wiringa, J. Carlson,* and V. R. Pandharipande†)

In the 1980's, the ground states of ^{2}H, ^{3}H, ^{3}He, and ^{4}He, and the low-energy scattering states of ^{5}He were studied with Hamiltonians of the form described in the previous section in an essentially exact fashion (limited only by statistical errors) by using the Green's function Monte Carlo (GFMC) method. Our work in the last few years has focused on extending these calculations to light p-shell nuclei and their excited states. These are the first calculations of the structure of such nuclei with realistic many-nucleon Hamiltonians and thus they also test the range of applicability of such Hamiltonians.

In the GFMC calculations, we operate on a trial wave function with the imaginary time propagator, $\exp[-(H'-E_0)\tau]$, where H' is a simplified Hamiltonian, E_0 is an estimate of the eigenvalue, and τ is the imaginary time. To save computer time, the trial wave function is a simplified form of the variational wave functions described in the previous section. The excited-state components of the trial wave function will then be damped out for large τ, leaving the exact lowest eigenfunction with the quantum numbers of the input variational wave function. The expectation value of H is computed for a sequence of increasing values of τ to determine the convergence. Our H' contains the reprojected v_8' part of the NN potential and full 3N potential. The small correction H-H' is computed perturbatively. The many-body propagator is written as a symmetrized product of exact two-body propagators, with the 3N potential treated in lowest order.

GFMC calculations for fermion systems suffer from the well-known sign problem in which the statistical error grows exponentially with imaginary time; in our original calculations, this effectively limited τ to 0.06 MeV^{-1}, which means that components of the trial wave function with excitation energies less than ~10 MeV were not appreciably damped out. In the last two years, we have solved this problem for nuclei by using "constrained path propagation". In this approach, configurations whose overlap with the trial wave function is small or negative are discarded with a probability such that the average overlap for the discarded configurations is zero. This procedure may not result in an upper bound, but for the very few cases in which it introduces a significant error, a few unconstrained steps result in reliable expectation values. With this method there is no sign problem and we can propagate to arbitrarily large τ. This year we have also realized that a symmetry of the even–A nuclei allows us to save almost 50 percent of the computer time in these cases.

The computer resources (both CPU time and memory) required by our present GFMC method increase exponentially with the number of nucleons. At present calculations of up to A=8 nuclei can be routinely made with propagation to τ = .2 MeV and we are beginning to explore A = 9; in the next few years we might be able to reach A=12. However using the present method for larger nuclei will not be practical. To overcome this limit we started work on a cluster-expansion GFMC method. This method, and the computer program, is based on our cluster VMC calculation of ^{16}O that was made a few years ago. In the cluster VMC, expectation values are expanded in terms corresponding to the number of nucleons whose spin and isospin degrees of freedom are active. The complete Jastrow wave function is used in every order of the expansion and thus all integrations are 3A-dimensional. To extend the method to GFMC, one writes the GFMC mixed estimate for a given τ as an N×3A dimensional integral where N is the number of time slices used to reach τ, and then makes the spin- and isospin-cluster expansion of this entire expectation value. Preliminary results obtained for ^{16}O and the Argonne v_8' potential using four-body clusters contained large statistical fluctuations. Alternate Monte Carlo sampling methods were tried with inconclusive results.

*Los Alamos National Laboratory; †University of Illinois, Urbana

b.3. Studies of Three-Nucleon Interactions in Nuclear Systems (S. C. Pieper, R. B. Wiringa, V. R. Pandharipande*, D. G. Ravenhall,* and J. Carlson†)

We have made GFMC calculations of the energies of 25 states for nuclei with $3 \leq A \leq 8$ using the Hamiltonian consisting of the Argonne v_{18} NN and Urbana IX 3N potentials. These calculations have shown that this Hamiltonian underbinds p-shell nuclei by 0.8 MeV in ^{6}Li to 5 MeV in ^{8}He. The error increases with both A and |N-Z|. However, with the exception of some underpredicting of the spin-orbit splittings, the excitation spectra of the nuclei are reasonably well reproduced. The rms error for the 10 ground states is 2.3 MeV and for the 15 excitation energies is 0.5 MeV; with no 3N potential at all these numbers are 7.3 and 0.5 MeV, respectively.

These results show that the simple Urbana 3N potentials, which have been used successfully for more than a decade in studies of s-shell nuclei and dense matter, need to be extended for work in the p-shell. In the last few years, we have been constructing improved "Illinois" models for the 3N potential. Our approach is to use theoretical guidance to suggest the structure of new terms, but to consider the coupling constants and short-range shapes of the potential to be adjustable. This is in the same spirit as the development of realistic NN potentials. We have considered a number of new terms. We find that new potential terms are often not perturbative, *i.e.*, an expectation value of the new term using the GFMC wave function from just Argonne v_{18} and Urbana IX may be misleading. Thus each new term must be added to the GFMC propagator and a new GFMC calculation made. Furthermore, as the strength of the new term is adjusted, the propagations must be repeated.

The dominant term of the Urbana potential is the Fujita-Miyazawa (FM) two-pion term with intermediate excitation of one nucleon to a Δ. We have now studied three-pion ring terms containing one and two Δ excitations. These are repulsive in s-shell nuclei and attractive in p-shell nuclei and correct the overall loss of binding energy with respect to both A and |N-Z|. The Tucson-Melbourne potential contains the FM term and a term arising from s-wave πN scattering; we have also considered a corrected s-wave term.

The FM terms in the Urbana 3N potentials and the new models that we first constructed have coupling constants that are about 1/2 the value suggested by soft pion physics. We have also made a model that has the stronger coupling constant; this required a significantly softer cutoff parameter (normally we use the same cutoff as is used in the NN potential). We find that we can obtain excellent fits to the $3 \leq A \leq 8$ binding energies with either class of 3N potential – the rms errors are $\leq$ 500 keV. However the strong coupling constant seems to result in a pion-condensed phase of nuclear matter at much too low a density. We are continuing to investigate this. Figure V-5 compares GFMC values of ground and excited state energies for Urbana IX and one of the new Illinois models to experimental values.

*University of Illinois, Urbana, †Los Alamos National Laboratory

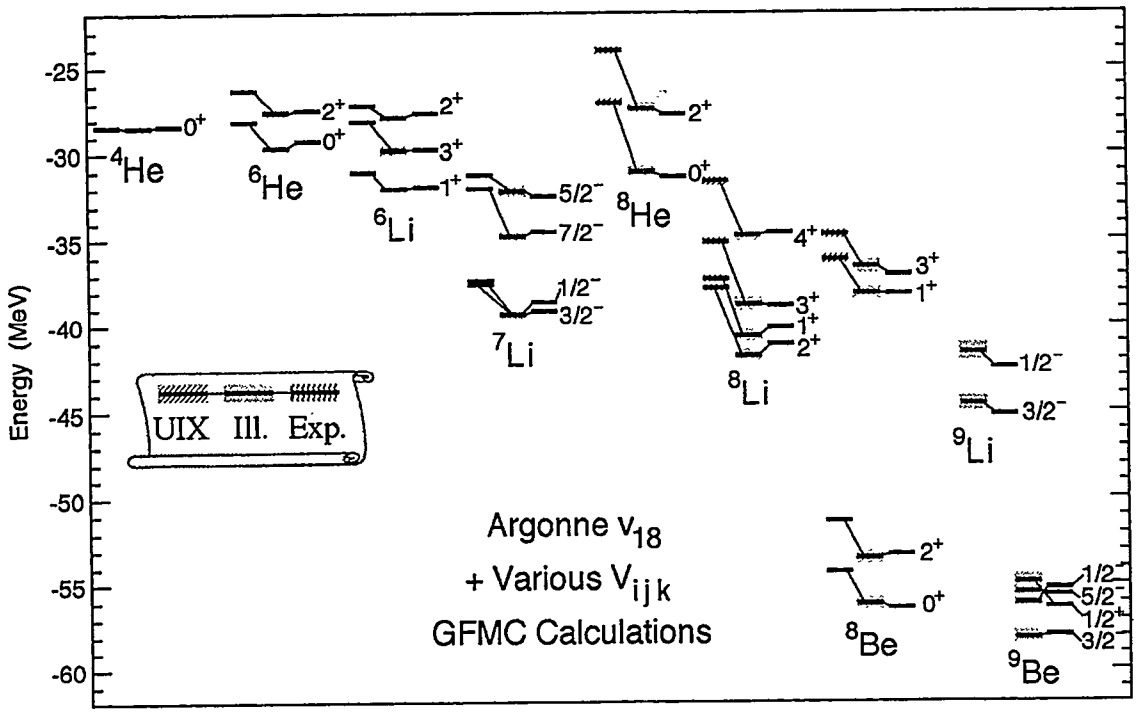

Fig. V-5. GFMC energies for A=4-9 nuclei using the Argonne v_{18} NN potential with either the Urbana IX or one of several new Illinois 3N potentials, compared to experiment.

b.4. Nuclear Structure Studies with (e,e'p) and (e,e'n) Reactions (R. B. Wiringa, L. Lapikás*, and J. Wesseling*)

In previous years we have calculated single-nucleon momentum distributions in many of the A ≤ 8 nuclei and a variety of cluster-cluster overlap wave functions, such as ⟨dpl^{3}He⟩, ⟨ddl^{4}He⟩, and ⟨αdl^{6}Li⟩. More recently we have begun studying overlaps such as ⟨^{6}He + pl^{7}Li⟩ and ⟨^{6}Li + nl^{7}Li⟩. These overlaps can be used to predict the results of exclusive (e,e'p) and (e,e'n) measurements and various pickup or stripping reactions. The spectroscopic factors obtained from these overlaps can be significantly different from the predictions of conventional shell models like that of Cohen and Kurath.

A recent test of these predictions is shown in Fig. V-6, where the ⟨^{6}He+pl^{7}Li⟩overlaps were used in a Coulomb distorted wave impulse approximation (CDWIA) analysis of previously unpublished ^{7}Li(e,e'p)^{6}He experiments performed at NIKHEF. Lapikás and Wesseling obtained spectroscopic factors to the 0^+ ground state of ^{6}He of 0.42(4) and to the 2^+ first excited state of 0.16(2), in excellent agreement with our predictions of 0.41 and 0.18, respectively. A letter reporting these results was recently published[1].

In contrast to the proton knockout, we predict there should be significantly less quenching in the ^{7}Li(e,e'n)^{6}Li reaction. We have provided our overlaps to an experimental group at MIT, and they are currently studying the feasibility of such an experiment with the new BLAST detector. We have also carried out initial calculations of overlaps in ^{9}Be, which is the next stable target above ^{7}Li, and we have predicted spectroscopic factors involving ^{7}He, which is being developed as a radioactive beam at ATLAS.

*NIKHEF

[1] L. Lapikás, J. Wesseling, and R. B. Wiringa, Phys. Rev. Lett. **82**, 4404 (1999).

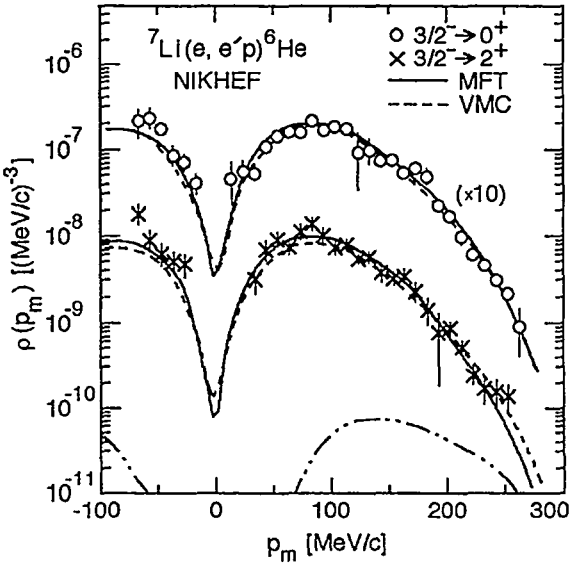

Fig. V-6. Experimental momentum distributions for the transitions to the ground state (circles) and first excited state (crosses) in the reaction ^{7}Li(e,e'p)^{6}He, compared to DCWIA calculations with meanfield (MFT) and variational (VMC) wave functions.

b.5. Radiative Capture Reactions for Astrophysical Applications (R. B. Wiringa and K. Nollett*)

Radiative capture reactions play a major role in many astrophysical processes, including primordial nucleosynthesis and stellar evolution. We are using the many-body quantum Monte Carlo wave functions discussed above to study radiative capture reactions involving light p-shell nuclei. Our first project is to obtain the low-energy cross section for ^{4}He(d,γ)^{6}Li. This reaction is the primary source of ^{6}Li in the big bang. The dominant nuclei synthesized in the big bang are ^{2}H, ^{3}He, ^{4}He, and ^{7}Li. Trace amounts of ^{6}Li should also have been made, although a primordial abundance has not yet been unambiguously identified in astronomical observations. The cross section at keV energies is sufficiently small that laboratory experiments have only established an upper bound, which could be orders of magnitude too high.

Our QMC wave functions are good for bound states, but are not as well developed for scattering states. Hence, we evaluate the appropriate electromagnetic matrix elements (primarily E2, E1, and M1) between a ^{6}Li ground state and a correlated α–d pair, which is then folded with a continuum α–d wave function obtained from a suitable optical potential. One of the interesting challenges has been to find ways of Monte Carlo sampling in the tail of the ^{6}Li ground state where most of the capture reaction will take place. We have also developed an improved variational wave function for ^{6}Li that at long range has the form of α and d clusters with the empirical separation energy. At present, we are able to reproduce the observed E2 cross section from the 3^+ resonance at 0.7 MeV to beyond 3 MeV, but our E1 cross section in the same regime, which is an order of magnitude smaller, is two times too large compared to experiment, although the experimental data has sizeable error bars. At the capture energies of interest for primordial nucleosynthesis, the E1 and E2 contributions are about equal.

We also expect to study a number of other interesting radiative capture reactions such as ^{4}He(^{3}H,γ)^{7}Li and ^{4}He(^{3}He,γ)^{7}Be, which also play an important role in primordial nucleosynthesis, and for which the experimental uncertainties are ~30%. A good warm-up exercise for these calculations will be the thermal neutron capture reactions ^{6}Li(n,γ)^{7}Li and ^{7}Li(n,γ)^{8}Li, which should provide a good test of our many-body wave functions, and for which good experimental data is available.

*University of Chicago

b.6. Microscopic Calculation of A = 6–8 Weak Decays (R. B. Wiringa and R. Schiavilla*)

Initial variational Monte Carlo calculations were made for the weak decays of ^{6}He, ^{7}Be, ^{8}He, ^{8}Li, and ^{8}B. The variational wave functions were obtained for our standard Hamiltonian containing the Argonne v_{18} two-nucleon potential and the Urbana IX three-nucleon potential. Consistent two-body axial current operators tuned to reproduce ^{3}H β-decay are included in the evaluations.

Our calculated Gamov-Teller (GT) matrix element for ^{6}He(β^-)^{6}Li is too large by 5%, while those for ^{7}Be(ε)^{7}Li and ^{7}Be(ε)^{7}Li* are 5% too low, compared to experiment. The two-body axial current contributes only a 1% increase in A=6 and 3% in A = 7. The branching ratio ^{7}Li*/^{7}Li is 10.2% compared to the experimental 10.5%. We are currently studying the sensitivity of these results to changes in the variational wave function, and plan to evaluate mixed estimates with the more precise GFMC wave functions in the near future. Nevertheless, the status of these *ab initio* calculations of A = 6–7 weak decays looks quite satisfactory.

The situation for A=8 weak decays is much more difficult. While the A=6–7 decays are between states of predominantly the same spatial symmetry, the ^{8}Li and ^{8}B decays involve transitions from the 2^+[31] ground states to the 2^+[4] first excited state of ^{8}Be, which is in fact a fairly broad resonance.

*TJNAF and Old Dominion University

The impulse approximation gives only 39% of the experimental GT matrix element; the two-body axial current is relatively more important here, but only boosts our result to 43%. The ^{8}He(β^-)^{8}Li decay proceeds from the 0^+[22] ground state to several 1^+[31] excited states. Again, we get less than 50% of the measured GT matrix element to the lowest ^{8}Li state; however, in the ^{8}He decays, the experimental data is less complete. Again, we will be investigating alternate variational wave functions and computing GFMC mixed estimates in the near future. However, these suppressed A=8 decays will probably require additional physics input to reach a satisfactory state.

b.7. Λ Single Particle Energies (A. R. Bodmer and Q. N. Usmani*)

After some revisions, this work was published with the above title.[1] We make microscopic calculations of the single particle energies B_Λ of hypernuclei (HN) in terms of ΛN and ΛNN potentials, which are phenomenological, but based on pion-exchange considerations. We also include a purely phenomenological space-exchange component in the ΛN potential. Since the data for the HN range from $_\Lambda$C to $^{208}_\Lambda$Pb realistic few-body calculations are not feasible. Our procedure is then based on a local density approach where the binding D(ρ,k) of a Λ hyperon of momentum k to nuclear matter of density ρ is calculated with the Fermi hypernetted chain (FHNC) method for densities $\rho \lesssim \rho_0$ where ρ_0 is the density of normal nuclear matter. From this we then obtain D(ρ) the Λ binding for k = 0, and m*(ρ) the effective mass. We also obtain corresponding effective ΛN and ΛNN potentials, which by suitable folding into the core-nucleus density distribution obtained from electron-scattering data, gives the Λ-core potential $U_\Lambda(\rho)$. This folding procedure is essential to obtain finite range effects due to the interactions, which play an important role especially for lighter and medium-heavy HN. The Schrodinger equation with $U_\Lambda(\rho)$ and m*(ρ(r)) is then solved to obtain the B_Λ for the HN and Λ angular momenta of interest. Another change compared to our earlier work is that we now use only a dispersive ΛNN potential for which we can make reliable calculations, which so far has not been achieved for the two-pion exchange ΛNN potential. However, we include a phenomenological ρ dependence for the strength W of the dispersive ΛNN potential, which allows for a two-pion-exchange contribution. This dependence is such that the effective strength becomes more repulsive at larger densities, and implies that this strength becomes more repulsive for large mass number A since lighter HN have relatively more surface. Our best fits in fact require a large ρ dependence. This then translates into an A-dependent strength for W, nicely consistent with variational Monte Carlo calculations of $^5_\Lambda$He which require W ≅ 0.01 MeV, whereas normal nuclear matter requires W ≅ 0.02 MeV. Thus without a density dependence, *i.e.* with a constant W, not only are the fits worse than with a density dependence but they also cannot be reconciled with $^5_\Lambda$He. The probable interpretation is in terms of a dispersive plus two-pion exchange ΛNN potential since the latter is known to give an attractive contribution for lighter HN as a result of the associated correlations, but is conjectured to give a less attractive and possibly even a repulsive contribution for larger ρ, and hence for heavier HN. D(ρ) has a saturation behavior, already previously known, with a maximum as a function of ρ, resulting from the interplay of the attractive contribution of the ΛN forces, very approximately proportional to ρ, and the repulsive ΛNN contribution very approximately proportional to ρ^2. The effect of the density dependence of the effective strength W is to produce a sharper and larger maximum of D(ρ) at a smaller $\rho \approx 0.125$ fm^3 than without the density dependence with the maximum at $\rho \approx 0.15$ fm^3. For the well depth we obtain $D(\rho_0) = 29 \pm 1$ MeV, well consistent with earlier values. The exchange fraction of the ΛN potential corresponds to $m^*_\Lambda(\rho_0) \approx 0.75\ m_\Lambda$ and to a ratio of p- to s-state ΛN potential strengths of ≈ 0.45, with considerably less uncertainty than the value obtained from Λp scattering. We have also included charge-symmetry breaking which leads to a difference between the Λ-proton and Λ-neutron interactions. An important new result is that charge-symmetry breaking becomes quite significant for heavy HN with a large neutron excess, and has a strength very well consistent with the value we obtained in earlier work from the A = 4 HN.

*Universiti Putra Malaysia, [1]Q. N. Usmani and A. R. Bodmer, Phys. Rev. C **60**, 055215 (1999)

b.8. Core-Nucleus Distortion in Hypernuclei (A. R. Bodmer and Q. N. Usmani*)

We are continuing our study of the effects of the spherical distortion of the core nucleus by the Λ in a hypernucleus. The response of the core is determined by an appropriately chosen energy-density functional which depends on the nuclear compressibility and which gives a very good description of the nuclear binding energies. The forcing action of the Λ is determined by the nuclear density dependence of the Λ binding in nuclear matter which is obtained from our work on the Λ-single energies. Because of the strongly repulsive ΛNN forces, this Λ binding saturates at a density not very much less than the central density of nuclei, and results in a core-nucleus distortion which is much less than would be obtained with only ΛN forces. The effects of core distortion turn out to be small even for light hypernuclei. Our results justify the usual assumption that spherical core distortion effects are small and can mostly be neglected.

*Universiti of Putra Malaysia

C. NUCLEAR STRUCTURE AND HEAVY-ION REACTIONS

This research focuses on nuclear structure in unusual regimes: nuclei far from stability, and superdeformed nuclei at high spin. We also study heavy-ion reactions near the Coulomb barrier. Much of this work is closely tied to experiments performed at ATLAS and at radioactive-beam facilities.

Our studies of drip-line nuclei focus on breakup reactions induced by the Coulomb and nuclear fields from a target nucleus. A critical issue is to develop a realistic description of breakup mechanisms as a necessary tool for extracting or testing the nuclear structure properties of drip-line nuclei. An example of particular interest to solar neutrino physics is the low-lying E1 strength of ^{8}B which determines the radiative proton capture on ^{7}Be in the sun. We have developed a single-particle model which reproduces the low-lying dipole strength of ^{8}B, extracted in recent Coulomb dissociation experiments. We have tested the model against other observables that are sensitive to the size of the valence proton state. Thus we find that the model is consistent with the measured cross sections of the predominantly nuclear-induced breakup on a carbon target.

We have extended our studies of drip-line nuclei to include the structure and decay of deformed proton emitters. This is described in a coupled-channels treatment of the particle-rotor model, supplemented with a Green's function technique. The calculation of decay rates is commonly performed by using complex energies. This is a difficult task because the decay widths of interest are extremely small. However, by employing the Green's function method it is sufficient to solve the coupled equations with an energy that is real. The results we obtain for the decay of low-spin states are quite encouraging in comparison to measurements. The decay from high-spin states, on the other hand, is much more difficult to predict. It is influenced by the Coriolis force, which is too strong without the effect of pairing.

Our studies of superdeformed nuclei, at both low and high spins, address the issues of possible new regions of superdeformation and hyperdeformation. Special emphasis is being put on the study of fission barriers at high spin, and the relation between fission barriers and the possibility of producing very extended nuclear shapes. Other areas of interest are the structure of heavy elements and superheavy elements, density dependence of two-body interactions, and the phenomenon of proton radioactivity. The techniques we use to study these problems are a deformed central potential approach for surveying nuclear structure over a large region, self-consistent mean-field calculations for more detailed studies of particular nuclides, and many-body wave functions when residual interaction effects are small and a mean-field approach is inadequate.

Much of our work is computer intensive and we are adapting our codes to exploit the massively parallel IBM SP supercomputer system at Argonne. The use of the SP system allows us to calculate energy surfaces as a function of angular momentum, using the Strutinsky method with cranking, in a four-dimensional deformation space consisting of quadrupole, octupole, hexadecapole, and necking degrees of freedom. We carried out studies of nuclear energy surfaces in nuclei with masses ranging from A~80 to A~200. We are analyzing these calculations to look for nuclei that are good candidates for experimental investigation of superdeformation. Our recent analysis of energy surfaces near A=100 suggests that very extended minima in several nuclides near ^{108}Cd are experimentally accessible. Experimental studies motivated by these calculations have led to the observation of a superdeformed band in ^{108}Cd. We have adapted our many-body code for parallel computer systems and have modified it so as to allow the use of general two-body matrix elements. We are using this code to study the nuclear structure of nuclides near the proton dripline. A complementary effort, in conjunction with J. L. Egido and L. M. Robledo, is also focused in this area. In the latter studies, we are using a Gogny interaction in the HFB approximation. We have completed an analysis of excited states in ^{256}Fm; the heaviest nuclide for which there is extensive spectroscopic information on non-intrinsic excited states. The pairing force strength obtained from this analysis will improve the reliability of future theoretical studies of superheavy elements.

c.1. Systematic Study of ^{8}B Breakup Cross Sections (H. Esbensen and K. Hencken*)

The low-lying E1 response of ^{8}B has recently been extracted from measurements of the $^{8}B \rightarrow {}^{7}Be + p$ breakup on a Pb target, namely, from longitudinal momentum distributions of ^{7}Be fragments[1], and from the decay energy spectrum[2]. Since the strength of the low-lying E1 response is closely related to the mean-square-radius of the valence proton in ^{8}B, it is useful to investigate whether it is consistent with other observables that are sensitive to the size of the valence proton density. In this work we have focussed on the one-proton removal cross section.

We describe the valence structure of ^{8}B in a two-body model, with an inert ^{7}Be core and a weakly bound proton. The nuclear induced breakup of ^{8}B is calculated in the eikonal approximation, whereas Coulomb dissociation is calculated to first order. We assume that the core of ^{8}B is identical to a free ^{7}Be nucleus and calibrate the core-target interaction so that the measured ^{7}Be interaction cross sections are reproduced.

The calculated one-proton removal cross sections are shown in Fig. V-7 for different targets as functions of the beam energy. The solid curves are the results we obtain when we adjust the structure model to reproduce the recently extracted E1 strength. The uncertainty in the extracted E1 strength and also in our calibration of the core-target interaction results in a total uncertainty of about 10% in the predicted cross sections. Thus we conclude that the predictions are consistent with measurements on a C target (except the one at 40 MeV/u, which falls outside the systematics). This is a nice result because the ^{8}B breakup on C is mainly induced by nuclear interactions. The dashed curves are based on a model that gives a 20% smaller E1 strength; the predictions of this model are clearly inconsistent with the C data.

The predicted cross sections on high-Z targets are larger than the data. This is ascribed to approximations we have made. Thus we treat the Coulomb and nuclear induced breakup as independent processes. Moreover, the radial dependence of the Coulomb form factors that we have used assumes that the target nucleus does not penetrate the valence proton density. A way to improve our description for high-Z targets is discussed below. This work has been submitted for publication.

*University of Basel, Switzerland

[1]B. Davids *et al.*, Phys. Rev. Lett. **81**, 2209 (1998)
[2]N. Iwasa *et al.*, Phys. Rev. Lett. **83**, 2910 (1999)

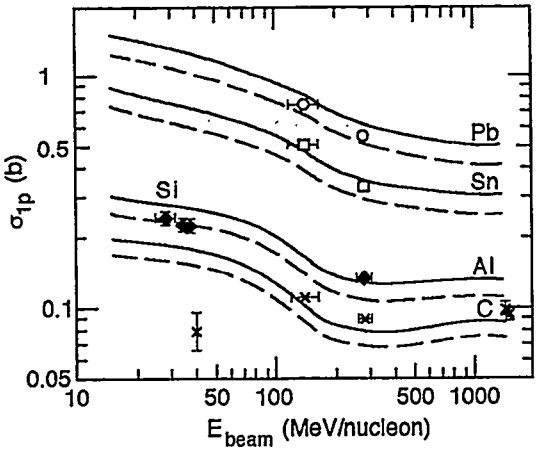

Fig. V-7. Calculated and measured one-proton removal cross sections for ^{8}B on C, Al, Si, Sn, and Pb targets, as functions of the ^{8}B beam energy. The solid curves are based on a model that reproduces the E1 strength extracted from recent experiments[1,2]. The dashed curves are based on a model that produces a 20% smaller E1 strength.

c.2. Coulomb-nuclear Interference in Breakup Reactions of ^{8}B (H. Esbensen)

The analyses of measured decay-energy spectra of ^{8}B have all lead to the conclusion that the E2 strength is strongly quenched[1]. The origin of the quenching has not yet been fully explained. Higher-order processes play a role at low beam energies[2] but they should be much less important at high energies. It was therefore surprising that the analysis of a measurement at 254 MeV/u also required a strong quenching of the E2 strength[1]. In this work I try to explain why a quenching is necessary even at high energy.

A general description of first-order Coulomb dissociation can be made in the distorted wave Born approximation. At high energies, it is sufficient to use a semiclassical description of the relative motion of projectile and target. The distorted waves, which are generated by nuclear interactions with the target, can be estimated in the eikonal approximation, whereas Coulomb excitation is treated to first-order. From these approximations one can derive the following expression for the decay energy spectrum:

$$\frac{d\sigma}{dE} = \frac{\mu}{\hbar^2 k}\int 2\pi b\,db \sum_{ljm} \left| \left\langle \psi_{kljm} \left| \left(e^{i\chi_N} - 1\right) + e^{i\chi_N}\,\Omega_C \right| \psi_{gs} \right\rangle \right|^2 .$$

Here χ_N is the nuclear eikonal phase, which depends on the impact parameter and the position of the valence proton with respect to the ^{7}Be core. The first term, *i.e.* the matrix element of $(e^{i\chi_N} - 1)$ between the ground state of ^{8}B and continuum states, is responsible for nuclear diffraction dissociation. The second term contains the operator Ω_C, which is responsible for the first-order Coulomb dissociation. It is multiplied by the eikonal factor $e^{i\chi_N}$, which suppresses the Coulomb dissociation operator when the valence proton penetrates the target nucleus and gets absorbed. The combined expression includes the interference between the Coulomb and nuclear induced breakup.

[1] N. Iwasa et al., Phys. Rev. Lett. **83**, 2910 (1999)
[2] H. Esbensen and G. F. Bertsch, Nucl. Phys. **A600**, 37 (1996)

The numerical calculation of the above expression is much more complicated and time-consuming than the 'conventional' calculation of Coulomb dissociation in which one ignores the influence of nuclear processes; they enter only via a cutoff in the integration over impact parameters. The conventional analyses also employ a multipole expansion of the Coulomb field from the target, which assumes that the target nucleus does not penetrate the density of the valence proton. This assumption is reasonable for tightly bound nuclei but it is questionable for a loosely bound nucleus like ^{8}B. By using the correct multipole expansion of the Coulomb field, and including the influence of the nuclear field as described above, one may be able to explain the empirical quenching of the Coulomb dissociation. This work is in progress.

c.3. Calculations of Proton Decay Rates of Spherical and Deformed Nuclei (C. N. Davids and H. Esbensen)

We have used a Green's function technique, based on the Gell-Mann-Goldberger transformation, to show that the "distorted wave" decay rates calculated by Aaberg[1] and the "exact" decay rates calculated by Maglione[2] for spherical proton emitters are mathematically equivalent[3,4]. Numerically the two methods give half-lives agreeing to within 0.005%. We have also extended the Green's function technique to cover the case of deformed proton emitters[3,4], and shown that the decay rates calculated by Maglione *et al.*[2] and Kadmensky and Bugrov[5] are equivalent.

[1] S. Aberg, P. B. Semmes, and W. Nazarewicz, Phys. Rev. C **56**, 1762 (1997); Phys. Rev. C **58**, 3011 (1998)
[2] E. Maglione et al., Phys. Rev. Lett. **81**, 538 (1998); Phys. Rev. C **59**, R589 (1999)
[3] C. N. Davids and H. Esbensen, Proceedings of the International Symposium on Proton-Emitting Nuclei, 6-9 October 1999, Oak Ridge, TN, AIP Conference Proceedings, in press (2000)
[4] C. N. Davids and H. Esbensen, Physical Review C in press (2000)
[5] V. P. Bugrov and S. G. Kadmensky, Sov. J. Nucl. Phys. **49**, 967 (1989), S. G. Kadmensky and V. P. Bugrov, Phys. of Atomic Nuclei **59**, 424 (1996)

c.4. Coupled-channels Treatment of Proton Emission (H. Esbensen and C. N. Davids)

Measurements of the proton decay of deformed nuclei beyond the proton drip line have previously been analyzed in a particle-rotor model, making use of several approximations. Thus the wave functions of the decaying states have been calculated by diagonalizing a deformed Hamiltonian in a spherical, single-particle basis. Moreover, this was done in the adiabatic limit, where the excitation energies of the core are set to zero. Since the decay rate is extremely sensitive to the energy of the emitted protons, we decided to improve the description by adopting the coupled channels approach, which allows us to include non-zero core excitation energies. Moreover, the radial wave functions are automatically generated by solving a set of coupled radial equations.

The decay rate of a resonance is determined by the amplitudes of the asymptotic radial wave functions at large distances. It is, however, very difficult to calculate the radial wave functions of a resonance accurately out to large distances, where the long-range Coulomb quadrupole coupling can safely be ignored. It requires that the resonance energy has been determined with extremely high precision, much better than 1 eV. A simple way to overcome this problem is to solve the coupled equation out to 10 to 20 fm. One can then use the Green's function method (GFM)[1] to extrapolate the wave function out into the asymptotic region and include the effect of the long-range Coulomb coupling to first order.

An example is illustrated in Table IV-3. for the decay from the $3/2^+$ ground state of ^{131}Eu to the 0^+ ground state and to the excited 2^+ and 4^+ states of the ^{130}Sm daughter nucleus. The first line gives the measured decay widths[2]. The second line gives the results of the coupled channels approach, which are in fair agreement with the measurement. The third line gives the results we obtain in the adiabatic limit. It is seen that the decay widths to the 2^+ and 4^+ states are grossly overestimated compared to the coupled-channels results.

Table V-3. Decay widths (in units of 10^{-20} MeV) for the $3/2^+$ ground state of ^{131}Eu to the 0^+ ground state and the 2^+ and 4^+ excited states of ^{130}Sm.

	Γ_{0+}	Γ_{2+}	Γ_{4+}
Experiment [2]	1.71	0.54	-
Coupled-channels method	1.83	0.99	3.16×10^{-8}
Adiabatic limit	2.05	83.9	13.7
Adiabatic limit + GFM	2.05	1.01	2.83×10^{-8}

The Green's function method can also be used to improve the results obtained in the adiabatic limit because it allows us to implement the correct energy of the emitted proton, when the daughter nucleus ends up in an excited state. The results we obtain are given in the fourth line. The decay widths to the 2^+ and 4^+ states are now strongly reduced but they are close to the values obtained in the coupled-channels calculation. The methods we have developed will be used to extract information about the structure of proton-rich nuclei from measurements of the decay rates and energies of the emitted protons.

[1]C. N. Davids and H. Esbensen, Phys. Rev. C in press (2000)
[2]A. A. Sonzogni et al., Phys. Rev. Lett. **83**, 1116 (1999)

c.5. Many-body Wave Functions (R. R. Chasman)

We are continuing the development of many-body variational wave functions that put pairing and particle-hole two-body interactions on an equal footing. The variational parameters are calculated with an iteration procedure. The complexity of the wave functions depends only on the number of levels included in the valence space, but does not depend on the number of nucleons in the system. In these wave functions, we conserve particle number and parity strictly by projecting states of good particle number and parity before carrying out the variational calculations. We have added a cranking term to the many-body Hamiltonian and modified the projection procedure to get states of good signature before variation. This allows us to study pairing collapse as a function of angular momentum. We have also extended the program to calculate spectroscopic factors involved in proton decay. This is useful for studies of nuclides near the proton drip line.

By using residual interaction strengths (*e.g.* the quadrupole interaction strength or pairing interaction strength) as generator coordinates, one gets many different wave functions; each having a different expectation value for the relevant interaction mode. Such wave functions are particularly useful when one is dealing with a situation in which a configuration interaction treatment is needed. This is particularly true

for an adequate treatment of pairing at high spin as well as for instances in which the single-particle level density is low. Because the same basis states are used in the construction of all of the many-body wave functions, it is possible to calculate overlaps and interaction matrix elements for the many-body wave functions obtained from different values of the generator coordinates (which are not in general orthogonal) easily. The valence space can contain a very large number of single-particle basis states, when there are constants of motion that can be used to break the levels up into groups.

Wave functions of this sort become more realistic as the size of each of the groups is increased. To increase this size, we have parallelized our code to run on the SP computer system. We have also modified our codes to handle arbitrary two-body matrix elements. This latter feature allows us to include Coulomb matrix elements easily. Together with J.L. Egido and L.M. Robledo, we have developed subroutines for calculating Gogny interaction matrix elements and Coulomb matrix elements for this many-body code.

As is the case with most non-linear problems, the results are sensitive to the choice of starting values for the variational parameters. We have been examining choices of starting points and other strategies for dealing with this problem. We have introduced a pseudo-annealing procedure, by adding a one-body off-diagonal matrix element to the interaction and then let the system cool slowly. This is of limited value. We have also constructed a starting wave function by maximizing its overlap with a configuration-interaction solution and then using this wave function as a new starting point for our minimization procedure. This has been moderately successful.

We have been more successful in improving our minimization procedure with some other strategies. First of all, we have found that making the changes in the variational amplitudes for proton and neutron amplitudes inversely proportional to the magnitude of the respective pairing correlations is very useful, when going from one iteration to the next. This helps the proton and neutron amplitudes converge at the same rate and we get improvements in the energy. We have found that our many-body wave functions are relatively resistant to large-scale structural changes so long as the relative phases of the variational amplitudes are not changed. We have been able to utilize this feature to get improvements in many-body wave functions by taking the results of a minimization and then restarting the iterative procedure with a wave function in which all positive amplitudes are replaced by +1 and all negative amplitudes are replaced by -1. This approach is particularly valuable for improving the energies of wave functions in metastable minima, because the new trial functions do not fall into the absolute minimum.

c.6. Very Extended Shapes in Nuclei (R. R. Chasman)

In the past few years, large computer resources have become available on the massively parallel processor IBM SP system at Argonne, in addition to the resources provided by NERSC. We have parallelized the code used to calculate single-particle spectra to exploit the SP system and have devoted a large part of our efforts to calculating energy surfaces in a four-dimensional shape space that includes reflection asymmetric shapes. We study the nuclear energy surfaces as a function of mass, charge, shape and angular momentum, using the Strutinsky method. In this approach, one makes quantum corrections to a smooth liquid drop behavior using the calculated single-particle energy levels. In earlier studies, we found that it is often not sufficient to use only quadrupole and hexadecapole deformations to describe very extended reflection-symmetric nuclear shapes. When we added a necking degree of freedom, we found previously unknown minima. These minima are characterized by very extended capsule shaped nuclei with axis ratios of 2.2:1 in the A=180 mass region. We have now added octupole deformation to this shape space. The inclusion of these two degrees of freedom in our shape space substantially increases our ability to describe nuclear shapes compared to a typical shape space consisting only of quadrupole and hexadecapole deformations. As parity is no longer a good quantum number when octupole deformation is included, the size of the matrices that we diagonalize

[1]R.R. Chasman, Workshop on the Science for an Advanced ISOL Facility, (1997) p. 69
[2]R.R. Chasman, PHY-9018-TH-98
[3]R.R. Chasman, Phys. Rev. Lett. **80**, 4610 (1998)
[4]R.R. Chasman Phys. Lett. B**219**, 227 (1989)

is doubled. In a typical calculation, we diagonalize matrices that are 600 × 600. Several thousand such diagonalizations are needed to determine energy surfaces.

There remains a need to test calculated fission barriers and to generally understand nuclear properties at the highest spins. Using the four-dimensional deformation space described above, we have analyzed the high-spin energy surfaces of the N=86 isotones going from Sn (Z=50) to Dy (Z=66). There is a high spin superdeformed minimum in all of these nuclides (~1.85:1 axis ratio) that becomes yrast at high spin. These shapes are well known experimentally in the Dy region.

We find that as the proton number decreases from Z=66 to Z=50, the fission barrier increases by roughly 10 MeV at a given angular momentum. The superdeformed minimum associated with N=86 is present for both Sn and Dy. This result suggests that we can extend the study of nuclear properties at extreme deformations to a new regime of angular momenta, with the availability of radioactive nuclear beam facilities. A preliminary version of this work has been published.[1]

We have extended our high spin Strutinsky calculations[2] to nuclei in the A=100 mass region. Many of the very extended minima that we find will be accessible with projectiles produced at an exotic beam facility. However, our calculations show very extended minima in nuclides in the vicinity of ^{108}Cd that are accessible using existing facilities. Recent experiments, inspired by these calculations, show a superdeformed rotational band in ^{108}Cd.

Several odd-parity excited states have been found in the superdeformed minima of the Hg region. Because of their low excitation energies, it had been thought that these states are very collective. Making use of a particle number conserving treatment of pairing, we found[3] that one can calculate the excitation energies of these states quite well as simple broken pair excitations; using conventional pairing force strengths and the single-particle levels that were obtained when superdeformation in this mass region was first[4] predicted. The transition matrix elements connecting these excited states to the superdeformed yrast band remain to be explained.

We are analyzing nuclides in the region $70 < A < 100$, searching for very extended minima.

c.7. Single-Particle States in the Heaviest Elements (R. R. Chasman and I. Ahmad)

The search for superheavy elements has been a major theme of nuclear structure research for the past twenty years. Theoretical predictions of the stability of superheavy elements depend crucially on the single-particle energy level spacings in the vicinity of 114 protons and 184 neutrons. Our approach is to learn as much as possible about these levels from spectroscopic studies of nuclides in the A=250 region. This is possible because there are members of the relevant spherical multiplets that drop rapidly in energy with increasing deformation, and are fairly close to the ground state in the strongly deformed nuclides near A=250. The orbitals that are important for fixing the shell corrections near N=184 are the $h_{11/2}$, $j_{13/2}$ and $k_{17/2}$ spherical states. For each of these spherical orbitals, there is a corresponding deformed orbital whose energy in the A=250 region is quite sensitive to one of these spherical states, *e.g.* the 1/2-[761] orbital that has already been identified in ^{251}Cf is quite sensitive to the energy of the spherical $j_{13/2}$ orbital. The position of the 1/2+[880] deformed orbital is very sensitive to the single particle energy of the $k_{17/2}$ spherical state. We have calculated signatures for the low-lying states in ^{251}Cf and the calculated energies and signatures are in good agreement with the experimentally observed (d,p) spectrum. We expect to see the high-J states in an (α,^{3}He) transfer reaction. As a ^{250}Cf target is not available, we have studied the high-J states in ^{249}Cm, which is an isotone of ^{251}Cf. The (α,^{3}He) experiment has been carried out and two high-J peaks have been observed at ~1.6 and 1.9 MeV. These peaks are candidates for the 1/2+ [880] band. Additional coincidence studies will be needed to make a definitive assignment. This study[1] has been published.

[1] I. Ahmad *et al.*, Nucl. Phys. **646**, 175 (1999)
[2] R. R. Chasman and I. Ahmad, Phys. Lett. B**392**, 255 (1997)
[3] I. Ahmad, R.R. Chasman and P. R. Fields, Phys. Rev. C (accepted for publication)

Using the Strutinsky method, we found[2] that we could get very good agreement with the known low-lying levels in ^{251}Cf using a Woods-Saxon potential. We have used the potential parameters generated from this fit to study the stability of superheavy elements. To determine potential parameters for protons in the heavy elements, we utilized data from our spectroscopic studies of ^{255}Md. These studies show the 1/2-[521] orbital to lie above the 7/2-[514] orbital, but the magnitude of the energy difference is not known. Determining the potential in this way, we extrapolate directly to the superheavy element region. As the usual zero-point correction to mass estimates is questionable in that it treats only the quadrupole deformation mode, we replaced this correction in our mass estimates by a term that depends quadratically on the sum of the proton and neutron shell corrections. This correction is easy to evaluate and gives quite reasonable corrections where masses are known. Using the potential parameters derived from the heaviest elements for which there is detailed spectroscopic information, we find that our calculated lifetimes are sufficiently long so as to be able to observe elements at least through Z=120.

In our analysis, we have assumed that the 1/2-[521] orbital lies just above the 7/2-[514] orbital in ^{255}Md. In fact, this level spacing is not yet known. Our estimates of superheavy element stability will be affected by the experimental value of this level spacing. We hope to determine this spacing through experimental studies, and thereby refine our estimates of superheavy element lifetimes. Another important feature in determining the binding energy of superheavy elements is the magnitude of the pairing interaction strength.

We have recently completed a study[3] of excited states in ^{256}Fm, which is the heaviest nucleus in which excited non-rotational states have been observed. We have used the I=7 negative parity state at 1426 keV in this nuclide to adjust the proton pairing interaction strength. Our calculated spectrum for other proton broken pair states is in good agreement with those that have been observed, and we predict many other such states between 1 and 2 MeV. Pinning down the proton pairing strength, in the heaviest nuclide where there is sufficient data to do so, improves the reliability of predictions of the stability and structure of yet heavier elements.

Additionally, we have studied[3] the decay of ^{255}Md to determine low-lying single-particle state assignments in ^{255}Fm and ^{251}Es. Through studies such as these, we hope to get an accurate picture of nuclear structure on both sides of the deformed neutron single particle gap at N=152 and the deformed proton gap at Z=100.

At present, we are analyzing excited states in ^{251}Cf populated in the alpha decay of ^{255}Fm. This will give further insight into nuclear structure beyond the N=162 deformed gap.

c.8. Studies of Nuclear Energy Surfaces (R. R. Chasman, J. L. Egido,* and L. M. Robledo*)

This collaborative research program is focused on the study of nuclear energy surfaces, with an emphasis on very deformed shapes using two complementary methods: 1) the Strutinsky method for making surveys of mass regions and; 2) Hartree-Fock calculations using a Gogny interaction to study specific nuclei that appear to be particularly interesting from the Strutinsky method calculations. The great advantage of the Strutinsky method is that one can study the energy surfaces of many nuclides (~300) with a single set of calculations. Although, the Hartree-Fock calculations are quite time consuming relative to the Strutinsky calculations, they determine the shape at a minimum without being limited to a few deformation modes. We have completed a study of ^{182}Os using both approaches. In our cranked Strutinsky calculations, that incorporate a necking mode deformation in addition to quadrupole and hexadecapole deformations, we found three well separated, deep, strongly-deformed minima. The first is

*Universidad Autonoma de Madrid

[1]R. R. Chasman and L.M. Robledo, Phys. Lett. B**351**,18 (1995)
[2]J. L. Egido, L.M. Robledo and R.R. Chasman, Phys. Lett. B**393**, 13 (1997)
[3]L. M. Robledo, J.L. Egido, and R.R. Chasman, Proceedings of the Conference on Nuclear Structure at the Limits, Argonne National Laboratory, Argonne, IL, July 22-26 (1996) p. 124
[4]C. N. Davids *et al.*, Phys. Rev. Lett. **76**,592 (1996)

characterized by nuclear shapes with axis ratios of 1.5:1; the second by axis ratios of 2.2:1 and the third by axis ratios of 2.9:1. We also studied this nuclide with the density-dependent Gogny interaction at I=60 using the Hartree-Fock method and found minima characterized by shapes with axis ratios of 1.5:1 and 2.2:1. A comparison of the shapes at these minima, generated in the two calculations, shows that the necking mode of deformation is extremely useful for generating nuclear shapes at large deformation that minimize the energy. The Hartree-Fock calculations are being extended to larger deformations in order to further explore the energy surface in the region of the 2.9:1 minimum.

With the recent availability of large computer resources on the SP system at Argonne, together with the continued availability of computing resources at NERSC, it is feasible to carry out Strutinsky calculations on a large four-dimensional grid in a deformation space that includes octupole deformation in addition to quadrupole, hexadecapole and necking deformations. We are carrying out this study of the A~180 region concentrating on the questions: 1) how do the inclusion of necking and reflection-asymmetric degrees of freedom modify nuclear energy surfaces and; 2) how soft are the many, known, very-deformed nuclear shapes in this region to octupole deformation?

We have completed[1] the first phase of these studies, using the Strutinsky method to calculate nuclear energy surfaces in the four-dimensional space discussed above. Comparing the results obtained with and without octupole deformation, we found major modifications of the energy surface in many nuclei in the region around ^{176}W. These effects are strong at all values of the angular momentum. There are reductions of the total energy of ~ 7 MeV for the necked-in shapes at the largest deformations. This feature can be understood in terms of incipient fission fragments. The reflection-asymmetric shape is necked-in in such a way as to exploit the large shell corrections associated with a strongly deformed fragment in the vicinity of ^{100}Zr and a spherical fragment in the vicinity of ^{80}Zr. The symmetric necked-in shape at these large deformations corresponds to two strongly-deformed incipient fission fragments near A=90 and is not favored. The effects are huge here, compared to typical octupole deformation energy gains of less than 1 MeV.

As in the case for Strutinsky method calculations, the introduction of reflection asymmetry doubles the basis space that must be used in Hartree-Fock calculations. We have extended the Hartree-Fock codes to allow us to calculate the properties of very-deformed reflection asymmetric shapes, using a one-center basis. We have finished a calculation[2] of the energy surface of ^{176}W at I=0, using the Gogny interaction. In these calculations, we also found a substantial lowering of the fission barrier when reflection asymmetric shapes are allowed. At I=0, where the Hartree-Fock calculations were carried out, the fission barrier is lowered by 4.5 MeV when reflection asymmertic shapes are included. At I=0, the reduction is 6.2 MeV in the Strutinsky calculations. The agreement between these two very different methods is impressive. In the Hartree-Fock calculations, the asymmetric division is into fission fragments of ^{66}Ni and ^{110}Pd.

We have recently broadened the area of our comparative studies to include low-spin studies in the neutron-deficient Pb region. In addition to HFB and Strutinsky calculations, we are applying the many-body wave functions discussed above, which go beyond mean-field approximations.

The neutron-deficient nuclides (N < 110) in the Pb region have states that are characterized by three distinct shapes; spherical, prolate and oblate. In the oblate and prolate states, there are low-lying single-particle states derived from spherical states on both sides of the Z=82 single-particle gap. Although this gap is roughly 4 MeV, there are states within a few hundred keV of ground in the neutron-deficient Tl(Z=81) and Bi(Z=83) isotopes that would be at ~ 4 MeV excitation, in the simplest single-particle picture. In addition, proton emission has been observed in the nuclide ^{185}Bi. We are making calculations of the properties of nuclides in this region using our many-body wave functions. In addition, we are also studying many of these same nuclides using the Gogny interaction in the HFB approximation.

Proton emission has been observed[4] in the light Pb nuclei. It seems that one might hope to use this phenomenon to extract some interesting spectroscopic data on nuclear shapes and orbitals in much the same way that one gets spectroscopic information through single-nucleon transfer reactions such as (d,p) and (d,t) reactions. In order to explore this possibility, we have developed a treatment of proton-emission spectroscopic factors using many-body wave functions. In the case that we have studied (^{185}Bi $\rightarrow$ ^{184}Pb), the energetics of the reaction are such that only the ground state is populated. We calculate a very small spectroscopic factor for the proton decay to the ground state. The small spectroscopic factor is largely due to the shape

difference between the deformed decaying state in ^{185}Bi and the ground state of ^{184}Pb, which is spherical. To understand this spectroscopic factor, it is necessary to have good wave functions for the initial and final states. Our systematic study of this region should provide us with improved wave functions.

D. ATOMIC THEORY AND FUNDAMENTAL QUANTUM MECHANICS

d.1. Interactions of High-Energy Photons with Matter (M. Inokuti)

In support of experimental work in atomic physics with the use of synchrotron radiation, theoretical studies are being conducted on the physics of Compton scattering by bound electrons, focusing on topics selected in view of basic importance, timeliness, and potential in applications.

When the photon energy greatly exceeds the binding energy of an electron, the effect of electron binding to an atom is largely understood in the framework of an impulse approximation, which accounts for the momentum of an electron at the instant of the Compton scattering. However, the physics remains to be explored for a more general case, where full details of atomic structure, described for instance in terms of the Green's function, need to be considered.[1] For a hydrogen-like atom, or within a simple-electron approximation, full analysis of the binding effect is theoretically feasible. Efforts are being made to elucidate basic points of the physics involved and to suggest items for experimental exploration.

Work on the Compton scattering by liquid water has been completed. Results of recent measurements by a group at Sendai were compared closely with an earlier semi-empirical determination of the Bethe surface (the strength of the Compton scattering plotted as a function of both energy transfer and momentum transfer), within the impulse approximation and a reasonably good agreement was found[1].

[1]M. Dingfelder and M. Inokuti, Radiat. Environ. Biophys. **38**, 93 (1999)

d.2. Interactions of Fast Charged Particles with Matter (M. Inokuti)

Stopping power, the total yield of ionization, its fluctuation, ionization cross sections, and other quantities related to the energy loss of fast charged particles penetrating through matter are important in many applications such as the detection of particles and the analysis of their charges and kinetic energies. A review of the current understanding of "W, F, and I: Three quantities basic to radiation physics" was published[1].

A monograph[2] on "Fundamentals of Plasma Chemistry" was edited. It contains nine articles reviewing fundamental aspects of the processing of material surfaces by use of low-temperature chemically active plasmas, including electron interactions with various atoms, molecules, and solid surfaces.

Another review on "Electron collision cross sections of atoms" has been produced for inclusion in a forthcoming volume on "Atomic Collisions" in the Landolt-Börnstein Numerical Data and Functional Relationships in Science and Technology, Springer-Verlag. This article reports on various cross sections for electron collisions with free atoms, and presents values recommended as best in the light of current knowledge.

[1]M. Inokuti, in the proceedings of the International Symposium in Commemoration of Professor Doke's Seventieth Birthday, eds. S. Kubota and J. Kikuchi (Waseda University Press, Tokyo 1999) p. 1.
[2]M. Inokuti and K. H. Becker (eds), Advances in Atomic, Molecular, and Optical Physics, Vol. 43, Fundamentals of Plasma Chemistry, (Academic Press, San Diego 1999) 166 pages.

d.3. Stochastic Variational Approach to Quantum Mechanical Few-body Problems (Kálmán Varga)

The quantum mechanical few-body problem is of fundamental importance for all branches of microphysics and it has substantially broadened with the advent of modern computers. This book gives a simple, unified recipe to obtain precise solutions to virtually any few-body bound state problem and presents its application to various problems in atomic, molecular, nuclear and solid state physics. The main ingredients of the methodology are wave function expansion in terms of Correlated Gaussians and optimization of the variational trial function by stochastic sampling. The book is written for physicists and, especially, for graduate students interested in quantum few-body physics[1].

[1] Y. Suzuki and K. Varga, "Stochastic Variational Approach to Quantum Mechanical Few-body Problems", Springer-Verlag (Berlin Heidelberg, 1998).

d.4. Multipositronic Systems (Kálmán Varga)

Recent calculations have given the very surprising result that a positron can cling to a neutral atom. The simplest such positronic atom is the Lie^+. We have explored the possibility of the formation of stable atoms/ions containing two or more positrons. It is shown that the H^- and the Li^- ions can bind not only one but two positrons. The binding energies of these double positronic atoms $E(H^-,e^+,e^+) = 0.57eV$ and $E(Li^-,e^+,e^+) = 0.15eV$ are somewhat smaller than those of their single positronic counterparts (E(HPs) = 1.06 eV and E(LiPs) = 0.32 eV). We have also found that a proton and two Ps^- positronium ions where $Ps^- = (e^+, e^-, e^-)$, can form a bound system.[1]

[1] K. Varga, Phys. Rev. Lett. **83**, 5471 (1999)

d.5. Force-Free Interactions and Nondispersive Phase Shifts in Interferometry (M. Peshkin)

In earlier work, I sharpened an observation of Zeilinger to prove that force-free interactions in a Mach-Zehnder interferometer lead to nondispersive, *i.e.*, energy-independent, phase shifts. That result can be useful in interpreting the results of certain types of interferometry experiments. Recently, a photon-interferometry experiment and a proposed neutron-interferometry experiment have been misinterpreted by their authors, who did not consider the nondispersivity test, as demonstrating a new kind of geometrical effect. I have corrected that interpretation and the ensuing discussion has led to a new proposed experiment. A Comment presenting this work has been accepted for publication by Foundations of Physics Letters.

d.6. A No-go Theorem for Matter-wave Interferometry with Application to Neutron Electric-Dipole Moment Experiments (M. Peshkin)

Work on this project has been completed. The no-go theorem addresses a recent proposal to measure the neutron electric-dipole moment (EDM) by novel interferometry techniques. Ultra-cold neutrons in a state described by some initial wave packet and polarized in the +z (vertical) direction are to be exposed to a strong external electric field gradient in the x direction. The resulting force F_x on the EDM will cause the initial wave packet to evolve into the coherent sum of two spatially different partial wave packets, one with σ_x =+1 and one with σ_x = -1. The two partial wave packets will differ little, their centroids being separated in x by an amount proportional to the EDM and equal to some femtometers if the EDM equals 10^{-25} e-cm. The spatial separation is then to be changed to a separation in horizontal momentum by letting the neutrons fall under the influence of gravity and reflecting them from a mirror set at 45 degrees to the vertical, after which the neutrons are to bounce along a long horizontal beam tube extending in the x direction. As the neutrons proceed along the beam tube, the relative phase of the two partial wave packets is expected to grow because of their different central momenta. That relative phase growth, which is proportional to the EDM and to the length of the beam tube, results in a rotation of the neutrons' polarization, to be measured at the end of the beam tube.

I have shown that if one measures the polarization in the most direct way, by catching the neutrons in a box and measuring the polarization at an instant, that will not work. The unitarity of the time evolution guarantees that the so-measured polarization will not change as the neutrons progress down the beam tube, contrary to semi-classical expectations. If, alternatively, one measures the polarization as the neutrons pass a place in the beam tube, then the rotation of the polarization, now time dependent, does grow proportionally to the length of the beam tube, but the expected rotation is too small to be measured in practice. In principle, separating the two wave packets by magnetic reflectors that act on the neutron's magnetic-dipole moment may enable an interferometric measurement of the EDM, but the practicalities of that scheme have not been investigated. A paper reporting this work has been accepted for publication in Nuclear Instruments and Methods in Physics Research, Section A.

d.7. Quantum Robots (P. Benioff)

Work on quantum robots was continued in 1999. A quantum robot is a mobile system with an on-board quantum computer and ancillary memory, output, and control systems. The quantum robot interacts with other quantum systems in its environment. The dynamics of the interaction is described by tasks that are alternating sequences of computation and action phases. Which type of phase is active depends on the state of the control system. Each computation phase determines the action for the next phase. Input includes the local state of the environment and states of the memory and output systems. The following action phase carries out the action determined in the previous computation phase. Local environmental observations may be needed. The task is complete when the desired goal is reached. Additional details including a description of the dynamics as a Feynman sum over phase paths are given elsewhere[1].

[1] P. Benioff, Phys. Rev. A **58** 893 (1998)

[2] L. K.Grover, in *Proceedings of 28th Annual ACM Symposium on Theory of Computing* ACM Press New York 1996, p. 212; Phys. Rev. Letters, **79** 325 (1997); G. Brassard, Science **275**, 627 (1997).

Study of a simple example of a search task was begun in which a quantum robot searches a 2-D region R of NxN sites to determine the site location of a particle. The idea here is to exploit quantum mechanical parallelism by putting the memory system in a superposition state

$$\psi = \frac{1}{N} \sum_{X,Y=0}^{N-1} |X,Y\rangle .$$

Here each state $|X,Y\rangle$ corresponds to a specific site of R to examine for the presence or absence of the particle. Since all sites of R are searched in parallel and coherently, the idea is to see if Grover's Algorithm[2] can be used to efficiently process the memory of the returned quantum robot to determine the location of the particle. If so one would have an example of a task that can be done more efficiently by a quantum robot than by any classical robot. During 1999 work had not progressed sufficiently to see if this was possible.

d.8. The Representation of Natural Numbers in Quantum Mechanics (P. Benioff)

Work was begun on conditions that a physical system must have in order that states of the system represent the natural numbers (nonnegative integers). That states of many physical systems satisfy the conditions is clear from the existence of classical computers and the projected existence of simple quantum computers[1]. However there are also many systems with no states suitable for representing the numbers.

Necessary conditions that must be satisfied are based on the relation

$$s = \sum_{j=1}^{L} k^{j-1} \underline{s}_j$$

between a string $\underline{s}$ of L digits with k values 0,1,...k-1 and the corresponding number s. The goal is to give, for a quantum system with L components, conditions that a tensor product basis state of the form $|\underline{s}\rangle = \bigotimes_{a\varepsilon A} |\underline{s}_a\rangle$ must satisfy so that the above equation is satisfied.

Work has progressed on describing necessary conditions for such a system. Some of them are the usual ordering conditions on the set A of L labels and on the k basis states for each component system. The new part is a dynamical condition based on these orderings. This is that there must exist operations that are *efficiently implementable physically* that correspond to the operations of addition of k^{j-1} for j =1,2,...,L. Work is progressing on describing these conditions in more detail.

[1] L. Vandersypen *et al*, Los Alamos Archives Report No. quant-ph/9910075; J. Ahn, T. Weinacht, and P. Bucksbaum, Science **287**, 463-465, (2000).

E. OTHER ACTIVITIES

e.1. International Workshop on Understanding Deconfinement in QCD (C. D. Roberts, D. Blaschke,* and F. Karsch†)

In partnership with D. Blaschke (University of Rostock) and F. Karsch (University of Bielefeld), C.D. Roberts organized an International Workshop on "Understanding Deconfinement in QCD" at the European Centre for Theory, Trento, Italy, 1-13 March 1999. The workshop's primary focus was QCD at nonzero baryon density, although nonzero temperature was also considered. Nonzero baryon density is a domain of QCD that is inaccessible with current lattice-QCD simulation algorithms because the integrand in the functional integral is complex. Hence this direct, quantitative approach cannot presently address questions as important as whether a quark-gluon plasma exists in the interior of dense astrophysical objects. The workshop brought together approximately sixty physicists whose specializations ranged from lattice-QCD and matrix models to Dyson-Schwinger equations and phenomenological models. The presentations described current research on overcoming the lattice-QCD problems at nonzero baryon density and the predictions of the more phenomenological approaches, which can already explore this domain. Representatives of the large CERN experimental collaborations were also present and gave up-to-date summaries of their results. We gathered written contributions together and published them in a proceedings volume[1], which should prove useful because much new material was presented at the meeting.

*University of Rostock, Germany, †University of Bielefeld, Germany

[1]Proceedings of the International Workshop on Understanding Deconfinement in QCD, eds. D. Blaschke, F. Karsch, and C.D. Roberts (World Scientific, Singapore, 2000)

e.2. Theory Institute on Advanced Calculational Methods in the Nuclear Many-body Problem (S. C. Pieper, R. Roncaglia, K. Varga, and R. B. Wiringa)

A Theory Institute on "Advanced Calculational Methods in the Nuclear Many-body Problem" was held during the week of August 2–6, 1999. The Institute brought together 45 theorists, including 15 postdocs and graduate students, representing 24 universities and laboratories, both domestic and foreign. A total of 28 talks were presented, on subjects ranging from the nucleon-nucleon interaction at the quark level to large-scale shell model calculations, and from low-energy astrophysical reactions to GeV electron scattering. The primary focus was on recent developments in computational methods that are used for microscopic nuclear many-body calculations, including Fadde'ev-Yakubovsky, resonating group, coupled-cluster, correlated-basis, and quantum Monte Carlo methods. The meeting included an excursion to downtown Chicago to see the "Cows on Parade" exhibition (www.cowsonparade.net) and an outdoor symphony concert. The program of Theory Institutes at Argonne has been sponsored by Frank Fradin, the Associate Laboratory Director for Physical, Biological and Computational Sciences, for ten years; this is the largest nuclear physics workshop in the series to date.

e.3. Twelfth Annual Midwest Nuclear Theory Get-Together (R. B. Wiringa)

The Theory Group hosted the Twelfth Annual Midwest Nuclear Theory Get-Together on September 24 and 25, 1999. Nuclear theorists from a number of midwest universities get together every fall to find out what different people and groups in the region are working on. The organizational duties rotate among the participants, but Argonne has become the regular meeting place by virtue of its facilities and central location. The organizer for 1999 was Bill Friedman of the University of Wisconsin. The meeting provides a good chance for students to broaden their horizons and get some practical speaking experience in a friendly atmosphere. The format is very informal, with an agenda of talks being volunteered at the beginning of the meeting. This year we had the largest attendance ever: 30 faculty, postdocs, and students from twelve different universities in Illinois, Indiana, Iowa, Michigan, Minnesota, Missouri, Ohio, and Wisconsin, along with the Argonne staff. Some 28 presentations were made over Friday afternoon and Saturday morning. Topics included light-front and effective field theories, QCD, quantum Monte Carlo methods, pionic fusion, relativistic heavy-ion collisions, and nuclear astrophysics. A good time was had by all.

OTHER EDUCATIONAL ACTIVITIES IN THE PHYSICS DIVISION

a. Enhancement of Minority Involvement in DOE Nuclear Physics Programs (B. Zeidman)

The ANL Physics Division, through its Minority Program, continues to attract highly qualified students who apply for participation in the programs of the Physics Division and other ANL divisions. The program is directed toward identification of physics departments with relatively strong programs and faculty interested in stimulating their students to pursue research, particularly in summer programs. Several returning, as well as new, minority physics majors participated in the ANL Summer Program during 1999. Over a dozen former participants are currently enrolled in programs leading to doctorates in physics. A Michigan State University student who spent several summers working with J. Nolen at ATLAS as an undergraduate is currently engaged in thesis research in accelerator physics under Nolen's direction. Another student at the University of Michigan is doing his thesis research in the ANL Physics Division.

The program is an ongoing effort based upon personal interactions with a substantial number of qualified minority students and faculty. During visits to the Physics Departments of HBCU colleges (Historically Black Colleges and Universities) and other institutions with large minority populations, lectures are presented and there are discussions of activities in physics at ANL and other laboratories, graduate programs, etc. Other activities include attendance at meetings of minority organizations, appointment as Adjunct Professor at Hampton University including supervision of graduate thesis research, and serving on the Advisory Boards of the Centers of Excellence at both Hampton University and Morehouse College.

b. Nuclear Physics Award for Faculty in Undergraduate Institutions (B. Zeidman)

The goal of the 'Faculty Program', is to enhance undergraduate science education through faculty awards for minority and HBCU faculty that will allow them to directly participate in the ANL Physics Division research program and increase the number of undergraduates involved in research. A participant has obtained independent funding for continuing research collaboration with ANL that involves several undergraduate students. Several minority faculty members and students have been involved in research collaborations with the Physics Division for the past few years and will return this year. In order to maximize the scope of the program, existing educational programs are being utilized to supplement support for some of the participants and more formal collaborative arrangements are being discussed.

c. Scientific Support of SciTech Museum Exhibits and Outreach Programs (D. Henderson)

SciTech (Science and Technology Interactive Center) is a hands-on science museum located in Aurora, Illinois, near Argonne. With the help of volunteers and institutional support from Argonne, Fermilab, and several technological companies, SciTech has become an acknowledged leader in developing exhibits to teach modern science in a museum context.

D. Henderson of the Physics Division serves voluntarily as an exhibit developer on a regular basis. Several other staff members volunteer from time to time. The Physics Division collaborates with SciTech in developing exhibits for the museum and for use in Argonne's public educational activities. These efforts involve no significant programmatic costs.

STAFF MEMBERS OF THE PHYSICS DIVISION

Listed below are the staff of the Physics Division for the year ending December 31, 1999. The program headings indicate only the individual's current primary activity.

SCIENTIFIC STAFF

EXPERIMENTAL NUCLEAR PHYSICS STAFF

Regular Staff

Irshad Ahmad, Ph.D., University of California, 1966
Birger B. Back, Ph.D., University of Copenhagen, 1974
* R. Russell Betts, Ph.D., University of Pennsylvania, 1972
Michael P. Carpenter, Ph.D., University of Tennessee, 1987
† Cary N. Davids, Ph.D., California Institute of Technology, 1967
‡ Stuart J. Freedman, Ph.D., University of California, 1972
Donald F. Geesaman, Ph.D., State University of N.Y., Stony Brook, 1976
Donald S. Gemmell, Ph.D., Australian National University, 1960
§ Walter F. Henning, Ph.D., Technical University of Munich, 1968
David J. Hofman, Ph.D., State University of New York, Stonybrook, 1994
¶ Harold E. Jackson, Jr., Ph.D., Cornell University, 1959
‖ Robert V.F. Janssens, Ph.D. Univ. Catholique de Louvain, Belgium, 1978
Cheng-lie Jiang, Ph.D. China Institute of Atomic Energy, 1960
Teng Lek Khoo, Ph.D., McMaster University, 1972
**Walter Kutschera, Ph.D., University of Graz, Austria, 1965
Torben Lauritsen, Ph.D., State University of New York, 1990
Christopher J. Lister, Ph.D., University of Liverpool, 1977
Zheng-tian Lu, Ph.D., University of California, Berkeley, 1994
†† Jerry A. Nolen, Jr., Ph.D., Princeton University, 1965
Thomas P. O'Neill, Ph.D., California Institute of Technology, 1994
Peter N. Ostroumov, Ph.D. Moscow Engineering and Physical Institute, 1982
Richard C. Pardo, Ph.D., University of Texas, 1976
David H. Potterveld, Ph.D., Caltech, 1988
Karl Ernst Rehm, Ph.D., Technical University, Munich, 1973
Paul Reimer, Ph.D. University of Illinois, 1996
Guy Savard, Ph.D., McGill University, 1988
¶ John P. Schiffer, Ph.D., Yale University, 1954
Dariusz Seweryniak, Ph.D., Uppsala University, 1994
Kenneth W. Shepard, Ph.D., Stanford University, 1970
Kenneth Teh, Ph.D., Vanderbilt University, 1988
Alan H. Wuosmaa, Ph.D., University of Pennsylvania, 1989

---

* Joint appointment with the University of Illinois-Chicago.
† Adjunct Professor, Vanderbilt University.
‡ On leave of absence at the University of California, Berkeley.
§ Director of the Physics Division until November 1999. On leave of absence at GSI, Darmstadt.
¶ Associate Director of the Physics Division. Joint appointment with the University of Chicago.
‖ Adjunct Professor, North Carolina State University and Adjoint Professor, Vanderbilt University.
** On leave of absence at the University of Vienna.
†† Director of the ATLAS Facility. Adjunct Professor, Michigan State University.

Special Appointments

Lowell M. Bollinger, Ph.D., Cornell University, 1951
William J. Childs, Ph.D., University of Michigan, 1956
F. Paul Mooring, Ph.D., University of Wisconsin, 1951
* Michael Paul, Ph.D., Hebrew University of Jerusalem, 1973
Gilbert J. Perlow, Ph.D., University of Chicago, 1940
G. Roy Ringo, Ph.D., University of Chicago, 1940
Ralph E. Segel, Ph.D., Johns Hopkins University, 1955
George E. Thomas, B.A., Illinois Wesleyan, 1943
† Ben Zeidman, Ph.D. Washington University, 1957

THEORETICAL NUCLEAR PHYSICS STAFF

Regular Staff

Richard R. Chasman, Ph.D., University of California, 1959
Henning Esbensen, Ph.D., University of Aarhus, 1977
§ Tsung-Shung Harry Lee, Ph.D., University of Pittsburgh, 1973
Steven C. Pieper, Ph.D., University of Illinois, 1970
Craig T. Roberts, Ph.D., Flinders University of South Australia, 1989
Robert B. Wiringa, Ph.D., University of Illinois, 1978

Special Appointments

Paul Benioff, Ph.D., University of California, 1959
Arnold R. Bodmer, Ph.D., Manchester University, 1953
Fritz Coester, Ph.D., University of Zurich, 1944
Mitio Inokuti, Ph.D., University of Tokyo, 1962
Dieter Kurath, Ph.D., University of Chicago, 1951
Robert D. Lawson, Ph.D. Stanford University, 1953
Harry J. Lipkin, Ph.D., Princeton University, 1950
¶ Vijay Pandharipande, Ph.D., University of Bombay, 1969
Murray Peshkin, Ph.D., Cornell University, 1951

---

* Special Term Appointee from the Hebrew University of Jerusalem, Israel.
† Special Term Appointee. Adjunct Professor, Hampton University.
§ Adjunct Professor, University of Pittsburgh.
¶ Special Term Appointee from the University of Illinois, Urbana.

TEMPORARY APPOINTMENTS

Postdoctoral Appointees

John Arrington (from California Institute of Technology, Pasadena, CA):
Medium-energy physics.
(Juny 1998--)

Jacques Bloch (from University of Durham, NC.):
Theoretical physics studies.
(September 1998-December 1999)

Joseph A. Caggiano (from Michigan State University, E. Lansing, MI):
(Heavy-Ion Research at ATLAS)
(March 1999-)

Philippe Collon (from University of Vienna, Austria):
Heavy-ion research at ATLAS)
(November 1999-)

Chun-Yen Chen (from Kansas State University, Manhattan, KS):
Medium-energy physics.
(March 1998--)

Dirk De Schepper (from MIT, Cambridge, MA):
Medium-energy physics.
(May 1997--)

Nigel George (from Brookhaven National Laboratory, Upton, NY):
Medium-energy physics.
(May 1999-)

Kawtar Hafidi (from CEN, Saclay, France):
Medium-energy physics.
(November 1999-)

Andreas Heinz (from GSI, Darmstadt, Germany):
Heavy-ion research at ATLAS.
(February 1999-)

Robert Kaye (from Florida State University, Tallahassee, FL):
Linac development.
(April 1998—July 1999)

Michael Kelly (from University of Washington, Seattle, WA):
Heavy-ion research at ATLAS
(June 1999-)

Filipe G. Kondev (from Australian National University, Canberra, Australia):
Heavy-ion research at ATLAS.
(February 1999-)

Yimin Li (from Peking University, China):
Medium-energy physics.
(February 1999-)

Douglas Moehs (from Texas A&M University, College Station, TX):
ATLAS operations and development.
(August 1998--)

Bryon Mueller (from California Institute of Technology, Pasadena, CA):
Medium-energy physics.
(June 1997--)

Maria Petra (from University of Illinois, Urbana, IL):
ATLAS operations and development.
(February 1998--)

Riad Rejoub (from University of Nevada, Reno, NV):
ATLAS Operations and development.
(June 1998—October 1999)

Renato Roncaglia (from Indiana University, Bloomington, IN):
Theoretical studies.
(September 1997—September 1999)

Sebastian Schmidt (from University of Rostock, Germany):
Theoretical studies.
(February 1999-)

* Jazmin Schwartz (from Yale University, New Haven, CT):
Heavy-ion research at ATLAS.
(August 1999-)

Alejandro Sonzogni (from University of Washington, Seattle, WA):
Heavy-ion research at ATLAS.
(May 1997—August 1999)

Juha Uusitalo (from University of Jyvaskyla, Jyvaskyla, Finland):
Heavy-ion research at ATLAS.
(April 1997—April 1999)

Kalman Varga (from Atomki, Debracen, Hungary):
Theoretical studies.
(April 1998--)

Ingo Wiedenhover (from University of Cologne, Cologne, France):
Heavy-ion research at ATLAS.
(September 1997--)

*Resident Graduate Student until August 1999.

TECHNICAL AND ENGINEERING STAFF

(and areas of activity)

Kevin G. Bailey (B.S. University of Nebraska, 1989).
Technical assistance, medium-energy physics.

Brian T. Batzka (B.S. University of Houston, 1992).
ATLAS lead operator.

* Peter J. Billquist
ECR heavy-ion source, ATLAS operation.

John M. Bogaty (A.A.S. DeVry, 1961).
Electrical systems, ATLAS operation and development.

Benny E. Clifft (A.S.E.E., DeVry, 1959).
Electrical systems, ATLAS operation and development.

† Joseph Falout (B.S.M.E. University of Illinois, 1970).
Experimental equipment design.

John P. Greene (M.S. DePaul University, 1982).
Target preparation.

† Ray E. Harden (A.A.S. Milwaukee School of Engineering, 1957).
ATLAS operator

† Dale J. Henderson (B.S. Elmhurst College, 1951).
Detector development, technical assistance, heavy-ion physics.

James M. Joswick (A.A.S. Milwaukee School of Engineering, 1964).
ATLAS experimental equipment maintenance, technical assistance, heavy-ion physics.

† Raymond B. Kickert
ATLAS experimental equipment maintenance, technical assistance, heavy-ion physics.

† Paul Markovich (B.S. Purdue University, 1972).
Surface chemistry, ATLAS development and operation.

Thomas P. Mullen (B.S. Marquette University, 1966).
Division ESH/QA engineer.

Floyd Munson, Jr. (A.A.S. DeVry, 1966, B.S. Lewis University, 1993).
Control system for ATLAS.

Bruce G. Nardi (A.A.S. Morton Jr. College, 1967; A.A.S. DeVry, 1969).
Electronics design and maintenance.

Tom O'Connor (M.S. DePaul University, 1995).
Technical assistance, medium-energy physics.

---

* In charge of Dynamitron operations.
† Special Term Appointee.

Tad Pennington (M.S. University of Missouri, 1989; M.S. University of Alabama, 1998)
Detector development, technical assistance, heavy-ion physics.

Deborah Quock (M.S. Rice University, 1985)
Technical assistance, ATLAS control system.

James R. Specht (A.A.S. DeVry, 1964).
Cryogenics engineer. ATLAS development and operation.

Philip Strickhorn (B.S. DeVry, 1990).
Electrical and technical assistance with ATLAS operations.

Richard Vondrasek (B.S. University of Chicago, 1990).
ATLAS operator.

Philip R. Wilt (Johnstown Technical School 1973).
Electronics design and maintenance.

Bruce J. Zabransky (M.S. University of Illinois, Chicago, 1973).
Mechanical Engineer.

Gary P. Zinkann (B.S. DeVry, 1975).
ATLAS operations supervisor.

ADMINISTRATIVE STAFF

* Allan Bernstein, M.B.A., Rosary College, 1986
* James E. Nelson, B.A., University of Illinois, 1975
† Karen J. Thayer

VISITORS AND STUDENTS

Long-Term Visitors (at Argonne more than 4 months)

Jason Clark (from University of Manitoba, Canada):
Heavy-ion research at ATLAS.
(May 1999-)

Christopher Fasano (from Monmouth College, Monmouth, IL):
Theoretical studies.
(February 1999-)

Hiroshi Fukutani (from University of Manitoba, Canada):
Heavy-ion research at ATLAS.
(May 1998—June 1999)

*Assistant Division Director
†Special Term Appointee

Subhendu Ghosh (from Nuclear Science Centre, New Delhi, India):
ATLAS development.
(August 1997—August 1999)

Boris Harss (from Technical University of Munich, Germany):
Heavy-ion research at ATLAS.
(June 1997—October 1999)

* Donald McLeod (from University of Illinois, Chicago, IL):
Heavy-ion research at ATLAS.
(June 1994--)

Michael Maier (from University of Heidelberg, Germany):
Heavy-ion research at ATLAS.
(April-October 1999)

Daniel Martin (from McGill University, Montreal, Quebec):
Heavy-ion research at ATLAS.
(November 1998—January 1999)

† Peter N. Ostroumov (from Moscow Engineering and Physical Institute, Russia):
ATLAS development.
(June-October 1999)

Gian-Luca Poli (from University of Milan, Italy):
Heavy-ion research at ATLAS.
(December 1999-)

Prakash Potukuchi (from Nuclear Science Centre, New Delhi, India):
ATLAS development.
(March 1996—September 1999)

Kumar Sharma (from University of Manitoba, Canada):
Heavy-ion research at ATLAS.
(July 1998--)

Sunniva Siem (from University of Oslo, Norway):
Heavy-ion research at ATLAS.
(January 1998—August 1999)

Rolf Siemssen (from KVI, Groningen, Netherlands):
Heavy ion rresearch at ATLAS.
(October 1998--)

James Stewart (from University of Liverpool, UK):
Medium-energy physics.
(March 1998—March 1999)

Joseph V. Vaz (from Universit of Manitoba, Canada):
Heavy-ion Research at ATLAS.
(November 1999-)

---

*Guest Faculaty Research Participant.
†Joined regular staff November 1999.

Short-Term Visitors (at ANL less than 4 months)

* Nour-eddi Berrah (Western Michigan University, Kalamazoo, MI):
Atomic physics research.
(October 1991--)

Chantal Boudreau (from McGill University, Montreal, Quebec):
Heavy-ion research at ATLAS.
(June-August 1999)

Scott Cohen (from University of Portland, Portland, OR):
Theoretical studies.
(May-June 1999)

Frank Dohrmann (from University of Hamburg, Germany):
Medium-energy physics.
(October-December 1999)

Susan Fischer (DePaul University, Chicago, IL):
Heavy-ion research at ATLAS.
(October 1998--)

Clive Halliwell (University of Illinois, Chicago, IL):
Heavy-ion research at ATLAS.
(June 1998--)

Jeffrey Hangst (University of Aarhus, Denmark):
Heavy-ion research at ATLAS.
(April 1995--)

* Edward Hohman (York Township High School, Lyons, IL):
Summer student coordinator.
(July 1999)

Mikhail Ivanov (JINR, Dubna, Russia):
Nuclear theory studies.
(September 1999)

Yori Kalinovsky (from Bogoliubov Lab. for Theoretical Physics, Russia):
Theoretical studies.
(April-May 1999)

Judith Katzy (University of Illinois, Chicago, IL):
Heavy-ion research at ATLAS.
(February 1998--)

* Wojciech Kucewicz (University of Illinois, Chicago, IL):
Heavy-ion research at ATLAS.
(April 1998--)

---

* Guest Faculty Research Participant.

Daniel Martin (from McGill University, Montreal, Quebec):
Heavy-ion research at ATLAS.
(November 1998-January 1999)

Falk Meissner (from DESY, Hamburg, Germany):
Medium-energy physics.
(March 1999)

Rachid Nouicer (University of Chicago, Chicago, IL):
Heavy-ion research at ATLAS.
(April 1998--)

Yau Wah (University of Chicago, Chicago, IL):
Heavy-ion research at ATLAS.
(January 1998--)

Resident Graduate Students

Hanan Amro (North Carolina State University, Raleigh, NC):
Heavy-ion research at ATLAS.
(January 1995-August 1999)

Larry Todd Brown (Vanderbilt University, Nashville, TN):
FMA development at ATLAS
(January 1994—December 1999)

Peter Cabauy (from University of Michigan, Ann Arbor, MI):
Theoretical studies.
(May-November 1999)

Patrick Crotty (University of Chicago, Chicago, IL):
Heavy-ion research at ATLAS.
(January 1998-January 1999)

David Gaskell (Oregon State University, Corvallis, OR):
Medium-energy physics.
(September 1998--)

Burt Holzman (University of Illinois, Chicago, IL):
Heavy-ion research at ATLAS.
(June 1997--)

Mauricio Portillo (Michigan State University, E. Lansing, MI):
Accelerator development.
(September 1995--)

Jennifer Ressler (from University of Maryland, College Park, MD):
Heavy-ion research at ATLAS.
(January 1999-)

* Jazmin Schwartz (Yale University, New Haven, CT):
Heavy-ion research at ATLAS.
(May 1995—August 1999)

*Postdoctoral appointee as of August 1999.

Guest Graduate Students

Khalefeh Abu Saleem (from Illinois Institute of Technology, Chicago, IL):
Heavy-ion research at ATLAS.
(June 1999-)

Francesca Borasi (University of Milan, Milan, Italy):
Heavy-ion research at ATLAS.
(November 1997—May 1999)

Andrew Cassidy (from McGill University, Montreal, Quebec):
Heavy-ion research at ATLAS.
(June-August 1999)

Xu Du (from Northwestern University, Evanston, IL):
Medium-energy physics.
(June 1999-)

Dipangkar Dutta (Northwestern University, Evanston, Illinois):
Medium-energy studies.
(June 1994—December 1999)

William Lee (from Georgia State University, Atlanta, GA):
Medium-energy physics.
(September-December 1999)

Kenneth Nollett (University of Chicago, Chicago, IL
Theoretical studies.
(May 1997—June 1999)

Undergraduate Students

Martin Alcorta (University of Chicago)
Teresa Barlow (Illinois Benedictine College)
Nathaniel Burke (North Central College)
Bobby Chapin (University of St. Francis)
Edward Collins (Tulane University)
Joseph Czernick (Benedictine University)
Scott Davis (University of Illinois-Urbana)
Sorge Diaz (Florida International University)
Jessica Dunmore (University of Hartford)
Javier Figueroa (Benedictine University)
Juan Figueroa (Benedictine University)
Eric Hemmeter (Bates College)
Lisa Lim (North Central College)
Brian Napolitano (College of DuPage)
Jennifer Nelson (University of Illinois-Urbana)
Jason Noeth (St. Norbert College)
Timothy Peceniak (North Central College)
Keri Unterzuber (North-Central College)
Michael Witt (North Central College)

Pre-College Program (Just Graduated from High School)
(June--August 1999)

Lindsay Deremer (Oak Park-River Forest High School)
Matthew Dickerson (Hinsdale Central High School)
Alice Lam (Downers Grove North High School)
Scott Styles (Bolingbrook High School)
Richard Vanswol (Chicago Christian High School)

High School Student Aide

Silvia Palomino (Joliet Central High School)
Angela Baity (Plainfield High School)

PUBLICATIONS DURING 1999

(The arrangement follows approximately the Table of Contents)

HEAVY-ION NUCLEAR PHYSICS RESEARCH

Ground-State Band and Deformation of the Z = 102 Isotope ^{254}No
P. Reiter, T. L. Khoo, C. J. Lister, D. Seweryniak, I. Ahmad, M. Alcorta, M. P. Carpenter, J. A. Cizewski, C. N. Davids, G. Gervais, J. P. Greene, W. F. Henning, R. V. F. Janssens, T. Lauritsen, S. Siem, A. A. Sonzogni, D. Sullivan, J. Uusitalo, I. Wiedenhöver, N. Amzal, P. A. Butler, A. J. Chewter, K. Y. Ding, N. Fotiades, J. D. Fox, P. T. Greenlees, R.-D. Herzberg, G. D. Jones, W. Korten, M. Leino, and K. Vetter
Phys. Rev. Lett. **82**, 509-512 (1999)

Decay Out of the Doubly-Magic Superdeformed Band in the N = Z Nucleus ^{60}Zn
C. E. Svensson, D. Rudolph, C. Baktash, M. A. Bentley, J. A. Cameron, M. P. Carpenter, M. Devlin, J. Eberth, S. Flibotte, A. Galindo-Uribarri, G. Hackman, D. S. Haslip, R. V. F. Janssens, D. R. LaFosse, T. J. Lampman, I. Y. Lee, F. Lerma, A. O. Macchiavelli, J. M. Nieminen, S. D. Paul, D. C. Radford, P. Reiter, L. L. Riedinger, D. G. Sarantites, B. Schaly, D. Seweryniak, O. Thelen, H. G. Thomas, J. C. Waddington, D. Ward, W. Weintraub, J. N. Wilson, C. H. Yu, A. V. Afanasjev, and I. Ragnarsson
Phys. Rev. Lett. **82**, 3400-3404 (1999)

Stellar Reactions with Short-Lived Nuclei: ^{17}F(p,α)^{14}O
B. Harss, J. P. Greene, D. Henderson, R. V. F. Janssens, C. L. Jiang, J. Nolen, R. C. Pardo, K. E. Rehm, J. P. Schiffer, R. H. Siemssen, A. A. Sonzogni, J. Uusitalo, I. Wiedenhöver, M. Paul, T. F. Wang, F. Borasi, R. E. Segel, J. Blackmon, M. S. Smith, A. Chen, and P. Parker
Phys. Rev. Lett. **82**, 3964-3967 (1999)

Discovery of Fine Structure in the Decay of the Highly Deformed Proton Emitter ^{131}Eu
A. A. Sonzogni, C. N. Davids, P. J. Woods, D. Seweryniak, M. P. Carpenter, J. J. Ressler, J. Schwartz, J. Uusitalo, and W. B. Walters
Phys. Rev. Lett. **83**, 1116-1118 (1999)

Transition Rates Between Mixed Symmetry States: First Measurement in ^{94}Mo
N. Pietralla, C. Fransen, D. Belic, P. von Brentano, C. Frieβner, U. Kneissl, A. Linnemann, A. Nord, H. H. Pitz, T. Otsuka, I. Schneider, V. Werner, and I. Wiedenhöver
Phys. Rev. Lett. **83**, 1303-1306 (1999)

Octupole Correlations in the Pu Isotopes: From Vibration to Static Deformation?
I. Wiedenhöver, R. V. F. Janssens, G. Hackman, I. Ahmad, J. P. Greene, H. Amro, P. K. Bhattacharyya, M. P. Carpenter, P. Chowdhury, J. Cizewski. D. Cline, T. L. Khoo, T. Lauritsen, C. J. Lister, A. O. Macchiavelli, D. T. Nisius, P. Reiter, E. H. Seabury, D. Seweryniak, S. Siem, A. Sonzogni, J. Uusitalo, and C. Y. Wu
Phys. Rev. Lett. **83**, 2143-2146 (1999)

Sympathetic Crystallization of Trapped Ions
P. Bowe, L. Hornekaer, C. Brodersen, M. Drewsen, J. S. Hangst, and J. P. Schiffer
Phys. Rev. Lett. **82**, 2071-2074 (1999)

Density Limitations in a Stored Laser-Cooled Ion Beam
N. Madsen, P. Bowe, M. Drewsen, L. H. Hornekaer, N. Kjaergaard, A. Labrador, J. S. Nielsen, J. P. Schiffer, P. Shi, and J. S. Hangst
Phys. Rev. Lett. **83**, 4301-4304 (1999)

Single Particle Signatures in High-Spin, Quasicontinuum States in ^{193,194}Hg from g-Factor Measurements
L. Weissman, R. H. Mayer, G. Kumbartzki, N. Benczer-Koller, C. Broude, J. A. Cizewski, M. Hass, J. Holden, R. V. F. Janssens, T. Lauritsen, I. Y. Lee, A. O. Macchiavelli, D. P. McNabb, and M. Satteson
Phys. Lett. **B446**, 22-27 (1999)

A New Measurement of the Strength of the Superallowed Fermi Branch in the Beta Decay of ^{10}C with GAMMASPHERE
B. K. Fujikawa, S. J. Asztalos, R. M. Clark, M.-A. Deleplanque-Stephens, P. Fallon, S. J. Freedman, J. P. Greene, I.-Y. Lee, L. J. Lising, A. O. Macchiavelli, R. W. MacLeod, J. C. Reich, M. A. Rowe, S.-Q. Shang, F. S. Stephens, and E. G. Wasserman
Phys. Lett. **B449**, 6-11 (1999)

Measurements of g-Factors of Excited States in Ba and Ce Nuclei Using γ Rays from Secondary Fission Fragments
A. G. Smith, G. S. Simpson, J. Billowes, J. L. Durell, P. J. Dagnall, S. J. Freeman, M. Leddy, A. A. Roach, J. F. Smith, A. Jungclaus, K. P. Lieb, C. Teich, B. J. P. Gall, F. Hoellinger, N. Schulz, I. Ahmad, J. Greene, and A. Algora
Phys. Lett. **B453**, 206-210 (1999)

Radioactive Decay of ^{80}Y and Low-Lying States in ^{80}Sr
J. Doring, A. Aprahamian, R. C. de Haan, J. Gorres, H. Schatz, M. Wiescher, W. B. Walters, L. T. Brown, C. N. Davids, C. J. Lister, and D. Seweryniak
Phys. Rev. C **59**, 59-70 (1999)

Second Proton and Neutron Alignments in the Doubly-Odd Nuclei ^{154,156}Tb
D. J. Hartley, J. L. Allen, T. B. Brown, F. G. Kondev, J. Pfohl, M. A. Riley, S. M. Fischer, R. V. F. Janssens, D. T. Nisius, P. Fallon, W. C. Ma, and J. Simpson
Phys. Rev. C **59**, 1171-1174 (1999)

High-K Isomers in Neutron-Rich Hafnium Nuclei At and Beyond the Stability Line
R. D'Alarcao, P. Chowdhury, E. H. Seabury, P. M. Walker, C. Wheldon, I. Ahmad, M. P. Carpenter, G. Hackman, R. V. F. Janssens, T. L. Khoo, C. J. Lister, D. Nisius, P. Reiter, D. Seweryniak, and I. Wiedenhöver
Phys. Rev. C **59**, R1227-R1231 (1999)

Yrast States of the Proton Drip Line Nucleus ^{106}Sb
D. Sohler, J. Cederkall, M. Lipoglavsek, Zs. Dombradi, M. Gorska, J. Persson, D. Seweryniak, I. Ahmad, A. Atac, R. A. Bark, J. Blomqvist, M. P. Carpenter, B. Cederwall, C. N. Davids, C. Fahlander, S. M. Fischer, H. Grawe, G. Hackman, R. V. F. Janssens, A. Johnson, A. Kerek, W. Klamra, J. Kownacki, C. J. Lister, S. Mitarai, D. Nisius, L.-O. Norlin, J. Nyberg, G. Poli, P. Reiter, J. J. Ressler, H. A. Roth, J. Schwartz, G. Sletten, J. Uusitalo, W. B. Walters, and M. Weiszflog
Phys. Rev. C **59**, 1324-1327 (1999)

Spectroscopy of the Proton Emitter ^{109}I
C.-H. Yu, A. Galindo-Uribarri, S. D. Paul, M. P. Carpenter, C. N. Davids, R. V. F. Janssens, C. J. Lister, D. Seweryniak, J. Uusitalo, and B. D. MacDonald
Phys. Rev. C **59**, R1834-R1838 (1999)

High-Spin Structure in ^{181,183}Au
W. F. Mueller, H. Q. Jin, J. M. Lewis, W. Reviol, L. L. Riedinger, M. P. Carpenter, C. Baktash, J. D. Garrett, N. R. Johnson, I. Y. Lee, F. K. McGowan, C.-H. Yu, and S. Cwiok
Phys. Rev. C **59**, 2009-2032 (1999)

Deformed Negative-Parity Excitations in ^{71}As
N. Fotiades, J. A. Cizewski, C. J. Lister, C. N. Davids, R. V. F. Janssens, D. Seweryniak, M. P. Carpenter T. L. Khoo, T. Lauritsen, D. Nisius, P. Reiter, J. Uusitalo, I. Wiedenhöver, A. O. Macchiavelli, and R. W. MacLeod
Phys. Rev. C **59**, 2919-2922 (1999)

Yrast Spectroscopy of N = 82,83 Isotopes ^{136}Xe and ^{137}Xe from ^{248}Cm Fission
P. J. Daly, P. Bhattacharyya, C. T. Zhang, Z. W. Grabowski, R. Broda, B. Fornal, I. Ahmad, T. Lauritsen, L. R. Morss, W. Urban, W. R. Phillips, J. L. Durell, M. J. Leddy, A. G. Smith, B. J. Varley, N. Schulz, E. Lubkiewicz, M. Bentaleb, and J. Blomqvist
Phys. Rev. C **59**, 3066-3070 (1999)

Proton Emission from the Closed Neutron Shell Nucleus ^{155}Ta
J. Uusitalo, C. N. Davids, P. J. Woods, D. Seweryniak, A. A. Sonzogni, J. C. Batchelder, C. R. Bingham, T. Davinson, J. deBoer, D. J. Henderson, H. J. Maier, J. J. Ressler, R. Slinger, and W. B. Walters
Phys. Rev. C **59**, R2975-R2978 (1999)

Proton and α Radioactivity Below the $Z = 82$ Shell Closure

G. Poli, C. N. Davids, P. J. Woods, D. Seweryniak, J. C. Batchelder, L. T. Brown, C. R. Bingham, M. P. Carpenter, L. F. Conticchio, T. Davinson, J. DeBoer, S. Hamada, D. J. Henderson, R. J. Irvine, R. V. F. Janssens, H. J. Maier, L. Müller, F. Soramel, K. S. Toth, W. B. Walters, and J. Wauters

Phys. Rev. C **59**, R2979-R2983 (1999)

Relative Quadrupole Deformations for Decoupled Structures in the Odd-Odd ^{130}Pr and ^{132}Pr Nuclei

F. G. Kondev, M. A. Riley, D. J. Hartley, T. B. Brown, R. W. Laird, M. Lively, J. Pfohl, R. K. Sheline, R. M. Clark, P. Fallon, D. G. Sarantites, M. Devlin, D. R. LaFosse, F. Lerma, R. Wadsworth, I. M. Hibbert, N. J. O'Brien, E. S. Paul, D. T. Joss, P. J. Nolan, S. L. Shepherd, D. E. Archer, and J. Simpson

Phys. Rev. C **59**, 3076-3085 (1999)

α-Decay Rates of ^{180,182,184}Pb and the Z = 82 Shell Closure

K. S. Toth, C. R. Bingham, J. C. Batchelder, L. T. Brown, L. F. Conticchio, C. N. Davids, R. J. Irvine, D. Seweryniak, D. M. Moltz, W. B. Walters, J. Wauters, and E. F. Zganjar

Phys. Rev. C **60**, 011302/1-5 (1999)

Differential Quadrupole Moment Measurements of the $1/2^+[660]$ ($i_{13/2}$) Neutron Intruder Band in ^{133}Nd and ^{135}Nd

F. G. Kondev, M. A. Riley, D. J. Hartley, T. B. Brown, R. W. Laird, M. Lively, J. Pfohl, R. K. Sheline, E. S. Paul, D. T. Joss, P. J. Nolan, S. L. Shepherd, R. M. Clark, P. Fallon, D. G. Sarantites, M. Devlin, D. R. LaFosse, F. Lerma, R. Wadsworth, I. M. Hibbert, N. J. O'Brien, J. Simpson, and D. E. Archer

Phys. Rev. C **60**, 011303/1-5 (1999)

Decay Properties of the New Isotopes ^{172}Hg and ^{173}Hg

D. Seweryniak, J. Uusitalo, M. P. Carpenter, D. Nisius, C. N. Davids, C. R. Bingham, L. T. Brown, L. Conticchio, D. J. Henderson, R. V. F. Janssens, W. B. Walters, J. Wauters, and P. J. Woods

Phys. Rev. C **60**, 031304/1-4 (1999)

Odd-Even Staggering in the $\pi_{g9/2}\nu_{g9/2}$ Band in ^{72}Br

N. Fotiades, J. A. Cizewski, C. J. Lister, C. N. Davids, R. V. F. Janssens, D. Seweryniak, M. P. Carpenter, T. L. Khoo, T. Lauritsen, D. Nisius, P. Reiter, J. Uusitalo, I. Wiedenhöver, A. O. Macchiavelli, and R. W. MacLeod

Phys. Rev. C **60**, 057302/1-3 (1999)

Interlayer Phase Correlation of the Vortex System Around the Coupling Transition in $Bi_2Sr_2CaCu_2O_y$ Containing Columnar Defects
Y. Tsuchiya, T. Hanaguri, H. Yasuda, A. Maeda, M. Sasase, K. Hojou, D. G. Steel, J. U. Lee, and D. J. Hofman
Phys. Rev. B **59**, 11568-11574 (1999)

Migration from the Normal to the Highly Deformed Minimum in ^{131}Nd
D. J. Hartley, W. Reviol, L. L. Riedinger, F. G. Kondev, A. Galindo-Uribarri, D. G. Sarantites, H. Q. Jin, D. R. LaFosse, S. M. Mullins, B. H. Smith, and J. N. Wilson
Phys. Rev. C **60**, 041301/1-5 (1999)

Fission Hindrance in Hot ^{216}Th: Evaporation Residue Measurements
B. B. Back, D. J. Blumenthal, C. N. Davids, D. J. Henderson, R. Hermann, D. J. Hofman, C. L. Jiang, H. T. Penttila, and A. H. Wuosmaa
Phys. Rev. C **60**, 044602/1-7 (1999)

Near Yrast Study of the *fpg* Shell Nuclei ^{58}Ni, ^{61}Cu and ^{61}Zn
S. M. Vincent, P. H. Regan, S. Mohammadi, D. Blumenthal, M. Carpenter, C. N. Davids, W. Gelletly, S. S. Ghugre, D. J. Henderson, R. V. F. Janssens, M. Hjorth-Jensen, B. Kharraja, C. J. Lister, C. J. Pearson, D. Seweryniak, J. Schwartz, J. Simpson, and D. D. Warner
Phys. Rev. C **60**, 064308/1-18 (1999)

Positron-Electron Pairs Produced in Heavy-Ion Collisions
I. Ahmad, Sam M. Austin, B. B. Back, R. R. Betts, F. P. Calaprice, K. C. Chan, A. Chishti, C. M. Conner, R. W. Dunford, J. D. Fox, S. J. Freedman, M. Freer, S. B. Gazes, A. L. Hallin, Th. Happ, D. Henderson, N. I. Kaloskamis, E. Kashy, W. Kutschera, J. Last, C. J. Lister, M. Liu, M. R. Maier, D. M. Mercer, D. Mikolas, P. A. A. Perera, M. D. Rhein, D. E. Roa, J. P. Schiffer, T. A. Trainor, P. Wilt, J. S. Winfield, M. Wolanski, F. L. H. Wolfs, A. H. Wuosmaa, A. R. Young, and J. E. Yurkon
Phys. Rev. C **60**, 064601/1-14 (1999)

Correlated Spins of Complementary Fragment Pairs in the Spontaneous Fission of ^{252}Cf
A. G. Smith, G. S. Simpson, J. Billowes, P. J. Dagnall, J. L. Durell, S. J. Freeman, M. Leddy, W. R. Phillips, A. A. Roach, J. F. Smith, A. Jungclaus, K. P. Lieb, C. Teich, B. J. P. Gall, F. Hoellinger, N. Schulz, I. Ahmad, J. P. Greene, and A. Algora
Phys. Rev. C **60**, 064611/1-4 (1999)

Time-Decay History of Normal-Deformation High-Spin States in ^{193,194}Hg
L. Weissman, R. H. Mayer, N. Benczer-Koller, C. Broude, J. A. Cizewski, M. Hass, J. Holden, R. V. F. Janssens, G. Kumbartzki, T. Lauritsen, I. Y. Lee, A. O. Macchiavelli, N. Matt, D. P. McNabb, and M. Satteson
Nucl. Phys. **A645**, 191-202 (1999)

Spectroscopy of Rn, Ra and Th Isotopes Using Multi-Nucleon Transfer Reactions
J. F. C. Cocks, D. Hawcroft, N. Amzal, P. A. Butler, K. J. Cann, P. T. Greenlees, G. D. Jones, S. Asztalos, R. M. Clark, M. A. Deleplanque, R. M. Diamond, P. Fallon, I. Y. Lee, A. O. Macchiavelli, R. W. MacLeod, F. S. Stephens, P. Jones, R. Julin, R. Broda, B. Fornal, J. F. Smith, T. Lauritsen, P. Bhattacharyya, and C. T. Zhang
Nucl. Phys. **A645**, 61-91 (1999)

Possible Observation of the $1/2^+[880]$ Orbital in $^{249}_{96}$Cm
I. Ahmad, B. B. Back, R. R. Chasman, J. P. Greene, T. Ishii, L. R. Morss, G. P. A. Berg, A. D. Bacher, C. C. Foster, W. R. Lozowski, W. Schmitt, E. J. Stephenson, and T. Yamanaka
Nucl. Phys. **A646**, 175-186 (1999)

Strength Distribution of γ-Transitions Deexciting Superdeformed Rotational Bands
A. P. Lopez-Martens, T. Dossing, T. L. Khoo, A. Korichi, F. Hannachi, I. J. Calderin, T. Lauritsen, I. Ahmad, M. P. Carpenter, S. M. Fischer, G. Hackman, R. V. F. Janssens, D. Nisius, P. Reiter, H. Amro, and E. F. Moore
Nucl. Phys. **A647**, 217-245 (1999)

High-Accuracy Mass Determination of Unstable Cesium and Barium Isotopes
F. Ames, G. Audi, D. Beck, G. Bollen, M. de Saint-Simon, R. Jertz, H.-J. Kluge, A. Kohl, M. Konig, D. Lunney, I. Martel, R. B. Moore, T. Otto, Z. Patyk, H. Raimbault-Hartmann, G. Rouleau, G. Savard, E. Schark, S. Schwarz, L. Schweikhard, H. Stolzenberg, J. Szerypo, and the ISOLDE Collaboration
Nucl. Phys. **A651**, 3-30 (1999)

Nuclear Physics: The Core of Matter, the Fuel of Stars
John P. Schiffer
Nucl. Phys. News **9**, 5-9 (1999)

Production of Neutron-Rich Isotopes by Cold Fragmentation in the Reaction ^{197}Au + Be at 950 *A* MeV
J. Benlliure, K.-H. Schmidt, D. Cortina-Gil, T. Enqvist, F. Farget, A. Heinz, A. R. Junghans, J. Pereira, and J. Taieb
Nucl. Phys. **A660**, 87-100 (1999)

Superdeformation in ^{193}Pb: Observation of Three Additional Excited Bands
D. Roßbach, A. N. Wilson, C. Barton, M. P. Carpenter, D. M. Cullen, H. Hübel, R. V. F. Janssens, S. L. King, A. Korichi, and A. T. Reed
Nucl. Phys. **A660**, 393-405 (1999)

α-Decay Characteristics of Neutron-Deficient ^{190,192}Po Nuclei and Alpha Branching Ratios of ^{186,188}Pb Isotopes

A. N. Andreyev, N. Bijnens, M. Huyse, P. Van Duppen, M. Leino, T. Enqvist, P. Kuusiniem, W. Trzaska, J. Uusitalo, N. Fotiades, J. A. Cizewski, D. P. McNabb, K. Y. Ding, C. N. Davids, R. V. F. Janssens, D. Seweryniak, M. P. Carpenter, H. Amro, P. Decrock, P. Reiter, D. Nisius, L. T. Brown, S. Fischer, T. Lauritsen, J. Wauters, C. R. Bingham, and L. F. Conticchio
J. Phys. G: Nucl. Part. Phys. **25**, 835-837 (1999)

Strangeness Production in High Density Baryon Matter

R. Ganz for the E917 Collaboration: B. B. Back, R. R. Betts, H. C. Britt, J. Chang, W. C. Chang, C. Y. Chi, Y. Y. Chu, J. B. Cumming, J. C. Dunlop, W. Eldredge, S. Y. Fung, R. Ganz, E. Garcia, A. Gillitzer, G. Heintzelman, W. F. Henning, D. J. Hofman, B. Holzman, J. H. Kang, E. J. Kim, S. Y. Kim, Y. Kwon, D. McLeod, A. Mignerey, M. Moulson, V. Nanal, C. Ogilvie, R. Pak, A. Ruangma, D. E. Russ, R. K. Seto, P. J. Stanskas, G. S. F. Stephans, H. Wang, F. L. H. Wolfs, A. H. Wuosmaa, H. Xiang, G. H. Xu, H. B. Yao, and C. M. Zou
J. Phys. G: Nucl. Part. Phys. **25**, 247-253 (1999)

Exploring the $I = 50 - 60\hbar$ Domain: Collective and Terminating Structures in ^{156}Dy, ^{159}Er and ^{160}Er

F. G. Kondev, M. A. Riley, J. Simpson, R. V. F. Janssens, A. V. Afanasjev, I. Ragnarsson, T. B. Brown, D. J. Hartley, M. P. Carpenter, P. Fallon, S. M. Fischer, T. L. Khoo, T. Lauritsen, W. C. Ma, J. F. Sharpey-Schafer, J. C. Lisle, and C. A. Kalfas
J. Phys. G: Nucl. Part. Phys. **25**, 897-899 (1999)

α-Decay Characteristics of Neutron-Deficient ^{190,192}Po Nuclei and Alpha Branching Ratios of ^{186,188}Pb Isotopes

A. N. Andreyev, N. Bijnens, M. Huyse, P. Van Duppen, M. Leino, T. Enqvist, P. Kuusiniemi, W. Trzaska, J. Uusitalo, N. Fotiades, J. A. Cizewski, D. P. McNabb, K. Y. Ding, C. N. Davids, R. V. F. Janssens, D. Seweryniak, M. P. Carpenter, H. Amro, P. Decrock, P. Reiter, D. Nisius, L. T. Brown, S. Fischer, T. Lauritsen, J. Wauters, C. R. Bingham, and L. F. Conticchio
J. Phys. G: Nucl. Part. Phys. **25**, 835-837 (1999)

High Spin States in ^{128}Ba

O. Vogel, R. S. Chakrawarthy, A. Dewald, P. Petkov, K. Jessen, J. Gableske, P. von Brentano, D. Bazzacco, A. Gizon, J. Gizon, S. Lunardi, D. R. Napoli, P. Pavan, C. Rossi Alvarez, and I. Wiedenhöver
Eur. Phys. J. A **4**, 323-325 (1999)

Identification of a High-K Isomer in Neutron-Rich ^{185}Ta

C. Wheldon, P. M. Walker, R. D'Alarcao, P. Chowdhury, C. J. Pearson, E. H. Seabury, I. Ahmad, M. P. Carpenter, D. M. Cullen, G. Hackman, R. V. F. Janssens, T. L. Khoo, D. Nisius, and P. Reiter
Eur. Phys. J. A **5**, 353-355 (1999)

New Excitation Scheme of ^{139}Cs
A. Nowak, W. Urban, W. Kurcewicz, T. Rząca-Urban, H. Mach, B. Fogelberg, J. L. Durell, M. J. Leddy, M. A. Jones, W. R. Phillips, A. G. Smith, B. J. Varley, M. Bentaleb, E. Lubkiewicz, N. Schulz, I. Ahmad, and L. R. Morss
Eur. Phys. J. A **6**, 1-3 (1999)

In-Beam Study of ^{254}No
M. Leino, H. Kankaanpaa, R.-D. Herzberg, A. J. Chewter, F. P. Heβberger, Y. Le Coz, F. Becker, P. A. Butler, J. F. C. Cocks, O. Dorvaux, K. Eskola, J. Gerl, P. T. Greenlees, K. Helariutta, M. Houry, G. D. Jones, P. Jones, R. Julin, S. Juutinen, H. Kettunen, T. L. Khoo, A. Kleinbohl, W. Korten, P. Kuusiniemi, R. Lucas, M. Muikku, P. Nieminen, R. D. Page, P. Rahkila, P. Reiter, A. Savelius, Ch. Schlegel, Ch. Theisen, W. H. Trzaska, and H.-J. Wollersheim
Eur. Phys. J. A **6**, 63-69 (1999)

First Observation of Excited States in the Neutron-Rich Nucleus ^{138}Te
F. Hoellinger, B. J. P. Gall, N. Schulz, W. Urban, I. Ahmad, M. Bentaleb, J. L. Durell, M. A. Jones, M. Leddy, E. Lubkiewicz, L. R. Morss, W. R. Phillips, A. G. Smith, and B. J. Varley
Eur. Phys. J. A **6**, 375-376 (1999)

Behavior of Intruder Based States in Light Bi and Tl Isotopes: the Study of ^{187}Bi α Decay
J. C. Batchelder, K. S. Toth, C. R. Bingham, L. T. Brown, L. F. Conticchio, C. N. Davids, R. J. Irvine, D. Seweryniak, W. B. Walters, J. Wauters, E. F. Zganjar, J. L. Wood, C. DeCoster, B. Decroix, and K. Heyde
Eur. Phys. J. A **5**, 49-52 (1999)

Nuclear Physics at the End of the Century
E. M. Henley and J. P. Schiffer
Rev. Mod. Phys. **71**, S205-S219 (1999)

Measured Level Lifetimes for the Coronal Transitions of Fe X and Fe XIV
D. P. Moehs and D. A. Church
Astrophys. J. **516**, L111-L113 (1999)

Nuclear Physics at the End of the Century
E. M. Henley and J. P. Schiffer
More Things in Heaven and Earth: A Celebration of Physics at the Millennium, ed. Benjamin Bederson (Springer Verlag, New York, 1999) pp. 345-369

Preparation of Actinide Targets by Molecular Plating for Coulomb Excitation Studies at ATLAS
John P. Greene, Robert V. F. Janssens, and Irshad Ahmad
Proceedings of the 19th World Conference of the INTDS (Nuclear Targets - Preparation, Characterization, and Use), Oak Ridge, TN, October 5-9, 1998; Nucl. Instrum. Methods **A438**, 119-123 (1999)

Structure and Formation Mechanism of the Transfermium Isotope ^{254}No
P. Reiter, T. L. Khoo, C. J. Lister, D. Seweryniak, I. Ahmad, M. Alcorta, M. P. Carpenter, J. A. Cizewski, C. N. Davids, G. Gervais, J. P. Greene, W. F. Henning, R. V. F. Janssens, T. Lauritsen, S. Siem, A. A. Sonzogni, D. Sullivan, J. Uusitalo, I. Wiedenhöver, N. Amzal, P. A. Butler, A. J. Chewter, K. Y. Ding, N. Fotiades, J. D. Fox, P. T. Greenlees, R.-D. Herzberg, G. D. Jones, W. Korten, M. Leino, and K. Vetter
Proceedings of Conference "Nuclear Structure '98", August 10-15, 1998, Gatlinburg, TN, ed. C. Baktash, AIP Conference Proceedings 482, pp. 121-126 (1999)

Proton and Cluster Emission at the Proton Drip Line
G. Poli, J. C. Batchelder, C. R. Bingham, D. J. Blumenthal, R. Bonetti, L. T. Brown, R. Collatz, L. Conticchio, C. N. Davids, J. de Boer, A. Guglielmetti, N. Gunn, D. J. Henderson, Z. Hu, R. J. Irvine, R. Kirchner, H. J. Maier, L. Mueller, P. B. Price, E. Roeckl, D. J. Seweryniak, F. Soramel, Y. Szerypo, K. S. Toth, W. B. Walters, B. A. Weaver, A. Westphal, and P. J. Woods
Proceedings of the 8th International Conference on Nuclear Reaction Mechanisms, Villa Monastero, Varenna, Italy, 9-14 June 1997, pp. 624-633 (1999)

The Status of APS, BESSRC, and NEET
I. Ahmad, R. W. Dunford, H. Esbensen, D. S. Gemmell, E. P. Kanter, B. Kraessig, U. Rutt, and S. H. Southworth
Atomic and Molecular Physics at High Brilliance Synchrotron Radiation Facilities, Proceedings of the 1998 International Workshop on Atomic and Molecular Physics at High Brilliance Synchrotron Radiation Facilities, Hyogo, Japan, 4-6 November 1998, pp. 19-30 (1999)

A Yrast Study of the A = 61 Isobars $^{61}_{29}$Cu and $^{61}_{30}$Zn
S. M. Vincent, P. H. Regan, S. Mohammadi, W. Gelletly, D. Blumenthal, M. P. Carpenter, C. N. Davids, R. V. F. Janssens, C. J. Lister, C. J. Pearson, J. Simpson, D. Seweryniak, J. Schwartz, and D. D. Warner
Proceedings of the International Conference on the Physics of Nuclear Structure at the Extremes, Lewes, Sussex, United Kingdom, June 17-19, 1998; J. Phys. G: Nucl. Part. Phys. **25**, 941-943 (1999)

Discrete Line Spectroscopy of $^{62}_{31}$Ga with AYEBALL

S. M. Vincent, P. H. Regan, D. Blumenthal, M. Carpenter, C. N. Davids, W. Gelletly, R. V. F. Janssens, C. J. Lister, D. Seweryniak, J. Schwartz, J. Simpson, and D. D. Warner

Proceedings of the International Conference on the Physics of Nuclear Structure at the Extremes, Lewes, Sussex, United Kingdom, June 17-19, 1998; J. Phys. G: Nucl. Part. Phys. **25**, 679-683 (1999)

High Spin States in ^{58}Ni

S. Mohammadi, P. H. Regan, S. M. Vincent, D. Blumenthal, M. Carpenter, C. N. Davids, W. Gelletly, R. V. F. Janssens, C. J. Lister, C. J. Pearson, J. Simpson, D. Seweryniak, and J. Schwartz

Proceedings of the International Conference on the Physics of Nuclear Structure at the Extremes, Lewes, Sussex, United Kingdom, June 17-19, 1998; J. Phys. G: Nucl. Part. Phys. **25**, 909-912 (1999)

Exclusive Studies of the GDR in Excited Nuclei

V. Nanal, B. B. Back, D. J. Hofman, G. Hackman, D. Ackermann, S. Fischer, D. Henderson, R. V. F. Janssens, T. L. Khoo, A. A. Sonzogni, and Y. Alhassid

Proceedings of GR98 Topical Conference on Giant Resonances, Varenna, Italy, May 11-16, 1998; Nucl. Phys. **A649**, 153c-156c (1999)

Proton Radioactivity - Spherical and Deformed

C. N. Davids, P. J. Woods, D. Seweryniak, A. A. Sonzogni, J. C. Batchelder, C. R. Bingham, T. Davinson, D. J. Henderson, R. J. Irvine, G. L. Poli, J. Uusitalo, and W. B. Walters

Proceedings of the International Workshop on Rare Nuclear Processes in Low Energy Heavy Ion Physics, New Delhi, India, 16-20 November 1998; Pramana - J. Phys. **53**, 269 (1999)

Superdeformation in the A = 150 and A = 190 Regions

M. P. Carpenter and R. V. F. Janssens

Proceedings of Nuclear Structure '98, August 10-15, 1998, Gatlinburg, TN, pp. 393-406 (1999)

Unsafe Coulomb Excitation of $^{240-244}$Pu

I. Wiedenhöver, R. V. F. Janssens, G. Hackman, I. Ahmad, J. P. Greene, H. Amro, M. P. Carpenter, D. T. Nisius, P. Reiter, T. Lauritsen, C. J. Lister, T. L. Khoo, S. Siem, J. Cizewski, D. Seweryniak, J. Uusitalo, A. O. Macchiavelli, P. Chowdhury, E. H. Seabury, D. Cline, and C. Y. Wu

Proceedings of Nuclear Structure '98, August 10-15, 1998, Gatlinburg, TN, pp. 527-534 (1999)

Unsafe Coulomb Excitation of $^{240-244}$Pu

R. V. F. Janssens, I. Wiedenhöver, G. Hackman, I. Ahmad, J. P. Greene, H. Amro, M. P. Carpenter, D. T. Nisius, P. Reiter, T. Lauritsen, C. J. Lister, T. L. Khoo, S. Siem, J. Cizewski, D. Seweryniak, J. Uusitalo, A. O. Macchiavelli, P. Chowdhury, E. H. Seabury, D. Cline, and C. Y. Wu

Proceedings of the International Conference on Perspectives in Nuclear Physics, Paradise Island, Bahamas, November 13-16, 1998, eds. J. H. Hamilton, H. K. Carter, and R. B. Piercey, World Scientific (Singapore, New Jersey, London, Hong Kong, 1999) pp. 47-56

Spectroscopy of Neutron-Rich Nuclei Populated in the Spontaneous Fission of ^{252}Cf and ^{248}Cm

A. G. Smith, G. S. Simpson, J. Billowes, J. L. Durell, W. R. Phillips, P. J. Dagnall, S. J. Freeman, M. Leddy, A. A. Roach, J. F. Smith, A. Jungclaus, K. P. Lieb, C. Teich, N. Schulz, B. J. P. Gall, F. Hoellinger, I. Ahmad, J. Greene, and A. Algora

Proceedings of Conference "Nuclear Structure '98", August 10-15, 1998, Gatlinburg, TN, ed. C. Baktash, AIP Conference Proceedings 481, pp. 283-293 (1999)

The Spectroscopy of ^{183}Tl: An Extreme Case of Prolate-Oblate Shape-Competition

W. Reviol, L. L. Riedinger, C. R. Bingham, W. Weintraub, D. Jenkins, R. Wadsworth, A. N. Wilson, S. Juutinen, K. Helariutta, M. P. Carpenter, R. V. F. Janssens, D. Seweryniak, J. Uusitalo, I. Wiedenhöver, C. J. Gross, K. S. Toth, J. C. Batchelder, and J. A. Cizewski

Proceedings of Conference "Nuclear Structure '98", August 10-15, 1998, Gatlinburg, TN, ed. C. Baktash, AIP Conference Proceedings 481, pp. 232-239 (1999)

How Far from Stability Can We Go Using Gammasphere and the FMA?

C. J. Lister

Proceedings of the International Nuclear Physics Conference 1998, August 24-28, 1998, Paris, France, ed. B. Frois, D. Goutte, and D. Guillemaud-Mueller; Nucl. Phys. **A654**, 691c-696c (1999)

Weak Interaction Studies with an On-Line Penning Trap Mass Spectrometer

G. Savard, R. C. Barber, F. Buchinger, J. E. Crawford, X. Feng, S. Gulick, G. Hackman, J. C. Hardy, J. K. P. Lee, R. B. Moore, K. S. Sharma, and J. Uusitalo

Proceedings of the International Nuclear Physics Conference 1998, August 24-28, 1998, Paris, France, ed. B. Frois, D. Goutte, and D. Guillemaud-Mueller; Nucl. Phys. **A654**, 961c-966c (1999)

K-Isomers in Hf Nuclei At and Beyond the Neutron-Rich Edge of β-Stability

P. Chowdhury, R. D'Alarcao, E. H. Seabury, P. M. Walker, C. Wheldon, I. Ahmad, M. P. Carpenter, G. Hackman, R. V. F. Janssens, T. L. Khoo, D. Nisius, and P. Reiter

Proceedings of the International Nuclear Physics Conference 1998, August 24-28, 1998, Paris, France, ed. B. Frois, D. Goutte, and D. Guillemaud-Mueller; Nucl. Phys. **A654**, 651c-654c (1999)

Nuclear Excitation by Electronic Transition (NEET)
I. Ahmad, R. W. Dunford, H. Esbensen, D. S. Gemmell, E. P. Kanter, B. Krässig, S. H. Southworth, and U. Rütt
Proceedings of the 19th Werner Brandt Workshop on the Interaction of Charged Particles with Matter, Bariloche, Argentina, 13-16 April, 1999, pp. 195-204 (1999)

Preparation of 1 mg/cm^2 ^{13}C Target
John P. Greene, George E. Thomas, Alejandro Garcia, Alexander Komives, and John O. Stoner Jr.
Proceedings of the 19th World Conference of the INTDS, Oak Ridge, TN, October 5-9, 1998; Nucl. Instrum. Methods **A438**, 52-57 (1999)

Results from Experiment E917 for Au + Au Collisions at the AGS
D. Hofman for the E917 Collaboration
Proceedings of the 14th International Conference on Ultra-Relativistic Nucleus Collisions, Torino, Italy, May 10-15, 1999; Nucl. Phys. **A661**, 75c-81c (1999)

Decay Out of the Yrast Superdeformed Band in ^{191}Hg
S. Siem, P. Reiter, T. L. Khoo, T. Lauritsen, M. P. Carpenter, I. Ahmad, H. Amro, I. Calderin, T. Dossing, S. M. Fischer, U. Garg, D. Gassman, G. Hackman, F. Hannachi, R. V. F. Janssens, B. Kharraja, A. Korichi, A. Lopez-Martens, E. F. Moore, D. Nisius, and C. Schuck
Proceedings of the International Conference on "The Nucleus: New Physics for the New Millennium", Faure, South Africa, January 18-22, 1999, eds. F. D. Smit, R. Lindsay, and S. V. Förtsch (Kluwer Academic/Plenum Publishers, New York 1999), pp. 431-434

Lifetime Measurements and Dipole Transition Rates for Superdeformed States in ^{190}Hg
H. Amro, R. V. F. Janssens, E. F. Moore, G. Hackman, S. M. Fischer, I. Ahmad, M. P. Carpenter, B. Crowell, T. L. Khoo, T. Lauritsen, D. Nisius, J. Timar, and A. Wilson
Proceedings of the International Conference on "The Nucleus: New Physics for the New Millenium", Faure, South Africa, January 18-22, 1999, eds. F. D. Smit, R. Lindsay, and S. V. Förtsch, (Kluwer Academic/Plenum Publishers, New York 1999), pp. 27-31

Gamma-Ray Array Physics
C. J. Lister
Proceedings of the International Conference on "The Nucleus: New Physics for the New Millennium", Faure, South Africa, January 18-22, 1999, eds. F. D. Smit, R. Lindsay, and S. V. Förtsch, (Kluwer Academic/Plenum Publishers, New York 1999) pp. 275-286

Proton Radioactivity - Spherical and Deformed
C. N. Davids, P. J. Woods, D. Seweryniak, A. A. Sonzogni, J. C. Batchelder, C. R. Bingham, T. Davinson, D. J. Henderson, R. J. Irvine, G. L. Poli, J. Uusitalo, and W. B. Walters
Proceedings of the XXXIII Zakopane School of Physics, Zakopane, Poland, 1-9 September 1998; Acta Physica Polonica **B30**, 555-563 (1999)

New Superdeformed Bands in ^{150}Gd

S. Ertürk, P. J. Twin, D. E. Appelbe, P. Fallon, C. W. Beausang, S. Asztalos, R. Krüken, T. Lauritsen, I. Y. Lee, A. O. Macchiavelli, and F. S. Stephens

Proceedings of the International Conference on "The Nucleus: New Physics for the New Millennium", Faure, South Africa, January 18-22, 1999, eds. F. D. Smit, R. Lindsay, and S. V. Förtsch (Kluwer Academic/Plenum Publishers, New York 1999), pp. 173-183

Lifetime Measurements and Dipole Transition Rates for Superdeformed States in ^{190}Hg

H. Amro, R. V. F. Janssens, E. F. Moore, G. Hackman, S. M. Fischer, I. Ahmad, M. P. Carpenter, B. Crowell, T. L. Khoo, T. Lauritsen, D. Nisius, J. Timar, and A. N. Wilson

International Conference on The Nucleus: New Physics for the New Millennium, Faure, South Africa, January 18-22, 1999, Book of Abstracts, p. 2 (1999)

Radiative Decay of High-Lying States in ^{24}Mg

C. J. Lister, A. H. Wuosmaa, J. Schwartz, D. Henderson, C. N. Davids, D. Seweryniak, R. V. F. Janssens, M. P. Carpenter, T. Lauritsen, P. Reiter, I. Wiedenhöver, J. Cizewski, and W. Catford

APS Centennial Meeting, March 20-26, 1999, Atlanta, GA; Bull. Am. Phys. Soc. 44, 985 (1999)

High Spin Spectroscopy of Plutonium Isotopes

I. Wiedenhöver, R. V. F. Janssens, G. Hackman, I. Ahmad, J. P. Greene, H. Amro, M. P. Carpenter, P. Reiter, T. Lauritsen, C. J. Lister, T. L. Khoo, S. Siem, J. Cizewski, D. Seweryniak, J. Uusitalo, A. O. Macchiavelli, P. Chowdhury, E. H. Seabury, D. Cline, and C. Y. Wu

APS Centennial Meeting, March 20-26, 1999, Atlanta, GA; Bull. Am. Phys. Soc. 44, 1298 (1999)

The PHOBOS Multiplicity Detector

A. H. Wuosmaa and the PHOBOS Collaboration

APS Centennial Meeting, March 20-26, 1999, Atlanta, GA; Bull. Am. Phys. Soc. 44, 1532 (1999)

Flow Signatures for 10.7 GeV/Nucleon Au + Au in Experiment E917 at the AGS

D. J. Hofman and the E917 Collaboration

APS Centennial Meeting, March 20-26, 1999, Atlanta, GA; Bull. Am. Phys. Soc. 44, 498 (1999)

Decay of ^{256}Md

I. Ahmad and R. R. Chasman

APS Centennial Meeting, March 20-26, 1999, Atlanta, GA; Bull. Am. Phys. Soc. 44, 1139 (1999)

Formation Mechanism of the Transfermium Isotope
P. Reiter, A. A. Sonzogni, T. L. Khoo, C. J. Lister, I. Ahmad, M. P. Carpenter, C. N. Davids, W. F. Henning, R. V. F. Janssens, T. Lauritsen, D. Seweryniak, S. Siem, J. Uusitalo, I. Wiedenhöver, P. A. Butler, N. Amzal, A. J. Chewter, P. T. Greenlees, R. D. Herzberg, G. Jones, M. Leino, K. Vetter, J. Cizewski, K-Y. Ding, N. Fotiades, and W. Korten
APS Centennial Meeting, March 20-26, 1999, Atlanta, GA; Bull. Am. Phys. Soc. 44, 1298 (1999)

Identification of Excited States in ^{125,126}Pr
D. R. LaFosse, T. Koike, C. J. Chiara, D. B. Fossan, K. Starosta, S. J. Freeman, M. J. Leddy, J. F. Smith, M. Devlin, F. Lerma, D. G. Sarantites, J. N. Wilson, R. Wadsworth, A. N. Wilson, C. N. Davids, R. V. F. Janssens, and D. Seweryniak
APS Centennial Meeting, March 20-26, 1999, Atlanta, GA; Bull. Am. Phys. Soc. 44, 1136 (1999)

Decay Out of the Yrast Band in ^{183}Tl
W. Reviol, C. R. Bingham, L. L. Riedinger, W. Weintraub, D. Jenkins, R. Wadsworth, A. Wilson, S. Juutinen, K. Helariutta, M. P. Carpenter, R. V. F. Janssens, D. Seweryniak, J. Uusitalo, I. Wiedenhöver, C. J. Gross, K. S. Toth, J. C. Batchelder, and J. A. Cizewski
APS Centennial Meeting, March 20-26, 1999, Atlanta, GA; Bull. Am. Phys. Soc. 44, 1137 (1999)

Entry Regions and Feeding Mechanisms of the Normal and M1 Bands in ^{196}Pb
N. Fotiades, J. A. Cizewski, K. Y. Ding, M. Cromaz, P. Fallon, I. Y. Lee, A. O Macchiavelli, D. Ward, R. V. F. Janssens, J. A. Becker, L. A. Bernstein, K. Hauschild, D. P. McNabb, and A. Gorgen
APS Centennial Meeting, March 20-26, 1999, Atlanta, GA; Bull. Am. Phys. Soc. 44, 1138 (1999)

Band Structure of ^{125}La
K. Starosta, C. J. Chiara, D. B. Fossan, T. Koike, D. R. LaFosse, S. J. Freeman, M. J. Leddy, J. F. Smith, M. Devlin, F. Lerma, D. G. Sarantites, J. N. Wilson, R. Wadsworth, A. N. Wilson, C. N. Davids, R. V. F. Janssens, and D. Seweryniak
APS Centennial Meeting, March 20-26, 1999, Atlanta, GA; Bull. Am. Phys. Soc. 44, 1139 (1999)

Laser Trapping for Noble Gas Trace Analysis
C.-Y. Chen, K. Bailey, D. J. Lin, Z.-T. Lu, T. P. O'Connor, and L. Young
APS Centennial Meeting, March 20-26, 1999, Atlanta, GA; Bull. Am. Phys. Soc. 44, 1152 (1999)

Superdeformation in ^{128}Ce
A. Galindo-Uribarri, S. D. Paul, D. Hartley, W. Reviol, L. L. Riedinger, O. Zeidan, M. Devlin, D. Sarantites, M. Carpenter, and D. Seweryniak
APS Centennial Meeting, March 20-26, 1999, Atlanta, GA; Bull. Am. Phys. Soc. 44, 1297 (1999)

Spectroscopy Study of the Proton Emitter ^{109}I
Chang-Hong Yu, A. Galindo-Uribarri, C. J. Gross, S. D. Paul, M. P. Carpenter, C. N. Davids, R. V. F. Janssens, C. J. Lister, D. Seweryniak, J. Uusitalo, and B. D. MacDonald
APS Centennial Meeting, March 20-26, 1999, Atlanta, GA; Bull. Am. Phys. Soc. 44, 1296 (1999)

High-Spin Structure in ^{116}Xe and ^{118}Xe
T. Koike, C. J. Chiara, D. B. Fossan, D. R. LaFosse, K. Starosta, S. J. Freeman, M. J. Leddy, J. F. Smith, M. Devlin, F. Lerma, D. G. Sarantites, J. N. Wilson, R. Wadsworth, A. N. Wilson, C. N. Davids, R. V. F. Janssens, and D. Seweryniak
APS Centennial Meeting, March 20-26, 1999, Atlanta, GA; Bull. Am. Phys. Soc. 44, 1296 (1999)

Exotic Rotational Band in ^{168}Hf
P. G. Varmette, B. Herskind, G. H. Hagemann, G. Sletten, A. Maj, M. Bergstrom, K. A. Schmidt, Wen-Chao Ma, S. W. Odegaard, M. P. Carpenter, T. Lauritsen, R. V. F. Janssens, T. L. Khoo, C. J. Lister, S. Siem, D. J. Hartley, L. L. Riedinger, J. Domsheit, H. Hubel, A. Bracco, S. Frattini, and B. Million
APS Centennial Meeting, March 20-26, 1999, Atlanta, GA; Bull. Am. Phys. Soc. 44, 1297 (1999)

G-Factor Measurement of Discrete, High Spin, Normal Deformation States in ^{193}Hg
T. J. Mertzimekis, N. Benczer-Koller, J. Holden, G. Kumbartzki, L. Weissman, M. Hass, K.-H. Speidel, R. V. F. Janssens, I. Y. Lee, and A. Macchiavelli
APS Centennial Meeting, March 20-26, 1999, Atlanta, GA; Bull. Am. Phys. Soc. 44, 1297 (1999)

Heating of Au^{197} Nuclei with 8 GeV/c Antiprotons
T. Lefort, L. Beaulieu, K. Kwiatkowski, W.-C. Hsi, V. E. Viola, L. Pienkowski, R. G. Korteling, R. Laforest, E. Martin, E. Ramakrishnan, D. Rowland, A. Ruangma, E. Winchester, S. J. Yennello, S. Gushue, L. P. Remsberg, B. Back, and H. Breuer
APS Centennial Meeting, March 20-26, 1999, Atlanta, GA; Bull. Am. Phys. Soc. 44, 1408 (1999)

Heating of Nuclear Matter with 8 GeV/c π^- and = p Beams
L. Beaulieu, T. Lefort, K. Kwiatkowski, W.-C. Hsi, V. E. Viola, L. Pienkowski, R. G. Korteling, R. Laforest, E. Martin, E. Ramakrishnan, D. Rowland, A. Ruangma, E. Winchester, S. J. Yennello, S. Gushue, L. P. Remsberg, B. Back, and H. Breuer
APS Centennial Meeting, March 20-26, 1999, Atlanta, GA; Bull. Am. Phys. Soc. 44, 1409 (1999)

Towards Improved Predictions for Photon-Atom Scattering
J. P. J. Carney, R. H. Pratt, R. W. Dunford, E. P. Kanter, B. Krassig, S. H. Southworth, L. Young, R. A. Bonham, P. Lykos
APS Centennial Meeting, March 20-26, 1999, Atlanta, GA; Bull. Am. Phys. Soc. 44, 1534 (1999)

Laboratory Studies of Nuclear Reactions in Stellar Explosions
K. Ernst Rehm
APS Centennial Meeting, March 20-26, 1999, Atlanta, GA; Bull. Am. Phys. Soc. 44, 396 (1999)

Status of the Phobos Experiment at RHIC
Steven Manley for the PHOBOS Collaboration
APS Centennial Meeting, March 20-26, 1999, Atlanta, GA; Bull. Am. Phys. Soc. 44, 634 (1999)

The Phobos DAQ
P. A. Kulinich for the PHOBOS Collaboration
APS Centennial Meeting, March 20-26, 1999, Atlanta, GA; Bull. Am. Phys. Soc. 44, 1409 (1999)

Multiplicity Measurements with the PHOBOS Detector
Michael Reuter for the PHOBOS Collaboration
APS Centennial Meeting, March 20-26, 1999, Atlanta, GA; Bull. Am. Phys. Soc. 44, 1532 (1999)

Silicon Pad Detectors for the PHOBOS Experiment
R. Nouicer for the PHOBOS Collaboration
APS Centennial Meeting, March 20-26, 1999, Atlanta, GA; Bull. Am. Phys. Soc. 44, 1532 (1999)

Compton Double Ionization of Helium in the Region of the Cross-Section Maximum
B. Kraessig, R. W. Dunford, D. S. Gemmell, S. Hasegawa, E. P. Kanter, H. Schmidt-Bocking, W. Schmitt, S. H. Southworth, Th. Weber, and L. Young
18th International Conference on X-Ray and Inner-Shell Processes, August 23-27, 1999, Chicago, IL, Book of Abstracts, B4, p. 152 (1999)

Forward-Backward Asymmetries of Atomic Photoelectrons
S. H. Southworth, B. Kraessig, E. P. Kanter, J. C. Bilheux, R. W. Dunford, D. S. Gemmell, S. Hasegawa, and L. Young
18th International Conference on X-Ray and Inner-Shell Processes, August 23-27, 1999, Chicago, IL, Book of Abstracts, B22, p. 170 (1999)

Nuclear Excitation by Electronic Transition in ^{189}Os
I. Ahmad, R. W. Dunford, H. Esbensen, D. S. Gemmell, E. P. Kanter, B. Kraessig, U. Rutt, and S. H. Southworth
18th International Conference on X-Ray and Inner-Shell Processes, August 23-27, 1999, Chicago, IL, Book of Abstracts, D26, p. 304 (1999)

Search for ^{8}Be Decays of High-Spin States in ^{24}Mg
A. H. Wuosmaa, I. Wiedenhöver, C. J. Lister, M. P. Carpenter, R. V. F. Janssens, H. Amro, A. Heinz, J. Caggiano, T. Lauritsen, D. Seweryniak, S. Siem, A. Sonzogni, M. Devlin, L. G. Sobotka, and D. G. Sarantites
1999 Fall Meeting of the APS Division of Nuclear Physics, Pacific Grove, CA, 20-23 October 1999; Bull. Am. Phys. Soc. 44, 36 (1999)

Spin Determination for High-Spin States of ^{24}Mg
I. Wiedenhöver, A. H. Wuosmaa, C. J. Lister, M. P. Carpenter, R. V. F. Janssens, H. Amro, P. Bhattacharyya, A. Heinz, J. Caggiano, F. G. Kondev, T. Lauritsen, D. Seweryniak, S. Siem, A. Sonzogni, M. Devlin, L. G. Sobotka, and D. G. Sarantites
1999 Fall Meeting of the APS Division of Nuclear Physics, Pacific Grove, CA, 20-23 October 1999; Bull. Am. Phys. Soc. 44, 36 (1999)

Enhanced Deformed Structures in the Neutron-Deficient Nucleus ^{178}Hg
M. P. Carpenter, F. G. Kondev, R. V. F. Janssens, M. Alcorta, L. T. Brown, C. N. Davids, T. L. Khoo, T. Lauritsen, C. J. Lister, D. Seweryniak, M. Sonzogni, J. Uusitalo, I. Wiedenhöver, P. Bhattacharyya, S. M. Fischer, W. Reviol, L. L. Riedinger, and R. Nouicer
1999 Fall Meeting of the APS Division of Nuclear Physics, Pacific Grove, CA, 20-23 October 1999; Bull. Am. Phys. Soc. 44, 65 (1999)

First Observation of Excited Structures in Neutron Deficient ^{177}Au and ^{178}Au Isotopes
F. G. Kondev, M. P. Carpenter, R. V. F. Janssens, M. Alcorta, L. T. Brown, C. N. Davids, T. L. Khoo, T. Lauritsen, C. J. Lister, D. Seweryniak, M. Sonzogni, J. Uusitalo, I. Wiedenhöver, P. Bhattacharyya, S. M. Fischer, W. Reviol, L. L. Riedinger, and R. Nouicer
1999 Fall Meeting of the APS Division of Nuclear Physics, Pacific Grove, CA, 20-23 October 1999; Bull. Am. Phys. Soc. 44, 64 (1999)

Gammasphere at ATLAS: Physics at the Limits
R. V. F. Janssens
1999 Fall Meeting of the APS Division of Nuclear Physics, Pacific Grove, CA, 20-23 October 1999; Bull. Am. Phys. Soc. 44, 14 (1999)

Measurement of ^{44}Ti(α,p)^{47}V Cross Sections at Energies of Astrophysical Interest
A. A. Sonzogni, K. E. Rehm, I. Ahmad, F. Brumwell, J. Caggiano, C. N. Davids, J. Greene, B. Harss, A. Heinz, D. Henderson, W. Henning, R. V. F. Janssens, C. L. Jiang, G. McMichael, J. Nolen, R. C. Pardo, J. P. Schiffer, D. Seweryniak, R. H. Siemssen, J. Uusitalo, I. Wiedenhöver, B. Zabransky, F. Borasi, R. E. Segel, M. Paul, and J. W. Truran
1999 Fall Meeting of the APS Division of Nuclear Physics, Pacific Grove, CA, 20-23 October 1999; Bull. Am. Phys. Soc. 44, 58 (1999)

Studying K-Isomers Populated in U + Hf Reactions with Gammasphere
R. D'Alarcao, P. Chowdhury, I. Shestakova, C. J. Pearson, Z. Podolyak, P. M. Walker, C. Wheldon, D. M. Cullen, I. Ahmad, M. Carpenter, R. V. F. Janssens, T. L. Khoo, F. G. Kondev, C. J. Lister, D. Seweryniak, and I. Wiedenhöver
1999 Fall Meeting of the APS Division of Nuclear Physics, Pacific Grove, CA, 20-23 October 1999; Bull. Am. Phys. Soc. 44, 65 (1999)

Production of Radioactive Ion Beams with an In-Flight Technique
B. Harss, R. C. Pardo, K. E. Rehm, J. Greene, R. V. F. Janssens, C. L. Jiang, J. Nolen, J. P. Schiffer, J. Specht, P. Wilt, B. Zabransky, F. Borasi, R. E. Segel, and T. F. Wang
1999 Fall Meeting of the APS Division of Nuclear Physics, Pacific Grove, CA, 20-23 October 1999; Bull. Am. Phys. Soc. 44, 57 (1999)

Rotational Bands in the Proton Emitters ^{131}Eu and ^{141}Ho
D. Seweryniak, C. N. Davids, A. Sonzogni, J. Uusitalo, M. P. Carpenter, A. Heinz, R. V. F. Janssens, T. L. Khoo, F. Kondev, C. J. Lister, P. Reiter, I. Wiedenhöver, P. J. Woods, T. Davinson, J. Ressler, W. B. Walters, J. A. Cizewski, K. Y. Ding, and N. Fotiades
1999 Fall Meeting of the APS Division of Nuclear Physics, Pacific Grove, CA, 20-23 October 1999; Bull. Am. Phys. Soc. 44, 51 (1999)

Superallowed β-Decay of $T_z = 0$ Nuclei with $A \geq 62$
G. C. Ball, P. Bricault, A. MacDonald, G. Boisvert, S. Bishop, J. D'Auria, J. Cerny, D. M. Moltz, J. Powell, J. C. Hardy, V. Iacob, G. Savard, J. R. Leslie, H.-M. Mak, and I. S. Towner
1999 Fall Meeting of the APS Division of Nuclear Physics, Pacific Grove, CA, 20-23 October 1999; Bull. Am. Phys. Soc. 44, 59 (1999)

Complex Band Interactions in ^{170}Er
C. Y. Wu, D. Cline, M. W. Simon, R. Teng, K. Vetter, M. P. Carpenter, R. V. F. Janssens, and I. Wiedenhöver
1999 Fall Meeting of the APS Division of Nuclear Physics, Pacific Grove, CA, 20-23 October 1999; Bull. Am. Phys. Soc. 44, 64 (1999)

The α-Decay Spectra of ^{183}Tl^{m} and ^{182}Tl
K. S. Toth, C. R. Bingham, J. C. Batchelder, C. N. Davids, D. Seweryniak, and W. B. Walters
1999 Fall Meeting of the APS Division of Nuclear Physics, Pacific Grove, CA, 20-23 October 1999; Bull. Am. Phys. Soc. 44, 65 (1999)

In-Beam Spectroscopy Study of Doubly-Odd Nucleus ^{182}Au

J. P. Zhang, W. C. Ma, R. B. Piercey, J. A. Winger, W. Liu, R. K. Vadapalli, P. G. Varmette, J. K. Hwang, C. J. Beyer, J. H. Hamilton, A. V. Ramayya, M. P. Carpenter, R. V. F. Janssens, and D. Ward

1999 Fall Meeting of the APS Division of Nuclear Physics, Pacific Grove, CA, 20-23 October 1999; Bull. Am. Phys. Soc. 44, 65 (1999)

Multiple Band Structures in ^{179}Au

W. F. Mueller, D. Balabanski, C. R. Bingham, D. Hartley, W. Reviol, L. L. Riedinger, O. Zeidan, M. P. Carpenter, R. V. F. Janssens, T. L. Khoo, F. Kondev, D. Seweryniak, J. Uusitalo, I. Wiedenhöver, D. Jenkins, and R. Wadsworth

1999 Fall Meeting of the APS Division of Nuclear Physics, Pacific Grove, CA, 20-23 October 1999; Bull. Am. Phys. Soc. 44, 66 (1999)

Population of Neutron-Rich Isotopes ^{208}Pb + ^{238}U Deep-Inelastic Collisions

G. J. Lane, R. M. Clark, M. A. Deleplanque, R. M. Diamond, P. Fallon, I. Y. Lee, A. O. Macchiavelli, F. S. Stephens, C. E. Svensson, K. Vetter, D. Ward, R. Broda, B. Fornal, A. P. Byrne, G. D. Dracoulis, R. V. F. Janssens, and I. Wiedenhöver

1999 Fall Meeting of the APS Division of Nuclear Physics, Pacific Grove, CA, 20-23 October 1999; Bull. Am. Phys. Soc. 44, 77 (1999)

^{5}He Ternary Spontaneous Fission Yields from ^{252}Cf and ^{235}U

J. K. Hwang, A. V. Ramayya, J. H. Hamilton, C. J. Beyer, J. Kormicki, X. Q. Zhang, A. Rodin, A. Formichev, J. Kliman, L. Krupa, G. M. Ter-Akopian, Uy. Ts. Oganessian, G. Hubarian, D. Seweryniak, R. V. F. Janssens, I. Ahmad, C. J. Lister, M. P. Carpenter, T. Lauritsen, I. Wiedenhöver, W. C. Ma, and R. B. Piercey

1999 Fall Meeting of the APS Division of Nuclear Physics, Pacific Grove, CA, 20-23 October 1999; Bull. Am. Phys. Soc. 44, 78 (1999)

Ternary Spontaneous Fission of ^{252}Cf

A. V. Ramayya, J. K. Hwang, J. H. Hamilton, C. J. Beyer, J. Kormicki, X. Q. Zhang, A. Rodin, A. Formichev, J. Kliman, L. Krupa, G. M. Ter-Akopian, Yu. Ts. Oganessian, G. Hubarian, D. Seweryniak, R. V. F. Janssens, I. Ahmad, C. J. Lister, M. P. Carpenter, T. Lauritsen, I. Wiedenhöver, W. C. Ma, R. B. Piercey, and J. D. Cole

1999 Fall Meeting of the APS Division of Nuclear Physics, Pacific Grove, CA, 20-23 October 1999; Bull. Am. Phys. Soc. 44, 78 (1999)

Structure of ^{6}He Studied by the ^{6}Li(t,^{3}He)^{6}He Reaction

T. Nakamaura, T. Aumann, D. Bazin, Y. Blumenfeld, R. Clement, T. Glasmacher, P. Lofy, A. Navin, B. Pritychenko, B. Sherrill, J. Yurkon, J. Caggiano, B. Danilin, and I. J. Thompson

1999 Fall Meeting of the APS Division of Nuclear Physics, Pacific Grove, CA, 20-23 October 1999; Bull. Am. Phys. Soc. 44, 35 (1999)

Observation of Diffraction Patterns at 10.8 GeV/Nucleon Au + Au Reactions
Birger Back (for the E917 Collaboration)
1999 Fall Meeting of the APS Division of Nuclear Physics, Pacific Grove, CA, 20-23 October 1999; Bull. Am. Phys. Soc. 44, 75 (1999)

Nuclear Temperature of 8 GeV/c π^-, p^- + Au
A. Ruangma, R. W. Ibbotson, R. LaForest, E. Martin, E. Ramakrishnan, D. J. Rowland, E. M. Winchester, S. J. Yennello, L. Beaulieu, W. Hsi, K. Kwiatkoski, T. Lefort, V. E. Viola, L. Pienkowski, R. G. Korteling, H. Breuer, S. Gushue, L. P. Remsberg, and B. Back
1999 Fall Meeting of the APS Division of Nuclear Physics, Pacific Grove, CA, 20-23 October 1999; Bull. Am. Phys. Soc. 44, 75 (1999)

Spectroscopy of ^{27}P and ^{23}Al with the S800 Spectrograph at MSU
J. A. Caggiano, D. Bazin, W. Benenson, B. Davids, R. Ibbotson, H. Scheit, B. Sherrill, J. Yurkon, A. Zeller, J. Greene, J. Nolen, A. Wuosmaa, M. Bhattacharya, A. Garcia, M. Wiescher, B. Blank, and M. Chartier
1999 Fall Meeting of the APS Division of Nuclear Physics, Pacific Grove, CA, 20-23 October 1999; Bull. Am. Phys. Soc. 44, 19 (1999)

Feeding of the Superdeformed Band in the N = Z Nucleus ^{60}Zn
C. E. Svensson, R. M. Clark, M. Cromaz, M. A. Deleplanque, R. M. Diamond, P. Fallon, G. J. Lane, I. Y. Lee, A. O. Macchiavelli, F. S. Stephens, K. Vetter, D. Ward, R. A. E. Austin, T. Rodinger, J. C. Waddington, M. P. Carpenter, R. V. F. Janssens, C. Andreoiu, D. Rudolph, M. Devlin, F. Lerma, and D. G. Sarantites
1999 Fall Meeting of the APS Division of Nuclear Physics, Pacific Grove, CA, 20-23 October 1999; Bull. Am. Phys. Soc. 44, 49 (1999)

Spectroscopy of $^{100}_{48}Cd_{52}$
R. M. Clark, M. Cromaz, M. A. Deleplanque, R. M. Diamond, P. Fallon, G. J. Lane, I. Y. Lee, A. O. Macchiavelli, F. S. Stephens, C. E. Svensson, K. Vetter, D. Ward, J. N. Wilson, M. Devlin, D. G. Sarantites, D. Appelbe, J. C. Waddington, M. P. Carpenter, R. V. F. Janssens, D. Seweryniak, I. Wiedenhöver, C. J. Chiara, D. B. Fossan, T. Koike, D. R. Lafosse, K. Starosta, D. Jenkins, N. Kelsall, R. Wadsworth, and B. Alex Brown
1999 Fall Meeting of the APS Division of Nuclear Physics, Pacific Grove, CA, 20-23 October 1999; Bull. Am. Phys. Soc. 44, 50 (1999)

Discovery of Fine Structure in the Decay of the Highly Deformed Proton Emitter ^{131}Eu
C. N. Davids, A. A. Sonzogni, P. J. Woods, D. Seweryniak, M. P. Carpenter, J. J. Ressler, J. Schwartz, J. Uusitalo, and W. B. Walters
1999 Fall Meeting of the APS Division of Nuclear Physics, Pacific Grove, CA, 20-23 October 1999; Bull. Am. Phys. Soc. 44, 51 (1999)

An Experimental Study of the Coulomb Dissociation of ^{8}B

B. Davids, Sam M. Austin, R. R. C. Clement, B. M. Sherrill, D. W. Anthony, P. A. Lofy, T. Aumann, T. Baumann, D. Bazin, T. Nakamura, J. Yurkon, C. N. Davids, and H. Esbensen

1999 Fall Meeting of the APS Division of Nuclear Physics, Pacific Grove, CA, 20-23 October 1999; Bull. Am. Phys. Soc. 44, 53 (1999)

A Technique for Studying Low Energy and Low Intensity Radioactive Beams: Coulomb Excitation of a Radioactive Beam of ^{78}Rb

Jazmin Schwartz, C. J. Lister, D. Henderson, C. Davids, R. V. F. Janssens, D. Nisius, P. Reiter, D. Seweryniak, S. M. Fischer, J. A. Cizewski, A. Aprahamian, R. Dehaan, and S. Vincent

1999 Fall Meeting of the APS Division of Nuclear Physics, Pacific Grove, CA, 20-23 October 1999; Bull. Am. Phys. Soc. 44, 71 (1999)

R&D RELATED TO A FUTURE RARE-ISOTOPE FACILITY

Status of the First Batch of Niobium Resonator Production for the New Delhi Booster Linac
Prakash N. Potukuchi, Subhendu Ghosh, K. W. Shepard
Proceedings of the Eighth International Conference on Heavy-ion Accelerator Technology, October 5 –9, 1998, Argonne, Illinois (1999) p. 236

Status of the Linac Booster for NSC Pelletron
A Roy, P.N. Prakash, B.P. Aajithkumar, S. Ghosh, T. Changrani, A. Sarkar, R. Mehta, B.K. Sahu, A. Choudhury, J. Chacko, J. Anthony, M.V. Suresh Babu, M. Kumar, S. A. Krishnan, A. Mandal, G. O. Rodrigues, R. Kumar, R. K. Bhowmik, G. K. Mehta, K. W. Shepard
Proceedings of the Eighth International Conference on Heavy-ion Accelerator Technology, October 5 –9, 1998, Argonne, Illinois (1999) p. 267

An Advanced ISOL Facility Based on ATLAS
J. A. Nolen, K. W. Shepard, R. C. Pardo, G. Savard, K.E. Rehm, J. P. Schiffer, W. F. Henning, C.L. Jiang, I. Ahmad, B. B. Back, R. A. Kaye, M. Petra, M. Portillo, J. P. Greene, B. E. Clifft, J. R. Specht, R.V.F.Janssens, R. H. Siemssen, I. Bomes, C. B. Reed, A. M. Hassanein
Proceedings of the Eighth International Conference on Heavy-ion Accelerator Technology, October 5 –9, 1998, Argonne, Illinois (1999) p. 477

Beam Tests Of The 12 MHz RFQ Rib Injector For ATLAS
R.A. Kaye, K.W. Shepard, B.E. Clifft, M. Kedzie
Proceedings of the Eighth International Conference on Heavy-ion Accelerator Technology, October 5 –9, 1998, Argonne, Illinois, p. 528 (1999)

Beam Tests Of The 12 MHz RFQ Rib Injector For ATLAS
R.A. Kaye, K.W. Shepard, B.E. Clifft, M. Kedzie
Proceedings of the 1999 Particle Accelerator Conference, March 29th - April 2nd, 1999, New York City, p. 524 (1999)

Prototype 350 MHz Niobium Spoke-Loaded Cavities
K. W. Shepard, M. Kedzie, J. R. Delayen, J. Mammosser, C. Piller
Proceedings of the 1999 Particle Accelerator Conference, March 29th - April 2nd, 1999, New York City, p. 955 (1999)

Status of the Niobium Resonator Construction Project for the New Delhi Booster Linac
P.N. Potukuchi, S. Ghosh, K.W. Shepard
Proceedings of the 1999 Particle Accelerator Conference, March 29th - April 2nd, 1999, New York City, p. 952 (1999)

A High-Power Heavy-Ion Driver Accelerator for an Advanced Rare-Isotope Accelerator Facility in the United States
P.N. Ostroumov, K. W. Shepard, J. A. Nolen, and R. C. Pardo
ICFA Beam Dynamics Newsletter, No. 20, August, 1999, p. 60

Experimental Characterization of Gridded Electrostatic Lens (GEL) Low-Energy Beam Transport (LEBT) for the Laser Ion Source (LIS) and Effect of a Wire Grid on the Extraction Electrode

P.N. Ostroumov (ANL), P. Fournier, N. Lisi, C. Meyer, R. Scrivens (CERN, PS Division)

PS/HP/Note 99-10, Technical Note, CERN, Switzerland, 1999

An Advanced ISOL Facility Based on ATLAS

J. A. Nolen, K. W. Shepard, R. C. Pardo, G. Savard, K. E. Rehm, J. P. Schiffer, W. F. Henning, C.-L. Jiang, I. Ahmad, B. B. Back. R. A. Kaye, M. Petra, M. Portillo, J. P. Greene, B. E. Clifft, J. R. Specht, R. V. F. Janssens, R. H. Siemssen, I. Gomes, C. B. Reed, and A. M. Hassanein

Proceedings of the 8th International Conference on Heavy Ion Accelerator Technology (HIAT98), Argonne, IL, October 5-9, 1998, ed. Kenneth W. Shepard, AIP Conference Proceedings **473**, 477-489 (1999)

Production Mechanisms and Expected Yields of Exotic Beams at the Proposed ISOL-Based Rare Ion Accelerator

J. A. Nolen, B. B. Back. C. L. Jiang, K. E. Rehm, and G. Savard

1999 Fall Meetings of the APS Division of Nuclear Physics, Pacific Grove, CA 20-23 October 1999; Bull. Am. Phys. Soc. **44**, 57 (1999)

ISOL Beams from Fragmentation: The Best of Both Worlds

G. Savard

1999 Fall Meeting of the APS Division of Nuclear Physics, Pacific Grove, CA 20-23 October 1999; Bull. Am. Phys. Soc. **44**, 57 (1999)

MEDIUM-ENERGY NUCLEAR PHYSICS RESEARCH

Observation of a Coherence Length Effect in Exclusive ρ^0 Electroproduction
K. Ackerstaff et al. (and the HERMES Collaboration)
Phys. Rev. Lett. **82**, 3025-3029 (1999)

Beam-Induced Nuclear Depolarization in a Gaseous Polarized Hydrogen Target
K. Ackerstaff et al. (and the HERMES Collaboration)
Phys. Rev. Lett. **82**, 1164-1168 (1999)

Parton Energy Loss Limits and Shadowing in Drell-Yan Dimuon Production
M. A. Vasiliev et al. (FNAL E866/NuSea Collaboration)
Phy. Rev. Lett. **83**, 2304-2307 (1999)

Coherent π^0 Photoproduction on the Deuteron Up to 4 GeV
D. G. Meekins, et al.
Phys. Rev. C **60**, 052201/1-4 (1999)

Ultra-Sensitive Isotope Trace Analyses with a Magneto-Optical Trap
C. Y. Chen, Y. M. Li, K. Bailey, T. P. O'Connor, L. Young, and Z.-T. Lu
Science **286**, 1139-1141 (1999)

Angular Dependence of the ^{1}H(e,e'K$^+$)Λ Cross Section
Jinseok Cha (and TJNAF E91-016 Collaboration)
1999 Fall Meeting of the APS Division of Nuclear Physics, Pacific Grove, CA, 20-23 October 1999; Bull. Am. Phys. Soc. 44, 47 (1999)

Probing High Momentum Components of the Nuclear Wave Function
John Arrington (and TJNAF E89-008 Collaboration)
1999 Fall Meeting of the APS Division of Nuclear Physics, Pacific Grove, CA, 20-23 October 1999; Bull. Am. Phys. Soc. 44, 48 (1999)

Longitudinal Pion Electroproduction in H, ^{2}H, and ^{3}He
David Gaskell (and TJNAF E91-003 Collaboration)
1999 Fall Meeting of the APS Division of Nuclear Physics, Pacific Grove, CA, 20-23 October 1999; Bull. Am. Phys. Soc. 44, 33 (1999)

Deep Inelastic Scattering Reactions on Nuclear Targets
Donald F. Geesaman
1999 Fall Meeting of the APS Division of Nuclear Physics, Pacific Grove, CA, 20-23 October 1999; Bull. Am. Phys. Soc. 44, 10 (1999)

Longitudinal Pion Electroproduction from H and ^{2}H at W = 1.9 GeV
Bryon Mueller (and TJNAF E91-003 and E92-021 collaboration)
1999 Fall Meeting of the APS Division of Nuclear Physics, Pacific Grove, CA, 20-23 October 1999; Bull. Am. Phys. Soc. 44, 33 (1999)

THEORETICAL PHYSICS

Nuclear Structure Studies with the ^{7}Li(e,e'p) Reaction
L. Lapikas, J. Wesseling, and R. B. Wiringa
Phys. Rev. Lett. **81**, 4404-4407 (1999)

Multipositronic Systems
Kalman Varga
Phys. Rev. Lett. **83**, 5471-5474 (1999)

Soft-Core Hyperon-Nucleon Potentials
Th. A. Rijken, V. G. J. Stoks, and Y. Yamamoto
Phys. Rev. C **59**, 21 (1999)

Soft-Core Baryon-Baryon Potentials for the Complete Baryon Octet
V. G. J. Stoks and Th. A. Rijken
Phys. Rev. C **59**, 3009 (1999)

Stability of Two- and Three-Dimensional Excitonic Complexes
J. Usukura, Y. Suzuki, and K. Varga
Phys. Rev. B **59**, 5652-5661 (1999)

Mean Field Exponents and Small Quark Masses
A. Holl, P. Maris, and C. D. Roberts
Phys. Rev. C **59**, 1751-1755 (1999)

A Simple Example of Definitions of Truth, Valifity, Consistency, and Completeness in Quantum Mechanics
Paul Benioff
Phys. Rev. A **59**, 4223-4237 (1999)

Nuclear Induced Breakup of Halo Nuclei
H. Esbensen and G. F. Bertsch
Phys. Rev. C **59**, 3240-3245 (1999)

Evidence for the Fourth P_{11} Resonance Predicted by the Constituent Quark Model
Simon Capstick, T.-S. H. Lee, W. Roberts, and A. Svarc
Phys. Rev. C **59**, R3002-R3004 (1999)

Isotopic Effect in ϕ Photoproduction at a Few GeV
A. Titov, T.-S. H. Lee, and H. Toki
Phys. Rev. C **59**, R2993-R2997 (1999)

Structure of the ϕ Photoproduction Amplitude at a Few GeV
A. I. Titov, T.-S. H. Lee, H. Toki, and O. Streltsova
Phys. Rev. C **60**, 035205/1-20 (1999)

Survey of Heavy-Meson Observables
M. A. Ivanov, Yu. L. Kalinovsky, and C. D. Roberts
Phys. Rev. D **60**, 034018/1-17 (1999)

Strange Hadron Matter and SU(3) Symmetry
V. G. J. Stoks and T.-S. H. Lee
Phys. Rev. C **60**, 024006/1-9 (1999)

Particle-Hole Folded-Diagram Calculation of the Hypernucleus $^{16}_{\Lambda}$O Using Meson-Exchange Interactions
Yiharn Tzeng, S. Y. Tsay Tzeng, T. T. S. Kuo, and T.-S. H. Lee
Phys. Rev. C **60**, 044305/1-13 (1999)

Describing a_1 and b_1 Decays
J. C. R. Bloch, Yu. L. Kalinovsky, C. D. Roberts, and S. Schmidt
Phys. Rev. D **60**, 111502/1-5 (1999)

Pair Creation: Back-Reactions and Damping
J. C. R. Bloch, V. A. Mizerny, A. V. Prozorkevich, C. D. Roberts, S. M. Schmidt, S. A. Smolyansky, and V. D. Vinnik
Phys. Rev. D **60**, 116011/1-7 (1999)

Nucleon Form Factors and a Nonpointlike Diquark
J. C. R. Bloch, C. D. Roberts, S. M. Schmidt, A. Bender, and M. R. Frank
Phys. Rev. C **60**, 062201/1-5 (1999)

Diquark Condensation and the Quark-Quark Interaction
J. C. R. Bloch, C. D. Roberts, and S. M. Schmidt
Phys. Rev. C **60**, 065108/1-7 (1999)

Reply to 'Comment on "Effective Q-Q Interactions in Constituent Quark Models" '
L. Ya. Glozman, Z. Papp, W. Plessas, K. Varga, and R. F. Wagenbrunn
Phys. Rev. C **61**, 019804/1-2 (1999)

Λ Single Particle Energies
Q. N. Usmani and A. R. Bodmer
Phys. Rev. C **60**, 055215/1-16 (1999)

Force-Free Interactions and Nondispersive Phase Shifts in Interferometry
Murray Peshkin
Found. Phys. **29**, 481-489 (1999)

Describing the Nucleon Electromagnetic Form Factors at High Momentum Transfers
L. Theußl, B. Desplanques, B. Silvestre-Brac, and K. Varga
Few-Body Systems Suppl. **10**, 403-406 (1999)

Goldstone-Boson-Exchange Dynamics in the Constituent-Quark Model for Baryons
R. F. Wagenbrunn, L. Ya. Glozman, W. Plessas, and K. Varga
Few-Body Systems Suppl. **10**, 387-390 (1999)

Hadronic Decays of Light and Strange Baryon Resonances in the GBE Constituent-Quark Model
A. Krassnigg, W. Plessas, L. Theuβl, K. Varga, and R. F. Wagenbrunn
Few-Body Systems Suppl. **10**, 391-394 (1999)

Quantum Monte Carlo Calculations for Light Nuclei
R. B. Wiringa
Proceedings of the Workshop on Electron Nucleus Scattering, EIPC, Marciana Marina (Isola d'Elba, Italy) 22-26 June 1998, eds. Omar Benhar, Adelchi Fabrocini, and Rocco Schiavilla (Edizioni Ets, Pisa 1999) pp. 85-101

Nonperturbative Effects in QCD at Finite Temperature and Density
C. D. Roberts
Proceedings of the Research Workshop on Deconfinement at Finite Temperature and Density, LCTA, Dubna, Russia, 1-25 October 1997; Phys. Part. Nucl. **30**, 223-257 (1999)

Recent Developments in Theories of Pion Production in Nucleon-Nucleon Collisions
T.-S. H. Lee
Proceedings of the 7th Conference on Mesons and Light Nuclei '98, Institute of Nuclear Physics, Prague, Czech Republic, 31 August-4 September 1998, eds. J. Adam, P. Bydzovsky, J. Dobes, R. Mach, J. Mares, M. Sotona, (World Scientific, Singapore 1999) pp. 379-390

The Bethe Surface of Liquid Water
Michael Dingfelder and Mitio Inokuti
Proceedings of the 9th L. H. Gray Workshop (an International Meeting on Computational Methods in Track Structure Simulation in Physical and Biological Sciences - Theory and Applications) Milton Hill House, Harwell, Oxfordshire, UK, 10-13 September 1998; Radiation and Environmental Biophysics **38**, 93-96 (1999)

Dyson Schwinger Equations: Connecting Small and Large Length-Scales
Craig Roberts
Proceedings of the International Conference on Nuclear and Particle Physics with CEBAF at Jefferson Lab, Dubrovnik, Croatia, 03-10 November 1998; Fizika B 8, 285-294 (1999)

Quantum Monte Carlo Calculations for Light Nuclei
R. B. Wiringa
Proceedings of the Second Workshop on Electronuclear Physics with Internal Targets and the BLAST Detector, MIT, Cambridge, MA, 28-30 May 1998, eds. Ricardo Alarcon and Richard Milner (World Scientific, Singapore 1999) pp. 308-325

Study of the Δ Structure and NΔ Interactions with N(e,e'π) and d(e,e'π) Reactions
T.-S. H. Lee
Proceedings of the Second Workshop on Electronuclear Physics with Internal Targets and the BLAST Detector, MIT, Cambridge, MA, 28-30 May 1998, eds. Ricardo Alarcon and Richard Milner (World Scientific, Singapore 1999) pp. 39-53

W, F, and I: Three Quantities Basic to Radiation Physics
Mitio Inokuti
Proceedings of International Symposium in Commemoration of Professor Doke's Seventieth Birthday, Waseda University, Tokyo, Japan, 29 March 1999, eds. S. Kubota and J. Kikuchi (1999) pp. 1-17

The Nuclear Breakup of Halo Nuclei Through Diffraction and Stripping
K. Hencken, G. Bertsch, and H. Esbensen
Proceedings of the International Nuclear Physics Conference (INPC98), August 24-28, 1998, Paris, France, ed. B. Frois, D. Goutte, and D. Guillemaud-Mueller; Nucl. Phys. **A654**, 669c-672c (1999)

Non-Mean-Field Variational Description of Light Nuclei and Baryons
Rezsö G. Lovas, Kálman Varga, and Yasuyuki Suzuki
Proceedings of the Workshop on Electron Nucleus Scattering, Elba International Physics Center, Marciana Marina (Isola d'Elba, Italy), eds. Omar Benhar, Adelchi Fabrocini, Rocco Schiavilla, 22-26 June 1998 (Edizioniets 1999) pp. 119-133

Developing and Using a Nuclear Standard Model
Robert B. Wiringa
APS Centennial Meeting, March 20-26, 1999, Atlanta, GA; Bull. Am. Phys. Soc. 44, 1299 (1999).

Quantum Monte Carlo Studies of Nuclear Structure in Light Nuclei
R. Wiringa
1999 Fall Meeting of the APS Division of Nuclear Physics, Pacific Grove, CA, 20-23 October 1999; Bull. Am. Phys. Soc. 44, 31 (1999)